Polymerization of Functionalized Olefins with Neutral Group Ten Catalysts

Thesis by

Todd Ross Younkin

In Partial Fulfillment
of the Requirements for the Degree of
Doctor of Philosophy

California Institute of Technology
Pasadena, California

2001

(Submitted May 18, 2001)

To My Family With Love

Acknowledgements

It seems that most Ph.D. candidates aren't afforded the opportunity to work on a project which is truly a group effort. However, the story I've told herein is based on the hard work of many talented individuals. We acted together to develop ideas for new synthetic procedures and catalysts—calling upon each other for the support necessary to bring these ideas to fruition. In hindsight, the project has provided invaluable lessons about human nature, science, and the number of beers it takes before a good idea is *truly* formulated.

The "Ni project" began a year before I arrived with the initial efforts of Chunming Wang and Rob Li—who laid the foundation for later success through the development of the first salicylaldimine catalysts. Stefan Friedrich, famed inventor of the *o*-anthracenyl ligand, joined the group as I arrived in California. He served as my friend and mentor, patiently explaining the techniques that helped a young, arrogant graduate student get his start. I will always appreciate his efforts, though I am continually disappointed that he didn't provide me with more of his meticulous ways.

The arrival of Jason Henderson was well timed, as the project was stagnating in my hands, and it needed a talented chemist who could prepare Stefan's ligand. Although we didn't always see eye to eye, I am happy to say that Jason helped me grow personally and that we communicate on a regular basis now that we're not fighting for recognition. I wish the best of luck to him and his beautiful family.

Eric Connor. *Oh Jesus.* I can't say enough about the impact he had on me personally, spiritually, and scientifically. Of course, his persistence is unrivaled—for over a year, he toiled with the preparation of the "nitrile catalyst". At the point where most people (including myself) would throw in the towel, he was just getting started. The most memorable experience I have of him is our road trip to "Polyolefins II" in Napa. As the only students at the conference, we (unselfishly) delivered, in tandem, a dynamic talk which gave us the spotlight in a room full of our favorite organometallic chemists. If you ever have the chance, join Connor for a Guinness and chat (not about chemistry!)—you'll learn about yourself and meet a good friend.

During the last few months, I've had the pleasure of working with Andrew Waltman and Stuart Cantrill. Working with Drew has forced me to think more about mentoring, an artform which I am only beginning to appreciate. I hope that the "demons" I've given him aren't too bad or difficult to overcome—I'm sure it's not anything that a few hours of therapy or medication can't cure. I'd love to stay, continuing the search for a "portal to the alternate universe where *the catalyst* already exists," but am proud instead to pass the buck to these fine lads. Best of luck, Stu and Drew—I only hope that I've not led you astray (too much).

To these seven people, I am truly indebted—your patience with my persistent questions, hardheaded nature, and personality has been much appreciated.

My advisor, Bob Grubbs, is the reason such a fine team was assembled. He has an amazing knack for finding the right people for a project and letting "the ball roll." He continually encouraged my ideas and served as a valuable mentor. His "hands off" approach has forced me to think on my own, a task which I still relish.

I'd like to thank my committee members, Professors John Bercaw, Dennis Dougherty, and Dave Tirrell, for their continuing guidance.

The "Ni project" always maintained close financial and scientific ties with industry. Initially, the project was funded by W. R. Grace as part of an ATP project through NIST. This was followed by funding from Cryovac (Sealed Air Corp.) and more recently, Rohm & Haas. The respective project managers for each company—Don Bansleben, Bill Roberts, and Willie Lau—were always excited about the work we had performed. Their questions and intellectual contribution were a large part of our success.

In addition, many people contributed to our project through their analysis of our catalysts and polymers. Andrew Najadi performed polymerizations under various conditions that increased our understanding of the anthracenyl catalyst. Galen Hatfield (W.R. Grace) and Jonathan J. Litzau (W.R. Grace/Cryovac) performed wondrous feats through ^{1}H and ^{13}C NMR analysis of (almost all) the polymers prepared. Joy Harris kindly performed GPC and thermal analysis of the polymer samples. Cathy Sarinsky and Scott Ross performed the magnetization transfer experiments discussed in Ch. 3, helping to elucidate the mode of *cis-/trans-* isomerization for the "nitrile" catalyst. Sonjong Hwang, very patiently performed the solid-state analysis of the polymers discussed in Ch. 4 (it turns out that PE has a ^{13}C relaxation time ~ 5000 seconds). Mona Shahgholi graciously assisted in the ^{18}O-labelling study outlined in Ch. 1. Larry Henling and Mike

Day were instrumental in the structural determinations depicted in this thesis and were nice enough to provide me with an explanation of the theory of X-ray diffraction approximately 20 times (not bad for 17 structures).

My fellow "classmates"—Chris Treadway, Melanie Sanford, Kirk Hansen, and Steve Szczepankiewicz—have served as a source of inspiration as well as good companions.

The Grubbs' group has served as my home for a number of years, and there are a bunch of people who are not only coworkers, but whom I'm proud to call close friends (in no particular order, guys): Eric Dias, David Lynn, Helen Elizabeth Blackwell, Adam Matzger, Anna Mapp, Melanie Sanford, Daniel O'Leary, Jennifer Love, Justin Gallivan, LJ (T. Jon Seiders), and Bill Ward. Thanks for your support and guidance. Other coworkers, such as J. P. Morgan, Arnab Chatterjee, Tom Kirkland, Marcus Weck, Andreas Kilbinger, Oren Scherman, Dan Sanders, Steve Goldberg, Hyunjin Kim, Choon Woo Lee, and Dean Toste (who else am I forgetting?) have been a source of both good ideas and an occasional spirit.

Rick Gerhart, Tom Dunn, Mike Roy, Ray Garcia, Guy Duremburg, Chris Smith, and Steve Gould all deserve a huge pay raise. In addition, I'd like to extend a special thanks to Dian Buchness, who (if and when I receive my degree) is the person who helped me jump through all of the appropriate hoops. The continual effort of these individuals has greatly eased my time at Caltech.

Unfortunately, there seemed to be a few people with whom I had problems associating—I wish them nothing but the best of luck in their future endeavors—but will continue to be amazed at how people can be motivated by such different forces.

Life at Caltech is not *always* work. California is unequaled for its outdoor activities—which occasionally provide the proper perspective on life. I will never forget memorable trips to Joshua Tree, Mt. Whitney, Yosemite, Sequoia, King's Canyon, and the Redwoods with friends like Dave, Ken Brameld, Kirk Hansen, Pavel Stroop, Alex Gibson, Mike Hill, and Wendy. Other forms of stress relief have come in the form of a round of golf. Thanks to anyone who I beat—if you beat me, then scram!

Thanks to my family for their undying support. I am truly a blessed man.

Finally, a special thanks to my newest family member—my lovely bride-to-be, Wendy Vascik. She is, above all, the woman of my dreams, and fills my every morning with sunshine (and the sound of a hairdryer). I've benefited from her patience, loving heart, constant encouragement, and unwavering support. I look forward to the wonderful twists and turns which life will provide both of us.

Abbreviations

acac	Acetylacetonate
acac*	Pentanoylacetonate
Ar	Aryl
BHE	β-hydrogen elimination
BHT	β-hydrogen transfer to monomer
^{n}Bu	*n*-Butyl
^{t}Bu	*tert*-Butyl
COD	1,5-cyclooctadiene
Cp	η^5-Cyclopentadiene
Cp*	η^5-Pentamethylcyclopentadiene
dppe	Bis(diphenyl)phosphinoethane
dppm	Bis(diphenyl)phosphinomethane
Et	Ethyl
et	Ethylene
^{i}Pr	Isopropyl
MA	Methyl acrylate
Me	Methyl
MMA	Methyl methacrylate
nacnac	N,N-diphenyl-β-diketimate
PCy_3	Tricyclohexylphosphine, $P(C_6H_{11})_3$
Ph	Phenyl
PPh_3	Triphenylphosphine, $P(C_6H_5)_3$
py	Pyridine
THP	*O*-tetrahydropyranyl
tmeda	tetramethylethylenediamine
VA	Vinyl acetate

Abstract

This thesis describes the preparation, characterization, and application of well-defined single-component group ten salicylaldimine complexes for the polymerization of ethylene to high molecular weight materials as well as the copolymerization of ethylene and functionalized olefins. After an initial introduction to the field, Chapter 2 describes the preparation of PPh_3 complexes that contain a series of modified salicylaldimine and naphthaldimine ligands. Such complexes were activated for polymerization by the addition of cocatalysts such as $Ni(COD)_2$ or $B(C_6F_5)_3$. As the steric demand of the ligand set increased—the molecular weight, polymerization activity, and lifetime of the catalyst was observed to increase. In fact, complexes containing "bulky" ligands, such as the $[^{Anthr,H}Sal]$ ligand (**2.5**), were found to be highly-active single component complexes for the polymerization of ethylene. Model hydrido compound were prepared—allowing for a better understanding of both the mechanism of polymerization and one mode of decomposition.

Chapter 3 describes the effect which additives play on neutral Ni^{II} polymerization catalysts such as **2.5**. The addition of excess ethers, esters, ketones, anhydrides, alcohols, and water do not deactivate the catalysts for polymerization. However, the addition of excess acid, thiols, and phosphines was observed to shut-down catalysis. Since excess phosphine was found to inhibit catalysis, "phosphine-free" complexes, such as the acetonitrile complex (**3.26**), were prepared. The acetonitrile complex was found to be the most active neutral polymerization catalyst prepared to date.

Chapter 4 outlines the use of catalyst **2.5** and **3.26** for the preparation of linear functionalized copolymers containing alcohols, esters, anhydrides, and ethers. Copolymers can be prepared with γ-functionalized-α-olefins, functionalized norbornenes, and functionalized tricyclononenes, with up to 30 mol% comonomer incorporation.

Chapter 5 outlines the preparation of a series of Pt^{II} alkyl/olefin salicylaldimine complexes which serve as models for the active species in the Ni^{II}-catalyzed polymerization process. Understanding the nature of the M-olefin interaction as a the electronic and steric properties of the salicylaldimine ligand is varied has allowed for a number of predictions about the design of future polymerization systems.

Table of Contents

Chapter 1: Homogeneous Late-Metal Catalysts for the Coordination Polymerization of Olefins

Chapter 2: Neutral Salicylaldimine Ni^{II} and Pd^{II} Complexes. The Development of Highly Active Single-Component Catalysts for the Polymerization of Ethylene to High Molecular Weight Products

Chapter 3: Variation of the Ancillary-Ligand in Neutral Ni$^{\text{II}}$ Salicylaldimine Catalysts. Preparation of Highly-Active, "Phosphine-Free Systems"—Rate of Catalysis, Polymer Microstructure, and Catalyst Stability

Chapter 4: Linear Functionalized Polyethylene Prepared with Single Component, Neutral Ni^{II} Salicylaldimine Complexes

Chapter 5: The Effect of Ligand Modification Upon Olefin Coordination in Neutral Pt^{II} Alkyl-Olefin Complexes. Implications for the Past Performance and Future Design of Neutral Ni^{II} Oligomerization and Polymerization Catalysts.

List of Figures, Tables, and Schemes

Chapter 1

Chapter 2

Chapter 3

Chapter 4

Chapter 5

Chapter 1

Homogeneous Late-Metal Catalysts for the Coordination Polymerization of Olefins

1.1. Polyolefins – An overview

Hydrocarbon-based polymers, termed "polyolefins" because of their traditional feedstock, are of crucial economic importance as reflected by current production rates that exceed 160 billion pounds annually.[1] In fact, they continually serve as the fastest growing segment of the polymer industry.[2] Polyethylene (PE), with sales exceeding 100 billion pounds annually (~ 60% of the market), is undoubtedly the most significant.[1,3] Three major classes of PE are currently marketed (Figure 1.1): (a) low density (LDPE), (b) high density (HDPE), and (c) linear low density (LLDPE).[1,3] LDPE is a branched homopolymer prepared in a high-temperature/high-pressure radical process that requires pressures exceeding 1500 atmospheres (22,500 psig).[4] Such free-radical polymerizations are unselective, producing both short- and long-chain branches without the need for other olefins. These "irregularities" affect both crystallinity and melt temperature (short-chain branching) as well as the rheology of the polymer melt (long-chain branches), bestowing upon LDPE a different performance profile than the linear homopolymers outlined below.[3]

In contrast to LDPE, HDPE is a linear, semicrystalline polymer, prepared commercially through use of Ziegler-Natta or chromium-based catalysts in a low-pressure process.[3] Owing to its increased crystallinity, HDPE demonstrates a greatly increased strength, toughness, and chemical resistance. Therefore, typical applications include use in grocery bags, blow-molded (i.e., milk, detergent, etc.) bottles, pipe, crates, tubing, and medical applications such as hip replacements.[3] These same features provide a material with decreased elasticity, poor impact strength at low temperatures, and little clarity. However, similar metal catalysts can produce ethylene copolymers, LLDPEs, containing 8-10% α-olefins (1-butene, 1-hexene, or 1-octene) that act to decrease the crystallinity and density (relative to HDPE), such that a polymer with properties similar to LDPE can be produced at lower pressures.[3]

In general, polyolefins are characterized by the combination of their strength, flexibility, and general utility over a wide temperature range.[3] However, the hydrophobic nature of these polymers leads to poor compatibility with other polymers and a low adhesion to surfaces such as wood and metal. *These impairments can be overcome by the incorporation of small amounts of polar functionalities* (2-20 mol %).[5]

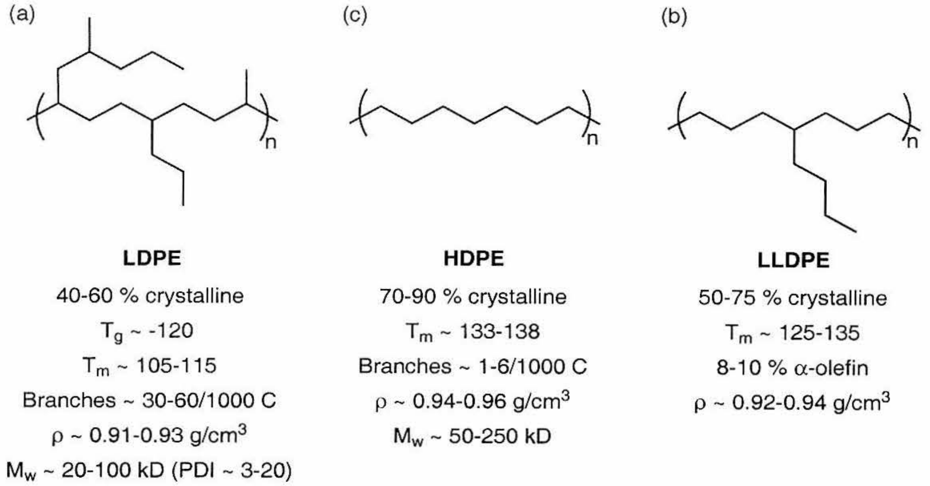

Figure 1.1. The three main classes of polyethylene (PE): (a) Low Density Polyethylene (LDPE), (b) Linear Lowest Density Polyethylene (LLDPE), and (c) High Density Polyethylene (HDPE).

1.2. Functionalized polyolefins and their commercial uses

The aforementioned low-pressure processes cannot incorporate these polar functionalities due to deactivation of the highly electrophilic metal catalysts.[1,3,6] Therefore, the ability to incorporate such species remains as the most attractive feature of the high-pressure radical process.[7] Copolymers containing vinyl acetate (VA), methyl acrylate (MA), methyl methacrylate (MMA), and acrylic acids are commercially prepared. Some of the applications for these copolymers are outlined in Table 1.1.

Table 1.1. Commercial uses for functionalized ethylene copolymers.

Comonomer	**Content (%)**	**Tradename(s)**	**Utility**
Methacrylate/ Methyl Methacrylate	15-30	*Lotryl* *Emac* *Optema*	Medical packaging, Disposable gloves, Hoses, Tubing
Acrylic/ Methacrylic Acid	15-20	*Nucrel* *Primacor*	Laminates for metal and glass fibers (automotive parts, construction materials), Adhesive films
Acrylic/ Methacrylic Acid[a] *(Ionomer)*	5-10	*Surlyn*	Golf ball covers, Wrestling mats, Rodeo Vests, Bacon packaging, Dog chew toys
Vinyl Acetate (VA)	2-20	*Elvax* *Ultrathene* *Escorene*	Squeeze toys, Hoses, Tubing, Insulation for wires/ cable, Footwear, Bottle cap liners, Meat, Poultry, and Frozen food packaging

[a] Author's personal favorite.

As desired, the polar functionalities in these polymers are distributed in a random fashion.[5] Unfortunately, the unselective radical process leads to formation of branched materials that have low crystallinity, and therefore, do not exhibit any of the properties associated with HDPE. Linear varieties of such copolymers have been prepared through multistep sequences.[8-11] Although such materials exhibit superior performance attributes for adhesion, wettability, and gas diffusion characteristics, their fabrication *via* olefin metathesis followed by subsequent hydrogenation of the unsaturated polymer (Figure 1.2) is prohibitively expensive. For these reasons, commercially relevant copolymers are still produced through high pressure free-radical techniques. Therefore, alternative methods that allows for the production of linear functionalized polyolefins using low pressure and commercial feedstocks (olefins) are highly attractive.[5]

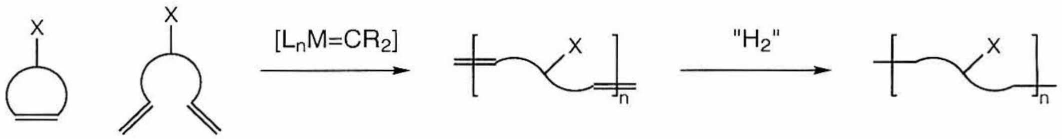

Figure 1.2. Olefin metathesis routes have been utilized for the preparation of linear functionalized polyolefins.

1.3. Late-metal catalysts for the preparation of functionalized polyethylenes

The polymerization of ethylene or α-olefins by the Ziegler-Natta or metallocene catalysts as described above follows two basic principles. These include chain growth *via* migratory insertion in an alkyl/olefin complex and chain transfer through a variety of mechanisms including β-hydride elimination (βHE) and β-transfer to monomer (βHT, not shown) (Figure 1.3).[12,13] Late-metal catalysts operate by a similar mechanism, but due to their increased propensity for chain transfer *via* βHE, they typically provide dimers or low molecular weight oligomers.[13,14] The functional-group tolerance required for the proposed coordination polymerization of ethylene and functionalized olefins, however, suggests that late-metal centers would provide good targets, as they demonstrate a much lower oxophilic nature. Therefore, the prime objective in the search for late transition metal complexes is the design of catalysts capable of producing high molecular weight products.[1,6]

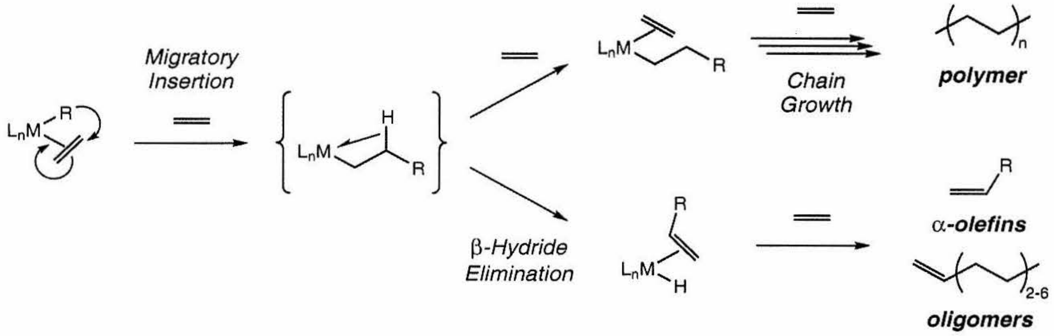

Figure 1.3. Polymerization/oligomerization mediated by a transition metal complex. Late-metal complexes typically prepare dimers or oligomers with ethylene or α-olefins.

1.4. Cationic Ni^{II}/Pd^{II} diimine catalysts allow for the polymerization of α-olefins and the copolymerization of functionalized olefins

In 1995, the polymerization community witnessed a "revolution" when Johnson, Killian, and Brookhart reported the use of cationic Ni^{II} and Pd^{II} α-diimine catalysts **1.1** and **1.2** for the polymerization of ethylene, *α-olefins*, and *cyclic olefins containing β-hydrogens* to high molecular weights.[1,15] Even more importantly, however, was the subsequent, seminal report on the copolymerization of ethylene/α-olefins with a variety of vinyl- functionalized olefins (such as vinyl acetate (VA), acrylate (MA), acrylic acid (AA)) by the Pd^{II} complexes.[1,16,17] As a consequence of the reversible chelation of the

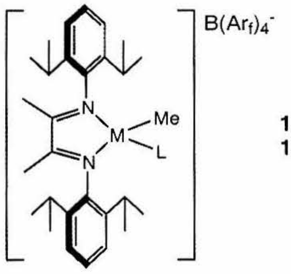

1.1 M = Ni
1.2 M = Pd

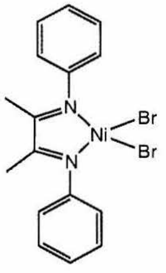

1.3

carbonyl groups from the monomer as shown in Figure 1.4, catalyst activity was found to decrease with increased comonomer incorporation.[1,16,17] However, copolymers containing up to 20 mol % of a commercially relevant monomer such as methyl acrylate could be prepared.[1,17]

Unfortunately, chain running (*vide infra*) results in the predominant incorporation of the functionality (such as acrylic groups) at the ends of branches in highly branched, amorphous copolymers. Similar to early metal systems, the Ni^{II} diimine systems form an intramolecular chelate with acrylic monomers that deactivate the catalyst and renders ethylene/acrylate copolymerizations unsuccessful. ***To date, there still remains no catalyst system capable of incorporating conventional polar monomers such as acrylates, methacrylates, and vinyl acetates directly into the backbone of a linear polyethylene.***[18]

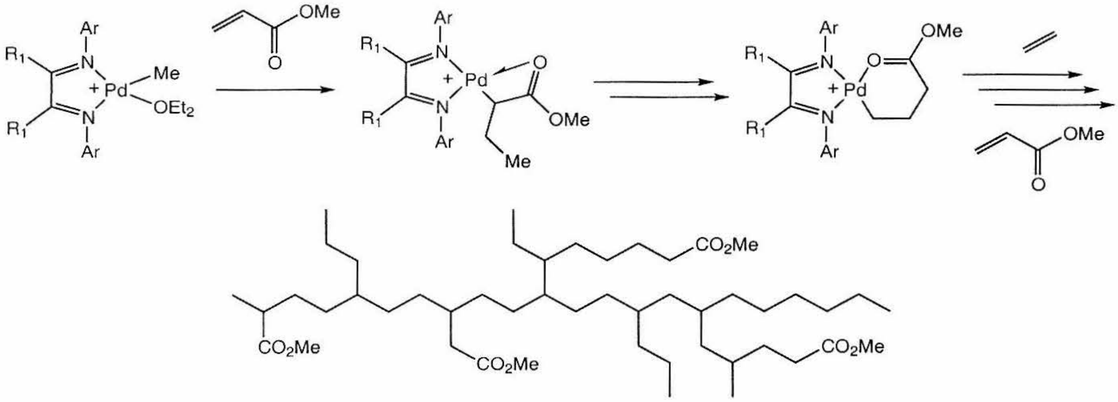

Figure 1.4. Copolymerization of ethylene and a vinyl-functionalized olefin (methyl acrylate) with cationic Pd^{II} catalysts yields amorphous polymer with functionality on the chain ends. Catalyst counterion, $[B(Ar_f)_4]^-$, omitted for clarity.

Although these cationic d^8 systems aren't successful for the preparation of linear functionalized polyolefins, understanding their polymerization behavior might allow for the design of improved systems. The complexes maintain several key features that allow for the formation of higher molecular weight products.[1,6] These include the use of (a) cationic (electrophilic) metal centers—resulting in rapid rates of olefin insertion [TOF_{Ni} ~ 4×10^6 g polymer $(\text{mol cat})^{-1}\cdot(\text{hr})^{-1}$], (b) sterically demanding ligands that act to disfavor chain transfer [$M_n > 100 \cdot 10^3$ g/mol (Ni^{II})], and (c) weakly coordinating counterions such as $[B(Ar_f)_4]^-$ or those generated from MAO.

The reduction of chain transfer rates was initially attributed to a slowing of the rate of associative displacement of the unsaturated polymer chain by ethylene (Figure 1.5).[1,15] Recent calculations, however, have proposed that an alternative chain termination pathway, namely βHT to monomer (Figure 1.5), may be operational, and that the barrier to βHT increases with the increasing steric demand of the ligand set.[19-23] Additional support for such termination mechanisms is evidenced by the fact that Ni^{II} complexes with a decreased steric demand (**1.3**) are highly active *oligomerization* catalysts for the conversion of ethylene to linear α-olefins.[1,24]

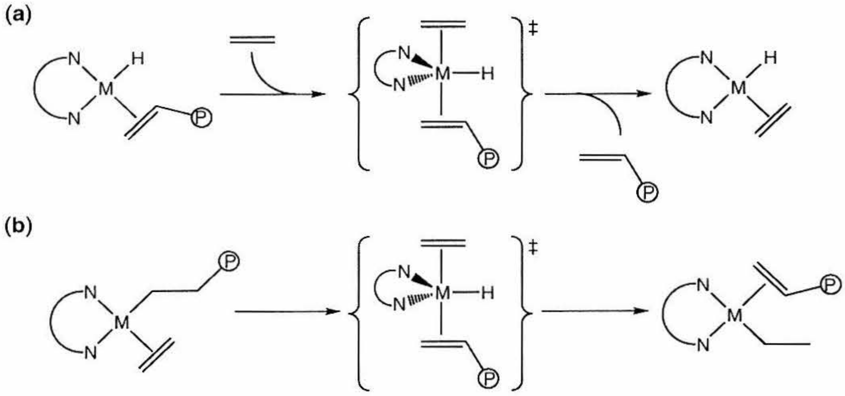

Figure 1.5. Proposed mechanisms for chain transfer/termination. (a) Associative displacement of polymer chain by free ethylene. (b) β-Hydrogen transfer (βHT) to monomer.

Stable, easily handled, discrete alkyl complexes of these cationic d^8 systems are available through the coordination of acetonitrile and benzonitrile. These weak donor ligands allow for highly active preparative-scale polymerizations.[1,25] The ether complex, which serves as an ideal precursor for low temperature ^1H NMR spectroscopy studies (*vide infra*) due to its increased lability, is available through protonation of a dimethyl precursor with $H^+(OEt_2)_2(BAr_f)_4$ in the presence of excess diethyl ether.[1,25]

Considering that these polymers are generated in low pressure processes, the resultant polyethylenes exhibit interesting polyolefin architectures. Polymers obtained with Ni^{II} complexes are moderately branched and exhibit a controlled response to both pressure and temperature (1-100 branches/1000 carbons—primarily methyl branches). In stark contrast, the amorphous polymers obtained with Pd^{II} catalysts (approximately 100 branches per 1000 carbon atoms) show no sign of a dependence on ethylene concentration. The Pd^{II} catalysts yield "branch on branch" architecture and have demonstrated an ability to prepare hyper-branched polymers.[1,26] All highly branched polyethylenes possess both even- and odd-number branches (C_1-C_5 and longer), which is believed to arise through a "chain-running" process (Figure 1.6).[1]

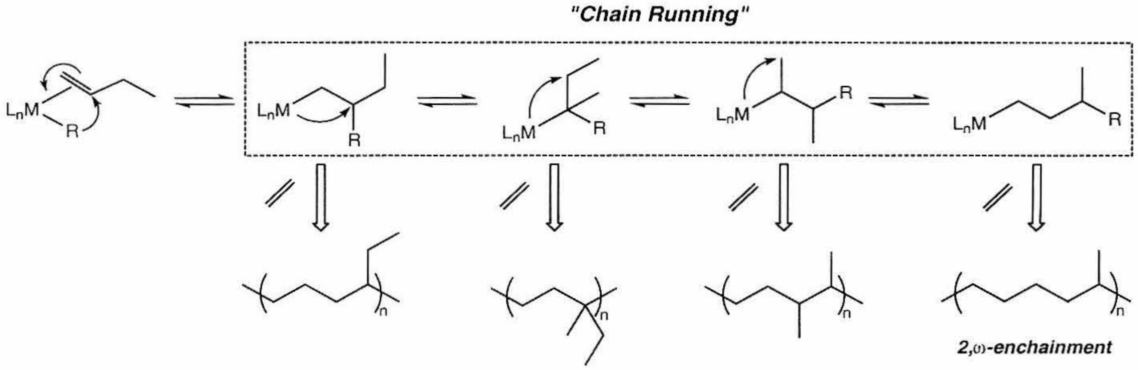

Figure 1.6. Chain running mechanism yields highly branched PE or "chain-straightened" poly(α-olefins).

Such "chain running" has also been observed with a catalyst prepared upon the combination of $(Me_3Si)_2N\text{-}P(=NSiMe_3)_2$ with either $Ni(COD)_2$ or $Ni(\eta^3\text{-allyl})_2$ in toluene.[27,28] The resulting species is believed to be *neutral*, as supported by comparison with the structurally determined Pd^{II} analog. The Ni^{II} catalyst mixture converts ethylene to a moderate M_w, branched polymer that possesses primarily methyl and some longer chain branches.[27] The mixture polymerizes α-olefins in a $2,\omega-$enchainment (Figure 1.6) yielding polymers that contain only methyl branches.[28]

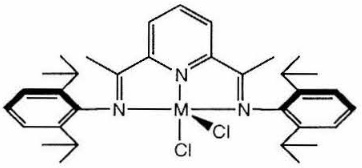

1.4 M = Fe
1.5 M = Co

1.5. Cationic Fe^{II} and Co^{II} catalysts for the preparation of linear polyolefins

The results outlined above for cationic d^8 complexes stimulated considerable industrial and academic interest in late transition metal polymerization catalysts. In the search for other suitable ligand structures, three different research groups independently reported cationic Fe^{II} and Co^{II} catalysts **1.4** and **1.5**.[29,30] In analogy to **1.1** and **1.2**, these complexes use tridentate bis(arylimino) pyridine ligands to shield the metal center. The Fe^{II} catalyst was found to polymerize ethylene to *highly linear*, crystalline high-density polyethylene (HDPE) at an astonishing rate [$TOF_{Ni} \sim 10^7$ g polymer (mol cat)$^{-1}\cdot$ (hr)$^{-1}$ at 40 bar] upon the addition of an activator such as MAO.[29-31] Broad and multimodal PDIs are observed as a result of chain transfer to aluminum as well as βHE.[29-31] Isotactic polypropylene (55-70% [mmmm]) can be prepared with moderate activities (TOF ~ 1.6 $\cdot$ 10^4 g polymer (mol cat)$^{-1}\cdot$ (hr)$^{-1}$.

Although variation of the bis(imino) pyridine core has only provided catalysts which exhibit very low activities,[32] removing the steric bulk of the *o*-aryl substituents in **1.4** yields, in analogy to **1.3**, catalysts for ethylene oligomerization.[33,34] Phenomenal activities (TOF up to 10^8) for the formation of >99% linear α-olefins were observed, far exceeding those reported for commercial SHOP catalysts.[1] The Co^{II} catalyst **1.5** is not so lucky, as it typically demonstrates activities that are much lower than **1.4** and, as such, has received less attention.[29,30,34] In addition, the Ru^{II} and Rh^{II} analogs are found to be inactive for polymerization.[35]

Although these catalysts prepare highly linear HDPE-type materials which greatly contrast those prepared by **1.1** and **1.2**, no reports on their functional group compatibility or the reaction with functionalized olefins have emerged. It is expected that these cationic

Fe^{II} d^6 catalysts exhibit an increased electrophilicity relative to the d^8 complexes, such as **1.1** and **1.2** and are, therefore, less tolerant of polar groups.

1.6. Neutral SHOP-type catalysts—Functional group tolerance and linear products

The Shell Higher Olefin Process (SHOP), a cornerstone of the petrochemical industry, is based on the production of C_8-C_{20} linear α-olefins through the oligomerization of ethylene with **1.6**. Originally developed by Keim *et al.* in the late-1960s and 1970s, this catalyst maintains high activities and selectivity for α-olefins as well as an unprecedented functional-group tolerance, such that catalysis with **1.6** is performed in a biphasic mixture (1,4-butanediol as a polar phase) allowing for the continuous separation of the nonpolar products.[36,37]

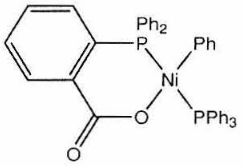

1.6

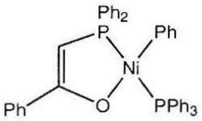

1.7

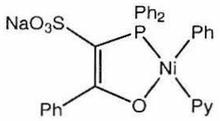

1.8

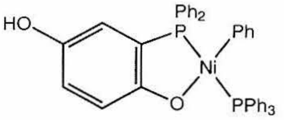

1.9

During the search for other complexes containing [P,O] chelating ligands, the similarly related complex, **1.7** was prepared. It also provided oligomeric materials (99% linear, 98% α-olefins, C_4-C_{30}) at 50 atm (750 psig) ethylene, 50 °C in toluene. Surprisingly, however, **1.7** was found to yield linear polyethylene in hexane under the same conditions.[1,18,38] Further development of similar [X,L] complexes led to the discovery of a variety of ethylene polymerization catalysts.[39] Most require higher pressures to convert ethylene to *linear* polyethylene and demonstrate low to moderate activities [TOF ~ 10^4 g polymer· (mol cat)$^{-1}$· (hr)$^{-1}$].[6,18]

Later, however, it was discovered that the addition of a "phosphine sponge," such as $Ni(COD)_2$, $Ni(CO)_4$, $Rh(acac)(C_2H_4)_2$, or trimethylamine-N-oxide allowed for the production of polyethylene at lower pressures.[40] It was proposed that these cocatalysts served to remove the strongly coordinating ligand ($L = PR_3$), freeing the coordination site necessary for polymerization to proceed.[40] Support for this hypothesis came from replacement of triphenylphosphine ligand with weakly coordinating groups, such as pyridine or triphenylphosphine oxide (**1.8**). These catalysts prepared high M_w without need for use of a cocatalyst.[40]

[P,O] complexes, such as **1.9**, containing electron-rich phosphorus ylides (L = CR_2PR_3) have also been investigated intensively.[1,6,41-44] They are single-component, activator-free precursors for both ethylene and acetylene polymerization.[41-44] Linear polyethylenes with very high molecular weights are accessible, with M_ws reported to be as high as $1 \cdot 10^6$ g mol^{-1} at elevated pressures (100 atm, 100 °C).[42] High productivities (TOF ~ $5 \cdot 10^4$ g polymer $\cdot$ (mol cat)$^{-1} \cdot$ (hr)$^{-1}$) were observed in typical polymerization experiments, with rates as high as 1.8×10^5 (17 atm ethylene).[41,42,44] These systems displayed high compatibility with functionalized species and were found to demonstrate activity in polar solvents, such as acetone, DMF, or alcohols.[42,43]

Attempts were made for the copolymerization of ethylene with methyl acrylate or vinyl acetate using 1.7-1.9 and have thus far been unsuccessful.[40] However, the copolymerization of monomers containing methylene spacers between the olefin and the polar functionality were successful, yielding low M_w (~ $10 \cdot 10^3$ g/mol) copolymers with low levels of comonomer incorporation (~ 4-18 weight %).[45]

Although evidence suggests that insertion of coordinated olefins in these neutral d^8 complexes proceeds from a four-coordinate intermediate,[37] an alternative insertion mechanism that could be operating is olefin insertion from a five-coordinate intermediate. In fact, researchers working with complexes of the type (pyca)Ni(Ph)L **1.10**, containing derivatives of 2-pyridine carboxylate (pyca), have proposed such a mechanism.[46,47] Triphenylphosphine complexes of this type (L = PPh_3) are single component catalysts for the conversion of ethylene to linear (low M_w) PE and allow for the copolymerization of ethylene and CO to yield alternating polyketones.[47] However, when electron-rich phosphines, such as PCy_3, PBn_3, and PMe_2Ph were used, the products were oligomeric (typically C_4-C_{10} at 80 °C with 40 atm ethylene).[46] Since the activity and product distribution of these [N,O] complexes was dependent on the nature of the L-group,[46,47] Cavell *et al.* proposed the mechanism depicted in Figure 1.7.[46] The propensity of Ni^{II} oligiomerization/polymerization complexes to form five-coordinate complexes is known,[48] and reactions involving Ni^{II} complexes often involve such five-coordinate complexes as intermediates or isolable complexes.[49]

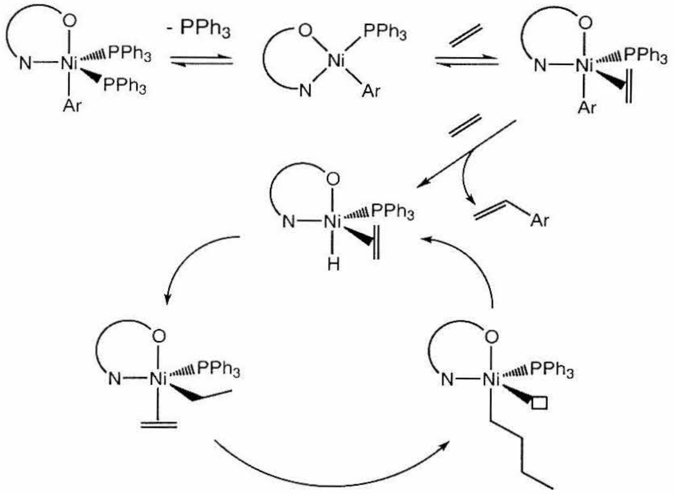

Figure 1.7. Postulated mechanism for the production of low molecular weight products by (pyca)Ni(PPh_3)Ph **1.10**.

Although polyethylene had been prepared with a variety of neutral complexes containing [P,O] and [N,O] chelates, such systems typically provide lower M_w polymers, require high operating pressures (typically in excess of 10 atm), and have not allowed for the copolymerization of ethylene and vinyl-functionalized monomers such as methyl acrylate.

1.7. Ethylene polymerization vs. oligomerization with late metal catalysts.

As previously outlined, the primary challenge in the discovery of late-metal polymerization systems is the development of catalysts that can prepare high molecular weight materials. Therefore, theoretical and mechanistic works that detail these subtle discrepancies is of utmost value. Chain growth with the cationic Ni^{II}/Pd^{II} diimine complexes and ethylene was monitored by low temperature ^1H NMR spectroscopy, leading to the determination that the alkyl/ethylene complex **1.11** is the catalyst resting state for the polymerization (Figure 1.8).[1,25,50] In early-metal polymerization systems, such alkyl/olefin intermediates are not observed due to the lack of π-backbonding (typically d^0).[12] Since migratory insertion of the alkyl group serves as the turnover-limiting step, chain growth is zero-order in the concentration of ethylene. Migratory insertion barriers were significantly lower for Ni ($\Delta G^{\ddagger}_{ins.}$ ~ 13-14 kcal/mol) compared to

Pd ($\Delta G^{\ddagger}_{ins.}$ ~ 17-18 kcal/mol), suggesting that Ni systems would deliver the highest TOFs.[1,25,50] Complexes containing the bulkiest ligands exhibited slightly lower insertion barriers.[1]

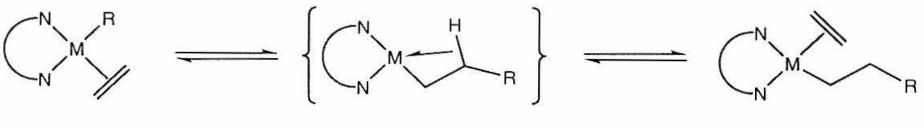

1.11

Figure 1.8. Mechanistic studies using low temperature ^{1}H NMR spectroscopy reveal that resting state of Ni^{II}/Pd^{II} catalysts during ethylene polymerization is the alkyl/olefin complex **1.11**.

Since the resting state of these polymerizations is the alkyl/olefin adduct, it appears that the limitation of most late-metal systems will be chain transfer, most likely through one of the two mechanisms outlined above.[1] The introduction of ligands with a large steric demand should suppress the rate of chain transfer relative to chain-growth, and therefore, increase the molecular weight of the resulting products. ***Note that an increase in the barrier to chain transfer, $\Delta G^{\ddagger}_{transfer}$, by ~ 3-4 kcal/mol will transform an oligomerization catalyst into a polymerization catalyst.***[18]

1.8. Neutral Ni^{II} salicylaldimine catalysts

Although cationic Pd^{II} diimine catalysts were successful for the copolymerization of ethylene and functionalized olefins, the materials are highly branched and contain functionality near the ends of the polymer chain, not along the backbone.[1] We believed that through the integration of the aforementioned studies, neutral Ni^{II} complexes could be prepared which would allow for the formation of *high molecular weight, linear, functionalized polyolefins*. The use of a neutral metal center would provide increased tolerance towards polar functionalities as evidenced by the behavior of complexes **1.6 - 1.9**. In addition, it was expected that a neutral catalyst would yield linear polymeric architectures. The introduction of well-placed steric "bulk" would assist in the production of high molecular weight products and allow for the formation of exclusively polymeric products at much lower operating pressures.

Initial investigations aimed at screening "bulky" bidentate ligands based on [P,O], [P,N], [N,N], and [N,O] chelates provided the pyrrole- and phenol-based catalysts, **1.12** and **1.13**, which showed promise for the oligomerization and polymerization of ethylene, respectively, upon addition of an electrophilic cocatalyst such as $Ni(COD)_2$ or $B(C_6F_5)_3$. In analogy with previous reports for cocatalyst activation in [P,O] complexes,[1,6,40] these cocatalysts were believed to act as a "phosphine sponge," binding the ancillary ligand (PPh_3) of precatalysts **1.12** and **1.13**.

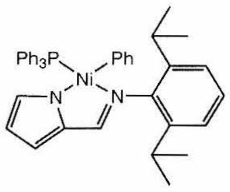

1.12
oligomers

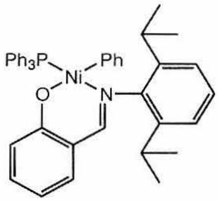

1.13
polymers

As **1.13** showed promise for the production of polymeric material, neutral Ni^{II} salicylaldimine complexes were the subject of further development. These Schiff base complexes were attractive because of the freedom and flexibility provided through easy tuning of the steric and electronic demand of the phenol-based ligand. In analogy with the studies outlined above by Brookhart, it was hoped that the introduction of sterically demanding substituents on both the benzimine and phenolic ring might serve to block the axial face of the metal center, yielding high molecular weight polymer through retardation of associative displacement.[1] It was additionally hoped that bulky groups would serve to decrease the rate of catalyst deactivation, shown to occur by ligand disproportionation and dimerization in analogy to [P,O] systems.[40,45,48]

At the outset of this research, several years ago, the goals of this project were to develop neutral Ni^{II} salicylaldimine catalysts which demonstrated a higher activity for the homopolymerization of ethylene, provide materials of increased molecular weights, allow for the convenient preparation of functionalized polyolefins, and understand how modification of the ligand set leads to changes in the rate of olefin polymerization as well as the product distribution. The salicylaldimine complexes **1.14-1.17** had been prepared *via* the short synthetic sequence outlined in Scheme 1.1. The phenols were purchased or prepared by nickel-catalyzed aryl-aryl coupling procedure. Formylation, followed by condensation of the corresponding salicylaldehydes with 2,6-diisopropylaniline, led to the appropriate ligand, which was subsequently bound to the metal center through preparation of the sodium salt and combination with Ni(PPh$_3$)$_2$PhCl. The behavior of complexes **1.13-1.17** for the polymerization of ethylene is where our gripping story begins.

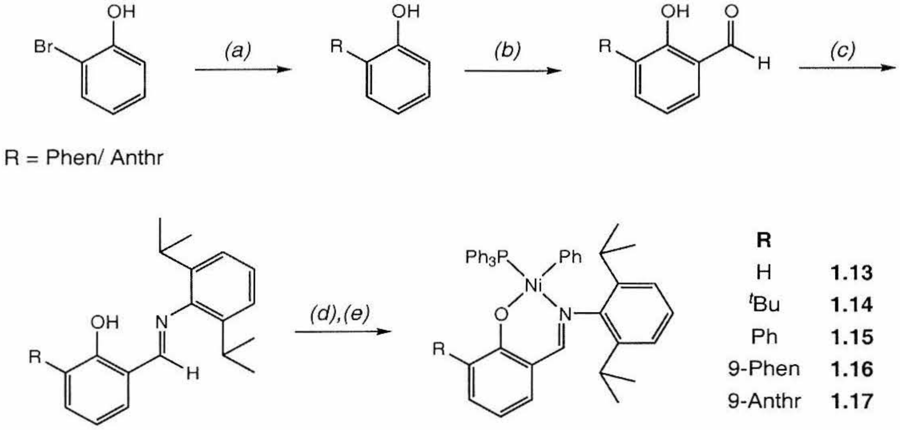

R	
H	**1.13**
^{t}Bu	**1.14**
Ph	**1.15**
9-Phen	**1.16**
9-Anthr	**1.17**

Scheme 1.1. Preparation of neutral Ni^{II} salicylaldimine complexes **1.13-1.17**. (a) Mg, ArBr, Ni(dppe)Cl$_2$, Δ. (b) (CH$_2$O)$_n$, SnCl$_4$, lutidine, Δ. (c) 2,6-(^{i}Pr)$_2$-C$_6$H$_3$, MeOH, cat. HCO$_2$H. (d) NaH, THF. (e) Ni(PPh$_3$)$_2$PhCl, benzene.

1.9 References

(1) Ittel, S. D.; Johnson, L. K.; Brookhart, M. *Chem. Rev.* **2000**, *100*, 1169-1203.

(2) Thayer, A. M. In *Chem. Eng. News*, 1995; Vol. 73, p 15.

(3) Odian, G. *Principles of Polymerization*; Third ed.; John Wiley & Sons, Inc.: New York, NY, 1991.

(4) Deckers, A.; Schulund, R.; Klimesch, R. In; 5,473,025: USA, 1995.

(5) Boffa, L. S.; Novak, B. M. *Chem. Rev.* **2000**, *100*, 1479-1493.

(6) Britovsek, G. J. P.; Gibson, V. C.; Wass, D. F. *Angew. Chem.-Int. Edit.* **1999**, *38*, 429-447.

(7) Doak, K. W. In *Encyclopedia of Polymer Science and Engineering*; Mark, H. F., Ed.; John Wiley & Sons, Inc.: New York, NY, 1986; Vol. 6, p 386.

(8) McLain, S. J.; McCord, E. F.; Arthur, S. D.; Hauptman, E.; Feldman, J.; Nugent, W. A.; Johnson, L. K.; Mecking, S.; Brookhart, M. *Abstr. Pap. Am. Chem. Soc.* **1997**, *213*, 154-PMSE.

(9) Wang, C.; Grubbs, R. H., Unpublished Results.

(10) Watson, M. D.; Wagener, K. B. *Macromolecules* **2000**, *33*, 5411-5417.

(11) Watson, M. D.; Wagener, K. B. *Macromolecules* **2000**, *33*, 8963-8970.

(12) Brintzinger, H. H.; Fischer, D.; Mulhaupt, R.; Rieger, B.; Waymouth, R. M. *Angew. Chem.-Int. Edit. Engl.* **1995**, *34*, 1143-1170.

(13) Crabtree, R. H. *The Organometallic Chemistry of the Transition Metals*; 3rd ed.; John Wiley & Sons, Inc.: New York, NY, 2001.

(14) Fischer, K.; Jonas, K.; Misbach, P.; Stabba, R.; Wilke, G. *Angew. Chem.-Int. Edit. Engl.* **1973**, *12*, 943-1026.

(15) Johnson, L. K.; Killian, C. M.; Brookhart, M. *Journal of the American Chemical Society* **1995**, *117*, 6414-6415.

(16) Johnson, L. K.; Mecking, S.; Brookhart, M. *Journal of the American Chemical Society* **1996**, *118*, 267-268.

(17) Mecking, S.; Johnson, L. K.; Wang, L.; Brookhart, M. *Journal of the American Chemical Society* **1998**, *120*, 888-899.

(18) Mecking, S. *Angew. Chem.-Int. Edit.* **2001**, *40*, 534-540.

(19) Deng, L. Q.; Margl, P.; Ziegler, T. *Journal of the American Chemical Society* **1997**, *119*, 1094-1100.

(20) Deng, L. Q.; Woo, T. K.; Cavallo, L.; Margl, P. M.; Ziegler, T. *Journal of the American Chemical Society* **1997**, *119*, 6177-6186.

(21) Musaev, D. G.; Froese, R. D. J.; Svensson, M.; Morokuma, K. *Journal of the American Chemical Society* **1997**, *119*, 367-374.

(22) Froese, R. D. J.; Musaev, D. G.; Morokuma, K. *Journal of the American Chemical Society* **1998**, *120*, 1581-1587.

(23) Musaev, D. G.; Froese, R. D. J.; Morokuma, K. *Organometallics* **1998**, *17*, 1850-1860.

(24) Killian, C. M.; Johnson, L. K.; Brookhart, M. *Organometallics* **1997**, *16*, 2005-2007.

(25) Tempel, D. J.; Johnson, L. K.; Huff, R. L.; White, P. S.; Brookhart, M. *Journal of the American Chemical Society* **2000**, *122*, 6686-6700.

(26) Guan, Z. B.; Cotts, P. M.; McCord, E. F.; McLain, S. J. *Science* **1999**, *283*, 2059-2062.

(27) Keim, W.; Appel, R.; Storeck, A.; Kruger, C.; Goddard, R. *Angew. Chem.-Int. Edit. Engl.* **1981**, *20*, 116-117.

(28) Mohring, V. M.; Fink, G. *Angew. Chem.-Int. Edit. Engl.* **1985**, *24*, 1001-1003.

(29) Britovsek, G. J. P.; Gibson, V. C.; Kimberley, B. S.; Maddox, P. J.; McTavish, S. J.; Solan, G. A.; White, A. J. P.; Williams, D. J. *Chem. Commun.* **1998**, 849-850.

(30) Small, B. L.; Brookhart, M.; Bennett, A. M. A. *Journal of the American Chemical Society* **1998**, *120*, 4049-4050.

(31) Britovsek, G. J. P.; Bruce, M.; Gibson, V. C.; Kimberley, B. S.; Maddox, P. J.; Mastroianni, S.; McTavish, S. J.; Redshaw, C.; Solan, G. A.; Stromberg, S.; White, A. J. P.; Williams, D. J. *Journal of the American Chemical Society* **1999**, *121*, 8728-8740.

(32) Britovsek, G. J. P.; Gibson, V. C.; Mastroianni, S.; Oakes, D. C. H.; Redshaw, C.; Solan, G. A.; White, A. J. P.; Williams, D. J. *Eur. J. Inorg. Chem.* **2001**, 431-437.

(33) Small, B. L.; Brookhart, M. *Journal of the American Chemical Society* **1998**, *120*, 7143-7144.

(34) Britovsek, G. J. P.; Mastroianni, S.; Solan, G. A.; Baugh, S. P. D.; Redshaw, C.; Gibson, V. C.; White, A. J. P.; Williams, D. J.; Elsegood, M. R. J. *Chem.-Eur. J.* **2000**, *6*, 2221-2231.

(35) Dias, E. L.; Brookhart, M.; White, P. S. *Organometallics* **2000**, *19*, 4995-5004.

(36) Lutz, E. F. *Journal of Chemical Education* **1986**, *63*, 202-203.

(37) Peuckert, M.; Keim, W. *Organometallics* **1983**, *2*, 594-597.

(38) Keim, W.; Kowaldt, F. H.; Goddard, R.; Kruger, C. *Angew. Chem.-Int. Edit. Engl.* **1978**, *17*, 466-467.

(39) Keim, W.; Appel, R.; Gruppe, S.; Knoch, F. *Angew. Chem.-Int. Edit. Engl.* **1987**, *26*, 1012-1013.

(40) Klabunde, U.; Mulhaupt, R.; Herskovitz, T.; Janowicz, A. H.; Calabrese, J.; Ittel, S. D. *J. Polym. Sci. Pol. Chem.* **1987**, *25*, 1989-2003.

(41) Starzewski, K. A. O.; Witte, J. *Angew. Chem.-Int. Edit. Engl.* **1985**, *24*, 599-601.

(42) Starzewski, K. A. O.; Witte, J. *Angew. Chem.-Int. Edit. Engl.* **1987**, *26*, 63-64.

(43) Starzewski, K. A. O.; Witte, J. *Angew. Chem.-Int. Edit. Engl.* **1988**, *27*, 839-840.

(44) Starzewski, K. A. O.; Born, L. *Organometallics* **1992**, *11*, 2701-2704.

(45) Klabunde, U.; Ittel, S. D. *Journal of Molecular Catalysis* **1987**, *41*, 123-134.

(46) Desjardins, S. Y.; Cavell, K. J.; Jin, H.; Skelton, B. W.; White, A. H. *J. Organomet. Chem.* **1996**, *515*, 233-243.

(47) Desjardins, S. Y.; Cavell, K. J.; Hoare, J. L.; Skelton, B. W.; Sobolev, A. N.; White, A. H.; Keim, W. *J. Organomet. Chem.* **1997**, *544*, 163-174.

(48) Heinicke, J.; He, M. Z.; Dal, A.; Klein, H. F.; Hetche, O.; Keim, W.; Florke, U.; Haupt, H. J. *Eur. J. Inorg. Chem.* **2000**, 431-440.

(49) Macgregor, S. A.; Lu, Z.; Eisenstein, O.; Crabtree, R. H. *Inorg. Chem.* **1994**, *33*, 3616-3618.

(50) Svejda, S. A.; Johnson, L. K.; Brookhart, M. *Journal of the American Chemical Society* **1999**, *121*, 10634-10635.

Chapter 2

Neutral Salicylaldimine Ni^{II} and Pd^{II} Complexes. The Development of Highly Active Single-Component Catalysts for the Polymerization of Ethylene to High Molecular Weight Products.

2.1. Abstract

Initial studies on ethylene polymerization with neutral Ni^{II} catalysts **2.1-2.5** were performed through combination with cocatalysts, such as $Ni(COD)_2$ or $B(C_6F_5)_3$. These mixtures polymerize ethylene at low to moderate pressures. TOFs increase as the size of the substituent in the *o*-position of the ligand increases, such that: **2.1** < **2.2** < **2.3** < **2.4** < **2.5**. Electronic modification of these catalysts show that electron-deficient ligands (*p*-CF_3 **2.12**, *p*-NO_2 **2.13**) provide higher activities and M_ws than their electron-rich partners (*p*-H **2.1**, *p*-OMe **2.11**). Several catalysts were prepared which contain both of these features, i.e., steric demand in the *o*-position and an electron withdrawing group (NO_2) in the *p*-position of the ligand. They exhibit a similar trend, with activity increasing: **2.29** < **2.30** < **2.31** < **2.32**. All of the catalysts investigated display brief lifetimes (~ 10-20 min), with the rate of decomposition related to structure, such that: **2.1** > **2.3** > **2.4** ~ **2.5**. These reactions are ill-defined, as evidenced by PDIs (M_w/M_n) often >> 2.

Ni^{II} salicylaldimine complexes with "bulky" ligand sets serve as single-component catalysts, allowing for the preparation of high molecular weight linear PE. Catalyst lifetimes were greatly increased by omitting the cocatalyst, with **2.5** exhibiting an "indefinite" existence for polymerization in toluene. Again, activity increases: **2.1** < **2.3** < **2.4** ~ **2.5**. Unlike the cocatalyst-mediated trials, electron-rich catalysts (*p*-H) display higher activities than electron deficient (*p*-NO_2) analogs. The synthetic route to catalyst **2.5** was optimized. Ligands **2.58**, **2.68**, and **2.69**, although difficult to prepare, yielded *in situ* catalysts which provided higher M_ws than **2.5**. A neutral Pd^{II} analog, **2.48**, was prepared. However, the addition of ethylene leads to styrene production and reduction of the metal center.

Spectroscopic analysis of polymerizations with **2.5** demonstrate a low initiation efficiency at ambient temperatures and pressures. The Ni^{II} hydride complex, **2.71**, did not exhibit an increased initiation efficiency. These results suggest that the active species is the "phosphine-removed" species **2.76**. Reaction of complex **2.71** with O_2 leads to formation of **2.75**, providing an understanding of how ethylene purity can affect the polymerization.

2.2. Cocatalyst-assisted polymerization of ethylene using neutral Ni^{II} salicylaldimine complexes

As outlined at the end of Chapter 1, our group had prepared a series of neutral Ni^{II} complexes **2.1-2.5** which were found to be active for the "cocatalyst-activated" polymerization of ethylene to moderate molecular weights. These polymerizations were accomplished by dissolving the appropriate catalyst in toluene, followed by injection of a solution of an electrophilic phosphine scavenger, such as $Ni(COD)_2$ or $B(C_6F_5)_3$. As proposed for other neutral Ni^{II} [P,O] systems, the phosphine scavengers were believed to bind PPh_3 more tightly than the "$[N,O]Ni^{II}R$" fragment, thereby serving to remove the coordinated phosphine and open a coordination site which allows for polymerization.[1,2]

Polymer was obtained at low to moderate pressures (4-20 atm) and ambient temperatures, with both the activity of the catalyst and the product distribution displaying a slight dependence on the pressure of the reaction. For example, the polymerization of ethylene with complex **2.1** at 60 psig (4.0 atm) provided PE with an $M_w \sim 3{,}400$ g/mol (2.0 g PE), whereas polymerization at 200 psig (13.3 atm) yielded an $M_w \sim 10{,}000$ (2.5 g PE).[3] This outcome was consistent with observations made using the SHOP system, where higher pressures were found to reduce the rate of chain termination.[1]

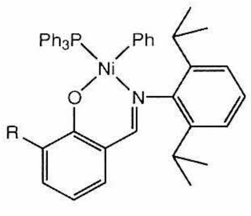

R	
H	**2.1**
^{t}Bu	**2.2**
Ph	**2.3**
9-Phen	**2.4**
9-Anthr	**2.5**

Attempts to homopolymerize ethylene with **2.1** and no "phosphine sponge" led to the observation of no ethylene uptake and provided no sign of either solid polyethylene or any oligomeric products (*vide infra*).[3] In contrast to $Ni(COD)_2$ or $B(C_6F_5)_3$, a number of other Lewis acid cocatalysts, such as 9-BBN, $B(Ph)_3$, and CuCl were found to be unsuccessful for the "activation" of complex **2.1**. However, $Rh(acac)(CH_2CH_2)_2$ has been employed successfully as a cocatalyst for polymerization with similar Ni^{II} salicylaldimine complexes.[4]

When **2.1** was combined with the appropriate phosphine scavenger (trial 2.1*a*), a 5-8 min induction period was followed by the rapid uptake of ethylene and a rise in the temperature of the reaction. For the SHOP system, based on neutral [P,O] Ni^{II} systems, it has been proposed that the induction period arises from the relatively slow insertion of ethylene into the Ni-Ph bond (stabilized by Ni-Ph backbonding to the arene π^* orbitals), followed by β-hydride elimination which generates an active "Ni-H" species. To date, low temperature ^1H NMR studies of ethylene consumption have failed to demonstrate the formation of styrene, leading us to conclude that the induction period may arise from the relatively slow abstraction of phosphine from the Ni^{II} center.

Table 2.1. Polymerization of ethylene by neutral Ni^{II} salicylaldimine complexes **2.1-2.5** upon addition of a "phosphine sponge".[a]

Entry	Complex	Cocatalyst	Yield PE (g)	TOF [b]	M_w ($\cdot 10^3$)	PDI (M_w/M_n)	Branches [c]
2.1*a*	**2.1**	$Ni(COD)_2$	2.0	0.16	3.4	1.5	45
2.1*b*	**2.2**	$Ni(COD)_2$	3.5	0.29	11.4	1.8	55
2.1*c*	**2.3**	$Ni(COD)_2$	4.0	0.33	23.3	2.3	40
2.1*d*	**2.4**	$Ni(COD)_2$	7.0	0.58	32.7	3.8	30
2.1*e*	**2.4**	$B(C_6F_5)_3$	7.0	0.58	49.5	6.8	35
2.1*f*	**2.5**	$Ni(COD)_2$	7.4	0.62	54.0	6.4	25
2.1*g*	**2.5**	$B(C_6F_5)_3$	5.0	0.42	23.8	7.2	50

[a] Polymerization conditions: 75 μmol of the appropriate catalyst, 150 μmol (2.0 eq.) of the "phosphine sponge," 90 mL of toluene, T = 25 °C. [b] TOF = Turnover Frequency. 10^6 g PE· (mol catalyst^{-1})· (hr^{-1}). [c] Total number of $C_1+C_2+C_3+C_4$ branches per 1000 carbons as determined by ^{13}C NMR.

The results of several ethylene polymerizations are summarized in trials 2.1*a-g*, outlined in Table 2.1. As previously shown for cationic late-metal systems,[5] chain migratory processes (which control the branch content of the resultant PE—see Figure 2.2) and chain termination reactions (which control M_w) were expected to be suppressed by the introduction of bulky substituents in the *o*-position of the salicylaldiminato ring. In fact, when complexes **2.2-2.5** were used as initiators, higher molecular weight polyethylene was obtained than with **2.1**, as the resultant polymer exhibits M_w values between 11,400 to 54,000. The polyethylene was moderately branched in all cases, but exhibited a slight decrease in the total number of branches (from 45 to 25/1000, as determined by ^{13}C NMR spectroscopy) when precatalysts containing larger groups in the *o*-position of the phenolic ring are utilized. Greater than 80-90% of the branches were methyl branches, with the remainder being longer (C_2 –C_6^+) branches (see Figure 2.1). In accord with research on other systems, these branches are believed to arise from β-hydride elimination followed by reinsertion in a [2,1]-fashion as shown in Figure 2.2.[2,5]

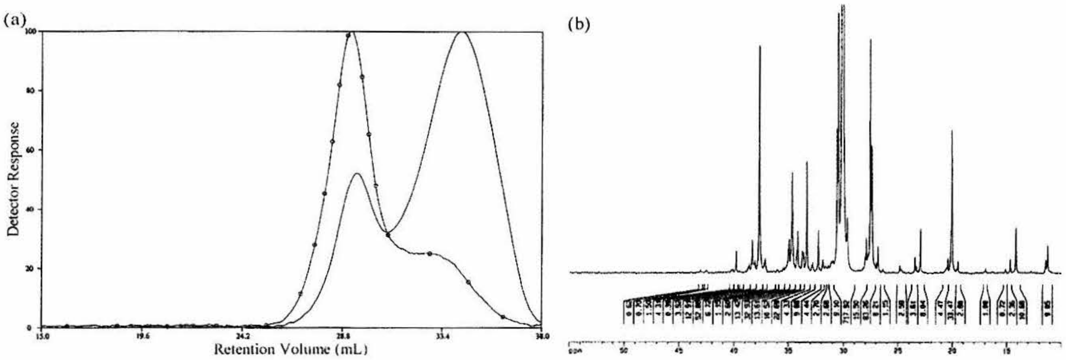

Figure 2.1. Polyethylene obtained from trial 2.1*d* using catalyst **2.4** and 2 eq. of $Ni(COD)_2$. (a) Dual detector (RI, DP) GPC trace demonstrating multimodal nature of PE. (b) ^{13}C NMR analysis demonstrated that the resultant PE has a “non-linear” character.

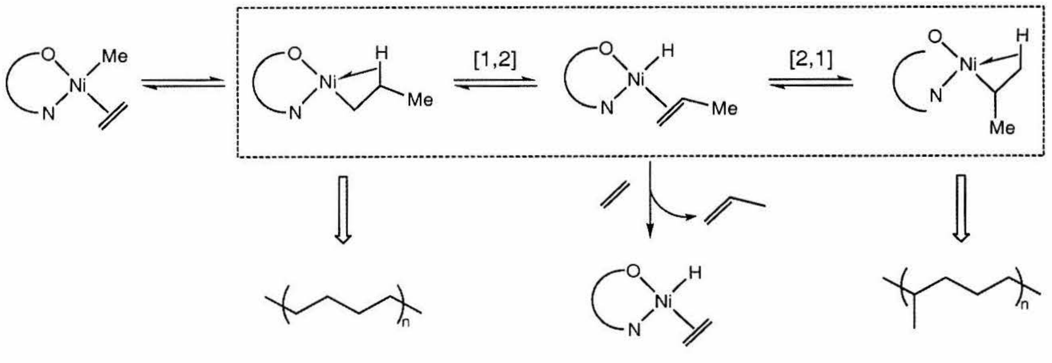

Figure 2.2. Mechanism which provides branched PE with neutral Ni^{II} catalysts such as **2.1-2.5**.

The retardation of chain transfer processes (increase in M_w) was ascribed to a slowing of the associative displacement of the unsaturated polymer chain from the metal center by free ethylene, in accordance with studies of cationic Ni^{II}/Pd^{II} diimine polymerization systems (Figure 2.2).[2,5] Recent calculations, however, have suggested that both cationic and neutral Ni^{II} systems undergo chain transfer by the direct β-hydrogen transfer (βHT) to incoming monomer,[6-9] and that the barrier for βHT increases with increasing bulk about the metal center. An additional theory suggests that the introduction of bulk around the metal center serves to "organize" the molecule, pushing the *cis*-coordinated olefin and alkyl chain together, thereby decreasing the barrier to insertion.[10] An energy difference of ~ 3-4 kcal/mol in the barrier to termination relative to insertion can account for the formation of moderate to high M_w polymer.[11] Chapter 5 will readdress some of these issues, but for now, it is important to realize that the resulting molecular weight increases as the steric demand of the ligand set increases (*vide infra*).

Under these "cocatalyzed" polymerization conditions, reactions with **2.2-2.5** were found to be highly exothermic, with temperatures rising 70-80 °C in a matter of minutes. No observed induction period was noted, which was attributed to an increased rate of phosphine abstraction or dissociation arising from the introduction of the bulky groups in the *ortho-* position of the phenolic ring. However, even when the temperature was maintained constant, the resulting polymer exhibited multimodal character (reflected by PDIs >> 2, see Figure 2.1(a)), indicating that multiple active sites are generated under the polymerization conditions, i.e., *the system is ill-defined.*

It is important to note that complexes **2.6** and **2.7**, which demonstrated reduced steric demands on the aryl imine substituent, were not found to be effective initiators for ethylene polymerization.[3] This phenomenon will be revisited in Chapter 3, as it may be a consequence of the rapid decomposition of the proposed active species. In addition, these results suggested that the benzimine-substituent remains coordinated to the metal center throughout the polymerization, as a less pronounced effect on the activity and product distribution for **2.6** and **2.7** would be expected if dissociation of the imine were crucial to activity. However, if imine dissociation is mandatory for polymerization, it could be argued that increasing the steric demand of the imine, without changing the electronic nature of the ligand set, would favor imine dissociation, such that ethylene polymerization rates would *increase* in the (observed) order: **2.6** < **2.7** < **2.1**.

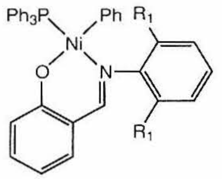

R_1	
H	**2.6**
Me	**2.7**
^{t}Bu	**2.8**

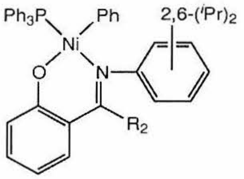

R_2	
Me	**2.9**
Ph	**2.10**

The use of ketimine based ligands instead of aldimines has exhibited a tremendous impact on the molecular weight of the resulting materials obtained with both cationic Fe^{II} and Ni^{II} systems.[2,12] However, attempts to prepare complex **2.8** (containing a 2,6-di(^{t}butyl) aryl imine) as well as the ketimine **2.9** and benzimine **2.10** compounds were unsuccessful as condensation of the appropriate aldehyde, acetophenone, or benzophenone with the sterically encumbered anilines did not provide any detectable amount of the appropriate ligands under any of the tested conditions. Since polymer was only produced with the 2,6-diisopropylaryl imine group, it has been a constant throughout

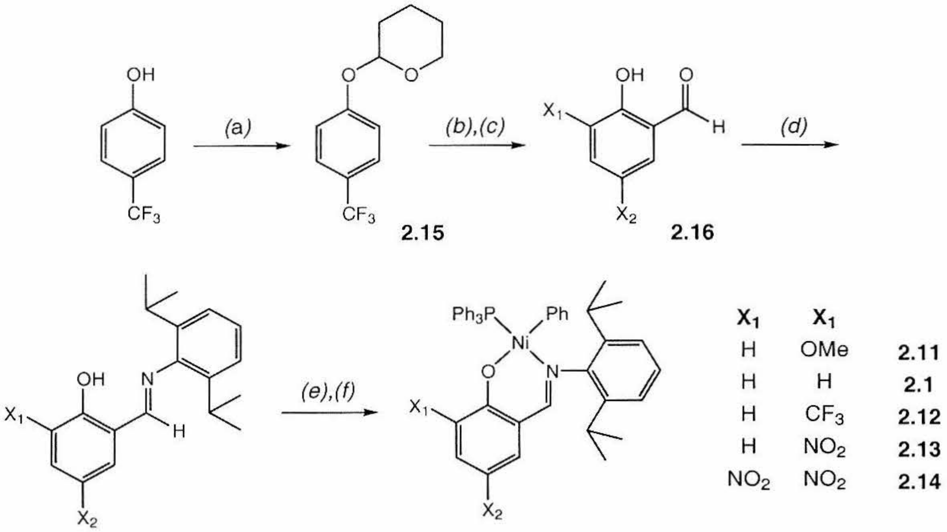

X$_1$ = H, X$_2$ = CF$_3$ (**2.17**)

X_1	X_1	
H	OMe	**2.11**
H	H	**2.1**
H	CF_3	**2.12**
H	NO_2	**2.13**
NO_2	NO_2	**2.14**

Scheme 2.1. Preparation of *p*-substituted salicylaldimine catalysts **2.11-2.14**. (*a*) DHP, CH_2Cl_2, PPTS, 25 °C, 95%. (*b*) ^{n}BuLi, THF, 0 °C. (*c*) DMF, H_2O, 75 %. (*d*) 2,6-(^{i}Pr$_2$)-$C_6H_3NH_2$, MeOH, cat. HCO_2H, ~ 85%. (*e*) NaH, THF, RT. (*f*) $Ni(PPh_3)_2PhCl$, C_6H_6, RT, ~ 85%.

the preparation of the new ligands described in this Chapter. Ligands which include a reduced steric demand on the benzimine will be revisited in Chapter 3. At this point, however, we set out to determine how further manipulation of the ligand set led to differences in the reactivity of these neutral systems.

2.3. The effect of electronic perturbation on the "cocatalyst-assisted" polymerization of ethylene

The effect which various electronic substituents play on the activity of the catalyst was investigated by the preparation of Ni^{II} complexes containing (*ortho-*), *para-*substituted salicylaldimine ligands **2.11-2.14** (Scheme 2.1). A few of the ligands were readily prepared by the condensation of the appropriate salicylaldehyde with 2,6-diisopropylaniline (**2.11** and **2.13-2.14**). Compound **2.12** was prepared by the short synthetic sequence outlined in Scheme 2.1. Protection of the *p*-cresol with 2,3-dihydropyran provided THP adduct **2.15** that is easily formylated with good regioselectivity by the addition of ^{n}BuLi and DMF at 0 °C in THF. Subsequent deprotection yielded **2.16** which condensed with 2,6-diisopropylaniline to provide the *p*-CF_3-ligand, **2.17**. In all cases, the appropriate sodium salts were obtained upon treatment of **2.11-2.14** with an excess of NaH in THF. The reaction of the (^{X1,X2}Sal)Na with *trans-*[NiCl(Ph)$(PPh_3)_2$][13] led to production of the Ni^{II} complexes **2.11-2.14** in good yields.[3,14] According to the NMR spectra, the diamagnetic Ni^{II} complexes adopt a square-planar geometry, as evidenced by good *narrow* lineshape in the ^1H NMR spectra of **2.11-2.14** and from the characteristic ^{31}P ($^4J_{PH}$ ~ 9 Hz) coupling observed for the ~*CH*=NAr~ proton *trans-* to the PPh_3.[15] The signals arising from the bound triphenylphosphine ligand in the ^{31}P NMR spectra of complexes **2.11-2.14** are observed between 24 and 27 ppm, in good agreement with the values previously obtained for complexes **2.1-2.5**.[3] There does not appear to be any correlation between the chemical shift of the bound PPh_3 and the electronic nature of the ligand (*p*-OMe (**2.11**) ~ 24.6, *p*-H (**2.1**) ~ 25.9, *p*-CF_3 ~ 26.1 (**2.12**), *p*-NO_2 ~ 25.5 (**2.13**)), possibly due to the *cis-* arrangement of the two groups.

Upon activation of these systems with either $Ni(COD)_2$ or $B(C_6F_5)_3$ as a phosphine sponge, polymerization activity was observed in all four systems (Table 2.2).

The electron-deficient complexes **2.13** and **2.14** demonstrated the highest activity, although the polymerization with complex **2.14** occurred with a relatively long induction period (approx. 20 min). The electron-rich complex **2.11** demonstrated the lowest TOF, but did not exhibit any apparent induction period. It is believed that these rates reflect the rate of insertion for the putative active species, such as **2.18,** as the electron-deficient species **2.13** and **2.14** are expected to yield systems with an increased electrophilic character relative to the electron-rich system **2.11**.

Table 2.2. Polymerization of ethylene with the electronically-modified catalysts **2.11-2.14.**[a]

Trial	Catalyst	Substituents: X_1 / X_2	Yield PE (g)	TOF[b]	T_m (°C)	M_w (*10^3)	PDI	Branches[c]
2.2*a*	**2.11**	H, OMe	1.0	0.08	98.0	7.3	1.7	53
2.2*b*	**2.1**	H, H	2.0	0.16	94.2	3.4	1.5	45
2.2*c*	**2.12**	H, CF_3	2.7	0.22	105.0	12.0	1.8	30
2.2*d*	**2.13**	H, NO_2	8.0	0.64	129.8	366.0	18.0	22
2.2*e*	**2.14**	NO_2, NO_2	7.7	0.62	129.0	239.0	14.0	15

[a] Polymerizations performed with 75 μmol of the appropriate catalyst, 150 μmol (2.0 eq.) of $Ni(COD)_2$, 100 psig ethylene, 90 mL of anhydrous toluene, T = 30 °C, t = 10 min. [b] TOF = Turnover Frequency. 10^6 g PE· (mol catalyst^{-1})· (hr^{-1}). [c] Total number of C_1+C_2+C_3+C_4 branches per 1000 carbons (as determined by ^{13}C NMR spectroscopy).

Although complex **2.13** and **2.14** exhibit the greatest activity, the molecular weight distributions (PDI) were high, again suggesting that multiple active sites persist for these "cocatalyzed" reactions. In the case of **2.13** and **2.14** it is proposed that the electrophilic cocatalysts coordinate to the NO_2 groups of the ligand, providing at least three different species **2.18-2.20** under the polymerization conditions. Similar interactions between the cocatalyst and ligand have been characterized for α-iminocarboxamidato Ni^{II} ethylene polymerization catalysts.[16] All three complexes **2.18-2.20** would be expected to yield different product distributions (large PDIs), and could explain the enormous jump in M_w observed when going from catalyst **2.12** to **2.13** and **2.14** (compare trials 2.2*c* to 2.2*d-e*). In addition, it should be noted here that complex **2.14** and the cocatalyst $B(C_6F_5)_3$

are the only salicylaldimine system, to date, which can reproducibly insert propylene to yield higher oligomeric materials.[2]

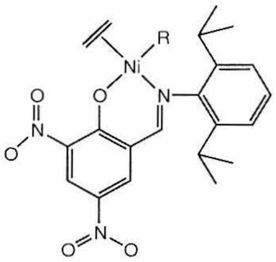

2.18

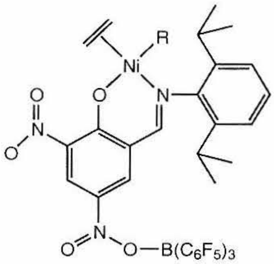

2.19

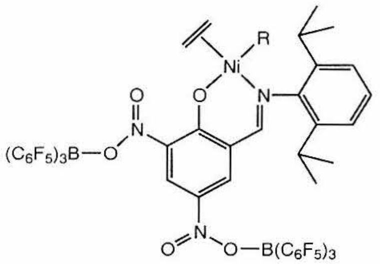

2.20

Since ligands with p-NO_2 groups provided complexes which demonstrated both (1) the highest activity for ethylene polymerization, as well as (2) the highest observed M_ws, we set out to prepare sterically demanding ligands with p-NO_2 groups in the hope of combining the two effects.

2.4. Combination of steric and electronic perturbation of salicylaldimines through nitration of a series of ligands

Nitration of salicylaldimines **2.21-2.24** was easily accomplished by the addition of HNO_3 to an HOAc solution of the appropriate salicylaldehyde with gentle heating (Scheme 2.2). The reactions typically proceed rapidly and the products were easily isolated as yellowish-orange solids by precipitating *via* the addition of water. The only atypical behavior observed during nitration was with the *o*-(9-anthracenyl)-salicylaldehyde (**2.24**), where it was observed that the 10-position of the anthracenyl ring underwent faster nitration than the *p*-position of the salicylaldehyde ring; therefore, the final product upon addition of two equivalents of HNO_3 was found to be **2.28**.

Condensation of 2,6-diisopropylaniline with **2.25-2.28** was quite facile as the aldehydes have an increased electrophilicity relative to their electron-rich analogs **2.21-2.24**. In addition, the presence of the p-NO_2 group(s) leads to an increased crystallinity, such that crystallization from MeOH served to drive the reaction to completion. Using the aforementioned protocols, the sodium salts were prepared and combined with $Ni(PPh_3)_2PhCl$ to yield complexes **2.29-2.32**.

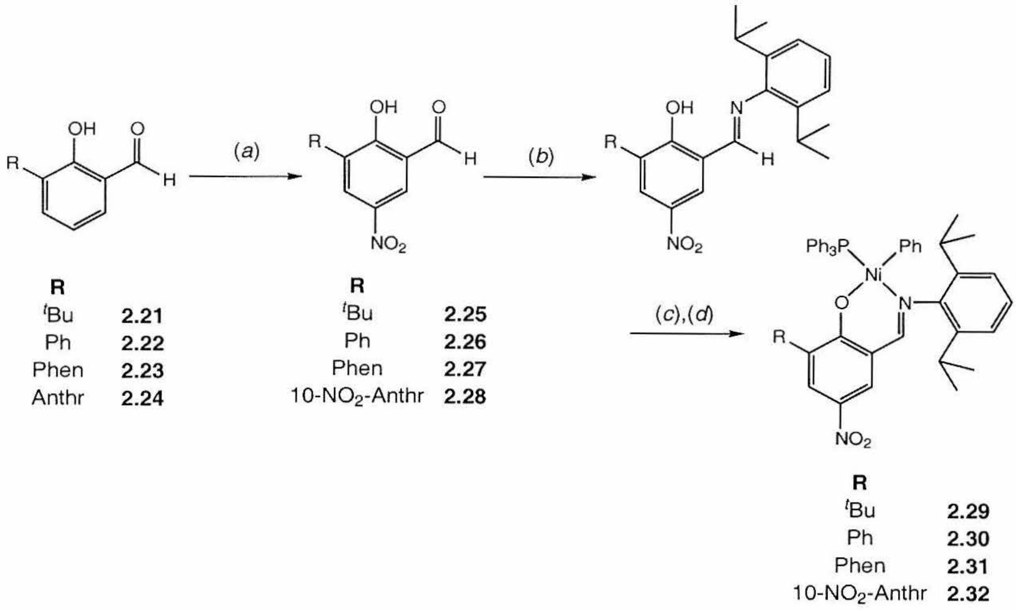

Scheme 2.2. Preparation of *p*-NO_2 substituted salicylaldimine complexes **2.29-2.32**. (*a*) HNO_3, HOAc, Δ. (*b*) 2,6-($^iPr_2$)-$C_6H_3NH_2$, MeOH, cat. HCO_2H, ~ 85%. (*c*) NaH, THF, RT. (*d*) $Ni(PPh_3)_2PhCl$, C_6H_6, RT, ~ 85%.

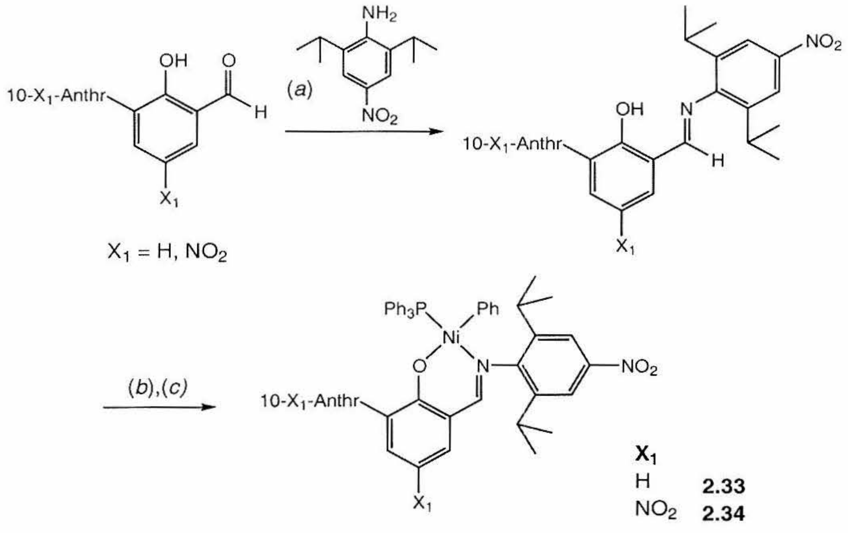

Scheme 2.3. Preparation of complexes **2.33** and **2.34** containing 2,6-diisopropyl-4-NO_2 benzimine ligands. (*a*) MeOH, cat. HCO_2H, Δ. (*b*) NaH, THF, 25 °C. (*c*) $Ni(PPh_3)_2PhCl$, C_6H_6, 25 °C, ~ 85%.

In addition, the effect of electron withdrawing groups on the *p*-substituent of the benzimine moiety was investigated through the preparation of two ligands containing the 4-NO_2-2,6-diisopropylbenzimine (Scheme 2.3), which were prepared *via* published methods from our group.[9] Generation of the corresponding sodium salts and metallation with $Ni(PPh_3)PhCl$ provided complexes **2.33** and **2.34** in good yield.

Table 2.3. Polymerization of ethylene with various electronically-modified catalysts **2.29-2.34**.[a]

Trial	Catalyst	*o*-Substituent	Yield PE (g)	TOF[b]	T_m (°C)	M_w ($*10^3$)	PDI [M_w/M_n]	Branches[c]
2.3*a*	**2.29**	^{t}Bu	3.2	0.25	102.3	3.4	1.5	25
2.3*b*	**2.30**	Ph	6.6	0.53	96.5	12.0	2.0	20
2.3*c*	**2.31**	9-Phen	7.8	0.63	100.8	6.0	2.1	25
2.3*d*	**2.32**	9-(10-NO_2)-Anthr	8.8	0.70	107.3	12.0	2.8	45
2.3*e*	**2.33**	Anthr	9.8	0.78	124.0	53.0	7.8	26
2.3*f*	**2.34**	10-NO_2-Anthr	9.9	0.79	ND[d]	47.0	6.4	32

[a] Polymerizations performed with 75 μmol of the appropriate catalyst, 150 μmol (2.0 eq.) of $Ni(COD)_2$, 100 psig ethylene, 90 mL of anhydrous toluene, T = 30 °C, t = 10 min. [b] TOF = Turnover Frequency. 10^6 g PE· (mol catalyst^{-1})· (hr^{-1}). [c] Total number of C_1+C_2+C_3+C_4 branches per 1000 carbons (as determined by ^{13}C NMR spectroscopy). [d] ND = not determined.

As outlined in Table 2.3, complexes **2.29-2.32** demonstrate the same reactivity trend as observed with the electron-rich analogs **2.2-2.5**, such that TOFs increase with the size of the substituent in the *o*-position of the phenolic ring: ^{t}Bu < Ph < Phen ~ Anthr (compare trials 2.3*a-d* to 2.1*b-g*). Also in agreement with trials 2.1*a-g*, the molecular weights are observed to increase slightly with the steric demand of the ligand. Polymerization with complex **2.32** provides a bit of an erratic data point (slightly higher branch content than **2.31**), which may arise because of the 10-NO_2- group. However, as shown below in Figure 2.3, the *o*-(9-anthracenyl) group is orthogonal to the phenolic ring, such that π-effects are expected to be minimal due to poor overlap, and any σ-effect would be expected to be weak as the distance between the EWG and the metal center is quite large.

The activity of the p-NO_2 benzimine complexes **2.33-2.34** is observed to be slightly higher than that observed with **2.5** and **2.32**. In accord with other polymerizations containing ligands with NO_2 groups, the observed M_ws are slightly higher, but very broad PDIs indicate that multiple species may persist under polymerization conditions.

2.5. Neutral Ni^{II} naphthaldimine complexes

In addition to the preparation of complexes such as **2.1-2.5** based on the salicyaldehyde framework, we sought to prepare and study derivatives based on 2-hydroxy-naphthaldimine. We believed that the use of these derivatives could allow for the design of ligands which imposed steric demands on the equatorial plane through substitution in the 8-position (*vide infra*). A series of substituted naphthaldimines were prepared, their Ni^{II} complexes were synthesized, and studied as polymerization catalysts.

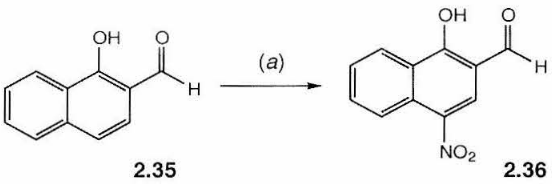

Scheme 2.4. Preparation of p-NO_2-naphthaldehyde. (*a*) HNO_3, HOAc, Δ, 85%.

Naphthyl-based ligands allow for easy modification at both the 4- and 8-positions of the naphthalene ring.[17,18] Nitration of the easily prepared 1-hydroxy-2-naphthaldehyde (**2.35**) provides **2.36** as outlined in Scheme 2.4.[19] Using techniques similar to those outlined in Scheme 2.1 and standard literature protocols, we prepared ligand **2.37** (Scheme 2.6) in a few steps from commercially available 2-methoxynaphthalene as shown in Scheme 2.5. The reaction of 2-methoxynaphthalene with ^tBuLi in cyclohexane followed by transmetallation to Mg provided the necessary Grignard reagent for a nickel-catalyzed aryl coupling with 4-bromotoluene, yielding **2.38** in ~ 60% yield.[17,18] Deprotection of the methyl ether with BBr_3 gave **2.39** in nearly quantitative yields.

Protection of the phenol with DHP (**2.40**) followed by formylation provided **2.41**, which could be deprotected in an acid catalyzed process to give 1-hydroxy-8-*p*-tolyl-naphthalene-2-carbaldehyde, **2.42** in ~ 34% overall yield after 5 steps.

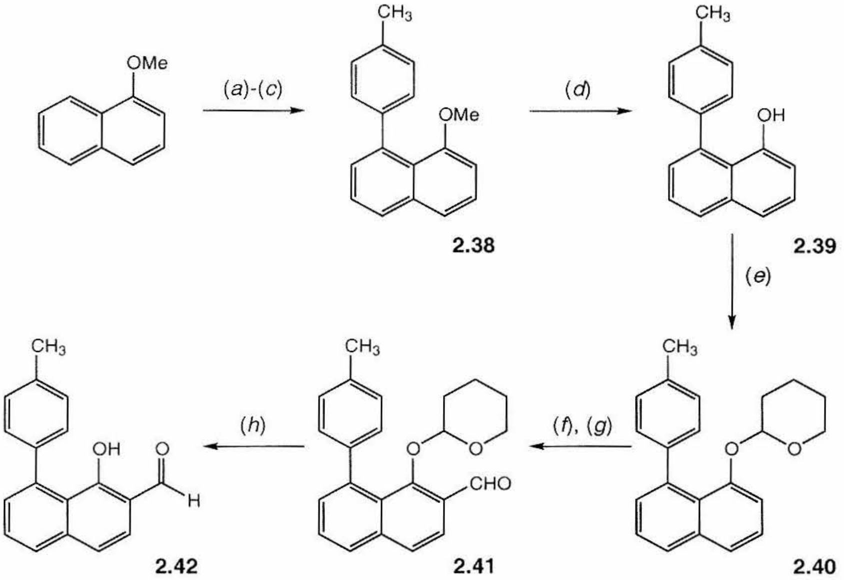

Scheme 2.5. Preparation of **2.42**. (*a*) ^{t}BuLi, cyclohexane, 25 °C. (*b*) $MgBr_2$, Et_2O, 25 °C. (*c*) 4-bromotoluene, Ni(dppe)Cl_2, THF, Δ, 40 hr. (*d*) BBr_3, CH_2Cl_2, -78 °C. (*e*) DHP, cat. PPTS, CH_2Cl_2, 25 °C. (*f*) ^{n}BuLi, Et_2O, 25 °C. (*g*) DMF, H_3O^+. (*h*) 3:1 EtOH:THF, cat. PPTS, Δ.

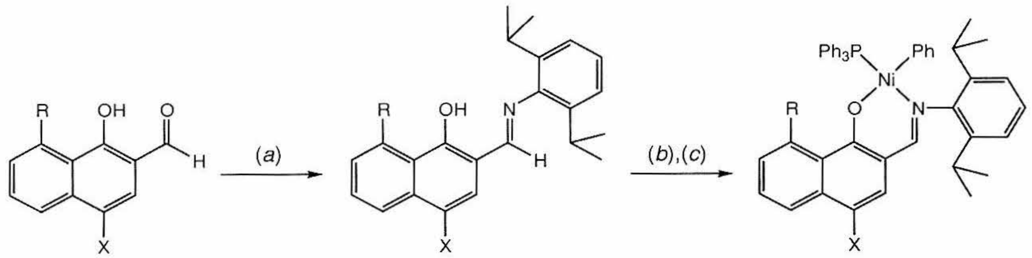

X	**R**	
H	H	**2.35**
NO_2	H	**2.36**
H	*p*-Tol	**2.42**

X	**R**	
H	H	**2.43**
NO_2	H	**2.44**
H	*p*-Tol	**2.37**

X	**R**	
H	H	**2.45**
NO_2	H	**2.46**
H	*p*-Tol	**2.47**

Scheme 2.6. Preparation of neutral Ni^{II} naphthaldimine complexes **2.45-2.47**. (*a*) 2,6-(^{i}Pr)$_2$-$NH_2C_6H_3$, MeOH, cat. HCO_2H. (*b*) NaH, THF. (*c*) Ni(PPh_3)PhCl, C_6H_6, 25 °C.

The condensation of naphthaldehydes **2.35**, **2.36**, and **2.42** with 2,6-diisopropylaniline led to formation of the naphthaldimines **2.37**, **2.43**, and **2.44** in good yield (Scheme 2.6). As observed for the salicylaldimines, these products were yellow to orange solids with several diagnostic ^{1}H NMR shifts including –C*H*MeMe' (sept, 2H, δ ~ 3.0, $^3J_{HH}$ ~ 7 Hz), –CH*MeMe'* (doublet, 12H, δ ~ 1.15 - 1.25 , $^3J_{HH}$ ~ 7 Hz), –C*H*=NAr (s, 1H, δ ~ 8.2), and in the case of **2.37**, a diagnostic resonance for the methyl group of the 8-tolyl substituent (s, 3H, δ = 2.40). Deprotonation of the naphthaldimines with NaH in THF, followed by reaction with $Ni(PPh_3)_2PhCl$ in benzene afforded the appropriate Ni^{II} adducts **2.45-2.47**, respectively. In agreement with salen complexes **2.1-2.5**, the naphthaldimine adducts are orange solids which demonstrate ^{31}P NMR resonances δ ~ 26 ppm. The $^4J_{PH}$ coupling of –C*H*=NAr (~ 8 Hz) suggests, in analogy to **2.1-2.5**, that the coordinated PPh_3 occupies the position *trans*- to the imine. Several attempts were made to crystallize **2.47** to determine how the 8-(*p*-tolyl)-substituent affected the nature of the Ni-PPh_3 bond. However, these complexes were extremely soluble and resisted all efforts for crystallization.

Table 2.4. Polymerization of ethylene by neutral Ni^{II} naphthaldimine complexes **2.45-2.47** upon addition of a "phosphine sponge".[a]

Entry	Complex	Cocatalyst	Yield	TOF[b]	M_w	PDI (M_w/M_n)	Branches[c]	T_m (°C)
2.4*a*	**2.45**	$Ni(COD)_2$	0.7	0.05	42.0	3.6	30	118.3
2.4*b*	**2.45**	$B(C_6F_5)_3$	2.3	0.18	59.0	4.8	25	118.0
2.4*c*	**2.46**	$Ni(COD)_2$	2.8	0.22	380.0	1.8	25	126.3
2.4*d*	**2.46**	$B(C_6F_5)_3$	6.9	0.55	10.0	2.9	29	73.8
2.4*e*	**2.47**	$Ni(COD)_2$	2.3	0.18	3.0	13.3	45	96.8
2.4*f*	**2.47**	$B(C_6F_5)_3$	5.3	0.42	15.0	2.1	65	113.0

[a] Polymerization conditions: 75 μmol of the appropriate catalyst, 150 μmol (2.0 eq.) of the appropriate cocatalyst, 90 mL of toluene, T = 30 °C. [b] TOF = Turnover Frequency. 10^6 g PE· (mol catalyst^{-1})· (hr^{-1}). [c] Total number of C_1+C_2+C_3+C_4 branches per 1000 carbons (as determined by ^{13}C NMR spectroscopy).

Ethylene polymerizations were performed with the three complexes (Trials 2.4*a*-*f*). In all cases, the activities of the naphthaldimine complexes were observed to be lower than their analogous salicylaldimine complexes (compare trials 2.4*c-d* to 2.2*d*). Disappointingly, complex **2.47** demonstrated both a low activity and produced extremely low molecular weight products even when compared to the unsubstituted naphthaldimine complex **2.45** (compare trials 2.4*a-b* with 2.4*e-f*). Comparing the activity and product distribution of catalyst **2.5**, which has steric protection provided for the axial coordination sites, with **2.47**, where the bulk is thrust into the frontside of the equatorial plane, suggested that the further development of salicylaldimine ligands should focus on providing increased protection of the axial sites to obtain catalysts with an increased activity which provide high molecular weight products (Section 2.10). In addition to these features, increasing the size of the ligand was predicted to increase catalyst lifetimes and provide PE with a lower branch content.

Several attempts were made to determine the nature of "cocatalyst activation" through investigation of the addition of $B(C_6F_5)_3$ to Ni^{II} complexes, such as **2.1-2.5**. ^{19}F NMR spectroscopic analysis of a freshly prepared mixture of **2.5** and 1-2 eq. of $B(C_6F_5)_3$ indicates the presence of many new species present in trace amounts; however, the complicated mixture made identification of any major products extremely difficult. Some evidence was observed for the $Ph_3P \cdot B(C_6F_5)_3$ adduct as a similar broad lump ($\delta \sim -15$ ppm) was observed in the ^{31}P NMR spectra for both a mixture of **2.5**/2.0 eq. $B(C_6F_5)_3$ and Ph_3P/1.0 eq. $B(C_6F_5)_3$. To date, however, these systems have been difficult to study as they are ill-defined mixtures.

2.6. Neutral Ni^{II} complexes serve as single-component catalysts—A fine example demonstrating the importance of control experiments

During the course of our studies, a control experiment performed using **2.5** in toluene without the addition of either $Ni(COD)_2$ or $B(C_6F_5)_3$ as a cocatalyst, led (to our surprise and delight) to the discovery that **2.5** is an active catalyst for the polymerization of ethylene without the use of any additives. To better understand the reason for the activity of **2.5**, we made several crystallization attempts, obtaining X-ray quality crystals from toluene at –50 °C over the course of a week.

The structure of **2.5** is presented in Figure 2.3. In the solid state, the molecule adopts a nearly ideal square-planar coordination geometry with the Ni displaced approximately 0.03 Å from the equatorial plane defined by N, O, P, and C(31). In agreement with the observation of $^4J_{PH}$ coupling to the imine, the 2,6-diisopropylbenzimine occupies the position *trans-* to the triphenylphosphine ligand with a nearly linear P-Ni-N angle (172.16(12)°). The phenyl group attached to Ni lies *trans-* to the phenoxide with an O-Ni-C31 angle of 166.2(2)°. The Ni-O, Ni-N, and Ni-C(31) bond distances are similar to those in known nickel complexes as outlined in Table 2.5.[20-24] For example, the Ni-PPh$_3$ bond of **2.5** (2.172(2) Å) is less than 0.01 Å longer than in Cavell's {Ni(PPh$_3$)(*o*-tolyl)[N,O]} complexes with the [N,O] bidentate ligand 2-pyridinecarboxylate (*d*(Ni-P) = 2.163(2) Å),[22] suggesting that in the solid state there is little or no steric interaction between the anthracene moiety and the *cis*-triphenylphosphine ligand. However, the anthracenyl unit swings out of the plane of the phenolato-fragment, forming an approximately 80° angle with the equatorial plane. The isopropyl groups of the arylimino moiety are also forced to sit in an arrangement perpendicular to the square plane, such that the substituents provide some steric protection of the axial positions above and below the metal center.

Table 2.5. Comparison of relevant bond lengths in **2.5** to other neutral Ni^{II} aryl/ phosphine complexes.

Complex	**Ni-PPh$_3$ (Å)**	**Ni-Ar (Å)**	**REF**
2.5	2.193 (1)	1.893 (2)	This Work
Ni[*O*C(Ph)CH*P*Ph$_2$](PPh$_3$)Ph	2.230 (3)	1.893 (4)	[Keim][20]
Ni[*O*C(Me)CH*P*Ph$_2$][*C*H$_2$P(^{i}Pr)$_3$]Ph	NA[a]	1.890 (4)	[Starzewski][21]
Ni[*p*-NO$_2$-pyca](PPh$_3$)*o*-tolyl	2.163 (2)	1.851 (7)	[Cavell][22]
Ni[pyca](PPh$_3$)*o*-tolyl	2.163 (2)	1.884 (5)	[Cavell][22]
Ni[pyca](PMePh$_2$)Mes	2.148 (2)	1.865 (8)	[Cavell][23]
Ni[P,O](PPh$_3$)Ph	2.212 (1)	1.921 (1)	[Gibson][24]

[a] NA = Not Applicable

Figure 2.3. X-ray analysis of Ni^{II} salicylaldimine complex **2.5**. Thermal ellipsoids are shown at 30% probability. All hydrogen atoms have been omitted for clarity.

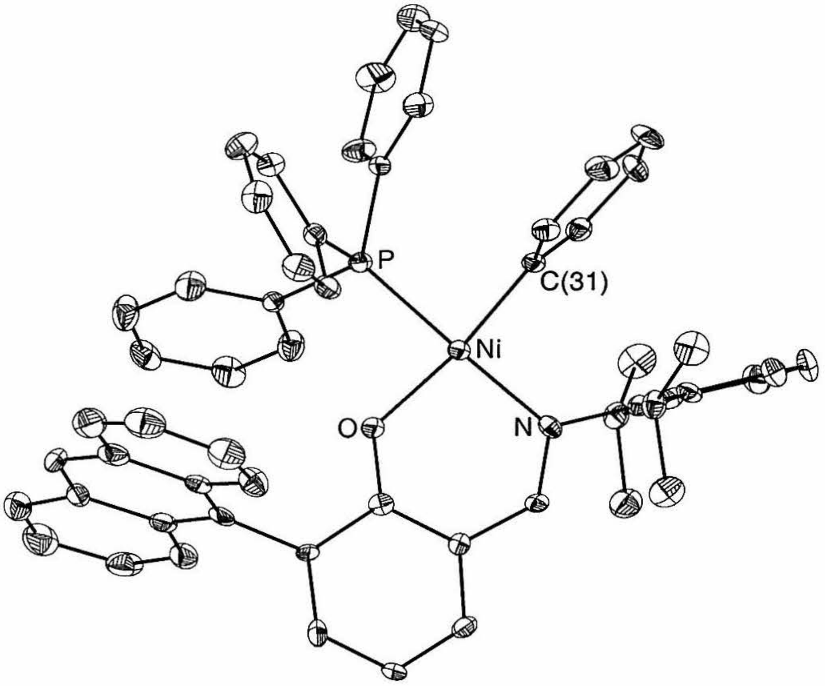

Table 2.6. Important bond lengths (Å) and bond angles (°) for **2.5**.

		Bond Lengths (Å)	
Ni-N	1.937(4)	Ni-O	1.910(3)
Ni-P	2.172(2)	Ni-C(31)	1.895(5)
		Bond Angles (°)	
N-Ni-O	94.5(2)	N-Ni-P	172.16(12)
N-Ni-C(31)	93.5(2)	O-Ni-P	87.51(11)
O-Ni-C(31)	166.2(2)	P-Ni-C(31)	86.0(2)

As shown in Table 2.7, PE can be obtained at similar rates as before (compare trials 2.7*a-g* with trials 2.1*a-g*, 2.3*a-f*, and 2.4*a-f*), but the productivity of the catalysts is *significantly* higher, with **2.5** exhibiting an "indefinite" lifetime for ethylene polymerization in a non-coordinating medium such as toluene. In accord with the polymerizations performed with "phosphine sponges," the activity and molecular weight are observed to increase and the branch content decreases as the size of the substituent in the *o*-position of the ligand increases: H (**2.1**) < ^{t}Bu (**2.2**) < Ph (**2.3**) < Phen (**2.4**) ~ Anthr (**2.5**). The molecular weight of the PE produced in these single-component polymerizations is significantly higher than the cocatalyzed reactions, with M_ws typically in the range of 70-300 · 10^3 g/mol. Clearly, this demonstrates that the cocatalyst, $Ni(COD)_2$ or $B(C_6F_5)_3$, had a significant interplay with the Ni^{II} center during the cocatalyzed polymerizations. The polyethylene obtained with **2.5** under single-component conditions also demonstrates a decreased branch content when compared to the previous trials employing $Ni(COD)_2$ or $B(C_6F_5)_3$.

Table 2.7. Single-component polymerization of ethylene with **2.1-2.4** at ρ = 100 psig.[a]

Trial	**Catalyst**	**Yield (g)**	**TOF[b]**	**M_w (10^3)**	**PDI**	**Branches[c]**	**T_m (°C)**
2.7*a*	**2.1**	0.8	0.01	11.4	2.3	42	95.3
2.7*b*	**2.3**	14.1	0.10	207.0	2.2	10	132.9
2.7*c*	**2.4**	40.4	0.30	207.0	2.4	8	129.5
2.7*d*	**2.5**	77.3	0.59	347.0	3.0	5	136.1
2.7*e*	**2.30**	16.1	0.12	247.0	3.2	10	127.8
2.7*f*	**2.31**	29.4	0.20	194.0	5.9	12	129.1
2.7*g*	**2.32**	28.2	0.22	252.0	2.7	6	134.0

[a] Polymerization performed with 65 μmol of the appropriate catalyst at 30 °C in 100 mL of anhydrous toluene, t = 120 min. [b] TOF = Turnover Frequency. 10^6 g PE· (mol catalyst^{-1})· (hr^{-1}). [c] Total number of C_1+C_2+C_3+C_4 branches per 1000 carbons, as determined by ^{13}C NMR spectroscopy.

Unlike the aforementioned similarities, the trend observed in rates of single-component polymerization activities is opposite to that observed upon cocatalyst activation, as the *p*-NO_2 species **2.30-2.32** demonstrate lower activities than their electron-rich analogs **2.2-2.5** (compare trials 2.7*b-e*, 2.7*c-f*, and 2.7*d-g*). These observations are consistent with a mechanism in which phosphine dissociation is the rate-limiting step, since the highly-withdrawing ligands of **2.30-2.32** should act to strengthen the Ni-PPh_3 bond. ^1H and ^{31}P NMR spectroscopic studies of ethylene polymerization (below) are in agreement with this hypothesis. Of course, hindsight suggests that we should have, at this point, began synthetic efforts towards electron-rich salen ligands with an increased steric demand—such investigations are underway.

2.7. Characteristics of polyethylene prepared with neutral Ni^{II} salicylaldimine complexes such as 2.5

The polyethylene obtained with complexes **2.4** and **2.5** is quite linear (typically ~ 5-25 branches/1000 carbons as determined by ^{13}C NMR spectroscopy) and of much higher molecular weight than samples prepared upon addition of a "phosphine sponge." The PDIs observed under these single-component conditions are typically ~ 1.8-2.3, suggesting that a well-defined homogeneous initiator is acting as a single-site catalyst.[25] As shown in Figures 2.4(a)-(c), spectroscopic analysis suggests that the linear polymers contain very few branches, with a typical branch analysis of the polymer demonstrating that > 95% of the branches are methyl groups. In polymers containing a higher branch content (for example, 20/1000 C's) obtained with **2.5** at slightly elevated temperatures, the following distribution was observed: 15 C_1, <1 C_2, <<<1 C_3, 1 C_4, 0 C_5, and 3 C_6^+, indicating that long-chain branching can occur.

As outlined in Table 2.7, decreased molecular weights and increased branch content were observed with complexes **2.1** and **2.3**. ^1H NMR spectroscopic analysis of low M_w PE samples prepared with **2.1** demonstrate signals at δ ~ 5.3 ppm. These signals are believed to arise from the olefinic $-CH=CH_2$ endgroup of the polymer in accord with a system that operates by β-hydride elimination and subsequent chain transfer (Figure 2.5).[26] Endgroup analysis can be performed using the experimental M_w [11,400 g/mol (determined vs. polystyrene standards) / 14.0 g/mol (PE: $CH_2=CH-(CH_2)_n-CH_3$, approximated as series of methylene groups) = 814 methylenes; Each methylene has 2 Hs = 1628 Hs; therefore, 1625 sp^3 hybridized CHs and 3 sp^2 hybridized CHs. This provides

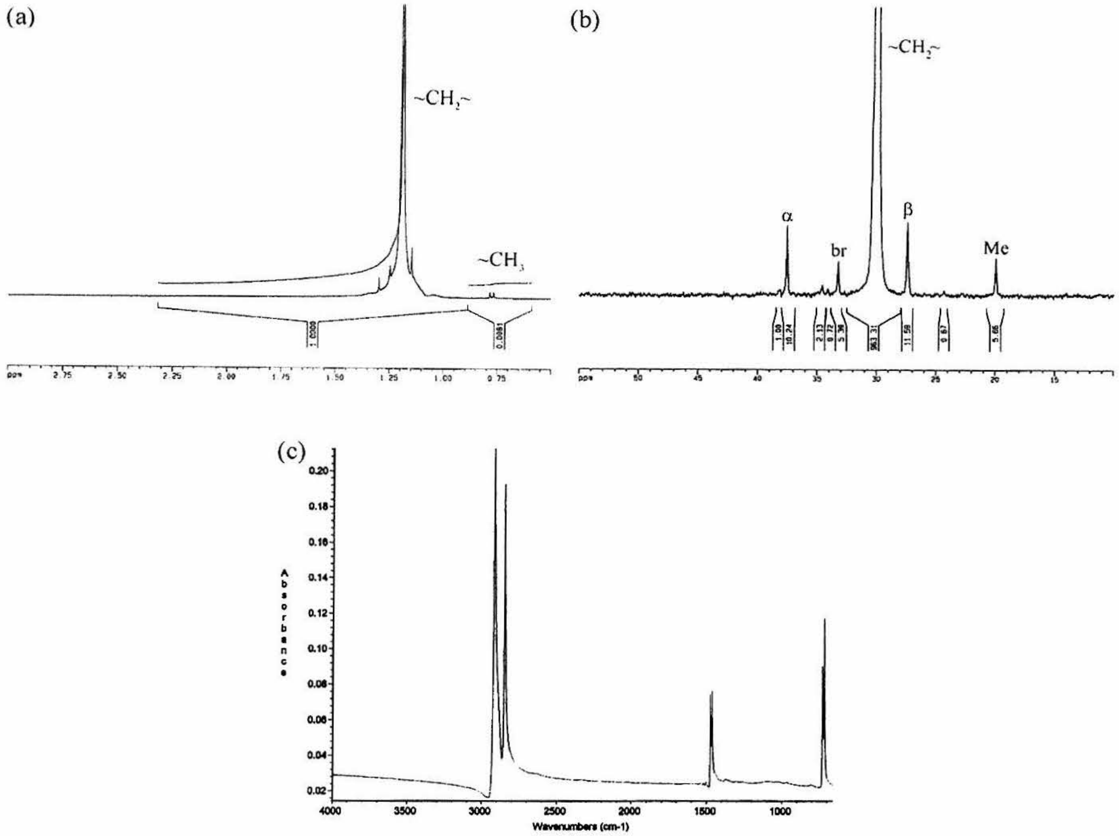

Figure 2.4. Typical ^1H/ ^{13}C NMR {(a) & (b), respectively} and IR spectra (c) of linear high molecular weight PE obtained using complex **2.5**. This PE sample contains ~ 5 branches/ 1000 Cs, has an $M_w \sim 350 \cdot 10^3$ g/mol (PDI = 2.2), and a $T_m = 136.5$ °C.

a theoretical value for olefinic CHs of 0.18%]. As shown in Figure 2.4, the experimental value is determined to be 0.21% (0.0023/1.0686), demonstrating that all of the polymer chain ends can be accounted for by a β-hydride elimination mechanism. In conjunction with the methyl branches often observed in PE obtained with these catalysts, it definitely appears that the complex can undergo β-hydride elimination, followed by reinsertion or displacement of the growing polymer chain from the metal center.

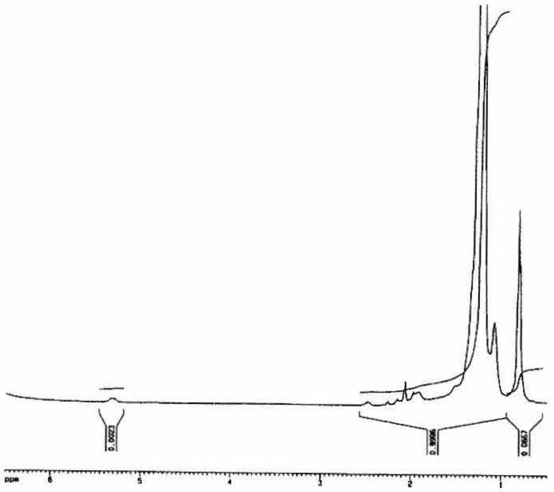

Figure 2.5. Endgroup analysis of low M_w PE suggests that chain termination occurs solely by β-hydride elimination with **2.1**.

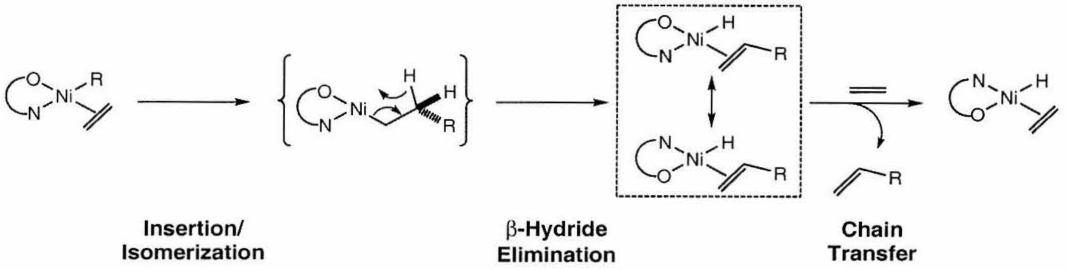

Figure 2.6. β-Hydride elimination operating with complex **2.1**. Endgroup analysis quantifies the polymer chain ends as olefins.

PE samples with higher molecular weights, obtained with complexes **2.2-2.5**, do not show any olefinic endgroups, due to the inherent sensitivity requirements of ^{1}H NMR spectroscopy (M_w of 11,400 (Figure 2.5) already at 0.2%; $M_w \sim 300.0 \cdot 10^3$ g/mol would have $\sim 7.0 \cdot 10^{-3}$% intensity). Phenyl resonances have not been observed as the "head" of the polymer chain, suggesting that the Ni-Ph species inserts ethylene, eliminates styrene, making a "Ni-H" species, which serves as the initiator for further polymerization. Again, however, the elimination of styrene from complexes **2.1-2.5** has not been observed. In fact, styrene can be incorporated into copolymers as outlined in Chapter 4.

The activity of catalyst **2.5** is observed to increase with temperature as shown in Table 2.8. However, they are susceptible to deactivation above 80 °C under polymerization conditions as evidenced by decreased productivities. The nature of this decomposition will be addressed in Chapter 3. The optimal operating temperatures, therefore, are between 45 and 50 °C. At these slightly elevated temperatures, complex **2.5** exhibits an activity of 1.0- $3.7 \cdot 10^6$ g PE ($mol^{-1}Ni$) (hr^{-1}). Such TOFs are comparable to "classical" metallocenes, such as $(Cp_2ZrMe)^+[B(C_6F_5)_4]^- = 4.5 \cdot 10^6$ g PE $\cdot$ ($mol^{-1}Zr$) $\cdot$ (hr^{-1}) and other highly active late metal cationic systems upon activation with a cocatalysts (MAO), for example ((Ar*N*=C(Me)C(Me)=*N*Ar)NiBr$_2$/MAO = $3.0 \cdot 10^6$ g PE ($mol^{-1}Ni$) (hr^{-1}) (Ar = 2,6-(^{i}Pr)$_2$C$_6$H$_3$).[2] However, at these temperatures both the rate of βHE and chain transfer are observed to increase drastically, such that the PE obtained has a lower molecular weight and higher branch content (compare trials 2.8*a-d*).

The effect of exposing catalyst **2.5** to different ethylene concentrations was investigated by performing a series of polymerizations at both 25 and 70 °C. As shown in Table 2.9, the nature of the products is greatly affected by temperature (compare trials 2.9*a-d/e*), but is less affected by changes in pressure (compare trials 2.9*a-c* or 2.9*d-h*). The TOF increases dramatically, however, with both an increase in temperature and/or pressure. In fact, Figure 2.7 demonstrates that the catalysts' response to ethylene is linear over the range of 15-90 psig (~ 1-6 atm)

Table 2.8. Polymerization of ethylene with **2.5** at different temperatures [ρ = 400 psig].[a]

Trial	Cat (μmol)	Temp (°C)	Yield (g)	TOF[b]	M_w (10^3)	PDI (M_w/M_n)	Branches[c]	T_m (°C)
2.8*a*	60	40	106.2	1.19	316.6	1.9	6	127.3
2.8*b*	60	55	89.0	0.99	131.3	2.0	8	124.3
2.8*c*	60	62	103.9	1.61	63.1	1.8	11	119.2
2.8*d*	60	70	196.0	3.76	38.9	1.8	20	115.8

[a] Reaction performed at the appropriate temperature in 100 mL anhydrous toluene for 60 min. [b] 10^6 g PE (mol^{-1} **2.5**) hr^{-1}. [c] Total number of $C_1+C_2+C_3+C_4$ branches per 1000 carbons, as determined by ^{13}C NMR spectroscopy.

Ethylene polymerization can be performed *in situ* with similar results to those obtained using the well-defined complex. For example, combination of the alkali salt of the desired ligand, (^{Anthr,H}Sal)Na, with a toluene solution of Ni(PPh$_3$)PhCl in a glass bomb, followed by immediate pressurization to 100 psig of ethylene, leads to the production of 38.3 g of linear polyethylene with $M_w = 348\cdot 10^3$ g/mol, PDI = 2.2, and T_m = 136.5 °C, demonstrating that the only major difference between the use of the well-defined initiator **2.5** and the catalyst prepared *in situ* is the rate of the reaction. This effect was ascribed to both the residence time required to prepare the active catalyst (~ 1 hr.) and the presence of an equivalent of free PPh$_3$—the effect of which will be elaborated upon in Chapter 3.

Table 2.9. Polymerization of ethylene with **2.5** at different pressures [T = 25 & 70 °C].[a]

Trial	**Cat (μmol)**	**Pressure (psig)**	**Yield (g)**	**TOF[b]**	**M_w (· 10^3)**	**PDI (M_w/M_n)**	**Branches[c]**	**T_m (°C)**
T = 25.0 °C								
2.9*a*	42	50	5.3	0.12	219.0	1.9	9	127.4
2.9*b*	42	224	30.6	0.52	294.0	1.9	13	130.6
2.9*c*	25	400	27.4	0.66	171.0	3.6	9	128.0
T = 70.0 °C								
2.9*d*	25	50	6.55	0.35	12.2	1.6	46	87.9
2.9*e*	42	50	19.0	0.45	11.3	1.6	49	88.3
2.9*f*	60	224	76.5	1.54	28.8	1.8	20	112.8
2.9*g*	42	250	27.7	0.66	34.5	1.8	24	115.3
2.9*h*	25	400	18.9[d]	5.79	37.0	1.8	19	115.5

[a] Reaction performed at the appropriate temperature in 100 mL anhydrous toluene for 60 min. [b] 10^6 g PE (mol^{-1}**2.5**) hr^{-1}. [c] Total number of $C_1+C_2+C_3+C_4$ branches per 1000 carbons, as determined by ^{13}C NMR. [d] Time = 8 min.

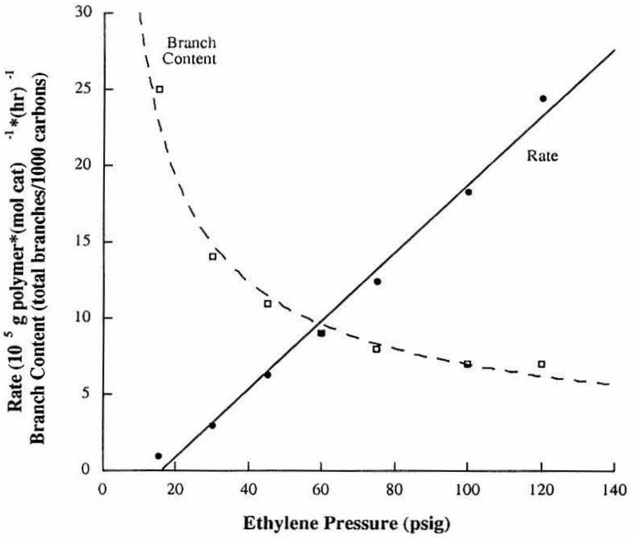

Figure 2.7. Variation of catalyst activity and branch content as a function of polymerization pressure with **2.5**.

2.8. Preparation of (^{Anthr,H}Sal)Pd(PPh$_3$)Ph 2.48 and the analysis of its reaction with ethylene

Cationic polymerization catalysts based on Ni^{II} and Pd^{II} diimine complexes demonstrate very different polymerization behaviors.[2] Ni^{II} catalysts allow for the preparation of moderately linear materials,[2,5] whereas polymers obtained with the Pd^{II} analog are highly branched.[2] The benefit of catalysis with the Pd^{II} initiators lies in their ability to incorporate functionalized olefins, such as acrylates, whereas Ni^{II} initiators are deactivated by a tight association of the carbonyl functionality as outlined in Chapter 1.[2] Very few reports, however, investigate the use of neutral Pd^{II} complexes for ethylene polymerization. In fact, [P,O]Pd(PPh$_3$)Ph, was found to undergo ethylene insertion followed by the rapid and irreversible β-hydride elimination of styrene and a reduction of the metal center. We sought to prepare the neutral Pd^{II} salicylaldimine complex, **2.48**, analogous to complex **2.5** to investigate its behavior for the polymerization of ethylene and α-olefins, in the hope that it might provide additional reactivity profiles or substrate scope.

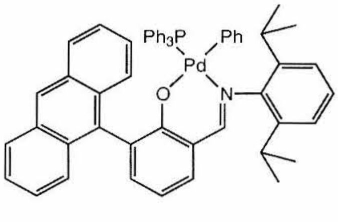

2.48

In analogy to the synthesis for **2.5**, complex **2.48** was prepared by the combination of Na($^{\text{Anthr,H}}$Sal) with $Pd(PPh_3)_2PhBr$[27] in C_6H_6. A yellow crystalline material was obtained *via* recrystallization of **2.48** in 1:3 benzene/hexane or pentane mixtures. Compound **2.48** exhibited many of the same diagnostic ^1H NMR (toluene-d_8, 300.0 MHz) handles as complex **2.5**, including two doublets at $\delta = 1.06$ and 1.19 (6H each, $^3J_{HH} = 7.0$ Hz) for the inequivalent –CH*Me*Me' and –CHMe*Me'*, a septet ($\delta = 3.62$, 2H, $^3J_{HH} = 7.0$ Hz) for –*CH*MeMe', and a doublet for –C*H*=NAr ($\delta = 8.17$, 1H, $^4J_{PH} \sim 9$ Hz), supporting the formation of the *trans-* geometry of **2.48**. The ^{31}P NMR spectrum exhibited a signal at δ 29.04 ppm.

Confirmation of the structure for **2.48**, shown in Figure 2.9, was obtained by X-ray analysis of crystals obtained from a benzene/pentane mixture. In analogy to the structure of **2.5**, the Pd^{II} species is square planar with a *trans*-arrangement of the coordinated PPh_3 and benzimine groups. The 9-anthracenyl and 2,6-diisopropylbenzimine groups are essentially orthogonal to the equatorial plane defined by N, O, P, and C(52) (79° and 88° respectively). All of the bond lengths are within standard distances for a d^8 Pd complex, with the Pd-O, -N, -P, and -C(52) lengths being, on average, ~ 0.13 Å longer than the same bonds in **2.5**. The largest observed difference between structures **2.5** and **2.48** is the "puckering" of the six-membered metal chelate defined by the phenolic ring, the imine, and the metal center. The chelate is canted away from the equatorial plane of the metal center by ~ 10-15°. This subtle change in the coordination of the salen fragment may provide insight into the degree of π-donation to each of the d^8 centers.

Unfortunately, the addition of 100-120 psig of ethylene to a toluene or benzene solution of **2.48** leads to the observation of a slow consumption of ethylene in conjunction with the formation of Pd^0 deposits. TLC analysis of the reaction (upon release of the pressure) leads to the observation of the free $^{\text{Anthr,H}}$Sal ligand as identified by comparison to an authentic sample of the ligand. No solid polymeric products were obtained upon the addition of excess acidified methanol.

The introduction of ~ 1 atm of ethylene to a solution of **2.48** in C_6D_6 led to the slow consumption of ethylene and **2.48** at similar rates as evidenced by the simultaneous disappearance of a singlet at $\delta = 5.3$ (CH_2CH_2) and the septet at $\delta = 3.6$ ppm (-C*H*MeMe′ of **2.48**). In agreement with the results outlined above for attempts at higher pressures of ethylene, appearance of the $^{\text{Anthr,H}}$Sal ligand was confirmed from its diagnostic ^{1}H NMR spectroscopic shifts. GC/MS analysis of the resulting mixture indicated that 1 eq.. of styrene was produced for every equivalent of the $^{\text{Anthr,H}}$Sal ligand. Therefore, in agreement with earlier studies for [P,O]Pd(PPh_3)Ph, we postulate that ethylene insertion into the Pd-Ph bond of **2.48** leads to the production of **2.49** which rapidly (and irreversibly) eliminates styrene *via* βHE followed by reduction of the metal center (Figure 2.8).

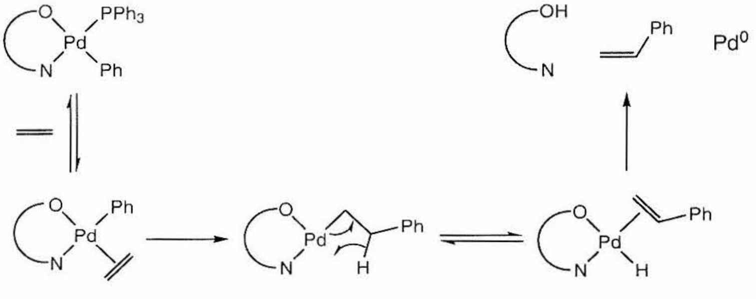

Figure 2.8. Neutral Pd^{II} salicylaldimine complex **2.48** is an inefficient catalyst for the polymerization of ethylene. Proposed mechanism of decomposition.

Figure 2.9. X-ray analysis of Pd^{II} salicylaldimine complex **2.48**. Thermal ellipsoids are shown at 30% probability. All hydrogen atoms have been omitted for clarity.

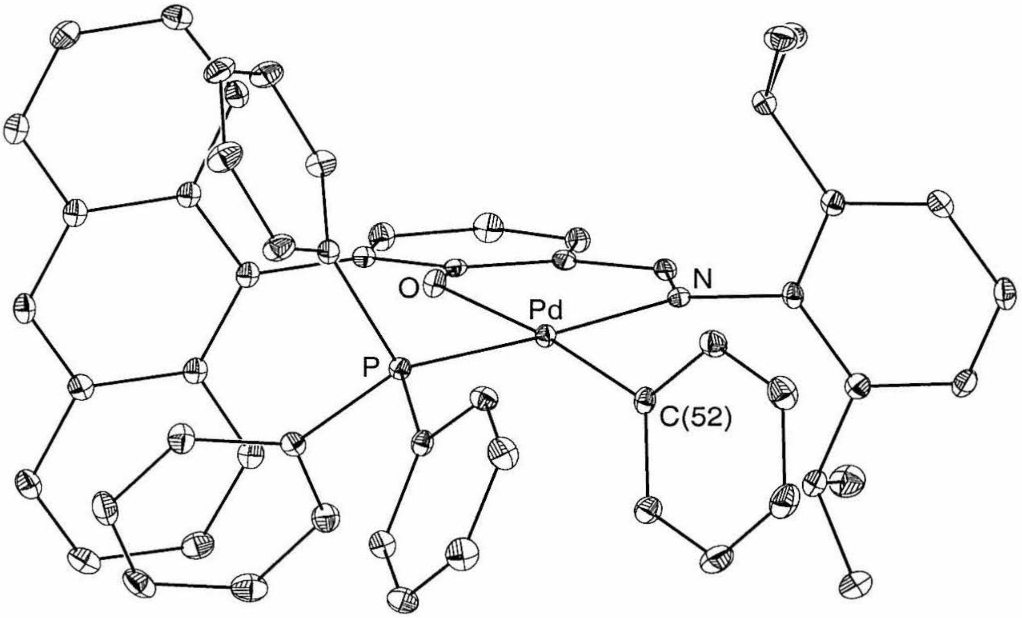

Table 2.10. Selected bond lengths (Å) and angles (°) for **2.48**.

		Bond Lengths (Å)	
Pd-N	2.0991(14)	Pd-O	2.0843(11)
Pd-P	2.2613(5)	Pd-C(52)	1.9956(17)
		Bond Angles (°)	
N-Pd-O	89.74(5)	N-Pd-P	177.11(4)
N-Pd-C(52)	93.06(6)	O-Pd-P	88.79(3)
O-Pd-C(52)	174.04(6)	P-Pd-C(52)	88.64(5)

2.9. Synthetic endeavors – A better synthetic route to o-anthracenyl ligand

Owing to the promise of neutral Ni^{II} complexes for the polymerization of ethylene in the presence of functionalities (Chapter 3) and the copolymerization of functionalized olefins (Chapter 4), we sought to prepare large batches of complex **2.5**. The previous route employed a nickel-catalyzed aryl coupling as the key step in the preparation of the $^{\text{Anthr,H}}$Sal ligand, i.e., formation of the trisubstituted biphenyl unit. In our hands, this reaction proved to be erractic, and therefore, alternative synthetic routes were sought which could prepare the *o*-anthracenyl ligand in good yield.

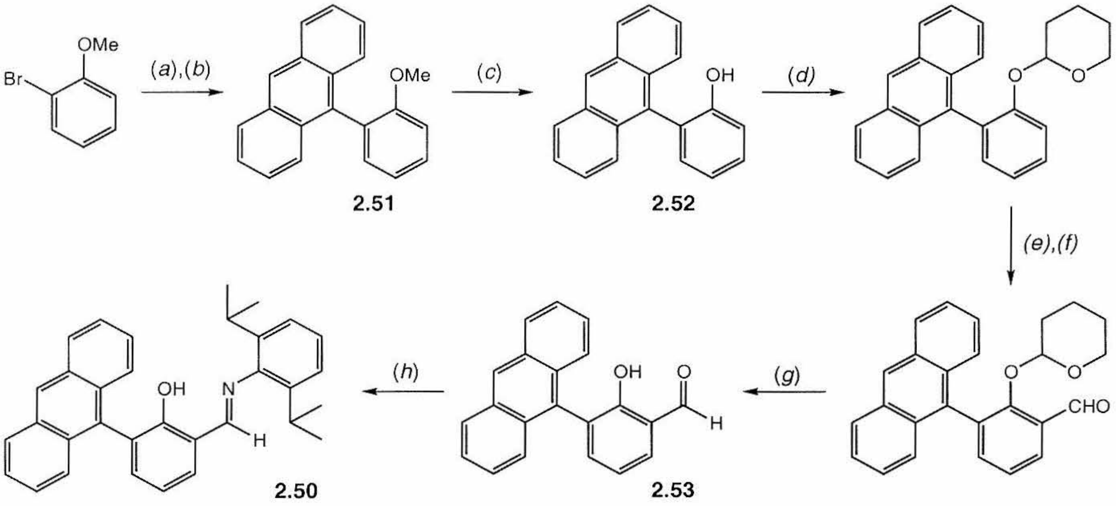

Scheme 2.7. Synthesis of ligand **2.50**. (*a*) Mg, THF; -10 °C, anthrone. (*b*) 3 N HCl. (*c*) BBr_3, CH_2Cl_2, -78 to 25 °C. (*d*) DHP, CH_2Cl_2, cat. PPTS. (*e*) ^{n}BuLi, THF. (*f*) DMF, 1 N HCl. (*g*) EtOH, cat. PPTS, Δ. (*h*) 2,6-(^{i}Pr)$_2$- $NH_2C_6H_3$, MeOH, cat. HCO_2H.

We developed a scalable route into ligand **2.50** based on the reported synthesis of *o*-(9-anthracenyl)-anisole (Scheme 2.7).[28,29] The key step, the reaction of the Grignard of *o*-bromoanisole with anthrone in THF at –10 °C, allows for the facile coupling of the two aryl units. Acidic workup (~ 3 N HCl) serves to aromatize the central ring of the anthracenyl moiety, providing **2.51** in yields ranging from 60-85% from the *o*-bromoanisole. Although use of the lithiate is reported, in our hands the organolithium reagent led to lower yields and the observation of anisole which presumably arises from deprotonation of anthrone instead of nucleophilic attack of the ketone.[28] Deprotection of the methyl ether in **2.51** was achieved with BBr_3 at -78 °C, yielding the phenol **2.52** in good yield. Subsequent protection of the phenol as the *O*-THP adduct allows for regioselective formylation using ^{n}BuLi and DMF. Mild deprotection with PPTS in EtOH yields the desired salicylaldehyde **2.53**, which can be converted to the desired ligand by condensation with 2,6-diisopropylaniline. Overall, the ligand is obtained in ~ 40% yield after 6 steps.

This methodology has successfully yielded a number of *o*-(9-anthracenyl) aromatic compounds such as **2.54-2.57** *via* the combination of anthrone with other Grignard reagents as depicted in Scheme 2.8. These ligands are currently being pursued as scaffolds for both neutral and cationic polymerization catalysts as continued interest in the nature of electronic perturbation of ligands containing the *o*-anthracenyl moiety. We are especially interested in pursuing an electron-rich (*p*-OMe, *p*-NMe_2, etc.) version of the (^{Anthr,H}Sal) ligand.

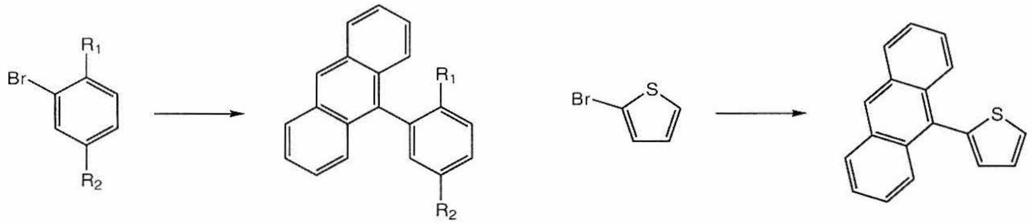

R_1	R_2	
OBn	OMe	**2.54**
OMe	OMe	**2.55**
OMe	CF_3	**2.56**

2.57

Scheme 2.8. Grignard catalyzed coupling to anthrone serves as an entry point for the preparation of a variety of potential ligands **2.54-2.57**.

2.10. The preparation of salen ligands which serve to provide further protection of the axial site of the metal

As previously outlined, the 9-anthracenyl group provides some shielding of the axial site of the metal center, exhibiting high TOFs and M_ws while providing polymer that is predominately linear. Unfortunately, however, the addition of 80 psig of propylene to a toluene solution of **2.5** leads to oligomeric products. We believed that the preparation of ligands which provided an increased protection of the metal center could allow for even higher M_w polyethylene and solid polypropylene by suppressing the rate of associative interchange of the growing polymer chain (Figure 2.2).

We sought to prepare a ligand containing the *m*-terphenyl linkage, such as that contained in **2.58** (Scheme 2.9), as preliminary molecular modeling illustrated that such a ligand would act to shield the top and bottom axial sites of the metal more efficiently than the *o*-anthracenyl group. Preparation of the parent phenol **2.56** was accomplished *via* the Pd-catalyzed coupling to iodobenzene in the presence of Cs_2CO_3 (albeit in low yield). The remaining sequence to **2.58** was analogous to that outlined for the preparation of **2.50** from **2.52** (Scheme 2.8).

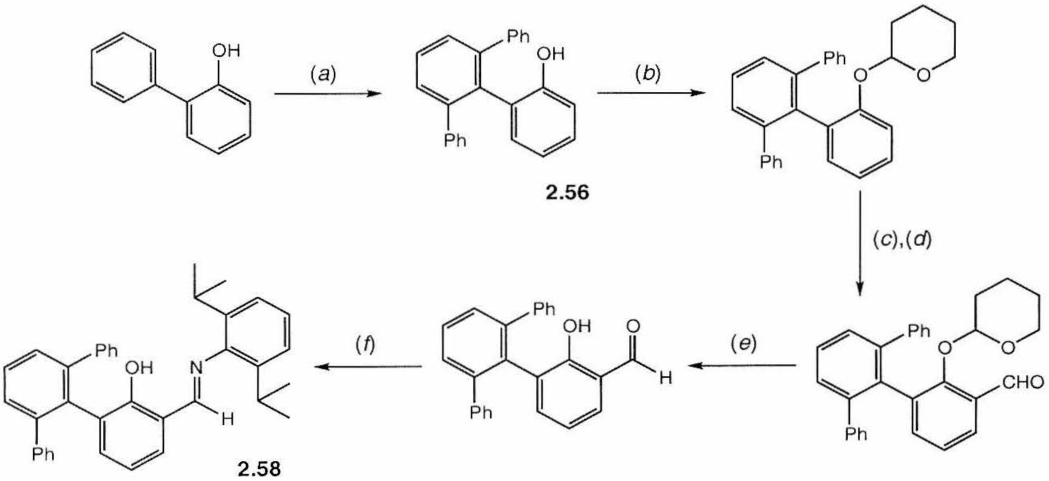

Scheme 2.9. Preparation of **2.58**. (*a*) Pd, Cs_2CO_3, 4 eq.. PhI, Δ, 6-20 %. (*b*) DHP, CH_2Cl_2, cat. PPTS. (*c*) ^{n}BuLi, THF, 0 °C. (*d*) DMF, H_3O^+. (*e*) EtOH, cat. PPTS, Δ. (*f*) 2,6-(^{i}Pr)$_2$- $NH_2C_6H_3$, MeOH, cat. HCO_2H.

However, a serious bottleneck in the reaction sequence was present in the preparation of **2.56**, namely the low-yielding Pd-catalyzed aryl-aryl coupling which serves as the first step of the reaction sequence. Although the procedure was repeated on several occasions on very large scales, the isolation of a reasonable amount of material was not possible. For this reason, a synthetic method which allowed for the formation of a *m*-terphenyl linkage in high yield was desired. Using a synthetic strategy employed for the preparation of hindered biphenyls,[30-32] the reaction of cyclopentadienones with disubstituted acetylenes could provide complex **2.59**, similar to **2.56**, *via* the process shown in Figure 2.9. We believed that the phenol would have to be protected to prevent undesired side reactions, as the reactions require temperatures in excess of 200 °C.

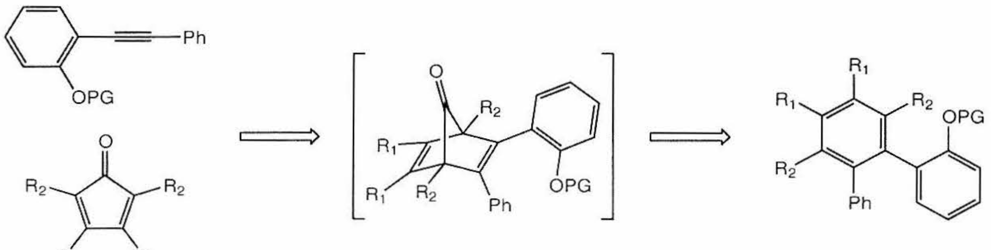

2.59

Figure 2.10. Retrosynthetic analysis of a *m*-terphenyl linkage using a substituted diphenylacetylene and a cyclopentadieneone derivative.

After several initial attempts to use a variety of protected diphenylacetylenes (PG = Me, Ac, THP), we masked the salicylaldehyde group as a benzofuran to attach that fragment to a phenylacetylene as outlined in Scheme 2.10. Preparation of benzofuran substituted species **2.63**, was expected to allow for the facile formation of a salicylaldehyde such as **2.66** through ozonolysis and saponification. According to literature reports, the alkylation of 2-bromophenol with propargyl chloride yielded the propargyl ether **2.60**, which undergoes Claisen cyclization to provide the bromo-substituted benzofuran **2.61** in good yields.[33] Unfortunately, coupling of the phenylacetylene with $Pd(PPh_3)_2Cl_2$/CuI in NEt_3 was incomplete after 15 hr. at reflux, and yielded a number of products as determined by GC/MS analysis. For this reason, the iodo-substituted benzofuran **2.62** was prepared in analogous fashion to the synthesis of **2.61**. The Pd/Cu mediated phenylacetylene coupling was facile with **2.61**, complete in nearly 30 minutes at room temperature, yielding **2.63** in almost quantitative yields.

Reaction of **2.63** with the commercially available tetraphenylcyclopentadienone was achieved through thermolysis (~ 260 °C, 2 hr.) in a vacuum sealed tube, yielding the desired product **2.64** in 87% yield upon precipitation from CH_2Cl_2 with hexanes.

Ozonolysis of **2.64** in CH_2Cl_2 at –78 °C, followed by saponification with 2.5 M NaOH in DME led to ~ 92% recovery of the desired salicylaldehyde **2.66**. However, the condensation of 2,6-diisopropylaniline led to a product, **2.68**, which demonstrated *very poor solubility* in all solvents tested. Strong evidence that it was the desired salicylaldimine **2.68** came from elemental analysis and mass spectrometry, which identified the material as both the right composition and correct mass/isotopic abundance.

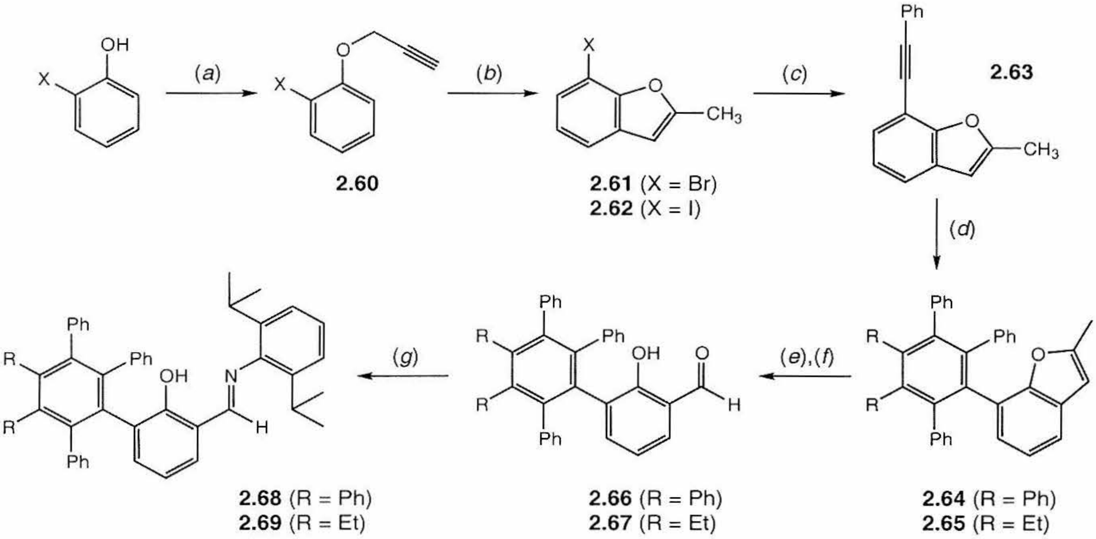

Scheme 2.10. Preparation of **2.68** and **2.69**. (*a*) $HCCCH_2Br$, K_2CO_3, DMF. (*b*) N,N-DEA, CsF, Δ. (*c*) PhCCH, NEt_3, CuI, $Pd(PPh_3)_2Cl_2$, Δ. (d) Appropriate cyclopentadienone, 260 °C, vacuum. (*e*) O_3, CH_2Cl_2, -78 °C. (*f*) 2.5 M NaOH, DME, Δ. (*g*) 2,6-$(^iPr)_2$-$NH_2C_6H_3$, C_6H_6, cat. PPTS.

Owing to the poor solubility of **2.68**, we prepared the "less crystalline" version, **2.69**, *via* removal of two of the aromatic groups (which are derived from the cyclopentadienone) and introduction of alkyl groups, in the hope of promoting increased solubility. Compound **2.63** was reacted with 2,5-diphenyl-3,4-diethyl cyclopentadienone (prepared in analogy to literature reports[30]) at 260 °C in a vacuum-sealed tube, providing **2.65** in good yield. The substituted benzofuran was ozonolyzed, saponified (**2.67**), and condensed with 2,6-diisopropylaniline, yielding **2.69**. This compound demonstrated a greatly increased solubility relative to **2.68**.

Several attempts were made to prepare well-defined polymerization initiators using ligands **2.58** and **2.69**. The sodium salt of both ligands could be prepared by the addition of NaH to a THF solution of **2.58** and **2.69**. Combination of these salts with $Ni(PPh_3)_2PhCl$ yielded yellowish-orange solutions that exhibited ^{31}P NMR signals at 22.88 and 22.41 ppm, respectively, similar to the shifts obtained with other salicylaldimine Ni^{II}-PPh_3 complexes. However, the ^{1}H NMR spectrum of each reaction was extremely broad and difficult to interpret. Attempts to isolate the desired products in each experiment proved to be elusive.

However, in analogy to the *in situ* polymerizations reported above for **2.5**, we attempted to generate catalysts containing ligands **2.58** and **2.69** and test them for polymerization. The combination of the sodium salts of **2.58** and **2.69** with 1 eq.. of $Ni(PPh_3)PhCl$, followed by pressurization to 100 psig, did lead to the production of polyethylene in both cases (Table 2.11). As shown in Table 2.11, the productivities of each ligand are lower than those typically observed for **2.5**. However, the molecular weights are higher, especially those observed in trial 2.11*b*. Ligands such as these exhibit

Table 2.11. *In situ* generation of ethylene polymerization catalysts using ligands **2.58** and **2.69**.[a]

Trial	Ligand	PE (g)	M_w ($\cdot$ 10^3)	PDI (M_w/M_n)	T_m (°C)	Branch Content[b]
2.11*a*	**2.5**	38.3	348.0	2.2	136.5	8
2.11*b*	**2.58**	7.9	532.0	2.1	135.8	6
2.11*c*	**2.69**	0.3	392.0	1.9	112.5	ND[c]

[a] Polymerization performed with 65 μmol of the appropriate sodium salt, 65 μmol (1.0 eq..) $Ni(PPh_3)_2PhCl$, 100 mL anhydrous toluene, 100 psig ethylene, T = 30 °C. [b] Total number of C_1+C_2+C_3+C_4 branches per 1000 carbons, as determined by ^{13}C NMR spectroscopy. [c] ND = not determined.

great promise in making polymer of increased molecular weight, however, the difficulty associated with their syntheses as well as the performance attributes of complex **2.5** led us to continue our investigations with the $^{\text{Anthr,H}}$Sal ligand.

2.11. Spectroscopic observation of ethylene polymerization with complex 2.5

Several attempts have been made to follow the insertion of ethylene into **2.5** using ^{1}H and ^{31}P NMR spectroscopy. To date, free PPh$_3$ (^{31}P NMR δ = - 4.5 ppm) has not been observed under any conditions. However, using a (dangerous) high pressure NMR tube and ~ 5-7 atm of ethylene, three phosphine species were observed as shown in Figure 2.10. They are tentatively assigned as: (a) the starting precatalyst **2.5**, (b) an alkyl complex of the type [N,O]Ni(PPh$_3$)R (where R = growing polymer chain), and (c) the hydride complex [N,O]Ni(PPh$_3$)H (the chain-terminated species ready to reenter the catalytic cycle). Further support for the presence of a "Ni-H" was present in the ^{1}H NMR spectrum as a shielded doublet which resonated at δ = - 27.2 ($^{2}J_{PH}$ = 136 Hz), similar to the closely related complex [Ph$_2$*P*CH$_2$C(CF$_3$)$_2$*O*]Ni(PCy$_3$)H (δ = -24.8, dd).[34] These results suggest, in agreement with earlier arguments concerning the activity of various

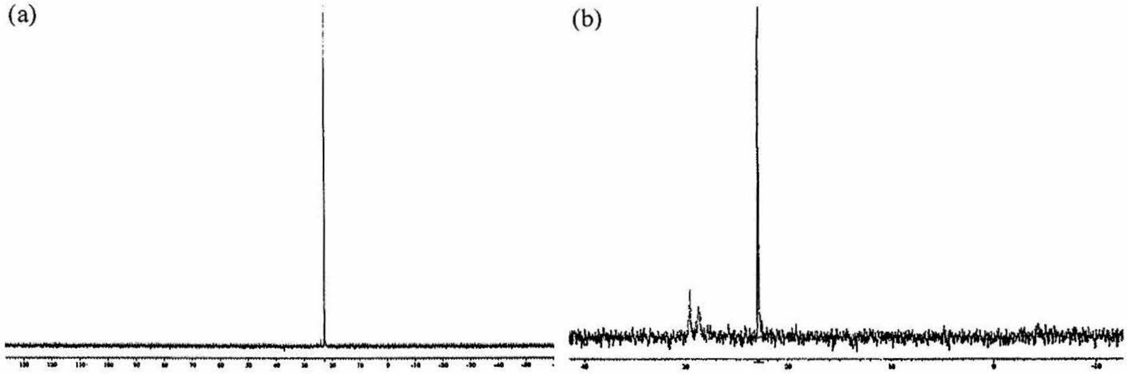

Figure 2.11. High pressure (~ 5 atm) reaction of ethylene and **2.5** demonstrates three species by ^{31}P NMR spectroscopy. (a) Initial unactivated complex, **2.5**. (b) Consumption of ethylene yields two new species, proposed to be [N,O]Ni(PPh$_3$)R and [N,O]Ni(PPh$_3$)H.

electronically modified catalysts, that the resting state of the polymerization is the ligated phosphine complex, and that phosphine dissociation *is* the rate-determining step in the polymerization of ethylene.

Exposure of a 0.02 M solution of **2.5** to ~ 1.5 atm of ethylene at low temperature, followed by warming to room temperature led to the observation of ethylene insertion at ~ -10 °C, followed by the disappearance of ethylene and the production of polymer (as observed by deposition of PE along the walls of the NMR tube). However, very little information could be obtained by ^{1}H or ^{31}P NMR spectroscopy as the signals for the catalyst remained essentially unchanged. These results suggest that the initiation efficiency under ambient temperatures and pressures is *very low* (less than 1%) and imply that insertion occurs from a four-coordinate active species.

2.12. Molecular motions observed in neutral Ni^{II} salicylaldimine complexes

One postulate for the increased single-component activity of complexes **2.4** and **2.5**, was that the large aryl substituents increase the rate of phosphine dissociation (the proposed rate determining step of the polymerization) through rotation or a "wiggling" motion which abuts the coordinated PPh_3. Although the Ni-PPh_3 bond length of **2.5** (Figure 2.3) does not suggest that lengthening of the Ni-Ph bound occurs with the *o*-anthracenyl group, several attempts were made to monitor the variable temperature ^{1}H NMR behavior of complexes such as **2.4** and **2.5**. The molecular motions of such complexes can be easily discerned by **2.4** and its *p*-NO_2 derivative, **2.31**, as these

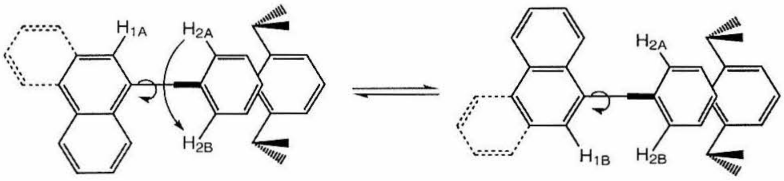

Figure 2.12. Use of C_s symmetric complexes allows for determination of molecular motions. Rotation barriers for Ni-Ph are calculated and shown in Table 2.12. Evidence for rotation about aryl-aryl bonds was not found.

Table 2.12. Variable temperature ^{1}H NMR studies determine the barriers for rotation about the Ni-Ar bond.

Trial	Complex	Conditions	T_c (°C)	k_{coal} (s^{-1})	$\Delta G^{\ddagger}$ (kcal/mol)
2.12*a*	**2.4**	0.02 M $CDCl_3$	35.4	91.3	15.3 (2)
2.12*b*	**2.31**	0.02 M $CDCl_3$	41.5	82.8	15.7 (2)
2.12*c*	**2.31**	0.02 M *o*-$C_6D_4Cl_2$	48.5	94.4	16.0 (2)
2.12*d*	**2.31**	0.02 M $CDCl_3$ 5 eq.. PPh_3	43.5	86.2	15.8 (2)
2.12*e*	**2.70**	0.02 M C_6D_6	50.0	173.1	15.6 (1)

complexes possess C_s symmetry at room temperature due to restricted rotation about the phenanthryl-phenoxide bond and the N-C^{ipso} bond. Therefore, diastereotopic nuclei on the phenyl group arise because the equatorial plane no longer serves as a mirror plane, providing aryl groups that sit with either an "up" or "down" orientation as shown in Figure 2.12.

The ^{1}H NMR spectra of these complexes demonstrates unequivocal $-CHMe_2$ groups as evidenced by two septets in the $\delta = 2.5\text{-}4.0$ region which integrate to 2H and four doublets around $\delta = 1.0\text{-}1.2$ totaling 12H. Complexes **2.4** and **2.31** were studied using variable temperature NMR. In all cases, the inequivalent protons of the –CH*Me*Me' and –CHMe*Me'* as well as the diagnostic H_{1A}/H_{1B} of the phenanthrene substituents undergo very little change as the temperature is raised. In fact, at higher temperatures above 100 °C, separate signals for the diastereotopic protons of both the aniline and the phenanthrene moieties begin to broaden and migrate slightly. However, decomposition occurs with prolonged exposure to temperatures above 100 °C. Therefore, ^{1}H NMR spectroscopy demonstrates no evidence for rotation about the o-phenanthrenyl-phenoxide bond or for the 2,6-diisopropylbenzimine up to 100 °C, suggesting that the barrier to rotation for each of these groups is greater than 20 kcal/mol. On the basis of these observations, rotation of the naphthalene or phenanthrene substituents or the 2,6-diisopropyl aryl fragment is probably negligible during the course of a polymerization reaction.

Coalescence is observed around 45 °C in each of the spectra, which was determined to be rotation about the Ni-Ph bond, exchanging the *o,o'* and the *m,m'* protons of the metal-bound aryl ligand. As seen in Table 2.12, the barrier for Ni-Ph group rotation is not impacted greatly by the electronic nature of the ligand. The barrier to Ni-Ph group rotation is also independent of the size of the *ortho-* substituent. For example, the *o*-Naphth complex **2.70** (prepared *via* analogous methods to those described for the initial synthesis of **2.5** – see experimental section)[3,14] demonstrates an almost identical $\Delta G^{\ddagger}_{rotation}$ for Ni-Ph.

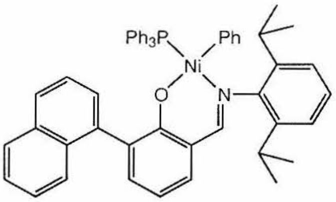

2.70

2.13. Neutral Ni^{II} salicylaldimine hydrido complexes as initiators

Small molecules, such as ethylene or carbon monoxide, have been documented in several cases to exhibit much lower barriers to insertion into metal-hydride bonds than the corresponding metal-aryl or metal-alkyl bond.[35] The increased migratory aptitude is attributed, in part, to the non-directional nature of a proton's σ-orbital when compared to the directionalized sp^3 and sp^2 orbitals of the alkyl and aryl fragments.[26,35] We sought to prepare the hydrido complexes **2.71** and **2.72** in an effort to (1) demonstrate that the Ni^{II} *hydrido* species could serve as a catalytically active complex, and hence exist within the proposed catalytic cycle, (2) prepare complexes which exhibited a lower barrier to initiation, allowing for the spectroscopic detection of initiation (observed as insertion of ethylene into the Ni-H bond), and (3) determine the susceptibility of the Ni-H species to deactivation, to better understand how complexes such as **2.5** are inactivated.

A literature search on d^8 hydrido complexes suggested that the isolation of such species would require the use of sterically demanding electron-rich phosphines such as P^iPr_3 or PCy_3. The precursor, $Ni(PCy_3)_2HCl$ (**2.73**), was selected because of its reasonable thermal stability and ease of synthesis from $Ni(PCy_3)_2Cl_2$ and $NaBH_4$.[36]

Complex **2.71** was easily be prepared *via* reaction of the Na, Cs, or Tl salt of the $^{\text{Anthr,H}}$Sal ligand with **2.73**, in C_6H_6 or THF at 25 °C (Scheme 2.11). Initial reactions were monitored by ^{1}H NMR spectroscopy (C_6D_6, 300.0 MHz), following the disappearance of the diagnostic Ni-H signal from **2.73** (δ = -24.41, t, $^2J_{PH}$ = 73.0 Hz). Support for the

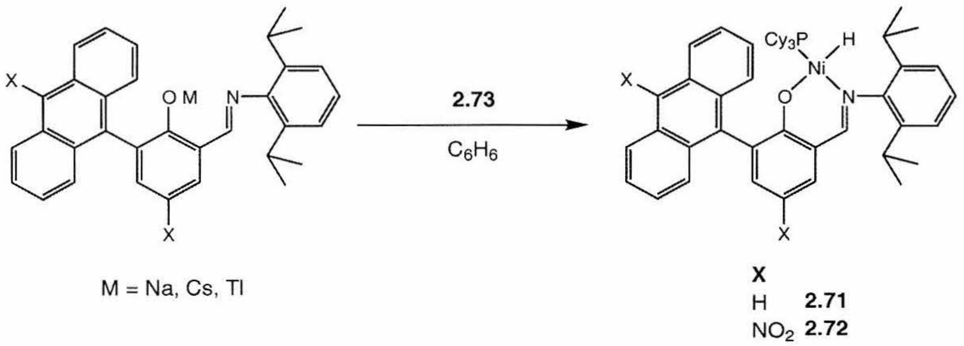

Scheme 2.11. The synthesis of Ni^{II} salicylaldimine hydrido complexes **2.71** and **2.72**.

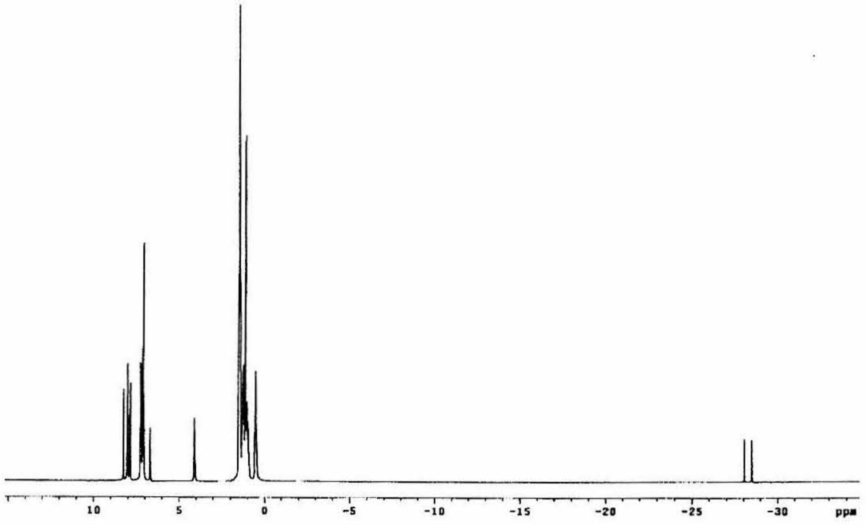

Figure 2.13. ^{1}H NMR of **2.71** (C_6D_6, 300.0 MHz). Diagnostic Ni-H signal observed at δ = –28.4 (d, $^2J_{PH}$ = 128 Hz from *cis*-PCy_3 ligand). The large coupling suggests the structure maintains a *trans*- geometry.

formation of **2.71** came from the appearance of a doublet at $\delta = -28.37$ (d, 1H, $^2J_{PH} = 128$ Hz) and the correlated ^{31}P signal at $\delta = 42.2$ (d, $^2J_{PH} = 128.5$ Hz), which suggested the formation of a complex containing one phosphine and a Ni-H. The large increase in the coupling constant, $\Delta(^2J_{PH}) = 55$ Hz, indicated that the new Ni-H occupied a position *trans-* to a stronger σ-donor than Cl, namely the phenoxide.[26] Furthermore, these values are similar to those observed for the proposed "[N,O]Ni(PPh_3)H" complex observed during experiments using higher pressures of ethylene (see section 2.6).

A single-crystal X-ray study confirmed the structure of the hydride complex **2.71** and provided structural information for the Ni^{II} hydride. Crystals of suitable quality were obtained by dissolving ~50 mg of the complex in a minimal amount of benzene, followed by the slow diffusion of acetonitrile into the benzene solution at 5 °C. As outlined in Figure 2.14, X-ray studies agree with the aforementioned ^1H and ^{31}P NMR results, which suggested that **2.71** is a square planar complex with a *trans-* arrangement. The Ni-N, Ni-O, and Ni-P bond distances of 1.88, 1.89, and 2.13 Å are a bit shorter than those observed for **2.5** (1.94, 1.91, and 2.17 Å, respectively). This is a bit surprising as PCy_3 has a significantly larger cone angle (170°) when compared to PPh_3 (145°), and appears to reflect the size of the Ni-aryl substituent in **2.5** as determined by the P-Ni-R angle (86.0(2)° for **2.5**, 77.0(6)° for **2.71**). Complex **2.71** is one of the few structurally characterized Ni^{II} complexes containing a terminal hydride.[37] The Ni-H bond length of 1.36(2) Å is in good agreement with the SHOP-type complex $\{Ph_2PCH_2C(CF_3)_2O\}$ $NiH(PCy_3)$ of 1.37(3) Å, demonstrating the similar nature of a d^8 hydride *trans* to an alkoxide or phenoxide.[34]

A similar synthetic procedure was employed for the synthesis of the *p*-NO_2-derivative **2.72** ($\delta = -28.702$, d, $^2J_{PH} = 128$ Hz), from the sodium salt of the nitrated ligand and **2.74**. However, during the synthesis of **2.72**, an additional species (**2.74**, present in ~ 5%) was observed as evidenced by a Ni-H signal at $\delta = 28.624$ (dd, $^2J_{PH} = 128$ Hz, $^2J_{PH} = 99$ Hz). The splitting pattern (doublet of doublets) of the hydride signal suggests that two phosphines are bound to the metal center in an asymmetric environment. This type of bonding arrangement rules out the square planar and

Figure 2.14. X-ray analysis of **2.71**. Thermal ellipsoids shown at 30% probability. All non-essential hydrogens have been omitted for clarity.

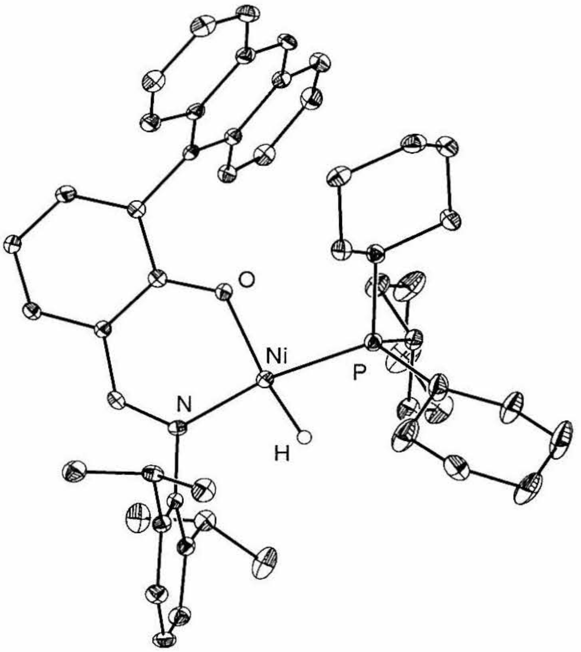

Table 2.13. Selected bond lengths (Å) and angles (°) for Ni^{II} complex **2.71**.

	Bond Lengths (Å)		
Ni-N	1.8861(14)	Ni-O	1.8983(11)
Ni-P	2.1339(5)	Ni-H	1.360(16)
	Bond Angles (°)		
N-Ni-O	95.15(5)	N-Ni-P	169.68(5)
N-Ni-H	92.9(6)	O-Ni-P	94.81(4)
O-Ni-H	171.2(6)	P-Ni-H	77.0(6)

symmetrical trigonal bipyramidal complexes shown in Figure 2.15. However, further evidence would be required to distinguish between the trigonal bipyramidal, square pyramidal, and square planar structures shown in Figure 2.15. Unfortunately, neither of these compounds could be isolated in analytical purity.

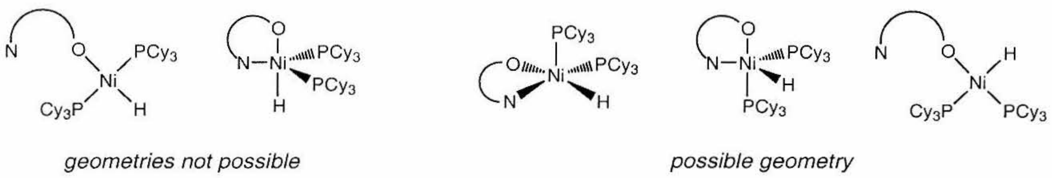

Figure 2.15. Possible structures for **2.74**.

The addition of 1.5 atm of ethylene to complex **2.71** in C_6D_6 at 65 °C leads to the observation of a decrease in ethylene concentration with no observable change in the ^1H NMR signals of complex **2.71** (Figure 2.13). Along with the consumption of ethylene came an increase in the ^1H NMR signals in the hydrocarbon region (~ 1 ppm), although the presence of PCy_3 in this region makes further analysis difficult. The lack of change in concentration of **2.71** suggests, as outlined above for experiments performed with **2.5**, that initiation efficiency is extremely low (< 1%) at ambient pressures and temperatures. There were no signs of other olefins, suggesting the formation of higher molecular weight polymer or chain termination by a mechanism other than β-hydride elimination. Unlike the trials performed with **2.5**, the system reached equilibrium (Figure 2.16), possibly suggesting that β-hydride elimination competes with ethylene insertion at this concentration (~ 1 eq.).

During the routine use of the hydride complex, **2.71**, it was observed that the Ni-H signal disappeared instantaneously upon exposure to the atmosphere. A new signal (δ = -9 ppm, bs, 1H) in the ^1H NMR spectrum appeared with the concomitant formation of $Cy_3P{=}O$, as evidenced by a signal at δ = 47.2 ppm in the ^{31}P NMR spectrum. Unusual IR signals were observed at 3341.0 (ν_{OH}), 2303.5, and 2197.0 cm^{-1}. Luckily, the material crystallized from both benzene and acetonitrile, allowing for its structural determination (Figure 2.17) as the bridging hydroxy complex **2.75**. The dimeric structure exhibits a

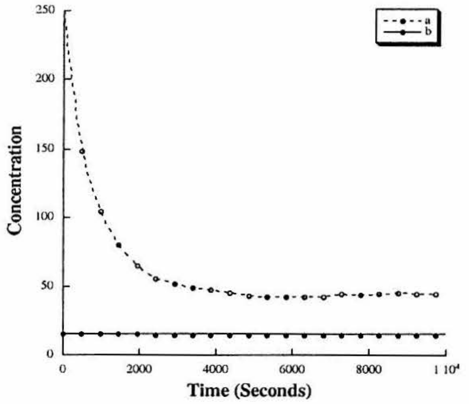

Fig. 2.16. Decrease in (a) ethylene concentration and (b) concentration of **2.71** vs. time. Equilibration suggests that insertion completes with β-hydride elimination at this concentration. No evidence for Ni-Et species was observed.

"puckered" N_2O_2 ring, in contrast to the neutral $[(Tp^{iPr2})Ni(\mu\text{-}OH)]_2$ and the cationic complex $\{(P^\wedge P)Ni(\mu\text{-}OH)\}_2[BF_4]_2$ in which the Ni_2O_2 core is almost planar.

It was believed that complex **2.75** arose from reaction of **2.71** with O_2 or H_2O. The addition of degassed water to a C_6D_6 solution of **2.71** led to the slow production of **2.75** over the span of ~ 3-4 hours. However, the introduction of ~ 1 eq.. of O_2 (*via* syringe) led to complete formation of **2.75** within 10 minutes at 25 °C. These observations suggested that the reaction occurs with O_2, and that the observation of **2.75** upon addition of H_2O might be due to O_2 contamination (*vide supra*). However, it should be noted that catalysts such as **2.5** do not exhibit long lifetimes in aqueous-based polymerizations.[4] It is also interesting to note that the cationic Ni^{II} diimine methyl adduct, $[(N,N)Ni(Me)(L)]B(Ar_f)_4$, reacts with water to produce a bridging hydroxide dimer by the liberation of methane.[38]

Figure 2.17. X-ray Analysis of **2.75.** Thermal ellipsoids shown at 30% probability. All nonessential hydrogen atoms have been omitted for clarity.

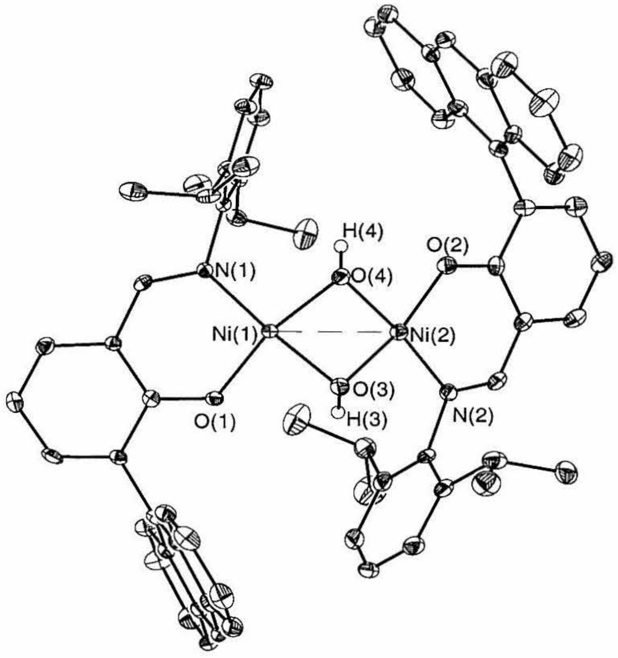

Table 2.14. Selected bond lengths (Å) and angles (°) for Ni^{II} complex **2.75**.

Bond Lengths (Å)

Ni(1)-N(1)	1.857(3)	Ni(1)-O(1)	1.835(2)
Ni(1)-O(3)	1.868(3)	Ni(1)-O(4)	1.867(3)
Ni(1)-Ni(2)	2.6966(7)	Ni(1)-H(3)	2.13(4)
O(3)-H(3)	0.77(3)	O(3)-O(4)	2.350(2)

Bond Angles (°)

N(1)-Ni(1)-O(1)	96.25(11)	N(1)-Ni(1)-O(4)	97.46(11)
N(1)-Ni(1)-O(3)	175.06(12)	Ni(1)-O(3)-Ni(2)	92.52(10)
Ni(1)-O(3)-H(3)	111(3)	O(3)-Ni(1)-O(4)	77.98(10)

For conclusive support that O_2 was the culprit, a 0.02 mM solution of **2.71** in toluene-d_8 was exposed to 1 atm of isotopically-labelled $^{18}O_2$. Upon exposure, the bright orange solution indicative of **2.71** rapidly darkened to a deep reddish-brown, followed by the precipitation of **2.75**. ^{1}H NMR spectroscopy clearly demonstrated that the hydride had been completely converted to **2.75**, as evidenced by loss of the "Ni-H" signal and appearance of the "Ni-OH" signal. IR analysis of the Ni-OH dimer indicated a ν_{OH} at 3341 cm^{-1} supporting evidence for the formation of Ni-^{18}OH. MS analysis of the $Cy_3P{=}O$ (Figure 2.18) shows that, indeed, that isotopically labeled $^{18}O_2$ was introduced as evidenced by the major species at *m/z* = 297.3 ($Cy_3P{=}O$ at 295.3). These results lead us to propose a mechanism (Figure 2.19) wherein **2.71** reacts with O_2 to yield an intermediate peroxy complex. This species rapidly liberates phosphine oxide and dimerizes to form **2.72**. The exact nature of this process (radical *vs.* insertion) is unknown, however, the addition of diazobenzene does not lead to any sign of insertion, possibly suggesting a radical pathway.

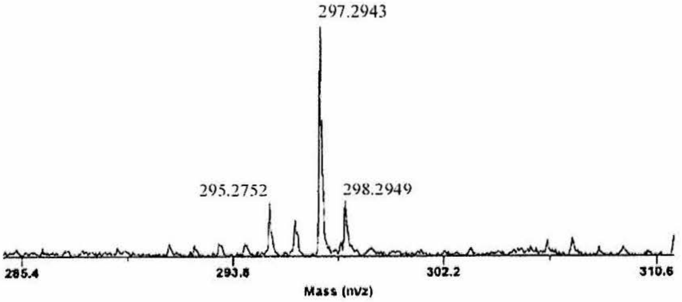

Figure 2.18. Hi-RES Mass Spec of $Cy_3P{=}^{18}O$ produced from reaction of **2.71** with $^{18}O_2$.

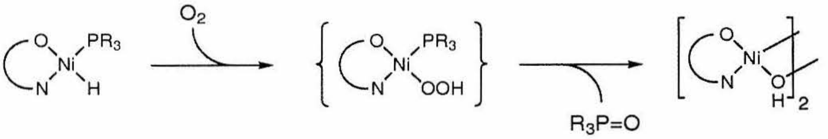

2.71

2.75

Figure 2.19. Postulated mechanism for formation of **2.75** from **2.71** with concomitant loss of phosphine oxide.

Attempts to polymerize ethylene by charging a glass bomb with **2.5** and reagent grade solvents under aerobic conditions do not allow for the production of polymer. In fact, the reaction of **2.5** with ~ 1 atm of ethylene followed by ~ 1 atm of O_2, leads to nearly quantitative formation of **2.75** over the course of 2 days. For these reasons, the exclusion of O_2 from polymerization trials with such neutral Ni^{II} catalysts is of utmost importance.

2.14. Conclusions

Neutral Ni^{II} salicylaldiminato complexes containing a variety of ligand sets have been developed. These complexes are active for the homopolymerization of ethylene at low to moderate pressures through "activation" with an electrophilic cocatalyst, such as $Ni(COD)_2$ or $B(C_6F_5)_3$. The resulting polymer is of low to moderate molecular weight (Mws ~ $2.0\text{-}70.0 \cdot 10^3$ g/mol) with a moderate degree of branching (~ 20-70 branches/ 1000 carbons). Bulky substituents in the *o*-position of the salicylaldiminato ring enhance the activity of the catalyst, increase molecular weights, and lower the number of branches in the resulting polyethylene. This phenomenon is supported by a model in which βHE and associative displacement of the polymer chain are reduced through an increase in the steric bulk of the ligand set. Electron-withdrawing groups in the *p*-position of the salicylaldiminato ring lead to considerable increases in the catalyst activity, although broad PDIs suggest that the reaction mixture contains a complex assortment of ill-defined active species, especially when the ligands contain NO_2 groups. The observed increases in activity probably reflect the reactivity of the putative active species as electron deficient systems, such as **2.14** and **2.15**, are expected to have a greatly increased electrophilic nature relative to their electron-rich analogs.

During single-component polymerizations (i.e., those without "cocatalyst"), a similar trend is observed for activity, such that increasing the steric demand of the ligand set leads to increases in activity, molecular weights, and very importantly, lifetime. However, the opposite trend is observed upon electronic modification, such that electron-withdrawing groups in the *p*-position of the ring yield catalysts with reduced relative activities. We believe that this observation reflects the decreased rate of phosphine dissociation, which has been determined through spectroscopic analysis to be the rate determining step.

The molecular weight of the PE obtained under single-component conditions is a product of the ligand employed during catalysis. As observed in other late-metal systems, increasing the steric demand of the ligand can lead to significant changes in the molecular weight, such that PE with an $M_w \sim 530 \cdot 10^3$ g/mol can be obtained with highly specialized ligand arrays. M_w and the branch content of the PE can be controlled through variation of both the temperature and pressure.

Neutral Pd^{II} salicylaldimine complexes do not exhibit the ability to form polymer due to a rapid β-hydride elimination followed by an irreversible reduction of the metal center.

The preparation of a Ni^{II} hydride species, **2.71**, allowed for similar observations to those obtained with **2.5**, namely that such complexes exhibit a low initiation (<1%) under ambient pressures and temperatures. These results clearly demonstrate that phosphine dissociation is the rate-determining step during polymerizations, and suggest that the active species is **2.76**. This hypothesis is additionally supported by their linear response to increased ethylene pressure over the range of 0 – 100 psig.

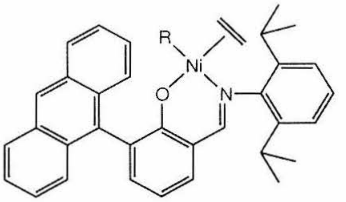

2.76

Surprisingly, the exposure of **2.71** to the atmosphere led to a rapid reaction which produced the bridging hyrdroxide complex **2.72**. Mechanistic studies have elucidated that the bridging hydroxide forms through reaction of **2.68** with O_2, leading to a proposed mechanism of formation which involves the formation of a Ni-peroxy species.

Table 2.15. Crystal Data and Structure Refinement for **2.5**, **2.48**, **2.68**, and **2.72**.

	2.5	**2.48**	**2.68**	**2.72**
Empirical Formula	$C_{71}H_{66}NNiOP$	$C_{51}H_{44}NOPPd\bullet C_6H_6$	$C_{51}H_{63}NOPNi\bullet 4(C_6H_6)$	$C_{66}H_{62}N_2Ni_2O_4\bullet \frac{1}{2}(N{\equiv}CCH_3)$
Formula Weight	1038.93	902.35	1108.14	1083.61
Crystallization Solvent	Toluene	C_6H_6/ pentane	C_6H_6/ CH_3CN	CH_3CN
Crystal Habit	Columnar	Square prism	Column	Square needle
Crystal Color	Yellow	Yellow	Orange	Reddish brown
Crystal Dimensions (mm^3)	0.48 x 0.10 x 0.07	148.00 x 0.39 x 0.15	0.31 x 0.19 x 0.19	0.44 x 0.07 x 0.05
Wavelength	0.71073 Å MoKα	0.71073 Å MoKα	0.71073 Å MoKα	0.71073 Å MoKα
Data Collection Temperature (K)	160(2)	98(2)	98(2)	98(2)
Unit Cell Dimensions (Å)	a=20.397(9) b=10.994(5) c=26.028(13)	a = 9.5473(5) b = 13.2077(7) c = 20.2788(10)	a = 10.2643(6) b = 23.5700(13) c = 26.2323(15)	a = 9.0540(9) b = 20.512(2) c = 29.299(3)
Unit Cell Dimensions (°)	β=107.85(4)	α= 73.9060(10) β= 87.2070(10) γ = 89.7660(10)	β= 99.6420(10)	β= 93.573(2)
Volume ($Å^3$)	5556(5)	2453.9(2)	6256.7(6)	5430.6(9)
Z	4	2	4	4
Crystal System	Monoclinic	Triclinic	Monoclinic	Monoclinic
Space Group	$P2_1/c$	P-1	$P2_1/n$	$P2_1/n$
Density(Calculated) Mg/m^3	1.242	1.221	1.176	1.325
Data/ Restraints/ Parameters	7234 / 0 / 731	11102 / 0 / 828	15058 / 0 / 1060	9567 / 0 / 931
Goodness-of-fit (GOF) on F^2	1.149	1.811	1.562	1.124
Final R Indices [I > 2σ(I)]	7234 reflections R1=0.0620 *w*R2=0.0896	9752 reflections R1=0.0301 *w*R2=0.0622	10020 reflections R1=0.0475 *w*R2=0.0664	5876 reflections R1=0.0466 *w*R2=0.0706
R Indices (All Data)	R1=0.1126 *w*R2=0.1067	R1=0.0356 *w*R2=0.0629	R1=0.0795 *w*R2=0.0690	R1=0.0886 *w*R2=0.0762

2.15. Acknowledgements

This work was sponsored by an ATP (Advanced Technology Program) between Caltech, W.R. Grace, and NIST. Additional funding was provided by the Cryovac division of the Sealed Air Corporation. NMR and GPC analysis were kindly provided by Galen Hatfield (W.R. Grace) and Jonathan J. Litzau (Cryovac). Larry Henling and Michael Day performed X-ray analysis of **2.5**, **2.48**, **2.68**, and **2.72** (twice). Mona Shahgholi assisted with the ^{18}O labelling experiment.

2.16. Experimental Section

General Considerations. The manipulations of all metal-containing complexes were performed using standard Schlenk techniques under an atmosphere of Argon or nitrogen. Argon, nitrogen, and ethylene were purified by passage through columns of BASF R3-11 catalyst (Chemalog) and 4 Å molecular sieves (Linde) or by passage through a Matheson 6410 oxygen scrubber. Solid organometallic compounds were transferred and stored in a nitrogen-filled glovebox (Vacuum atmospheres). All other reactions were performed under aerobic conditions unless otherwise stated. NMR spectra were recorded using either a JEOL 400 (^{1}H, 400 MHz; ^{19}F, 161.4 MHz; ^{31}P, 161.4 MHz; ^{13}C, 100.0 MHz), with chemical shifts referenced to internal solvent resonances and reported relative to tetramethylsilane. ^{31}P NMR data is referenced to external 85% H_3PO_4, where PPh_3 has a chemical shift of –5.4 ppm.

Materials. All organic materials were obtained from Aldrich Chemical Co. unless otherwise stated. Inorganic materials were purchased from the Strem Chemical Co. $Ni(PPh_3)_2PhCl$, $Ni(PCy_3)_2HCl$, and $Pd(PPh_3)_2PhBr$ were prepared using the appropriate literature procedures.

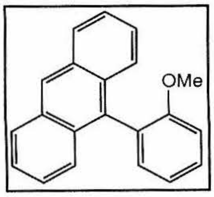

General Synthetic Methods.

Method A—Anthracenyl coupling *via* reaction of Grignard with Anthrone. Preparation of 9-(2-Methoxy-phenyl)-anthracene (2.51):

Synthesized in analogy to literature methods.[28,29] The crude product was recrystallized from CH_3CN, providing 60-80% of the desired product as pale yellow crystals. The melting point matched literature values (MP = 176-177 °C).[28,29] $C_{21}H_{16}O$ FW = 284.35. **^{1}H NMR** (CD_2Cl_2, 400.0 MHz): δ 4.531 (s, 3H), 7.01-7.07 (m, 2H), 7.154 (dd, 1H, $^3J_{HH}$ = 6.9 Hz, $^4J_{HH}$ = 2.1 Hz), 7.27-7.42 (m, 5H), 7.536 (dd, 2H, $^3J_{HH}$ = 8.7 Hz, $^4J_{HH}$ = 1.2 Hz), 7.976 (dd, 2H, $^3J_{HH}$ = 8.4 Hz, $^4J_{HH}$ = 0.6 Hz), 8.467 (s, 1H). **^{13}C NMR** (CD_2Cl_2, 75.4 MHz): δ 116.08, 121.13, 124.54, 125.91, 126.37, 125.67, 128.27, 128.99, 130.24, 130.45, 131.21, 132.02, 132.62, 154.29. **IR** (KBr pellet, cm^{-1}): 734.8, 755.9, 782.1, 794.0, 854.2, 903.8, 934.3, 1021.6, 1047.5, 1109.0, 1163.3, 1178.0, 1244.3, 1268.4, 1295.1, 1356.0, 1432.0, 1463.4, 1480.0, 1491.1, 1578.0, 1597.8, 2832.0, 2934.1, 3021.4, 3046.4. **EA** (Calcd./Found): C 88.70 (88.62), H 5.67 (5.66), N 0.00 (0.00).

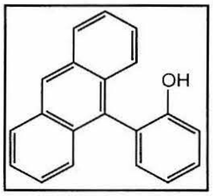

2-Anthracen-9-yl-phenol (2.52): The methyl ether (**2.51**) (17.7 g, FW = 284.36, 62.2 mmol) was dissolved in 50 mL of CH_2Cl_2 and cooled to –78 °C with an external dry ice/acetone bath, followed by the addition of BBr_3 (100 mL, 1.0 M, 100.0 mmol, 1.6 eq.). The reaction was warmed to room temperature, quenched by the addition of water, and concentrated by rotary evaporation under reduced pressure. Column chromatography with 80/20 hexanes/ethyl acetate as the eluant yielded 12.25 g (73 %) of the desired product. $C_{20}H_{14}O$, FW = 270.33. **^{1}H NMR** (CD_2Cl_2, 300.0 MHz): δ 4.531 (s, 1H), 7.01-7.07 (m, 2H), 7.154 (dd, 1H, $^3J_{HH}$ = 6.9 Hz, $^4J_{HH}$ = 2.1 Hz), 7.27-7.42 (m, 5H), 7.536 (dd, 2H, $^3J_{HH}$ = 8.7 Hz, $^4J_{HH}$ = 1.2 Hz), 7.976 (dd, 2H, $^3J_{HH}$ = 8.4 Hz, $^4J_{HH}$ = 0.6 Hz), 8.467 (s, 1H). **^{13}C NMR** (CD_2Cl_2, 75.4 MHz): δ 116.08, 121.13, 124.54, 125.91, 126.37, 125.67, 128.27, 128.99, 130.24, 130.45, 131.21, 132.02, 132.62, 154.29. **IR** (KBr pellet, cm^{-1}): 736.2, 803.5, 851.7, 897.5, 1031.5, 1175.6, 1204.9, 1284.0, 1338.5, 1359.4, 1441.4, 1459.4, 1470.5, 1490.2, 1568.7, 1614.3, 3048.8, 3472.0. **EA** (Calcd./Found): C 88.86 (88.29), H 5.22 (5.18), N 0.00 (0.00). **MP**: 186-187.5 °C.

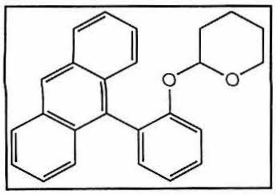

Method B—Protection of a phenol as O-THP ether: Preparation of 2-(2-Anthracen-9-yl-phenoxy)-tetrahydropyran: To a solution of the phenol (**2.52**) (9.97 g, FW = 270.32, 29.5 mmol) in 100 mL of CH_2Cl_2 was added 3,4-dihydro-2*H*-pyran (4 mL, FW = 84.12, δ = 0.922, 3.71 g, 44.1 mmol, 1.50 eq.) and a catalytic amount of PPTS (~ 10 mg). The mixture was stirred at room temperature for 3 days (monitored by TLC), washed twice with water (2x50 mL), and evaporated to yield 10.81 g (nearly quantitative) of the desired crude product. $C_{25}H_{22}O_2$, FW = 354.44. **^{1}H NMR** ($CDCl_3$, 300.0 MHz): δ 0.84-1.44 (m, 6H), 3.37-3.62 (m, 2H), 5.31 (m, 1H), 7.15-7.55 (m, 8H), 7.66 (d, 1H, $^3J_{HH}$ = 8.7 Hz), 7.75 (d, 1H, $^3J_{HH}$ = 9.0 Hz), 8.03 (d, 2H, $^3J_{HH}$ = Hz), 8.48 (s, 1H). **^{13}C NMR** ($CDCl_3$, 75.4 MHz): δ 17.7, 24.9, 30.0, 61.6, 61.9, 96.1, 96.4, 115.3, 115.8, 121.4, 121.7, 124.7, 125.2, 126.0, 126.6, 127.1, 127.5, 127.8, 128.2, 128.6, 129.0, 130.2, 131.3, 132.5, 132.9, 133.9, 155.4. **EA** (Calcd./Found): C 84.72 (84.60), H 6.26 (6.09), N 0.00 (0.00).

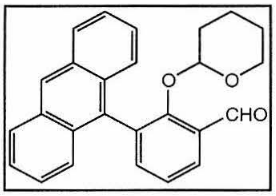

Method C—Formylation of O-THP-ethers: Synthesis of 3-Anthracen- 9- yl- 2-(tetrahydro-pyran- 2-yloxy)-benzaldehyde: To a solution of the aforementioned THP-protected ether (10.81 g, FW = 354.44, 30.5 mmol) in 250 mL of anhydrous Et_2O, cooled with an external ice bath, was added 38 mL of 1.6N ^{n}BuLi (in hexanes). A precipitate formed rapidly. The cooling bath was removed and the mixture was stirred at room temperature for 2.5 hours, at which point DMF (6 mL, FW = 73.10, δ = 0.944, 77.4 mmol, 2.5 eq.) was slowly added. After an additional 16 hours at room temperature, the reaction was quenched by the addition of water. Extraction and concentration of the organic phase led to isolation of 11.50 g (98%) of the desired product. $C_{26}H_{22}O_3$, FW = 382.45. **^{1}H NMR** ($CDCl_3$, 300.0 MHz): δ 0.56-1.27 (m, 6H), 2.87 (m, 1H), 3.43 (m, 1H), 4.26 (m, 1H), 7.38-7.50 (m, 5H), 7.57-7.61 (m, 2H), 7.69 (dd, 1H, $^3J_{HH}$ = 7.8 Hz, $^4J_{HH}$ = 1.2 Hz), 8.03-09 (m, 3H), 8.54 (s, 1H), 10.62 (s, 1H). **^{13}C NMR** ($CDCl_3$, 75.4 MHz): δ 19.5, 24.6, 29.9, 64.2, 102.4, 124.6, 125.5, 126.1, 126.2, 126.5, 127.6, 128.0, 128.7, 130.0, 130.8, 131.2, 131.3, 131.9, 132.9, 139.5, 159.0, 191.8. **EA** (Calcd./Found): C 81.65 (81.21), H 5.80 (5.96), N 0.00 (0.00).

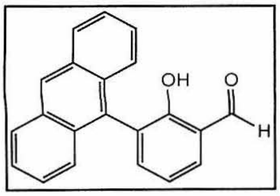

Method D—Formation of substituted salicylaldehydes: Synthesis of 3-Anthracen-9-yl-2-hydroxy-benzaldehyde (2.53):

The protected aldehyde (12.0 g, FW = 382.45, 31.4 mmol) was dissolved in 100 mL of MeOH and 50 mL THF. A catalytic amount of PPTS (~ 20 mg) was added, and the solution was refluxed for 16 hours. The solution was concentrated by rotary evaporation under reduced pressure and the residue was washed with cold acetone to yield the desired product as a yellow solid 3.0 g (34%) (Higher yields can be obtained by column chromatography). $C_{21}H_{14}O_2$, FW = 298.33. **^{1}H NMR** ($CDCl_3$, 300.0 MHz): δ 7.25 (t, 1H, $^3J_{HH}$ = 7.8 Hz), 7.37-7.51 (m, 4H), 7.60-7.62 (m, 3H), 7.77 (dd, 1H, $^3J_{HH}$ = Hz, $^4J_{HH}$ = Hz), 8.08 (d, 2H, $^3J_{HH}$ = Hz), 8.56 (s, 1H), 10.05 (s, 1H), 11.22 (s, 1H). **^{13}C NMR** ($CDCl_3$, 75.4 MHz): δ 120.02, 120.95, 125.28, 125.91, 126.11, 127.52, 127.60, 128.77, 130.35, 130.82, 131.49, 134.02, 140.36, 159.88, 196.86. **EA** (Calcd./Found): C 84.55 (84.12), H 4.73 (4.77), N 0.00 (0.00).

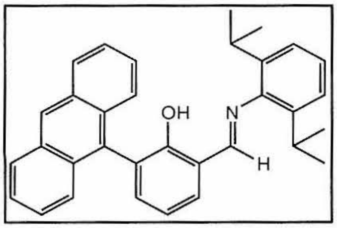

Method E—Condensation to yield salicylaldimines: Preparation of 2-Anthracen-9-yl-6-[(2,6-diisopropyl-phenylimino)-methyl]-phenol (2.50): To a slurry of **2.53** (2.0 g, FW = 298.33, 6.70 mmol) in 25 mL of MeOH was added 2,6-diisopropylaniline (1.50 mL, FW = 177.29, d = 0.939, 1.41 g, 7.95 mmol, 1.18 eq.) and a catalytic amount of formic acid (~ 7 drops). The mixture was stirred at room temperature for 4.5 hours, with precipitation of the product as a yellow powder. The precipitate was collected by filtration, washed with 30 mL of cold MeOH, and dried *in vacuo* to give 2.55 g (83%) of the desired product. $C_{33}H_{31}NO$, FW = 457.61. **^{1}H NMR** ($CDCl_3$, 300.0 MHz): δ 1.23 (d, 12H, $^3J_{HH}$ = 6.9 Hz), 3.09 (sept, 2H, $^3J_{HH}$ = 6.9 Hz), 7.23 (bs, 3H), 7.41-7.52 (m, 6H), 7.61 (dd, 1H, $^3J_{HH}$ = 9.0 Hz, $^4J_{HH}$ = 1.6 Hz), 7.84 (d, 2H, $^3J_{HH}$ = 8.7 Hz), 8.12 (d, 2H, $^3J_{HH}$ = 8.1Hz), 8.52 (s, 1H), 8.59 (s, 1H), 13.33 (s, 1H). **^{13}C NMR** ($CDCl_3$, 75.4 MHz): δ 23.81, 23.21, 118.99, 119.07, 123.41, 125.23, 125.62, 125.69, 126.69, 127.04, 127.30, 128.47, 128.77, 130.47, 131.64, 132.36, 132.46, 136.81, 138.94, 146.26, 159.63, 166.85. **EA** (Calcd./Found): C 86.61 (86.48), H 6.83 (6.95), N 3.06 (3.16).

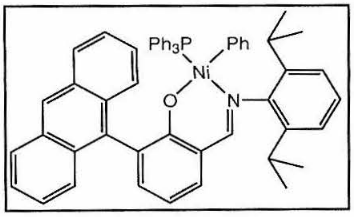

Method F—Synthesis of (Sal)Ni(PPh$_3$)Ph Complexes: Preparation of (^{Anthr,H}Sal)Ni(PPh$_3$)Ph (2.5): A 50 mL

Schlenk flask was charged with ^{Anthr,H}Sal ligand (500 mg, FW = 457.61, 1.1 mmol) and excess NaH (131 mg, FW = 24.01, 5.5 mmol, 5.0 eq..), followed by evacuation of the flask and addition of an Argon atmosphere. Anhydrous THF (10 mL) was transferred by cannula to the Schlenk flask, at which time, intense bubbling was observed as H_2 was released. After one hour of stirring at room temperature, the solution was filtered through a celite plug (to remove unwanted NaH) to a second Schlenk flask, where the THF was removed under reduced pressure, providing the sodium salt as a pale yellow solid. The salt was dissolved in 10 mL of anhydrous benzene, and transferred *via* cannula to a flask containing $Ni(PPh_3)_2PhCl$ (758 mg, FW = 695.85, 1.1 mmol, 1.0 eq..). The solution was allowed to react at room temperature for 1.5 hours, at which time, it was filtered through a celite plug (to remove NaCl) to a second flask and concentrated to ~ 1.5 mL. The deep reddish-brown benzene solution was layered with excess pentane and stored in the freezer (5 °C) overnight. Yellow crystals formed, which were isolated by removal of the supernatant *via* cannula filtration, followed by several pentane washes (3 x 20 mL) to provide 783 mg g (84%) of **2.5**. $C_{57}H_{50}NNiOP$, FW 854.71. **^{1}H NMR** (C_6D_6, 400 MHz): δ1.14 (d, 6H, $^3J_{HH}$ = 6.6 Hz), 1.18 (d, 6H, $^3J_{HH}$ = 6.6 Hz), 4.17 (sept., 2H, $^3J_{HH}$ = 6.6 Hz), 6.19 (t, 2H, $^3J_{HH}$ = 7.3 Hz), 6.29 (t, 1H, $^3J_{HH}$ = 7.3 Hz), 6.58-6.63 (m, 6H), 6.73-6.78 (m, 3H), 6.82 (d, 1H, $^3J_{HH}$ = 6.9 Hz), 6.88 (d, 1H, $^3J_{HH}$ = 8.0 Hz), 6.89 (s, 1H), 6.95-7.21 (m, 15H), 7.61 (d, 2H, $^3J_{HH}$ = 8.4 Hz), 7.82 (d, 2H, $^3J_{HH}$ = 8.08 Hz), 7.83 (s, 1H), 8.15 (d, 1H, $^4J_{PH}$ = 11.3 Hz). **^{13}C NMR** (C_6D_6, 75.4 MHz): δ 22.6, 25.6, 28.9, 114.2, 119.9, 121.2, 122.8, 124.5, 124.7, 124.9, 125.8 (d, $^1J_{PC}$ = 34.3 Hz), 127.3 (d, $^3J_{PC}$ = 9.8 Hz), 128.4, 129.0 (d, $^4J_{PC}$ = 1.6 Hz), 130.6, 130.8, 131.5, 131.8, 133.5 (d, $^2J_{PC}$ = 10.1 Hz), 134.7, 136.6, 137.4, 138.3, 140.7, 145.2, 146.4, 150.1, 165.2, 166.7. **^{31}P NMR** (C_6D_6, 161.9 MHz): δ 22.7 (s). **EA** (Calcd./Found): C 80.10 (79.77), H 5.90 (6.09), N 1.64 (1.49).

Crystal Structure of Complex 2.5 (^{Anthr,H}Sal)Ni(PPh$_3$)Ph (Appendix A)—Crystals suitable for X-ray structure determination were grown from a solution of **2.5** in toluene at –20 °C over a few days. The yellow crystal used for data collection had dimensions 0.48 × 0.10 × 0.07 mm. The X-ray diffraction data were collected by using a CAD-4 diffractometer with graphite-monochromated Mo Kα radiation. Unit cell parameters were determined by a least-squares analysis of 25 automatically centered reflections in the range 8.6° < θ< 10.9°. Data were collected at 160 K in the range θ= 1.6-22.5°. A total of 16 164 reflections were collected, 7238 of which were independent. A set of 4691 reflections with $F_o^2 > 2\sigma(F_o^2)$ were observed. The structure was solved by direct methods using the SHELXS-86 program. Hydrogen atoms appeared in the difference Fourier map. They were restrained to these positions during refinement, and their U_{iso} values were fixed at 1.1 times the $U_{eq.}$ value of the attached atom. Refinement was full-matrix least squares on F^2 using SHELXL-93.

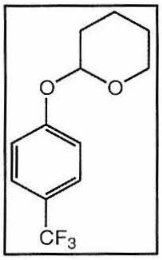

2-(4-Trifluoromethyl-phenoxy)-tetrahydro-pyran (2.15): Using method A with α,α,α-trifluoro-p-cresol (5.07 g, FW = 162.11, 31.2 mmol), 30 mL of CH_2Cl_2, 3,4-dihydro-2*H*-pyran (2.92 g, FW = 84.12, d = 0.922, 34.7 mmol, 1.1 eq..), and a catalytic amount of PPTS. The desired product was purified by passage through a plug of silica (using 90/10 Hexanes/Ethyl acetate) to remove any unreacted phenol, yielding 7.31 g (95%) of the product as a white solid. $C_{12}H_{13}F_3O_2$, FW = 246.23. **TLC** (R_f product ~ 0.95 in 90 Hex/10 EA). **^{1}H NMR** (CD_2Cl_2, 400.0 MHz): δ 1.58-2.05 (m, 6H), 5.50 (t, 1H, $^3J_{HH}$ = 3.3 Hz) ,7.159 (d, 2H, $^3J_{HH}$ = 8.8 Hz), 7.570 (d, 2H, $^3J_{HH}$ = 8.8 Hz). **^{13}C NMR** (CD_2Cl_2, 75.4 MHz): δ 19.05, 25.52, 30.60, 62.49, 96.82, 116.85, 123.68 (q, $^2J_{CF}$ = 32.6 Hz), 125.08 (q, $^1J_{CF}$ = 270.8 Hz), 127.13 (q, $^3J_{CF}$ = 3.8 Hz), 160.29. **^{19}F NMR** (CD_2Cl_2, 161.4 MHz): δ –62.9 (s). **EA** (Calcd./Found): C 58.54 (58.03), H 5.32 (5.30), N 0.00 (0.00).

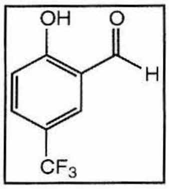

2-Hydroxy-5-trifluoromethyl-benzaldehyde (2.16): Sequential use of method B and C using **2.15** (5.0 g, FW = 246.23, 20.3 mmol), 40 mL of THF, 1.25 eq.. of ^{n}BuLi, and 1.25 eq.. of anhydrous DMF provided 3.86 g of the desired product (72%). ***Alternative synthesis:*** To a solution of α,α,α-trifluorocresol (7.1 g, FW = 162.11, 43.8 mmol) and 2,6-lutidine (1.9 g, FW = 107.16, 17.6 mmol, 0.4 eq..) in toluene (80 mL) was slowly added $SnCl_4$ (1.2 g, FW = , 44.0 mmol, 1.0 eq..). The reaction stirred at room temperature for 20 minutes, at which time, paraformaldehyde (3.2 g, FW ~ 30, 106.0 mmol, 2.41 eq..) was added. The reaction was heated to 110 °C and stirred at that temperature for 12 hours. Upon cooling to ambient temperature, the reaction mixture was poured into water (250 mL), and acidified to pH ~ 1 by the addition of concentrated HCl. The mixture was then extracted with diethyl ether (500 mL), the organic layer was washed twice with brine, and dried over Na_2SO_4. The solvent was removed by rotary evaporation to leave a yellow oil. The oil was loaded onto a silica gel column and eluted with hexanes: ethyl acetate (6:1) to provide 1.0 g (12%) of the desired product as a white powder. $C_8H_5F_3O_2$, FW = 190.12. **^{1}H NMR** (C_6D_6, 400.0 MHz): δ 7.21-7.91 (m, 12H), 9.91 (s, 1H), 11.32 (s, 1H). **EA** (Calcd./Found): C 50.54 (50.65), H 2.65 (2.64), N 0.00 (0.00).

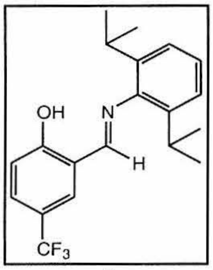

2-[(2,6-Diisopropyl-phenylimino)-methyl]-4-trifluoromethyl-phenol (2.17): Using method D with **2.16** (0.80 g, FW = 190.12, 4.0 mmol), 2,6-diisopropylaniline (0.80 g, FW = 177.29, 4.5 mmol, 1.13 eq..), methanol (10 mL), and formic acid (~0.1 mL) provided 1.25 g (85%) of the desired product. $C_{20}H_{22}F_3NO$, FW = 349.39. **^{1}H NMR** (C_6D_6, 400.0 MHz): δ 1.24 (d, 12H, $^3J_{HH}$ = 6.9 Hz), 2.99 (sept., 2H, $^3J_{HH}$ = 6.9 Hz), 7.21-7.68 (m, 7H), 8.41 (s, 1H), 13.72 (s, 1H). **^{13}C NMR** (C_6D_6, 75.4 MHz): δ 23.6, 28.4, 118.2, 121.5, 122.8, 123.5, 125.5, 129.5, 138.7, 145.5, 163.99, 165.8. **EA** (Calcd./Found): C 68.75 (68.77), H 6.35 (6.41), N 6.35 (3.92).

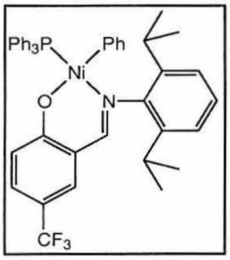

(^{H,CF3}Sal)Ni(PPh3)Ph (2.12): Using method E with **2.17** (0.45 g, FW = 349.39, 1.25 mmol), excess NaH (150 mg, FW = 24.01, 6.25 mmol, 5.0 eq..), and THF (10 mL); followed by anhydrous benzene (15 mL) and $Ni(PPh_3)_2PhCl$ (0.86 g, FW = 695.85, 1.25 mmol) provided 0.68 g (74%) of the desired product after several pentane washes. $C_{44}H_{41}F_3NNiOP$, FW = 746.46. **^{1}H NMR** (C_6D_6, 400.0 MHz): δ 0.95 (d, 6H, $^3J_{HH}$ = 6.9 Hz), 1.24 (d, 6H, $^3J_{HH}$ = 6.9 Hz), 3.94 (sept., 2H, $^3J_{HH}$ = 6.9 Hz), 6.19 (d, 1H, $^3J_{HH}$ = 8.8 Hz), 6.29 (t, 1H, $^3J_{HH}$ = 7.4 Hz), 6.36 (t, 1H, $^3J_{HH}$ = 7.3 Hz), 6.98-7.68 (m, 21H). **^{13}C NMR** (C_6D_6, 75.4 MHz): δ 22.2, 25.5, 28.7, 118.4, 121.4, 122.4, 122.6, 123.3, 125.2, 126.1, 128.0, 128.3, 129.9, 130.4, 130.9, 131.7, 134.2, 137.5, 140.1, 149.0, 165.8, 170.5. **EA** (Calcd./Found): C 77.14 (76.92), H 8.09 (8.07), N 4.50 (4.52).

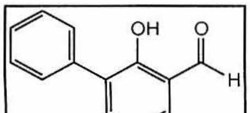

2-Hydroxy-5-nitro-biphenyl-3-carbaldehyde (2.26): $C_{13}H_9NO_4$, FW = 243.21. **^{1}H NMR** ($CDCl_3$, 400.0 MHz): δ 7.42-7.52 (m, 3H), 7.606 (d, 2H, $^3J_{HH}$ = 8.4 Hz), 8.495 (d, 1H, $^4J_{HH}$ = 4.2 Hz), 8.543 (d, 1H, $^4J_{HH}$ = 4.2 Hz), 10.044 (s, 1H), 12.168 (s, 1H). **^{13}C NMR** ($CDCl_3$, 75.0 MHz): δ 119.75, 128.65, 128.71, 128.92, 129.25, 131.84, 132.24, 134.06, 140.56, 163.61, 196.07. **EA** (Calcd./Found): C 64.20 (64.81), H 3.73 (3.92), N 5.76 (5.82).

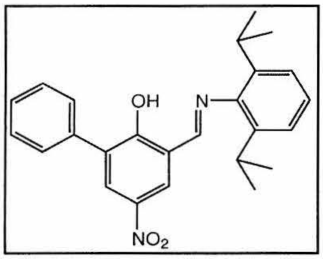

3- [(2,6- Diisopropyl- phenylimino) - methyl] – 5 - nitro-biphenyl -2-ol: $C_{25}H_{26}N_2O_3$, FW = 402.49. **^{1}H NMR** ($CDCl_3$, 400.0 MHz): δ 1.193 (d, 12H, $^3J_{HH}$ = 7.0 Hz), 2.953 (sept., 2H, $^3J_{HH}$ = 7.0 Hz), 7.228 (bs, 3H), 7.41-7.46 (m, 1H), 7.508 (t, 2H, $^3J_{HH}$ = 7.0 Hz), 7.716 (dd, 2H, $^3J_{HH}$ = 7.0 Hz, $^4J_{HH}$ = 1.5 Hz), 8.332 (d, 1H, $^4J_{HH}$ = 3.0 Hz), 8.421 (d, 1H, $^4J_{HH}$ = 3.0 Hz), 8.433 (s, 1H), 14.850 (s, 1H). **^{13}C NMR** ($CDCl_3$, 75.0 MHz): δ 23.71, 28.37, 117.71, 123.61, 126.59, 127.49, 128.52, 128.62, 128.93, 129.40, 131.66, 135.30, 138.96, 139.78, 144.26, 164.93, 165.91. **EA** (Calcd./Found): C 74.60 (74.38), H 6.51 (6.62), N 6.96 (6.72).

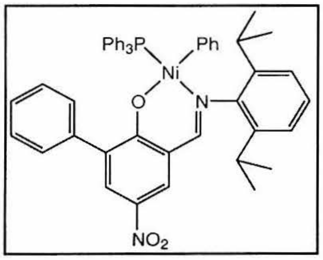

(^{Ph,NO2}Sal)Ni(PPh$_3$)Ph (2.30): $C_{49}H_{45}N_2NiO_3P$, FW = 799.58. **^{1}H NMR** (C_6D_6, 400.0 MHz): δ 1.07 (d, 6H, $^3J_{HH}$ = 7.0 Hz), 1.15 (d, 6H, $^3J_{HH}$ = 7.0 Hz), 3.96 (sept., 2H, $^3J_{HH}$ = 7.0 Hz), 6.15 (t, 2H, $^3J_{HH}$ = 7.3 Hz), 6.28 (t, 1H, $^3J_{HH}$ = 7.3 Hz), 6.60 (t, 2H, $^3J_{HH}$ = 7.3 Hz), 6.68-6.75 (m, 6H), 6.82-6.86 (m, 8H), 6.91-6.98 (m, 6H), 7.44 (t, 6H, $^3J_{HH}$ = 8.0 Hz), 7.64 (d, 1H, $^4J_{PH}$ = 11.0 Hz), 8.03 (d, 1H, $^4J_{HH}$ = 3.0 Hz), 8.28 (d, 1H, $^4J_{HH}$ = 3.0 Hz). **^{13}C NMR** (C_6D_6, 75.0 MHz): δ 22.5, 23.4, 28.9, 107.4, 118.6, 121.5, 122.8, 125.2 (d, $^4J_{PC}$ = 1.9 Hz), 126.3 (d, $^3J_{PC}$ = 7.1 Hz), 128.3, 128.5, 128.7, 129.3, 130.8 (d, $^1J_{PC}$ = 44.4 Hz), 130.9, 134.0 (d, $^2J_{PC}$ = 10.1 Hz), 134.7, 136.1, 136.2, 136.3, 137.6, 140.0, 144.2, 148.9, 166.1, 167.7. **^{31}P NMR** (C_6D_6, 161.9 MHz): δ 21.8 (s). **EA** (Calcd./Found): C 73.61 (73.80), H 5.67 (5.78), N 3.50 (3.39).

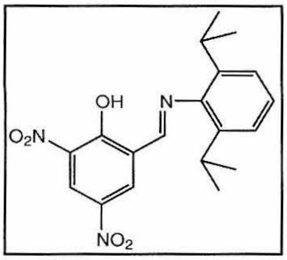

2-[(2,6-Diisopropyl-phenylimino)-methyl]-4,6-dinitro-phenol: $C_{19}H_{21}N_3O_5$, FW = 371.39. **^{1}H NMR** (C_6D_6, 400.0 MHz): δ 1.24 (d, 12H, $^3J_{HH}$ = 6.9 Hz), 2.96 (sept., 2H, $^3J_{HH}$ = 6.9 Hz), 7.25-7.43 (m, 3H), 8.32 (bs, 1H), 8.53 (d, 1H, $^4J_{HH}$ = 3.0 Hz), 9.04 (d, 1H, $^4J_{HH}$ = 3.0 Hz), 16.30 (bs, 1H). **^{13}C NMR** ($CDCl_3$, 75.0 MHz): δ 23.8, 28.8, 107.4, 117.6, 124.4, 128.0, 129.7, 134.3, 134.9, 139.9, 141.7, 166.6, 168.6. **EA** (Calcd./Found): C 61.45 (61.20), H 5.70 (5.79), N 11.31 (11.31).

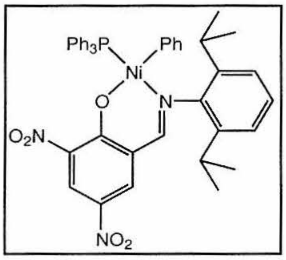

(^{NO2,NO2}Sal)Ni(PPh$_3$)Ph (2.14): $C_{43}H_{40}N_3NiO_5P$, FW = 768.48. **^{1}H NMR** (C_6D_6, 400.0 MHz): δ 0.98 (d, 6H, $^3J_{HH}$ = 7.0 Hz), 1.16 (d, 6H, $^3J_{HH}$ = 7.0 Hz), 3.83 (sept., 2H, $^3J_{HH}$ = 7.0 Hz), 6.23 (t, 2H, $^3J_{HH}$ = 7.3 Hz), 6.35 (t, 1H, $^3J_{HH}$ = 7.3 Hz), 6.80 (t, 2H, $^3J_{HH}$ = 7.3 Hz), 6.83 (d, 2H, $^3J_{HH}$ = 7.3 Hz), 6.92 (t, 1H, $^3J_{HH}$ = 7.3 Hz), 6.98-7.08 (m, 12H), 7.38 (d, 1H, $^4J_{PH}$ = 7.0 Hz), 7.50-7.55 (m, H), 7.71 (d, 1H, $^4J_{HH}$ = 3.0 Hz), 8.22 (d, 1H, $^4J_{HH}$ = 3.0 Hz). **^{13}C NMR** ($CDCl_3$, 75.0 MHz): δ 22.5, 25.9, 29.0, 107.4, 121.9, 122.5, 123.0, 125.3 (d, $^1J_{PC}$ = 37.4 Hz), 125.5, 126.8, 128.1 (d, $^3J_{PC}$ = 10.2 Hz), 129.4, 130.3, 133.1, 134.0, 134.1 (d, $^2J_{PC}$ = 10.2 Hz), 136.8 (d, $^4J_{PC}$ = 2.3 Hz), 139.6, 141.9, 142.5, 143.2, 148.2, 162.1, 164.6. **^{31}P NMR** (C_6D_6, 161.9 MHz): δ 24.3 (s). **EA** (Calcd./Found): C 67.21 (67.07), H 5.25 (5.39), N 5.47 (5.31).

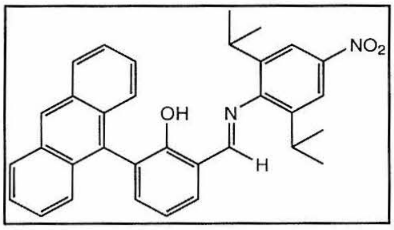

2-Anthracen-9-yl-6-[(2,6-diisopropyl-4-nitro-phenylimino)-methyl]-phenol: $C_{33}H_{30}N_2O_3$, FW = 502.60. **^{1}H NMR** ($CDCl_3$, 300.0 MHz): δ 1.18 (d, 12H, $^3J_{HH}$ = 6.6 Hz), 3.03 (sept., 2H, $^3J_{HH}$ = 6.6 Hz), 7.22 (t, 1H, $^3J_{HH}$ = 7.2 Hz), 7.37-7.57 (m, 6H), 7.72 (d, 2H, $^3J_{HH}$ = 8.7 Hz), 8.03 (s, 2H), 8.06 (d, 2H, $^3J_{HH}$ = 8.7 Hz), 8.42 (s, 1H), 8.53 (s, 1H), 12.48 (s, 1H). **^{13}C NMR** ($CDCl_3$, 75.4 MHz): δ 23.22, 28.38, 118.36, 119.16, 119.42, 125.10, 125.63, 126.30, 127.24, 127.31, 128.67, 130.27, 131.46, 131.66, 132.79, 132.86, 137.64, 140.61, 145.61, 159.33, 166.91. **EA** (Calcd./Found): C 78.86 (78.59), H 6.02 (6.11), N 5.57 (5.29).

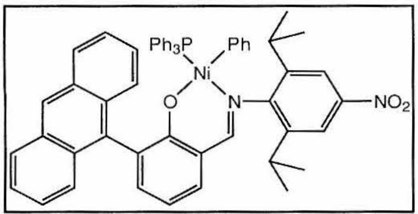

(^{Anthr,H}Sal^{NO2})Ni(PPh$_3$)Ph (2.33): $C_{57}H_{49}N_2NiO_3P$, FW = 899.71. **^{1}H NMR** (C_6D_6, 400.0 MHz): δ 0.94 (d, 6H, $^3J_{HH}$ = 7.0 Hz), 1.06 (d, 6H, $^3J_{HH}$ = 7.0 Hz), 4.06 (sept., 2H, $^3J_{HH}$ = 7.0 Hz), 6.04 (t, 2H, $^3J_{HH}$ = 7.3 Hz), 6.16 (t, 1H, $^3J_{HH}$ = 7.3 Hz), 6.55-6.61 (m, 6H), 6.62 (t, 2H, $^3J_{HH}$ = 7.3 Hz), 6.68 (d, 1H, $^3J_{HH}$ = 8.0 Hz), 6.71-6.77 (m, 3H), 6.96-7.15 (m, 15H), 7.60 (d, 2H, $^3J_{HH}$ = 8.4 Hz), 7.75 (d, 2H, $^3J_{PH}$ = 8.8 Hz), 7.81 (s, 1H), 7.92 (s, 2H), 7.93 (d, 1H, $^3J_{HH}$ = 8.4 Hz). **^{13}C NMR** (CD_2Cl_2, 75.4 MHz): δ 22.4, 25.5, 29.4, 114.2, 118.7, 119.5, 121.4, 124.8, 125.0, 125.3, 125.8, 127.5 (d, $^3J_{PC}$ = 9.8 Hz), 127.7, 128.4, 129.3, 130.3, 130.6, 130.9, 131.6, 133.5 (d, $^2J_{PC}$ = 10.1 Hz), 135.0, 136.1, 137.4 (d, $^4J_{PC}$ = 1.4 Hz), 138.7, 143.3, 145.5 (d, $^1J_{PC}$ = 50.5 Hz), 146.1, 156.0, 165.5, 166.1. **^{31}P NMR** (C_6D_6, 161.9 MHz): δ 23.30 (s). **EA** (Calcd./Found): C 76.10 (75.97), H 5.49 (5.42), N 3.11 (3.18).

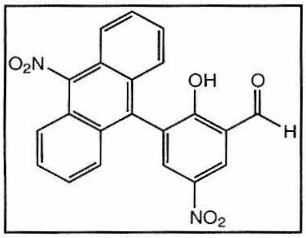

2-Hydroxy- 5-nitro- 3- (10- nitro- anthracen- 9- yl) – benzaldehyde: $C_{21}H_{12}N_2O_6$, FW = 388.34. **^{1}H NMR** ($CDCl_3$, 300.0 MHz): δ 7.25-7.70 (m, 6H), 7.96-8.05 (m, 2H), 8.48 (d, 1H, $^4J_{HH}$ = 2.1 Hz), 8.82 (d, 1H, $^4J_{HH}$ = 2.1 Hz), 10.17 (s, 1H), 11.82 (s, 1H). **^{13}C NMR** ($CDCl_3$, 75.4 MHz): δ 119.8, 121.8, 122.0, 125.5, 127.3, 128.0, 128.7, 129.6, 130.0, 131.9, 134.0, 140.6, 145.6, 164.1, 195.5. **EA** (Calcd./Found): C 64.95 (64.64), H 3.11 (3.58), N 7.21 (6.57).

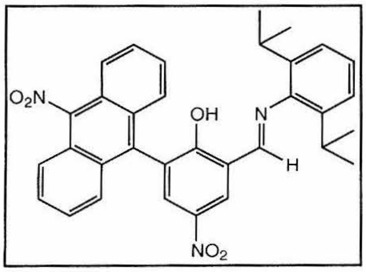

2-[(2,6-Diisopropyl-phenylimino)-methyl]-4-nitro-6-(10-nitro-anthracen-9-yl)-phenol: $C_{33}H_{29}N_3O_5$, FW = 547.62. **^{1}H NMR** ($CDCl_3$, 300.0 MHz): δ 1.19 (d, 12H, $^3J_{HH}$ = 6.9 Hz), 2.95 (sept., 2H, $^3J_{HH}$ = 6.9 Hz), 7.22 (bs, 3H), 7.55 (t, 2H, $^3J_{HH}$ = 7.8 Hz), 7.69 (t, 2H, $^3J_{HH}$ = 8.4 Hz), 7.76 (d, 2H, $^3J_{HH}$ = 8.7 Hz), 7.99 (d, 2H, $^3J_{HH}$ = 8.7 Hz), 8.40 (d, 1H, $^4J_{HH}$ = 2.7 Hz), 8.57 (s, 1H), 8.62 (d, 1H, $^4J_{HH}$ = 2.7 Hz), 14.86 (s, 1H). **^{13}C NMR** ($CDCl_3$, 75.4 MHz): δ 23.7, 28.4, 107.4, 117.8, 121.9, 122.3, 123.7, 126.2, 126.9, 127.1, 127.5, 128.8, 129.0, 129.9, 131.2, 133.8, 139.0, 139.7, 143.7, 165.5, 166.0. **EA** (Calcd./Found): C 72.38 (72.12), H 5.34 (5.05), N 7.67 (7.30).

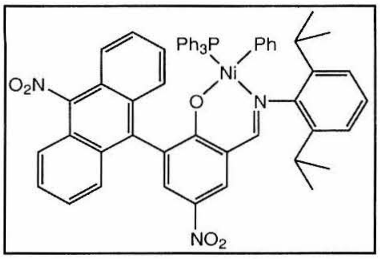

($^{10\text{-NO2-Anthr,NO2}}$Sal)Ni(PPh$_3$)Ph (2.32): $C_{57}H_{48}N_3NiO_5P$, FW = 944.70. **^{1}H NMR** (C_6D_6, 400.0 MHz): δ 1.07 (d, 6H, $^3J_{HH}$ = 7.0 Hz), 1.13 (d, 6H, $^3J_{HH}$ = 7.0 Hz), 4.03 (sept., 2H, $^3J_{HH}$ = 7.0 Hz), 6.11 (t, 2H, $^3J_{HH}$ = 7.6 Hz), 6.22 (t, 1H, $^3J_{HH}$ = 7.3 Hz), 6.61 (m, 6H), 6.69 (d, 2H, $^3J_{HH}$ = 7.3 Hz), 6.71-6.75 (m, 3H), 6.80-6.84 (m, 4H), 6.91-7.05 (m, 9H), 7.39 (d, 2H, $^3J_{HH}$ = 8.8 Hz), 7.64 (d, 2H, $^3J_{HH}$ = 8.8 Hz), 7.82 (d, 1H, $^4J_{PH}$ = 8.4 Hz), 7.93 (d, 1H, $^4J_{HH}$ = 3.2 Hz), 8.32 (d, 1H, $^4J_{HH}$ = 3.2 Hz). **^{13}C NMR** (C_6D_6, 75.4 MHz): δ 22.4, 25.4, 29.0, 102.6, 119.0, 121.3, 121.6, 122.0, 122.9, 125.2 (d, $^3J_{PC}$ = 1.7 Hz), 125.7, 126.4, 127.1 (d, $^1J_{PC}$ = 39.8 Hz), 128.3, 128.5, 129.3, 129.4, 130.0, 130.7, 131.7, 132.1, 133.1 (d, $^2J_{PC}$ = 10.2 Hz), 136.0, 136.9, 137.3, 139.7, 143.5, 144.2, 144.4, 149.0, 166.1, 168.5. **^{31}P NMR** (C_6D_6, 161.9 MHz): δ 24.8 (s). **EA** (Calcd./Found): C 72.38 (72.12), H 5.34 (5.05), N 7.67 (7.30).

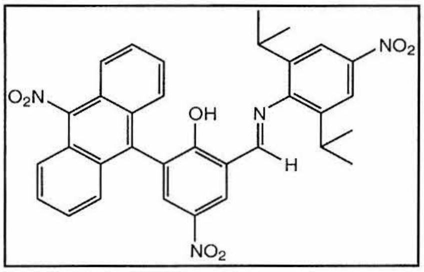

2-[(2,6-Diisopropyl-4-nitro-phenylimino)-methyl]-4-nitro- 6- (10- nitro- anthracen-9-yl)-phenol: $C_{33}H_{28}N_4O_7$, FW = 592.60. **^{1}H NMR** ($CDCl_3$, 300.0 MHz): δ 1.21 (d, 12H, $^3J_{HH}$ = 6.9 Hz), 2.95 (sept., 2H, $^3J_{HH}$ = 6.9 Hz), 7.50-7.56 (m, 2H), 7.65-7.71 (m, 4H), 7.99 (d, 2H, $^3J_{HH}$ = 9.0 Hz), 8.07 (s, 2H), 8.43 (d, 1H, $^4J_{HH}$ = 2.4 Hz), 8.43 (d, 1H, $^4J_{HH}$ = 2.4 Hz), 8.55 (s, 1H), 8.63 (d, 1H, $^4J_{HH}$ = 2.4 Hz), 13.60 (s, 1H). **^{13}C NMR** ($CDCl_3$, 75.4 MHz): δ 23.2, 28.6, 117.7, 119.3, 121.9, 125.8, 127.1, 127.4, 128.7, 129.0, 129.7, 131.7, 133.0, 140.2, 140.5, 145.5, 146.2, 149.9, 164.3, 165.8. **EA** (Calcd./Found): C 66.88 (66.65), H 4.76 (4.92), N 9.45 (9.65).

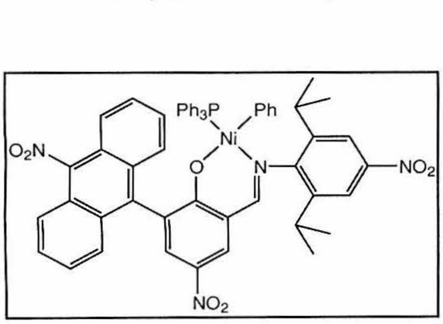

($^{10\text{-NO2-Anthr,NO2}}$Sal^{NO2})Ni(PPh$_3$)Ph (2.34): $C_{57}H_{47}N_4NiO_7P$, FW = 989.71. **^{1}H NMR** (C_6D_6, 400.0 MHz): δ 0.86 (d, 6H, $^3J_{HH}$ = 6.8 Hz), 1.02 (d, 6H, $^3J_{HH}$ = 6.8 Hz), 3.91 (sept., 2H, $^3J_{HH}$ = 6.8 Hz), 5.97 (t, 2H, $^3J_{HH}$ = 7.3 Hz), 6.10 (t, 1H, $^3J_{HH}$ = 7.3 Hz), 6.50-6.64 (m, 8H), 6.71 (t, 3H, $^3J_{HH}$ = 6.2 Hz), 6.76-7.05 (m, 10H), 7.33 (d, 2H, $^4J_{PH}$ = 9.0 Hz), 7.61 (d, 2H, $^3J_{HH}$ = 8.0 Hz), 7.62 (d, 1H, $^4J_{PH}$ = 9.7 Hz), 7.89 (s, 2H), 7.92 (d, 1H, $^4J_{HH}$ = 3.1 Hz), 8.33 (d, 1H, $^4J_{HH}$ = 3.1 Hz). **^{13}C NMR** ($CDCl_3$, 75.4 MHz): δ 22.3, 25.6, 29.7, 102.5, 118.9, 121.5, 122.0, 122.3, 122.8, 123.2, 125.9, 126.5, 127.3, 127.8 (d, $^3J_{PC}$ = 9.9 Hz), 128.5, 128.7, 129.0, 129.4, 129.8, 131.4, 132.4, 133.0, 133.4 (d, $^2J_{PC}$ = 10.0 Hz), 136.0, 137.1, 142.8, 146.6, 149.6, 154.5, 166.3, 172.1, 173.4. **^{31}P NMR** (C_6D_6, 161.9 MHz): δ 25.0 (s). **EA** (Calcd./Found): C 69.18 (69.38), H 4.79 (4.92), N 5.66 (5.82).

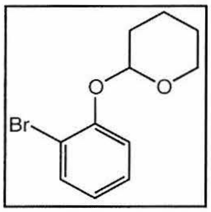

2-(2-Bromo-phenoxy)-tetrahydro-pyran: Prepared from o-bromophenol (49.81 g, FW = 173.01, 0.288 mol), 25 mL of CH_2Cl_2, 3,4-dihydro-2*H*-pyran (26.6 g, FW = 84.12, d = 0.922, 0.317 mol, 1.1 eq..), and a catalytic amount of PPTS as described in method A. Yielded 70.4 g (95 %) of the desired product. $C_{11}H_{13}BrO_2$, FW = 257.12. **^{1}H NMR** ($CDCl_3$, 400.0 MHz): δ 1.58-1.78 (m, 3H), 1.80-1.90 (m, 1H), 1.92-2.02 (m, 1H), 2.10-2.23 (m, 1H), 3.598 (d, 1H, $^3J_{HH}$ = 5.7 Hz), 3.866 (dt, 1H, $^3J_{HH}$ = 4.4 Hz, $^4J_{HH}$ = 1.2 Hz), 5.538 (s, 1H), 6.708 (t, 1H, $^3J_{HH}$ = 7.3 Hz), 7.080 (d, 1H, $^3J_{HH}$ = 8.0 Hz), 7.255 (t, 1H, $^3J_{HH}$ = 7.3 Hz), 7.768 (d, 1H, $^3J_{HH}$ = 8.0 Hz). **^{13}C NMR** ($CDCl_3$, 100.4 MHz): δ 18.47, 25.36, 30.36, 61.75, 87.59, 96.44, 96.58, 115.17, 115.30, 123.29, 123.43, 129.37, 129.51, 139.27, 139.41, 155.59. **EA** (Calcd./Found): C 51.38 (51.63), H 5.10 (5.32), N 0.00 (0.00).

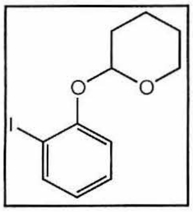

2-(2-Iodo-phenoxy)-tetrahydro-pyran: Prepared in analogous fashion to that above with 2-iodophenol (21.42 g, FW = 220.01, 97.36 mmol), 150 mL CH_2Cl_2, 3,4-dihydro-2*H*-pyran (8.60 g, FW = 84.12, d = 0.922, 9.33 mL, 1.05 eq..), and a catalytic amount of PPTS, providing 27.24 g (92%) of the desired product. $C_{11}H_{13}IO_2$, FW = 304.12. **^{1}H NMR** ($CDCl_3$, 400.0 MHz): δ 1.58-1.78 (m, 3H), 1.80-1.90 (m, 1H), 1.92-2.02 (m, 1H), 2.10-2.23 (m, 1H), 3.598 (d, 1H, $^3J_{HH}$ = 5.7 Hz), 3.866 (dt, 1H, $^3J_{HH}$ = 4.4 Hz, $^4J_{HH}$ = 1.2 Hz), 5.538 (s, 1H), 6.708 (t, 1H, $^3J_{HH}$ = 7.3 Hz), 7.080 (d, 1H, $^3J_{HH}$ = 8.0 Hz), 7.255 (t, 1H, $^3J_{HH}$ = 7.3 Hz), 7.768 (d, 1H, $^3J_{HH}$ = 8.0 Hz). **^{13}C NMR** ($CDCl_3$, 100.4 MHz): δ 18.47, 25.36, 30.36, 61.75, 87.59, 96.44, 96.58, 115.17, 115.30, 123.29, 123.43, 129.37, 129.51, 139.27, 139.41, 155.59. **EA** (Calcd./Found): C 43.44 (43.83), H 4.31 (4.53), N 0.00 (0.00).

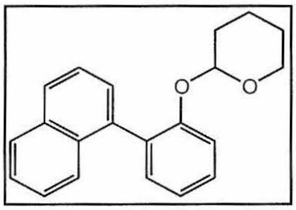

2-(2-Naphthalen-1-yl-phenoxy)-tetrahydro-pyran: Using a Ni-catalyzed aryl-coupling similar to literature methods with 2-iodophenol (21.42 g, FW = 220.01, 97.36 mmol), 150 mL CH_2Cl_2, 3,4-dihydro-2*H*-pyran (8.60 g, FW = 84.12, d = 0.922, 9.33 mL, 1.05 eq..), and a catalytic amount of PPTS $C_{21}H_{20}O_2$, FW = 304.38. **^{1}H NMR** ($CDCl_3$, 300.0 MHz): δ 0.84-1.44 (m, 6H), 3.37-3.62 (m, 2H), 5.31 (m, 1H), 7.15-7.55 (m, 8H), 7.66 (d, 1H, $^3J_{HH}$ = 8.7 Hz), 7.75 (d, 1H, $^3J_{HH}$ = 9.0 Hz), 8.03 (d, 2H, $^3J_{HH}$ = Hz), 8.48 (s, 1H). **^{13}C NMR** ($CDCl_3$, 75.4 MHz): δ 17.7, 24.9, 30.0, 61.6, 61.9, 96.1, 96.4, 115.3, 115.8, 121.4, 121.7, 124.7, 125.2, 126.0, 126.6, 127.1, 127.5, 127.8, 128.2, 128.6, 129.0, 130.2, 131.3, 132.5, 132.9, 133.9, 155.4. **EA** (Calcd./Found): C 82.86 (82.45), H 6.62 (6.54), N 0.00 (0.00).

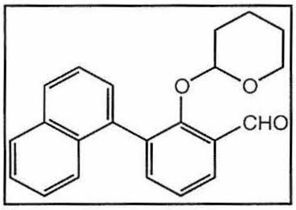

3- Naphthalen- 1- yl- 2- (tetrahydro- pyran- 2- yloxy)-benzaldehyde: $C_{22}H_{20}O_3$, FW = 332.39. **^{1}H NMR** ($CDCl_3$, 300.0 MHz): δ 0.56-1.27 (m, 6H), 2.87 (m, 1H), 3.43 (m, 1H), 4.26 (m, 1H), 7.15-7.55 (m, 8H), 7.66 (d, 1H, $^3J_{HH}$ = 8.7 Hz), 7.75 (d, 1H, $^3J_{HH}$ = 9.0 Hz), 8.03 (d, 2H, $^3J_{HH}$ = Hz), 8.48 (s, 1H). **^{13}C NMR** ($CDCl_3$, 75.4 MHz): δ 19.5, 24.6, 29.9, 64.2, 102.4, 124.6, 125.5, 126.1, 126.2, 126.5, 127.6, 128.0, 128.7, 130.0, 130.8, 131.2, 131.3, 131.9, 132.9, 139.5, 159.0, 191.8. **EA** (Calcd./Found): C 79.50 (80.01), H 6.06 (6.13), N 0.00 (0.00).

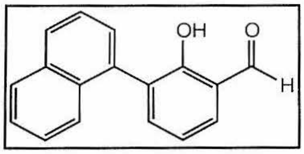

2-Hydroxy-3-naphthalen-1-yl-benzaldehyde: $C_{17}H_{12}O_2$, FW = 248.28. **^{1}H NMR** (CD_2Cl_2, 300.0 MHz): δ 7.211 (t, 1H, $^3J_{HH}$ = 7.8 Hz), 7.45-7.74 (m, 7H), 7.983 (d, 2H, $^3J_{HH}$ = 7.8 Hz), 10.025 (s, 1H), 11.389 (s, 1H). **^{13}C NMR** (CD_2Cl_2, 75.4 MHz): δ 120.18, 121.12, 125.79, 126.28, 126.33, 126.45, 128.00, 128.66, 128.69, 129.75, 132.17, 133.91, 134.08, 135.09, 139.34, 159.56, 197.31. **EA** (Calcd./Found): C 82.24 (83.38), H 4.87 (4.92), N 0.00 (0.00).

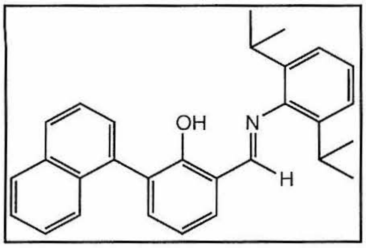

2-[(2,6-Diisopropyl-phenylimino)-methyl]-6-naphthalen-1-yl-phenol: $C_{29}H_{29}NO$, FW = 407.55. **^{1}H NMR** (CD_2Cl_2, 300.0 MHz): δ 1.181 (d, 6H, $^3J_{HH}$ = 6.9 Hz), 1.196 (d, 6H, $^3J_{HH}$ = 6.9 Hz), 3.045 (sept., 2H, $^3J_{HH}$ = 6.9 Hz), 7.127 (t, 1H, $^3J_{HH}$ = 7.8 Hz), 7.18-7.23 (m, 3H), 7.43-7.55 (m, 5H), 7.585 (t, 1H, $^3J_{HH}$ = 7.8 Hz), 7.753 (dd, 1H, $^3J_{HH}$ = 8.4 Hz, $^4J_{HH}$ = 0.9 Hz), 7.91-7.96 (m, 2H), 8.440 (s, 1H), 13.356 (s, 1H). **^{13}C NMR** (CD_2Cl_2, 75.4 MHz): δ 23.85, 23.88, 28.63, 119.07, 119.14, 123.55, 125.71, 126.07, 126.17, 126.60, 127.98, 128.25, 128.53, 129.23, 132.28, 132.50, 133.90, 135.69, 136.22, 139.14, 146.45, 159.28, 167.31. **EA** (Calcd./Found): C 85.47 (85.33), H 7.17 (7.08), N 0.00 (0.00).

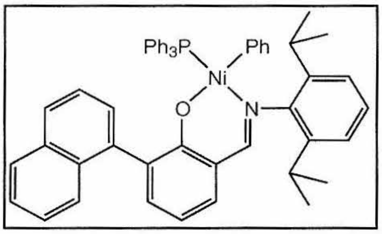

(^{Napth}Sal)Ni(PPh$_3$)Ph (2.70): Using method E with the ^{Naphth,H}Sal ligand (0.435 g, FW = 407.55, 1.07 mmol), NaH (72.3 mg, FW = 24.00, 3.01 mmol, 2.81 eq..), and Ni(PPh3)2PhCl (0.744 g, FW = 695.85, 1.07 mmol, 1.0 eq.) in 20 mL of benzene. The product was obtained by recrystallization from benzene with pentane. Dried in vacuo orange-red crystals 472 mg (81%). $C_{53}H_{48}NNiOP$, FW = 804.62. **^{1}H NMR** (C_7D_8, 500.0 MHz): δ 0.871 (d, 3H, $^3J_{HH}$ = 6.5 Hz), 0.958 (d, 3H, $^3J_{HH}$ = 6.5 Hz), 1.227 (d, 3H, $^3J_{HH}$ = 7.0 Hz), 1.480 (d, 3H, $^3J_{HH}$ = 6.5 Hz), 3.421 (sept., 1H, $^3J_{HH}$ = 7.0 Hz), 4.598 (sept., 1H, $^3J_{HH}$ = 6.5 Hz), 6.099 (t, 1H, $^3J_{HH}$ = 7.5 Hz), 6.199 (t, 1H, $^3J_{HH}$ = 7.3 Hz), 6.258 (t, 1H, $^3J_{HH}$ = 6.8 Hz), 6.352 (d, 1H, $^3J_{HH}$ = 7.5 Hz), 6.445 (t, 1H, $^3J_{HH}$ = 7.5 Hz), 6.536 (dt, 1H, $^3J_{HH}$ = 8.0 Hz, $^4J_{HH}$ = 1.5 Hz), 6.630 (q, 6H, $^3J_{HH}$ = 7.0 Hz), 6.716 (d, 1H, $^3J_{HH}$ = 7.0 Hz), 6.796 (t, 3H, $^3J_{HH}$ = 7.5 Hz), 6.88-6.99 (m, 3H), 7.08-7.12 (m, 3H), 7.18-7.23 (m, 3H), 7.320 (bt, 6H, $^3J_{HH}$ = 7.0 Hz), 7.496 (d, 1H, $^3J_{HH}$ = 8.0 Hz), 7.831 (d, 1H, $^3J_{HH}$ = 8.0 Hz), 7.999 (d, 1H, $^4J_{PH}$ = 9.5 Hz). **^{31}P NMR** (C_6D_6, 161.0 MHz): δ 22.44 (s). **EA** (Calcd./Found): C 79.11 (78.99), H 6.01 (6.10), N 1.74 (1.76).

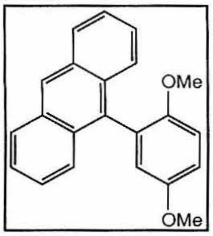

9-(2,5-Dimethoxy-phenyl)-anthracene (2.55): $C_{22}H_{18}O_2$, FW = 314.38. ^{1}**H NMR** (CD_2Cl_2, 300.0 MHz): δ 3.580 (s, 3H), 3.801 (s, 3H), 6.863 (dd, 1H, $^{4}J_{HH}$ = 2.7 Hz, $^{5}J_{HH}$ = 0.9 Hz), 7.07-7.15 (m, 2H), 7.382 (ddd, 2H, $^{3}J_{HH}$ = 7.8 Hz, $^{3}J_{HH}$ = 6.6 Hz, $^{4}J_{HH}$ = 1.2 Hz), 7.488 (ddd, 2H, $^{3}J_{HH}$ = 8.1 Hz, $^{3}J_{HH}$ = 6.6 Hz, $^{4}J_{HH}$ = 1.2 Hz), 7.648 (dd, 2H, $^{3}J_{HH}$ = 8.7 Hz, $^{4}J_{HH}$ = 0.9 Hz), 8.076 (dd, 2H, $^{3}J_{HH}$ = 9.0 Hz, $^{4}J_{HH}$ = 1.5 Hz), 8.524 (s, 1H). ^{13}**C NMR** (CD_2Cl_2, 75.4 MHz): δ 56.18, 56.66, 112.81, 114.41, 118.52, 125.53, 125.77, 126.87, 127.03, 128.34, 128.72, 130.60, 131.77, 133.99, 152.55, 154.06. **EA** (Calcd./Found): C 84.05 (83.83), H 5.77(5.74), N 0.00 (0.00).

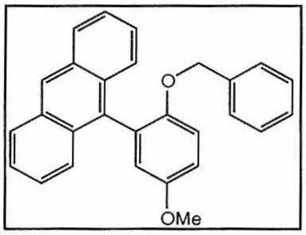

9-(2-Benzyloxy-5-methoxy-phenyl)-anthracene (2.54): $C_{28}H_{22}O_2$, FW = 390.47. ^{1}**H NMR** (CD_2Cl_2, 300.0 MHz): δ 3.79 (s, 3H), 4.84 (s, 2H), 6.77-6.80 (m, 2H), 7.01-7.14 (m, 6H), 7.390 (ddd, 2H, $^{3}J_{HH}$ = 7.8 Hz, $^{3}J_{HH}$ = 6.6 Hz, $^{4}J_{HH}$ = 1.2 Hz), 7.492 (ddd, 2H, $^{3}J_{HH}$ = 8.1 Hz, $^{3}J_{HH}$ = 6.6 Hz, $^{4}J_{HH}$ = 1.2 Hz), 7.686 (dd, 2H, $^{3}J_{HH}$ = 8.7 Hz, $^{4}J_{HH}$ = 0.9 Hz), 8.085 (dd, 2H, $^{3}J_{HH}$ = 9.0 Hz, $^{4}J_{HH}$ = 1.5 Hz), 8.54 (s, 1H). ^{13}**C NMR** (CD_2Cl_2, 75.4 MHz): δ 56.19, 71.38, 114.42, 115.25, 118.51, 125.53, 125.78, 126.93, 127.13, 127.22, 127.75, 128.44, 128.75, 129.36, 130.64, 131.80, 133.92, 137.68, 151.43, 154.40. **EA** (Calcd./Found): C 84.05 (83.83), H 5.77(5.74), N 0.00 (0.00).

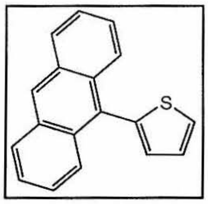

2-Anthracen-9-yl-thiophene (2.57): Anthrone (0.435 g, FW = 407.55, 1.07 mmol), is dissolved in THF and added to the lithiate at –78°C. The reaction mixture was gradually warmed to room temperature and stir at room temperature for three hours. 240 mL of 0.5 M HCl were added. The product was recovered by column chromatography (95/5 Hexane/Ethyl Acetate) giving 5.52 g (26 %) as a yellow solid. $C_{18}H_{12}S$, FW = 260.35. ^{1}**H NMR** (CD_2Cl_2, 300.0 MHz): δ 7.19(m, 2H), 7.3 (m, 1H), 7.45 (m, 2H), 7.63 (m, 2H), 7.84 (d, J_{HH} = 6 Hz, 2H), 8.03 (d, J_{HH} = 6 Hz, 2H), 8.53 (s, 1H). ^{13}**C NMR** (CD_2Cl_2, 75.4 MHz): δ 125.6, 126.2, 126.8, 127.0, 127.5, 128.2, 128.6, 129.0, 129.8, 131.5, 132.2, 139.2. **EA** (Calcd./Found): C 83.04 (82.49), H 4.65 (4.58), N 0.00 (0.00).

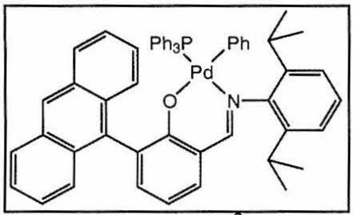

(^{Anthr}Sal)Pd(PPh$_3$)Ph (2.48): **^{1}H NMR** (C_6D_6, 400 MHz): δ1.14 (d, 6H, $^3J_{HH}$ = 6.6 Hz), 1.18 (d, 6H, $^3J_{HH}$ = 6.6 Hz), 4.17 (sept., 2H, $^3J_{HH}$ = 6.6 Hz), 6.19 (t, 2H, $^3J_{HH}$ = 7.3 Hz), 6.29 (t, 1H, $^3J_{HH}$ = 7.3 Hz), 6.58-6.63 (m, 6H), 6.73-6.78 (m, 3H), 6.82 (d, 1H, $^3J_{HH}$ = 6.9 Hz), 6.88 (d, 1H, $^3J_{HH}$ = 8.0 Hz), 6.89 (s, 1H), 6.95-7.21 (m, 15H), 7.61 (d, 2H, $^3J_{HH}$ = 8.4 Hz), 7.82 (d, 2H, $^3J_{HH}$ = 8.08 Hz), 7.83 (s, 1H), 8.15 (d, 1H, $^4J_{PH}$ = 11.3 Hz). **^{13}C NMR** (C_6D_6, 75.4 MHz): δ 22.6, 25.6, 28.9, 114.2, 119.9, 121.2, 122.8, 124.5, 124.7, 124.9, 125.8 (d, $^1J_{PC}$ = 34.3 Hz), 127.3 (d, $^3J_{PC}$ = 9.8 Hz), 128.4, 129.0 (d, $^4J_{PC}$ = 1.6 Hz), 130.6, 130.8, 131.5, 131.8, 133.5 (d, $^2J_{PC}$ = 10.1 Hz), 134.7, 136.6, 137.4, 138.3, 140.7, 145.2, 146.4, 150.1, 165.2, 166.7. **^{31}P NMR** (C_6D_6, 161.9 MHz): δ 22.7 (s). **EA** (Calcd./Found): C 80.10 (79.77), H 5.90 (6.09), N 1.64 (1.49).

Crystal Structure of Complex 2.48 (Appendix B). Crystals suitable for X-ray structure determination were grown from a solution of **2.48** in benzene at room temperature by the slow infusion of pentane over a few days. The orange crystal used for data collection had dimensions 1.48 × 0.39 × 0.15 mm^3. The X-ray diffraction data were collected by using a CCD area detector diffractometer with graphite-monochromated Mo Kα radiation (0.71073 Å). Unit cell parameters were determined by a least-squares analysis of 25 automatically centered reflections in the range 2.25° < θ< 28.18°. Data were collected at 98 K. A total of 42656 reflections were collected, 11102 of which were independent. A set of 9752 reflections with $F_o^2 > 2\sigma(F_o^2)$ were observed. The structure was solved by direct methods using the SHELXS-97 program. Hydrogen atoms appeared in the difference Fourier map. Their were unrestrained during refinement, and their U_{iso} values were fixed at 1.1 times the $U_{eq.}$ value of the attached atom. Refinement was full-matrix least squares on F^2 using SHELXL-97.

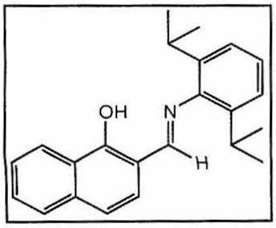

2- [(2,6- Diisopropyl- phenylimino)- methyl]- naphthalen- 1- ol (2.43): $C_{23}H_{25}NO$, FW = 331.45. **^{1}H NMR** ($CDCl_3$, 300.0 MHz): δ 1.23 (d, 12H, $^3J_{HH}$ = 6.9 Hz), 3.13 (sept., 2H, $^3J_{HH}$ = 6.9 Hz), 7.18-

7.27 (m, 5H), 7.53 (dt, 1H, $^3J_{HH}$ = 6.9 Hz, $^4J_{HH}$ = 1.2 Hz), 7.62 (dt, 1H, $^3J_{HH}$ = 6.9 Hz, $^4J_{HH}$ = 1.2 Hz), 7.75 (d, 1H, $^3J_{HH}$ = 7.8 Hz), 8.19 (s, 1H), 8.52 (dd , 1H, $^3J_{HH}$ = 7.5 Hz, $^4J_{HH}$ = 0.6 Hz), 14.67 (s, 1H). **^{13}C NMR** ($CDCl_3$, 75.4 MHz): δ 23.8, 28.4, 110.8, 117.4, 123.6, 124.5, 125.7, 126.6, 127.1, 127.5, 127.6, 129.7, 136.7, 140.8, 142.6, 164.8, 167.3. **EA** (Calcd./Found): C 83.34 (83.04), H 7.60 (7.61), N 4.23 (4.32).

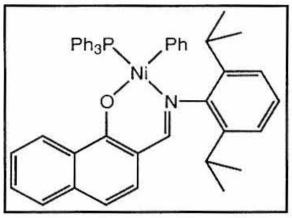

(Napthaldimine)Ni(PPh$_3$)Ph (2.45): $C_{47}H_{44}NNiOP$: FW 728.54. **^{1}H NMR** (C_6D_6, 400 MHz): δ 1.11 (d, 6 H, $^3J_{HH}$ = 7.0 Hz), 1.30 (d, 6 H, $^3J_{HH}$ = 7.0 Hz), 4.14 (sept., 2 H, $^3J_{HH}$ = 7.0 Hz), 6.29-7.71 (m, 29 H), 8.03 (d, 1H, $^4J_{PH}$ = 9.2 Hz). **^{13}C NMR** (C_6D_6, 75 MHz): δ 22.6, 25.6, 28.8, 112.2, 114.5, 121.4, 122.6, 124.0, 125.2, 125.8, 127.0, 128.4, 129.6, 129.8, 130.3, 131.2, 131.8, 133.8, 134.0, 134.4 (d, $^2J_{PC}$ = 10.0 Hz), 137.7, 140.7, 146.7 (d, $^1J_{PC}$ = 48.8 Hz), 150.3, 165.0, 165.2. **^{31}P NMR** (C_6D_6, 161 MHz): δ 27.2 (s). **EA** (Calcd./Found): C 77.49 (77.63), H 6.09 (6.25), N 1.92 (2.08).

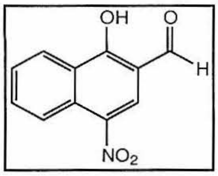

1-Hydroxy-4-nitro-naphthalene-2-carbaldehyde (2.36): A solution of 1-hydroxy-naphthalene-2-carbaldehyde **10** (8.31 g, FW = 172.19, 48.2 mmol) in 25 mL of glacial HOAc was cooled to 0°C using an external bath of acetone and ice. Upon cooling, 3.4 mL of conc. HNO_3 (4.76 g, d = 1.40 g/mL, FW = 63.01, 75.5 mmol, 1.6 eq..) was added dropwise to the solution, causing the formation of a thick slurry. After 30 minutes of stirring at 0 °C, the slurry was poured over 300 mL of ice, precipitating the desired product **10**. The deep orange product was isolated by filtration, washed several times with H_2O (3 x 50 mL), and dried *in vacuo* yielding 3.65 g (35 %). $C_{11}H_7NO_4$: FW 217.18. **^{1}H NMR** ($CDCl_3$, 300 MHz): δ 7.71 (t, 1H, $^3J_{HH}$ = 7.8 Hz), 7.92 (t, 1H, $^3J_{HH}$ = 7.8 Hz), 8.58 (s, 1H), 8.58 (d, 1H, $^3J_{HH}$ = 8.2 Hz), 8.79 (d, 1H, $^3J_{HH}$ = 9.0 Hz), 10.02 (s, 1H), 13.18 (s, 1H). **^{13}C NMR** ($CDCl_3$, 75 MHz): δ 107.4, 112.0, 120.0, 124.1, 125.1, 127.7, 127.8, 134.0, 134.4, 165.9, 195.5. **EA** (Calcd./Found): C 60.83 (60.90), H 3.25 (4.06), N 6.45 (6.60).

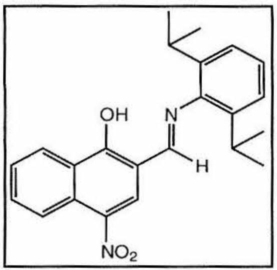

2-[(2,6-Diisopropyl-phenylimino)-methyl]-4-nitro-naphthalen-1-ol (2.44): $C_{23}H_{24}N_2O_3$: FW 376.46. **^{1}H NMR** ($CDCl_3$, 300 MHz): δ 1.24 (d, 12 H, $^3J_{HH}$ = 6.9 Hz), 3.08 (sept., 2H, $^3J_{HH}$ = 6.9 Hz), 7.26 (m, 2H), 7.38 (m, 1H), 7.56 (m, 1H), 7.77 (m, 1H), 7.94 (d, 1H, $^3J_{HH}$ = 11.1 Hz), 8.33 (s, 1H), 8.55 (dd, 1H, $^3J_{HH}$ = 8.1 Hz, $^4J_{HH}$ = 1.2 Hz), 8.75 (d, 1H, $^3J_{HH}$ = 8.7 Hz), 14.77 (s, 1H). **^{13}C NMR** ($CDCl_3$, 75 MHz): δ 23.7, 28.6, 106.7, 124.2, 124.3, 126.3, 126.7, 129.1, 129.5, 129.9, 132.4, 132.9, 134.8, 135.5, 143.0, 163.8, 179.5. **EA** (Calcd./Found): C 73.38 (73.33), H 6.43 (6.37), N 7.44 (7.13).

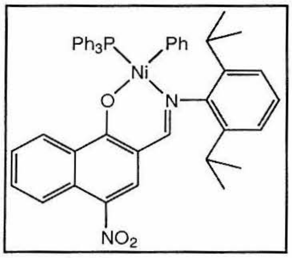

(NO_2Napthaldimine)Ni(PPh_3)Ph (2.46): $C_{47}H_{43}N_2NiOP$: FW 773.55. **^{1}H NMR** (C_6D_6, 400 MHz): δ 1.02 (d, 6H, $^3J_{HH}$ = 6.9 Hz), 1.24 (d, 6H, $^3J_{HH}$ = 6.9 Hz), 3.96 (sept., 2H, $^3J_{HH}$ = 6.9 Hz), 6.71-7.68 (m, 27H), 8.29 (s, 1H), 9.01 (d, 1H, $^4J_{PH}$ = 8.8 Hz). **^{13}C NMR** (C_6D_6, 75 MHz): δ 22.8, 25.8, 29.1, 110.9, 122.0, 123.0, 124.4, 125.4, 125.7 (d, $^4J_{PC}$ = 1.7 Hz), 126.2, 126.5, 128.4, 128.8, 130.0 (d, $^2J_{PC}$ = 10.1 Hz), 130.2, 130.7, 131.3 (d, $^3J_{PC}$ = 3.6 Hz), 133.2, 134.0, 134.4 (d, $^2J_{PC}$ = 10.1 Hz), 137.5 (d, $^3J_{PC}$ = 2.4 Hz), 140.4, 144.8 (d, $^1J_{PC}$ = 49.4 Hz), 165.6, 168.8, 168.9. **^{31}P NMR** (C_6D_6, 161 MHz): δ 26.5 (s). **EA** (Calcd./Found): C 72.98 (73.19), H 5.60 (5.75), N 3.62 (3.38).

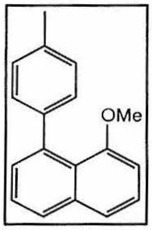

8-(*p*-tolyl)-1-methoxynapthalene (2.38): Under an atmosphere of Argon, 1-methoxynapthalene (5 mL, d = 1.090, 5.45 g, FW = 158.20, 34.5 mmol) was dissolved in 28 mL of freshly degassed cyclohexane. ^{t}BuLi (25 mL, 1.7 N in pentane, 42.5 mmol, 1.23 eq..) was added slowly to the reaction mixture at room temperature. The mixture was stirred at room temperature for two days. Freshly prepared $MgBr_2$, obtained from the reaction of Mg (1.02 g, FW = 24.31, 41.9 mmol) with 1,2-dibromoethane (3.4 mL, d = 2.18, 7.41 g, FW = 187.87, 39.4 mmol) in 60 mL of anhydrous THF. To a solution of 4-bromotoluene (5.02 g, FW = 171.04, 29.4 mmol) and Ni(dppe)Cl_2 (445 mg, FW = 528.05, 0.84 mmol, 0.25 eq..). The material was recovered by column chromatography, yielding 8.3 g (62%) of the desired product. $C_{18}H_{16}O$: FW 248.33. **^{1}H NMR** ($CDCl_3$, 300 MHz): δ 2.41 (s, 3H), 3.49 (s, 3H), 6.78

(dd, 1H, $^3J_{HH}$ = 7.5 Hz, $^4J_{HH}$ = 0.9 Hz), 7.13-7.50 (m, 8H), 7.78 (dd, 1H, $^3J_{HH}$ = 8.1 Hz, $^4J_{HH}$ = 1.2 Hz). **^{13}C NMR** ($CDCl_3$, 75 MHz): δ 21.2, 55.2, 106.1, 121.2, 123.5, 125.4, 125.9, 127.3, 127.4, 128.6, 129.1, 135.1, 135.7, 138.9, 142.4, 156.7. **EA** (Calcd./Found): C 87.06 (87.34), H 6.49 (6.54), N 0.00 (0.00).

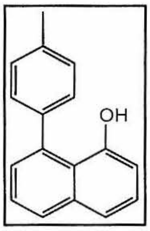

8-*p*-Tolyl-naphthalen-1-ol (2.39): $C_{17}H_{14}O$: FW 234.30. **^{1}H NMR** ($CDCl_3$, 300 MHz): δ 2.45 (s, 3H), 5.57 (s, 1H), 6.91 (dd, 1H, $^3J_{HH}$ = 7.5 Hz, $^4J_{HH}$ = 1.2 Hz), 7.19 (dd, 1H, $^3J_{HH}$ = 7.1 Hz, $^4J_{HH}$ = 1.2 Hz), 7.31-7.45 (m, 6H), 7.50 (dd, 1H, $^3J_{HH}$ = 8.3 Hz, $^4J_{HH}$ = 1.2 Hz), 7.84 (dd, 1H, $^3J_{HH}$ = 8.3 Hz, $^4J_{HH}$ = 1.2 Hz). **^{13}C NMR** ($CDCl_3$, 75 MHz): δ 21.2, 111.6, 120.9, 121.3, 124.8, 126.8, 128.4, 128.5, 129.3, 129.6, 135.6, 138.0, 138.5, 153.0. **EA** (Calcd./Found): C 87.15 (87.31), H 6.02 (6.12), N 0.00 (0.00).

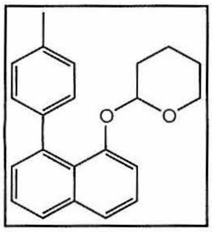

2-(8-*p*-Tolyl-naphthalen-1-yloxy)-tetrahydro-pyran (2.40): $C_{22}H_{22}O_2$: FW 318.42. **^{1}H NMR** ($CDCl_3$, 300 MHz): δ 0.85-1.58 (m, 6H), 2.38 (s, 3H), 3.48 (m, 1H), 3.62 (m, 1H), 5.25 (m, 1H), 7.11-7.45 (m, 8H), 7.52 (dd, 1H, $^3J_{HH}$ = 8.4 Hz, $^4J_{HH}$ = 1.2 Hz), 7.78 (dd, 1H, $^3J_{HH}$ = 8.4 Hz, $^4J_{HH}$ = 1.2 Hz). **^{13}C NMR** ($CDCl_3$, 75 MHz): δ 17.6, 21.1, 25.0, 29.8, 61.4, 96.9, 109.8, 121.8, 124.9, 126.1, 127.5, 127.6, 127.7, 128.6, 129.4, 135.2, 135.7, 138.6, 143.0, 154.2. **EA** (Calcd./Found): C 82.99 (83.17), H 6.96 (7.18), N 0.00 (0.00).

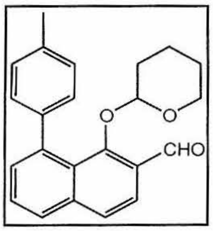

1-(Tetrahydro-pyran-2-yloxy)-8-*p*-tolyl-naphthalene-2-carbaldehyde (2.41): $C_{23}H_{22}O_3$: FW 346.43. **^{1}H NMR** ($CDCl_3$, 300 MHz): δ 0.90-1.51 (m, 6H), 2.41 (s, 3H), 3.02 (m, 1H), 3.67 (m, 1H), 4.24 (m, 1H), 7.15-7.29 (m, 3H), 7.37 (dd, 1H, $^3J_{HH}$ = 7.2 Hz, $^4J_{HH}$ = 1.2 Hz), 7.43-7.47 (m, 1H), 7.57 (dd, 1H, $^3J_{HH}$ = 8.1 Hz, $^3J_{HH}$ = 7.2 Hz), 7.73 (d, 1H, $^3J_{HH}$ = 8.7 Hz), 7.84 (dd, 1H, $^3J_{HH}$ = 8.1 Hz, $^4J_{HH}$ = 1.2 Hz), 7.92 (d, 1H, $^3J_{HH}$ = 8.7 Hz), 10.52 (s, 1H). **^{13}C NMR** ($CDCl_3$, 75 MHz): δ 21.1, 21.3, 24.8, 29.5, 65.8, 103.4, 122.3, 125.0, 125.7, 127.8, 128.1, 128.3, 129.1, 131.2, 131.6, 136.5, 139.4, 139.5, 140.0, 157.6, 191.7. **EA** (Calcd./Found): C 79.74 (80.01), H 6.40 (6.52), N 0.00 (0.00).

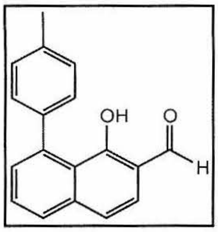

1-Hydroxy-8-p-tolyl-naphthalene-2-carbaldehyde (2.42): $C_{18}H_{14}O_2$: FW 262.31. **^{1}H NMR** ($CDCl_3$, 300 MHz): δ 2.43 (s, 3H), 7.19-7.46 (m, 7H), 7.59 (dd, 1H, $^3J_{HH}$ = 8.1 Hz, $^3J_{HH}$ = 8.1 Hz), 7.74 (dd, 1H, $^3J_{HH}$ = 8.1 Hz, $^3J_{HH}$ = 1.2 Hz), 9.87 (s, 1H), 12.81 (s, 1H). **^{13}C NMR** ($CDCl_3$, 75 MHz): δ 21.3, 114.9, 120.0, 122.1, 126.9, 127.5, 127.9, 128.7, 129.5, 130.1, 136.2, 138.9, 140.6, 142.0, 163.5, 195.9. **EA** (Calcd./Found): C 82.42 (82.60), H 5.38 (5.51), N 0.00 (0.00).

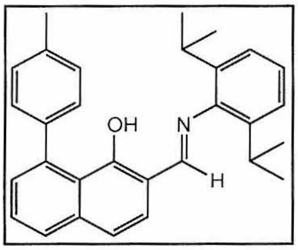

2- [(2,6- Diisopropyl- phenylimino)- methyl] - 8- *p*- tolyl-naphthalen-1-ol (2.37): $C_{30}H_{31}NO$: FW 421.59. **^{1}H NMR** ($CDCl_3$, 300 MHz): δ 1.12 (d, 12H, $^3J_{HH}$ = 6.9 Hz), 2.40 (s, 3H), 2.95 (sept, 2H, $^3J_{HH}$ = 6.9 Hz), 7.11-7.26 (m, 8H), 7.34 (d, 2H, $^3J_{HH}$ = 8.1 Hz), 7.53 (dd, 1H, $^3J_{HH}$ = 8.1 Hz, $^3J_{HH}$ = 7.8 Hz), 7.70 (dd, 1H, $^3J_{HH}$ = 8.1 Hz, $^4J_{HH}$ = 1.2 Hz), 8.10 (d, 1H, $^4J_{HH}$ = 2.7 Hz) , 14.44 (s, 1H). **^{13}C NMR** ($CDCl_3$, 75 MHz): δ 21.4, 23.6, 28.1, 111.7, 117.8, 123.3, 124.1, 126.2, 127.4, 127.8, 127.9, 128.4, 128.8, 129.8, 135.7, 137.9, 140.4, 141.5, 141.7, 142.9, 164.5, 167.5. **EA** (Calcd./Found): C 85.47 (85.48), H 7.41 (7.34), N 3.32 (2.92).

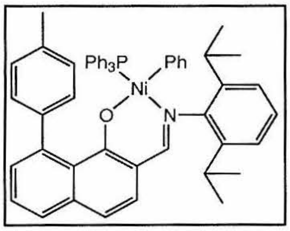

{8-(*p*-tolyl)-1-hydroxy-2-napthaldimine}Ni(PPh_3)Ph (2.47): $C_{54}H_{50}NNiOP$,FW = 818.68. **^{1}H NMR** (C_6D_6, 400 MHz): δ 1.20 (d, 6H, $^3J_{HH}$ = 6.6 Hz), 1.37 (d, 6H, $^3J_{HH}$ = 6.6 Hz), 2.15 (s, 3H), 4.20 (sept., 2H, $^3J_{HH}$ = 6.6 Hz), 6.13-7.27 (m, 31H), 7.56 (dd, 1H, $^3J_{HH}$ = 8.1 Hz, $^4J_{HH}$ = 0.9 Hz), 7.89 (d, 1H, $^3{}_{HH}$ = 7.3 Hz). **^{13}C NMR** (C_6D_6, 75 MHz): δ 21.8, 23.2, 26.1, 29.2, 114.4, 115.3, 117.1, 121.3, 123.0, 125.3, 125.9, 126.6, 127.5, 127.7, 128.6, 129.0, 129.1, 129.2, 129.6, 131.2 (d, $^1J_{PC}$ = 43.8 Hz), 134.5, 134.7 (d, $^2J_{PC}$ = 19.1 Hz), 138.3 (d, $^4J_{PC}$ = 1.5 Hz), 139.8, 140.8, 141.7, 142.2, 147.1, 149.7, 163.9, 167.1. **^{31}P NMR** (C_6D_6, 161 MHz): δ 27.5 (s). **EA** (Calcd./Found): C 79.23 (79.41), H 6.16 (6.30), N 1.71 (1.52).

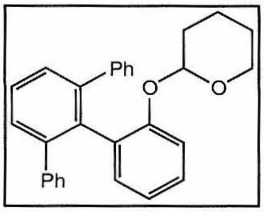

2- (2',6'- Diphenyl- biphenyl-2- yloxy)- tetrahydro- pyran: $C_{29}H_{26}O_2$, FW = 406.52. **^{1}H NMR** ($CDCl_3$, 300 MHz): δ 0.85-1.58 (m, 6H), 2.38 (s, 3H), 3.48 (m, 1H), 3.62 (m, 1H), 5.25 (m, 1H), 7.11-7.45 (m, 8H), 7.52 (dd, 1H, $^3J_{HH}$ = 8.4 Hz, $^4J_{HH}$ = 1.2 Hz), 7.78 (dd, 1H, $^3J_{HH}$ = 8.4 Hz, $^4J_{HH}$ = 1.2 Hz). **^{13}C NMR** ($CDCl_3$, 75 MHz): δ 17.6, 21.1, 25.0, 29.8, 61.4, 96.9, 109.8, 121.8, 124.9, 126.1, 127.5, 127.6, 127.7, 128.6, 129.4, 135.2, 135.7, 138.6, 143.0, 154.2. **EA** (Calcd./Found): C 82.99 (83.17), H 6.96 (7.18), N 0.00 (0.00).

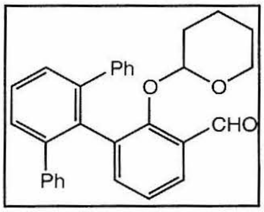

2',6'-Diphenyl-2-(tetrahydro-pyran-2-yloxy)- biphenyl- 3-carbaldehyde: $C_{30}H_{26}O_3$, FW = 434.53. **^{1}H NMR** ($CDCl_3$, 400 MHz): δ 1.38-1.77 (m, 6H), 3.18 (m, 1H), 3.47 (m, 1H), 4.74 (t, 1H, $^3J_{HH}$ ~ 1.2 Hz), 6.92 (t, 1H, $^3J_{HH}$ ~ 7.2 Hz), 7.00-7.68 (m, 15H), 10.04 (s, 1H). **^{13}C NMR** ($CDCl_3$, 75 MHz): δ 17.6, 21.1, 25.0, 29.8, 61.4, 114.9, 120.0, 122.1, 126.9, 127.5, 127.9, 128.7, 129.5, 130.1, 136.2, 138.9, 140.6, 142.0, 163.5, 195.9. **EA** (Calcd./Found): C 82.42 (82.60), H 5.38 (5.51), N 0.00 (0.00).

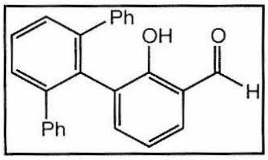

2',6'-Diphenyl-2-hydroxy-biphenyl-3-carbaldehyde: $C_{25}H_{18}O_2$, FW = 350.41. **^{1}H NMR** ($CDCl_3$, 300 MHz): δ 6.68 (t, 1H, $^3J_{HH}$ = 7.2 Hz), 7.04-7.51 (m, 15H), 9.68 (s, 1H), 10.91 (s, 1H). **^{13}C NMR** ($CDCl_3$, 100 MHz): δ 118.81, 119.79, 126.41, 126.45, 127.44, 127.69, 127.97, 129.13, 129.19, 129.49, 132.75, 133.47, 139.79, 141.62, 142.73, 159.05, 196.41. **EA** (Calcd./Found): C 85.69 (85.79), H 5.18 (5.37), N 0.00 (0.00).

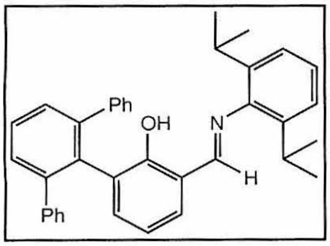

2',6'-Diphenyl-3-[(2,6-diisopropyl-phenylimino)-methyl]-biphenyl-2-ol (2.58): $C_{37}H_{35}NO$, FW = 509.68. **^{1}H NMR** ($CDCl_3$, 300 MHz): δ 1.18 (d, 12H, $^3J_{HH}$ = 6.9 Hz), 2.82 (sept, 2H, $^3J_{HH}$ = 6.9 Hz), 6.68 (t, 1H, $^3J_{HH}$ = 7.3 Hz), 6.98 (dd, 1H, $^3J_{HH}$ = 8.08, $^2J_{HH}$ = 2.2), 7.11 (dd, 1H, $^3J_{HH}$ = 8.08, $^2J_{HH}$ = 2.2), 7.18-7.23 (m, 8H), 7.27-7.30 (m, 3H), 7.50-7.59 (m,3H), 8.14 (s, 1H), 11.95 (bs, 1H). **^{13}C NMR** ($CDCl_3$, 75 MHz): δ 23.37, 28.03, 117.68, 117.93, 123.17, 125.33, 126.19, 127.27, 127.44, 127.73, 128.91, 129.14, 129.34, 131.11, 134.60, 136.18, 138.65, 142.03, 142.75, 145.95, 158.79, 166.28, . **EA** (Calcd./Found): C 87.19 (88.01), H 6.92 (6.98), N 2.75 (2.87).

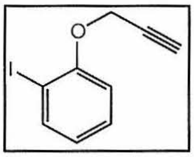

1-Iodo-2-prop-2-ynyloxy-benzene (2.60): Iodophenol (FW = 220.01; 9.92 g; 45.0 mmol) and K_2CO_3 (FW = 138.21; 8.08 g; 58.5 mmol; 1.3 eq..) were placed in a 200 mL RB flask with a magnetic stirbar. The solids were immersed in 75 mL of anhydrous DMF. The resulting orange slurry was stirred at room temperature for 5 minutes, followed by the addition of propargyl bromide (FW = 118.97; d = 1.335; 8.70 g; 6.52 mL; 58.5 mmol; 1.3 eq..) to the mixture slowly *via* syringe. The reaction was monitored periodically by TLC. After stirring at room temperature for 13 hours, the reaction was diluted with 75 mL of H_2O, acidified to pH ~ 5 with HCl, and extracted twice with Et_2O. The organic fractions were combined and washed with 75 mL of 1 N NaOH and brine (2x75 mL). The pale yellow organic layer was dried over K_2CO_3, filtered, and the solvent was removed by rotary evaporation. The product was purified by kugelrohr distillation (175 °C; ~ 300 mm Hg) to provide 10.2 g (88%) as a pale yellow oil. GC ($100_{5\ \mathrm{min}}$—15 °C/min—$300_{5\mathrm{min}}$) 8.3 min. C_9H_7IO, FW 257.95. **^{1}H NMR** (C_6D_6, 300 MHz): δ 1.94 (t, 1H, $^4J_{HH}$ = 2.4 Hz), 4.11 (d, 2H, $^4J_{HH}$ = 2.4 Hz), 6.37 (dt, 1H, $^3J_{HH}$ = 7.5 Hz, $^4J_{HH}$ = 1.5 Hz), 6.54 (dd, 1H, $^3J_{HH}$ = 8.1 Hz, $^4J_{HH}$ = 1.2 Hz), 6.90 (dt, 1H, $^3J_{HH}$ = 7.5 Hz, $^4J_{HH}$ = 1.5 Hz), 7.62 (dd, 1H, $^3J_{HH}$ = 7.5 Hz, $^4J_{HH}$ = 1.5 Hz). **^{13}C NMR** (C_6D_6, 75 MHz): δ 56.6, 76.2, 78.3, 86.9, 112.9, 123.3, 129.3, 139.9, 156.6. **IR** (Neat, cm^{-1}): 925, 1014, 1057, 1123, 1164, 1214, 1253, 1296, 1372, 1455, 1471, 1574, 1673, 1770, 1900, 2009, 2123, 2867, 2919, 3061, 3279. **EA** (Calcd./Found): C 41.89 (41.68), H 2.73 (2.79), N 0.00 (0.00). **MS/EI-Hi Res** (Calcd./Found): 257.95 (257.9543(6))

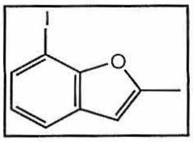

7-Iodo-2-methyl-benzofuran (2.62): Anhydrous CsF (FW = 151.90; 6.6 g; 43.4 mmol) was placed in an oven-dried 100 mL RB flask. The salt was flame-dried twice under vacuum and placed under an inert atmosphere of argon. The RB flask was then charged with **2.60** (FW = 258.07; 8.0 g; 31.0 mmol; 0.7 eq..) and 50 mL of N,N-diethylaniline (DEA) and capped with a reflux condensator. The reaction was heated to reflux with an external heating mantle. It gradually darkened to a brownish-black suspension, with its progress monitored by GC. After 16 hours at reflux, the reaction was cooled, poured into a vessel with 200 mL of Et_2O and passed through a short bed of celite to remove any undesired Cs salts. The dark red-brown filtrate was extracted with 4 M HCl (3x150 mL) and brine (150 mL), dried over $MgSO_4$, filtered, and the solvent was stripped by rotary evaporation. The desired product was obtained by kugelrohr distillation (120 °C; ~ 2 mm Hg) to give 6.5 g (81%) of the product as a pale yellow oil. C_9H_7IO: FW 257.95. GC ($100_{5\ \mathrm{min}}$—15 °C/min—$300_{5\mathrm{min}}$) 8.8 min. **^{1}H NMR** (C_6D_6, 300 MHz): δ 1.90 (d, 3H, $^4J_{HH}$ = 1.1 Hz), 5.96 (d, 1H, $^4J_{HH}$ = 1.1 Hz), 6.64 (t, 1H, $^3J_{HH}$ = 7.7 Hz), 7.12 (dd, 1H, $^3J_{HH}$ = 7.7 Hz, $^4J_{HH}$ = 0.9 Hz), 7.45 (dd, 1H, $^3J_{HH}$ = 7.7 Hz, $^4J_{HH}$ = 0.9 Hz). **^{13}C NMR** (C_6D_6, 75 MHz): δ 13.8, 75.0, 103.9, 120.3, 124.5, 129.6, 132.5, 155.5, 156.1. **IR** (Neat, cm^{-1}): 938, 999, 1045, 1131, 1177, 1231, 1256, 1293, 1417, 1469, 1588, 1614, 1626, 1652, 1770, 1842, 1909, 2343, 2360, 2847, 2919, 2953, 3055, 3111. **EA** (Calcd./Found): C 41.89 (41.81), H 2.73 (2.33), N 0.00 (0.00). **MS/EI-Hi Res** (Calcd./Found): 257.95 (257.9543(4)).

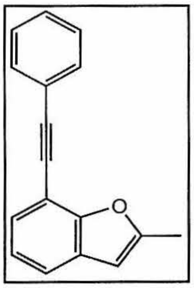

2-Methyl-7-phenylethynyl-benzofuran (2.63): $C_{17}H_{12}O$, FW = 232.28. **^{1}H NMR** (CD_2Cl_2, 400 MHz): δ 2.53 (s, 3H), 6.46 (s, 1H), 7.20 (t, 1H, $^3J_{HH}$ = 7.7 Hz), 7.40-7.76 (m, 7H). **^{13}C NMR** (C_6D_6, 75 MHz): δ 14.23, 30.96, 84.51, 93.67, 103.22, 106.95, 121.11, 122.86, 123.52, 127.10, 128.84, 128.91, 129.74, 129.84, 132.00, 132.85, 154.77, 156.79. **EA** (Calcd./Found): C 87.90 (87.74), H 5.21 (5.28), N 0.00 (0.00).

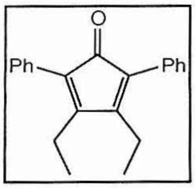

3,4-Diethyl-2,5-diphenyl-cyclopenta-2,4-dienone: Charged a 250 mL 3-neck RB flask with 1,3-diphenylacetone (12.60 g, FW = 210.28, 59.92 mmol), 50 mL of 95% ethanol, and 1,8-diazabicyclo[5.4.0]undec-7-ene (DBU) (1.0 g, FW = 152.24, δ = 1.018, 6.57 mmol, 0.1 eq.). 3,4-Hexanedione (13.88 g, FW = 114.15, d = 0.939, 121.64 mmol, 2.03 eq..) was added to the orange-yellow solution dropwise over 15 minutes. The deep red solid was purified by repeated recrystallization from methanol, providing 2.83 g (16%). $C_{21}H_{20}O$, FW = 288.38. **^{1}H NMR** (400.0 MHz, CD_2Cl_2): δ 1.249 (t, 6H, $^3J_{HH}$ = 7.6 Hz), 2.633 (q, 4H,

$^3J_{HH}$ = 7.6 Hz), 7.32-7.46 (m, 10H). **^{13}C NMR** (100.0 MHz, CD_2Cl_2): δ 14.02, 20.00, 125.60, 127.63, 128.54, 129.77, 132.14, 158.92, 201.61. **EA** (Calcd./Found): C 87.46 (86.99), H 6.99 (7.19), N 0.00 (0.00).

(^{Anthr,H}Sal)Cs salt: The (^{Anthr,H}Sal) ligand (496 mg, FW = 457.61, 1.08 mmol) and CsOH H_2O (230 mg, FW = 167.93, 1.49 mmol, 1.38 eq..) were placed in an oven-dried Schlenk flask and evacuated for several hours. 10 mL of anhydrous THF were added, providing a pale yellow solution which quickly darkened to a deep orange color. After 4 hours of stirring at room temperature, the reaction mixture was passed through a celite plug to remove any undesired salts. The solvent was stripped *in vacuo* to provide a bright yellow powder which was dried overnight under vacuum.

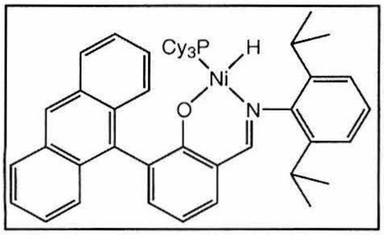

(^{Anthr,H}Sal)Ni(PCy$_3$)H (2.71): The Cs salt (438 mg, FW = 589.51, 0.743 mmol) and Ni(PCy$_3$)HCl (492 mg, FW = 656.03, 0.749 mmol, 1.02 eq..) were placed in an oven-dried 20 mL vial with a small stirbar. 15 mL of anhydrous THF was added to the vial, and the reaction was allowed to stir at room temperature for 3 days (to ensure completion), at which point the reaction was passed through a teflon filter, providing a deep red solution. The THF was removed *in vacuo* to provide a yellowish-orange precipitate. Recrystallization was performed by dissolving the product in a minimal amount of benzene, adding excess CH_3CN, and cooling the mixture to –78 °C with an external dry ice/acetone bath. Removal of the mother liquor by cannula filtration left 532 mg (90%) of the product as a yellowish-orange ppt. $C_{51}H_{64}NNiOP$, FW = 796.73. **^{1}H NMR** (C_6D_6, 300 MHz): δ -28.37 (d, 1H, $^2J_{PH}$ = 128 Hz), 0.50 (q, 6H, $^2J_{HH}$ = 12.8 Hz), 1.01 (m, H), 1.13 (d, 6H, $^3J_{HH}$ = 7.0 Hz), 1.25 (q, J_{HH} = 6.9 Hz), 1.43 (d, J = Hz 6.9 Hz), 1.49 (d, 6H, $^3J_{HH}$ = 7.0 Hz), 4.08 (sept., 2H, $^3J_{HH}$ = 7.0 Hz), 6.68 (t, 1H, $^3J_{HH}$ = 7.7 Hz), 7.86 (d, 2H, $^3J_{HH}$ = 8.4 Hz), 8.25 (s, 1H). **^{13}C NMR** (C_6D_6, 75.4 MHz): δ 23.90, 25.57, 27.23, 27.65 (d, $^3J_{PC}$ = 10.4 Hz), 29.20, 30.46, 33.55 (d, $^2J_{PC}$ = 21.8 Hz), 114.22, 121.05, 123.76, 125.42, 125.55, 126.25, 126.29, 128.95, 129.07, 131.81, 132.21, 132.72, 135.35, 137.89, 138.39, 140.03, 156.57, 164.71, 166.62. **^{31}P NMR** (C_6D_6, 121.4 MHz): δ 42.2 (d, $^2J_{PH}$ = 128.5 Hz). **EA** (Calcd./Found): C 76.88 (76.62), H 8.10 (7.96), N 1.76 (1.83).

Crystal Structure of Complex 2.71 (Appendix C). Crystals suitable for X-ray structure determination were grown from a solution of **2.71** in benzene at room temperature by the slow infusion of acetonitrile over a few days. The orange crystal used for data collection had dimensions 0.31 × 0.19 × 0.19 mm^3. The X-ray diffraction data were collected by using a CCD area detector diffractometer with graphite-monochromated Mo Kα radiation (0.71073 Å). Unit cell parameters were determined by a least-squares analysis of 25 automatically centered reflections in the range 1.57° < θ< 28.54°. Data were collected at 98 K in the range θ = 1.57-28.51°. A total of 127512 reflections were collected, 15058 of which were independent. A set of 10020 reflections with $F_o^2 > 2\sigma(F_o^2)$ were observed. The structure was solved by direct methods using the SHELXS-97 program. Hydrogen atoms appeared in the difference Fourier map. Their were unrestrained during refinement, and their U_{iso} values were fixed at 1.1 times the $U_{eq.}$ value of the attached atom. Refinement was full-matrix least squares on F^2 using SHELXL-97.

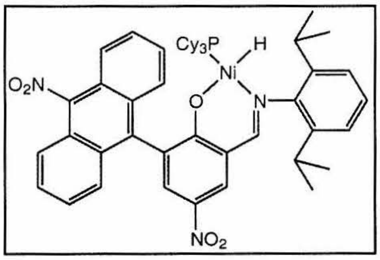

NO_2-Hydride Complex (2.72): **^{1}H NMR** (C_6D_6, 300.0 MHz): δ-28.702 (d, 1H, $^2J_{PH}$ = 128 Hz), 0.511 (bq, 6H, $^2J_{HH}$ = 12.3 Hz), 0.87-1.23 (m, 12H), 1.215 (d, 6H, $^3J_{HH}$ = 6.9 Hz), 1.34-1.54 (m, 15H), 1.449 (d, 6H, $^3J_{HH}$ = 6.9 Hz), 3.843 (sept., 2H, $^3J_{HH}$ = 6.9 Hz), 7.12-7.18 (m, 4H), 7.27-7.35 (m, 3H), 7.730 (dt, 2H, $^3J_{HH}$ = 8.7 Hz, $^4J_{HH}$ = 1.2 Hz), 7.776 (d, 1H, $^4J_{PH}$ = 7.5 Hz), 7.938 (dt, 2H, $^3J_{HH}$ = 8.7 Hz, $^4J_{HH}$ = 1.2 Hz), 8.136 (d, 1H, $^3J_{HH}$ = 3.3 Hz), 8.398 (d, 1H, $^3J_{HH}$ = 3.3 Hz). **^{13}C NMR** (toluene-d_8, 75.4 MHz): δ 23.32, 24.97, 26.70, 27.09 (d, $^2J_{PC}$ = 10.6 Hz), 29.90, 32.98 (d, $^1J_{PC}$ = 21.5 Hz), 113.51, 120.44, 124.58, 124.88, 125.22, 127.41, 127.72, 128.30, 128.63, 128.95, 131.22, 131.52, 132.16, 134.79, 137.79, 139.36, 155.97, 164.09, 166.01.

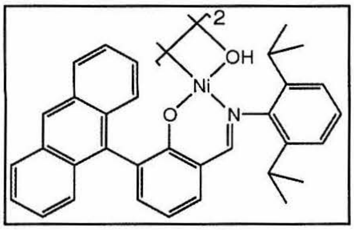

[(^{Anthr}Sal)Ni(OH)]$_2$ (2.75): **^{1}H NMR** (CD$_2$Cl$_2$, 400.0 MHz): δ –9.340 (s, 1H), 1.028 (d, 6H, $^3J_{HH}$ = 5.9 Hz), 1.268 (d, 6H, $^3J_{HH}$ = 5.9 Hz), 4.265 (sept., 2H, $^3J_{HH}$ = 5.9 Hz), 6.215 (d, 2H, $^3J_{HH}$ = 7.3 Hz), 6.589 (t, 1H, $^3J_{HH}$ = 7.3 Hz), 6.704 (t, 1H, $^3J_{HH}$ = 7.3 Hz), 6.942 (s, 1H), 7.004 (d, 1H, $^3J_{HH}$ = 7.3 Hz), 7.087 (d, 1H, $^3J_{HH}$ = 8.8 Hz), 7.30-7.46 (m, 6H), 7.986 (d, 2H, $^3J_{HH}$ = 8.8 Hz), 8.328 (s, 1H).

Crystal Structure of Complex 2.75 (Appendix D). Crystals suitable for X-ray structure determination were grown from a solution of **2.75** in benzene at room temperature by the slow infusion of acetonitrile over a few days. The orange crystal used for data collection had dimensions 0.31 × 0.19 × 0.19 mm^3. The X-ray diffraction data were collected by using a CCD area detector diffractometer with graphite-monochromated Mo Kα radiation (0.71073 Å). Unit cell parameters were determined by a least-squares analysis of 25 automatically centered reflections in the range 1.57° < θ< 28.54°. Data were collected at 98 K in the range θ = 1.57-28.51°. A total of 127512 reflections were collected, 15058 of which were independent. A set of 10020 reflections with $F_o^2 > 2\sigma(F_o^2)$ were observed. The structure was solved by direct methods using the SHELXS-97 program. Hydrogen atoms appeared in the difference Fourier map. Their were unrestrained during refinement, and their U_{iso} values were fixed at 1.1 times the $U_{eq.}$ value of the attached atom. Refinement was full-matrix least squares on F^2 using SHELXL-97.

2.17. References

(1) Klabunde, U.; Ittel, S. D. *Journal of Molecular Catalysis* **1987**, *41*, 123-134.

(2) Ittel, S. D.; Johnson, L. K.; Brookhart, M. *Chem. Rev.* **2000**, *100*, 1169-1203.

(3) Li, R. T. In *Division of Chemistry and Chemical Engineering*; California Institute of Technology: Pasadena, CA, 1997; p 156.

(4) Bauers, F. M.; Mecking, S. *Macromolecules* **2001**, *34*, 1165-1171.

(5) Johnson, L. K.; Killian, C. M.; Brookhart, M. *J. Am. Chem. Soc.* **1995**, *117*, 6414-6415.

(6) Deng, L. Q.; Margl, P.; Ziegler, T. *J. Am. Chem. Soc.* **1997**, *119*, 1094-1100.

(7) Deng, L. Q.; Woo, T. K.; Cavallo, L.; Margl, P. M.; Ziegler, T. *J. Am. Chem. Soc.* **1997**, *119*, 6177-6186.

(8) Froese, R. D. J.; Musaev, D. G.; Morokuma, K. *J. Am. Chem. Soc.* **1998**, *120*, 1581-1587.

(9) Chang, S.; Jones, L.; Wang, C. M.; Henling, L. M.; Grubbs, R. H. *Organometallics* **1998**, *17*, 3460-3465.

(10) Rappe, A. T.; Skiff, W. M.; Casewit, C. J. *Chem. Rev.* **2000**, *100*, 1435-1456.

(11) Mecking, S. *Angew. Chem.-Int. Edit.* **2001**, *40*, 534-540.

(12) Britovsek, G. J. P.; Gibson, V. C.; Wass, D. F. *Angew. Chem.-Int. Edit.* **1999**, *38*, 429-447.

(13) Hiodai, M.; Kashiwagi, T.; Ikeuchi, T.; Uchida, Y. *J. Organometal. Chem.* **1971**, *30*, 279-282.

(14) Wang, C. M.; Friedrich, S.; Younkin, T. R.; Li, R. T.; Grubbs, R. H.; Bansleben, D. A.; Day, M. W. *Organometallics* **1998**, *17*, 3149-3151.

(15) Klein, H.-F.; Bickelhaupt, A. *Inorganica Chimica Acta* **1996**, *248*, 111-114.

(16) Lee, B. Y.; Bazan, G. C.; Vela, J.; Komon, Z. J. A.; Bu, X. *J. Am. Chem. Soc.* **2001**, *ASAP*.

(17) Shirley, D. A. C., C. F. *J. Organometal. Chem.* **1969**, *20*, 251-252.

(18) Coll, G.; Morey, J.; Costa, A.; Saa, J. M. *J. Org. Chem.* **1988**, *53*, 5345-5348.

(19) Canales, J.; Olea, C.; Mena, G.; Valenzuela, J.; Costamagna, J.; Vargas, J. *Bol. Soc. Chil. Quim.* **1990**, *35*, 287-297.

(20) Keim, W.; Kowaldt, F. H.; Goddard, R.; Krüger, C. *Angew. Chem. Int. Ed. Engl.* **1978**, *17*, 466-467.

(21) Starzewski, K. A. O.; Born, L. *Organometallics* **1992**, *11*, 2701-2704.

(22) Desjardins, S. Y.; Cavell, K. J.; Hoare, J. L.; Skelton, B. W.; Sobolev, A. N.; White, A. H.; Keim, W. *J. Organomet. Chem.* **1997**, *544*, 163-174.

(23) Desjardins, S. Y.; Cavell, K. J.; Jin, H.; Skelton, B. W.; White, A. H. *J. Organomet. Chem.* **1996**, *515*, 233-243.

(24) Gibson, V. C.; Tomov, A.; White, A. J. P.; Williams, D. J. *Chem. Commun.* **2001**, 719-720.

(25) Odian, G. *Principles of Polymerization*; Third ed.; John Wiley & Sons, Inc.: New York, NY, 1991.

(26) Crabtree, R. H. *The Organometallic Chemistry of the Transition Metals*; 3rd ed. ed.; John Wiley & Sons, Inc.: New York, NY, 2001.

(27) Moser, W. R.; Wang, A. W.; Kildahl, N. K. *J. Am. Chem. Soc.* **1988**, *110*, 2816-2820.

(28) Dickerman, S. C.; Klein, M.; Vermont, G. B. **1964**.

(29) Nakamura, M.; Oki, M. *Bull. Chem. Soc. Jpn.* **1975**, *48*, 2106-2111.

(30) Barton, J. W.; Shepherd, M. K. *J. Chem. Soc.-Perkin Trans. 1* **1986**, 961-966.

(31) Barton, J. W.; Shepherd, M. K.; Willis, R. J. *J. Chem. Soc.-Perkin Trans. 1* **1986**, 967-971.

(32) Seiders, T. J.; Elliott, E. L.; Grube, G. H.; Siegel, J. S. *J. Am. Chem. Soc.* **1999**, *121*, 7804-7813.

(33) Ishii, H.; Ohta, S.; Nishioka, H.; Hayashida, N.; Harayama, T. *Chem. Pharm. Bull.* **1993**, *41*, 1166-1168.

(34) Muller, U.; Keim, W.; Kruger, C.; Betz, P. *Angew. Chem.-Int. Edit. Engl.* **1989**, *28*, 1011-1013.

(35) Brookhart, M.; Hauptman, E.; Lincoln, D. M. *J. Am. Chem. Soc.* **1992**, *114*, 10394-10401.

(36) Saito, T.; Munakata, H.; Imoto, H., Eds. *Nickel and Palladium Chlorohydridobis(phosphine) complexes.*

(37) Aresta, M.; Quaranta, E.; Dibenedetto, A.; Giannoccaro, P.; Tommasi, I.; Lanfranchi, M.; Tiripicchio, A. *Organometallics* **1997**, *16*, 834-841.

(38) Svejda, S. A.; Johnson, L. K.; Brookhart, M. *J. Am. Chem. Soc.* **1999**, *121*, 10634-10635.

Chapter 3

Variation of the Ancillary-Ligand in Neutral Ni^{II} Salicylaldimine Catalysts. Preparation of Highly Active, "Phosphine-Free Systems" —Rate of Catalysis, Polymer Microstructure, and Catalyst Stability.

3.1 Abstract

Ethylene polymerization studies performed with catalyst **3.1** in the presence of excess functionalized additives, such as ethers, esters, amines, alcohols, ketones, amides, phosphines, thiols, thioethers, and acids have led to an increased understanding of the requirements necessary to maintain high activity for the polymerization of ethylene with neutral Ni^{II} catalysts. The addition of excess PPh_3 to the reaction led to a dramatic decrease in polymerization activity. In addition, exchange reactions between **3.1** and PCy_3 appear to follow a dissociative mechanism. These observations suggested that a "phosphine-free" catalyst would demonstrate increased activities for the polymerization of olefins and possibly allow for the use of olefins that are less reactive than ethylene.

Several attempts were made for the preparation of "phosphine-free" neutral Ni^{II} complexes. Oxidative addition of the phenolic ($^{Anthr,H}Sal$) ligand to Ni^0 sources, such as $Ni(COD)_2$ and $Ni(PPh_3)_4$ was unsuccessful. The η^3-allylic complex, **3.20**, could be easily prepared, but did not exhibit catalytic properties. This has been attributed to a lack of initiation. The reaction of phenolic ($^{Anthr,H}Sal$) ligands to $(tmeda)NiMe_2$ allows for formation of complexes of the type ($^{Anthr,H}Sal$)Ni(L)Me, where L = Py (**3.22**), Lutidene (**3.23**), and $NCCH_3$ (**3.26**). The study of these complexes as catalysts for ethylene polymerization has allowed for an increased understanding of the polymerization process.

The bulk of ligand set has been determined to be crucial to the success of the catalyst, as ligands containing a lower steric demand than $^{Anthr,H}Sal$ have led to the production of bis(salicylaldimine) Ni^{II} species, **3.31** – **3.33**, providing an understanding of how **3.1** and **3.26** are deactivated during the polymerization process.

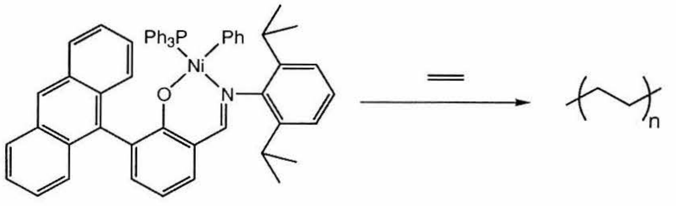

3.1

3.2 Testing the scope of a new polymerization catalyst

The previous chapter highlights the unexpected discovery that neutral Ni^{II} salicylaldimine complexes, such as **3.1**, were single-component systems capable of polymerizing ethylene to high molecular weight polymer at low to moderate pressures. In this chapter, we illustrate our efforts to determine how variation of the ancillary ligand, L, modifies the activity of these neutral systems. We sought to determine the functional group compatibility of our catalysts as well as increase their reactivity, especially towards olefins less reactive than ethylene (Chapter 4). Initially, we determined the compatibility of **3.1** through screening the polymerization with **3.1** in the presence of various additives.

3.3 The effect of additives on the polymerization of ethylene with Ni^{II} salicylaldimine catalysts

The use of different solvents for the coordination polymerization of ethylene and α-olefins is known to effect both the rate of polymerization and the nature of the products observed with homogeneous metallocene catalysts. The cationic nature of these complexes means that polar species can not only lead to differences in the contact-ion pair distances, but can slow or shut down catalysis through ligation.[1] Neutral complexes, such as **3.5 - 3.6**, with their less electrophilic nature, have demonstrated a greatly increased tolerance towards functionalized species when compared to metallocenes as **3.5** can operate in an aqueous environment and **3.6** in 1,4-butane-diol.[2] However, their behavior can still be greatly affected by the choice of solvent used for the reaction. For example, system **3.5** produces linear α-olefins in toluene, but yields high molecular weight polyethylene in hexane.[3] Given the tolerance of **3.5 – 3.6** to polar species (see Chapter 1), we believed that catalyst **3.1** should be sufficiently tolerant of oxygen and nitrogen functionalities as to allow for the preparation of polyethylene in the presence of polar additives or in a polar media.

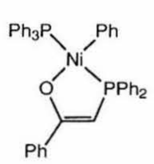

3.5

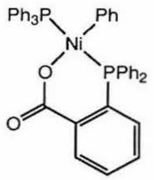

3.6

Catalyst **3.1** was screened for functional group compatibility by performing polymerizations upon the addition of a gross excess of a functionalized additive. Greater than 1000 equivalents of an ether, ester, ketone, alcohol, and even water, did not prevent the polymerization of ethylene by complex **3.1**. As outlined in trials 3.1*b-j*, complex **3.1** is capable of preparing higher molecular weight PE (M_w ~ 30.0-250.0· 10^3 g/ mol) in the presence of such functionalized species. Other reports of similar behavior with [P,O] complexes yield lower molecular weight products or require much higher operating pressures.[4-6]

Table 3.1. Ethylene homopolymerization with **3.1** in the presence of functionalized additives.[a]

Trial	**Functionalized Additive**	**Yield PE (g)**	**TOF[b]**	**M_w (*10^3)**	**PDI (M_w/ M_n)**	**T_m (°C)**	**Branches[c]**
3.1*a*	*None[d],[e]*	66.7	1.02	70.0	5.5	120.1	25
3.1*b*	Et_2O	30.5	0.47	241.0	2.0	135.2	3
3.1*c*	Ethyl Acetate	6.7	0.10	188.0	2.0	136.6	3
3.1*d*	Acetone	10.1	0.15	131.0	3.7	127.8	13
3.1*e*	Water	3.5	0.05	90.1	2.0	129.6	4
3.1*f*	DMF	3.5	0.05	30.0	4.9	126.0	5
3.1*g*	CH_3NO_2	2.8	0.04	140.0	2.4	133.2	5
3.1*h*	Ethanol	0.8	0.01	46.6	3.0	129.2	17
3.1*i*	Triethylamine	0.3	0.01	28.2	2.6	129.3	22
3.1*j*	Pyridine	0	--	--	--	--	--

[a] Polymerization reactions were performed with 65 μmol (0.72 mM) of catalyst **3.1** with 80 mL anhydrous toluene plus 10 mL of the appropriate additive at 100 psig ethylene. Temperature control (T~ 30°C) was maintained through use of an external ice bath. [b] TOF = Turnover Frequency. 10^6 g PE (mol. catalyst^{-1}) (hr.$^{-1}$). [c] Total number of C_1+C_2+C_3+C_4 branches per 1000 carbons. [d] Volume of toluene was doubled during the course of the reaction to a significant increase in the viscosity of the solution. [e] Reaction exothermed uncontrollably, leading to a fluxuation in the reaction temperature.

Table 3.1 outlines a few subtle nuances. As expected, to a first approximation, the rate of polymerization increases as the basicity of the additive decreases (compare all trials to 3.1*a* performed in toluene). The use of weakly coordinating species such as ethers, ketones, and esters, yields high polyethylene returns, high TOFs, and moderate to high molecular weights (trials 3.1*b*-*d*). The use of strongly coordinating bases, however, such as triethylamine and pyridine, lead to the production of only a *trace* amount of PE. As the pyridine complex, **3.3**, demonstrates activity for ethylene polymerization, it appears that the presence of a gross excess of these coordinating additives shifts the equilibrium shown in Figure 3.1 to the left, thereby forcing the catalyst to remain dormant.

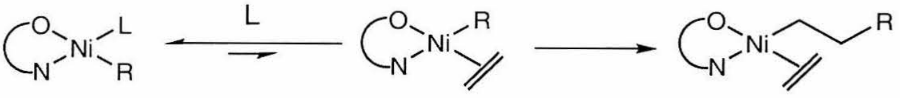

Figure 3.1. The addition of functionalized additives can slow catalysis with **3.1**.

The use of protic solvents, such as water and ethanol (trials 3.1*e* and 3.1*h*), leads to the observation of polymerization in which most of the production occurs at the initial stages of the reaction (~ 10-20 min). Coupled to the low productivity and lower molecular weights of the resultant PE, these results suggest that catalyst **3.1** is decomposing in the presence of protic species, possibly *via* cleavage of the ligand or polymer chain from the metal center. Recently, analogous observations have been postulated as the mode of deactivation for Ni^{II} salicylaldimine catalysts in aqueous-based polymerizations.[7]

Interestingly, the addition of ethereal solvents (trial 3.1*b*) led to products with a higher M_w and lower branch content than trials performed with catalyst **3.1** in toluene (trial 3.1*a*). In order to better understand the nature of this enhancement, we performed a series of polymerizations with various ethers. As outlined in Table 3.2, a number of ethereal additives can be employed during the polymerization of ethylene. There does

Table 3.2. Ethylene polymerization with catalyst **3.1** and ethereal additives.[a]

Trial	Additive	Yield PE (g)	TOF[b]	M_w (*10^3)	PDI (M_w/M_n)	T_m (°C)	Branches[c]
3.2*a*	*None*[d],[e]	66.7	1.02	70.0	5.5	120.1	25[d]
3.2*b*	Anisole	2.5	0.04	184.0	2.6	136.0	4
3.2*c*	$^{n}Bu_2O$	3.2	0.05	184.0	2.3	134.7	4
3.2*d*	Diglyme	6.3	0.10	189.0	2.1	136.4	2
3.2*e*	1,4-Dioxane	9.4	0.14	197.0	2.2	136.5	3
3.2*f*	Tetraglyme	25.4	0.39	179.0	2.4	131.4	5
3.2*g*	THF	25.7	0.39	258.0	2.2	132.6	8
3.2*h*	Triglyme	36.5	0.56	218.0	2.2	134.4	4
3.2*i*	Et_2O[d],[e]	43.0	0.66	165.0	2.2	126.5	34[d]
3.2*j*	DME	70.9	1.09	270.0	2.4	135.5	3

[a] Polymerizations performed with 65 μmol (0.72 mM) of catalyst **3.1** with 80 mL of anhydrous toluene plus 10 mL of the appropriate additive at 100 psig ethylene. Temperature control (T ~ 30 °C) was maintained through use of an external ice bath. [b] TOF = Turnover Frequency. 10^6 g PE (mol. catalyst^{-1}) (hr.$^{-1}$). [c] Total number of C_1+C_2+C_3+C_4 branches per 1000 carbons. [d] Volume of toluene was doubled during the course of the reaction to a significant increase in the viscosity of the solution. [e] Reaction exothermed uncontrollably, leading to a fluxuation in the reaction temperature.

Table 3.3. Polymerization of ethylene with catalysts **3.7-3.11** in the presence of Lewis bases.[a]

Trial	Catalyst	Yield PE (g)	TOF[b]	M_w (*10^3)	PDI (M_w / M_n)	T_m (°C)	Branches[c]
3.3*a*	**3.7**	8.2	0.26	68.0	4.7	120.3	26
3.3*b*	**3.8**	26.0	0.40	257.0	2.4	130.8	16
3.3*c*	**3.9**	14.6	0.22	161.0	6.8	127.8	18
3.3*d*	**3.10**	25.4	0.38	194.0	5.9	129.1	12
3.3*e*	**3.11**	25.8	0.38	72.3	5.7	121.9	19

[a] Polymerizations performed with 65 μmol (0.72 mM) of the appropriate catalyst with 80 mL of anhydrous toluene plus 10 mL of the appropriate additive at 100 psig ethylene. Temperature control (T ~ 30 °C) was maintained through use of an external ice bath. [b] TOF = Turnover Frequency. 10^6 g PE (mol. catalyst^{-1}) (hr.$^{-1}$). [c] Total number of C_1+C_2+C_3+C_4 branches per 1000 carbons.

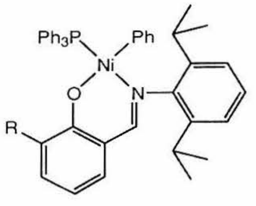

R	
Ph	**3.7**
Phen	**3.8**

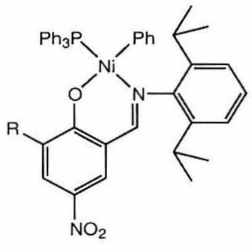

R	
Ph	**3.9**
Phen	**3.10**
10-NO2-Anthr	**3.11**

not appear to be a logical trend to the activity of catalyst **3.1** in the presence of such ethers, as the least basic ether (anisole, trial 3.2b) demonstrates the lowest TOF while polydentate ethers such as DME provide TOFs which rival the activity of **3.1** in toluene.

The polymerizations of ethylene with other Ni^{II} salicylaldimine complexes were investigated in the presence of ethers, such as Et_2O and DME, to determine if similar increases in the molecular weight of the resultant polymer could be observed. As outlined in Table 3.3, results with catalysts **3.7-3.11** are sporadic, indicating in some cases that the addition of ether may change the product distribution. The nature of this "ether effect" is not known, but it is believed that the presence of functionalized additives may act to alter the rate of βHE by solvation of the "active species".

The addition of a thiols, thioethers, and excess pyridine all act to disable complex **3.1** as evidenced by a color change in some cases and the lack of further ethylene uptake. The addition of acids deactivated the catalyst under polymerization conditions, and no polymer was produced. ^1H NMR spectroscopic studies reveal that catalyst **3.1** decomposes *via* protonation of the salicylaldimine ligand and its decomplexation from the metal center.

Excess phosphine leads to a tremendous decrease in the activity of **3.1** as well as the molecular weight of the resultant PE. In addition, the branch contents increases with increasing PR_3 (Table 3.4). For example, 1 equivalent (equiv.) of PPh_3 was added (trial 3.4*b*), the catalyst's activity was cut in half, while 100 equivalents of PPh_3 stopped the polymerization altogether (trial 3.4*f*). Furthermore, when 1 equiv. of tricyclohexylphosphine, PCy_3 (a more basic and coordinating ligand), was added, a more than twofold reduction in catalyst activity was observed. The M_w is observed to decrease dramatically between these trials (from 240.0 to $4.2 \cdot 10^3$ g/mol) while the branch content increases slightly (6 – 47 branches/ 1000).

Similar observations have been observed with (pyca)Ni(PR_3)(*o*-Tol).[8,9] When PR_3 = $P(CH_2Ph)_3$ **3.12**, PCy_3 **3.13**, $PMePh_2$ **3.14**, and PMe_2Ph **3.15**, linear oligomeric products are formed at 40 bar. When PR_3 = PPh_3 **3.16**, higher molecular weight polyethylene is obtained. However, in the presence of excess PPh_3, the rate of oligomerization with **3.16** as well as the molecular weight are observed to decrease. The researchers argued that the extent of phosphine control over the nature of the active species suggests that the phosphine remains coordinated in oligomerization trials with **3.12-3.15** (Figure 3.2). Insertion was postulated to occur through a four-coordinate intermediate with **3.16** in the absence of free ligand, however, the addition of excess PPh_3 drives catalyst **3.16** to the oligomerization cycle on the left of Figure 3.2, leading to the production of low M_w products.

Table 3.4. The Polymerization of Ethylene with **3.1** in the Presence of Excess PR_3 (R = Ph, Cy).[a]

Trial	**PR_3**	**Eq. PR_3**	**Yield (g)**	**TOF[b]**	**M_w ($x10^3$)**	**PDI**	**Branch Content[c]**
3.4a	*None*	0	30.5	0.348	237.0	2.2	6
3.4b	PPh_3	0.1	18.0	0.205	194.0	2.2	7
3.4c	PPh_3	1.0	4.2	0.048	158.7	2.1	8
3.4d	PPh_3	5.0	0.7	0.008	78.4	2.1	10
3.4e	PPh_3	10.0	0.2	0.002	4.2	1.6	47
3.4f	PPh_3	100.0	0	--	--	--	--
3.4g	PCy_3	1.0	0.8	0.009	103.0	3.4	5

[a] Polymerizations performed at 100 psig (~6.7 atm) ethylene, 67 μmol (0.61 mM) catalyst **3.1**, the appropriate amount of PR_3, 90 mL anhydrous toluene, T ~ 25.0 °C. [b] TOF = Turnover Frequency = 10^6 g PE (mol. cat^{-1}) (hr^{-1}). [c] Total number of $C_1+C_2+C_3+C_4$ branches per 1000 carbons.

A study on the influence of various phosphine ligands on the activity and selectivity of phenyl (2-diphenylphosphanylphenolato) (phosphine) Ni^{II} catalysts reached similar conclusions.[10] It was established that complexes containing weakly bound phosphines (such as PPh_3, $P(p\text{-}Tol)_3$, $P(p\text{-}X\text{-}C_6H_4)_3$ (X = Cl > Me > F)) yielded α-olefins of higher molecular weight, whereas complexes with strongly coordinated ligands, such as PMe_3, PMe_2Ph, and PCy_3 gave lower molecular weight α-olefins (C_4 to C_{24}) with a much lower catalytic activity.[10]

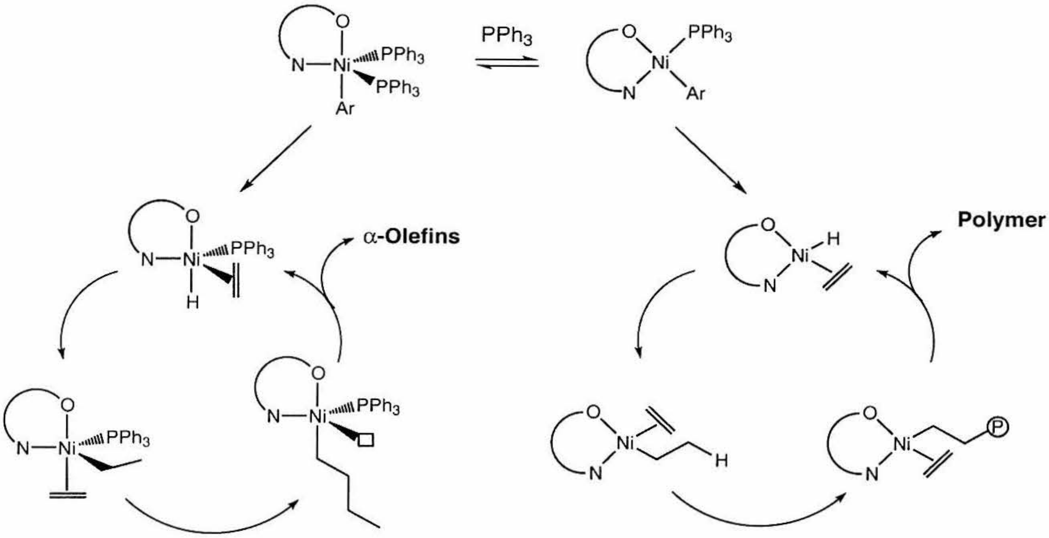

Figure 3.2. Proposed mechanism for the production of both low and high molecular weight products with **3.12-3.16**. Mechanism **A**—insertion from a five-coordinate species produces low M_w at low rates. Mechanism **B**—insertion from four-coordinate species yields high M_w with high TOFs.

It is possible that catalyst **3.1** operates by two mechanisms, inserting ethylene from both four- and five- coordinate species. As outlined in Chapter 2, the low initiation efficiency of catalyst **3.1** indicates that a very small percentage of the complex initiates, which we believed indicated that a small amount of the four coordinate olefin species, $[O,N]Ni(CH_2CH_2)H$, is generated and consumes ethylene rapidly. However, the observation of a postulated 18e$^-$ hydrido species $[O,N]Ni(PCy_3)H$, suggests that the formation of a five-coordinate species is feasible, and therefore, prohibits the dismissal of mechanism A (Figure 3.2).

3.4. Phosphine Exchange Studies.

As excess PPh_3 and PCy_3 act to slow catalyst **3.1** during polymerization, we sought to determine the behavior of **3.1** upon addition of these phosphines. The addition of up to 10 equivalents of PPh_3 provided a complete lack of any NMR evidence for ligand exchange or dissociation, even upon warming to 100 °C. However, the addition of two equivalents of PCy_3 to a C_6D_6 solution of **3.1** led to complete phosphine exchange overnight at 80 °C, yielding the tricyclohexylphosphine analog **3.17**.

To determine the mechanism of this exchange, we monitored the kinetics of the exchange at a variety of temperatures. Assuming that the process is first order in both [**3.1**] and [PCy_3], allows for the determination of second-order rate constants ($M^{-1}s^{-1}$) at different temperatures through monitoring the disappearance of **3.1**/appearance of **3.17** by ^1H NMR (Figure 3.3(a)).

Table 3.5. Exchange rates for complex **3.1** with PCy_3.[a]

Trial	Temp (°C)	Rate (M^{-1} s^{-1})
3.5*a*	50	$9.70\cdot 10^{-6}$
3.5*b*	62	$3.56\cdot 10^{-5}$
3.5*c*	70	$1.45\cdot 10^{-4}$
3.5*d*	78	$3.47\cdot 10^{-4}$

[a] Conditions: [2.5 mM] Complex 3.1, 0.6 mL C_6D_6, [2.6 mM] (1.04 equiv.) PCy_3, at the appropriate temperature.

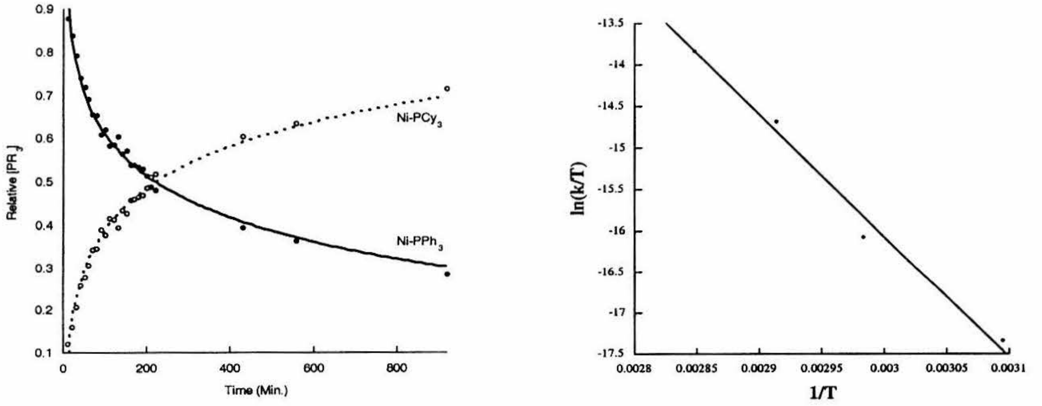

Figure 3.3. Exchange reaction between **3.1** and PCy_3. (a) Monitoring the change in concentration of **3.1** and **3.17** vs. time. (b) Eyring plot of the rates in Table 3.5.

The Eyring plot, shown in Figure 3.3(b), provides the enthalpic and entropic terms for this exchange process ($\Delta S^\ddagger = 7.4$ cal: mol^{-1} K^{-1}, $\Delta H^\ddagger = 28.8$ kcal mol^{-1}, $\Delta G^\ddagger_{298} =$ 26.6 kcal mol^{-1}). The high positive values for $\Delta S^\ddagger$ suggest the reaction proceeds through a dissociative pathway as shown in Figure 3.4(a), and not by an associative pathway as shown in Figure 3.4(b).[11]

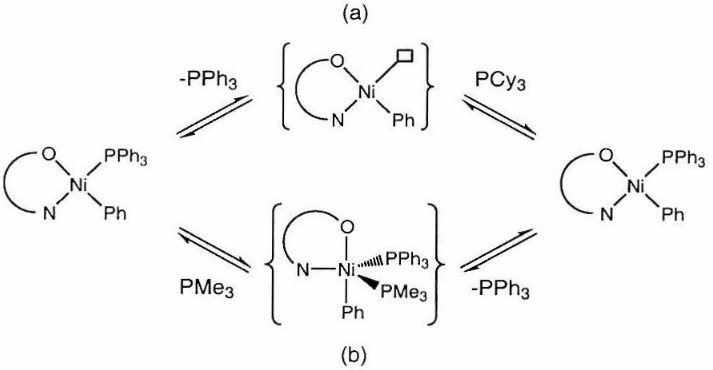

Figure 3.4. Mechanism of phosphine exchange with complex **3.1**. (a) Dissociative pathway. (b) Associative pathway.

Obviously, however, the exchange of **3.1** with a large, electron-rich phosphine such as PCy_3 (pK_a PCy_3H^+ ~ 9, cone angle ~ 170°)[11] may proceed through a different mechanism than coordination of ethylene, a small, π-donating ligand. In combination with the fact that PPh_3 exchange is not observed by ^{1}H NMR under any conditions with **3.1**, the extreme differences in rate between ethylene coordination ($>>10^4$ M^{-1} s^{-1}) and PCy_3 coordination ($<<10^{-6}$ M^{-1} s^{-1}) at room temperature suggest that these exchange processes may operate by different mechanisms.

Further support for the operation of two mechanisms comes from observations made upon the addition of PMe_3 and PEt_3 to complex **3.1**. These phosphines are similar in basicity to PCy_3 (pK_a PR_3H^+ ~ 9) but maintain much smaller sizes, with cone angles of ~ 104° and 114°, respectively.[11] The addition of 1.1 equivalents of PMe_3 to a solution of **3.1** in CD_2Cl_2 leads to the observation of instantaneous exchange at –78 °C, yielding **3.18**. Warming this sample to room temperature leads to the observation of rapid exchange between the 0.1 equivalents of excess PMe_3 and **3.18**. The addition of PEt_3

under similar conditions led to the complete formation of **3.19** within 20 minutes at –78 °C. Although the enthalpic and entropic numbers were not obtained for these reactions, their rapid rate and the observation of dynamic exchange at room temperature suggest that an associative pathway (such as that depicted in Figure 5.4(b)) is operational. These results indicate that both dissociation or displacement can occur in such Ni^{II} salicylaldimine complexes. These observations are in line with those made for **3.16**, where variation of the ligand set led to an observed changes in the mechanistic pathway.[9]

3.5. Synthesis of phosphine-free catalysts

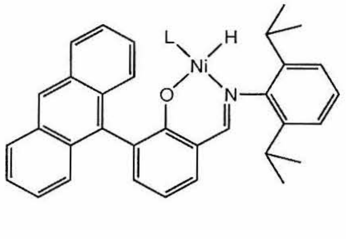

3.2

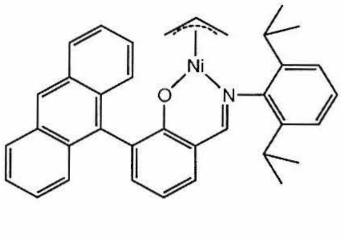

3.3

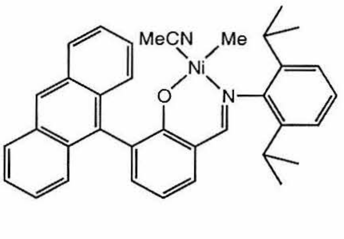

3,4

The addition of PR_3 to catalyst **3.1** is suggested to occur through phosphine dissociation or displacement. As the activity of catalyst **3.1** is directly correlated to the concentration of PPh_3 (Table 3.4), we believed that catalysts with increased TOFs or efficiency could be prepared through replacement of the coordinated "soft" base (PPh_3) in **3.1** with a "harder" ligand, such as an ether, nitrile, pyridine, or amine. Another possibility would be the use of η^3-allylic or η^5-cyclopentadienyl type ligands which could serve to both stabilize the precursor and act as the initiation site.

Several methods were envisioned as possible routes into these "phosphine-free" complexes through adaptation of methods used for the preparation of [P,O] (SHOP)-type complexes. First, the oxidative addition of the phenolic ligands to a Ni^0 source, such as $Ni(COD)_2$ or $Ni(PPh_3)_4$, could yield a complex of the type, [N,O]Ni(L)H, which were shown in Chapter 1 to successfully serve as a polymerization initiators. Second, reaction of the phenolic ligand with nickelocene, Cp_2Ni, could liberate an equivalent of cyclopentadiene and generate [N,O]NiCp. [P,O] complexes of this nature have demonstrated the ability to serve as oligomerization catalysts. Thirdly, the preparation of an [N,O]Ni(η^3-allyl) compound by reaction of the sodium salt of the ligand with [(η^3-

allyl)Ni(μ-X)]$_2$. Finally, it was believed that the reaction of the phenolic ligand with one of a few "stable" d^8 dialkyl complexes such as (phen)NiMe$_2$ or (tmeda)NiMe$_2$,, might lead to the liberation of methane and ligation of the desired phenol. The later two methods have proved to be successful in preparing a variety of square planar, (^{Anthr,H}Sal)NiCH$_3$(L) compounds where L was pyridine or nitrile.

3.6. *Oxidative addition of the Ligand to Ni^0 source*

Attempts to prepare a Ni^{II} hydrido species in a fashion analogous to those commonly employed for [P,O] ligands,[3,12,13] namely oxidative addition of the phenol to a Ni^0 source have thus far been unsuccessful. For example, the addition of the ^{Anthr,H}SalOH ligand to an equimolar solution of Ni(COD)$_2$ in 0.7 mL (0.1 mM) of anhydrous C_6D_6 led to no detectable reaction over the course of a week at room temperature. Heating the solution to 60 °C led to the observation of the free phenol and decomposition of the Ni(COD)$_2$. Attempts to perform such an oxidative addition through reaction of the phenol with Ni(PPh$_3$)$_4$ were similarly unsuccessful. These results may suggest that thermodynamics disfavors the formation of a [N,O]Ni(L)H where L is not a sterically demanding phosphine such as PCy$_3$ or PPh$_3$ (see Chapter 2).

3.7. *Salicylaldimine π-Allylic and η^5-cyclopentadienyl compounds of Ni^{II}—Ineffective initiators for ethylene polymerization*

Compounds of Ni^{II} containing π-allylic groups have had a large role in oligomerization, polymerization, and cyclization by group ten complexes ("nickel effect").[14] In fact, the addition of alkylaluminum reagents to Ni(PR$_3$)(η^3-allyl)Br led to a species capable of polymerizing ethylene and oligomerizing propylene. We believed that the preparation of Ni^{II} allylic species with the sterically demanding (^{Anthr,H}Sal) ligand might allow for the facile preparation of highly-active phosphine-free systems. Additionally, several [P,O] complexes containing η^5-cyclopentadienyl groups have been prepared and used as precatalysts for the oligomerization of ethylene by addition of the appropriate acylmethylphosphine, Ph$_2$PCH$_2$C(O)R to Cp$_2$Ni. Liberation of cyclopentadiene leads to formation of the appropriate [P,O]Ni(η^5-Cp) adduct which is believed to initiate by "slipping" to the [P,O]Ni(η^3-Cp) followed by insertion of ethylene into the Ni-cyclopentadienyl bond.

The π-allylic Ni^{II} salicylaldimine complex, **3.20**, was easily prepared in one step through combination of Cs(^{Anthr,H}Sal) with the [(η^3-allyl)NiX]$_2$ dimer (where X = Cl or Br) in C_6H_6. The reaction proceeded to completion within minutes at 25 °C as determined by ^{1}H NMR through observation of the disappearance of the starting materials. Isolation of the allyl compound was accomplished by filtration of the reaction mixture through a celite plug to remove unwanted Cs salts, followed by removal of the remaining solvent, yielding the desired product as a yellow powder in ~ 54% yield. Several attempts were made to recrystallize **3.20**, with the only success being the use of pentane at – 40 °C, which provided small yellow crystals of the desired product over the course of a week (albeit in low yield).

Several peaks in the ^{1}H NMR These include *two* septets (δ= 3.30/ 3.57, 1H, $^3J_{HH}$ = 6.9 Hz, –C*H*MeMe') and *four* doublets (δ= 1.20/ 1.23/ 1.26/ 1.31, 3H, $^3J_{HH}$ = 6.9 Hz, –CH*MeMe'*) which indicate that the equatorial plane does not serve as a plane of symmetry for the molecule. Four of the π-allylic substituents resonate in the δ= 2.2-3.1 ppm range, while the methine is clearly observed as a complex multiplet at δ= 5.35 ppm. Such splitting patterns indicated that the lowest energy geometry is that containing the allyl moiety perpendicular to the equatorial plane, in good agreement with other salicylaldimine d^8 (M= Ni, Pd) allylic complexes. None of the resonances displayed any sign of broadening, suggesting that the structure is static at 25 °C on the NMR timescale.

Unfortunately, these easily prepared complexes are inactive for the polymerization of ethylene under the conditions tested. For example, pressurization of a solution of **3.20** to 120 psig of ethylene at 40 °C led to little ethylene consumption and no sign of α-olefin or polymer production. As the reaction was not observed to darken, suggesting that decomposition does not occur, we attributed this lack of reactivity to the inability of complex **3.20** to insert ethylene into the robust p-allylic group.

The addition of the ^{Anthr,H}Sal ligand to nickelocene, NiCp$_2$, did not lead to the formation of any product. In fact, no reaction was observed between the phenol and NiCp$_2$ after two weeks at 80 °C in C_6D_6.

3.8. Pyridine and lutidine (2,6-dimethylpyridine) complexes

Several attempts were made to afford a pyridine/aryl complex of the type [N,O]Ni(Py)Ph *via* the addition of pyridine-N-oxide to a solution of complex **3.1** in C_6D_6. It was hoped that dissociation of the PPh_3, might lead to its oxidation to phosphine-N-oxide, and lead to the generation of the pyridine adduct **3.21**. However, addition of either equimolar or excess pyridine-N-oxide to complex **3.1** in C_6D_6 led to the observation of only a trace amount of new product after a week at 75 °C.

Owing to our inability to prepare such phosphine-free complexes from Ni^0 or $Ni^{II}(PPh_3)$ sources, we attempted to react the phenolic ligands with $Ni(tmeda)Me_2$ in the hope of liberating methane and leading to the formation of the desired complex.

$Ni(tmeda)Me_2$ was prepared by literature methods through the reaction of $MgMe_2$ with $Ni(tmeda)(acac)_2$. It is a highly-sensitive precursor, and must be stored in an anaerobic environment in the solid-state at low temperature (-30 °C). The addition of the $^{\text{Anthr,H}}$Sal ligand to in pyridine or lutidine (2,6-dimethylpyridine) solution leads to formation of the monomethyl adducts **3.22** and **3.23**, respectively, with concomitant liberation of CH_4. The products crystallized from solution as brownish-red crystals.

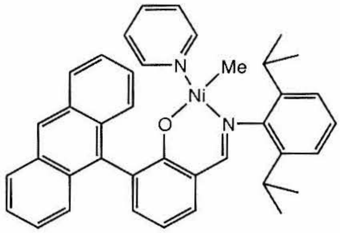

3.22

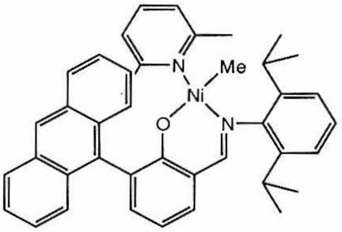

3.23

The ^1H NMR of **3.22** and **3.23** is similar in nature to those described for **3.1** in Chapter 2. The Ni-Me signal is found to resonate upfield of TMS at $\delta \sim -1.25$ (similar to the major species of **5.26** outlined below). Two doublets and a septet are observed for the $-CHMe_2$ groups of the substituted benzimine, suggesting that the complexes are square planar with an equatorial mirror plane cutting perpendicular to the benzimine group. In addition, a *trans-* relationship is believed to be the geometry of the complex as the $-CH{=}NAr$ groups show similar chemical shifts to those observed in **3.1**.

Surprisingly, complexes **3.22** and **3.23** exhibit poor activity in the polymerization of ethylene. Their TOFs are approximately one order of magnitude lower than those obtained with **3.1** under the same conditions.

3.9. Ethers—THF and Et_2O

Several attempts were made to prepare complexes where L = Et_2O (**3.24**) or THF (**3.25**) *via* the addition of 1 equivalent of the phenolic (^{Anthr,H}Sal) ligand to (tmeda)NiMe_2 in the appropriate ethereal solvent. ^1H NMR studies suggested that the preparation of these adducts were unsuccessful—leading to decomposition, which may be attributed to the weak basicity of the sp^3-hybridized ethers. These results agree with the fact that catalyst **3.1** is highly active for the polymerization of ethylene in THF or Et_2O (*vide supra)* and are in good agreement with the equilibrium described in Figure 3.1.

Similar observation have been made for cationic d^8 complexes. For example, attempts to prepare $\{[N,N]Pd(OEt_2)Me\}[B(Ar_f)_4]$ through halide abstraction of the precursor, [N,N]PdMeCl, in Et_2O led to the sole isolation of the chloride-bridged dimer, $\{[N,N]PdMe(\mu\text{-}Cl)\}_2[B(Ar_f)_4]$.[15]

3.10. Acetonitrile complex

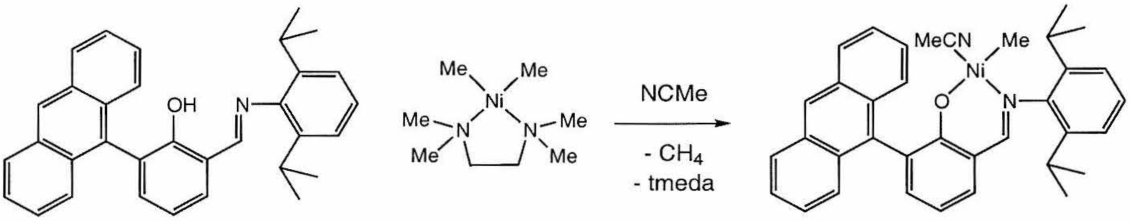

The use of nitriles, such as CH_3CN or PhCN, as labile ligands for d^8 polymerization catalysts, such as $\{Pd(NCMe)_4\}[BF_4]_2$, is well-documented. [1,15] We hoped that the use of these ligands might allow for the easy preparation of a stable phosphine-free system and, yet, generate a catalyst which exhibited *increased* activity relative to complex **3.1**. The nitrile complex **3.26** was prepared by mixing 1 equivalent of the (^{Anthr,H}Sal) ligand with (tmeda)NiMe_2 in ~ 0.05 M

Figure 3.5. X-ray analysis of Ni^{II} salicylaldimine complex **3.26**. Thermal ellipsoids are shown at 30% probability. All non-essential hydrogen atoms have been omitted for clarity.

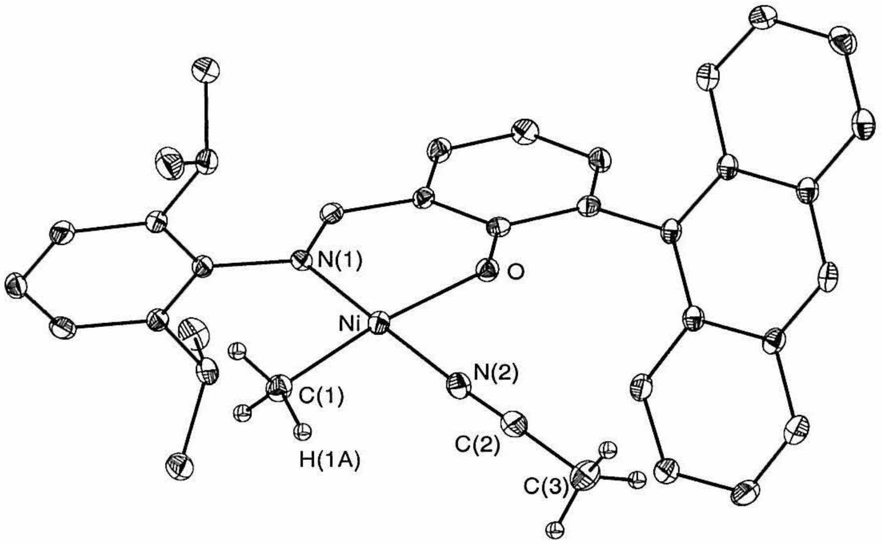

Table 3.6. Important bond lengths (Å) and bond angles (°) for complex **3.26**.

Bond Lengths (Å)

Ni-N(1)	1.8872(16)	Ni-O	1.9107(13)
Ni-N(2)	1.8588(19)	Ni-C(1)	1.931(2)

Bond Angles (°)

N(1)-Ni-O	94.12(6)	N(1)-Ni-N(2)	177.34(7)
N(1)-Ni-C(1)	92.88(9)	O-Ni-N(2)	83.87(6)
O-Ni-C(1)	172.72(9)	N(2)-Ni-C(1)	89.07(9)
N(2)-C(2)-C(3)	178.3(3)	Ni-C(1)-H(1A)	109.3(11)

anhydrous acetonitrile. The evolution of gas (methane) was observed over the course of 2-3 hours at room temperature. After sitting overnight at room temperature (~ 10 hours), X-ray quality reddish-brown crystals of **3.26** deposited from the solution allowing for confirmation of the structure of **3.26** as shown in Figure 3.5.

In analogy to the structure of complex **3.1** (Chapter 2), the nitrile complex 3.26 sits in a square planar arrangement containing C(1), N(1), O, and N(2). The 9-anthracenyl and 2,6-diisopropyl phenyl groups are approximately perpendicular to the equatorial plane, but the departure away from 90° is in accord with an environment that is less crowded than in complex **3.1**.

^{1}H NMR spectroscopy of complex **3.26** demonstrates the presence of two *isomers*- (3:1 ratio) with Ni-Me resonances at $\delta = -1.53$ and -0.98 (CD_2Cl_2). The major isomer in solution is the *trans*- isomer as evidenced by dissolution of crystals used for the structural determination at low temperature and ^{1}H NOE spectroscopy experiments on **3.26**. The isomeric ratio was not found to change with temperature, remaining 3:1 from –40 °C to 30 °C. Using equation (3.1) and the relative abundances of both the *cis*- and *trans*- isomers at 298 K, difference in ground state energies of 0.65 kcal/mol.

$$\Delta(\Delta G^\circ) = -RT[\ln(K_{cis/trans})] \sim 0.65 \text{ kcal/mol} \quad (3.1)$$

3.11. Study of Isomerization with ^{1}H NMR Magnetization Transfer Techniques

Magnetization transfer experiments allow for the determination of rates which occur slower than those accessible by line broadening analysis. The range of actual rate constants which can be obtained depend on the relaxation rates of the nuclei of interest. The magnetization transfer is accomplished by inverting the appropriate ^{1}H NMR signal (or population) at one of the exchanging sites and watching the inverted population "wash" into the second exchanging site. As shown in Figures 3.6 and 3.7, magnetization transfer techniques were used to successfully observe *cis-/trans-* isomerization in complex **3.26**.

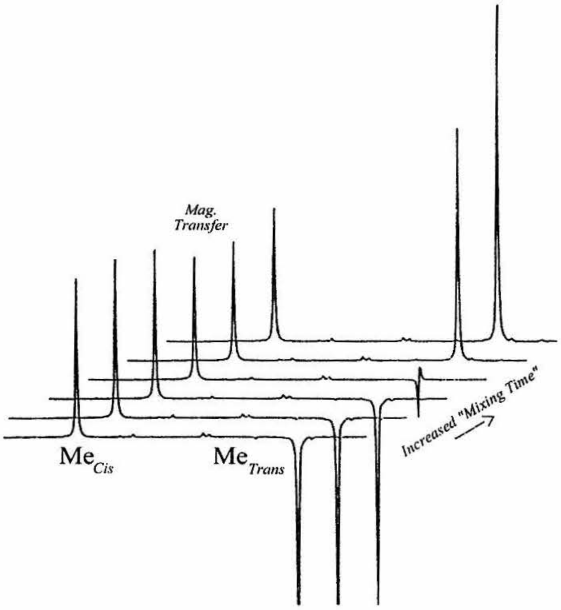

Figure 3.6. Magnetization transfer experiments between *cis*- and *trans*- isomer of **3.26.**

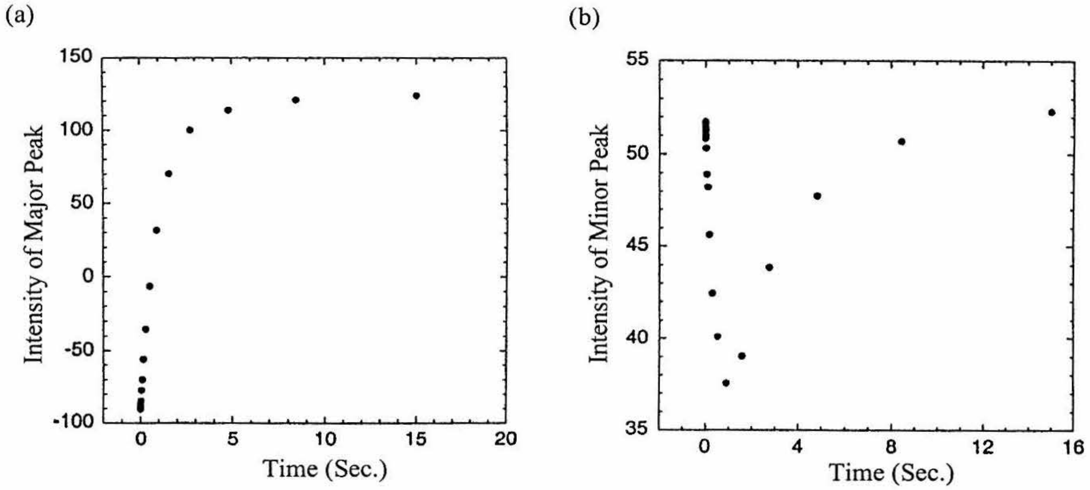

Figure 3.7. Magnetization transfer from major {*trans*- **(a)**} to minor {*cis*- **(b)**} isomer. [**3.26**] = 40 μmol. T = 10 °C in CD_2Cl_2.

By determining the rates a variety of temperatures (between –20 °C and 10 °C) an estimate for the barrier to isomerization was obtained ($\Delta G^{\ddagger}$ ~ 17 kcal/mol). As the addition of excess acetonitrile did not lead to any observed change in the rate of isomerization, we propose that *cis-/trans-* isomerization for **3.26** occurs through a tetrahedral species as depicted in Figure 3.8. The nature of this isomerization is still under intense investigation in our group as it may provide catalysts with increased activity or higher molecular weight products (Chapter 5).

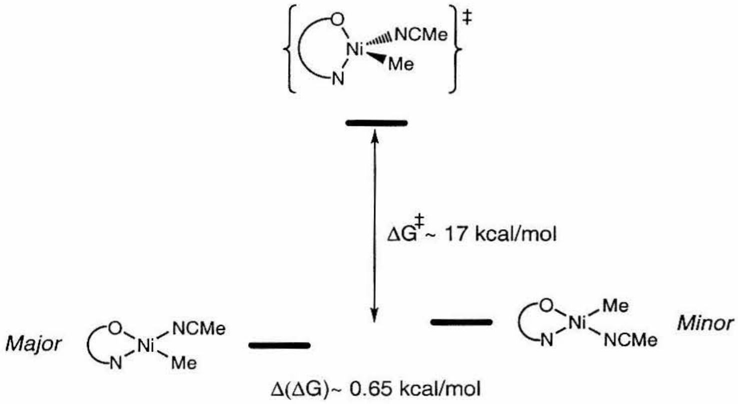

Figure 3.8. Proposed mechanism of *cis-/trans-* isomerization in **3.26**.

Complex **3.26** is generally found to be less stable than the analogous phosphine catalyst **3.1**. It can be stored for a prolonged period of time under an inert atmosphere at –20 °C, but will decompose in the solid state at room temperature over a few weeks. In contrast to **3.1**, it appears to be mildly sensitive to the atmosphere when in solution. The observation of ^{1}H NMR signals at $\delta \sim -7$ to -10 suggests that Ni-OH species are formed in some cases (Chapter 2). In addition, bis(salicylaldimine) complexes (*vide infra*) are occasionally observed with the decomposition of **3.26**.

Catalysts **3.26** is highly active for the polymerization of ethylene. Table 3.7 compares both catalyst **3.1** and **3.26** against the neutral SHOP-type complex, **3.5**, and the cationic Ni^{II} (**3.27**) and Fe^{II} (**3.28**) complexes outlined in Chapter 1.

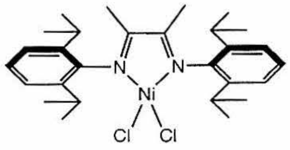

3.27

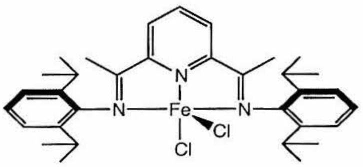

3.28

Table 3.7. Comparison of neutral Ni^{II} salicylaldimine catalysts **3.1** and **3.26** to other late-metal oligomerization/polymerization systems.[a],[b]

Trial	**Catalyst**	**TOF** **(g PE) (mol cat^{-1}) (hr^{-1})**	**M_w (10^3)**	**PDI**	**Branches[b]**
3.7*a*	**3.1** [a]	$1.2 \cdot 10^6$	190.0	11.7	15
3.7*b*	**3.26** [a]	$4.0 \cdot 10^6$	88.2	12.6	18
3.7*c*	**3.5** [a]	***$4.4 \cdot 10^4$***	***2.6***	1.5	12
3.7*d*	**3.1** [b]	$1.0 \cdot 10^6$	236.0	2.2	5
3.7*e*	**3.26** [b]	$2.1 \cdot 10^6$	56.0	10.9	9
3.7*f*	**3.27** [c]	$1.2 \cdot 10^6$	132.0	1.3	***86***
3.7*g*	**3.28** [c]	$2.3 \cdot 10^6$	34.4	18.3	**<1**

[a] Polymerization performed in a steel autoclave with 1000 mL benzene at 500 psig ethylene at 40 °C. [b] Polymerization performed in 90 mL toluene at 100 psig ethylene at 40 °C. [c] Same conditions as (b) plus 1000 eq. MMAO (in toluene) employed as cocatalyst. Total volume = 90 mL toluene. [d] Total number of C_1+C_2+C_3+C_4 branches per 1000 carbons as determined by ^{13}C NMR.

As clearly outlined in **Table 3.7**, all of the complexes except the [P,O]-based SHOP system, **3.5**, exhibit similar abilities to prepare high molecular weight PE. Neutral complexes **3.1** and **3.26** as well as the cationic complexes **3.27-3.28** provide very high activities, on the order of $1 \cdot 10^6$ g PE· (mol.cat^{-1}) · (hr^{-1}). Similar molecular weights were obtained under these conditions. A notable difference, however, is observed in the branch content of the resulting polymers. The cationic Fe^{II} system, **3.28**, provides a perfectly linear polymer, whereas **3.1** and **3.26** yield polymers with a low/moderate branch content and **3.27** provides high levels of branching.

3.12. Polymerizations of ethylene with ligands of reduced steric demand – in situ polymerizations and attempts to prepare well-defined complexes

Attempts to reduce the steric demand of the salicylaldimine ligand led to an interesting results. The addition of salicylaldimine ligands such as **3.29** (2,6-H) or **3.30** (2,6-Me), leads to rapid formation of the bis(salicylaldimine) complex **3.31** and **3.32**

Figure 3.9. X-ray analysis of Ni^{II} salicylaldimine complex **3.31**. Thermal ellipsoids are shown at 30% probability. All non-essential hydrogen atoms have been omitted for clarity.

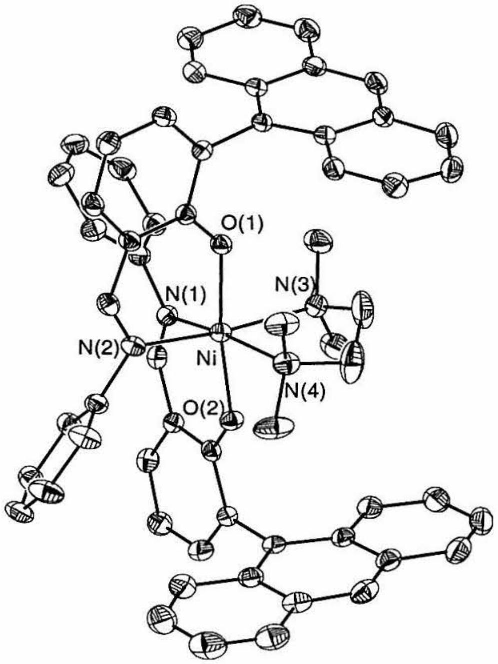

Table 3.8. Selected bond lengths (Å) and bond angles (°) for complex **3.31**.

Bond Lengths (Å)

Ni-O(1)	1.9959(11)	Ni-O(2)	1.9991(11)
Ni-N(1)	2.1289(14)	Ni-N(2)	2.1383(14)
Ni-N(3)	2.2517(14)	Ni-N(4)	2.2263(14)

Bond Angles (°)

N(1)-Ni-O(1)	96.84(5)	N(1)-Ni-O(2)	87.67(5)
N(1)-Ni-N(3)	91.34(5)	N(1)-Ni-N(4)	168.98(6)
O(1)-Ni-N(3)	84.20(5)	O(1)-Ni-N(4)	92.10(5)

respectively. The structure of **3.31** was confirmed by X-ray analysis as shown in Figure 3.9.

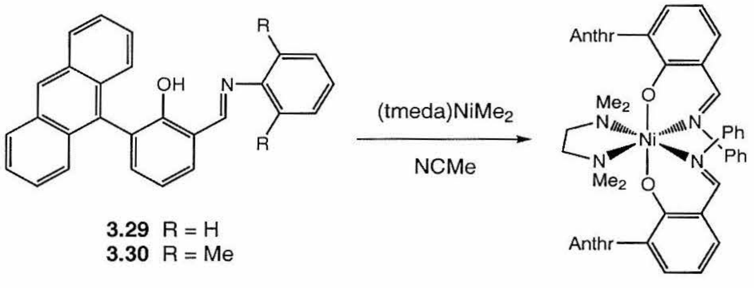

3.29 R = H
3.30 R = Me

3.31

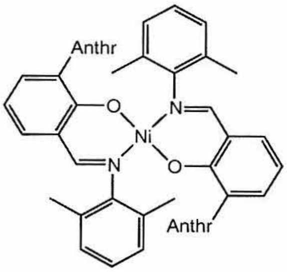

3.32

Although attempts to prepare such bis(salicylaldimine) structures using (tmeda)$NiMe_2$ and two equivalents of the ^{Anthr,H}Sal ligand have not led to the recovery of the analogous complex **3.33**, some signs of such a process were observed in the ^1H NMR as the resonances for Ni-CH_3 and Ar-OH are observed to decrease as a new septet $\delta \sim 5$ ppm grows into the spectra. This species has been identified as **3.33** by an independent synthesis.

The addition of 1 eq. of (^{Anthr,H}Sal)Na to $Ni(PPh_3)_2$C12 leads to the formation of **3.33** in 50% yield. The reaction medium instantly changes to a deep orange color upon addition of the sodium salt, which may indicate the formation of **3.34**. Upon concentration, however, the color darkens to a greenish-brown and the recovered material contains ~ 50% of (unreacted?) $Ni(PPh_3)_2Cl_2$ and 50% of **3.33** (structure confirmed by X-ray analysis—see Figure 3.10). These observations suggest that disproportionation of **3.34** leads to the formation of **3.33**.

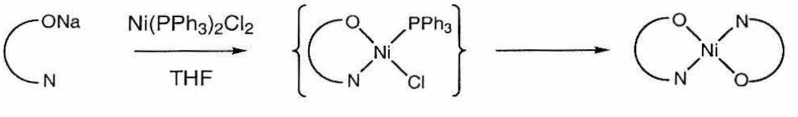

3.34 **3.33**

Of significant note is the fact that **3.33** is unstable to moisture, which greatly contrasts the behavior of other bis(salicylaldimine) complexes of d^8 metals. This may be a consequence of the size of the ligand which acts to destabilize **3.33**. In fact, a

Figure 3.10. X-ray analysis of Ni^{II} salicylaldimine complex **3.33**. Thermal ellipsoids are shown at 30% probability. All non-essential hydrogen atoms have been omitted for clarity.

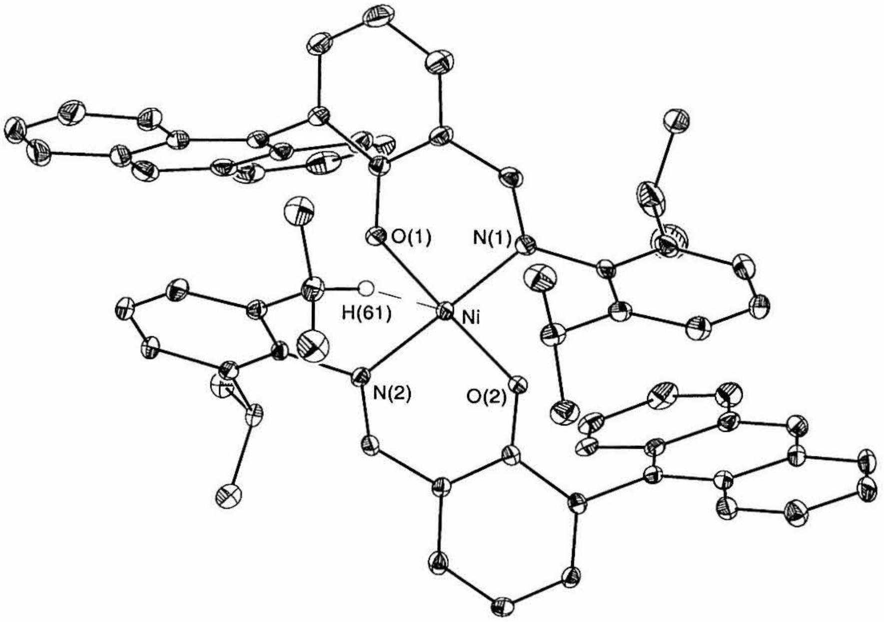

Table 3.9. Selected bond lengths (Å) and bond angles (°) for complex **3.33**.

Bond Lengths (Å)			
Ni-N	1.937(4)	Ni-O	1.910(3)
Ni-P	2.172(2)	Ni-C(31)	1.895(5)
Bond Angles (°)			
N-Ni-O	94.5(2)	N-Ni-P	172.16(12)
N-Ni-C(31)	93.5(2)	O-Ni-P	87.51(11)
O-Ni-C(31)	166.2(2)	P-Ni-C(31)	86.0(2)

comparison of the structure of **3.33** with that of $(^{H,H}Sal)_2Ni$ **3.35** (Appendix E) demonstrates that the bulky groups of the ligand lead to a significant distortion from a square planar geometry (31.2°), providing insight as to how to stabilize **3.1** and **3.26** from forming such decomposition products.

Similar observations have been observed for a variety of Ni^{II} alkyl complexes. For example, heating a pyridine solution of $NiCH_2CH_3(acac)PPh_3$ to 70 °C leads to a disproportionation reaction as outlined in Eq. (3.2).[16] The disproportionation is believed to produce $(PPh_3)_2Ni(CH_2CH_3)_2$ which liberates an equivalent of ethane. In addition, attempt to prepare [P,O] SHOP-type systems by the oxidative addition of the appropriate ligand to $Ni(COD)_2$ or addition of the appropriate phenol to NiCp2 have led to the discovery of trace amounts of the bis(ligand) structure, *cis*-$[Ni(Ph_2P(o\text{-}C_6H_4O)]$, as a minor biproduct.[10]

$$2\ NiCH_2CH_3(acac)(PPh_3) + 2\ Py \rightarrow Ni(acac)\cdot 2Py + (PPh_3)_2Ni(C_2H_4) + C_2H_6 \qquad (3.2)$$

3.13. Conclusions

The activity of Ni^{II} salicylaldimine catalyst **3.1** in ethylene polymerizations was found to increase as the relative basicity of the ancillary ligand, L, decreases, such that activity increases in the order:

$$Cy_3P{=}CH_2 < Ph_3P{=}CH_2 < Cy_3P < Py \sim Lut < Ph_3P < Et_3N < NCMe < THF \sim OEt_2$$

Ligand exchange reactions between complex **3.1** and different phosphines led to evidence that the catalyst can operate by both an "associative" and "dissociative" mechanism. Combining this knowledge and the lessons learned about which polar functionalities are detrimental to the success of **3.1**, we set out to prepare a variety of "phosphine-free" complexes. The η^3-allylic compound, **3.20**, was found to be catalytically inactive under all conditions tested. We attribute this to an inability of such a species to initiate since no decomposition is observed. The use of allyl species with an increased propensity to initiate may yield salicylaldimine complexes of Ni^{II} which are active for ethylene polymerization at lower pressures in the absence of a cocatalyst.

Pyridine and lutidine adducts, **3.22-3.23**, were successfully prepared. They unexpectedly exhibited lower TOFs than **3.1**, but are also increasingly stable than other "phosphine-free" complexes, further support for the equilibrium presented in Figure 3.1.

The nitrile catalyst **3.26** exhibits very high rates in ethylene polymerization, two- to four-fold greater than **3.1** under identical conditions. Complex **3.26** exists in solution as two isomers, with the major species as the *trans-* isomer. The difference in their ground state energies, $\Delta(\Delta G^{\circ})$ = 0.65 kcal/mol at 298 K. The barrier to their isomerization, $DG^{\ddagger} \sim 17$ kcal/mol, was determined using ^{1}H NMR magnetization transfer techniques. As the addition of free acetonitrile did not change the rate of isomerization drastically, we propose that the isomerization proceeds through a tetrahedral intermediate. The nature of this isomerization and the energy difference between the two isomers may have a substantial impact on the performance of neutral Ni^{II} catalysts (see Chapter 5).

Several attempts were made to prepare complexes containing less steric demand than those imparted by the ^{Anthr,H}Sal ligand. However, when the steric demand is decreased on either side of the ligand, the thermodynamic driving force is the production of the bis(salicylaldimine) structures **3.31-3.33**. The nature of this disproportionation reaction provides insight about the mode of deactivation of catalyst **3.1** and **3.26**.

Table 3.10. Crystal Data and Structure Refinement for **3.26**, **3.31**, **3.33**, and **3.35**.

	3.26	**3.31**	**3.33**	**3.35**
Empirical Formula	$C_{36}H_{36}N_2NiO$	$C_{60}H_{52}N_4Ni\ O_2$	$C_{66}H_{60}N_2NiO_2$ $2(CH_3CN)$	$C_{38}H_{44}N_2NiO_2$
Formula Weight	571.38	919.77	971.91 (82.06)	619.46
Crystallization Solvent	Acetonitrile	CH_2Cl_2/ CH_3CN	CH_3CN	CH_3CN
Crystal Habit	Blade	Needle	Thin chunk	Rhomboid
Crystal Color	Dichroic yellow/brown	Greenish-yellow	Dark Brown	Olive Green
Crystal Dimensions (mm^3)	0.36 x 0.22 x 0.06	0.37 x 0.22 x 0.19	0.259 x 0.185 x 0.148	0.37 x 0.27 x 0.185
Wavelength	0.71073 Å MoKα	0.71073 Å MoKα	0.71073 Å MoKα	0.71073 Å MoKα
Data Collection Temperature (K)	98(2)	98(2)	93(2)	93(2)
Unit Cell Dimensions (Å)	a=18.0982(13) b=14.4000(10) c=22.3830(16)	a=17.8013(6) b=19.2789(6) c=27.0247(9)	a=10.8701(8) b=28.890(2) c=18.3122(14)	a=8.0050(5) b=10.1054(6) c=11.0123(7)
Unit Cell Dimensions (°)	α= 90 β= 90 γ = 90	α= 90 β= 90 γ = 90	β= 97.8390(10)	α=113.5190(10) β=97.4260(10) γ=97.6730(10)
Volume ($Å^3$)	5833.3(7)	9274.6(5)	5697.0(7)	793.01(8)
Z	8	8	4	1
Crystal System	Orthorhombic	Orthorhombic	Monoclinic	Triclinic
Space Group	Pbca	Pbca	$P2_1/c$	P-1
Density (Calculated) Mg/m^3	1.301	1.317	1.229	1.297
Data/ Restraints/ Parameters	4213 / 0 / 505	11208/ 0/ 812	13770 / 15 / 901	3382/ 0/ 284
Goodness-of-fit (GOF) on F^2	1.913	1.805	1.499	2.406
Final R Indices [$I > 2\sigma(I)$]	4213 reflections R1=0.0287 *w*R2=0.0518	7057 reflections R1=0.0439 *w*R2=0.0566	8132 reflections R1=0.0499 *w*R2=0.0778	3260 reflections R1=0.0288 *w*R2=0.0711
R Indices (All Data)	R1=0.0387 *w*R2=0.0527	R1=0.0833 *w*R2=0.0589	R1=0.0985 *w*R2=0.0818	R1=0.0297 *w*R2=0.0713

3.14. Acknowledgements

This work was sponsored by an ATP (Advanced Technology Program) between Caltech, W.R. Grace, and NIST. Additional funding was provided by the Cryovac division of the Sealed Air Corporation. NMR and GPC analysis were kindly provided by Galen Hatfield (W.R. Grace) and Jonathan J. Litzau (Cryovac). Larry Henling and Michael Day performed X-ray analysis of **3.26**, **3.31**, **3.33**, and **3.35**.

3.15. Experimental Section

General Considerations. The manipulations of all metal-containing complexes were performed using standard Schlenk techniques under an atmosphere of Argon or nitrogen. Argon, nitrogen, and ethylene were purified by passage through columns of BASF R3-11 catalyst (Chemalog) and 4 Å molecular seives (Linde) or by passage through a Matheson 6410 oxygen scrubber. Solid organometallic compounds were transferred and stored in a nitrogen-filled glovebox (Vacuum atmospheres). All other reactions were performed under aerobic conditions unless otherwise stated. NMR spectra were recorded using either a JEOL 400 (^{1}H, 400 MHz; ^{19}F, 161.4 MHz; ^{31}P, 161.4 MHz; ^{13}C, 100.0 MHz), with chemical shifts referenced to internal solvent resonances and reported relative to tetramethylsilane. ^{31}P NMR data is referenced to external 85% H_3PO_4, where PPh_3 has a chemical shift of –5.4 ppm.

Materials. All organic materials were obtained from Aldrich Chemical Co. unless otherwise stated. Inorganic materials were purchased from the Strem Chemical Co. $MgMe_2$, (tmeda)Ni(acac)$_2$, (tmeda)NiMe$_2$, and [(η^3-allyl)NiBr]$_2$ were prepared using the appropriate literature procedures.

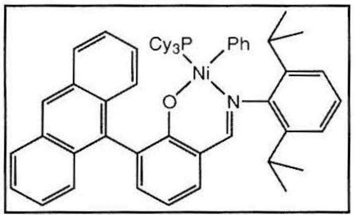

($^{\mathrm{Anthr}}$Sal)Ni(Ph)PCy$_3$ (3.17): $C_{57}H_{68}NNiOP$, FW = 872.82. **^{1}H NMR** (C_6D_6, 300 MHz): 0.50 (q, 6H, $^2J_{HH}$ = 12.8 Hz), 1.01 (m, H), 1.13 (d, 6H, $^3J_{HH}$ = 7.0 Hz), 1.25 (q, J_{HH} = 6.9 Hz), 1.43 (d, J = Hz 6.9 Hz), 1.49 (d, 6H, $^3J_{HH}$ = 7.0 Hz), 4.08 (sept., 2H, $^3J_{HH}$ = 7.0 Hz), 6.68 (t, 1H, $^3J_{HH}$ = 7.7 Hz), 7.86 (d, 2H, $^3J_{HH}$ = 8.4 Hz), 8.25 (s, 1H). **^{31}P NMR** (C_6D_6, 121.4 MHz): δ 21.0 (s). **EA** (Calcd./Found): C 78.44 (77.63), H 7.85 (6.25), N 1.60 (2.08).

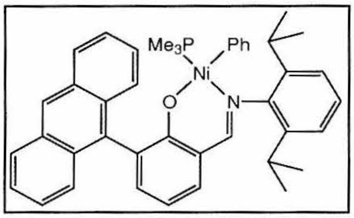

($^{\mathrm{Anthr}}$Sal)Ni(Ph)PMe$_3$ (3.18): **^{1}H NMR** (C_6D_6, 300 MHz): δ -0.148 (m, 9H), 1.02 (d, 6H, $^3J_{HH}$ = 6.9 Hz), 1.25 (d, 6H, $^3J_{HH}$ = 6.9 Hz), 3.69 (sept., 2H, $^3J_{HH}$ = 7.0 Hz), 6.23-6.33 (m, 3H), 6.74-6.85 (m, 4H), 6.95 (d, 2H, $^3J_{HH}$ = 6.7 Hz), 7.23-7.52 (m, 7H), 7.73 (d, 2H, $^3J_{HH}$ = 8.4 Hz), 8.02 (d, 2H, $^3J_{HH}$ = 8.4 Hz), 8.44 (s, 1H). **^{31}P NMR** (CD_2Cl_2, 121.4 MHz): δ -8.9 (s). **EA** (Calcd./Found): C 78.44 (77.63), H 7.85 (6.25), N 1.60 (2.08).

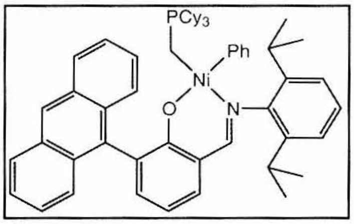

($^{\mathrm{Anthr}}$Sal)Ni(Ph)(CH$_2$PCy$_3$): $C_{58}H_{70}NNiOP$, FW = 886.85. **^{1}H NMR** (C_6D_6, 300.0 MHz): δ -0.258 (d, 2H, $^2J_{HH}$ = 8.1 Hz), 0.62-0.70 (m, 6H), 0.77-0.88 (m, 9H), 1.117 (d, 6H, $^3J_{HH}$ = 3.9 Hz), 1.27-2.10 (m, 18H), 1.345 (d, 6H, $^3J_{HH}$ = 3.9 Hz), 4.045 (sept., 2H, $^3J_{HH}$ = 3.9 Hz), 6.517 (t, 1H, $^3J_{HH}$ = 4.5 Hz), 6.60-6.63 (m, 3H), 6.897 (d, 2H, $^3J_{HH}$ = 4.8 Hz), 6.975 (t, 1H, $^3J_{HH}$ = 7.3 Hz), 7.12-7.15 (m, 3H), 7.18-7.25 (m, 3H), 7.474 (d, 2H, $^3J_{HH}$ = 4.5 Hz), 7.808 (d, 2H, $^3J_{HH}$ = 4.5 Hz), 8.068 (s, 1H), 8.173 (s, 1H), 8.307 (d, 2H, $^3J_{HH}$ = 5.4 Hz). **^{31}P NMR** (C_6D_6, 121.4 MHz): δ 32.7 (s). **EA** (Calcd./Found): C 78.55 (79.33), H 7.96 (8.13), N 1.58 (1.62).

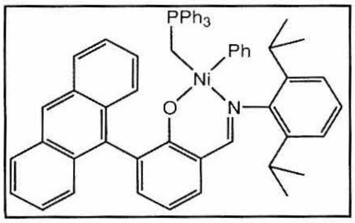

($^{\mathrm{Anthr}}$Sal)Ni(Ph)(CH$_2$PPh$_3$): $C_{58}H_{52}NNiOP$, FW = 868.71. **^{1}H NMR** (C_6D_6, 300.0 MHz): δ 0.809 (d, 2H, $^2J_{PH}$ = 13.5 Hz), 1.088 (d, 6H, $^3J_{HH}$ = 7.0 Hz), 1.206 (d, 6H, $^3J_{HH}$ = 7.0 Hz), 3.987 (sept., 2H, $^3J_{HH}$ = 7.0 Hz), 6.25-6.37 (m, 3H), 6.564 (t, 1H, $^3J_{HH}$ = 7.8 Hz), 6.678 (dt, 6H, $^3J_{HH}$ = 7.5 Hz, $^4J_{PH}$ = 2.7 Hz), 6.78-6.89 (m, 10H), 6.986 (d, 2H, $^3J_{HH}$ = 6.6 Hz), 7.03-7.22 (m, 8H), 7.680 (d, 2H, $^{3}J_{HH}$ = 8.4 Hz), 7.907 (s, 1H), 7.963 (s, 1H), 8.077 (d, 2H, $^{3}J_{HH}$ = 8.7 Hz). **^{13}C NMR** (C_6D_6, 75.4 MHz): δ -1.30 (d, $^{3}J_{HH}$ = 21.5 Hz), 23.4, 26.6, 29.0, 110.9, 122.0, 123.0, 124.4, 125.4, 125.7 (d, $^{4}J_{PC}$ = 1.7 Hz), 126.2, 126.5, 128.4, 128.8, 130.0 (d, $^{2}J_{PC}$ = 10.1 Hz), 130.2, 130.7, 131.3 (d, $^{3}J_{PC}$ = 3.6 Hz), 133.2, 134.0, 134.4 (d, $^{2}J_{PC}$ = 10.1 Hz), 137.5 (d, $^{3}J_{PC}$ = 2.4 Hz), 140.4, 144.8 (d, $^{1}J_{PC}$ = 49.4 Hz), 165.6, 168.8, 168.9. **^{31}P NMR** (C_6D_6, 121.4 MHz): δ 34.2 (s). **EA** (Calcd./Found): C 78.55 (78.23), H 7.96 (7.73), N 1.58 (1.52).

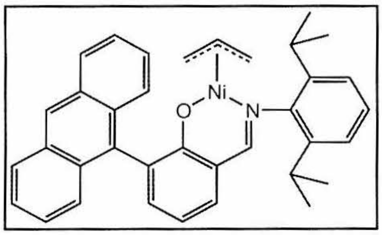

(^{Anthr}Sal)Ni(η^3-CH_2CHCH_2) (3.20): $C_{47}H_{43}N_2NiOP$: FW 773.55. **^{1}H NMR** (CD_2Cl_2, 500.0 MHz): δ 1.205 (d, 3H, $^{3}J_{HH}$ = 7.0 Hz), 1.229 (d, 3H, $^{3}J_{HH}$ = 7.0 Hz), 1.265 (d, 3H, $^{3}J_{HH}$ = 7.0 Hz), 1.314 (d, 3H, $^{3}J_{HH}$ = 7.0 Hz), 2.315 (dd, 1H, $^{3}J_{HH}$ = 7.0 Hz, $^{3}J_{HH}$ = 2.0 Hz), 2.343 (d, 3H, $^{2}J_{HH}$ = 12.5 Hz), 2.562 (d, 3H, $^{2}J_{HH}$ = 12.5 Hz), 3.03-3.06 (m, 1H), 3.308 (sept., 1H, $^{3}J_{HH}$ = 7.0 Hz), 3.567 (sept., 1H, $^{3}J_{HH}$ = 7.0 Hz), 5.31-5.39 (m, 1H), 6.795 (dd, 1H, $^{3}J_{HH}$ = 8.0 Hz, $^{3}J_{HH}$ = 7.0 Hz), 7.22-7.26 (m, 3H), 7.38-7.45 (m, 3H), 7.48-7.53 (m, 2H), 7.849 (dd, 1H, $^{3}J_{HH}$ = 9.0 Hz, $^{4}J_{HH}$ = 1.0 Hz), 7.933 (dd, 1H, $^{3}J_{HH}$ = 9.0 Hz, $^{4}J_{HH}$ = 1.0 Hz), 8.08-8.11 (m, 3H), 8.514 (s, 1H). **EA** (Calcd./Found): C 76.86 (76.22), H 6.28 (6.33), N 4.60 (4.47).

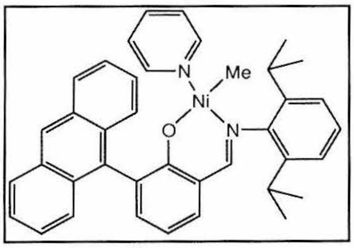

(^{Anthr}Sal)Ni(Me)Py (3.22): **^{1}H NMR** (C_6D_6, 400 MHz): δ -0.32 (s, 3H), 1.02 (d, 6H, $^{3}J_{HH}$ = 6.9 Hz), 1.24 (d, 6H, $^{3}J_{HH}$ = 6.9 Hz), 3.96 (sept., 2H, $^{3}J_{HH}$ = 6.9 Hz), 6.71-7.68 (m, 20H), 8.32 (s, 1H). **^{13}C NMR** (C_6D_6, 75 MHz): δ 22.8, 25.8, 29.1, 110.9, 122.0, 123.0, 124.4, 125.4, 125.7 (d, $^{4}J_{PC}$ = 1.7 Hz), 126.2, 126.5, 128.4, 128.8, 130.0 (d, $^{2}J_{PC}$ = 10.1 Hz), 130.2, 130.7, 131.3 (d, $^{3}J_{PC}$ = 3.6 Hz), 133.2, 134.0, 134.4 (d, $^{2}J_{PC}$ = 10.1 Hz), 137.5 (d, $^{3}J_{PC}$ = 2.4 Hz), 140.4, 144.8 (d, $^{1}J_{PC}$ = 49.4 Hz), 165.6, 168.8, 168.9. **EA** (Calcd./Found): C 76.86 (76.22), H 6.28 (6.33), N 4.60 (4.47).

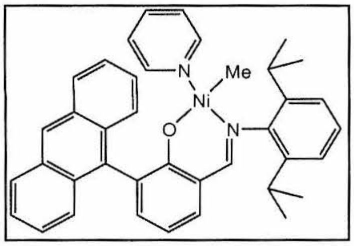

(^{Anthr}Sal)Ni(Me)Lut (3.23): **^{1}H NMR** (C_6D_6, 400 MHz): δ -0.42 (s, 3H), 1.06 (d, 6H, $^{3}J_{HH}$ = 6.6 Hz), 1.37 (d, 6H, $^{3}J_{HH}$ = 6.6 Hz), 1.45 (s, 3H), 1.52 (s, 3H), 4.20 (sept., 2H, $^{3}J_{HH}$ = 6.6 Hz), 6.13-7.27 (m, 16H), 7.56 (dd, 1H, $^{3}J_{HH}$ = 8.1 Hz, $^{4}J_{HH}$ = 0.9 Hz), 8.23 (s, 1H). **^{13}C NMR** (C_6D_6, 75 MHz): δ -3.2, 21.8, 23.2, 23.8, 26.1, 29.2, 114.4, 115.3, 117.1, 121.3, 123.0, 125.3, 125.9, 126.6, 127.5, 127.7, 128.6, 129.0, 129.1, 129.2, 129.6, 131.2, 134.5, 134.7, 138.3, 139.8, 140.8, 141.7, 142.2, 147.1, 149.7, 163.9, 167.1. **EA** (Calcd./Found): C 77.25 (77.35), H 6.64 (6.24), N 4.39 (4.26).

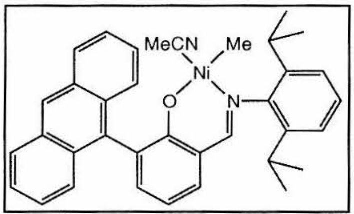

(^{Anthr}Sal)Ni(Me)NCMe (3.26): **^{1}H NMR** (CD_2Cl_2, 300 MHz): (M = Major; m = minor) δ -1.45 (s, 3H—M), -0.95 (s, 3H—m), 1.15 (d, 6H, $^{3}J_{HH}$ = 6.6 Hz—M), 1.18 (d, 6H, $^{3}J_{HH}$ = 6.6 Hz—m), 1.25 (d, 6H, $^{3}J_{HH}$ = 6.6 Hz—M), 1.28 (d, 6H, $^{3}J_{HH}$ = 6.6 Hz—m), 1.85 (s, 3H—m), 1.92 (s, 3H—M), 3.80 (sept, 2H, $^{3}J_{HH}$ = 6.6 Hz—M), 3.98 (sept, 2H, $^{3}J_{HH}$ = 6.6 Hz—M), ~6.60 (t, 2H, $^{3}J_{HH}$ = 7.3 Hz—M/m), 7.02-8.0 (m, 28H—M/m), 8.4 (s, 2H—M/m). **^{13}C NMR** (C_6D_6, 75.4 MHz): δ -2.4, 22.6, 25.6, 28.9, 114.2, 119.9, 121.2, 124.5, 124.7, 125.8, 127.3, 128.4, 129.0, 130.6, 130.8, 131.8, 133.5, 134.7, 137.4, 138.3, 140.7, 145.2, 146.4, 150.1, 165.2, 166.7. **EA** (Calcd./Found): C 75.67 (75.58), H 6.35 (6.46), N 4.90 (5.01)

Crystal Structure of Complex 3.26 (Appendix F): Crystals of suitable quality for X-ray analysis were obtained from the reaction of ^{Anthr,H}Sal ligand (60 mg, FW = 457.61, 131 μmol) with (tmeda)NiMe$_2$ (28 mg, FW = 204.90, 137 μmol, 1.05 eq.) in 3.0 mL of anhydrous acetonitrile (~ 45 mM) upon standing overnight at room temperature. The yellowish-brown crystal used for data collection had dimensions 0.36 × 0.22 × 0.06 mm^3. The X-ray diffraction data were collected by using a CCD area detector diffractometer with graphite-monochromated Mo Kα radiation (0.71073 Å). Unit cell parameters were determined by a least-squares analysis of 25 automatically centered reflections in the range 2.66° < θ< 23.30°. Data were collected at 98 K in the range θ = 1.82-23.32°. A total of 47311 reflections were collected, 4213 of which were independent. The structure was solved by direct methods using the SHELXS-97 program. Hydrogen atoms appeared in the difference Fourier map. Their were unrestrained during refinement, and their U_{iso} values were fixed at 1.1 times the U_{eq} value of the attached atom. Refinement was full-matrix least squares on F^2 using SHELXL-97.

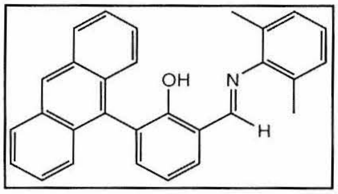

2-Anthracen-9-yl-6-[(2,6-dimethyl-phenylimino)-methyl]-phenol: $C_{29}H_{23}NO$, FW = 401.50. **^{1}H NMR** (C_6D_6, 300.0 MHz): δ 1.897 (s, 6H), 6.858 (s, 2H), 6.872 (t, 1H, $^3J_{HH}$ = 7.2 Hz), 7.08-7.30 (m, 7H), 7.812 (s, 1H), 7.861 (dd, 2H, $^3J_{HH}$ = 8.5 Hz, $^4J_{HH}$ = 0.9 Hz), 7.966 (dd, 2H, $^3J_{HH}$ = 8.7 Hz, $^4J_{HH}$ = 0.9 Hz), 8.269 (s, 1H), 13.480 (s, 1H). **^{13}C NMR** (C_6D_6, 75.4 MHz): δ 18.61, 118.97, 119.40, 125.24, 125.73, 127.18, 127.48, 127.82, 128.53, 128.56, 128.89, 131.15, 132.06, 132.38, 133.13, 136.87, 148.39, 160.43, 167.11. **EA** (Calcd. for $C_{29}H_{23}NO$ 0.5 C_3H_6O/Found): C 85.09 (84.65), H 6.09 (5.63), N 3.25 (3.44).

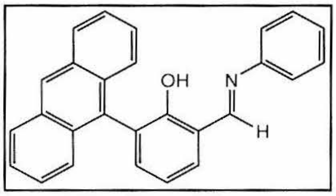

2-Anthracen-9-yl-6-phenyliminomethyl-phenol: $C_{27}H_{19}NO$, FW = 373.45. **^{1}H NMR** (C_6D_6, 300.0 MHz): δ 6.858 (s, 2H), 6.872 (t, 1H, $^3J_{HH}$ = 7.2 Hz), 7.08-7.30 (m, 7H), 7.812 (s, 1H), 7.861 (dd, 2H, $^3J_{HH}$ = 8.5 Hz, $^4J_{HH}$ = 0.9 Hz), 7.966 (dd, 2H, $^3J_{HH}$ = 8.7 Hz, $^4J_{HH}$ = 0.9 Hz), 8.269 (s, 1H), 13.480 (s, 1H). **^{13}C NMR** (C_6D_6, 75.4 MHz): δ 18.61, 118.97, 119.40, 125.24, 125.73, 127.18, 127.48, 127.82, 128.53, 128.56, 128.89, 131.15, 132.06, 132.38, 133.13, 136.87, 148.39, 160.43, 167.11. **EA** (Calcd. for $C_{29}H_{23}NO$ 0.5 C_3H_6O/Found): C 85.09 (84.65), H 6.09 (5.63), N 3.25 (3.44).

Crystal Structure of Complex 3.31 (Appendix G): Crystals suitable for X-ray structure determination were grown from a solution of **3.31** in methylene chloride at room temperature by the slow infusion of acetonitrile over a few days. The greenish-yellow crystal used for data collection had dimensions 0.37 × 0.22 × 0.19 mm^3. The X-ray diffraction data were collected by using a CCD area detector diffractometer with graphite-monochromated Mo Kα radiation (0.71073 Å). Unit cell parameters were determined by a least-squares analysis of 25 automatically centered reflections in the range 2.16° < θ< 27.01°. Data were collected at 98 K. A total of 154074 reflections were collected, 11208 of which were independent. A set of 7057 reflections with $F_o^2 > 2\sigma(F_o^2)$ were observed. The structure was solved by direct methods using the SHELXS-97 program. Hydrogen atoms appeared in the difference Fourier map. Their were unrestrained during refinement, and their U_{iso} values were fixed at 1.1 times the U_{eq} value of the attached atom. Refinement was full-matrix least squares on F^2 using SHELXL-97.

Crystal Structure of Complex 3.33 (Appendix H): Crystals suitable for X-ray structure determination were grown from a solution of **3.33** from a supersaturated acetonitrile solution by slow cooling. The dark brown crystal used for data collection had dimensions 0.259 × 0.185 × 0.148 mm^3. The X-ray diffraction data were collected by using a CCD area detector diffractometer with graphite-monochromated Mo Kα radiation (0.71073 Å). Unit cell parameters were determined by a least-squares analysis of 25 automatically centered reflections in the range 2.35° < θ< 26.39°. Data were collected at 98 K. A total of 104083 reflections were collected, 13770 of which were independent. A set of 8132 reflections with $F_o^2 > 2\sigma(F_o^2)$ were observed. The structure was solved by direct methods using the SHELXS-97 program. Hydrogen atoms appeared in the difference Fourier map. Their were unrestrained during refinement, and their U_{iso} values were fixed at 1.1 times the U_{eq} value of the attached atom. Refinement was full-matrix least squares on F^2 using SHELXL-97.

3.16. References

(1) Britovsek, G. J. P.; Gibson, V. C.; Wass, D. F. *Angew. Chem.-Int. Edit.* **1999**, *38*, 429-447.

(2) Peuckert, M.; Keim, W. *Organometallics* **1983**, *2*, 594-597.

(3) Keim, W.; Kowaldt, F. H.; Goddard, R.; Kruger, C. *Angewandte Chemie-International Edition in English* **1978**, *17*, 466-467.

(4) Starzewski, K. A. O.; Witte, J. *Angewandte Chemie-International Edition in English* **1985**, *24*, 599-601.

(5) Starzewski, K. A. O.; Witte, J. *Angewandte Chemie-International Edition in English* **1987**, *26*, 63-64.

(6) Starzewski, K. A. O.; Born, L. *Organometallics* **1992**, *11*, 2701-2704.

(7) Bauers, F. M.; Mecking, S. *Macromolecules* **2001**, *34*, 1165-1171.

(8) Desjardins, S. Y.; Cavell, K. J.; Jin, H.; Skelton, B. W.; White, A. H. *J. Organomet. Chem.* **1996**, *515*, 233-243.

(9) Desjardins, S. Y.; Cavell, K. J.; Hoare, J. L.; Skelton, B. W.; Sobolev, A. N.; White, A. H.; Keim, W. *J. Organomet. Chem.* **1997**, *544*, 163-174.

(10) Pietsch, J.; Braunstein, P.; Chauvin, Y. *New J. Chem.* **1998**, *22*, 467-472.

(11) Crabtree, R. H. *The Organometallic Chemistry of the Transition Metals*; 3rd ed. ed.; John Wiley & Sons, Inc.: New York, NY, 2001.

(12) Heinicke, J.; Koesling, M.; Brull, R.; Keim, W.; Pritzkow, H. *Eur. J. Inorg. Chem.* **2000**, 299-305.

(13) Heinicke, J.; He, M. Z.; Dal, A.; Klein, H. F.; Hetche, O.; Keim, W.; Florke, U.; Haupt, H. J. *Eur. J. Inorg. Chem.* **2000**, 431-440.

(14) Fischer, K.; Jonas, K.; Misbach, P.; Stabba, R.; Wilke, G. *Angewandte Chemie-International Edition in English* **1973**, *12*, 943-1026.

(15) Ittel, S. D.; Johnson, L. K.; Brookhart, M. *Chem. Rev.* **2000**, *100*, 1169-1203.

(16) Yamamoto, A.; Yamamoto, T.; Saruyama, T.; Nakamura, Y. *Journal of the American Chemical Society* **1973**, *95*, 4073-4074.

Chapter 4

Linear Functionalized Polyethylene Prepared with Single Component, Neutral Ni^{II} Salicylaldimine Complexes

4.1 Abstract

Neutral Ni^{II} Salicylaldimine catalysts **4.1** (L = PPh_3, R = Ph) and **4.2** (L = NCMe, R = Me) have been used for the copolymerization of ethylene with monomers containing esters, alcohols, anhydrides, and amides, providing linear functionalized polyethylenes with moderate to high molecular weights. α-Olefins and polycyclic olefin comonomers containing such functionality have been incorporated directly into the polyethylene backbone. The degree of comonomer incorporation is found to relate to monomer structure, such that: tricyclononenes (TCN) > norbornenes (NB) > α-olefins >> α,α-disubstituted olefins >> vinyl- or allyl-functionalized olefins. Sequential insertions have not been observed for norbornenes or tricyclononenes under any conditions, believed to be a consequence of the steric demand of these polycyclic olefins. Through variation of the polymerization conditions, it was possible to achieve a wide range of comonomer incorporation (extending from 0.1 to 30 mol %) while maintaining a linear structure. The performance of Ni^{II} catalysts **4.1** and **4.2** with a variety of comonomers is presented. The presence of acidic functionality, such as an alcohol, leads to decreased molecular weights and brief catalyst lifetimes, suggesting that the growing polymer chain can be cleaved from the metal center. The characterization of the resultant copolymers using thermal analysis, molecular weight determination, and both solid state and solution ^1H and ^{13}C NMR techniques has demonstrated that the materials contain a linear microstructure—rare for functionalized polyethylenes prepared in a single step from olefinic monomers.

4.2 Introduction

The incorporation of functionality into the hydrocarbon backbone of polyolefins is expected to drastically expand the scope of polyolefin applications by improving polymer adhesion, miscibility, paintability, toughness, and gas diffusion characteristics.[1,2] In addition, the introduction of reactive groups along the polyolefin backbone could allow for mild chemical modification, and therefore, further alteration by chemists.[3] Such new materials, however, can only find use as high performance thermoplastic materials if the polymers demonstrate both a high molecular weight and a crystalline melting point (T_m).[4-6] Poly(ethylene-co-alkyl acrylate), prepared by a radical process that employs extremely high pressure and temperature (2000 atm, >200 °C), provides a good example of how current technology cannot meet these requirements. The conditions necessary for the preparation of this polymer are unselective, yielding a highly branched material that displays a depressed melting point ($T_m \sim$ 100 °C, compare to linear PE ~ 135 °C), and therefore, fails to meet the criteria for a thermoplastomer.[7] In addition, the extreme temperatures and pressures required for such radical reactions requires a significant investment for operation.

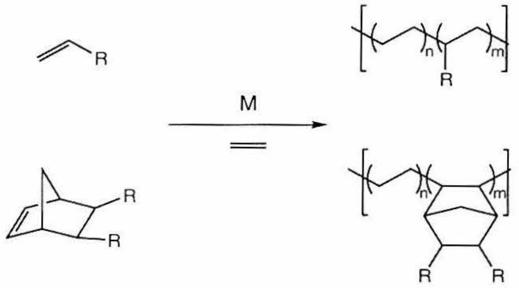

Figure 4.1. Copolymerization of functionalized olefins with transition metal catalysts—preparation of linear functionalized olefins.

An alternative approach which could provide linear functionalized polymers is the coordination polymerization of olefins with transition metal complexes (Figure 4.1). Traditionally, olefin polymerization catalysts, based on *highly electrophilic* early-metal systems, are easily deactivated by the presence of functionalized olefins, trace amounts of moisture, oxygen, or other impurities.[1] Heteroatoms have been incorporated into polyethylene using such highly sensitive metallocene catalysts, but this requires either: (1)

masking the functionality as an innocuous species (such as a borate), (2) pre-complexation of the functional group by a stoichiometric amount of Lewis acid, or (3) by using specially designed "bulky" monomers which disfavor coordination of the functionality to the active site of the catalyst.[3]

Increased promise is expected with late metal catalysts, as they typically display greater tolerance for polar functionalized compounds.[2,8,9] For example, a neutral Ni^{II} catalyst based on an anionic [P,O] chelate is employed industrially in the Shell Higher Olefin Process (SHOP) to generate ethylene oligomers in *1,4-butane-diol*. These systems are also reported to incorporate functional groups into ethylene oligomers, although the activity and molecular weight of the corresponding products are extremely low.[2,8] Better TOF's and higher molecular weight products could be obtained, but required the use of high ethylene pressures (~ 50 atm.) and/or a co-catalyst such as $Ni(COD)_2$.[2,10] In addition, the use of long-chain ω-functionalized-α-olefins, with methylene "spacers" which serve to separate the functionality from the olefin, were required for incorporation of functional groups into the polymer backbone.[10,11] Goodall *et al.* has recently used similar catalysts to prepare ethylene copolymers with functionalized norbornenes. Generally, the norbornene content was high in these materials (>40%), providing *amorphous* materials which exhibited T_gs ranging from 30 – 300+ °C, depending on the content and nature of the bicyclic comonomer.

Higher molecular weight polymers of ethylene and α–olefins can be prepared using cationic Ni^{II} and Pd^{II} diimine complexes with "bulky" ligand sets.[8] Unfortunately, the Ni^{II} diimine system forms an intramolecular chelate with acrylic monomers which deactivates the active form of the catalyst and renders ethylene/acrylate copolymerizations unsuccessful.[12] Remarkably, however, the cationic Pd^{II} systems allow for both methyl acrylate insertion and the subsequent insertion of ethylene.[13,14] This catalyst operates by a hydride elimination/ reinsertion reaction cycle, providing 4-, 5- and then 6- membered chelates successively, each with the carbonyl of the acrylate coordinated to the metal (Figure 4.2). The ring expanded 6-membered chelate allows for the insertion of ethylene, with up to 20 mol % of methyl acrylate incorporated into the polymer.[13,14] Although this serves as the premier example of ethylene/ acrylate copolymerization by a transition-metal catalyst, the materials are not thermoplastomers.

The copolymers exhibit glass transition temperatures (T_g) in the range of –67 °C to –77 °C because they are *highly branched* (~100 branches per 1000 carbons), and are found to contain acrylic functionality at the end of the branches, not along the polymer backbone.[14]

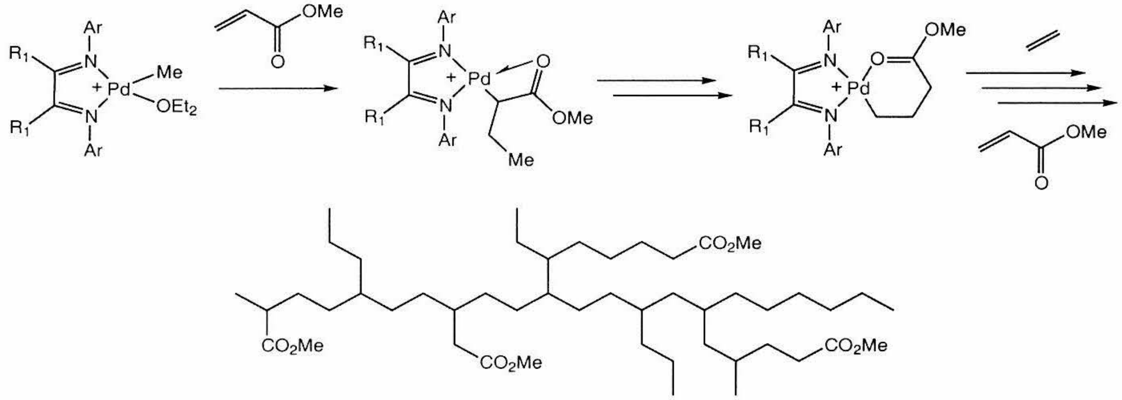

Figure 4.2. Copolymerization of ethylene and acrylate by cationic Pd^{II} diimine catalysts.

Other efforts to prepare functionalized hydrocarbon-based polymers include the polymerization of norbornenes containing esters and free carboxylic acids. Such monomers can be homopolymerized to high molecular weight *via* an insertion mechanism with either neutral Ni^{II} or cationic Pd^{II} catalysts.[15-17] Although reports indicate that ethylene/ norbornene copolymers with cationic d^8 systems are unsuccessful, Goodall *et al.* discovered that by reducing the steric demand of the diimine ligands, Pd^{II} systems could be used for the preparation of random copolymers of methyl acrylate and norbornene with a wide control over comonomer content.

In the previous two chapters, we have outlined the preparation and characteristics of neutral Ni^{II} catalysts **4.1** (L = PPh_3, R = Ph) and **4.2** (L = NCMe, R = Me) (Figure 4.3). These complexes provide high molecular weight, linear polyethylene in the presence of polar solvents such as ethers, esters, alcohols, amides, amines, and even water.[18,19] In fact, since our initial report, similar complexes have been utilized for the preparation of high molecular weight polyethylene in water, although the lifetime of the catalyst was observed to decrease greatly in an aqueous media.[20] Both catalysts contain a specifically-tailored, sterically demanding salicylaldimine ligand which acts to increase both the activity and lifetime. They operate at low ethylene pressures (~ 15-100 psig, 1-7 atm) and allow for reaction with olefins which are less reactive than ethylene (*vide infra*). They do not require the addition of highly-sensitive cocatalysts, and thereby allow for the introduction of most functionalities into the reactor.

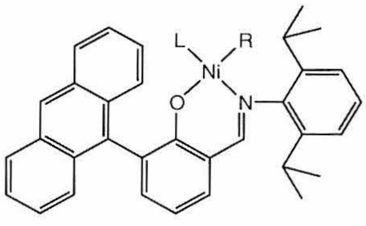

4.1 L = PPh_3 R = Ph
4.2 L = NCMe R = Me

Figure 4.3. Catalysts used for the preparation of linear functionalized polyolefins.

In this chapter, we report the preparation of a series of linear ethylene / functionalized olefin copolymers which range from semicrystalline materials (T_m ~ 80 - 128 °C; 0.1 - 6 mol % comonomer incorporation) to amorphous materials (Tg ~ 72 °C; 30 mol % comonomer incorporation). The polymerizations are discussed according to increasing reactivity of the monomer substructure: (1) vinyl- and allyl-functionalized olefins, (2) ω-functionalized-α-olefins, (3) functionalized norbornenes (NBs), and (4) functionalized tricylcononenes (TCNs). The characterization of these copolymers is presented, clearly demonstrating that crystallinity decreases for the linear copolymers as comonomer incorporation increases.

4.3 Results and Discussion

As outlined in the previous two chapters, the resting state of the catalyst is believed to be the *trans-* ligated species, where L (PPh_3 (**4.1**) or $NCCH_3$ (**4.2**)) occupies the coordination site *cis-* to the growing polymer chain (Figure 4.4). Although dissociation of this ancillary ligand from the metal center leads to formation of the same "active" species for both precatalysts **4.1** and **4.2**, ^1H NMR experiments clearly demonstrate an increased rate of initiation with complex **4.2** under the same conditions. It is believed that this is the reason polymerizations conducted at lower ethylene pressures are more productive with catalyst **4.2** (Ch. 3), and may be the rationale for higher comonomer incorporation with **4.2** than **4.1** (*vide infra*).

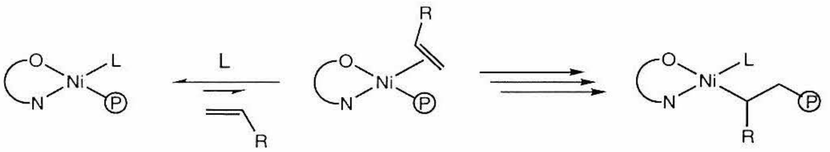

Figure 4.4. Proposed resting state for polymerization with catalysts **4.1** (L = PPh_3) and **4.2** (L = NCMe).

4.4 Copolymerization of ethylene with vinyl or allylic functionalized olefins (n < 2)

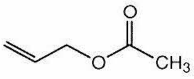

4.3

4.4

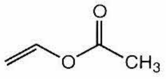

4.5

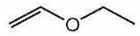

4.6

The addition of allylic- and vinyl- functionalized olefins **4.3** – **4.6**, allows for the production of polyethylene with catalyst **4.1** as illustrated in Table 4.1. The polymer return is lower than what is typically observed for ethylene homopolymerizations (Chapter 2 & 3), with ethylene consumption decreasing steadily over time, indicating that catalyst **4.1** is deactivated. Unfortunately, ^{1}H/ ^{13}C NMR analysis of the polymeric products obtained in trial 4.1*a-g* did not indicate signals in the δ 30-70 ppm region, expected to arise from methylene carbons next to the oxygen-containing functionalities in monomers **4.3** - **4.6**. In addition, IR spectra of each polymer provided no evidence of a ν_{CO} for **4.3** and **4.5** or a ν_{OH} for **4.4**, again indicating that polar comonomer incorporation was not achieved. As polymer can be obtained with these systems, the results suggest that the electronic nature of these electron-rich olefins is unfavorable for either binding to the metal center (i.e., association) or for migratory insertion to occur with these monomers. However, the reduced polymer yield may suggest that insertion of monomers **4.3-4.6** is followed by rapid decomposition.

The addition of electron-deficient monomers, such as acrylonitrile, acrylamide, and methyl acrylate, lead to the instant deactivation of catalysts **4.1** and **4.2** as determined by a lack (or halt) of ethylene consumption and in some cases a color change. The nature of catalyst deactivation was of great concern to us, since the functional groups contained in each monomer (nitrile, amide, and ester, respectively) allow for successful ethylene homopolymerizations (Chapter 3) with catalysts **4.1** and **4.2**. Again, decomposition of the catalyst suggested that insertion of the monomer might be occurring. In analogy to other reports, intramolecular chelation could be inhibiting polymer chain growth.[12] Decomposition could occur through one of the previously outlined pathways (Chapters 2 & 3) or in another (yet undetermined) fashion.

Table 4.1. Attempted copolymerization of ethylene with vinyl and allyl functionalized monomers **4.3-4.6**.[a]

Trial	Comonomer	Comonomer (mL)	PE (g)	M_w (*10^3)	PDI (M_w/M_n)	T_m (°C)	Branch Content[b]
4.1*a*	**4.3**	10	0.07	14.3	2.6	123	12
4.1*b*	**4.4**	10	0.28	12.7	2.0	124	6
4.1*c*	**4.5**	10	0.71	36.4	2.9	130	6
4.1*d*	**4.6**	10	2.05	93.9	3.5	130	5
4.1*e*	**4.6**	20	3.13	98.6	2.9	130	5
4.1*f*	**4.6**	50	3.85	78.2	2.0	129	6
4.1*g*	**4.6**	100	3.17	63.8	2.2	127	7

[a] Copolymerizations performed with 65 μmol catalyst **4.1** using 90 psig (~ 7 atm) ethylene at T = 25 °C. Volume of solvent + comonomer = 100 mL. (b) Total number of $C_1+C_2+C_3+C_4$ branches per 1000 carbons as determined by ^{13}C NMR studies.

To better understand the nature of the reaction between **4.1** and methyl acrylate, both complex **4.1** and the analogous Pd^{II} complex, (^{Anthr,H}Sal)Pd(PPh_3)Ph **4.7**, were heated to 80 °C in toluene-d_8 with 5 eq. of methyl acrylate. The expected product, *trans*-methyl cinnamate **4.8** (in analogy with the Heck reaction), was indeed produced in nearly quantitative yields (96%) (identified by GC/MS against an authentic sample) after heating Pd^{II} complex **4.7** for 4 days at 80 °C (Figure 4.5). In addition to the presence of a trace amount of **4.9** (2%), Pd^0 and free (^{Anthr,H}Sal) ligand were observed, suggesting that [2,1]-insertion of acrylate (predominant pathway) is followed by β-hydride elimination, and decomposition *via* reductive elimination of the ligand (Ch. 2).

A similar solution of methyl acrylate and catalyst **4.1**, showed complete consumption of **4.1** within just 2 hours at 80 °C, but the ^{1}H NMR spectrum did not exhibit signals which suggested the βHE route outlined above was operational (no free (^{Anthr,H}Sal) ligand (ArOH ~ 14 ppm) or Ni^0 observed). In addition, none of the diagnostic

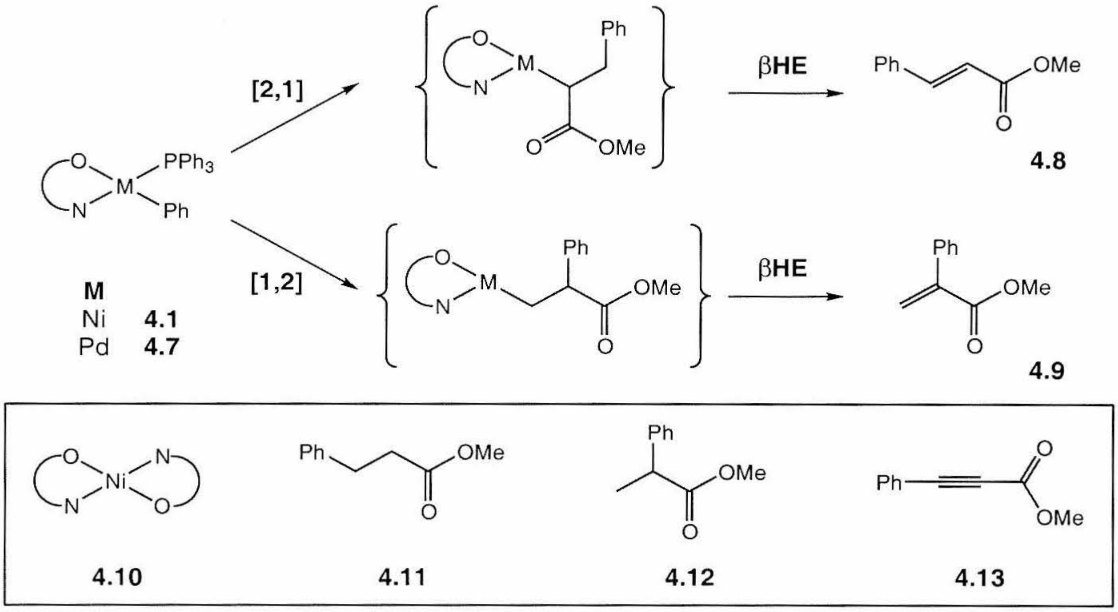

Figure 4.5. Reaction of methyl acrylate with Ni^{II} catalyst **4.1** and Pd^{II} complex **4.7**.

resonances for "Ni-OH" ($\delta \sim -9$ ppm), or "Ni-H" ($\delta \sim -29$ ppm) were present. Instead, observation of a deshielded –C*H*Me$_2$ signal ($\delta \sim 4.5$), indicates the possible formation of the bis(salicylaldimine) structure, (N^O)$_2$Ni **4.10**, although the spectrum is quite complex. GC/MS analysis of the products indicate the presence of both **4.8** (18%) and **4.9** (3%) in a slightly different ratio than observed with Pd^{II} complex **4.7**, however, the major product is the *reduced* form of **4.8** and **4.9**, namely **4.11** (68%) and **4.12** (9%). In addition, a trace amount (3%) of the oxidized product, **4.13**, and some species with a mass of 250 (the product of double insertion followed by reduction) are observed. The nature of this process is currently under further investigation as it may provide the necessary insight to allow ethylene and methyl acrylate copolymerization with neutral Ni^{II} catalysts.

4.5. Copolymerization of Ethylene and Functionalized α-Olefins (n ≥ 2)

Initially, we tested the commercially available ethyl undecylenoate **4.14** to determine whether catalysts **4.1** and **4.2** would incorporate ω-functionalized α-olefins and

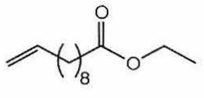

4.9

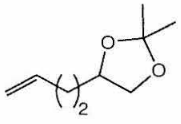

4.10

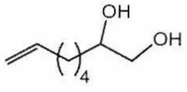

4.11

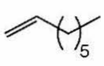

4.12

produce high molecular weight polymers. Trials 4.2*a-d* (Table 4.2) outlines our success with catalysts **4.1** and **4.2**. In analogy to observations for ethylene homopolymerization, the acetonitrile catalyst **4.2** demonstrates a slightly elevated activity for copolymerization trials as compared to the phosphine-containing catalyst **4.1** (compare trials 4.2*c-d* to 4.2*a-b*). The observed turnover frequencies for both catalysts are on the order of ~ 2 •10^5 grams of polymer• (mol. catalyst^{-1})• (hr.$^{-1}$), approximately one order of magnitude lower than ethylene homopolymerizations performed in a "non-coordinating" solvent (such as toluene or benzene, TOF ~ 2-6 •10^6). These values compare well with the rate observed for ethylene polymerization in a coordinating medium (for example, acetone ~8 •10^5 or ethyl acetate ~6.8 •10^5, Chapter 3). Rate suppression, however, is probably not a result of the coordination of the functional moiety to the metal center, as a three-fold increase in the concentration of comonomer **4.14** leads to only a minor decrease (if any) in the

Table 4.2. Direct comparison of catalyst **4.1** and **4.2** for the copolymerization of ethylene and ethyl undecylenoate **4.14**.[a]

Trial	Catalyst	Comon. 4.14 [M]	TOF [b] (•10^6)	Branch Content [c]	T_m (°C)	Comon. Incorp. [d]
4.2*a*	**4.1**	0.62	0.18	9	125	0.2
4.2*b*	**4.1**	2.07	0.13	10	122	1.8
4.2*c*	**4.2**	0.62	0.19	5	118	1.0
4.2*d*	**4.2**	2.07	0.19	6	108	3.8
4.2*e*	**4.2**	NEAT	0.03	ND[e]	ND[e]	10.0

[a] Conditions: 25 μmol catalyst (2.5 mM), Volume of toluene + comonomer (Comon.) **4.14** = 10.0 mL, 120 psig (~ 8 atm) ethylene, reaction time = 15 minutes, 40 °C bath. [b] TOF = (g polymer)•(mol cat)$^{-1}$•(hr.)$^{-1}$. [c] Total C_1+C_2+C_3+C_4 branches per 1000 carbons as determined by ^{13}C NMR. [d] Incorporation = mole %. [e] ND = not determined.

activity of catalysts **4.1** and **4.2** (compare trials 4.2*a-b* and 4.2*c-d*). In all likelihood, the decreased TOF is a reflection of the decreased insertion rate for α-olefins, as polymerization rates are identical to ethylene/octene copolymerizations in a non-coordinating medium (*vide infra*).

Higher incorporation of **4.14** into the copolymer is obtained by both catalysts when the concentration of monomer **4.14** is increased (^{13}C NMR analysis below). In addition, the incorporation of comonomer is generally higher with the acetonitrile catalyst **4.2** than the phosphine catalyst **4.1** (Figure 4.6). As the ligated species is the proposed resting state, we believe that the higher incorporation of the less reactive comonomer, such as **4.14**, is, in part, a manifestation of the increased lability of the acetonitrile relative to PPh_3, such that the comonomer can *compete with ethylene* for the active site.

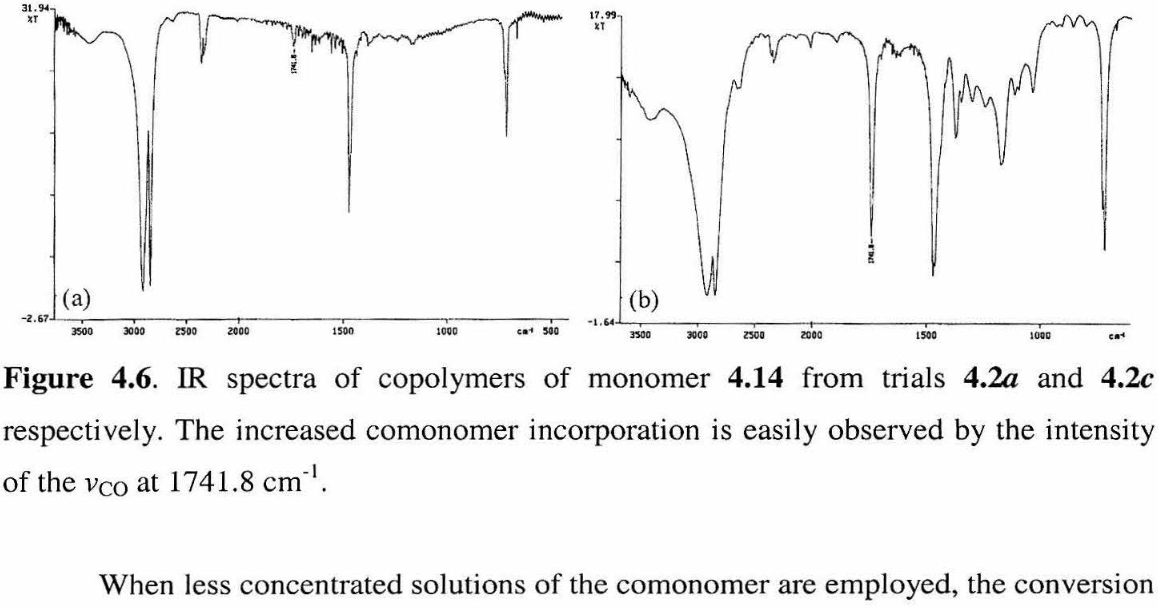

Figure 4.6. IR spectra of copolymers of monomer **4.14** from trials **4.2*a*** and **4.2*c*** respectively. The increased comonomer incorporation is easily observed by the intensity of the ν_{CO} at 1741.8 cm^{-1}.

When less concentrated solutions of the comonomer are employed, the conversion of **4.14** into the polymer is quite low (Table 4.2, Trial 4.3*c*) allowing for the formation of high molecular weight, linear copolymers. The thermal profile of these copolymers puts them in range with high density polyethylenes (HDPE). When the polymerization is run in "neat" ω-functionalized α-olefin, comonomer incorporation into the polyethylene can reach levels as high as 10 mole %, providing material similar in nature to linear low density polyethylene (LLDPE).[4] With high levels of comonomer incorporation, the resulting polymer exhibits a greatly decreased melting point (T_m) in accord with model polymer behavior (compare trials 4.2*c-e*).

^{13}C NMR spectra of poly(ethylene-co-ethyl undecylenoate)s of different compositions are displayed in Figure 4.7. The concentration of functionalized olefin is greater than the number of branches (compare the intensity of the C_1 peak of monomer **4.14** with peak from methyl branch in Figure 4.7). Even in high comonomer samples, such as trial **4.2*e***, there are no signals ascribed to a double insertion of the g-functionalized-a-olefin. Both spectra illustrate that catalysts **4.1** and **4.2** produce materials with a pure microstructure when compared to functionalized polyethylenes produced *via* free radical polymerization methods or with cationic late-metal catalysts.

Table 4.3. Copolymerization of ethylene and γ-functionalized-α-olefin comonomers using catalyst **4.2**.[a]

Trial	**Comon. [M]**	**M_w (•10^3)**	**PDI (M_w/M_n)**	**Branch Content[b]**	**T_m (°C)**	**TON Ethylene[c]**	**TON Comon.[c]**	**Comon. Incorp.[d]**
4.3*a*	**4.14** [3.61]	176	2.4	8	125	5396	17	0.4
4.3*b*	**4.14** [2.16]	204	2.1	7	128	6011	10	0.2
4.3*c*	**4.14** [0.72]	165	2.5	8	124	12400	25	0.2
4.3*d*	**4.15** [0.72]	172	2.3	5	124	6080	19	0.2
4.3*e*	**4.16** [0.72]	54	2.4	8	125	1362	5	0.3

[a] Conditions: 65 μmol catalyst (0.72 mM), 90 mL toluene, appropriate comonomer concentration (listed above), 100 psig ethylene, 40 °C bath, reaction time = 8 hrs. [b] Total $C_1+C_2+C_3+C_4$ branches per 1000 carbons as determined by ^{13}C NMR. [c] TON = mol. olefin converted· (mol catalyst^{-1}). [d] Incorporation = mol %.

α-Olefins with free alcohols (**4.15**) can be incorporated (Trial 4.3*d*). Again, the lifetime of the catalyst and the molecular weight of the polymer are affected, in agreement with of these systems in the polymerization of ethylene in the presence of methanol or water. Deactivation is believed to arise from protonation of the ligand or polymer chain. Protecting the diol functionality as a dioxolane in monomer **4.16**, leads to higher TONs for catalyst **4.2** and increased molecular weight (compare Trials 4.3*d-e*).

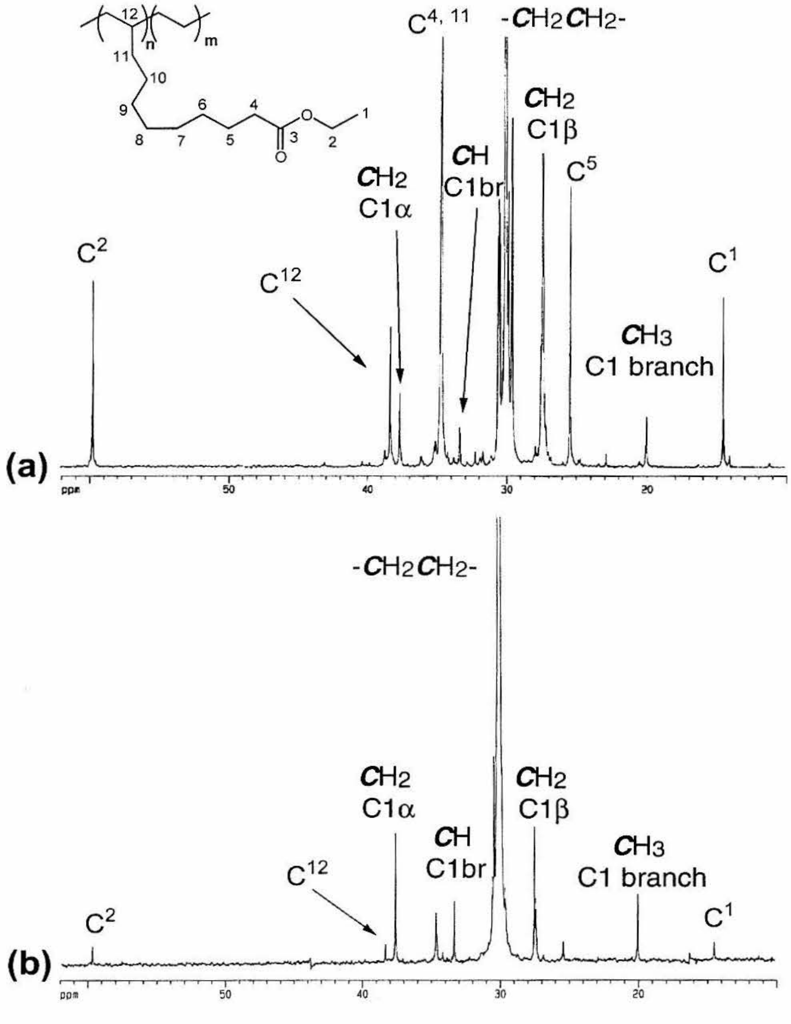

Figure 4.7. ^{13}C NMR (75% $C_6H_3Cl_3$, 25% C_6H_6, 400 MHz, 130 °C) of ethylene/ ethyl undecylenoate (**4.14**) copolymer produced by catalyst **4.2**, containing (a) 10 mol% **4.14** and (b) 0.4 mol% of **4.14**.

Table 4.4. Copolymerization of ethylene and 1-octene (**4.17**) with catalysts **4.1** and **4.2**.[a]

Trial	Catalyst	1-Octene mL (mM)	TOF[b]	M_w (•10^3)	PDI (M_w/M_n)	Branch Content[c]	Comon. Incorp. [d]	T_m (°C)
4.4a	**4.2**	0.1 (2.2)	5.27	12.8	3.30	58	1.7	111.5
4.4b	**4.2**	0.5 (10.5)	2.75	8.8	2.50	67	2.4	104.8
4.4c	**4.1**	1.0 (22.5)	3.27	ND[e]	ND[e]	76	1.7	120.0
4.4d	**4.2**	1.0 (22.5)	2.48	9.3	2.10	66	4.0	89.4
4.4e	**4.2**	2.5 (55.0)	1.22	7.4	3.40	82	6.5	Bd[f]
4.4f	**4.2**	10.0 (235.0)	0.95	3.3	2.10	106	12.5	Bd[f]
4.4g[g]	**4.2**	10.0 (235.0)	0.36	~ 0.4	ND[e]	ND[e]	NA[h]	ND[e]
4.4h	**4.1**	1.0 (22.5)	0.85	ND[e]	ND[e]	75	3.2	103.2
4.4i	**4.2**	1.0 (22.5)	0.92	ND[e]	ND[e]	85	3.5	100.7

[a] Conditions: 28 μmol catalyst (2.8 mM), Volume of toluene + comonomer **4.17** = 10 mL, 120 psig ethylene, 40 °C bath, reaction time=1 h. [b] Turn Over Frequency (TOF) = 10^5 g (polymer)•(mol catalyst)$^{-1}$•(hr.)$^{-1}$. [c] Total C_1+C_2+C_3+C_4 branches per 1000 carbons as determined by ^{13}C NMR. [d] Comonomer Incorporation = mol %. [e] ND = Not Determined. [f] Bd = broad. [g] Oligomerization conditions: 28 μmol catalyst (2.8 mM), 10 mL comonomer **4.17**, 0 psig ethylene, 40 °C bath, reaction time=1 h. [h] NA = Not applicable since ethylene is not present.

The copolymerization of 1-octene (**4.17**) was performed under similar conditions in order to better understand the role which ω-functionality plays on the polymerization (Table 4.4). In accord with previous observations, the α–olefin content (1-12.5 mole %, Trial 4.4*a-f*) was observed to increase with an increasing concentration of the comonomer. The resulting polymers demonstrated very low molecular weights (~ 3-10· 10^3 g/mol) and low melting points which appear to correlate to the degree of α-olefin incorporation. The samples obtained from trials 4.4*e* and 4.4*f* were amorphous, "tacky" polymers which demonstrated broad melting points just above room temperature.

Importantly, the absence of ethylene (trial 4.4*e*) led to the oligiomerization of 1-octene by **4.2** (DP = 2-4). ^{1}H NMR and GC/MS studies of 1-octene oligomerization demonstrated complete consumption of **4.17** within 1 hour at 25 °C, coupled to the production of a slew of products with M_w ~ 112 (C_8), 224 (C_{16}), 336 (C_{24}), and 448 (C_{32}) indicating, importantly, that isomerization is competitive with oligomerization.

A few notable differences exist between these copolymerizations and the aforementioned copolymerization of ethylene and γ-functionalized-α-olefins, such as **4.14**. First and foremost, the presence of functional groups on the monomer appears to have only a slight effect on the amount of comonomer incorporated into the polymer. Polymerizations performed at similar concentrations led to a slightly increased α-olefin content for 1-octene (neat ~ 12.5 mol % incorp.) over the γ-functionalized-α-olefins **4.14** (neat ~ 10 mol % incorp.) (compare Tables 4.3 and 4.4). However, the molecular weight of the 1-octene copolymers are *much* lower than the functionalized polymers (compare trials 4.4a-f to 4.3a-e).

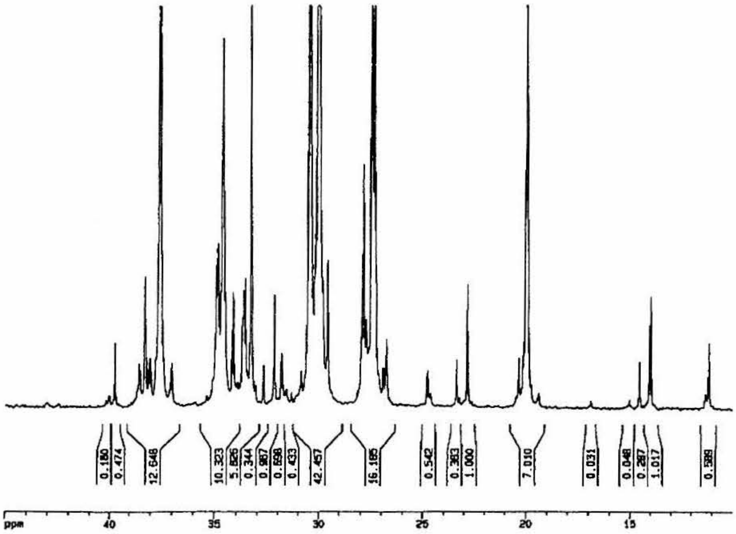

Figure 4.8. ^{13}C NMR analysis of copolymer of ethylene and 1-octene (**4.17**) prepared with catalyst **4.19** (Trial 4.5*d*).

^{1}H and ^{13}C NMR analysis of the ethylene/ 1-octene copolymers highlights the fact that copolymers with **4.17** have a large degree of complex branching when compared to the polymers typically obtained with Ni^{II} catalysts **4.1** and **4.2** (Figure 4.8) A comparison of the ^{13}C NMR of copolymers obtained with 1-octene or ethyl undecylenoate at similar incorporation levels, suggests that different mechanisms might be operational for the two monomers. Based on the aforementioned oligomerization results, it is plausible that isomerized products of 1-octene are inserted during the polymerization, yielding octene copolymers with a high branch content. In accord with results outlined in Ch. 3, the presence of functional groups (in this case, esters) may decrease the rate of βHE and therefore decrease the branch content and increase the molecular weight of polymers obtained from **4.14**. As a preliminary test to this hypothesis, the copolymerization of ethylene and **4.17** was performed with **4.1** and **4.2** (Trials 4.4*h-i*). An examination of the ^{13}C NMR branch analysis of the copolymers shows that similar results are obtained to trials 4.4*c-d*, performed in toluene, indicating that coordinating groups (in this case, ether), do not yield polymers with fewer branches. Therefore, the nature of the difference between polymerizations of unfunctionalized and ω-functionalized-α-olefins remains unclear at this time.

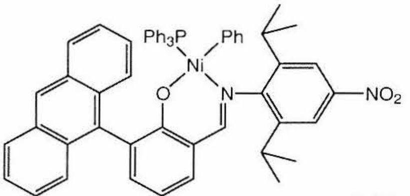

4.18

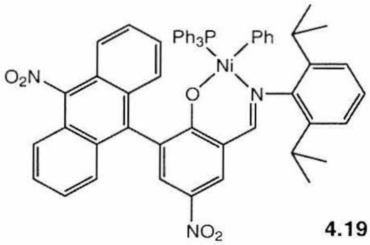

4.19

Table 4.5. Copolymerization of ethylene and **4.17** using catalysts **4.1-2** and **4.18-19**.[a]

Trial	Catalyst	Yield (g)	TOF[b]	T_m (°C)	C_1	C_2	C_3	C_4	C_5	C_6^+	Total Branch Conent[c]	Comonomer Incorp.[d]
4.5a	**4.1**	2.16	0.33	120.0	56	4	2	3	3	8	76	1.7
4.5b	**4.2**	1.76	0.25	89.4	36	4	2	3	3	18	66	4.0
4.5c	**4.18**	0.23	0.03	125.7	61	5	3	3	3	9	84	2.0
4.5d	**4.19**	0.08	0.01	111.4	63	6	3	4	3	9	88	2.1

[a] Conditions: 28 μmol catalyst (2.8 mM), Volume of toluene + comonomer **4.17** = 10 mL, 120 psig ethylene, 40 °C bath, reaction time=1 hr. [b] TOF (Turn Over Frequency) = 10^6 g· (mol^{-1})· (hr^{-1}). [c] Total C_1+C_2+C_3+C_4 branches per 1000 carbons as determined by ^{13}C NMR. [d] Incorporation = mol %.

Table 4.5 demonstrates the activity of a series of catalysts containing similar steric demand, but differing electronic properties. Complexes **4.18** and **4.19**, with nitrated phenolic and arylimine groups, respectively, demonstrate decreased activity for copolymerizations with 1-octene. These results are in agreement with earlier rates displayed for the single-component polymerization of ethylene using catalysts **4.1**, **4.2**, **4.18** and **4.19**. The decreased activity of **4.18** provides further support for the current mechanism—in which imine remains coordinated to the metal center—as the decreased σ-donor ability of the nitrated aryl group would be expected to increase the rate of imine dissociation, thereby increasing the activity of catalyst **4.18** relative to **4.1** or **4.2**, if such a mechanism were operational.

4.6. Copolymerization of functionalized norbornene monomers

Although α-olefins are successfully copolymerized with ethylene, it was believed that the use of olefins with an increased reactivity might allow for the preparation of copolymers that displayed an increased comonomer content. Norbornene monomers contain ~ 19.2 kcal/mol of ring strain, strain energy 14.4 kcal/mol of which can be relieved *via* insertion to the saturated bicyclic structure. This has been considered as an important factor for their increased activity relative to α-olefins.[21] In addition, β-hydrogen elimination reaction occurs rarely with norbornene monomers, due to the unfavorable *syn*- periplanar geometry which must be attained to eliminate the β-hydrogen of the bicyclic monomer.[22]

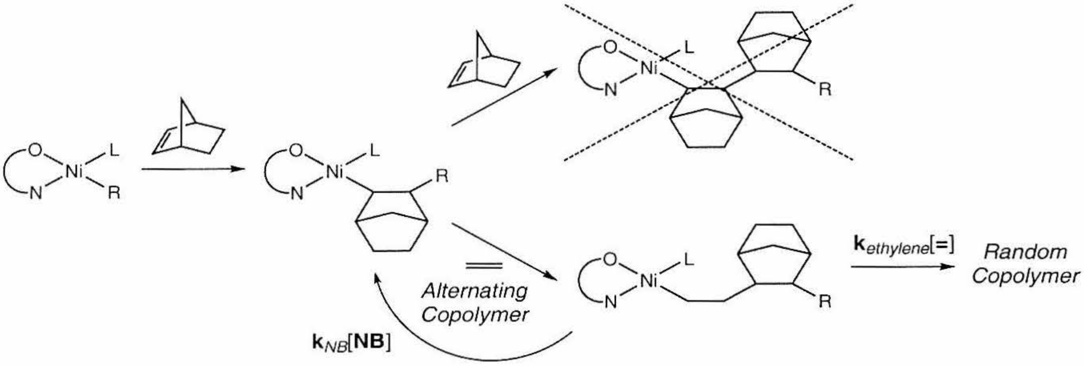

Figure 4.9. Polymerization of norbornene with neutral Ni^{II} catalysts **4.1** and **4.2**.

Neutral Pd^{II} salicylaldimine complexes demonstrate activity for the homopolymerization of norbornene. However, the addition of an α-olefin such as 1-hexene does not allow for chain transfer, instead leading to reduction of the metal center presumably through insertion, βHE, and reductive elimination of the ligand. For this reason, the full extent of their norbornene polymerization character was not investigated. The homopolymerization of norbornene or functionalized norbornenes with catalysts **4.1** and **4.2** has not been observed under any conditions tested to date.[1] Coupled to the results outlined below for copolymerizations, these results suggest that the double insertion of NBs are prohibited for the Ni^{II} centers. This effect is most likely a steric one, with the extreme size of the Ni-(σ-norbornyl) fragment unable to attain the appropriate geometry for a sequential norbornene insertion. Although the appropriate conditions have not been found, at low concentrations of ethylene, it is expected that these catalysts should be successful for the preparation of strictly alternating ENB (or ETCN) copolymers (Figure **4.5**).

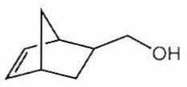

4.20

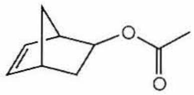

4.21

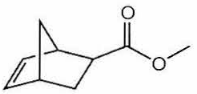

4.22

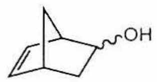

4.23

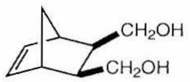

4.24

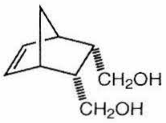

4.25

Copolymerizations with **4.1** and **4.2** have been successful with NBs such as **4.20-4.25**. The data for these polymerizations (Table 4.6), demonstrates that the NBs are readily incorporated into the polyethylene backbone with an improved incorporation (mol %) relative to the γ-functionalized-α-olefins. Although the norbornene monomers are incorporated at high levels, the overall TOF is slightly lower those observed for ω-functionalized α-olefins. It is likely that this reflects the reduced rate of insertion of ethylene into the metal norbornene bond due to steric factors. These polycyclic ethylene copolymers give lower molecular weight materials, but the comonomer yield into the polymer is frequently higher (~ 5 mol %).

---

[1] Norbornene was successfully polymerized in 40-85% yield (M_w's~150-550·10^3 g/mol) upon combination of neutral Ni^{II} salicylaldimine complexes, such as **2.3**, with the electrophilic $B(C_6F_5)_3$ reagent. However, ^{1}H NMR and GPC data clearly demonstrate that the (unknown) active species is not the same as that postulated for olefin polymerization with catalysts **4.1** and **4.2**.

Table 4.6. Ethylene copolymerization with catalysts **4.1** and **4.2** in the presence of functionalized norbornene monomers **4.20-4.23**.[a]

Trial	Cat.	Monomer [M]	Ethylene [psig]	TON Ethylene[b]	TON Mon	Branch	Mw	PDI	Tm	Comon Incorp
4.6*a*	**4.1**	4.20	100	458	34	9	17	1.6	105	5.0
4.6*b*	**4.1**	4.21	100	1540	39	9	70	2.1	110	4.0
4.6*c*	**4.2**	4.22	100	2474	60	9	74	1.6	109	2.0

[a] Conditions: 65 μmol (0.72 mM), catalyst, 90 mL toluene, comonomer, 40 °C bath, reaction time 8 h. [b] TON (Turn over number) = mol. substrate converted· (mol. catalyst^{-1}). [c] Total Me+Et+Pr+Bu branches per 1000 carbons. [d] in g•mol^{-1} [e] Mol %, determined by ^{13}C NMR. [f] No branches observed. [g] No T_m observed. [h] 2,6-di-tert-butylpyridine added to monomer solution prior to reaction. [i] Data not recorded.

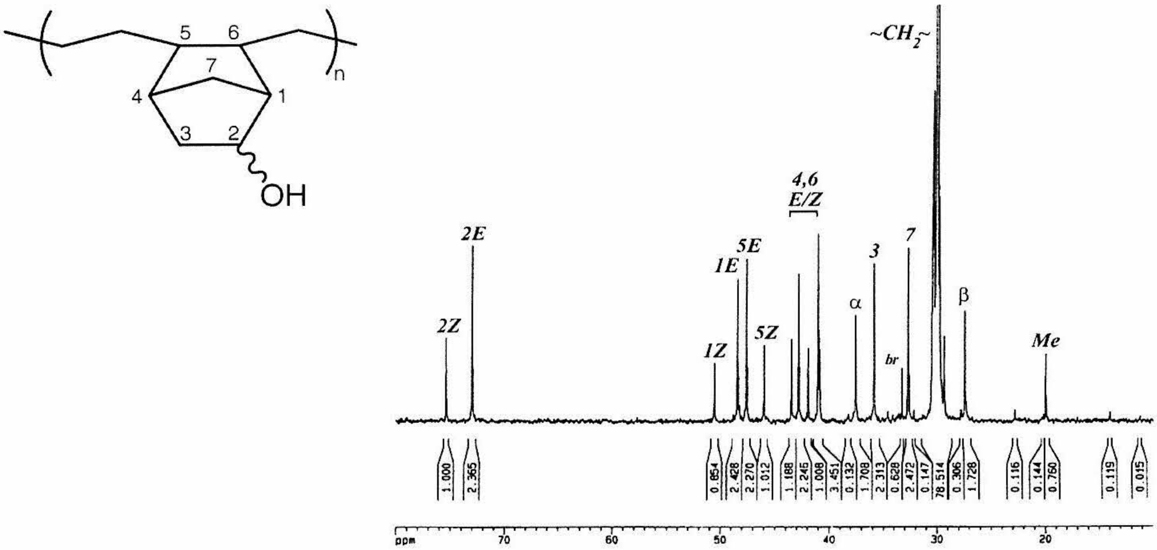

Figure 4.10. ^{13}C NMR of copolymer prepared with monomer **4.23**, incorporation of *endo-*/ *exo-* isomers in same ratio as monomer feed (70/30 *endo-*/*exo-*).

The neutral Ni^{II} complexes **4.1** and **4.2** do not appear to have a preference for reaction with either the *endo-* or *exo-* geometry of norbornene monomers. For example, five separate copolymerization trials were performed with 5-norbornen-2-ol (monomer **4.23** = 72 *endo-* /28 *exo-*) at a variety of different pressures, temperatures, and reaction times. In all five cases, copolymerizations led to formation of a polymer containing between 3-7 mol % of monomer **4.23** with approximately the same *endo*- /*exo*- ratio as found in the starting monomer feed [70.3/29.7 %, 73.5/26.5 %, 70.7/29.3 %, 68.4/31.6 %, and 71.7/28.3 %], as determined by ^{13}C NMR integration (Figure 4.6).

Further support for this notion came from testing the polymerization of monomers **4.24** and **4.25** with catalysts **4.1-2**. Using 1.0 mM solutions of catalyst **4.1-2**, 100 eq. of olefin **4.24** and **4.25**, and 120 psig of ethylene provided the same rate (~ $1.5 \cdot 10^4$ g polymer· (mol cat.$^{-1}$)· (hr.$^{-1}$)), similar yields of polymer (~ 0.3 g), and identical levels of comonomer incorporation (~ 0.2-0.3%) for all four trials. The reactions were extremely short-lived, however, with polymer only forming (rapidly) at the initial stage of the reaction (1-5 minutes). Again, this is believed to arise from protonation of the ligand/ polymer chain and cleavage from the metal center by the alcohol functionality. However, the lack of a difference in reactivity for the *endo*- or *exo*- norbornene isomer is extremely significant as often times, cationic d^8 systems and *endo*- monomers form a strong chelate which can deactivates the catalyst or slow the polymerization rate significantly. In fact, many times, painstaking effort has been taken to ensure that all traces of the *endo*-isomer are removed before polymerization with cationic catalysts.

4.7. Copolymerization of Ethylene and Functionalized Tricyclononene Monomers

Tricyclononene monomers (**4.26-4.29**) contain a fused cyclobutane ring pointed in an *exo*- orientation. It was predicted that these monomers would be more reactive than the aforementioned norbornenes and therefore incorporated more readily than their norbornene analogs. This is a consequence of the fused four-membered ring, which acts to increases the ring strain by an additional 5-10 kcal/mol. In addition, although no preference was observed between *endo*- and *exo*- functionalities, the use of a TCN framework holds the functionality further away from the olefin and, presumably, the metal center. The monomers are easily prepared in one step by thermolysis of commercially available quadricyclane and the appropriately substituted olefin, as described by Tabushi (Scheme 4.1). Monomers **4.26-4.29** were prepared and tested in copolymerization trials using catalysts **4.1** and **4.2**.

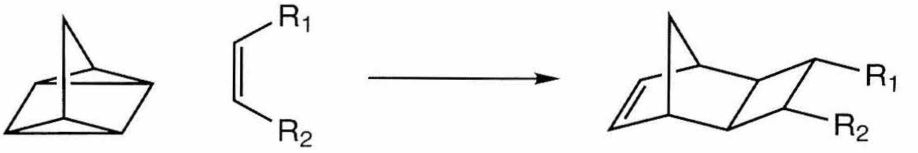

Scheme 4.1. Synthesis of TCN Monomers **4.26-4.29** in analogy to literature reports.

4.26

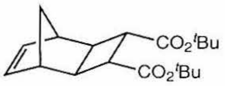

4.27

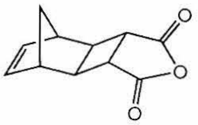

4.28

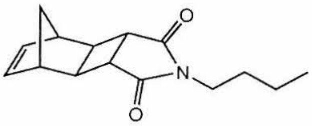

4.29

The copolymerization data obtained for ethylene and **4.26** using catalyst **4.2** is displayed in Table 4.7 (Trials 4.7*a-d*). The molecular weight of the resultant polymer increases slightly as the ethylene pressure is increased from 1 atm to 7 atm. In addition, the comonomer incorporation is observed to decrease with increasing ethylene pressure. When applying a lower pressures of ethylene (~ 5 psig), very high levels of comonomer incorporation (31 mol %) can be obtained with the highly reactive TCN monomers. Unfortunately, however, greatly decreased TON are observed for both ethylene and the polycyclic comonomer at these low ethylene pressures. Such low TONs may arise from incomplete catalyst initiation or catalyst decomposition as suggested above and in Ch. 2 & 3.

Polymers with increasing comonomer incorporation reflect a corresponding decrease in their melt transition temperature, T_m. With 2 mol % TCN, the copolymer exhibits a relatively sharp spike around 112 °C (T_m), and a second broad exotherm at 280-310°C, which has been assigned to the thermal cleavage of the *tert*-butyl ester moiety. At 6 mol % of comonomer **4.26** (Trial 4.7*b*), the T_m appears broadened as the increased (yet random) comonomer content in the polymer gives a decrease in the crystallinity of the polymer chain, leading to the production of a number of "states" with slightly differing crystallinity (Figure 4.11). The sample containing 30 mol % comonomer incorporation (Trial 4.7*a*), showed an endothermic transition between 68 °C and 75 °C (maximum ~ 71 °C) that is assigned as the T_g in accord with literature reports. No endotherm attributed to a Tm was observed. Again, these results are in good agreement with data obtained for unfunctionalized ENB (ethylene/norbornene) copolymers made with metallocenes catalysts.[23]

^{13}C NMR spectroscopic analysis of these ethylene copolymers indicate that the branch content is generally low (less than 15 branches per 1000 carbons), with methyl branches being the most prevalent (Trials 4.7 *b, c* and *d* contain 11, 14 and 14 methyl branches per 1000 carbons respectively) (Figure 4.9). As with the studies for norbornene polymerization, ^{13}C NMR analysis of the TCN copolymers indicates no evidence for the enchainment of comonomer diads, even in the sample containing 30 mol

Table 4.7. Ethylene Polymerization with catalysts **4.1** and **4.2** in the presence of monomers **4.26-4.29**.[a]

Trial	R	Comon /Ni	Ethylene (psig)	TON[b] Ethylene (Comon)	Branch Content[c]	M_w $(\bullet 10^3)$d)	PDI $[M_w/M_n]$	T_m (°C)	Comon. Incorp.e)
4.7a	4.26	0.14	<5	102 (51)	ND	30	1.2	[g]	31
4.7b	4.26	0.15	10	2014 (129)	11	55	1.6	80	6
4.7c	4.26	0.15	30	2600 (123)	14	41	1.6	90	4
4.7d	4.26	0.36	100	8585 (200)	14	76	2.3	112	2
4.7e	4.27	0.18	100	1360 (5)	5	59	2.9	124	0.3
4.7f[h]	4.28	0.02	20	3240 (20)	43	ND[*i*]	ND[*i*]	112	0.5
4.7g	4.29	0.13	100	7600 (8)	7	ND[*i*]	ND[*i*]	124	0.1

[a] Conditions: 65 μmol (0.72 mM), catalyst, 90 mL toluene, comonomer, 40 °C bath, reaction time 8 h, performed with catalyst **4.2**. [b] TON (Turn Over Number) = mol. substrate converted· (mol. catalyst^{-1}). [c] Total Me+Et+Pr+Bu branches per 1000 carbons. [d] in g•mol^{-1} [e] Mol %, determined by ^{13}C NMR. [f] No branches observed. [g] No T_m observed. [h] 2,6-di-tert-butylpyridine added to monomer solution prior to reaction. [i] ND = Not determined.

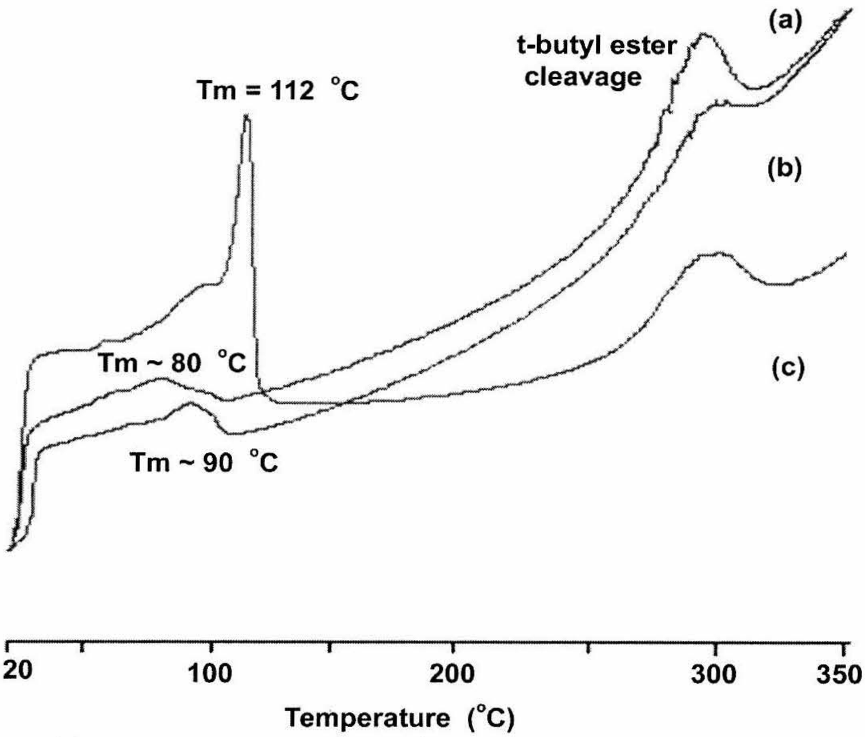

Figure 4.11. DSC heating curves for copolymers of ethylene and monomer **4.26**. Analysis performed under aerobic conditions with heating rate of 5 °C/min (after cooling from first cycle to 140 °C at 10 °C/min). Exotherms demonstrated for melt transition (T_m ~ 80-115 °C) and thermal cleavage of the ^{t}Bu ester (~ 300 °C).

% comonomer. The diad resonances would be expected to occur with a shift downfield of δ 46.0 ppm, in agreement with norbornene diads in P(ENB) prepared by metallocenes.[24] In addition, as previously stated, homopolymer has not been obtained from any of the TCN monomers upon combination with catalysts **4.1** or **4.2**. Although we have not yet found the appropriate conditions and/or comonomer, the theoretical limit of TCN incorporation for catalysts **4.1** and **4.2** is likely to be 50 mole% (Figure 4.5), i.e. it should be possible to form strictly alternating ethylene/TCN copolymers with these catalysts.

It is likely that sequential NB or TCN insertion is prohibited due to the size of the ligand set, as is frequently exhibited with metallocene systems.[25] Reducing the steric demand of the salicylaldimine ligand may yield a catalyst which can prepare polymers containing NB or TCN contents greater than 50 mol %. However, such catalysts are expected to exhibit shorter lifetimes (as catalyst decomposition is intimately linked to the size of the ligand – Ch. 3) and yield lower M_ws since associative displacement will be increasingly facile. A similar strategy has been utilized by *Goodall et al.*—namely Ni^{II} and Pd^{II} catalysts containing modified ligands allowed for the production of previously inaccessible ethylene-norbornene copolymers.

It should also be noted that monomer **4.26** contains the acid sensitive *tert*-butyl ester group, which can be seen from the ^{13}C NMR spectrum (Figure 4.12) of the copolymer from Trial ***4.7a*** remains fully intact. We believe this is a good illustration of the mild nature of the neutral Ni^{II} catalysts, and additionally demonstrates an advantage over cationic complexes which are prone to generate acidic byproducts during the polymerization that lead to cleavage of the ester moiety.

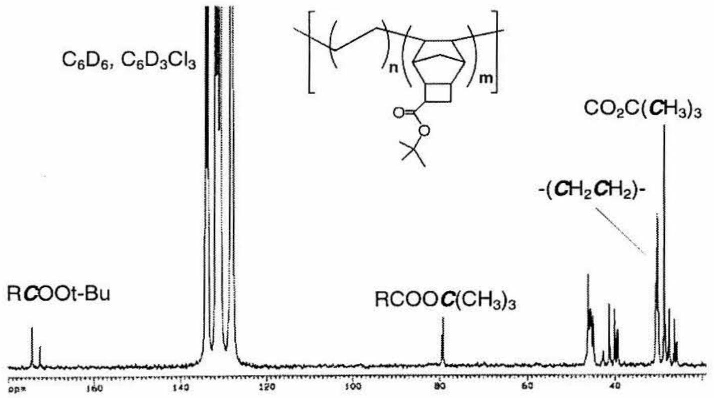

Figure 4.12. ^{13}C NMR (75% $C_6H_3Cl_3$, 25% C_6H_6, 400 MHz, 130 °C) of a copolymer of ethylene and monomer **4.26** produced by catalyst **4.2**, containing 31 mol% of **4.26**.

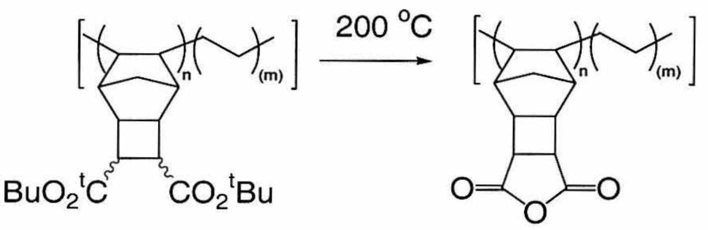

Scheme 4.2. Thermal treatment of the copolymer obtained from ethylene and monomer **4.27** leads to polyethylene containing anhydride functionalities.

The di-*tert*-butyl ester monomer, **4.27**, was easily prepared and incorporated into polyethylene (Trial **4.7*e***). Conversion of the di-*tert*-butyl ester functionality in this copolymer to an anhydride was accomplished *via* heating the functionalized polyethylene to 200 °C under reduced atmospheric pressure (Scheme 4.2). It could be imagined that this simple conversion could be effected in a polymer melt during processing of the polymer.

The introduction of an anhydride functionality could be accomplished in a more direct fashion by the copolymerization of **4.28** with ethylene as demonstrated in Trial 4.7*f*). Initially, catalyst TONs were low, but they could be increased by treating the anhydride monomer solution with a proton sponge to remove trace amounts of acid, as carboxylic acids have been shown to protonate the ligand from the metal catalyst (Ch. 3). The structures of the anhydride/ethylene copolymers prepared from both **4.27** and **4.29** were found to be similar by NMR analysis. The imide, **4.29**, prepared from monomer **4.28**, was also incorporated in to ethylene polymers, with the proceeding in a noticeably controlled fashion. This observation is reflected in the high ethylene TON (Trial 4.7*g*) and again outlines the fact that some functionalities tend to stabilize the nickel complexes, preventing a number of detrimental reactions (Chapter 3) during the course of the polymerization.

No low molecular weight polyethylene fractions were ever observed with the TCN comonomers, as concentration of a fraction of the methanol used to precipitate the polymer followed by ^{1}H NMR analysis of that fraction yielded only unreacted monomer and the $^{\text{Anthr,H}}$Sal ligand. Monomers **4.26** and **4.27** were found to contain *anti:syn* isomer ratios of 40:60 and 45:55, respectively, upon preparation as outlined in Figure 4.7. However, the TCN monomers differed from the aforementioned TCN monomers in that a reactivity difference between stereoisomers *was* observed. The ratio of isomers found in the methanol upon polymer precipitation indicated that the *anti-* isomer is consumed faster than the syn isomer. The preference for this isomer is reflected by the isomer ratio present in the isolated polymers (as determined by ^{13}C NMR spectroscopic analysis). This difference in reactivity is most likely due to the steric demand of the ^{t}Bu groups, as the *anti-* arrangement places the bulk away from the reacting olefin.

4.8. Solid-state ^{13}C NMR studies to determine crystallinity of copolymers

Solid-state ^{13}C NMR studies have been performed to better understand the nature of the crystalline domains within polyethylenes containing comonomer **4.9**. The samples examined ranged in comonomer content from 0.1 mol % to 3.8 mol %, typical in comonomer content to most of the functionalized polymers outlined in this chapter. Spectra from these samples exhibited solid-state ^{13}C NMR signals between 26 - 35 ppm for the methylene carbons of both the side-chain branches and the backbone of the polymer. The NMR spectra were fit to three Lorentzian lines as outlined in Figure 4.13. The broad upfield peak at 31.3 ppm (FWHM of 126 Hz) represents the methylene carbons in the amorphous phase, whereas the two narrow peaks at 32.8 and 34.1 ppm (FWHM 30-45 Hz) are indicative of methylene carbons in a crystalline phase.[26,27] Two separate crystalline peaks indicate the presence of crystallographically distinct phases, which are referred to as the orthorhombic phase (32.8 ppm, OCP) and the monoclinic phase (34.1 ppm, MCP) according to previous reports.[26] Quantitation of the three distinct phases was carried out from the spectral peak area of the fitted Lorentzian curves, and is summarized in Table 4.8. The content of the crystalline phase for all samples examined was over 60%. In samples with very low comonomer content (Trials 4*a-c*), over 20% of the crystalline phase is found to be in the MCP without any external forces acting to process the polymer (simply isolated by precipitation).

Table 4.8. Relative ratio of the crystalline phases as determined by Solid State ^{13}C MAS NMR.[a]

Trial	Comonomer Incorp. (Mol %)	Crystalline Fraction (%)	Fraction—OCP (%)	Fraction—MCP (%)
4.8*a*	0.2	63.3	36.6	26.7
4.8*b*	0.2	65.5	34.6	30.9
4.8*c*	0.4	60.5	32.1	28.4
4.8*d*	3.8	66.7	56.1	10.6

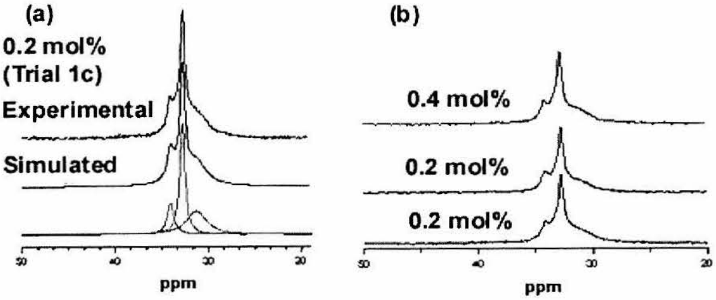

Figure 4.13. ^{13}C solid state NMR spectra of functionalized polyethylene containing monomer **4.9**. (a) Shows the experimentally obtained spectra (top), the Lorentzian fit (bottom), and the simulated curve (middle). (b) Solid state spectra obtained experimentally for polyethylenes with different monomer loadings (Trials 4.3*a*-*c*).

4.9. Conclusions

Neutral late transition metal catalysts **4.1** and **4.2** have been shown to be useful for the preparation of linear, functional-group-containing, high-molecular-weight, ethylene copolymers under mild laboratory conditions directly from functionalized olefinic monomers. In some cases, high TONs were observed for catalysts **4.1** and **4.2** demonstrating their tolerance of certain functionalities. Probably the most notable exception comes from the use of alcohol-containing monomers, which lead to reduced molecular weights, low polymer returns, and short catalyst lifetimes.

Comonomer content typically falls in the range of 0-10 mol % incorporation for ω-functionalized-α-olefins such as ethyl undecylenoate **4.9**. Catalyst TONs typically decrease in the presence of increased comonomer. Strained cyclic olefin monomers, such as tricyclononene (TCN) and norbornene (NB) monomers allow for much higher incorporation into the polyethylene backbone (up to 30 mol %). Although we have not yet found the appropriate conditions and/or comonomer, such cyclic olefins may be reactive enough to prepare ethylene copolymers with up to 50 mol % functionalized olefin (possibly alternating) as the double insertion of NBs or TCNs is not observed. With the linear functionalized polymers examined using both solid and solution-phase studies, the crystallinity is found to decreases drastically as the incorporation mol % increases, in agreement with model polymers prepared in a sequential fashion. Analysis of the copolymers suggests that ~ 10 mol % incorporation of a functionalized olefin can lead to significant changes in the properties of the polymer.

Post polymer modification of these functionalized polyolefins can allow for further modification of the polymers prepared by catalysts **4.1** and **4.2**. For example, the indirect incorporation of anhydride groups was demonstrated by thermolysis of a copolymer prepared with a monomer containing vicinal di-*tert*-butyl ester groups, **4.27**.

The promise of catalysts **4.1** and **4.2** is in their ability to polymerize monomers with ethers, esters, amides, anhydrides, and alcohols. However, these studies serve merely as a stepping stone to potential neutral catalysts which will some day make a large variety of functionalized polymeric materials.

4.10. Acknowledgement

Support has been provided by the National Institute for Standards and Technology (as part of the ATP program), W. R. Grace, and the Cryovac Division of the Sealed Air Corporation. A huge bit of thanks goes to Galen Hatfield (W. R. Grace) and Johnathan Litzau (Cryovac) for their wonderful GPC and NMR analyses of endless polymer samples. Sonjong Hwang, Caltech, was instrumental in solid-state analysis of these polymers.

4.11. Experimental Section

General Considerations. All manipulations and polymerizations were carried out in an N_2-filled drybox or using standard air-sensitive or vacuum line techniques under Argon. Argon was purified by passage through columns of BASF RS-11 (Chemalog) and Linde 4-Å molecular sieves or by passage through a Matheson O_2 scrubber Matheson Model 6410 Oxygen Absorbing Purifier. Ethylene was also purified by passage through a Matheson O_2 scrubber Matheson Model 6410 Oxygen Absorbing Purifier.

Materials. Solvents are rigorously degassed in 18 L reservoirs and passed through two sequential purification columns. Protic contaminants are removed with activated alumina, while a supported copper catalyst is used to remove trace oxygen from hydrocarbons.[28] Compound **4.1** was synthesized by the published procedure.[18] Catalyst **4.2** was prepared and characterized as described in Chapter 2. Compound **4.11** was prepared from commercially available hex-1-ene epoxide, by hydrolysis in dilute H_2SO_4 at room temperature for 15 hours. Extraction with diethyl ether was followed stirring in the presence of Na_2SO_4. The diethyl ether was removed using reduced pressure to give the diol. Subsequent protection using methoxy-propene in the presence of amberlyst resin gave the dioxolane **4.11**. Characterization matched published data.[29,30]

Preparation of Tricyclo[4.2.1.$0^{0,0}$]non-7-ene-3-carboxylic acid t-butyl ester (4.26). Quadricyclane (12 mL) and t-butyl acrylate (92 mL) was placed in a thick walled Schlenk tube. The components were degassed and then sealed under an atmosphere of nitrogen.

The reaction mixture was heated to 96 °C for 8 hours. The product was obtained by distillation. Isolated yield with respect to quadricyclane 80%. (bp: 120 °C / 1.00 mmHg). NMR spectroscopy revealed an *endo-* and an *exo-* isomer to be present (ratio 3:1). Assignment of the *endo-* isomer: **^{1}H NMR** ($CDCl_3$, 300 MHz, 25 °C): δ 5.90, 5.91 (2H, bs), 2.68 (1H, bs), 2.60 (1H, bs), 2.28-2.27 (m, 2H), 2.20 (m, 1H), 1.98 (d, 1H, $^3J_{HH}$ = 9.3 Hz), 1.61 (d, 1H, $^3J_{HH}$ = 10.0 Hz) 1.41 (s, 9H), 1.26 (d, 1H, $^3J_{HH}$ = 10.0 Hz). **^{13}C NMR** ($CDCl_3$, 75.47 MHz, 25 °C): δ 175.32, 135.78, 134.57, 79.76, 44.04, 43.83, 40.41, 40.27, 38.37, 34.11, 28.03, 23.66. **IR** (KBr, cm^{-1}): 1718.3 cm^{-1} [ν_{CO}]. **EA** (Calcd./Found): C 76.33 (76.41), H 9.15 (9.12), N 0.00 (0.00).

Tricyclo[4.2.1.0^{0,0}]non-7-ene-3,4-dicarboxylic acid t-butyl ester (4.27): The previously reported tricyclononene adduct of quadricyclane and maleic anhydride (**4.28**) was hydrolyzed by addition of the white solid to a flask containing NaOH and 100 mL of H_2O upon refluxing for 8 hours. The water was subsequently removed to provide a white solid (**4.28**), which was dried under reduced pressure. 50 mL of t-BuOH, the white solid and 1.5 mL of conc. H_2SO_4 was placed into a glass bomb with a pressure gauge. 70 mL of isobutlyene gas was condensed in the glass bomb (-70 °C). The flask was allowed to warm to room temperature. After stirring the reaction for 8 hours, the flask was heated to 84 °C (70 psig in flask) for 3 hours. The flask was cooled to –70 °C and the isobutylene gas was allowed to evaporate. The oil that remained was dissolved in pentane and washed with a saturated water solution of K_2CO_3. After drying the pentane layer with $MgSO_4$, 22.0 g of crude product was obtained which crystallized upon standing. The product (**4.27**) was purified by column chromatography with 90/10 hexanes/ethyl acetate. NMR spectroscopy shows both *endo-* and *exo-* isomers in a 1:3 ratio at 25 °C. $C_{14}H_{20}O_2$. *Endo* isomer—**^{1}H NMR** ($CDCl_3$, 300 MHz): δ1.3-1.5 (m, 20H), 2.23 (m, 2H, $^3J_{HH}$ = 2.1 Hz), 2.58 (m, 2H, $^3J_{HH}$ = 3.5 Hz), 2.74 (bs, 2H), 5.97 (bs, 2H). **^{13}C NMR** ($CDCl_3$, 75 MHz): δ28.1, 37.9, 40.8, 40.9, 43.5, 80.4, 135.3, 172.3. *Exo* isomer—**^{1}H NMR** ($CDCl_3$, 300 MHz): δ1.26 (s, 1H), 1.43 (m, 18H), 2.02 (m, 1H), 2.12 (m, 2H, $^3J_{HH}$ = 9.3 Hz), 3.14 (bs, 2H), 3.34 (m, 2H, $^3J_{HH}$ = 9.6 Hz), 5.98 (bs, 2H). **^{13}C NMR** ($CDCl_3$, 75 MHz): δ28.1, 37.9, 41.8, 42.9, 80.0, 136.5, 169.9. **IR** (KBr, cm^{-1}): 1721.5 [ν_{CO}]. **EA** (Calcd./Found): C 71.22 (71.22), H 8.81 (8.76), N 0.00 (0.00).

Synthesis of N-Butyl-tricyclo[4.2.1.0^{0,0}]non-7-ene-3,4-dicarboxylimide (4.29). The previously reported adduct of quadricyclane and maleic anhydride (**4.28**) was placed in a flask with toluene and 1.1 equivalents of n-butyl amine. The mixture was refluxed for 12 hours using a dean-stark apparatus. The product was isolated by distillation to give a light yellow solid. Isolated yield with respect to the anhydride starting material 85%. (bp: 142 °C / 0.25 mm/Hg). **^{1}H NMR** ($CDCl_3$, 300 MHz, 25 °C): δ 6.01 (bs, 2H), 3.51 (t, 2H, $^3J_{HH}$ = 7.2 Hz), 2.94 (bs, 2H), 2.65 (bs, 2H), 2.10 (bs, 2H), 1.6-1.2 (m, 6H), 0.89 (t, 3H, $^3J_{HH}$ = 7.5 Hz). **^{13}C NMR** ($CDCl_3$, 75.47 MHz, 25 °C): δ 179.10, 135.81, 44.54, 41.71, 41.05, 40.95, 38.92, 30.10, 20.37, 14.05. **IR** (KBr): 1769.3 cm^{-1}, 1697.2 cm^{-1} [ν_{CO}]. **EA** (Calcd./Found): C 73.44 (73.34), H 7.81 (7.94), N 5.71 (5.76).

General Procedure for Polymerization of Ethylene with Comonomers by Ni Complexes 4.1 and 4.2. A 6 oz or 12 oz Fisher-Porter glass pressure bottle was charged with the appropriate amount of Ni complex under an atmosphere of nitrogen (for polymerizations at 14 atm (200 psig) an 200 mL autoclave was used). Toluene (80 mL) was then cannula transferred into the reactor, followed by a solution of comonomer, in toluene (10 mL). The ethylene pressure was raised to the particular value and maintained for the specified times. MeOH/HCl workup afforded the polyethylene, which was filtered and dried under vacuum.

General Procedure for High-Resolution Liquid ^{13}C Nuclear Magnetic Resonance Characterization of Polyethylene Copolymers. It has been shown by Randall, that the NOE factor for many polyethylene systems is nearly full and constant for all carbons of the copolymer. Therefore, WALTZ decoupling sequences were used for improved signal-to-noise and thus allow the number of scans to be reduced. This is important when the polymer of interest is sparingly soluble in the solvent blend. When the integrations do not agree with each other using WALTZ, an inverse-gated experiment was run to check if some of the signals were being selectively enhanced. Little difference in the integration was observed in most polyethylenes, by making calculations based on averaging several signals, any error was minimized. Other things that were considered, were the potentially long relaxation times (T1's) of end groups (e.g., methyls, methylenes at/near the end of the polymer chain), these signals were not used for quantitation since they will not have fully relaxed when the next pulse fires and as a result signal is lost in these carbons. In a typical copolymer, the branch, alpha, and beta carbons were used to integrate. The sum of all of these signals were made and then divided by the number of carbons they are attributed to so as to get an averaged integration unit per carbon for that constituent. A 90 degree pulse (based on main methylene resonance at 30.0 ppm) and at least 32K data points were collected on a Bruker DMX-400 MHz NMR instrument with high temperature capabilities. 3000 scans, with a 10 second recycle delay, which amounts to an 8 hour run, constituted a typical experiment. This was to satisfy the requirements for signal-to-noise (ASTM method D-5017-96). The NMR solvent mixture is given below for 10 mm tubes and was found to work well for most polyolefins. ~150 mg sample, added in small aliquots, 2.0 ml 1,2,4-trichlorobenzene (protonated), 0.75 ml benzene-d6 (lock), 0.25 ml hexamethyldisiloxane (internal reference). Dissolution heating block and NMR experiment were maintained at 130 °C (good temperature control is very important, as benzene-d6 begins to boil around 130 °C, and going above this could prove disastrous). Small slits in the top of the NMR tube caps were cut to avoid pressure build up in the tube.

GPC analysis was determined by employing the waters 150 GPCV liquid chromatograph. It is equipped with three detectors, a Waters differential refractometer, a Waters single capillary viscometer and a Wyatt DAWN DSP light scattering detector. Several samples were prepared to yield an approximate 0.1 weight % solution in 1,2,4-trichlorobenzene. Four Waters high temperature µstyragel columns (10^6, 10^5, 10^4, 10^3 Angstrom) at 140 °C were used to determine the MWDs of the polymers. The instrument was calibrated with TSK narrow polydispersity polystyrene standards. A 'universal calibration' curve was created to determine their MWDs. The data was collected and calculated using the Water's Millenium.

Solid-state ^{13}C NMR experimental procedure: All ^{13}C magic angle spinning (MAS) NMR experiments were carried out with Bruker DSX 200 (50 MHz for ^{13}C) and a 7mm CPMAS probe except for a sample of 10 mol % comonomer incorporation which Bruker DSX 500 (125 MHz for ^{13}C) and a 4mm BL CPMAS probe were used simply because of limited amount of sample. 160 mg of polymer powder was packed in a 7 mm MAS rotor and was spun at 4.0 kHz at 4.7 T. The ^{13}C Block decay signal was acquired using a 4μs 90 ^{o} pulse with high power H-decoupling and the typical repetition time used was 500 s. The spin-lattice relaxation times were estimated to be ~80s and 0.1 s at 4.7 T for the crystalline and amorphous phases, respectively. There was no noticeable NMR signal growth observed when the repetition time was increased to 1000s.

Selected Spectral Data From Reported Copolymers. **Ethylene-Ethylundecylenoate Copolymer** (0.4 mol % of comonomer). **DSC** (25 to 150 °C, 15 °C/min second heating cycle): T_m = 125.2 °C. M_w = 176,000, PDI = 2.4. **IR** (KBr): 1742.0 cm^{-1} [ν_{CO}]. **^{1}H NMR** (C_7H_8, 300 MHz, 90 °C): δ 3.95 ($C(O)OCH_8CH_3$), 1.40-1.30 with max. at 1.38, 1.39, 1.36, 1.34, 1.32, 0.91 (CH_3, branch). **^{13}C NMR** (75% $C_6H_3Cl_3$, 25% C_6H_6, 400 MHz, 130 °C): δ

^{13}C Chemical Shift	**Assignment**
172.46	C^3
59.71	C^2
38.24	C^{12br}
37.53	C1α
34.57	$C^{13\alpha}$, C^{11}
33.25	$C1_{br}$
30.50	C1δ
30.5-29.7 with peak maxima at 30.47, 30.35, 29.97, 29.77	CH_2 backbone, C1δ, C^6, C^7, C^8, C^9
27.47, 27.31	C1β C^{10} ,$C^{14\alpha}$
25.32	C^5
19.94	CH_3 of a C1 branch
14.43	C^1
11.17	CH_3 of a C2 branch

Results obtained for ^{13}C NMR spectroscopic analysis for branch content of copolymer:

C1/ 1000C	**C2/ 1000C**	**C3/ 1000C**	**C4/ 1000C**	**C5/ 1000C**	**C6+/ 1000C**	**Total*/ 1000C**	**Mole% Comonomer**
6	<1	nd	nd.	nd	1	8	1.0 %

nd = not detected

Ethylene-Tricyclo[4.2.1.0^{0,0}]non-7-ene-3-carboxylic acid t-butyl ester Copolymer (Comonomer content 5.8 mol %): **DSC** (25 to 150 °C, 15 °C/min second heat): Tm = broad, with maximum at 80 °C. **IR** (KBr): 1727.4 cm^{-1} [ν_{CO}]. **^{1}H NMR** (C_6H_5Br, 300 MHz, 90 °C): δ Broad resonances between 2.2 and 0.7 ppm corresponding to the cyclic protons of the tricyclononene unit with maxima at 2.97, 2.32, 2.13, 1.9, 1.73, 1.64, 1.27 ($C(O)OC(CH_3)_3$), 1.15 (CH_2-CH_2), 0.75, 0.71. **^{13}C NMR** (75% $C_6H_3Cl_3$, 25% C_6H_6, 400 MHz, 130 °C): δ 174.37 (endo-C^{10}), 172.40 (exo-C^{10}), 79.37, 79.15 (exo and endo C^{11}), 46.04, 45.56, 45.31, 42.50, 41.14, 39.93, 32.50, 30.4-30.1 with maxima at 30.42, 30.36, 30.02 (CH_2-CH_2) 27.7-28.4 with maxima at 28.64, 28.48 (C^{12}), 19.96 (C1 branch CH_3). Ratio of endo and exo isomers incorporated in polymer; 1.25:1.

Results obtained for ^{13}C NMR spectroscopic analysis for branch content of copolymer:

C1/ 1000C	**C2/ 1000C**	**C3/ 1000C**	**C4/ 1000C**	**C5/ 1000C**	**C6+/ 1000C**	**Total*/ 1000C**	**Mole% Comonomer**
10	nd	nd	nd	nd	6	11	5.8%

* Does not include negative bias of up to 30% for branch level determination by ^{13}C NMR.

Tricyclonenene isomer content in the final copolymers

Comonomer Content (Mol %)	**Endo-**	**Exo-**
31	70	30
6.0	65	37

Ethylene-Tricyclo[4.2.1.0^{0,0}]non-7-ene-3,4-dicarboxylic acid t-butyl ester (Comonomer content 0.6 mol %): **IR** (KBr): 1736.6 cm^{-1} [ν_{CO}]. **^{13}C NMR** (75% $C_6H_3Cl_3$, 25% C_6H_6, 400 MHz, 130 °C): δ

^{13}C Chemical Shift	Assignment
171.58	C^{10}, C^{13}
79.82	C^{11}, C^{15}
45.33	C^{8}, C^{7}
44.40	C^{3}, C^{4}
43.54, 43.48	C^{1}, C^{6}, C^{2}, C^{5}
37.58	$C1\alpha$
34.64	C^{9}
33.30	$C1_{br}$
30.50	$C1\delta$
30.5-30.0 max. at 30.40, 30.01, 29.58	CH_2 backbone
28.58	C^{12}, C^{15}
27.47	$C1\beta$
23.37	CH_3 of a C4 branch
22.86	CH_3 of a C5 branch
20.30	$C1_1$ (CH_3 of a C1 branch)
14.53	CH_3 of a C3 branch
11.17	CH_3 of a C2 branch

Results obtained from ^{13}C NMR spectroscopic analysis for the branch content of the ethylene copolymer.

C1/ 1000C	C2/ 1000C	C3/ 1000C	C4/ 1000C	C5/ 1000C	C6+/ 1000C	Total*/ 1000C	Mole% Comonomer
27	3	1	1	2	3	37	0.6%

* Does not include negative bias of up to 30% for branch level determination by ^{13}C NMR.

Additional assignments for carbons from an Ethylene-Tricyclo[4.2.1.0^{0,0}]non-7-ene3,4-dicarboxylic acid t-butyl ester Copolymer (prepared from monomer containing both *exo*- and *endo*- isomers). (Comonomer content 0.5 mol %).

^{13}C Chemical Shift	Assignment
169.55	C^{10}, C^{13}
79.62	C^{11}, C^{15}
46.60	C^{8}, C^{7}
44.13, 42.90	C^{2}, C^{5}, C^{3}, C^{4}
41.51	C^{1}, C^{6}

Ethylene-Tricyclo[4.2.1.0^{0,0}]non-7-ene-3,4-dicarboxylic anhydride (Comonomer content 0.3 mol %): Polymerization was conducted under standard conditions. 2,6-Di-tertbutyl pyridine (2 equivalent to Ni catalyst) was added as a proton sponge to scavenge any trace amounts of acid contained in the anhydride monomer. **DSC** (25 to 150 °C, 15 °C/min second heat): T_m = 124.6 °C, M_w = 159000, PDI = 3.0. **IR** (KBr): 1861.8 cm^{-1}, 1794.0 cm^{-1} [ν_{CO}]. **^{13}C NMR** (75% $C_6H_3Cl_3$, 25% C_6H_6, 400 MHz, 130 °C): δ

^{13}C Chemical Shift	Assignment
172.17	C^{10}, C^{11}
46.18	C^{3}, C^{4}
44.93, 44.75	C^{1}, C^{2}, C^{5}, C^{6}
43.54, 43.48	C^{7}, C^{8}
37.53	$C1\alpha$
33.25	$C1_{br}$
30.46	$C1\delta$
30.5-30.0 max. at 30.36, 30.17, 29.97	CH_2 backbone
27.43	$C1\beta$
23.34	CH_3 of a C4 branch
22.83	CH_3 of a C5 branch
20.32	$C1_1$ (CH_3 of a C1 branch)
14.01	CH_3 of a C3 branch
11.15	CH_3 of a C2 branch

Results obtained for ^{13}C NMR spectroscopic analysis for branch content of copolymer:

C1/ 1000C	**C2/ 1000C**	**C3/ 1000C**	**C4/ 1000C**	**C5/ 1000C**	**C6+/ 1000C**	**Total*/ 1000C**	**Mole% Comonomer**
27	3	1	1	2	3	37	0.4%

* Does not include negative bias of up to 30% for branch level determination by ^{13}C NMR.

Ethylene-Tricyclo[4.2.1.0^{0,0}]non-7-ene- n-butyl-dicarboximido Copolymer (Comonomer content 0.6 mol % as determined by elemental analysis): **IR** (KBr): 1773.6 cm^{-1}, 1707.8 cm^{-1} [ν_{CO}]. **EA** (Found) C 85.59, H 14.19, N 0.29. **^{1}H NMR** (C_6H_5Br, 300 MHz, 90 °C): δ 3.38 CH_2N, 2.30, 2.07, 1.79, 1.5-0.7 with maxima at 1.42, 1.29, 1.15 (CH_2-CH_2), 0.74, 0.72. **^{13}C NMR** (75% $C_6H_3Cl_3$, 25% C_6H_6, 400 MHz, 130 °C): δ

^{13}C Chemical Shift	**Assignment**
178.04	C^{11}, C^{10}
46.35	C^7, C^8
45.0-44.9 max. at 45.09, 44.99	C^1, C^2, C^3, C^4, C^5, C^6
42.17	C^{12}
37.58	$C1_\alpha$
34.63	C^9
33.30	$C1_{br}$
30.39	$C1_\delta$
30.4-29.8 max. at 30.20, 30.01	CH_2 backbone
27.46	$C1_\beta$
20.30	$C1_1$ (CH_3 of a C1 branch)

^{13}C NMR analysis of the branch content within the copolymer shows that 7 branches per 1000 carbons are present. Only methyl (C1) branches are detected.

4.12. References

(1) Boffa, L. S.; Novak, B. M. *Chem. Rev.* 2000, *100*, 1479-1493.

(2) Britovsek, G. J. P.; Gibson, V. C.; Wass, D. F. *Angew. Chem.-Int. Edit.* 1999, *38*, 429-447.

(3) Novak, B. M.; Tanaka, H. *Abstr. Pap. Am. Chem. Soc.* 1999, *217*, U414-U414.

(4) Fatou, J. G.; Macia, I. G.; Marco, C.; Gomez, M. A.; Arribas, J. M.; Fontecha, A.; Aroca, M.; Martinez, M. C. *J. Mater. Sci.* 1996, *31*, 3095-3107.

(5) Watson, M. D.; Wagener, K. B. *Macromolecules* 2000, *33*, 5411-5417.

(6) Watson, M. D.; Wagener, K. B. *Macromolecules* 2000, *33*, 8963-8970.

(7) Marr, D. W. M. *Macromolecules* 1995, *28*, 8470-8476.

(8) Ittel, S. D.; Johnson, L. K.; Brookhart, M. *Chem. Rev.* 2000, *100*, 1169-1203.

(9) Mecking, S. *Angew. Chem.-Int. Edit.* 2001, *40*, 534-540.

(10) Klabunde, U.; Roe, D. C.; Ittel, S. D. *Abstr. Pap. Am. Chem. Soc.* 1987, *193*, 285-INOR.

(11) Klabunde, U.; Ittel, S. D. *Journal of Molecular Catalysis* 1987, *41*, 123-134.

(12) Correia, S. G.; Marques, M. M.; Ascenso, J. R.; Ribeiro, A. F. G.; Gomes, P. T.; Dias, A. R.; Blais, M.; Rausch, M. D.; Chien, J. C. W. *J. Polym. Sci. Pol. Chem.* 1999, *37*, 2471-2480.

(13) Johnson, L. K.; Mecking, S.; Brookhart, M. *J. Am. Chem. Soc.* 1996, *118*, 267-268.

(14) Mecking, S.; Johnson, L. K.; Wang, L.; Brookhart, M. *J. Am. Chem. Soc.* 1998, *120*, 888-899.

(15) Mehler, C.; Risse, W. *Makromolekulare Chemie-Rapid Communications* 1992, *13*, 455-459.

(16) Mathew, J. P.; Reinmuth, A.; Melia, J.; Swords, N.; Risse, W. *Macromolecules* 1996, *29*, 2755-2763.

(17) Goodall, B. L.; McIntosh, L. H.; Rhodes, L. F. *Macromol. Symp.* 1995, *89*, 421-432.

(18) Wang, C. M.; Friedrich, S.; Younkin, T. R.; Li, R. T.; Grubbs, R. H.; Bansleben, D. A.; Day, M. W. *Organometallics* 1998, *17*, 3149-3151.

(19) Younkin, T. R.; Conner, E. F.; Henderson, J. I.; Friedrich, S. K.; Grubbs, R. H.; Bansleben, D. A. *Science* 2000, *287*, 460-462.

(20) Bauers, F. M.; Mecking, S. *Macromolecules* 2001, *34*, 1165-1171.

(21) Wiberg, K. B. *Angew. Chem.-Int. Edit. Engl.* 1986, *25*, 312-322.

(22) Mehler, C.; Risse, W. *Macromolecules* 1992, *25*, 4226-4228.

(23) Rische, T.; Waddon, A. J.; Dickinson, L. C.; MacKnight, W. J. *Macromolecules* 1998, *31*, 1871-1874.

(24) Arndt-Rosenau, M.; Beulich, I. *Macromolecules* 1999, *32*, 7335-7343.

(25) McKnight, A. L.; Waymouth, R. M. *Macromolecules* 1999, *32*, 2816-2825.

(26) Vanderhart, D. L.; Khoury, F. *Polymer* 1984, *25*, 1589-1599.

(27) Han, O. C.; Chae, S. A.; Han, S. G.; Woo, S. K. *Bull. Korean Chem. Soc.* 1996, *17*, 1074-1077.

(28) Pangborn, A. B.; Giardello, M. A.; Grubbs, R. H.; Rosen, R. K.; Timmers, F. J. *Organometallics* 1996, *15*, 1518-1520.

(29) Boaz, N. W. *Tetrahedron: Asymmetry* 1995, *6*, 15-16.

(30) Ramaswamy, S.; Oehlschlager, A. C. *Tetrahedron* 1991, *47*, 1145-1156.

Chapter 5

The Effect of Ligand Modification Upon Olefin Coordination in Neutral Pt^{II} Alkyl-Olefin Complexes. Implications for the Past Performance and Future Design of Neutral Ni^{II} Oligomerization and Polymerization Catalysts.

5.1 Abstract

This chapter reports the synthesis, characterization, and study of neutral salicylaldimine Pt^{II} alkyl/ olefin complexes of the type: $\{\mathit{O}C_6H_3X_1X_2(CH{=}\mathit{N}\text{-}Ar)\}Pt(R)(CH_2CH_2)$ [R = Et, Ar = $2,6\text{-}(^iPr)_2C_6H_3$: X_1 = 9-Anthr, X_2 = H (**5.15**); X_1 = H, X_2 = OMe (**5.20**); X_1 = H, X_2 = H (**5.21**); X_1 = H, X_2 = Br (**5.22**); X_1 = H, X_2 = NO_2 (**5.23**); X_1 = 9-(10-NO_2-Anthr), X_2 = NO_2 (**5.24**); X_1 = NO_2, X_2 = NO_2 (**5.25**)], [R = Et, Ar = C_6H_5: X_1 = NO_2, X_2 = NO_2 (**5.36**)], [R = Me, Ar = $2,6\text{-}(^iPr)_2C_6H_3$: X_1 = 9-Anthr, X_2 = H (**5.17**)], and $[\{\mathit{O}C_6H_3X_1X_2(CH{=}\mathit{N}\text{-}Ar)\}Pt(Me)(\mu\text{-}COD)]_2$ [Ar = $2,6\text{-}(^iPr)_2C_6H_3$, X_1 = 9-Anthr, X_2 = H (**5.20**)]. Variation of the salicylaldimine ligand has provided an understanding of how perturbation of the steric and electronic framework of the ligand leads to changes in the coordination and behavior of the alkyl and η^2-olefinic moieties. Analogous neutral complexes of the type, $[L,L']Pt(Et)(CH_2CH_2)$ [L,L'] = 2-pyridinecarboxylate (pyca) (**5.31**), acetylacetonate (acac) (**5.32**), and a β-diiminate (nacnac) (**5.35**)] were also prepared and studied. All complexes containing asymmetric bidentate ligands display two isomeric forms, *cis-* and *trans-*, with the *cis-* geometry (olefin bound *trans-* to the anionic group) as the ground state in solution when R = Et, and the *trans-* geometry is the ground state when R = Me. There exists a linear free energy relationship between the energy of the two isomers $\Delta(\Delta G°)$ for **5.20-5.24** and the electronic nature of the chelate, suggesting that good π-donors provide an increased stability to the *cis-* adduct by increasing the degree of Pt-olefin π-backbonding. These results are supported by the observed barrier to olefin rotation, $\Delta G^{\ddagger}_{298}$ which increases slightly in the order: **5.25** < **5.24** < **5.23** < **5.22** < **5.15** < **5.21** < **5.20**. Olefin exchange is observed at room temperature between free ethylene and the *trans-* isomers of complexes **5.15**, **5.24**, and **5.25**, both isomers of **5.31**, and **5.32** (T_c ~ -50 °C). Understanding trends concerning ethylene self-exchange led to the design of complex **5.36**, which freely exchanges ethylene with both isomers at room temperature. Lineshape analysis of the exchange for **5.36** demonstrates that the barrier for olefin interchange is lower for the *trans-* isomer ($\Delta S^{\ddagger}$ = -33.4 cal mol^{-1} K^{-1}, $\Delta H^{\ddagger}$ = -2.66 kcal mol, $\Delta G^{\ddagger}_{298}$ = 7.30 kcal/mol) than the *cis-* isomer ($\Delta S^{\ddagger}$ = -39.2 cal mol^{-1} K^{-1}, $\Delta H^{\ddagger}$ = -1.80 kcal mol, $\Delta G^{\ddagger}_{298}$ = 9.89 kcal/mol.), and that both isomers undergo self-exchange by an associative mechanism. Combining all of the data results in an olefin binding energy

scale: **5.25** < **5.24** < **5.23** < **5.22** < **5.15** < **5.21** < **5.20**, where the *cis-* isomer has a higher binding affinity than the *trans-*. A mechanism for Ni^{II} oligomerization and polymerization is proposed which suggests that bidentate ligands with π-donating anions and good σ-donors should be targets for Ni^{II} polymerization catalysts, whereas anions which are coupled to a π-acidic partner should yield oligomerization catalysts.

5.2 Understanding the metal-catalyzed polymerization processes—a brief overview

A vast amount of effort has been directed towards understanding the steps in the metal-catalyzed polymerization of unsaturated molecules such as ethylene and α-olefins. The knowledge obtained from such studies has often enabled the rational development of new and improved catalyst systems.[1-3] One basic requirement is the formation of $L_nM(\eta^2$-alkene)R complexes of essentially *cis-* configuration, since the 1,2-insertion of η^2-coordinated olefins into a metal-alkyl, -aryl, or -hydride bond is believed to occur by a migration of the nucleophilic alkyl group to the unsaturated species (Figure 5.1).[4] The transition state for olefin insertion requires a coplanar M-C-C-R arrangement which often collapses to a β-agostic species (**5.1**) before binding an additional equivalent of olefin to yield **5.2**.[4] The observation (to a spectroscopically detectable level) or isolation of complexes such as **5.1** which are relevant to polymerization is exceptional.[5-8] Alkyl/olefin complexes, such as **5.2**, are more prevalent in the literature (with d^n complexes where $n \neq 0$), but many of these complexes are kinetically stable and do not perform insertion.[9-13] Two notable exceptions include $[Cp^*\{(MeO)_3P\}MR(C_2H_4)]^+$ {where M = $Co^{III/}$ or $Rh^{III/}$ and R = H or Et}[14,15] and $(L_n)_2M(\eta^2\text{-}CH_2{=}CHR)H$ {where M = $Nb^{III/}$ or $Ta^{III/}$, L_n = Cp or

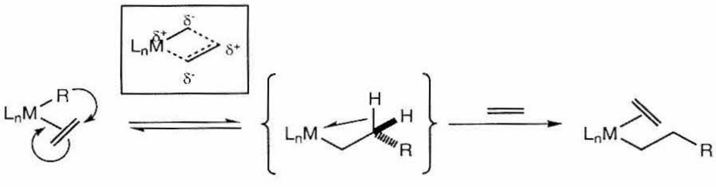

5.1 **5.2**

Figure 5.1. Migratory insertion of an alkyl group to the η^2-bound olefin (the reverse is β-hydride elimination). Fundamental studies suggest the intermediacy of a β-agostic structure such as depicted in **5.1**.

Cp*, and R = H, Me, or p-C_6H_4X},[16-18] both of which have served as valuable models for the active site in polymerizations using early- and late-metal catalysts, respectively.

Attaining an understanding of polymerization systems which operate with high turnover frequencies (approaching the rate of diffusion) is difficult, since few techniques have been developed that can both provide detailed information as well as accumulate data on the appropriate timescale [NMR "Timescale" ~ 10^1–10^6/sec. (slow but diagnostic); "IR Timescale" ~ 10^{12}/sec. (fast but less informative)].[4] The recent surge of interest in using late-transition metal insertion catalysts to prepare functionalized polyolefins has, in fact, provided a few examples of such highly active systems which can prepare high molecular weight polymers. These catalysts are based on cationic Fe^{II}, Co^{II}, Ni/Pd^{II} and neutral Ni^{II} metal centers.[19-21] Many *very similar complexes*, however, are observed to produce *oligomeric materials* or exhibit *much lower* rates of polymerization. Although high-throughput techniques may allow for an expedient, serendipitous solution to the challenge at hand,[22] it can be said with certainty that the understanding of late-metal polymerization systems is still in it's infancy.

Some information has been put forth about the barrier to insertion, propagation, and isomerization with alkyl diimine complexes of Ni^{II} and Pd^{II}.[20,23-25] Monitoring ethylene insertion at low temperatures indicated that $(N\text{^}N)M(R)(CH_2{=}CH_2)^+$ (similar to **5.2**) is the resting state for ethylene polymerizations for both Ni and Pd complexes.[20,24] The barrier for migratory insertion is slightly lower for Ni^{II} ($\Delta G_{Ni}^{\ddagger}$ = 13-14 kcal/mol) than for Pd^{II} ($\Delta G_{Pd}^{\ddagger}$ = 17-19 kcal/mol).[20,24] When propylene is the monomer, the insertion barriers are similar ($\Delta G_{Ni}^{\ddagger}$ = 14 kcal/mol; $\Delta G_{Pd}^{\ddagger}$ = 18-19 kcal/mol),[20,24,25] but the resting state for the Ni^{II} species was found to be the β-agostic structure (**5.1**) whereas the Pd^{II} resting state remains the olefin adduct **5.2**. Variation of the ligand set or monomer, however, can change this delicate balance, as the resting state for cyclopentene polymerization with Pd^{II} has been determined to be the β-agostic alkyl species (**5.1**).[20] Additional studies determined the migratory insertion barriers for acrylate ($\Delta G_{Pd}^{\ddagger}{}_{298}$ ~ 16-17 kcal/mol) as well as the ΔG for ethylene/acrylate binding = 4.9 kcal/mol.[26]

The preparation of model compounds–isoelectronic to the proposed intermediate(s)—has long served as an informative tool for the study of catalytic systems.[16,27] Recently, such strategies have targeted highly-active late-metal cationic systems through the preparation of $\mathrm{Pt^{II}}$ (**5.3**), $\mathrm{Ru^{II}}$ (**5.4**) and $\mathrm{Rh^{III/}}$ (**5.5**) alkyl/ olefin complexes (Figure 5.2).[11,13,28,29] Structural studies have elucidated the geometry of the catalyst resting state as well as the dependence of ligand structure on the position of the counterion. [13,28-30]

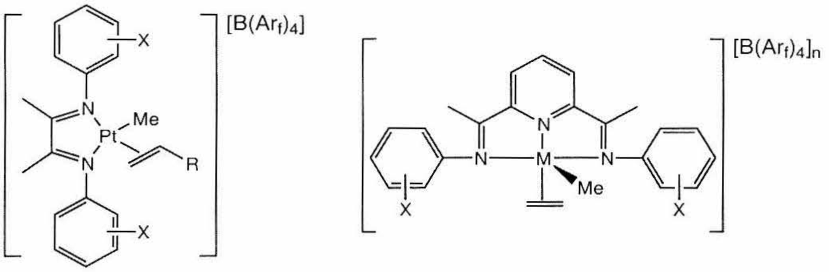

5.3

M = Ru n = 1 **5.4**
M = Rh n = 2 **5.5**

Figure 5.2. Model compounds of cationic highly active late-metal polymerization catalysts.

This chapter outlines the synthesis, characterization, and study of a series of neutral $\mathrm{Pt^{II}}$ alkyl/olefin complexes, such as **5.6** and **5.7**, which serve as kinetically stable model systems of the putative active species (**5.8**) in the $\mathrm{Ni^{II}}$-catalyzed polymerization process outlined in Chapters 2-4. We hoped that **5.6** and **5.7** would provide valuable information about: (a) the nature and importance of the olefin and alkyl chain geometries in **5.8** during polymerization, including differences between the ground state structures of the *cis-/ trans-* isomers, (b) how modification of the ligand structure gives rise to

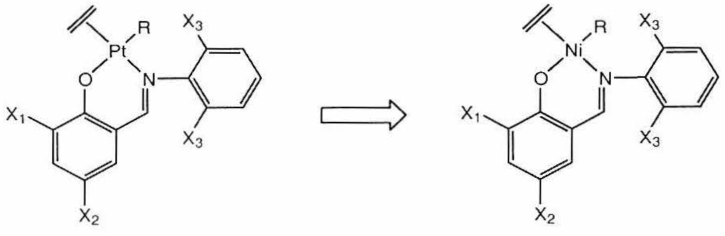

R = CH_3 **5.6**
R = CH_2CH_3 **5.7**

5.8

increased or decreased π-backbonding to the η^2-coordinated olefin, (c) how variation of the chelate affects the rate of β-hydride elmination, (d) the factors which affect the associative displacement of the growing polymer chain, and (e) elucidation of the rate of ligand exchange between ethylene and other donors, such as $NCCH_3$, pyridine, phosphines, etc. In addition, the preparation of complexes containing other anionic bidentate ligands, such as 2-pyridine carboxylate (pyca), acetylacetonate (acac), and a β-diiminate (nacnac), have provided crucial information about possible differences between Ni^{II} catalysts for oligomerization and polymerization.

5.3. Synthesis and Characterization of Neutral Salicylaldimine Pt^{II} Alkyl / Olefin Complexes

Pt^{II} olefin complexes are among the oldest class of organometallic complexes known, with Ziese initially reporting $K[Pt(C_2H_4)Cl_3]\ H_2O$ in 1830.[31] Since then, Pt^{II} olefin adducts have been extensively studied because of their increased kinetic stability relative to Ni^{II} or Pd^{II} analogs that are often of greater use in catalysis.[4] Insertion of olefins into Pt-aryl bonds are well-studied,[32] but only a handful of reports describe insertion into a Pt^{II} alkyl bond. These rare systems capitalize on the relief of ring strain or the formation of exceptionally strong metal-alkyl bonds as the driving force.[33-35] Recently, however, the aforementioned studies on Pt^{II} alkyl/olefin complexes bearing diimine ligands (**5.3**) show that the insertion of acrylates is possible in a fashion similar to the well-documented Pd^{II} systems.[20] Unfortunately, these Pt^{II} compounds are not effective initiators for the polymerization of ethylene or α-olefins.[11,28,29]

We envisioned the synthesis of complexes **5.6** and **5.7** using adaptation on well-known methods (Scheme 5.1). Reaction of the Na, Cs, or Tl salt of the appropriate ligand with either $\{MePt(CH_2{=}CH_2)(\mu\text{-}Cl)\}_2$ (**5.9**)[9,10] or $\{EtPt(CH_2{=}CH_2)(\mu\text{-}Cl)\}_2$ (**5.10**)[12] could provide **5.6** and **5.7** *via* liberation of the chloride salt. A second salt metathesis route involves the reaction of the ligand salt with the well-studied complex Pt(COD)MeCl (**5.11**) forming Pt(Sal)Me(η^2-COD) (**5.12**) that could be transformed to **5.6** by displacement of the η^2-coordinated COD with ethylene. Finally, in analogy to the synthesis of phosphine-free Ni^{II} and Pd^{II} salicylaldimine complexes described in Chapter 3, the reaction of the phenolic ligand with either (η^4-COD)$PtMe_2$ (**5.13**) or (tmeda)$PtMe_2$

(**5.14**)[36,37] could provide complex **5.6** with the concomitant liberation of methane. As outlined below, three synthetic routes could allow for the successful of the desired Pt^{II} alkyl/olefin complexes.

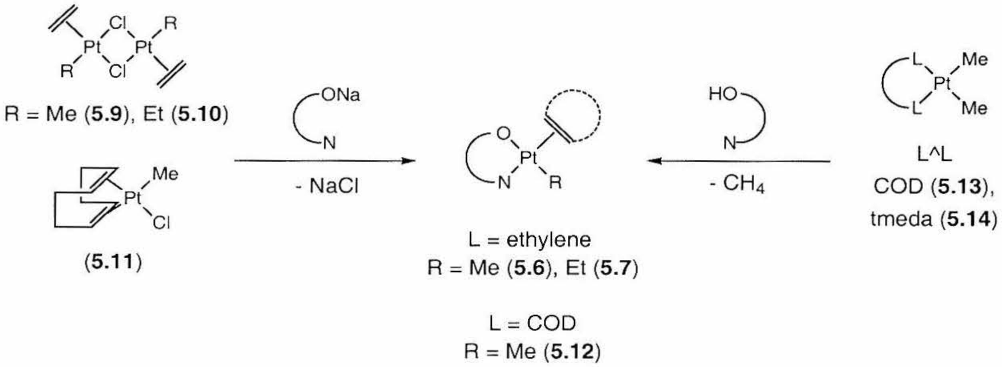

Scheme 5.1. Proposed synthesis of Pt^{II} Alkyl/Olefin salicylaldimine complexes **5.6, 5.7**, and **5.12**.

The availability of **5.10** from commercially available $K_2[PtCl_4]$ in one step was very attractive and was used exclusively for the preparation of the remainder of the Pt^{II} compounds described later.[12] In addition, although it was unclear at the onset whether the presence of β-hydrogens in **5.7** would lead to a decreased stability due to β-hydrogen elimination (βHE), such compounds appear to have an *increased* stability relative to the related methyl compounds (**5.6**). In addition, the preparation of ethyl complexes such as **5.7** has allowed the study of rates of β-hydrogen elimination.

The reported synthesis of **5.10**, *via* reaction of ethylene (800-900 psig) and H_2O upon $K_2[PtCl_4]$ proves to be a high yielding, reliable, and scalable procedure.[12] Dimer **5.10** could be isolated as an off-white solid from $CHCl_3$. It is moderately stable in the solid-state at low temperature (-30 °C), but darkens to a blackish-gray material over a couple of weeks at room temperature, under both aerobic and anaerobic conditions. Fortunately, compound **5.10** can be easily rejuvenated by dissolution in $CHCl_3$ followed by passage through a plug of celite with very little mass loss (~ 15% after two months). The dimer possesses diagnostic ^1H NMR ($CDCl_3/C_6D_6$) signals for the coordinated ethylene, $Pt(CH_2{=}CH_2)$ $\delta = 3.70/3.22$ (s, 4H, $^2J_{PtH} \sim 80$ Hz), as well as the pendant ethyl group, $PtCH_2CH_3$ δ= 1.22/1.13 (q, 2H, $^2J_{PtH}$ ~ 80 Hz) and $PtCH_2CH_3$ δ= 0.72/0.79 (t, 3H, $^2J_{PtH}$ ~ 38 Hz).

Mixing **5.10** with one equivalent of Na(^{Anthr,H}Sal) in C_6D_6 at ambient temperature led to a rapid consumption (< 10 min) of the starting materials as evidenced by loss of the diagnostic ^{1}H NMR signals for **5.10** and the sodium salt. In conjunction with the disappearance of these signals, two new species assigned initially as **5.15*M*** (*MAJOR*) and **5.15*m*** (*minor*), were present in an ~ 83/17 ratio as evidenced by the diagnostic ^{1}H NMR signals outlined in Table 5.1. The similarity between both the ^{1}H NMR splitting patterns and integrations suggested that the two species were intimately related, possibly as geometrical isomers. The isopropyl groups of the ligand serves as an excellent probe for the local geometry of the metal center. The observation of two doublets for –CHMe*Me'* and –CH*Me*Me' as well as a septet for –*CH*MeMe' mandates that the imine is (on the NMR timescale) constrained to an environment which differentiates the forward and backward methyl groups while maintaining equivalent methine shifts. Such patterns are typical for square planar d^8 salicylaldimine complexes (Chapters 2 & 3) with an equatorial mirror plane perpendicular to the aryl group of the benzimine, and suggests that dissociation of the imine does not readily occur at room temperature, i.e., that rotation about the N-C^{ipso} bond is restricted.

The Pt^{II}-ethylene signals are singlets which resonate at δ = 2.8 (**5.15*M***) and 3.9 ppm (**5.15*m***) and maintain sharp ^{195}Pt-satellites (which arise from a ^{1}H coupling to ^{195}Pt, I = ½, 33% natural abundance). These results indicate that any exchange processes, such as the reversible dissociation of C_2H_4, are slow at 25 °C, and that rapid rotation of the η^2-coordinated olefin occurs about the Pt-olefin axis.[10] The ethylene chemical shift values are upfield relative to the range typical observed for four coordinate alkyl/ olefin complexes (4.4 – 4.8 ppm), which may be caused by the presence of the perpendicular aryl group on the ^{Anthr,H}Sal ligand.[11,38] The signals for the Pt^{II} ethyl groups fall within the expected range for square planar Pt^{II} complexes and demonstrate sharp ^{195}Pt satellites within the expected values ($^2J_{PtH}$ ~ 80 Hz, $^3J_{PtH}$ ~ 40 Hz).[12]

Further support for the presence of geometrical isomers (with rapid rotation about the Pt-olefin axis) was found using ^{13}C NMR, that displays signals for two platinum-bound olefins, with the major signal resonating at δ = 55.1 ($^1J_{PtC}$ = 264 Hz) and the

Table 5.1. ^{1}H NMR (300.0 MHz, C_6D_6, T = 25°C) data for (^{Anthr,H}Sal)Pt^{II} ethyl/ethylene complexes **5.15*M*** and **5.15*m***.

Group	**5.15*M* (83%)**	**5.15*m* (17%)**
PtCH$_2$***CH$_3$***	0.909 ($^3J_{PtH}$ = 33.6 Hz)	0.240 ($^3J_{PtH}$ = 44.4 Hz)
Pt***CH$_2$***CH$_3$	1.085 ($^2J_{PtH}$ = 78.0 Hz)	0.476 ($^2J_{PtH}$ = 86.4 Hz)
Pt(***CH$_2$***=***CH$_2$***)	2.754 ($^2J_{PtH}$ = 67.8 Hz)	3.898 ($^2J_{PtH}$ = 63.3 Hz)
CH***Me***Me', CHMe***Me'***	1.024, 1.340	1.093, 1.273
C***H***MeMe'	3.107	3.271
C***H***=NAr	8.228 ($^3J_{PtH}$ = 22.5 Hz)	8.041 ($^3J_{PtH}$ obscured)

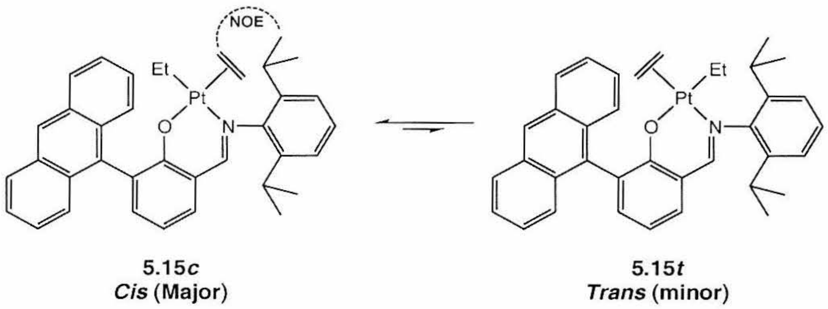

minor at δ = 67.5 ($^1J_{PtC}$ = 237 Hz). Based on these preliminary observations, **5.15*M*** and **5.15*m*,** were postulated as *trans*- and *cis*- geometrical isomers.

Originally, the major species (**5.15*M***) was proposed to be the *trans*- isomer, **5.15*t***, based on the NMR data for the related complex Pt(CH_2CH_2)(Py)MeCl **5.16**, where two of the three possible isomers were observed-- the *trans* (**5.16*t***, 75%, Pt-et δ 3.53) and *cis* (**5.16*c***, 25%, Pt-et δ = 4.12).[10] The *cis*- isomer with the strong σ-donating methyl group *trans*- to the ethylene was not observed.[10] The authors argued that the stability of the *trans*- arrangement was due, in part, to the high *trans*- influence of the methyl group that "labilizes" pyridine in **5.16*c***. Although the chemical shifts differ by ~ 0.75 ppm, the $^2J_{PtH}$ ~ 68 Hz for the coordinated ethylene of **5.15*M*** was in good agreement with that for **5.16*t*** ($^2J_{PtH}$ = 72 Hz).

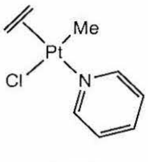

5.16*t*
75 %

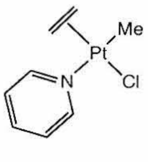

5.16*c*
25 %

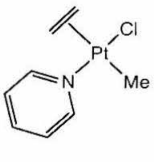

5.16
Not Observed

^{1}H NOESY NMR analysis led to the surprising discovery that the major species in solution was, in fact, the *cis-* isomer as evidenced by an NOE between the sp^2-hybridized olefin protons and the forward pointing –CHMe*Me'* group of the aryl imine. Further confirmation of the structure of the major species **5.15*c*** was obtained by X-ray analysis. Yellow crystals of suitable quality were prepared by the slow vapor diffusion of hexane into a saturated solution of **5.15** in toluene at room temperature over five days. Figure 5.3 depicts the structure of **5.15*c***, clearly demonstrating the *cis-* nature of the complex, as the phenoxide and the alkyl groups (both X-type donors) are bound in a *syn*-arrangement. Dissolution of the crystals at –78 °C in CD_2Cl_2 confirmed that the ground state structure, both in the solid state and in solution, is that of the *cis-* isomer **5.15*c***. Allowing the solution to stand at ambient temperature overnight led to equilibration of the sample to the same ratio observed just after formation from **5.10** (83 **5.15*c***/17 **5.15*t***), indicating that the isomers can equilibrate (albeit slowly) to reach the thermodynamic equilibrium.

The structure of **5.15*c*** will be discussed in further detail (*vide infra*), but several immediate observations should be noted. The Pt^{II} complex is in a square planar coordination environment with the η^2-bound ethylene perpendicular to the coordination plane defined by Pt, N, O, and C(3). The Pt-C(1)-H(1A) and Pt-C(1)-H(1B) angles are larger than 90°, suggesting π-backbonding from Pt into the π* of the h2-coordinated olefin,[31] and is in agreement with other square planar Pt^{II} alkyl/olefin complexes.[12,28,29,31] As observed for other structures possessing the $^{\text{Anthr,H}}$Sal ligand, the 9-anthracenyl and 2,6-diisopropylaryl groups are nearly orthogonal to the equatorial plane. There is a slight degree of disorder in the 2,6-diisopropyl phenyl group, suggesting that the aryl moiety is slightly flexible in the solid state, and therefore, likely mobile in solution.

Thermolysis of **5.15** leads to reduction of the metal center with the simultaneous production of free ligand as observed in the ^{1}H NMR by the diagnostic phenolic proton at

Figure 5.3. X-ray analysis of *cis*-($^{\mathrm{Anthr,H}}$Sal)Pt(Et)(et) **5.15*c***. Thermal ellipsoids are shown at 30% probability. All nonessential hydrogen atoms have been omitted for clarity.

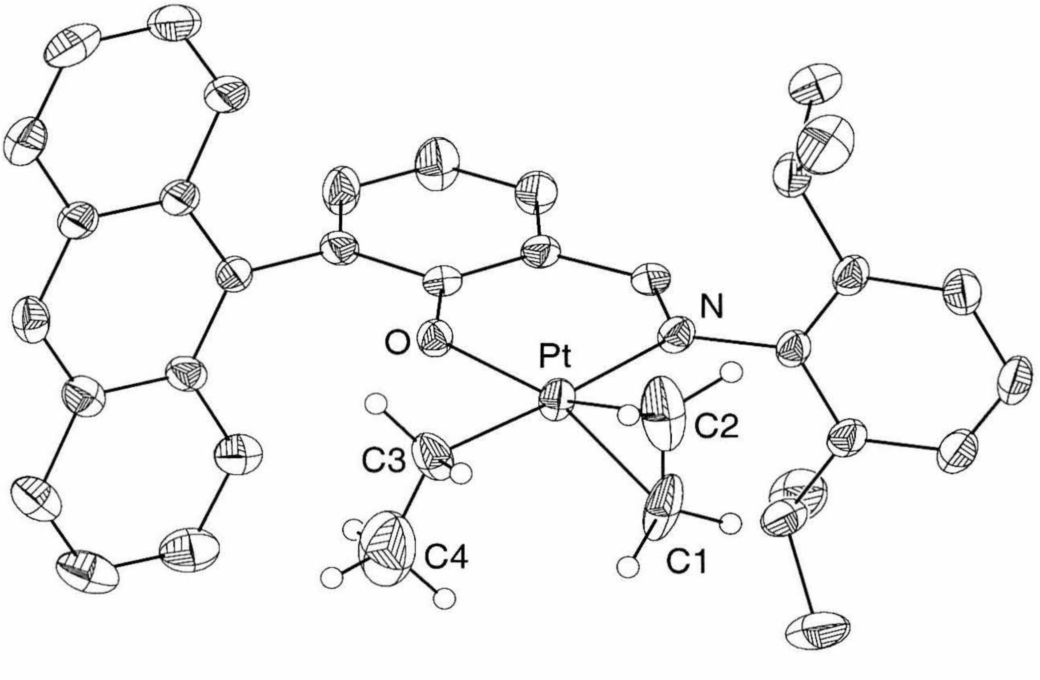

Table 5.2. Selected bond lengths (Å) and bond angles (°) for **5.15*c***.

	Bond Lengths (Å)		
Pt-N	2.126(4)	Pt-O	2.004(3)
Pt-C(1)	2.084(5)	Pt-C(2)	2.090(6)
C(1)-C(2)	1.404(8)	Pt-C(3)	2.033(5)
C(3)-C(4)	1.433(8)	N-C(5)	1.296(5)
	Bond Angles (°)		
N-Pt-O	90.25(13)	N-Pt-C(1)	96.66(19)
N-Pt-C(2)	96.2(2)	N-Pt-C(3)	174.79(16)
O-Pt-C(1)	162.2(2)	O-Pt-C(2)	156.0(2)
O-Pt-C(3)	84.54(16)	Pt-C(1)-H(1A)	116.6
Pt-C(1)-H(1B)	116.6	C(1)-Pt-C(2)	39.3(2)
C(1)-Pt-C(3)	88.3(2)	C(2)-Pt-C(3)	88.6(2)
Pt-C(3)-C(4)	109.6(4)	Pt-N-C(26)	120.8(3)

~ δ= 14 ppm (and by TLC against an authentic sample of the $^{\text{Anthr,H}}$Sal ligand) and ~ 1-2 equivalents of ethylene as evidenced by a singlet at ~ δ= 5.3 ppm by ^{1}H NMR. No hydrocarbon species or other olefinic products were detected, suggesting that migratory insertion does not occur under these conditions.[28] Studies pertaining to this decomposition will be addressed later in section 5.6. This decomposition limits the ceiling temperature for experiments with **5.15**. For example, magnetization transfer experiments aimed at determining the rate of isomerization, were performed rapidly at temperatures up to 70 °C, with some sign of decomposition. Under these conditions, no isomerization was observed. The fact that equilibration of an isomerically pure sample required 10-15 hours at 25 °C suggests that the barrier to isomerization is high ($\Delta G^{\ddagger}_{\text{isomerization}} \geq$ 20 kcal/ mol) for **5.15*c*** to **5.15*t***.

Other efforts to prepare ($^{\text{Anthr,H}}$Sal)Pt$^{\text{II}}$ alkyl/ olefin complexes were also successful. The addition of ($^{\text{Anthr,H}}$Sal)Na to **5.9** again led to the rapid and quantitative formation of the alkyl species, **5.17**, the methyl analog of **5.15**. Upon formation, the ratio of isomers (85 *Major* /15 *minor*) was similar to that observed for the ethyl complex (**5.15**). The Pt$^{\text{II}}$-ethylene signals resonated at δ= 3.22 (**5.17M**) and δ= 2.59 (**5.17m**), identical in chemical shift to the resonances for the ethyl compound **5.15**, but in inverse proportions suggesting that the favored isomer of the methyl compound in solution was **5.17*t***, the exact opposite of the ethyl compound. The compound was isolated as a single isomer by recrystallization from benzene and pentane at 5°C. Confirmation of the major isomer's structure (*trans*-) was supported by the observation of a strong NOE between the Pt-Me and the forward –CHMe*Me'*.

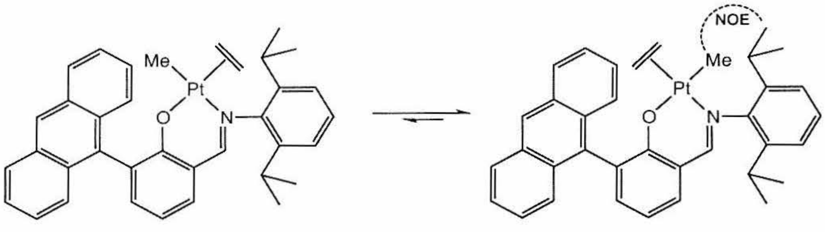

5.17*c*
Cis (minor)

5.17*t*
Trans (Major)

A solution of **5.17** in CD_2Cl_2 was monitored at room temperature by ^{1}H NMR and decomposition was observed over a 24-hour period. Although no oxidation products were observed, the well-known tendency of Pt^{II} compounds with "hard" ligand sets to oxidize suggests that oxidative addition of the chlorinated solvent such as methylene chloride might have been responsible for the complex's decay.[4,31] Similar behavior is observed for **5.15**, but requires one to two weeks at 25°C in CD_2Cl_2.

Attempts to prepare **5.12** by the addition of a phenolic ligand, such as ^{Anthr,H}Sal, to (COD)$PtMe_2$ **5.13** (Scheme 5.1) in C_6D_6 did not provide any evidence for methane liberation or ligation of the phenol, even upon prolonged heating at 80°C. The addition of one equiv. of PPh_3 to a ^{Anthr,H}Sal/(COD)$PtMe_2$ mixture, in hope that the phosphine might serve as a "promoter", led to the rapid and quantitative formation of *c*-$(PPh_3)_2PtMe_2$ (**5.18**) in 50% conversion (as evidenced by direct comparison to literature reports of the ^1H and ^{31}P NMR shifts for **5.18**).[39,40] Prolonged heating of the phenolic ligand with **5.18** at 80°C did not lead to any observable change over the course of a week. In a similar fashion, no reaction was observed between the ^{Anthr,H}Sal phenol and (tmeda)$PtMe_2$ **5.14**,[36,37] although a similar reaction has been successful for the preparation of other complexes of the type (Sal)Pt(L)Me, albeit in poor yield.[41]

The addition of the (^{Anthr,H}Sal)M {M = Na or Cs} to (COD)PtMeCl (**5.11**) in C_6D_6 leads to the rapid formation of what appears to be two species, based on sets of Pt-*Me*, -C*H*Me_2, and Pt-olefin signals in a 1:1 ratio. The methyl groups, which appear at $\delta = -0.20$ ($^2J_{PtH} \sim 82$ Hz, *trans*) and $\delta = -0.02$ ppm ($^2J_{PtH} \sim 75$ Hz, *cis*), suggest that the mixture could the *cis*- and *trans*- isomers of $Pt^{II}(\eta^2$-COD)(^{Anthr,H}Sal)Me, ***5.19c/t***. Unfortunately, the mixture quickly ($t_{1/2} \sim 1$ hour at 25°C) liberates an equivalent of free 1,5-COD. Studying the mode of olefin interchange or isomerization of **5.19** would be interesting, as it might proceed through a short-lived five-coordinate complex, such as $Pt^{II}(\eta^4$-COD)(^{Anthr,H}Sal)Me (***5.19p***). Understanding the nature this five-coordinate species could be beneficial for future ligand design. Although trigonal bipyramidal Pd^{II} and Pt^{II} complexes are well-known in the literature, almost all employ neutral bidentate ligands such as bipy or phen.[38] Typically, however, they exhibit the geometry outlined in ***5.19p***, with strong σ-donors in the axial sites and softer L-type ligands in the equatorial plane.

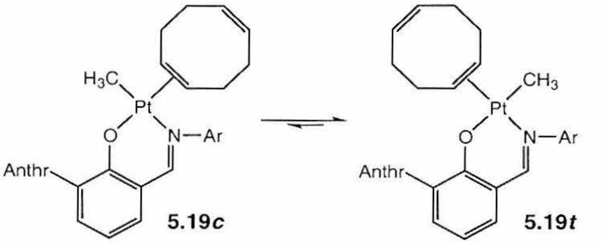

5.19*c* **5.19*t***

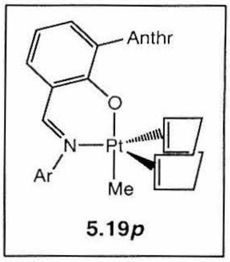

5.19*p*

Recrystallization of the mixture from benzene/hexane or benzene/pentane provided **5.19*d***, the nature of which was confirmed by X-ray diffraction analysis (Figure 5.4). As proposed, $[(^{\mathrm{Anthr,H}}\mathrm{Sal})\mathrm{PtMe}(\mu\text{-COD})]_2$ **5.19*d***, maintains a *trans-* geometry. The ^{1}H NMR signal for the Pt-Me group in **5.19*d*** is in good agreement with both the chemical shift and $^2J_{\mathrm{PtH}}$ observed for **5.17**, providing further evidence that the methyl adducts **5.17** and **5.19*d*** have a *trans-* ground state in both the solid state and solution. The diffraction data for **5.19*d*** will be readdressed below.

5.4. Modification of electronic and steric effects

To determine how the perturbation of both the electronic and steric parameters of the salicylaldimine ligand affects the metal center and the aforementioned equilibrium between *cis-* and *trans-* isomers, a series of Pt$^{\mathrm{II}}$ ethyl complexes, **5.20-5.25**, containing different groups in both the *ortho-* and *para-* positions of the phenolic moiety were synthesized and studied. The ligands were easily prepared by the condensation of one equiv. of 2,6-diisopropyl aniline with the 5-mono- or 3,5-di-substituted salicylaldehydes as outlined in previous chapters (Figure 5.5). Deprotonation of the ligand with NaH (preferred), NaO^{t}Bu, KO^{t}Bu, or CsOH, followed by reaction with the Pt$^{\mathrm{II}}$ precursor **5.10** in C_6D_6, leads to the clean formation of products **5.20-5.25** in quantitative yields as determined by ^{1}H NMR (Table 5.4). The formation of both *cis-* (**5.20*c*-5.25*c***) and *trans-* (**5.20*t*-5.25*t***) isomers was evident by a comparison of the chemical shift and $^NJ_{\mathrm{PtC}}$ for the diagnostic ^{1}H NMR resonances of the bound Pt-et and Pt-Et groups against the previously presented data obtained for complexes **5.15** and **5.17**. As shown in Table 5.4, the group occupying the position *trans-* to the phenoxide typically exhibits an upfield chemical shift and a larger value for $^NJ_{\mathrm{PtH}}$. These observations show that the hard, anionic

Figure 5.4. X-ray analysis of *trans*-[($^{\text{Anthr,H}}$Sal)PtMe(μ-COD)]$_2$ **5.19*d***. Thermal ellipsoids are shown at the 30% probability level. All non-essential hydrogen atoms have been omitted for clarity.

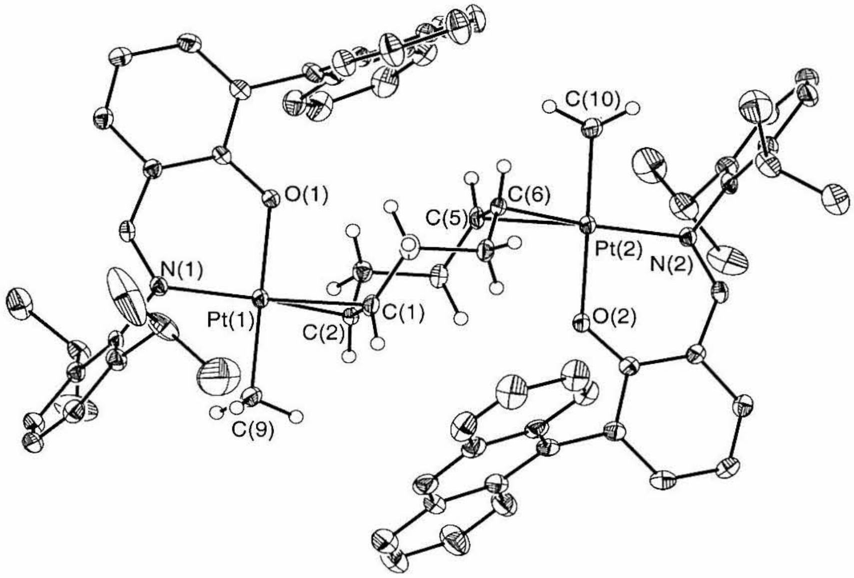

Table 5.3. Selected bond lengths (Å) and bond angles (°) for **5.19*d***.

	Bond Lengths (Å)		
Pt(1)-N(1)	2.053(3)	Pt(2)-N(2)	2.047(3)
Pt(1)-O(1)	2.095(2)	Pt(2)-O(2)	2.101(2)
Pt(1)-C(1)	2.152(4)	Pt(2)-C(5)	2.142(4)
Pt(1)-C(2)	2.143(4)	Pt(2)-C(6)	2.146(4)
C(1)-C(2)	1.391(6)	C(5)-C(6)	1.378(6)
Pt(1)-C(9)	2.036(4)	Pt(2)-C(10)	2.040(4)
	Bond Angles (°)		
N(1)-Pt(1)-O(1)	90.14(11)	N(1)-Pt(1)-C(9)	91.28(15)
N(1)-Pt(1)-C(1)	160.78(15)	N(1)-Pt(1)-C(2)	161.43(15)
O(1)-Pt(1)-C(1)	88.59(15)	O(1)-Pt(1)-C(2)	90.87(13)
O(1)-Pt-C(9)	177.17(17)	Pt(1)-C(1)-H(1)	103(2)
Pt(1)-C(1)-C(8)	117.8(3)	C(1)-Pt-C(2)	37.78(15)

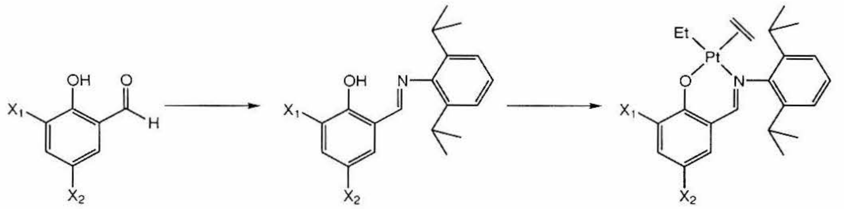

X_1	X_2	
H	OMe	5.20
H	H	5.21
H	Br	5.22
H	NO_2	5.23
10-NO_2-Anthr	NO_2	5.24
NO_2	NO_2	5.25

Figure 5.5. Synthesis of Pt^{II} ethyl/ ethylene complexes **5.20-5.25**. (*a*) 2,6-(^{i}Pr)$_2$-C_6H_3, MeOH, Δ, cat. HCO_2H; 65-86%. (*b*) NaH, THF; **5.10**, C_6D_6, 60-80%.

Ar*O*$^-$ exhibits a greater *trans*- influence compared to the aryl imine, -CH=*N*Ar,[4,10,31] often considered to be borderline on the "hard"/"soft" acid table.[42] ^{1}H NMR shifts for the Pt-et resonance of the *cis*- isomers (~ 2.7 ppm) demonstrate a sharp singlet ($\Delta\upsilon_{1/2}$ ~ 3 Hz, $^2J_{PtH}$ ~ 65-70 Hz), whereas the signal for the *trans*- isomer (~ 3-4 ppm) is broadened considerably ($\Delta\upsilon_{1/2}$ ~ 12 Hz, T = 25°C) in several cases (Figure 5.6). Broadening of Pt^{II}-olefin signals has often been attributed to olefin exchange processes.[10,11,28,29]

All reactions were monitored by ^{1}H NMR to ensure complete formation of the desired compound(s) before isolation. Interestingly, the equilibrium established at the initial stage of the reaction is the same as that established upon isolation of isomerically pure crystals and slow equilibration (*vide supra*). The neutral Pt^{II} complexes are recrystallized using primarily benzene/hydrocarbon or benzene/acetonitrile mixtures at ambient or low temperature {~ -30 to 10°C)}. The complexes proved to be susceptible to decomposition over prolonged periods of time, especially at elevated temperatures or in halogenated solvents. Again, it is believed that oxidative addition to a Pt^{IV} species might be the decomposition pathway, but conclusive evidence has not been obtained.

Dissolution of the isolated complexes **5.20-5.25** in C_6D_6, led to the observation that the ratio of the isomers ($K_{cis/trans}$) present at 25°C was dependent on the electronic nature of the ligand, with a decreased $K_{cis/trans}$ when using ligands with electron withdrawing groups. Figure 5.6 demonstrates the difference between compounds **5.23** and **5.25**, which utilize the *p*-NO_2 and *o,p*-$(NO_2)_2$ ligands, respectively. Remarkably, the lower energy isomer shifts from ***5.23c*** to ***5.25t***. The values of $K_{cis/trans}$ for a series of compounds are outlined in Table 5.5. The difference in free energy between the two isomers can be calculated using eq. (5.1). Comparison of trials **5.15**, **5.24**, and **5.25**,

Table 5.4. Diagnostic ^{1}H NMR signals for Pt^{II} alkyl/ethylene complexes.

Compound	**Ligand (X$_1$, X$_2$)**	**Eq. Ratio**	**Pt*CH$_2$*R δ (ppm)**	**^{2}J$_{PtH}$ (Hz)**	**PtCH$_2$*CH$_3$* δ (ppm)**	**^{3}J$_{PtH}$ (Hz)**	**Pt(*CH$_2$=CH$_2$*) δ (ppm)**	**^{2}J$_{PtH}$ (Hz)**
Salicylaldimines								
5.20*t*	H,OMe	5	0.22	82	0.28	40	3.45	65
5.20*c*		95	1.04	78	0.86	33	2.85	78
5.21*t*	H,H	12	0.47	85	0.24	43	3.91	63
5.21*c*		88	1.08	77	0.91	36	2.76	68
5.22*t*	H,Br	15	0.42	88	0.25	41	3.18	81
5.22*c*		85	1.04	75	0.88	36	2.68	68
5.15*t*	Anthr,H	17	0.48	86	0.24	44	3.90	63
5.15*c*		83	1.09	78	0.91	34	2.75	68
5.23*t*	H,NO$_2$	28	0.58	82	0.25	41	4.01	65
5.23*c*		72	1.12	80	0.92	36	2.88	70
5.24*t*	NO$_2$Anthr,NO$_2$	32	0.42	85	0.06	42	3.26	62
5.24*c*		68	0.25	77	-0.48	31	2.70	72
5.36*t*	NO$_2$, NO$_2$ (Ph)	53	0.62	80	0.27	39	3.09	76
5.36*c*		47	1.17	81	0.83	36	4.06	68
5.25*t*	NO$_2$, NO$_2$	58	0.62	86	0.19	43	4.13	68
5.25*c*		42	1.19	78	0.83	35	2.99	75
5.17*t*	Anthr,H	87	-0.14	76	[c]	[c]	3.22	60
5.17*c*		13	0.16	70	[c]	[c]	2.59	67
Other Ligands								
5.31	Pyca	75	1.14	80	0.90	38	3.55	70
5.31		25	1.24	76	0.98	35	4.06	71
5.32	Acac[d]	NA[e]	1.14	79	0.72	37	3.49	70
5.35	Nacnac[d]	NA[e]	-0.01	68	0.42	39	2.80	64

[a] C$_6$D$_6$, T = 25°C. [b] signals obscured in ^{1}H NMR. [c] R = Methyl. [d] Generated *in situ* (CD$_2$Cl$_2$) T = 25°C. [e] NA = Not Applicable. Ligand is symmetric, therefore, no isomers present.

$$\Delta(\Delta G°) = -RT[\ln(K)] = -RT[\ln(Pt_{cis}/Pt_{trans})] \qquad (5.1)$$

reveals that that modification of the size of the substituent in the *ortho-* position of the phenolic ring has very little impact on Δ(ΔG°). In fact, it appears that the 9-anthracenyl-

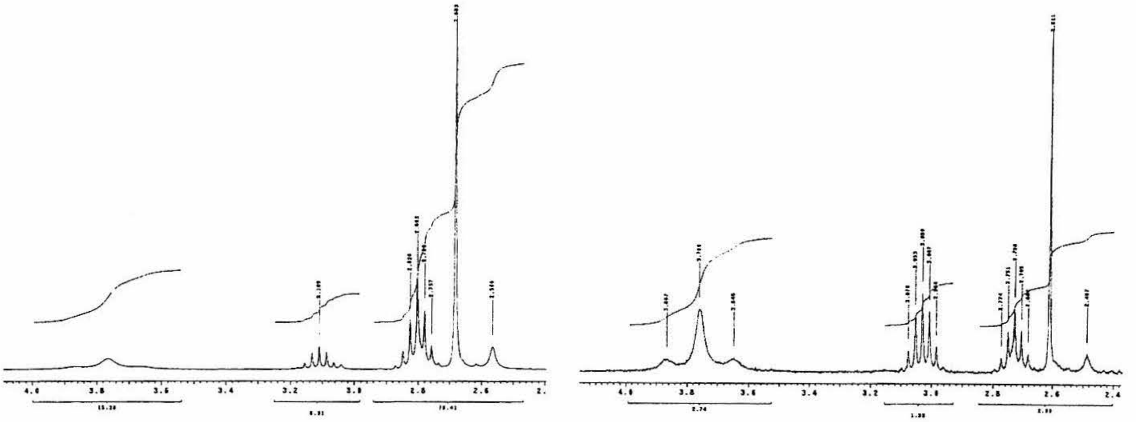

Figure 5.6. Comparison of ^1H NMR (C_6D_6, T = 25°C) of (*a*) **5.23** and (*b*) **5.25**, demonstrating variation of the concentration of *cis-* and *trans-* isomers through modification of the ligand architecture.

Table 5.5. Variation of *cis-/ trans-* ratio by ligand modification.[a],[b]

Compound	X_1	X_2	R	Cis	Trans	K	$\Delta(\Delta G°)$[c]	σ_p^+ [d]
5.20	H	OMe	Ar	95	5	19.00	-1.71 (6)	-0.78
5.21	H	H	Ar	88	12	7.33	-1.16 (4)	0
5.22	H	Br	Ar	85	15	5.67	-1.01 (3)	0.15
5.15	Anthr	H	Ar	83	17	4.88	-0.96 (6)	-
5.31	Pyca	-	-	75	25	3.00	-0.65 (2)	-
5.23	H	NO_2	Ar	72	28	2.57	-0.59 (3)	0.79
5.24	10-NO_2Anthr	NO_2	Ar	68	32	2.13	-0.44 (5)	-
5.33	**Acac***	-	-	50	50	1.00	0.00 (4)	
5.36	NO_2	NO_2	Ph	47	53	0.89	0.07 (3)	-
5.25	NO_2	NO_2	Ar	42	58	0.72	0.19 (4)	-
5.16[e]	(Py)(Me)Pt(et)Cl	-	-	25	75	0.33	~ 0.66	-
5.17[f]	Anthr	H	Ar	18	82	0.22	0.88 (4)	-
5.19[g]	Anthr	H	Ar	ND[h]	>99	-	-	-

[a] Conditions: 15 μmol Pt^{II} complex, 0.7 mL C_6D_6 (~ 21 mM), T = 25 °C (298.2 K). [b] Ar = 2,6-$(^iPr)_2C_6H_3$, Ph = C_6H_6. [c] Calculated according to equation (5.1) using T = 298.2 K and R = 1.987 cal (mol^{-1}) (K^{-1}). [d] Values for σ^{p+} taken from reference [43]. [e] Values extrapolated from reference [10]. [f] Alkyl group = methyl. [g] Alkyl group = methyl; olefin = η^2-COD. [h] ND = none detected.

substituents serve merely as a very large σ-withdrawing groups (falling somewhere between the σ-withdrawing power of Br and NO_2). The 9-anthracenyl groups are believed to have little effect on the π-system, since they are nearly orthogonal to the phenolic ring as observed in Figures 5.3 and 5.4. Variation of the size of the aryl group on the benzimine has a more pronounced effect on the $K_{cis/trans}$ (compare trials **5.25** and **5.26**). This nature of this effect is unclear since removal of the isopropyl groups provides a complex which can freely rotate around the N-C^{ipso} bond, and can therefore, impact the π-system of the ligand.

Through consideration of the four *p*-substituted salicylaldimine complexes in Table 5.5 (**5.20-5.23**), a linear free energy relationship was generated by plotting $\log(K_{cis/trans})$ vs. σ in accord with equation **5.2**. Good correlation was observed when σ^{p+} parameters were used (Figure 5.7).[43]

$$\text{Log}\,(K/K_o) = \rho\sigma \qquad (5.2)$$

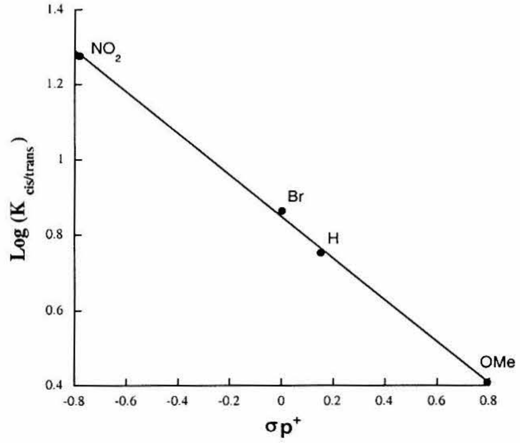

Figure 5.7. Hammet Plot for $K_{Cis/Trans}$. A good correlation was found for σ^{p+} (m = -1.806, $R^2 = 0.998$) that may indicate the *cis*- isomer is stabilized by electron-rich groups that can stabilize a developing positive charge generated upon π-backbonding from the metal center to the η^2-coordinated olefin.

As outlined in Figure 5.7, the Hammett plot has excellent agreement with σ^{P+} parameters.[43] The *trans-* relationship of the bound ethylene (in the major *cis-* isomer) to the phenoxide anion, requires that π-donation from the phenol contribute to the $\mathbf{d_{xz}}$ orbital from which the olefin would receive any π-backbonding contribution to it's π* orbital. It is proposed that π-donation builds up a positive charge on the phenoxide that can be stabilized through delocalization by π-donor groups, such as NMe_2 and OMe, strengthening the metal-olefin interaction and increasing the stability of the *cis-* isomer. As electron-withdrawing groups, such as NO_2 or the orthogonal 9-anthracenyl substituents, are placed on the phenolic ring, the π-donor ability of the phenoxy group decreases, thereby decreasing the amount of π-backbonding available until finally with **5.25**, the olefin prefers to bind in the *trans-* arrangement.

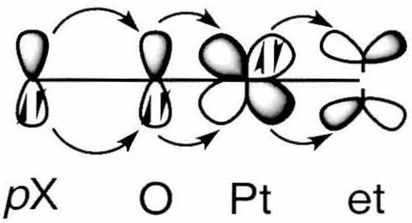

The relative importance of these subtle energy differences is unknown. Recent calculations have suggested that neutral Ni^{II} salicylaldimine systems may undergo insertion from only one "side", as the barrier to insertion is calculated to be as much as 10-15 kcal/mol higher from the *trans-* isomer than from the *cis-* isomer (Figure 5.8). The combination of the results outlined in Table 5.5 and these calculations, suggests that electron-rich π-donating ligands will provide a catalyst with the largest $\Delta(\Delta G^{\circ}_{cis/trans})$, and therefore, provide the possibility to prepare higher molecular weight products. In addition, as outlined below, olefins bound *trans-* to the imine have an increased lability relative to those *cis-* to the imine. Neither of these factors take the barrier to isomerization, of which little information is available, into consideration. However, researchers have demonstrated that such mechanisms can be operational for CO/olefin copolymerization using d^8 complexes with asymmetric ligands.[44,45]

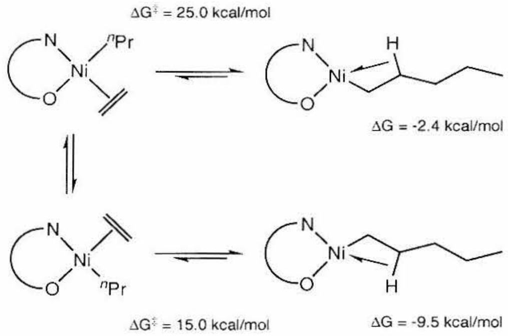

Figure 5.8. Proposed mechanism for ethylene insertion with neutral Ni^{II} salicylaldimine complexes – Future design for polymerization catalysts may explore asymmetric ligands that are good π-donors.

Since the lower energy isomer of **5.25** was determined to be the *trans-* geometry in solution, crystals were grown in an attempt to structurally characterize the ethyl isomer opposite to **5.15*c***. In fact, crystallization of **5.25** from benzene and hexane by vapor diffusion yielded bright yellow crystals that were determined to be **5.25*t*** by X-ray. The structure of the *trans-* isomer **5.25*t*** is depicted in Figure 5.9. A relevant difference of the bond lengths between Pt-N and Pt-O of the two isomers (**5.15*c*** and **5.25*t***) is observed, confirming the stronger *trans-* influence of the anionic alkyl group with respect to the η^2-coordinated olefin.[31,42] Further discussion on the structures of **5.15**, **5.19**, **5.25**, and **5.29** will be addressed shortly.

5. 5. Other bidentate ligand sets—[P,O], Pyca, Acac, and Nacnac Pt^{II} alkyl/ olefin complexes

A literature search provides a number of examples of neutral Ni^{II} catalysts which will oligomerize ethylene.[19,20,46] Typically, however, higher molecular weight products are observed with asymmetric ligand sets, such as [P,O], [N,O], and [P,N], which may provide additional support for the insertion/isomerization mechanism outlined above. To learn more about the similarities and differences between symmetric and asymmetric ligand sets, we sought to extend our studies of neutral Pt^{II} alkyl/ olefin complexes to ligands that have seen attention in Ni^{II} oligomerization/ polymerization catalysts. Some well-studied

Figure 5.9. X-ray analysis of *trans*-(^{NO2,NO2}Sal)Pt(Et)(et) **5.25*t***. Thermal ellipsoids are shown at 30% probability. All nonessential hydrogen atoms have been omitted for clarity.

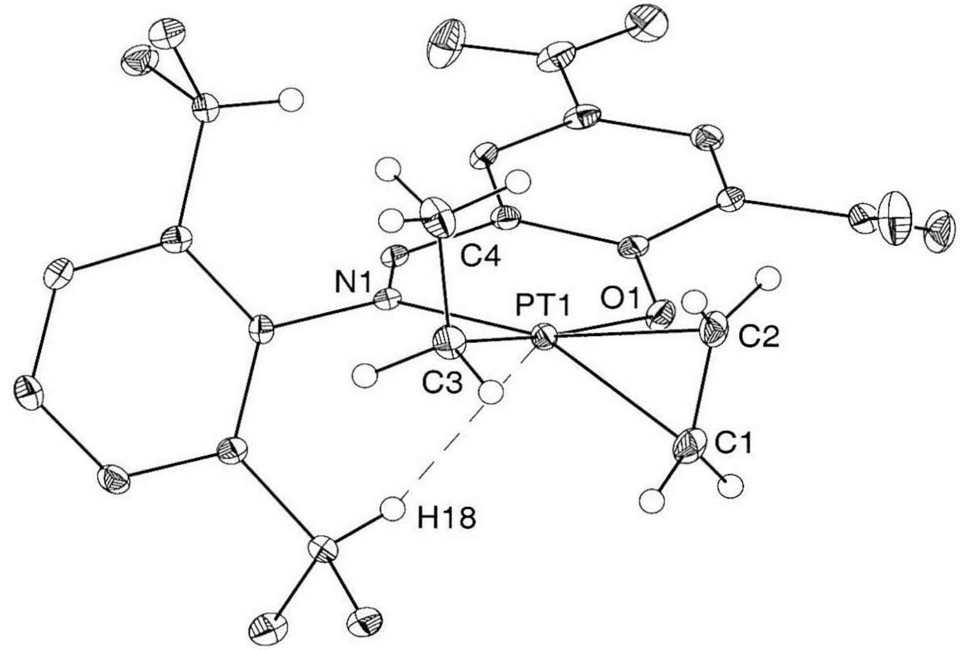

Table 5.6. Selected bond lengths (Å) and bond angles (°) for **5.25*t*.**

		Bond Lengths (Å)	
Pt-N(1)	2.070(2)	Pt-O(1)	2.1196(18)
Pt-C(1)	2.120(3)	Pt-C(2)	2.114(3)
C(1)-C(2)	1.380(4)	Pt-C(3)	2.029(3)
C(3)-C(4)	1.521(4)	Pt-H(18)	2.794(4)
		Bond Angles (°)	
N(1)-Pt-O(1)	89.84(8)	N(1)-Pt-C(1)	155.21(11)
N(1)-Pt-C(2)	165.85(10)	N(1)-Pt-C(3)	94.85(11)
O(1)-Pt-C(1)	86.66(10)	O(1)-Pt-C(2)	86.08(10)
O(1)-Pt-C(3)	172.51(10)	Pt-C(1)-H(1A)	105.7(17)
Pt-C(1)-H(1B)	108.3(17)	C(1)-Pt-C(2)	38.04(12)
C(1)-Pt-C(3)	91.46(13)	C(2)-Pt-C(3)	87.97(13)
Pt-C(3)-C(4)	110.2(2)	C(3)-Pt-H(18)	93.64(10)

systems include: (1) The [P,O] shop-type ligands,[20,21,46,47] (2) acac and acac-F_6,[47,48] (3) 2-pyridine-carboxylate (or pyca),[49,50] and (4) β-diketimates such as nacnac.[51,52] In addition, the Pt^{II} alkyl/phosphine complexes (pyca)PtEt(PPh_3) (**5.26**) and (acac)PtEt(PPh_3) (**5.27**) have previously been reported and studied as models for Pd^{II} carbonylation catalysts based on the same framework.[53,54]

5.6. [P,O] ligands

Several attempts were made to isolate complexes **5.28** and **5.29** (Figure 5.10). Neutral Ni^{II} complexes which utilize these ligand sets are found to be highly active for the oligomerization of ethylene to linear α-olefins or low molecular weight PE.[19,20,55] Using synthetic procedures analogous to those outlined above with the known Na salt of each ligand,[56] led to the rapid consumption of starting material **5.10**, followed by the observed liberation of free ethylene (gas evolution) and the production of an unknown product of poor solubility that did not contain signals indicative of a Pt-et interaction. Owing to the rapid reaction rate ($t_{1/2}$ ~ 2 min.), which agrees with rates observed for the preparation of other Pt^{II} alkyl/olefin complexes (and is faster than the reaction of **5.10** with PPh_3 ($t_{1/2}$ ~ 30 min.)), it is proposed that complex ***5.30c/t*** initially forms *via* loss of the appropriate chloride salt. In accord with the results presented above, the carboxylate (poor π-donor) destabilizes ***5.30c*** relative to ***5.30t***, and, therefore, the instability of these complexes may be due to the large *trans*- influence of the aryl phosphine group that drives the bound olefin from the metal center in ***5.30t***.[31,42]

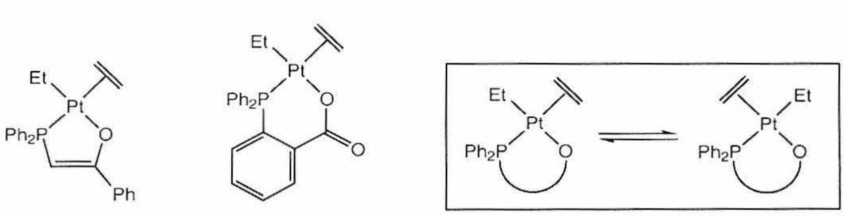

5.28 **5.29** **5.30*t*** **5.30*c***

Figure 5.10. Attempts for the preparation of neutral Pt^{II} [P,O] complexes **5.28** and **5.29** were unsuccessful. It is proposed that **5.30** forms, but is unstable due to the loss of ethylene.

5.7. 2-Pyridine-carboxylate (pyca)

The [N,O] ligand, 2-pyridine-carboxylate has been the source of many thorough studies on ethylene polymerization and carbonylation with d^8 complexes by Cavell *et al.* and, as such, serves as a necessary benchmark against which to compare the salicylaldimine complexes presented in this thesis.[49,50] On a first principles basis, the pyridine of the pyca ligand and the imine of the salen ligand are similar in their electronic nature $\{pK_a\ R_1(R_2{=}N)H^+ \sim 9\text{-}10\}$,[43] both chelates form a six-membered ring with the metal center which are fairly rigid in both the solid state and solution (as evidenced by X-ray and NMR studies).[49,50] The main differences between these scaffolds arise from the intrinsic difference between the phenolate and the carboxylate.

(Pyca)Pt(Et)et **5.31** was prepared in an analogous fashion to the previously outlined salicylaldimine alkyl/olefin complexes by combining the sodium salt of 2-pyridine-carboxylate with **5.10** in C_6D_6. The sodium salt was readily prepared *in situ* by the reaction of the commercially available carboxylate with 1.0 equiv. of NaO^{t}Bu. The reaction of Na(Pyca) with **5.10** was rapid and complete within 30 minutes at room temperature. Both the *cis-* and *trans-* isomers were observed in ~ 3:1 ratio as evidenced by their Pt-et signals at δ= 3.53 (*MAJOR,* $^2J_{PtH}$ = 70 Hz) and δ= 4.06 (*minor,* $^2J_{PtH}$ obscured), with further support from the ^{13}C NMR Pt-et signals at δ= 56.81 ($^1J_{PtC}$ ~ 221 Hz) and δ= 58.48 ($^1J_{PtC}$ ~ obscured). ^1H NOESY was inconclusive as no strong NOE enhancements were observed. However, in accordance with the data for salicylaldimine complexes **5.15** and **5.20-5.25**, it was proposed that the major species was the *cis-* isomer, **5.31*c***. During its preparation, the minor Pt-et (**5.31*t***) resonance was extremely broad at 25 °C ($\Delta\nu_{1/2}$ ~ 60 Hz), suggesting that an exchange process was readily occuring.[10,31] It is possible that the synthesis of **5.31** liberates a trace amount of free ethylene, which readily exchanges with **5.31*t*** (*vide infra*) as purification of **5.31** leads to a much sharper signal ($\Delta\nu_{1/2}$ ~ 8 Hz) that exhibits coupling to the ^{195}Pt metal center ($^2J_{HH}$ = 71.0 Hz).

Compound **5.31** was isolated as colorless X-ray quality crystals by dissolving the sample in CH_2Cl_2, layering with pentane, and placing in the freezer (-78 °C) for 1 week, and allowed for a confirmation of the structure of **5.31*c*** in the solid state. The structure contains four molecules in the asymmetric unit, of which molecule D is shown in Figure 5.11 as it best represents the "average" structure. An overlay of the four molecules

Figure 5.11. X-ray analysis of *cis*-(pyca)Pt(Et)(CH_2CH_2) **5.31**, molecule D (*see text*). Thermal ellipsoids displayed at 30% probability.

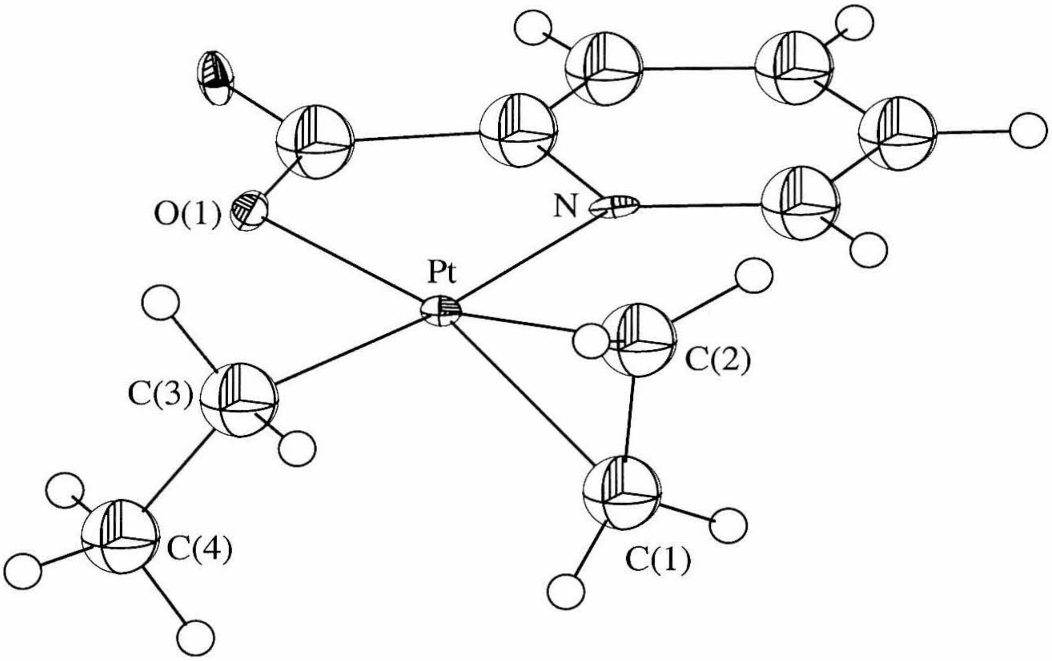

Table 5.7. Selected bond lengths (Å) and bond angles (°) for **5.31**.

	Bond Lengths (Å)		
Pt-N	2.126(4)	Pt-O(1)	2.004(3)
Pt-C(1)	2.084(5)	Pt-C(2)	2.090(6)
C(1)-C(2)	1.404(8)	Pt-C(3)	2.033(5)
C(3)-C(4)	1.433(8)	O(1)-C(5)	1.284(9)
	Bond Angles (°)		
N-Pt-O(1)	90.25(13)	N-Pt-C(1)	96.66(19)
N-Pt-C(2)	96.2(2)	N-Pt-C(3)	174.79(16)
O(1)-Pt-C(1)	162.2(2)	O(1)-Pt-C(2)	156.0(2)
O(1)-Pt-C(3)	84.54(16)	Pt-C(1)-H(1A)	116.6
Pt-C(1)-H(1B)	116.6	C(1)-Pt-C(2)	39.3(2)
C(1)-Pt-C(3)	88.3(2)	C(2)-Pt-C(3)	88.6(2)
Pt-C(3)-C(4)	109.6(4)	O(1)-C(5)-O(2)	122.4(7)

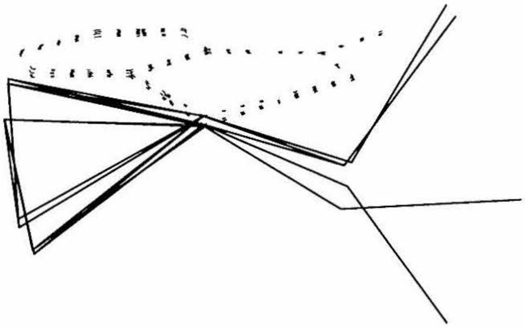

Figure 5.12. Overlay of the four molecules from asymmetric unit for **5.31** (Temp = 98 °K). Several degrees of freedom are observed for the Pt-ethyl and η^2-coordinated ethylene ligands of **5.31*c***.

(Figure 5.12--without constraints), provides a snapshot of how the Pt-ethyl and η^2-coordinated ethylene ligands interact. The preferred orientation of the olefin is perpendicular to the equatorial plane (defined by O(1), N, Pt, C(3)), as is typical for Pt^{II} olefin complexes.[31] However, Figure 5.12 clearly shows a slight up and down "wag" (~ 9°) with respect to the equatorial plane. The ethyl group appears to swing from "above" the molecule to "below" through a 180° arc pointed away from the molecule. Rotation of the ethyl group in a 360° fashion around the Pt-C(3) bond should have a much higher barrier as it will lead to contact between the methyl group and the bound olefin. The motions suggested Figure 5.12 are in good agreement with low temperature ^{1}H NMR of **5.31*c***, as the ethyl group is observed to freely rotate at –90 °C whereas the olefin "freezes out" at –80 °C.

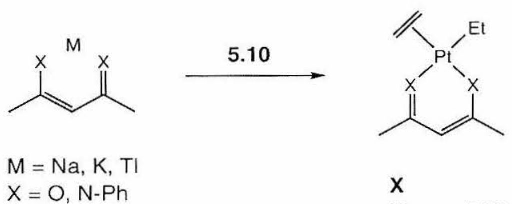

M = Na, K, Tl
X = O, N-Ph

X	
O	5.32
N-Ph	5.35

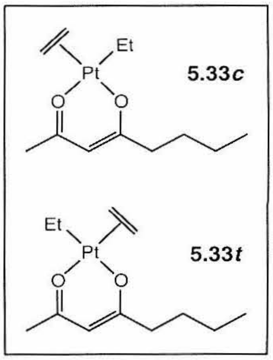

5.33*c*

5.33*t*

5.8. Symmetric anionic chelates - acac (5.32), acac (5.33), and nacnac (5.35)*

The acac complex was easily prepared by combination of the commercially available K(acac) H_2O with **5.10**. As shown in Figure 5.13(a), the crude ^{1}H NMR is very clean, with evidence for the ligand, Pt-et, and Pt-Et in the appropriate ratios. The methyl groups of the backbone are diastereotopic at T= 25 °C, implying that ethyl/ethylene epimerization is slow at this temperature, in agreement with the observed slow isomerization for **5.15**. The Pt-CH_2CH_3 signals are deshielded slightly with respect to **5.15**, **5.20-5.25**, and **5.31**, suggesting that the charge density at the methylene and methyl carbons are lower than observed in the aforementioned Pt^{II} alkyl/olefin adducts. Rotation about the Pt^{II}-olefin bond is facile, as again determined by the observation of a singlet with sharp ^{195}Pt satellites from (δ= 3.49, $^2J_{PtH}$ = 70.0 Hz). Isolation of **5.32** proved challenging as the material decomposes within a few hours at room temperature, even under anaerobic conditions. However, further confirmation of the postulated structure was obtained by reacting **5.32** with one equivalent of PPh_3, providing the known compound (acac)Pt(PPh_3)Et in quantitative yield, as determined by ^{1}H and ^{31}P NMR.[57]

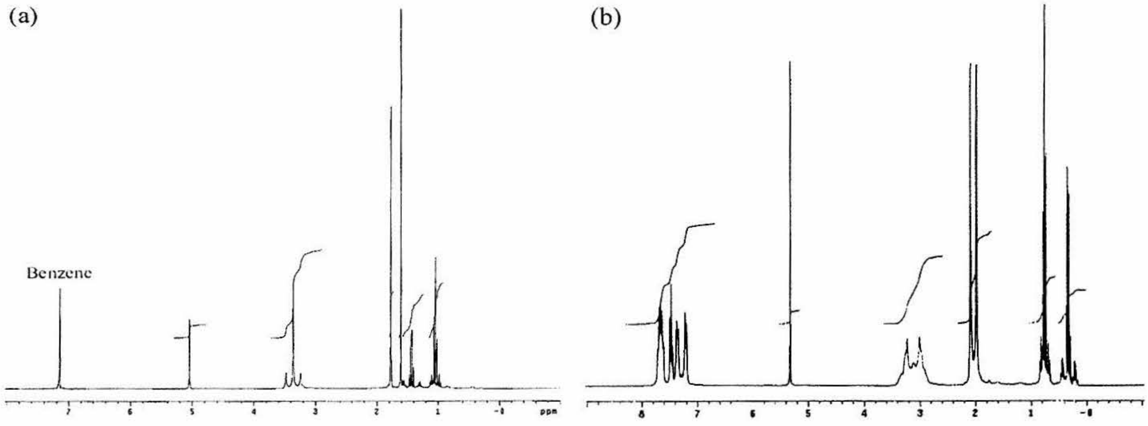

Figure 5.13. ^{1}H NMR spectra of (acac)Pt(Et)et (a; **5.32**) and (nacnac)Pt(Et)et (b; **5.34**) at 25°C in C_6D_6. Note that the methyl groups of both ligands are diastereotopic, suggesting that ethylene/ethyl site epimerization does not readily occur at room temperature. In addition, rotation about the Pt-et bond is facile for **5.32** (Pt-et = singlet), but is slow for **5.34** (split into a broad AA'BB' pattern).

Several attempts have been made to prepare the fluorinated version, (hfacac)Pt(Et)et, yet all efforts have been unsuccessful, providing a complicated mixture of products which rapidly decompose *via* metal center reduction.

Unlike the asymmetric N^O systems described in **Table 5.5**, the use of acac as a scaffold provides a single complex. To ensure that both the "cis" and "trans" isomers of a symmetric complex, such as **5.32**, are energetically equivalent, we prepared the asymmetric acac* complex (acac* = oct-2-en-4-one) **5.33**. Combination of the sodium salt of 2,4-octanedione with **5.10** provided a set of products with Pt-CH_2CH_3 (δ= 0.79/ 0.83 ppm) and $C(H)_{acac}$ (δ= 5.17/ 5.20 ppm), resonances similar to those observed for **5.32**. Only one Pt-et signal (δ 3.37 ppm; $^2J_{PtH}$ = 71.4 Hz) was observed for both species, but it is believed that the similar environments of the *cis*- and *trans*- isomers leads to coincidental chemical shifts. Indeed, the two isomers, **5.33*c/t***, were present in a 1:1 ratio ($K_{cis/trans}$ = 1.0) indicating that $\Delta(\Delta G°) \sim 0$ kcal/mol. The observation of both species by ^1H NMR provides further evidence that isomerization between the *cis*- and *trans*- forms is slow at room temperature and (in a unimolecular fashion) may be a high energy process. Attempts to isolate **5.33** were unsuccessful as the material decomposed to Pt^0 and free 2,4-octanedione.

The production of oligomeric products by (acac)Ni(R)L complexes is easily explained by modern rationale as protection of the metal center, through the use of a sterically demanding ligand set, has become a central theme (requirement?) for polymerization to higher molecular weight products by late-metals catalysts.[19,20] Although the introduction of "bulk" near the metal is more effective with *N*-based anions, such as nacnac (nacnac = N,N-bis(phenyl)-β-diketimate), performing the quick and dirty "switch-er-oo" does not lead to the desired revolutionary results and a sudden ability to prepare high molecular weight polymer. For example, the β-diketimate complex, (nacnac)Ni(Et)L **5.34** demonstrates *very low activity* with ethylene and produces *oligomers of ethylene in the* C_{10} – C_{20} *range.*[51,52] In order to better understand this unexpected result as well as the subtle electronic differences between the acac and nacnac ligand, we prepared complex **5.35**. We employed the N-Ph group (rather than 2,6-diisopropylphenyl) because of the ease of preparation and to reduce the importance of the "steric" component in our model system.

The addition of Na(nacnac) to **5.10** led to quantitative conversion to **5.35** (Figure 5.13(b)).[58,59] As observed in **5.32**, the methyl groups of the ligand are diastereotopic, suggesting that the barrier to isomerization is higher than ~ 15 kcal/mol. The aryl region exhibits some dynamic movement which can be "frozen out" at low temperatures, indicating the possibility of rotation about the N-C^{ipso} axis. Unlike all of the aforementioned complexes, however, **5.35** exhibits a broad series of peaks around 2.8-3.2, similar to the AA'BB' pattern observed in Pt^{II} ethylene complexes at low temperature where olefin rotation is restricted. As highlighted below, this complex demonstrates the highest barrier to olefin rotation (>14 kcal/mol) known for a square planar Pt^{II} complex, and may provide suggestions for future ligand design. Unfortunately, attempts to isolate this compound has been unsuccessful. Complexes of this nature will be the focus of further investigation as the introduction of a ligand with increased steric demands might allow for isolation of an analogous species.

5.9. Nature of the η^2-coordinated olefin—A comparison of the X-ray data for 5.15, 5.20, 5.25, and 5.31

Although the history of Pt^{II} olefin complexes is rich in structural data, only a handful of alkyl-olefin complexes, both four- and five- coordinate, have been the subject of X-ray analysis, with most of the studies having been performed over the last decade.[31,38,60] Although the overwhelming scattering power of Pt (Z = 78) can introduce significant error, the bond angles and lengths of the complexes presented in this chapter are in good agreement with their behavior in solution.

As previously outlined, the geometrical modification of the coordinated ethylene in complexes **5.15**, **5.20**, **5.25**, and **5.31** upon binding to Pt^{II} are similar to those observed in other three-, four-, and five- coordinate Pt olefin species, i.e., the substituents of the η^2-coordinated olefin are bent away from the metal center. This effect has been explained by a combination of olefin π to metal σ-donation and metal to π^* π-backbonding model as put forward by Dewar, Chatt, and Duncanson.[31] Both components of the bonding occur simultaneously in a synergistic fashion to strengthen the metal-alkene interaction and weaken the olefinic bond.

The out of plane displacement of the olefinic substituents (hydrogens for **5.15**, **5.25**, and **5.31**; μ-COD methylene groups for **5.20**) has been used to indicate the extent of π-backbonding present in the Pt-(olefin) bond.[31] In addition, shorter metal-olefin distances and longer carbon-carbon distances indicate an increased degree of π-backbonding. Therefore, structural data obtained from these complexes allows for a direct correlation of how π-backbonding changes as a function of the isomer studied or the ligand used. Comparison of these structures suggests that π-backbonding decreases in the order: **5.15** > **5.31** > **5.25** > **5.20** (Table 5.8).

Comparing these neutral Pt^{II} alkyl/olefin complexes to some previously reported cationic species such as those reported by Fusto,[28] Templeton,[60] and Ganis,[29] suggests that the extent of π-backbonding is much greater in neutral complexes, especially the *cis*-isomer **5.25**. Efforts are underway to structurally characterize an electron-rich complex, such as **5.20**, since it is expected that the structural changes will be more pronounced.

Table 5.8. Comparison of Bond Lengths (Å) and angles in Pt^{II} alkyl/olefin complexes.

	Compound		Pt-C(1) (Å)	Pt-C(2) (Å)	C(1)-C(2) (Å)	C(1)-Pt-C(2) (°)	Pt-alkyl (Å)
	Cationic						
--	$[\text{PtMe(et)(daethyph)}]\text{BF}_4$ [b]						
--	$[\text{k}^2\text{(Hpz')BHpz'}_2\text{)PtMe(et)}][\text{BAr'}_4]$[c]		2.114(6)	2.171(8)	1.181(14)	32.0(4)	2.048(4)
--	$\text{PtMe(CH}_2\text{CHCO2Me)(N\^{}N)]BF}_4$[d]		2.10 (3)	2.18 (4)	1.36 (5)		2.04 (4)
	Neutral						
5.15	*c*-($^{\text{Anthr,H}}$Sal)Pt(Et)et		2.084(5)	2.090(6)	1.404(8)	39.3(2)	2.033(5)
5.31	*c*-(pyca)Pt(Et)et	D	2099(9)	2.094(9)	1.375(13)	38.3(4)	2.051(9)
5.25	*t*-($^{\text{NO2,NO2}}$Sal)Pt(Et)et		2.120(3)	2.114(3)	1.380(4)	38.04(12)	2.029(3)
5.10	$[\text{PtEt(et)Cl}]_2$[e]		2.13 (2)	2.12 (2)	1.41 (3)		2.04 (2)
5.20	[($^{\text{Anthr,H}}$Sal)Pt(Me)(μ-COD)]$_2$	Pt(1)	2.152(4)	2.143(4)	1.391(6)	37.78(15)	2.036(4)
		Pt(2)	2.142(4)	2.146(4)	1.378(6)	37.49(15)	2.040(4)

[a] The carbon-carbon distance in free ethylene = 1.337(2) Å. [b](Fusto)[28] [c](Reinartz)[60] [d](Ganis)[29] [e](Basickes)[12]

However, this statement is supported by the observation that the η^2-coordinated olefinic protons and carbons are found outside the range typical for square planar Pt^{II}-olefin complexes, reflecting shielded values that support an increased amount of sp^3-hybridized character at the olefin.[31,38]

5.10. Barrier to olefin rotation

As previously discussed, the ^1H NMR resonance for η^2-coordinated olefin in all complexes (and each isomer) except for (nacnac)Pt(Et)et **5.35** is found to be a singlet at 25 °C, demonstrating that rapid rotation about the Pt-et axis is facile. This effect has been previously observed in a number of Pt-olefin complexes and is attributed to rapid rotation about the Pt-(et) bond.[31] At –90°C, the ^1H NMR (300 MHz, CD_2Cl_2) spectrum of **5.21** demonstrates an Pt-ethylene signal with a AA'BB' pattern with ^{195}Pt coupling as shown in Figure 5.14.

The complex splitting arises because rotation about the Pt-et axis has slowed sufficiently at –90°C as to "freeze out" the rotation, providing "inside"/"outside" and "top"/"bottom" protons with respect to the equatorial plane. As the sample is warmed (Figure 5.14), the peaks move together, approaching the coalesence temperature, $T_c \sim -10°C$. The rate of ethylene rotation at the coalesence temperature (k_{coal}) can be determined from the distance of the peaks (in Hz or s^{-1}) at the low temperature limit as expressed in equation **5.3**.[4] The barrier for ethylene rotation of each isomer ($\Delta G^{\ddagger}_{rotation}$), **5.21*c*** and **5.21*t***, can be calculated from the same low temperature splitting ($\Delta\nu$ in Hz) and T_c (K) as described by equation **5.4**.[4] By varying the temperature and monitoring the lineshape of the Pt-et resonances, the coalescence temperatures were determined for the complexes outlined in **Table 5.9**.

$$k_{coal} = 2p(\Delta\nu) = 2.2214(\Delta\nu) = 241.9\ s^{-1} \qquad (5.3)$$

$$\Delta G = 19.14\ (T_c)\ (9.97 + \log\ (T_c/dv) \qquad (5.4)$$

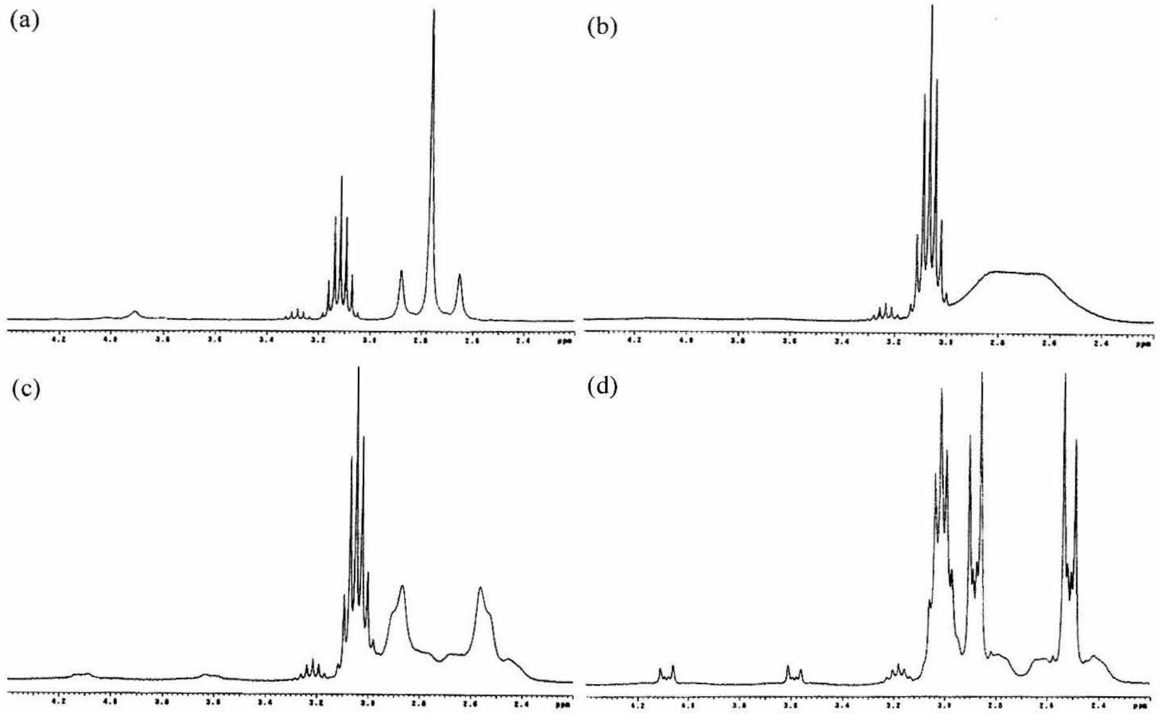

Figure 5.14. Variable temperature ^{1}H NMR studies to determine the barrier to Pt-et rotation in complex **5.21**. (a) 25 °C, (b) –14 °C, (c) –30 °C, and (d) –60 °C. T_c for both isomers ~ 10°C. Rotation barriers: *cis*- ($\Delta G^{\ddagger}_{298}$ = 12.2 kcal/mol), *trans*- ($\Delta G^{\ddagger}_{298}$ = 12.2 kcal/mol).

As shown in **Table 5.9**, all of the complexes have a $\Delta G^{\ddagger}_{rotation}$ of ~ 10-12 kcal/mol. The values are similar for both isomers, with a very slight difference on the "extreme" ends such that $\Delta G^{\ddagger}_{rotation}$ is higher for the *cis*- isomer with electron-rich ligands, such as **5.20**, and inherently lower for the *cis*- isomer with electron-deficient ligands (especially once the steric demand of the 2,6-diisopropylaryl imine is removed—see **5.36**). On average, the frequency of rotation (k_{coal}) is greater for the *trans*- isomer than the *cis*- isomer, again supporting the fact that the degree of π-backbonding is greater for ethylene when in the *cis*- configuration. Lineshape analysis of the ^{1}H NMR data for **5.36** provides an Eyring plot for olefin rotation of the *trans*- isomer (**5.36*t***). The entropic and enthalpic terms ($\Delta S^{\ddagger}_{rotation}$ = 3.1 cal mol^{-1} K^{-1}, $\Delta H^{\ddagger}_{rotation}$ = -11.8 kcal mol^{-1},

$\Delta G^{\ddagger}_{rotation,298}$ = -12.7 kcal mol^{-1}) provide further support that the exchange process is, in fact, olefin rotation.

A similar trend has been observed with Pt^{II}-olefin adducts, for a different reason.[9] For example, Ziese's dimer, [(et)PtCl(μ-Cl)]$_2$, demonstrates a broad singlet without discernable ^{195}Pt satellites at temperatures as low as –90 °C, indicating a rapid exchange process. The methyl analog, **5.9**, shows a higher barrier to rotation about the Pt-et axis, such that decoalescence is observed at - 40 °C.[10] The researchers argued that the presence of the strong σ-donating methyl group acts to increased the π-backbonding, such that the propensity for olefin dissociation or rotation in **5.9** is much lower than when compared to the parent dimer.

Table 5.9. Ethylene rotation barrier in Pt^{II} alkyl/olefin compounds.

Complex	Ligand (X_1, X_2)	$k_{coal(cis)}$ (s^{-1})	$\Delta G^{\ddagger}_{cis}$ (kcal/mol)	$k_{coal(trans)}$ (s^{-1})	$\Delta G^{\ddagger}_{trans}$ (kcal/mol)
5.20^{500}	H, OMe	400	12.4 (1)	558	12.3 (1)
5.21	H, H	340	12.2 (1)	520	12.2 (1)
5.15^{500}	Anthr, H	241	11.9 (1)	130	12.0 (1)
5.23 ^{500}	H, NO$_2$	392	11.8 (1)	514	12.0 (1)
5.24^{300}	10-NO$_2$-Anthr, NO$_2$	170	11.6 (1)	110	11.6 (1)
5.25	NO$_2$, NO$_2$	360	11.2 (1)	510	11.4 (1)
5.36^{300}	NO$_2$, NO$_2$ (Ph)	[c]	[c]	333	11.1 (1)
5.31	Pyca	[c]	[c]	510	10.6 (1)
5.32^{300}	Acac[d],[e]	242	10.4 (1)	-	-
5.35^{300}	Nacnac[d],[e]	189	> 14	-	-

[a] ^{1}H NMR {500.0 MHz}, 0.5 mM in CD$_2$Cl$_2$. [b] ^{1}H NMR {300.0 MHz}, 0.5 mM in CD$_2$Cl$_2$. [c] No low temperature limit detected (free rotation rapid at –90 °C). (d) Symmetrical ligand employed, isomers are equivalent structures. [e] Generated *in situ*.

5.11. Isomerization between cis- and trans- isomers

Attempts to observe isomerization between the *cis*- and *trans*- structures using magnetization transfer experiments has failed, as outlined above, leading to a preliminary assessment that the isomerization of neutral salicylaldimine Pt^{II} complexes such as **5.15** has a relatively high barrier when ~ 25 kcal/mol or greater for each of the complexes tested.

Complexes **5.32**, **5.33**, and **5.35**, demonstrate similar behavior at 25 °C as evidenced by the presence of diastereotopic methyl groups of the ligand in both the ^{1}H and ^{13}C NMR. Gentle heating of these mixtures leads to the very rapid decomposition of the alkyl/olefin with concomitant loss of ethylene, the protonated ligand, and Pt^0.

5.12. Ethylene self-exchange reactions

A majority of the substitution reactions of ligands on Pt^{II} centers occurs *via* five-coordinate intermediates, and therefore it was expected that the exchange between bound and free ethylene would occur through an associative pathway.[4,31,38] Attempts to observe the ethylene exchange reaction in electron-rich complexes such as **5.20** - **5.21** involved the addition of ~ 1 atm of ethylene to a J-Young NMR tube containing a 0.5 mM solution of the appropriate complex in CD_2Cl_2. Such olefin interchange, as outlined in Figure 5.15 was not observed at room temperature with either isomer.

Conversely, the addition of ~ 1 atm. of ethylene to a 0.5 mM solution of **5.15** in toluene-d_8 leads to an exchange between free ethylene and ethylene coordinated in the *trans-* arrangement (Figure 5.16). Heating the mixture of **5.25** and ethylene to 100°C shows some sign of broadening for the free ethylene peak at δ= 5.3 ppm, but the signal for **5.25*c*** remains sharp (Δν ~ 6 Hz), suggesting that at 100 °C the exchange between free ethylene and ethylene in the *cis-* arrangement is slow. The observed discrepancy in reactivity suggests that a large difference in the barrier to ethylene exchange can exist for the *cis-* and *trans-* isomers (~ 5 kcal/mol for **5.25*c*** vs. **5.25*t***). Further investigation of these results are ongoing.

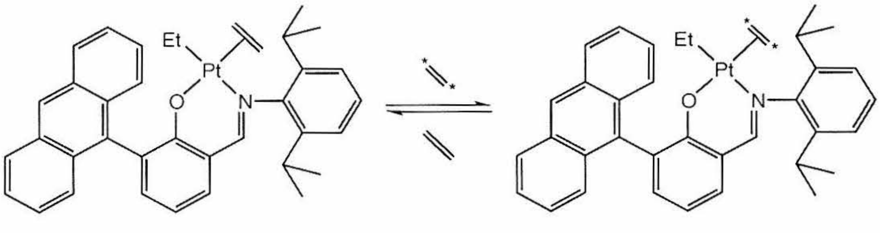

Figure 5.15. Degenerate exchange of ethylene with **5.15**. Model for the associative displacement of a growing polymer chain.

In contrast, the addition of ~1.0 atm of ethylene to Pt(pyca)Et(ethylene) (**5.31**) at 25 °C results in a rapid olefin exchange, for both the *cis*- and *trans*- isomers.[28] Several attempts were made to observe the dynamics of olefin interchange through lowering the temperature. With both 1 atm of ethylene (~ 12 eq. ethylene) and 7 equivalents of ethylene (both determined by integration at –90 °C) facile olefin exchange was observed at –90 °C. Reduction of the number of ethylene equivalents introduced failed to significantly slow the rate of olefin exchange. The Pt^{II} complexes, $PtR(pyca)PPh_3$ R = Me and Et operate *via* ligand dissociation or displacement during carbonylation. [53,54] Such a mechanism could be operational in these studies, and could lead to the drastically lower barrier to olefin exchange when compared to **5.25**.

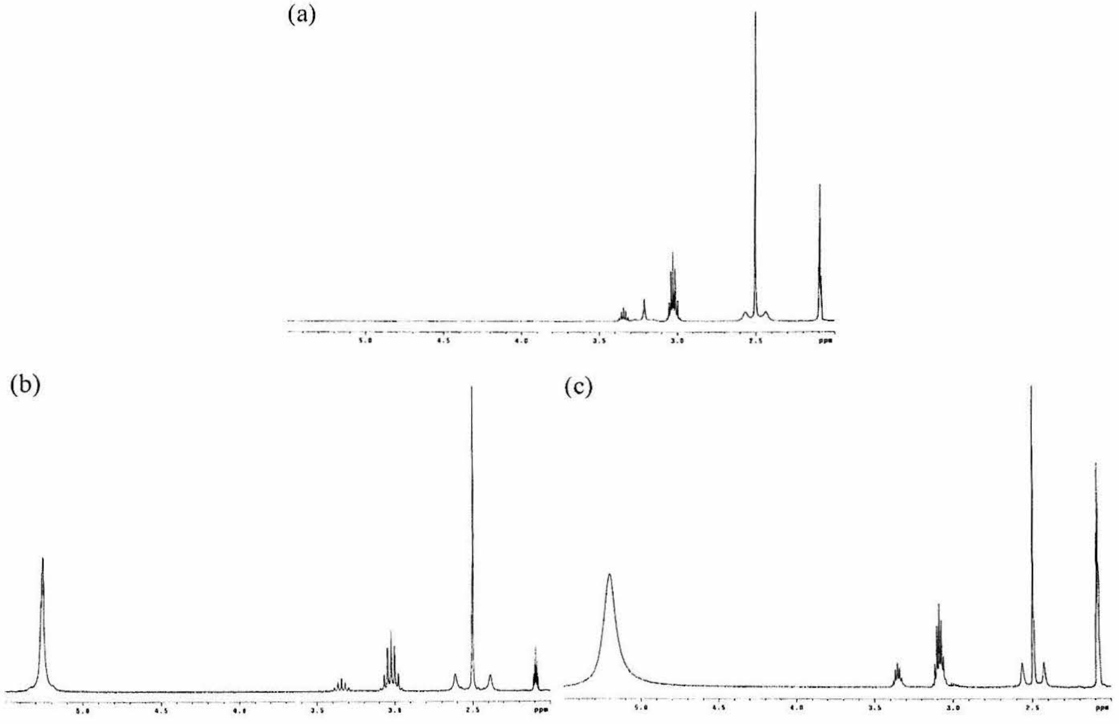

Figure 5.16. The addition of ~ 1 atm. ethylene to **5.25** (toluene-d_8). (a) No ethylene, 25 °C (500 MHz), (b) 1 eq. ethylene, 25 °C (300 MHz), ***5.25t*** exchanges. (c) 1 eq. ethylene, 100 °C (500 MHz), ***5.25c*** still very sharp signal (trace amount of phenol from reductive elimination observed as septet at 3.5 ppm).

The acac complex **5.32** was also observed to undergo exchange with free ethylene at room temperature. In this case, however, the rate of interchange was slowed at –90°C (although the signals were broad and lacked ^{195}Pt satellites). Warming a solution of **5.32** and ~ 1.5 equivalents of ethylene allowed for the determination of T_c = –50°C. In agreement with the increased π-backbonding in the nacnac adduct **5.35**, exposure of a 0.5 M solution (CD_2Cl_2) led to no evidence of ethylene exchange at room temperature.

This preliminary data suggests that the barrier to olefin interchange was related to the pK_a of the free anion (ROH), as ethylene exchange rates increased in the order: pyca (**5.31**, < -90°) > acac (**5.32**, -50°) > **5.25** (**5.25*t***, 25°) > nacnac (T_c > 25°) ~ **5.20-5.21** (T_c > 25°). In conjunction with the previously outlined data, ethylene exchange is related to the strength of the Pt^{II}-olefin bond, suggesting that an electron-deficient salicylaldimine complex could provide the best opportunity to observe olefin exchange. In addition, it was proposed that the bulky 2,6-diisopropylaryl imine groups were the reason for the high barrier to ethylene exchange in **5.25*c***. For these reasons, complex **5.36** was prepared from the commercially available precursors by the procedure previously discussed.

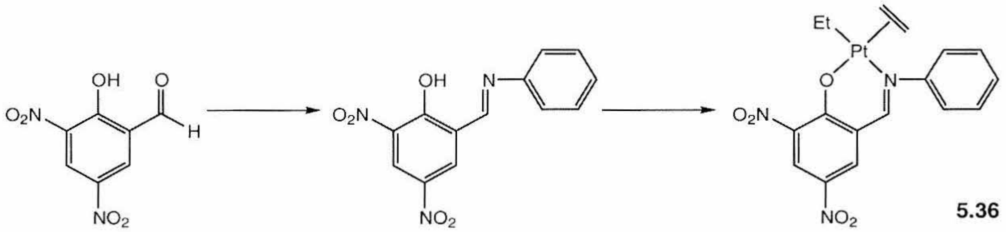

5.36

The *cis*- to *trans*- ratio of **5.36** (47/53) (Table 5.5) is in good agreement with the closely related complex **5.25**, but may reflect the subtle effect of changing the steric demand at the nitrogen fragment of the ligand as the ratios are not identical. The barrier to olefin rotation was also in agreement with the previously outlined results (Table 5.9), although it should be noted that the low temperature limit for olefin rotation of the *cis*-isomer could not be detected. This may reflect that the barrier to olefin rotation is inherently higher for complexes containing a 2,6-diisopropylaryl imine as rotation of the olefin might lead to close contact of the groups, thereby, increasing the barrier.

The addition of approximately 1 equivalent of ethylene to a 0.5 mM solution of **5.36** led to the observation of a coalesced ^{1}H NMR spectrum at room temperature. Again, variable temperature ^{1}H NMR studies provided further information. At –90°C, all three of the individual peaks were observed (free ethylene, **5.36c,** and **5.36t**). As per the spectrum without ethylene, the Pt-olefin signal for **5.36*t*** was split into the "frozen" AA'BB' pattern, while the lineshape for **5.36*c*** remained as a singlet. Warming the sample led to the determination of the coalescence temperature for the *trans*- isomer ($T_c \sim -35$ °C), followed by the *cis*- isomer ($T_c \sim 20$ °C). Lineshape analysis of the ^{1}H NMR spectra at a series of temperatures provided the exchange rates listed in Table 5.10, allowing for the kinetic parameters necessary for an Eyring plot [ln(k/T) vs. 1/T] (Figure 5.17).

From the Eyring plot in Figure 5.17, it was determined that the exchange between free ethylene and **5.36*t*** has $\Delta S^\ddagger = -33.4$ cal mol^{-1} K^{-1}, $\Delta H^\ddagger = -2.66$ kcal mol, $\Delta G^\ddagger_{298} = 7.30$ kcal/mol, while **5.36*c*** has : $\Delta S^\ddagger = -39.2$ cal mol^{-1} K^{-1}, $\Delta H^\ddagger = -1.80$ kcal mol, $\Delta G^\ddagger_{298} = 9.89$ kcal/mol. The highly negative values of $\Delta S^\ddagger$ suggest that olefin interchange occurs by an associative mechanism outlined in Figure 5.18.[4] These results have significant implications for the development of polymerization catalysts based on a neutral Ni^{II} framework. It appears that the use of electron rich systems may lead to an increased barrier/decreased rate for ethylene exchange, thereby leading to an increase in the molecular weight of the insertion products.

Table 5.10. Ethylene exchange rates for **5.36*c*** and **5.36*t***. Calculated from lineshape analysis of variable temperature ^{1}H NMR spectra using gNMR.

Temp. (K)	k_{Cis} (s^{-1})	k_{Trans} (s^{-1})
183	$7.0\cdot 10^1$	$1.2_5\cdot 10^2$
218	$1.8\cdot 10^2$	$4.5\cdot 10^2$
223	$2.1\cdot 10^2$	$5.5\cdot 10^2$
228	$2.3_5\cdot 10^2$	$6.7_5\cdot 10^2$
233	$2.5\cdot 10^2$	$7.7_5\cdot 10^2$
238	$2.9_5\cdot 10^2$	ND[a]

[a]ND = Not determined.

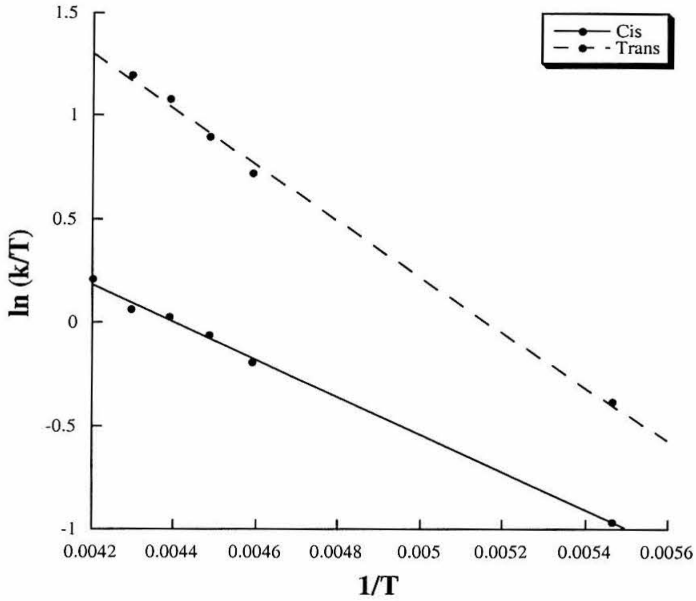

Figure 5.17. Eyring Plot for Olefin Exchange between free ethylene and **5.36**. ***Cis-Isomer***: $\Delta S^{\ddagger} = -39.2$ cal mol^{-1} K^{-1}, $\Delta H^{\ddagger} = -1.80$ kcal mol, $\Delta G^{\ddagger}_{298} = 9.89$ kcal/mol. ***Trans-Isomer***: $\Delta S^{\ddagger} = -33.4$ cal mol^{-1} K^{-1}, $\Delta H^{\ddagger} = -2.66$ kcal mol, $\Delta G^{\ddagger}_{298} = 7.30$ kcal/mol.

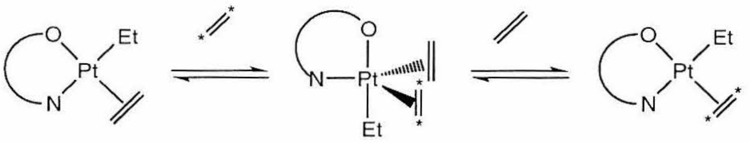

Figure 5.18. Associative ethylene exchange for 5.36*c* and 5.36*t* (5.36*c* shown as example).

5.13. Ligand Exchange Reactions

The reaction of **5.15** with phosphines, pyridine, and $NCCH_3$ was investigated to determine relative rates of displacement of ethylene for various ligands. The addition of 2 µL of acetonitrile, ether, or acetone to a 5 mM solution of **5.15** in C_6D_6 led to no observable change over a week at 25 °C, demonstrating that the association constant for these species is lower than that of ethylene. This is in agreement with the polymerization results depicted in Chapter 3, where the addition of excess nitrile, ether, or ketones led to small perturbations of the rates of polymerization. Surprisingly, although the addition of pyridine to polymerizations with neutral Ni^{II} salicylaldimine systems is quite detrimental (Chapter 3), the alkaloid was very slow to react with **5.15**, building up concentration of the pyridine adduct ***5.37t*** steadily over the course of a week at 25 °C. The ^1H NMR demonstrates the formation of a single isomer that is believed to be the *trans-* isomer in analogy with the chemical shifts and $^NJ_{PtH}$ for the *trans-* isomers listed above, as well as the phosphine adducts outlined below.

The addition of one equiv. of PPh_3 leads to the quantitative and rapid displacement (~ 30 min) of ethylene in **5.15** at 25 °C and two new products, ***5.38c*** and ***5.38t***, appear as evidenced by two new septets in the ^1H NMR at $\delta = 3.74$ ppm and $\delta = 3.89$ ppm. The starting material is completely consumed, followed by a slow isomerization of the kinetic product, ***5.38c***, to the thermodynamic product, ***5.38t***. The increased stability of the *trans-* isomer is most likely due to the *trans-* effect of the anionic phenolate group which acts to destabilize the phosphine *trans-* to it. It is interesting to note that PPh_3 can access both the *cis-* and *trans-* geometries as this aspect may prove to be crucial to catalysis.

Crystals of good quality were obtained from a concentrated solution of **5.38** in benzene upon cooling to 10 °C for 24 hours. As demonstrated in Figure 5.19, the Pt^{II} structure is square planar in analogy to the Ni^{II} and Pd^{II} complexes reported in Chapter 2. As determined by solution phase ^1H NMR techniques, the PPh_3 group occupies the position opposite the imine, again confirming that the thermodynamic product is ***5.38t***. The 9-anthracenyl and aryl imine moieties are perpendicular to the equatorial plane, but interestingly there are several degrees of freedom for the 2,6-diisopropylphenyl imino group. The Pt-P bond length of 2.20 Å is similar to the distance observed in other complexes such as $Pt(COMe)(pyca)(PPh_3)$ 2.22 Å,[54] when *trans-* to a nitrogen-based ligand. The ethyl group is slightly raised out of the equatorial plane, which may be a consequence of Pt-Et/Pt-PPh_3 interactions.

Figure 5.19. X-ray Diffraction Analysis of *t*-($^{\mathrm{Anthr,H}}$Sal)Pt(Et)PPh$_3$ **5.38**.

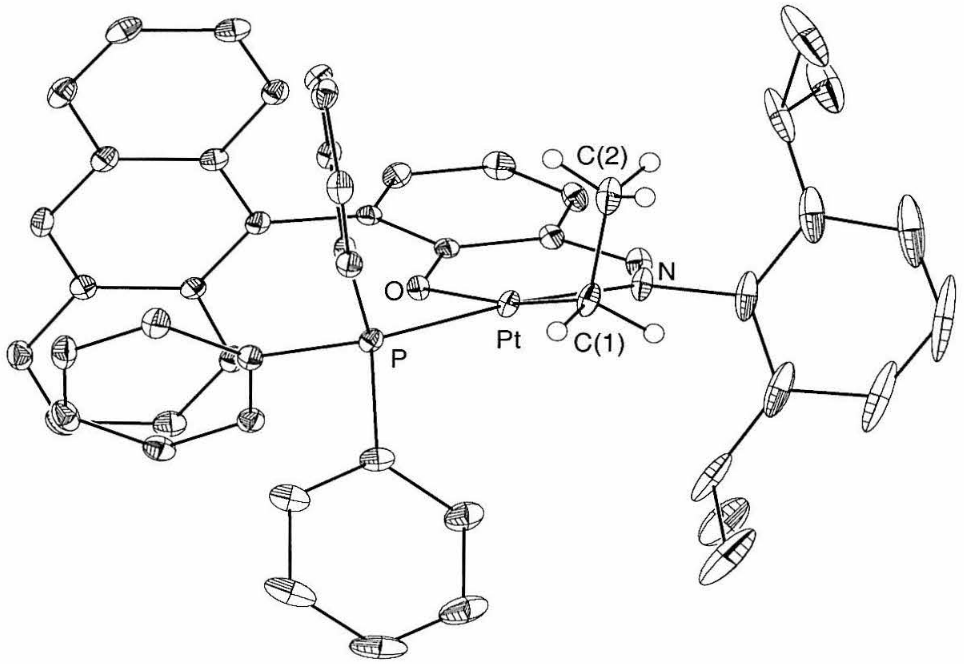

Table 5.11. Selected bond lengths (Å) and bond angles (°) for **5.38**.

	Bond Lengths (Å)		
Pt-N	2.094(2)	Pt-O	2.0954(15)
Pt-P	2.2047(7)	Pt-C(1)	2.062(2)
C(1)-C(2)	1.518(4)	N-C(3)	1.307(3)
	Bond Angles (°)		
N-Pt-O	89.69(7)	N-Pt-P	174.51(6)
N-Pt-C(1)	93.21(9)	O-Pt-P	90.78(5)
O-Pt-C(1)	171.33(9)	Pt-C(1)-C(2)	110.49(19)
C(1)-Pt-P	87.11(8)	Pt-N-C^{ipso}	123.33(16)

Unlike the addition of PPh_3, the addition of one equiv. of PCy_3 to a solution of **5.15** in 0.7 mL C_6D_6 leads to the sole formation of *trans*-(^{Anthr}Sal)Ni(PCy_3)Et **5.39*t*** as evidenced by the ^{1}H NMR signals of the $-CHMe_2$ group at δ= 3.95 ppm which slowly appear over 2.5 hours at 25 °C. ^{1}H NOESY demonstrated an NOE enhancement between the Pt-CH_2*CH_3* and the isopropyl groups of the aryl imine, providing further evidence for the *trans*- arrangement of **5.39**. In addition, $^4J_{PH}$ of the CH=NAr proton indicatives a *trans*- geometry, as such coupling would not be expected to be observed if PCy_3 and the imine were in a *cis*- arrangement.

These exchange reactions have demonstrated that the rate of association for the (^{Anthr,H}Sal)Pt(Et)L group is in the following (decreasing) order: PPh_3 > PCy_3 > Py > et > NCMe ~ $CH_3C(O)CH_3$ ~ Et_2O.

5.14. β-hydride elimination

One of the motivations for the preparation of these Pt^{II} model systems was to study the rate (and mechanism) for either migratory insertion or (the reverse process) β-hydride elimination (βHE). To date, no products which suggest that migratory insertion occurs have ever been observed. The preparation of hydrido- analogs might allow for the observation of ethylene migration as hydride has been shown in some cases to have a 10^6-10^8 greater aptitude for migration and such a process has been implicated in several catalytic cycles.

As previously mentioned, thermolysis of several of the Pt^{II} compounds leads to reductive elimination of the ligand and a reduction of the metal center. This is believed to occur through β-hydride elimination followed by loss of the respective phenol and ethylene, as outlined in Figure 5.20. Support for this mechanism was obtained upon thermolysis of **5.15** at 100 °C in toluene-d_8. The clean transformation of **5.15** to the (^{Anthr,H}Sal) ligand and ethylene was joined by the formation of Pt^0 mirror along the inside of the NMR tube. The rate of decomposition was suppressed by the presence of ethylene, as decomposition of **5.15** at 100 °C was complete within 2 hours in the absence of ethylene, yet after the addition of 2 equivalents of ethylene, the species **5.15** was still present after 36 hours of heating at 100 °C.

Figure 5.20. β-hydride elimination and reductive elimination leads to decomposition of **5.15**.

The pyridine complex **5.37*t*** and triphenylphosphine complex **5.38*t*** also undergo reductive elimination at elevated temperature, liberating ethylene and the free ligand. These reactions were observed at a much slower rate, taking several days at 80 °C in C_6D_6. The tricylcohexylphosphine adduct, **5.39*t*** was found to be stable, unchanged after two months of heating at 80 °C in C_6D_6. We believe this result suggests that βHE occurs from the 14e$^-$ square planar species which is not easily accessed with the strong σ-donating PCy_3.Contrary to our expectations, the addition of excess PPh_3 led to an increase in the rate of the decomposition of **5.38*t*** as outlined in Figure 5.21. Studies pertaining to the nature of this enhancement are ongoing.

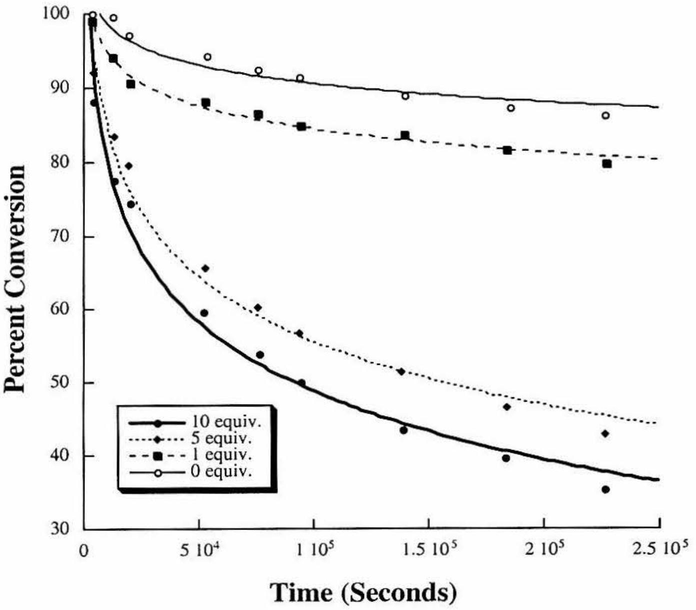

Figure 5.21. Rate of decomposition for **5.38*t*** *increases* upon addition of excess PPh_3.

5.15. Conclusions

This chapter outlines the preparation of a series of neutral Pt^{II} alkyl/ olefin complexes which are in all cases the putative active species for oligomerization and/ or polymerization of ethylene with Ni^{II} complexes of the same ligand set. Variation of the electronic nature of salicylaldimine ligands lead to a very ordered progression, with electron-rich π-donors, such as **5.20**, demonstrating the highest $K_{cis/trans}$ (bias for the *cis*-isomer) and electron-deficient systems, such as **5.25**, preferring a *trans*- arrangement. A linear free energy relationship for *p*-substituted derivatives **5.20-5.23** suggests that π-donors increase the degree of Pt-to-ethylene π-backbonding, thereby strengthening the metal-olefin interaction. These results are in agreement with X-ray structures of both isomers (**5.15*c*** and **5.25*t***), which suggest that the *cis*- isomer demonstrates a slightly increased metallocyclopropane character as described by the Dewar-Chatt-Duncanson model.[31] The barrier to olefin rotation is observed to increase slightly in the same direction, such that π-rich systems such as **5.20** and **5.35** provide the highest barrier to rotation.

The decreased association of ethylene with electron-deficient systems suggested that they might readily exchange with free ethylene. In fact, ethylene exchange was observed with **5.15*t***, **5.24*t***, **5.31**, and **5.32**. These systems led to the design of **5.36** with an electron deficient anion and a less bulky imine fragment. **5.36** readily exchanges ethylene at room temperature. Low temperature ^1H NMR studies reveal that the *cis*-isomer has a lower rate of exchange compared to the *trans*- isomer. Lineshape analysis provided the entropic and enthalpic terms for ethylene exchange with each isomer, suggesting that the mechanism of exchange is *via* an associative interchange.

Ligand exchange readily occurs with the ethylene of **5.15** displaced fastest by phosphines such as PPh_3 and PCy_3. Pyridine exchanges in a very slow manner, and the weak s-donors, NCMe, Et_2O, and acetone, are not observed to exchange after 1 week at 25°C.

Some of the complexes (**5.32**, **5.33**, and **5.35**) could not be isolated as they darken to Pt^0 *via* reductive elimination. Studies performed with **5.15**, **5.37**, and **5.38**, demonstrate that b-hydride elimination, followed by reductive elimination is the major pathway of thermal decomposition for Pt^{II} salicylaldimine complexes. The addition of excess ethylene to **5.15** suppressed the rate of decomposition, suggesting that βHE might depend on the loss of olefin. The pyridine and PPh_3 adducts decompose slower than **5.15**, with the addition of PPh_3 having an unexpected *accelerating* effect in the reduction process. The PCy_3 adduct does not decompose thermally to any appreciable extent.

These studies may provide direction towards the rational design of new late-metal catalysts which can prepare either high or low molecular weight products in the presence of functionalized groups.

Table 5.10. X-ray analysis data and structure refinement for **5.15**, **5.20**, **5.25**, **5.31**, and **5.38**.

	5.15	**5.20**	**5.25**	**5.31**	**5.38**
Empirical Formula	$C_{37}H_{39}NOPt$	$C_{76}H_{78}N_2O_2Pt_2$ 2.5(C_6D_6)	$C_{23}H_{29}N_3O_5Pt$	$C_{10}H_{13}NO_2Pt$	$C_{53}H_{49}NOPPt$ C_6H_6
Formula Weight	708.78	1636.85	622.58	374.30	1020.10
Crystallization Solvent	Toluene/ Hexane	Benzene/ Hexane	Benzene/ Hexane	Pentane/ CH_2Cl_2	Benzene
Crystal Habit	Prism	Block	Blocks	Blade	Trapezoidal
Crystal Color	Yellow	Yellow/Orange	Deep Yellow	Colorless	Canary Yellow
Crystal Dimensions (mm^3)	0.326 x 0.215 x 0.178	0.24 x 0.22 x 0.21	0.23 x 0.19 x 0.13	0.24 x 0.18 x 0.14	0.30 x 0.22 x 0.16
Wavelength	0.71073 Å MoKα	0.71073 Å MoKα	0.71073 Å MoKα	0.71073 Å MoKα	0.71073 Å MoKα
Data Collection Temperature (K)	293(2)	98(2)	98(2)	98(2)	98(2)
Unit Cell Dimensions (Å)	a=11.8674(12) b=17.1171(18) c=15.1623(16)	a=14.8073(12) b=18.2407(15) c=28.508(2)	a=8.1765(5) b=12.3539(7) c = 12.5292(7)	a=8.0940(4) b=16.8013(8) c=15.1965(7)	a=9.9116(8) b=12.0112(9) c=22.3876(17)
Unit Cell Dimensions (°)	β = 95.320(2)	β=102.0860(10)	α=85.3990(10) β=73.4250(10) γ = 70.7300	β= 90.4890(10)	α=74.8710(10) β=79.6870(10) γ= 67.6700(10)
Volume (Å^3)	3066.7(6)	7529.3(11)	1144.91(11)	2066.49(17)	2370.4(3)
Z	4	4	2	8	2
Crystal System	Monoclinic	Monoclinic	Triclinic	Monoclinic	Triclinic
Space Group	$P2_1/c$	$P2_1/n$	P-1	$P2_1$	P-1
Density (Calculated) Mg/m^3	1.535	1.444	1.806	2.406	1.429
Data/ Restraints/ Parameters	7322/ 0/ 366	18204/ 0/ 1076	5316 / 0 / 405	9591 / 1 / 310	10776 / 0 / 788
Goodness-of-fit (GOF) on F^2	1.364	1.802	1.464	1.947	1.455
Final R Indices [$I > 2\sigma(I)$]	5009 reflections R1=0.0363 wR2=0.0712	13902 reflections R1=0.0419 wR2=0.0630	4959 reflections R1=0.0204 wR2=0.0408	9423 reflections R1=0.0324 wR2=0.0687	9839 reflections R1=0.0248 wR2=0.0489
R Indices (All Data)	R1=0.0599 wR2=0.0738	R1=0.0626 wR2=0.0649	R1=0.0225 wR2=0.0411	R1=0.0331 wR2=0.0688	R1=0.0282 wR2=0.0493

5.16. Acknowledgements

T. Jon Seiders provided (η^4-COD)PtMeCl (**5.11**), (η^4-COD)PtMe$_2$ (**5.13**), and several valuable suggestions. Antek Wong-Foy kindly provided a sample of (tmeda)PtMe$_2$ (**5.14**), while Seva Rostovtsev provided [Pt(μ-Cl)(CH$_3$)(C$_2$H$_4$)]$_2$ (**5.9**) and relevant data from his own research. Dr. Chris Brandow assisted in the lineshape analysis of ^{1}H NMR spectra for olefin rotation and ethylene interchange. Dr. Mike Day and Larry Henling were invaluable for their crystallography efforts. Funding was provided by the Rohm & Haas Coorporation.

5.17. Experimental section

General Considerations. All manipulations and reactions were performed using standard Schlenk techniques unless otherwise noted. Argon was purified by passage through a Matheson 6410 O$_2$ removal system. Deuterated solvents were obtained from Cambridge Isotope Laboratories (99 atom % D), and degassed by drying over CaH$_2$, distilling, and degassing with three freeze-pump-thaw cycles. All organic reagents were purchased from Aldrich and used without further purification unless otherwise noted. Ethyl acrylate and norbornene were purified prior to use by passage through neutral alumina. [Pt(μ-Cl)(C$_2$H$_5$)(C$_2$H$_4$)]$_2$ (**5.10**),[12] (COD)PtMeCl (**5.11**), and (COD)PtMe$_2$ (**5.13**) were prepared using literature methods. [Pt(μ-Cl)(CH$_3$)(C$_2$H$_4$)]$_2$ (**5.9**) and (tmeda)PtMe$_2$ (**5.14**) were prepared through literature procedures and generously donated by the Bercaw group.[10] The salicylaldimine ligands used for the preparation of complexes **5.20**, **5.21**, **5.23**, and **5.25** were prepared as previously reported. [61,62]

Physical and Analytical Measurements. Nuclear magnetic resonance (NMR) data were recorded on either a Varian Mercury 300 {^{1}H (300 MHz), ^{13}C (75 MHz), ^{31}P (121 MHz)} or a Varian Inova 500 {^{1}H (500 MHz), ^{13}C (125 MHz, ^{31}P (202 MHz)}. Chemical shifts were referenced to internal solvent resonances and are reported relative to tetramethylsilane. NMR experiments on air-sensitive samples were conducted in J. Young Teflon-sealed NMR tubes. Elemental analysis was provided by Midwest Microlabs (Indianapolis, IN).

General Synthesis of Pt^{II} Alkyl/Olefin Complexes: [Pt(μ-Cl)(C_2H_5)(C_2H_4)]$_2$ (**5.10**) and the sodium salt of the appropriate ligand were weighed into a 2-dram vial, followed by addition of 0.6 mL C_6D_6. All syntheses were monitored by ^{1}H NMR and were found to be finished within 10-20 minutes at 25°C. Upon completion of the reaction, the mixture was filtered through either a Teflon filter or a celite plug to remove any undesired particulates. The solution was concentrated by rotary evaporation under reduced pressure and recrystallized in the manner outlined below. Although all syntheses were performed under anaerobic conditions, the starting materials and products appeared to be stable to atmospheric conditions for a few months in the solid state and days in solution at room temperature unless otherwise stated.

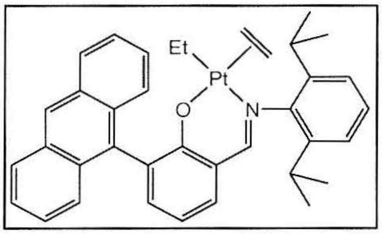

(^{Anthr,H}Sal)Pt(CH_2CH_3)(CH_2=CH_2) (5.15): The reaction was performed with the sodium salt of the ^{Anthr,H}Sal ligand (264 mg, FW = 551.70 (1 eq. THF), 0.48 mmol) and **5.10** (138 mg, FW = 575.30, 0.240 mmol, 0.50 equiv.) in 8 mL anhydrous benzene. After 12 hours at room temperature, the reaction was filtered, the product was isolated, and recrystallization was achieved by dissolving the product in a minimal amount of benzene, layering with pentane, and placing in the freezer (-5 °C) for 2 days, yielding 226 mg (66%) of the desired product as yellow crystals. *Cis (Major):* **^{1}H NMR** (CD_2Cl_2, 300.0 MHz): δ0.909 (t, 3H, $^3J_{HH}$ = 8.1 Hz, $^3J_{PtH}$ = 33.6 Hz), 1.024 (d, 6H, $^3J_{HH}$ = 6.9 Hz), 1.085 (q, 2H, $^3J_{HH}$ = 7.8 Hz, $^2J_{PtH}$ = 78.0 Hz), 1.340 (d, 6H, $^3J_{HH}$ = 6.9 Hz), 2.754 (s, 4H, $^2J_{PtH}$ = 67.8 Hz), 3.107 (sept., 2H, $^3J_{HH}$ = 6.9 Hz), 8.228 (s, 1H, $^3J_{PtH}$ = 22.5 Hz). **^{13}C NMR** (C_6D_6, 75.4 MHz): δ 9.05 ($^NJ_{PtC}$ = Hz), 14.26 ($^NJ_{PtC}$ = Hz), 22.33, 26.07, 28.06, 55.14 ($^1J_{PtC}$ = 255.1 Hz), 116.69, 123.70, 135.37, 138.86, 140.89, 164.04. *Trans (Minor)*: **^{1}H NMR** (CD_2Cl_2, 300.0 MHz): δ 0.240 (t, 3H, $^3J_{HH}$ = 8.1 Hz, $^3J_{PtH}$ = 44.4 Hz), 0.476 (q, 2H, $^3J_{HH}$ = 8.1 Hz, $^2J_{PtH}$ = 86.4 Hz), 1.093 (d, 6H, $^3J_{HH}$ = 6.9 Hz), 1.273 (d, 6H, $^3J_{HH}$ = 6.9 Hz), 3.898 (s, 4H, $^2J_{PtH}$ = 63.3 Hz), 3.271 (sept., 2H, $^3J_{HH}$ = 6.9 Hz), 8.041 (s, 1H, $^3J_{PtH}$ obscured). **^{13}C NMR** (C_6D_6, 75.4 MHz): δ -3.99, 15.23, 22.72, 25.49, 28.36, 67.53 ($^1J_{PtC}$ obscured), 165.20. **EA** (Calcd./ Found): C 62.70 (62.94), H 5.55 (5.45), N 1.98 (1.89).

Crystal Structure of 5.15 (Appendix I): Crystals suitable for X-ray structure determination were grown from a solution of **5.15** in toluene by the infusion of hexane over a week at room temperature. The yellow crystal used for data collection had dimensions 0.326 × 0.215 × 0.178 mm^3. The X-ray diffraction data were collected by using a CCD area detector diffractometer with graphite-monochromated Mo Kα radiation (0.71073 Å). Unit cell parameters were determined by a least-squares analysis of 25 automatically centered reflections in the range $2.37° < \theta < 27.17°$. Data were collected at 293 K in the range $\theta = 1.72\text{-}28.41°$. A total of 45188 reflections were collected, 7322 of which were independent. A set of 5009 reflections with $F_o^2 > 2\sigma(F_o^2)$ were observed. The structure was solved by direct methods using the SHELXS-97 program. Hydrogen atoms were placed at calculated distances and their U_{iso} values were fixed at 1.1 times the U_{eq} value of the attached atom. Refinement was full-matrix least squares on F^2 using SHELXL-97.

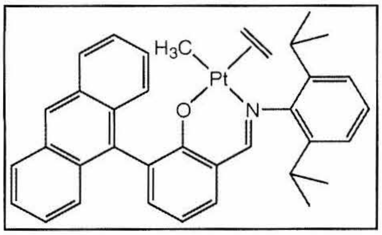

(^{Anthr,H}Sal)Pt(CH_3)(CH_2=CH_2) (5.17): To a solution of $[PtMe(ethylene)Cl]_2$ (15 mg, FW = 576.30, 84 μmol)[10] in 0.7 mL of C_6D_6, was added the sodium salt of the ^{Anthr,H}Sal ligand (16 mg, FW = 457.31, 168 μmol, 2.0 eq.). The reaction was monitored by ^{1}H NMR, with completion occuring within minutes at room temperature. The desired product was obtained by recrystallization from benzene/pentane to yield 60%. $C_{36}H_{37}NOPt$, FW = 694.76. *Major (trans) isomer:* **^{1}H NMR** (CD_2Cl_2, 300.0 MHz): δ –0.472 (s, 3H, $^2J_{PtH}$ = 76.2 Hz), 1.164 (d, 6H, $^3J_{HH}$ = 6.9 Hz), 1.231 (d, 6H, $^3J_{HH}$ = 6.9 Hz), 3.134 (s, 4H, $^2J_{PtH}$ = 61.8 Hz), 3.270 (sept., 2H, $^3J_{HH}$ = 6.9 Hz), 6.795 (dd, 1H, $^3J_{HH}$ = 8.1 Hz, $^3J_{HH}$ = 6.9 Hz), 7.245 (s, 3H), 7.35-7.46 (m, 5H), 7.556 (dd, 1H, $^3J_{HH}$ = 7.2 Hz, $^4J_{HH}$ = 2.1 Hz), 7.427 (dd, 2H, $^3J_{HH}$ = 8.7 Hz, $^4J_{HH}$ = 1.2 Hz), 8.058 (dd, 2H, $^3J_{HH}$ = 8.4 Hz, $^4J_{HH}$ = 1.2 Hz), 8.212 (s, 1H, $^3J_{PtH}$ obscured), 8.478 (s, 1H). *Minor (cis) isomer:* **^{1}H NMR** (C_6D_6, 300.0 MHz): δ 0.158 (s, 3H, $^2J_{PtH}$ = 70.1 Hz), 0.859 (d, 6H, $^3J_{HH}$ = 7.2 Hz), 1.014 (d, 6H, $^3J_{HH}$ = 7.2 Hz), 2.589 (s, 4H, $^2J_{PtH}$ = 66.6 Hz), 3.059 (sept., 2H, $^3J_{HH}$ = 7.2 Hz), 6.778 (dd, 1H, $^3J_{HH}$ = 7.7 Hz, $^3J_{HH}$ = 6.9 Hz), 6.884 (bs, 1H), 6.96-7.23 (m, 6H), 7.411 (bs, 1H), 7.579 (dd, 1H, $^3J_{HH}$ = 7.2 Hz, $^4J_{HH}$ = 1.8 Hz), 7.881 (d, 2H, $^3J_{HH}$ = 9.0 Hz), 8.054 (d, 2H, $^3J_{HH}$ = 8.4 Hz), 8.179 (bs, 1H, $^3J_{PtH}$ obscured), 8.293 (s, 1H). **EA** (Calcd./ Found): C 62.23 (62.46), H 5.37 (5.69), N 2.02 (1.89).

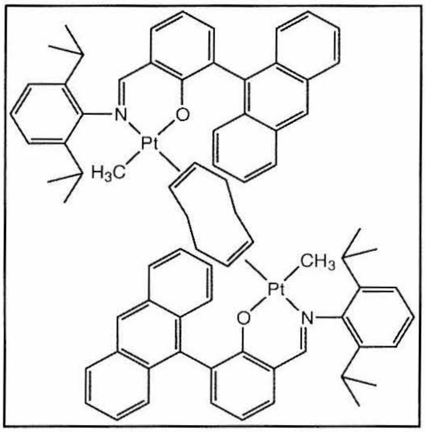

[(^{Anthr,H}Sal)Pt(CH$_3$)]$_2$(μ-COD) **5.19*d***: (η^4-COD)PtMeCl (15 mg, FW = 576.30, 84 μmol) and (^{Anthr,H}Sal)Na (16 mg, FW = 457.31, 168 μmol, 2.0 eq.) $C_{42}H_{45}NOPt$, FW = 774.89. ^{1}**H NMR** (CD_2Cl_2, 300.0 MHz): δ –0.470 (s, 3H, $^2J_{PtH}$ = 75.0 Hz), 1.179 (d, 6H, $^3J_{HH}$ = 6.9 Hz), 1.23-1.35 (m, 4H), 1.340 (d, 6H, $^3J_{HH}$ = 6.9 Hz), 2.664 (bs, 2H, $^2J_{PtH}$ = Hz), 3.265 (sept., 2H, $^3J_{HH}$ = 6.9 Hz), 6.604 (dd, 1H, $^3J_{HH}$ = 8.1 Hz, $^3J_{HH}$ = 6.9 Hz), 7.19-7.35 (m, 6H), 7.552 (dd, 2H, $^3J_{HH}$ = 0.9 Hz, $^3J_{HH}$ = 7.8 Hz), 7.794 (dd, 2H, $^3J_{HH}$ = 0.6 Hz, $^3J_{HH}$ = 7.8 Hz), 8.054 (s, 1H), 8.187 (s, 1H). **EA** (Calcd./ Found): C 65.10 (65.28), H 5.85 (5.98), N 1.81 (1.99).

Crystal Structure of 5.19*d* (Appendix L): Crystals suitable for X-ray structure determination were grown from a solution of **5.19*d*** in benzene by the infusion of hexane over a week at room temperature. The yellow crystal used for data collection had dimensions 0.24 × 0.22 × 0.21 mm^3. The X-ray diffraction data were collected by using a CCD area detector diffractometer with graphite-monochromated Mo Kα radiation (0.71073 Å). Unit cell parameters were determined by a least-squares analysis of 25 automatically centered reflections in the range $2.23° < \theta < 28.52°$. Data were collected at 98 K in the range θ = 1.46-28.53°. A total of 154834 reflections were collected, 18204 of which were independent. A set of 13902 reflections with $F_o^2 > 2\sigma(F_o^2)$ were observed. The structure was solved by direct methods using the SHELXS-97 program. Hydrogen atoms were located in the difference Fourier map. Their U_{iso} values were fixed at 1.1 times the U_{eq} value of the attached atom. Refinement was full-matrix least squares on F^2 using SHELXL-97.

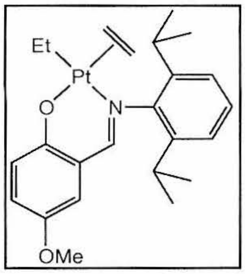

$(^{H,OMe}Sal)Pt(CH_2CH_3)(CH_2{=}CH_2)$ (5.20): The reaction was performed with sodium salt of the ^{H,OMe}Sal ligand (4.3 mg, FW = 333.40, 12.7 μmol) and **5.10** (14.6 mg, FW = 575.30, 25.4 μmol, 0.50 equiv.) in 0.7 mL C_6D_6. After filtration and isolation, recrystallization was achieved by dissolving the product in a minimal amount of benzene, layering with MeOH, and placing in the freezer (-5 °C) for 2 days, yielding 20 mg (70%) of the desired product as pale yellow crystals. $C_{24}H_{33}NO_2Pt$, FW = 562.60. *Cis (Major):* **^{1}H NMR** (CD_2Cl_2, 500.0 MHz): δ 0.909 (t, 3H, $^3J_{HH}$ = 7.4 Hz, $^3J_{PtH}$ = 36.0 Hz), 1.024 (d, 6H, $^3J_{HH}$ = 6.9 Hz), 1.080 (q, 2H, $^3J_{HH}$ = 7.4 Hz, $^2J_{PtH}$ obscured), 1.340 (d, 6H, $^3J_{HH}$ = 6.9 Hz), 2.758 (s, 4H, $^2J_{PtH}$ = 67.8 Hz), 3.111 (sept., 2H, $^3J_{HH}$ = 6.9 Hz), 6.71-6.76 (m, 1H), 7.084 (dd, 1H, $^3J_{HH}$ = 8.7 Hz, $^4J_{HH}$ = 0.6 Hz), 7.23-7.27 (m, 4H), 7.49-7.57 (m, 1H), 8.244 (s, 1H, $^3J_{PtH}$ = 22.2 Hz). **^{13}C NMR** (CD_2Cl_2, 100.0 MHz): δ 8.13, 15.38, 22.70, 26.30, 28.57, 56.02 ($^2J_{PtC}$ obscured), 63.21, 116.18, 119.11, 124.30, 125.80, 128.88, 141.55, 145.36, 151.16, 153.15, 160.45, 164.10. *Trans (Minor)*: **^{1}H NMR** (CD_2Cl_2, 500.0 MHz): δ 0.909 (t, 3H, $^3J_{HH}$ = 7.4 Hz, $^3J_{PtH}$ = 36.0 Hz), 1.024 (d, 6H, $^3J_{HH}$ = 6.9 Hz), 1.080 (q, 2H, $^3J_{HH}$ = 7.4 Hz, $^2J_{PtH}$ obscured), 1.340 (d, 6H, $^3J_{HH}$ = 6.9 Hz), 2.758 (s, 4H, $^2J_{PtH}$ = 67.8 Hz), 3.111 (sept., 2H, $^3J_{HH}$ = 6.9 Hz), 6.71-6.76 (m, 1H), 7.084 (dd, 1H, $^3J_{HH}$ = 8.7 Hz, $^4J_{HH}$ = 0.6 Hz), 7.23-7.27 (m, 4H), 7.49-7.57 (m, 1H), 8.244 (s, 1H, $^3J_{PtH}$ = 22.2 Hz). **^{13}C NMR** (CD_2Cl_2, 100.0 MHz): δ 8.13, 15.38, 22.70, 26.30, 28.57, 56.02 ($^2J_{PtC}$ obscured), 63.21, 116.18, 119.11, 124.30, 125.80, 128.88, 141.55, 145.36, 151.16, 153.15, 160.45, 164.10. **EA** (Calcd./ Found): C 51.24 (51.52), H 5.91 (5.62), N 2.49 (2.55).

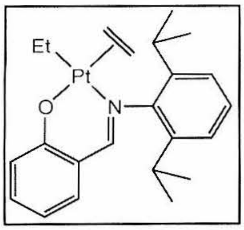

$(^{H,H}Sal)Pt(CH_2CH_3)(CH_2{=}CH_2)$ (5.21): The reaction was performed with the sodium salt of the ^{H,H}Sal ligand (17.0 mg, FW = 303.37, 56.2 μmol) and **5.10** (15.4 mg, FW = 575.30, 26.8 μmol,) in 0.7 mL C_6D_6. After filtration and isolation, recrystallization was achieved by dissolving the product in a minimal amount of benzene, layering with MeOH, and placing in the freezer (-5 °C) for 2 days, yielding 20 mg (70%) of the desired product as pale yellow crystals. $C_{23}H_{31}NOPt$, FW = 532.58. **Cis (Major): ^{1}H NMR** (CD_2Cl_2, 300.0 MHz): δ 0.909 (t, 3H, $^3J_{HH}$ = 7.4 Hz, $^3J_{PtH}$ = 36.0 Hz), 1.024 (d, 6H, $^3J_{HH}$

= 6.9 Hz), 1.080 (q, 2H, $^3J_{HH}$ = 7.4 Hz, $^2J_{PtH}$ = 77.2 Hz), 1.340 (d, 6H, $^3J_{HH}$ = 6.9 Hz), 2.758 (s, 4H, $^2J_{PtH}$ = 67.8 Hz), 3.111 (sept., 2H, $^3J_{HH}$ = 6.9 Hz), 6.71-6.76 (m, 1H), 7.084 (dd, 1H, $^3J_{HH}$ = 8.7 Hz, $^4J_{HH}$ = 0.6 Hz), 7.23-7.27 (m, 4H), 7.49-7.57 (m, 1H), 8.244 (s, 1H, $^3J_{PtH}$ = 22.2 Hz). **^{13}C NMR** (CD_2Cl_2, 75.4 MHz): δ 7.98, 15.37, 22.64, 26.17, 28.34, 56.24 ($^2J_{PtC}$ = 263.0 Hz), 116.80, 120.42, 121.71, 123.71, 123.92, 127.58, 135.69, 135.85, 141.12, 144.57, 163.99. **Trans (Minor): ^{1}H NMR** (CD_2Cl_2, 300.0 MHz): δ 0.239 (t, 3H, $^3J_{HH}$ = 7.5 Hz, $^3J_{PtH}$ = 42.6 Hz), 0.474 (q, 2H, $^3J_{HH}$ = 7.5 Hz, $^2J_{PtH}$ = 85.2 Hz), 1.092 (d, 6H, $^3J_{HH}$ = 6.9 Hz), 1.274 (d, 6H, $^3J_{HH}$ = 6.9 Hz), 3.275 (sept., 2H, $^3J_{HH}$ = 6.9 Hz), 3.909 (s, 4H, $^2J_{PtH}$ = 62.4 Hz), 6.50-6.55 (m, 1H), 6.798 (bd, 1H, $^3J_{HH}$ = 8.7 Hz), 7.18-7.22 (m, 1H), 7.24-7.33 (m, 3H), 7.39-7.45 (m, 1H), 8.056 (s, 1H, $^3J_{HH}$ obscured). **^{13}C NMR** (CD_2Cl_2, 75.4 MHz): δ 3.55, 12.39, 22.80, 25.56, 28.51, 66.97 ($^2J_{PtC}$ obscured), 114.55, 118.68, 121.46, 122.18, 124.18, 126.74, 136.25, 136.71, 141.10, 143.06, 164.57. **EA** (Calcd./ Found): C 51.87 (51.26), H 5.87 (5.65), N 2.63 (2.59).

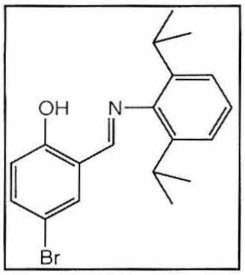

4-Bromo-2-[(2,6-diisopropyl-phenylimino)-methyl]-phenol: A solution of 5-bromo-salicylaldehyde (164 mg, FW = 201.02, 0.816 mmol) and formic acid (~ 0.1 mL) in methanol (3 mL), was added 2,6-diisopropyl-aniline (145 mg, FW = 177.29, 0.817 mmol, 1.0 eq.). The colorless solution gradually yellowed to a bright yellow solution. The reaction was monitored by TLC, with complete consumption occurring in about 2 hours. The solution was passed through a celite plug, concentrated, and recrystallized from acetonitrile to provide 226 mg (77%) of the desired product as pale yellow needles. $C_{19}H_{22}BrNO$, FW = 360.29. **^{1}H NMR** ($CDCl_3$, 300.0 MHz): δ 1.193 (d, 12H, $^3J_{HH}$ = 6.9 Hz), 2.958 (sept., 2H, $^3J_{HH}$ = 6.9 Hz), 7.004 (d, 1H, $^3J_{HH}$ = 8.4 Hz), 7.211 (s, 3H), 7.483 (bs, 1H), 7.510 (dd, 1H, $^3J_{HH}$ = 8.4 Hz, $^4J_{HH}$ = 2.4 Hz), 8.246 (s, 1H), 13.018 (bs, 1H). **^{13}C NMR** ($CDCl_3$, 75.4 MHz): δ 23.61, 28.24, 110.49, 119.33, 119.76, 123.27, 125.79, 134.16, 135.92, 138.53, 145.23, 160.17, 165.28. **IR** ($CHCl_3$, cm^{-1}): 783.7, 824.2, 853.7, 1169.1 (s), 1276.0 (s), 1350.6, 1364.1, 1385.4, 1428.2, 1474.4 (s), 1570.6, 1625.3 (s), 2871.6, 2929.5, 2966.6 (s), 3067.3. **EA** (Calcd./ Found): C 63.34 (63.33), H 6.15 (6.09), N 3.89 (3.88).

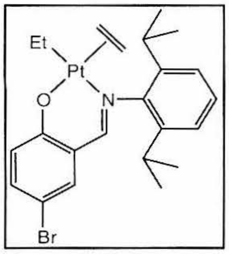

(^{H,Br}Sal)Pt(CH$_2$CH$_3$)(CH$_2$=CH$_2$) (5.22): The reaction was performed with the sodium salt of the ^{H,Br}Sal ligand (58.7 mg, FW = 382.27, 153.6 μmol) and **5.10** (22.1 mg, FW = 575.30, 76.8 μmol, 0.50 equiv.) in 0.7 mL C_6D_6. After filtration and isolation, recrystallization was achieved by dissolving the product in a minimal amount of benzene, layering with pentane, and placing in the freezer (-5 °C) for 2 days, yielding 20 mg (70%) of the desired product as pale yellow crystals. $C_{23}H_{31}NOPt$, FW = 532.58. **Cis (Major): ^{1}H NMR** (CD$_2$Cl$_2$, 300.0 MHz): δ 0.909 (t, 3H, $^3J_{HH}$ = 7.4 Hz, $^3J_{PtH}$ = 36.0 Hz), 1.024 (d, 6H, $^3J_{HH}$ = 6.9 Hz), 1.080 (q, 2H, $^3J_{HH}$ = 7.4 Hz, $^2J_{PtH}$ = 77.2 Hz), 1.340 (d, 6H, $^3J_{HH}$ = 6.9 Hz), 2.758 (s, 4H, $^2J_{PtH}$ = 67.8 Hz), 3.111 (sept., 2H, $^3J_{HH}$ = 6.9 Hz), 6.71-6.76 (m, 1H), 7.084 (dd, 1H, $^3J_{HH}$ = 8.7 Hz, $^4J_{HH}$ = 0.6 Hz), 7.23-7.27 (m, 4H), 7.49-7.57 (m, 1H), 8.244 (s, 1H, $^3J_{PtH}$ = 22.2 Hz). **^{13}C NMR** (CD$_2$Cl$_2$, 75.4 MHz): δ 7.98, 15.37, 22.64, 26.17, 28.34, 56.24 ($^2J_{PtC}$ = 263.0 Hz), 116.80, 120.42, 121.71, 123.71, 123.92, 127.58, 135.69, 135.85, 141.12, 144.57, 163.99. **Trans (Minor): ^{1}H NMR** (CD$_2$Cl$_2$, 300.0 MHz): δ 0.239 (t, 3H, $^3J_{HH}$ = 7.5 Hz, $^3J_{PtH}$ = 42.6 Hz), 0.474 (q, 2H, $^3J_{HH}$ = 7.5 Hz, $^2J_{PtH}$ = 85.2 Hz), 1.092 (d, 6H, $^3J_{HH}$ = 6.9 Hz), 1.274 (d, 6H, $^3J_{HH}$ = 6.9 Hz), 3.275 (sept., 2H, $^3J_{HH}$ = 6.9 Hz), 3.909 (s, 4H, $^2J_{PtH}$ = 62.4 Hz), 6.50-6.55 (m, 1H), 6.798 (bd, 1H, $^3J_{HH}$ = 8.7 Hz), 7.18-7.22 (m, 1H), 7.24-7.33 (m, 3H), 7.39-7.45 (m, 1H), 8.056 (s, 1H, $^3J_{HH}$ obscured). **^{13}C NMR** (CD$_2$Cl$_2$, 75.4 MHz): δ 3.55, 12.39, 22.80, 25.56, 28.51, 66.97 ($^2J_{PtC}$ obscured), 114.55, 118.68, 121.46, 122.18, 124.18, 126.74, 136.25, 136.71, 141.10, 143.06, 164.57. **EA** (Calcd./ Found): C 51.87 (51.26), H 5.87 (5.65), N 2.63 (2.59).

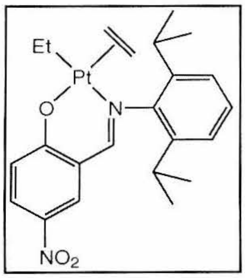

(^{H,NO2}Sal)Pt(CH$_2$CH$_3$)(CH$_2$=CH$_2$) (5.23): The reaction was performed with the sodium salt of the ^{H,NO2}Sal ligand (58.7 mg, FW = 382.27, 153.6 μmol) and **5.10** (22.1 mg, FW = 575.30, 76.8 μmol, 0.50 equiv.) in 0.7 mL C_6D_6. After filtration and isolation, recrystallization was achieved by dissolving the product in a minimal amount of benzene, layering with pentane, and placing in the freezer (-5 °C) for 2 days, yielding 20 mg (70%) of the desired product as pale yellow crystals. $C_{23}H_{30}N_2O_3Pt$, FW = 577.57. **^{1}H NMR** (CD$_2$Cl$_2$, 300.0 MHz): δ 0.239 (t, 3H, $^3J_{HH}$ = 7.5 Hz, $^3J_{PtH}$ = 42.6 Hz), 0.474 (q, 2H, $^3J_{HH}$ = 7.5 Hz, $^2J_{PtH}$ = 85.2 Hz), 1.092 (d, 6H, $^3J_{HH}$ =

6.9 Hz), 1.274 (d, 6H, $^3J_{HH}$ = 6.9 Hz), 3.275 (sept., 2H, $^3J_{HH}$ = 6.9 Hz), 3.909 (s, 4H, $^2J_{PtH}$ = 62.4 Hz), 6.50-6.55 (m, 1H), 6.798 (bd, 1H, $^3J_{HH}$ = 8.7 Hz), 7.18-7.22 (m, 1H), 7.24-7.33 (m, 3H), 7.39-7.45 (m, 1H), 8.056 (s, 1H, $^3J_{HH}$ obscured). **^{13}C NMR** (CD_2Cl_2, 75.4 MHz) δ -2.68, 8.21, 15.17, 22.62, 22.77, 25.60, 26.21, 26.25, 28.26, 28.49, 58.28 ($^2J_{PtC}$ = 269.8 Hz), 69.07 ($^2J_{PtC}$ = 231.0 Hz), 119.76, 122.82, 122.89, 123.98, 124.16, 124.35, 128.10, 128.26, 130.08, 130.43, 130.48, 133.13, 134.88, 134.91, 137.96, 140.62, 141.65, 143.91, 163.35, 163.38, 166.32, 169.30. **EA** (Calcd./ Found): C 47.83 (47.52), H 5.24 (5.16), N 4.85 (4.82).

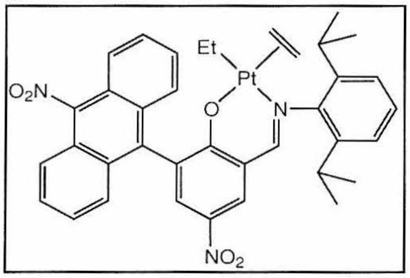

(^{NO_2Anthr,NO_2}Sal)Pt(CH_2CH_3)(CH_2=CH_2) (5.24): The reaction was performed with sodium salt of the ^{10NO2Anthr,H}Sal ligand (31.8 mg, FW = 641.69, 49.6 μmol) and **5.10** (14.3 mg, FW = 575.30, 24.8 μmol, 0.5 eq.) in 0.7 mL C_6D_6. After filtration, recrystallization was achieved by layering with hexane, allowing for equilibration (~ 3 days), and placing in the freezer (-5 °C) for a week, yielding 15 mg (38 %) of the desired product as yellowish-brown clumps. *Major (cis-) Isomer:* **^{1}H NMR** (CD_2Cl_2, 300 MHz) δ -0.475 (t, 3H, $^3J_{HH}$ = 7.8 Hz, $^3J_{PtH}$ ~ 30.6 Hz), 0.254 (q, 2H, $^3J_{HH}$ = 7.8 Hz, $^2J_{PtH}$ = 77.4 Hz), 1.108 (d, 6H, $^3J_{HH}$ = 6.9 Hz), 1.328 (d, 6H, $^3J_{HH}$ = 6.9 Hz), 2.705 (s, 4H, $^2J_{PtH}$ = 71.4 Hz), 3.055 (sept., 2H, $^3J_{HH}$ = 6.9 Hz), 7.25-7.30 (m, 3H), 7.538 (dd, 2H, $^3J_{HH}$ = 8.5 Hz, $^3J_{HH}$ = 6.6 Hz), 7.696 (dd, 2H, $^3J_{HH}$ = 8.7 Hz, $^3J_{HH}$ = 6.6 Hz), 7.851 (d, 2H, $^3J_{HH}$ = 9.0 Hz), 7.961 (d, 2H, $^3J_{HH}$ = 9.0 Hz), 8.340 (s, 1H), 8.486 (bs, 1H), 8.546 (bs, 1H). **^{13}C NMR** (CD_2Cl_2, 75.4 MHz) δ -2.24, 8.65, 14.88, 22.59, 22.75, 22.96, 25.60, 26.23, 28.55, 28.77, 58.45 ($^2J_{PtC}$ = 278.2 Hz), 71.04 ($^2J_{PtC}$ = 219.3 Hz), 123.60, 124.16, 124.34, 125.32, 126.99, 128.47, 128.69, 131.29, 133.58, 135.14, 137.37, 140.19, 141.27, 142.14, 143.51, 162.53, 165.83. *Minor (trans-) Isomer:* **^{1}H NMR** (CD_2Cl_2, 300 MHz) δ 0.063 (t, 3H, $^3J_{HH}$ = 7.2 Hz, $^3J_{PtH}$ = 42.4 Hz), 0.424 (q, 2H, $^3J_{HH}$ = 7.2 Hz, $^2J_{PtH}$ = 84.7 Hz), 1.175 (d, 6H, $^3J_{HH}$ = 6.9 Hz), 1.269 (d, 6H, $^3J_{HH}$ = 6.9 Hz), 3.240 (sept., 2H, $^3J_{HH}$ = 6.9 Hz), 3.258 (s, 4H, $^2J_{PtH}$ = 61.8 Hz), 7.25-7.30 (m, 3H), 7.519 (dd, 2H, $^3J_{HH}$ = 8.8 Hz, $^3J_{HH}$ = 6.6 Hz), 7.675 (dd, 2H, $^3J_{HH}$ = 7.8 Hz, $^3J_{HH}$ = 6.6 Hz), 7.832 (d, 2H, $^3J_{HH}$ = 8.7 Hz), 7.950 (d, 2H, $^3J_{HH}$ = 9.0 Hz), 8.354 (s, 1H), 8.500 (bs, 1H), 8.557 (bs, 1H). **^{13}C**

NMR (CD_2Cl_2, 75.4 MHz) δ -2.24, 8.65, 14.88, 22.59, 22.75, 22.96, 25.60, 26.23, 28.55, 28.77, 58.45 ($^2J_{PtC}$ = 278.2 Hz), 71.04 ($^2J_{PtC}$ = 219.3 Hz), 123.60, 124.16, 124.34, 125.32, 126.99, 128.47, 128.69, 131.29, 133.58, 135.14, 137.37, 140.19, 141.27, 142.14, 143.51, 162.53, 165.83. **EA** (Calcd./ Found): C 54.36 (54.73), H 3.16 (3.33), N 14.63 (14.67).

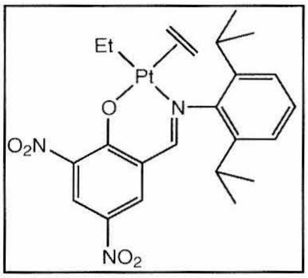

$\{^{NO_2,NO_2}Sal)\}Pt(CH_2CH_3)(CH_2{=}CH_2)$ (5.25): $C_{23}H_{29}N_3O_5Pt$, FW = 622.57. **^{1}H NMR** (CD_2Cl_2, 300 MHz) δ 0.193 (t, 3H, $^3J_{HH}$ = 7.8 Hz, $^3J_{PtH}$ = 42.6 Hz), 0.6195 (q, 2H, $^3J_{HH}$ = 7.5 Hz, $^3J_{PtH}$ = 86.3). **^{13}C NMR** (CD_2Cl_2, 75 MHz) δ -2.24, 8.65, 14.88, 22.59, 22.75, 22.96, 25.60, 26.23, 28.55, 28.77, 58.45 ($^2J_{PtC}$ = 278.2 Hz), 71.04 ($^2J_{PtC}$ = 219.3 Hz), 123.60, 124.16, 124.34, 125.32, 126.99, 128.47, 128.69, 131.29, 133.58, 135.14, 137.37, 140.19, 141.27, 142.14, 143.51, 162.53, 165.83. **EA** (Calcd. for $C_{23}H_{29}N_3O_5Pt$ 0.5 C_6H_6/ Found): C 47.20 (47.43), H 4.87 (4.84), N 6.35 (6.31).

Crystal Structure of 5.25 (Appendix J): Crystals suitable for X-ray structure determination were grown from a solution of **5.25** in benzene by slow vapor diffusion with hexane over a week at room temperature. The yellow crystal used for data collection had dimensions 0.23 × 0.19 × 0.13 mm^3. The X-ray diffraction data were collected by using a CCD area detector diffractometer with graphite-monochromated Mo Kα radiation (0.71073 Å). Unit cell parameters were determined by a least-squares analysis of 25 automatically centered reflections in the range $2.41° < \theta < 28.17°$. Data were collected at 93 K in the range θ = 1.70-28.29°. A total of 23715 reflections were collected, 5316 of which were independent. A set of 4959 reflections with $F_o^2 > 2\sigma(F_o^2)$ were observed. The structure was solved by direct methods using the SHELXS-97 program. Hydrogen atoms were located in the difference Fourier map. Their U_{iso} values were fixed at 1.1 times the U_{eq} value of the attached atom. Refinement was full-matrix least squares on F^2 using SHELXL-97.

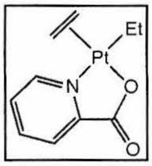

(Pyca) Pt(CH_2CH_3)(CH_2=CH_2) (5.31): A solution of **5.10** (28.3 mg, FW = 575.30, 49.2 μmol, 0.50 equiv.) in 0.7 mL of CD_2Cl_2 was added to a vial containing the sodium salt of 2-pyridine-carboxylate (26.8 mg, FW = 272.32, 98.4 μmol). The solution was thouroughly mixed at room temperature for 20 minutes, passed through a teflon filter to remove undesired particulates, and placed in a J-Young NMR tube for observation. Conversion was quantitative as observed by ^{1}H NMR (CD_2Cl_2). $C_9H_{16}O_2Pt$, FW = 351.30. *Major isomer (cis-)*—^{1}**H NMR** (CD_2Cl_2, 500.0 MHz): δ 0.90 (t, 3H, $^3J_{HH}$ = 7.5 Hz, $^2J_{PtH}$ = 38.0 Hz), 1.14 (q, 2H, $^3J_{HH}$ = 7.5 Hz, $^2J_{PtH}$ = 80 Hz), 3.54 (s, 4H, $^2J_{PtH}$ = 70.0 Hz), 7.67-7.69 (m, 1H), 7.89 (d, 1H, $^3J_{HH}$ = 5.0 Hz), 8.11 (td, 1H, $^3J_{HH}$ = 8.0 Hz, $^4J_{HH}$ = 1.5 Hz), 8.26 (d, 1H, $^3J_{HH}$ = 5.0 Hz). *Minor isomer (trans-)*—^{1}**H NMR** (CD_2Cl_2, 500.0 MHz): δ 0.98 (t, 3H, $^3J_{HH}$ = 8.0 Hz, $^2J_{PtH}$ = 35.0 Hz), 1.14 (q, 2H, $^3J_{HH}$ = 8.0 Hz, $^2J_{PtH}$ = 76 Hz), 4.06 (s, 4H, $^2J_{PtH}$ = 71.0 Hz), 7.84 (q, 1H, $^3J_{HH}$ = 4.5 Hz), 8.17 (m, 1H), 8.22 (m, 1H), 8.58 (d, 1H, $^3J_{HH}$ = 8.5 Hz). **EA** (Calcd./ Found): C 32.09 (31.98), H 3.50 (3.44), N 3.74 (3.65).

Crystal Structure of 5.31 (Appendix K): Crystals suitable for X-ray structure determination were grown from a solution of **5.31** in dichloromethane by the infusion of pentane over a week at room temperature. The colorless crystal used for data collection had dimensions 0.24 × 0.18 × 0.14 mm^3. The X-ray diffraction data were collected by using a CCD area detector diffractometer with graphite-monochromated Mo Kα radiation (0.71073 Å). Unit cell parameters were determined by a least-squares analysis of 25 automatically centered reflections in the range 2.43° < θ < 28.40°. Data were collected at 98 K in the range θ = 1.81-28.48°. A total of 30908 reflections were collected, 9591 of which were independent. A set of 9423 reflections with $F_o^2 > 2\sigma(F_o^2)$ were observed. The structure was solved by direct methods using the SHELXS-97 program. Hydrogen atoms were placed at calculated distances and their U_{iso} values were fixed at 1.1 times the U_{eq} value of the attached atom. Refinement was full-matrix least squares on F^2 using SHELXL-97.

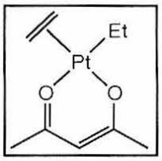

{Acac}Pt(CH_2CH_3)($CH_2{=}CH_2$) (5.32): A solution of **5.10** (28.3 mg, FW = 575.30, 49.2 μmol, 0.50 equiv.) in 0.7 mL of CD_2Cl_2 was added to a vial containing K(acac) H_2O (26.8 mg, FW = 272.32, 98.4 μmol). The solution was thouroughly mixed at room temperature for 20 minutes, passed through a teflon filter to remove undesired particulates, and placed in a J-Young NMR tube for observation. Conversion was quantitative as observed by ^1H NMR (CD_2Cl_2). Attempts to isolate this compound were unsuccessful, even at low temperature under anaerobic conditions. However, addition of 1 eq. of PPh_3 led to complete conversion (< 1hr. at 25°C) to the known compound (acac)Pt(PPh_3)Et.[57] $C_9H_{16}O_2Pt$, FW = 351.30. **^{1}H NMR** (C_6D_6, 300.0 MHz): δ 1.043 (t, 3H, $^3J_{HH} = 7.5$ Hz, $^3J_{PtH} = 36.9$ Hz), 1.436 (q, 2H, $^3J_{HH} =$ 7.5 Hz, $^2J_{PtH} = 78.6$ Hz), 1.607 (s, 3H), 1.774 (s, 3H), 3.363 (s, 4H, $^2J_{PtH} = 71.1$ Hz), 5.046 (s, 1H). **^{13}C NMR** (C_6D_6, 75.4 MHz): δ –1.24, 15.69, 27.06, 28.65, 56.42 ($^1J_{PtC}$ =275.4 Hz), 101.46 ($^3J_{PtC} = 56.7$ Hz), 183.70.

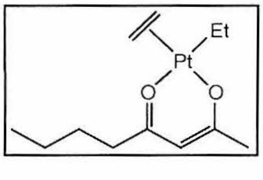

{Acac*}Pt(CH_2CH_3)($CH_2{=}CH_2$) (5.33): A solution of **5.10** (28.3 mg, FW = 575.30, 49.2 μmol, 0.50 equiv.) in 0.7 mL of CD_2Cl_2 was added to a vial containing the sodium salt of 2,4-octanedione (26.8 mg, FW = 272.32, 98.4 μmol). The solution was thouroughly mixed at room temperature for 20 minutes, passed through a teflon filter to remove undesired particulates, and placed in a J-Young NMR tube for observation. Conversion was quantitative as observed by ^1H NMR (CD_2Cl_2). Attempts to isolate this compound were unsuccessful, even at low temperature under anaerobic conditions. However, ^1H NMR assignments are in excellent agreement with compound **5.32**. $C_{12}H_{22}O_2Pt$, FW = 393.38. **^{1}H NMR** (CD_2Cl_2, 300.0 MHz): d 0.780 (t, 3H, $^3J_{HH} = 7.2$ Hz), 0.822 (t, 3H, $^3J_{HH} = 7.2$ Hz), 1.653 (s, 3H), 1.813 (s, 3H).

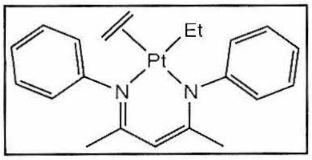

{Nacnac}Pt(CH_2CH_3)($CH_2{=}CH_2$) (5.35): A solution of **5.10** (28.3 mg, FW = 575.30, 49.2 μmol, 0.50 equiv.) in 0.7 mL of CD_2Cl_2 was added to a vial containing Na(PhNC(Me)CHC(Me)NPh)[58,59](26.8 mg, FW = 272.32, 98.4 μmol). The solution was thouroughly mixed at room temperature for 20 minutes, passed through a teflon filter to remove undesired particulates, and placed in a J-Young NMR tube for observation. Conversion was quantitative as observed by ^{1}H NMR (CD_2Cl_2). Attempts to isolate this compound were unsuccessful, even at low temperature under anaerobic conditions. $C_{21}H_{26}N_2Pt$, FW = 501.52. **^{1}H NMR** (CD_2Cl_2, 300.0 MHz): δ -0.010 (q, 2H, $^3J_{HH}$ = 7.2 Hz, $^2J_{PtH}$ = 68.1 Hz), 0.420 (t, 3H, $^3J_{HH}$ = 7.2 Hz, $^3J_{PtH}$ = 39.3 Hz), 1.645 (s, 3H), 1.754 (s, 3H), 2.795 (m, 4H, $^2J_{PtH}$ ~ 64.4 Hz), 5.001 (s, 1H), 6.893 (d, 2H, $^3J_{HH}$ = 7.5 Hz), 7.042 (d, 2H, $^3J_{HH}$ = 7.5 Hz), 7.149 (t, 2H, $^3J_{HH}$ = 7.5 Hz), 7.29-7.39 (m, 4H). ^{13}C NMR (CD_2Cl_2, 75.4 MHz): δ 7.87 ($^1J_{PtC}$ = 686.4 Hz), 16.45 ($^2J_{PtC}$ = 37.4 Hz), 26.05, 26.79 ($^3J_{PtC}$ = 31.1 Hz), 60.70 ($^1J_{PtC}$ = 227.7 Hz), 99.33 ($^3J_{PtC}$ = 47.4 Hz), 123.25, 125.15, 125.25, 126.16, 127.88, 128.52, 149.61, 151.71, 158.06, 160.43.

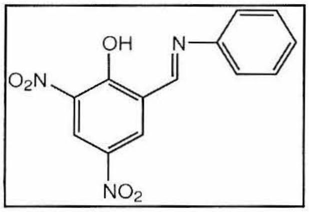

2,4-Dinitro-6-phenyliminomethyl-phenol:3,5-dinitrosalicylaldehyde (150.6 mg, FW = 212.12, 0.710 mmol) and a catalytic amount of formic acid (~ 0.1 mL) were dissolved in 10 mL of MeOH at room temperature. Aniline (66.1 mg, FW = 93.13, 0.710 mmol, 1.0 eq.) was added to the solution, leading to the immediate precipitaion of a bright orange solid. The reaction was stirred at room temperature for additional half hour, at which point the orange solid was collected on a glass frit and washed several times with methanol (3 x 60 mL). The orange solid was harvested and dried in vacuo to provide 196 mg (97%) of the desired product. Note: This material demonstrates very low solubility in most solvents. $C_{13}H_9N_3O_5$, FW = 287.23. **^{1}H NMR** (C_3D_6O, 300 MHz) δ 1.193 (d, 12H, $^3J_{HH}$ = 6.9 Hz), 2.958 (sept., 2H, $^3J_{HH}$ = 6.9 Hz), 7.004 (d, 1H, $^3J_{HH}$ = 8.4 Hz), 7.211 (s, 3H), 7.483 (bs, 1H), 7.510 (dd, 1H, $^3J_{HH}$ = 8.4 Hz, $^4J_{HH}$ = 2.4 Hz), 8.246 (s, 1H), 13.018 (bs, 1H). **^{13}C NMR** (C_3D_6O, 75.4 MHz) δ 23.61, 28.24, 110.49, 119.33, 119.76, 123.27, 125.79, 134.16, 135.92, 138.53, 145.23, 160.17, 165.28. **EA** (Calcd./ Found): C 54.36 (54.82), H 3.16 (3.47), N 14.63 (XXX).

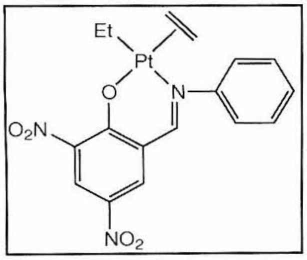

(^{NO_2,NO_2}Sal^{Ph})Pt(CH_2CH_3)(CH_2=CH_2) (5.36): Prepared by the combination of the sodium salt with **5.10**. Recrystallized by dissolution of the product in CH_2Cl_2, followed by slow diffusion of hexane into the CH_2Cl_2 layer at –78°C over 5 days. Yielded

15 mg (65 %). $C_{17}H_{17}N_3O_5Pt$, FW = 538.41. *Major (trans) species:* **^{1}H NMR** (CD_2Cl_2, 300 MHz) δ 0.265 (t, 3H, $^3J_{HH}$ = 7.8 Hz, $^3J_{PtH}$ = 38.7 Hz), 0.620 (q, 2H, $^3J_{HH}$ = 7.8 Hz, $^2J_{HH}$ = 79.8 Hz), 4.060 (s, 4H, $^2J_{PtH}$ = 68.1 Hz), 7.272 (d, 2H, $^3J_{HH}$ = 7.5 Hz), 7.32-7.51 (m, 3H), 8.470 (s, 1H, $^3J_{PtH}$ = 21.0 Hz), 8.502 (d, 1H, $^3J_{HH}$ = 3.0 Hz), 8.859 (d, 1H, $^3J_{HH}$ = 3.0 Hz). **^{13}C NMR** (CD_2Cl_2, 75.4 MHz) δ 23.61, 28.24, 110.49, 119.33, 119.76, 123.27, 125.79, 134.16, 135.92, 138.53, 145.23, 160.17, 165.28. *Minor (cis) species:* **^{1}H NMR** (CD_2Cl_2, 300.0 MHz) δ 0.826 (t, 3H, $^3J_{HH}$ = 7.5 Hz, $^3J_{PtH}$ = 36.0 Hz), 1.170 (q, 2H, $^3J_{HH}$ = 7.5 Hz, $^2J_{HH}$ = 81.2 Hz), 3.090 (s, 4H, $^2J_{PtH}$ = 75.9 Hz), 6.990 (d, 2H, $^3J_{HH}$ = 7.8 Hz), 7.32-7.51 (m, 3H), 8.409 (s, 1H, $^3J_{PtH}$ = 86.7 Hz), 8.466 (d, 1H, $^3J_{HH}$ = 3.3 Hz), 8.840 (d, 1H, $^3J_{HH}$ = 3.3 Hz). **^{13}C NMR** (CD_2Cl_2, 75.4 MHz) δ 23.61, 28.24, 110.49, 119.33, 119.76, 123.27, 125.79, 134.16, 135.92, 138.53, 145.23, 160.17, 165.28. **EA** (Calcd./ Found): C 37.92 (XXX), H 3.18 (XXX), N 7.80 (XXX).

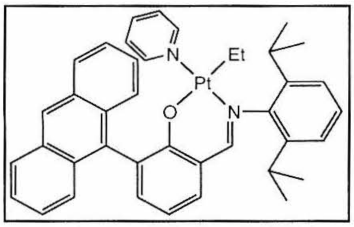

(^{Anthr,H}Sal)Pt(CH_2CH_3)(Py) (**5.37**): The ethylene adduct, **5.15** (13.8 mg, FW = 708.79, 19.5 µmol) and PPh_3 (5.1 mg, FW = 262.28, 19.5 µmol, 1.0 eq.) were added to a 2-dram vial and dissolved in 0.7 mL of anhydrous C_6D_6. The reaction was monitored by ^{1}H NMR, with **5.15** being completely consumed within 10 minutes at 25°C. Initially, two isomers were observed in a ratio of 83 (kinetic) /17 (thermodynamic). The kinetic (*cis*-) isomer was converted to the thermodynamic (*trans*-) isomer within 12 hours at 30°C. Recrystallization was achieved by layering the benzene solution with excess acetonitrile to give 7.4 mg (41%) as orange crystals. $C_{40}H_{40}N_2OPt$, FW = 759.84. **^{1}H NMR** ($CDCl_3$, 300.0 MHz) δ -0.187 (t, 3H, $^3J_{HH}$ = 7.8 Hz, $^3J_{PtH}$ = 51.6 Hz), 0.245 (dq, 2H, $^3J_{HH}$ = 7.8 Hz, $^3J_{PH}$ = 2.7 Hz, $^2J_{PtH}$ = 79.2 Hz), 1.258 (d, 6H, $^3J_{HH}$ = 6.9 Hz), 1.300 (d, 6H, $^3J_{HH}$ = 6.9 Hz), 3.765 (sept., 2H, $^3J_{HH}$ = 6.9 Hz), 6.598 (dd, 1H, $^3J_{HH}$ = 7.8 Hz, $^3J_{HH}$ = 6.9 Hz), 6.814 (dt, 6H, $^3J_{HH}$ = 7.8 Hz, $^4J_{PH}$ = 2.1 Hz), 7.00-7.40 (m, 18H), 7.662 (d, 2H, $^3J_{HH}$ = 9.0 Hz), 7.768 (d, 2H, $^3J_{HH}$ = 8.4 Hz), 8.018 (s, 1H), 8.338 (d, 1H, $^4J_{PH}$ = 12.0 Hz, $^3J_{PtH}$ = 63.6 Hz). **EA** (Calcd./ Found): C 63.23 (62.89), H 5.31 (5.35), N 3.69 (3.65).

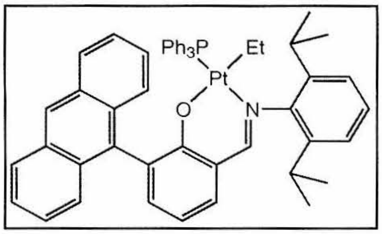

(^{Anthr,H}Sal)Pt(CH$_2$CH$_3$)(PPh$_3$) (**5.38**): The ethylene adduct, **5.15** (13.8 mg, FW = 708.79, 19.5 μmol) and PPh$_3$ (5.1 mg, FW = 262.28, 19.5 μmol, 1.0 eq.) were added to a 2-dram vial and dissolved in 0.7 mL of anhydrous C_6D_6. The reaction was monitored by ^{1}H NMR, with **5.15** being completely consumed within 10 minutes at 25 °C. Initially, two isomers were observed in a ratio of 83 (kinetic) /17 (thermodynamic). The kinetic (*cis-*) isomer was converted to the thermodynamic (*trans-*) isomer within 12 hours at 30 °C. Recrystallization was achieved by layering the benzene solution with excess acetonitrile to give 7.4 mg (41%) as orange crystals. $C_{53}H_{50}NOPPt$, FW = 943.02. *Kinetic (cis-) product:* **^{1}H NMR** (CDCl$_3$, 300.0 MHz) δ 3.765 (sept., 2H, $^3J_{HH}$ = 6.9 Hz). **^{31}P NMR** (C_6D_6, 121 MHz) δ 15.12 ($^1J_{PtP}$ = 4996 Hz). *Thermodynamic (trans-) product*: **^{1}H NMR** (CDCl$_3$, 300.0 MHz) δ -0.187 (t, 3H, $^3J_{HH}$ = 7.8 Hz, $^3J_{PtH}$ = 51.6 Hz), 0.245 (dq, 2H, $^3J_{HH}$ = 7.8 Hz, $^3J_{PH}$ = 2.7 Hz, $^2J_{PtH}$ = 79.2 Hz), 1.258 (d, 6H, $^3J_{HH}$ = 6.9 Hz), 1.300 (d, 6H, $^3J_{HH}$ = 6.9 Hz), 3.765 (sept., 2H, $^3J_{HH}$ = 6.9 Hz), 6.598 (dd, 1H, $^3J_{HH}$ = 7.8 Hz, $^3J_{HH}$ = 6.9 Hz), 6.814 (dt, 6H, $^3J_{HH}$ = 7.8 Hz, $^4J_{PH}$ = 2.1 Hz), 7.00-7.40 (m, 18H), 7.662 (d, 2H, $^3J_{HH}$ = 9.0 Hz), 7.768 (d, 2H, $^3J_{HH}$ = 8.4 Hz), 8.018 (s, 1H), 8.338 (d, 1H, $^4J_{PH}$ = 12.0 Hz, $^3J_{PtH}$ = 63.6 Hz). **^{13}C NMR** (C_6D_6; 75 MHz) δ 7.87 ($^1J_{PtC}$ = 686.4 Hz), 16.45 ($^2J_{PtC}$ = 37.4 Hz), 26.05, 26.79 ($^3J_{PtC}$ = 31.1 Hz), 60.70 ($^1J_{PtC}$ = 227.7 Hz), 99.33 ($^3J_{PtC}$ = 47.4 Hz), 123.25, 125.15, 125.25, 126.16, 127.88, 128.52, 149.61, 151.71, 158.06, 160.43. **^{31}P NMR** (C_6D_6; 121 MHz) δ 17.07 ($^1J_{PtP}$ = 4655 Hz). **EA** (Calcd. for $C_{53}H_{50}NOPPt$ C_6H_6/ Found): C 69.40 (69.31), H 5.53 (5.51), N 1.37 (1.43).

Crystal Structure of 5.38*t* (Appendix M): Crystals suitable for X-ray structure determination were grown from a saturated solution of **5.38** in benzene by cooling the vial to 5 °C for one week. The canary yellow crystal used for data collection had dimensions 0.30 × 0.22 × 0.16 mm^3. The X-ray diffraction data were collected by using a CCD area detector diffractometer with graphite-monochromated Mo Kα radiation (0.71073 Å). Unit cell parameters were determined by a least-squares analysis of 25 automatically centered reflections in the range 2.23° < θ < 28.35°. Data were collected at 98 K in the range θ = 1.88-28.34°. A total of 34869 reflections were collected, 10776 of which were independent. A set of 9839 reflections with $F_o^2 > 2\sigma(F_o^2)$ were observed. The structure was solved by direct methods using the SHELXS-97 program. Hydrogen atoms were located in the difference Fourier map. Their U_{iso} values were fixed at 1.1 times the U_{eq} value of the attached atom. Refinement was full-matrix least squares on F^2 using SHELXL-97.

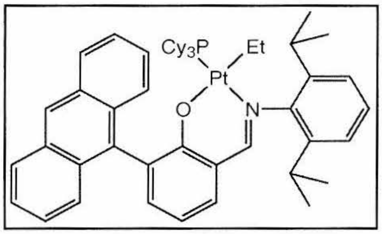

(^{Anthr,H}Sal)Pt(CH_2CH_3)(PCy_3) (5.38): The ethylene adduct, **5.15** (13.8 mg, FW = 708.79, 19.5 μmol) and PCy_3 (5.1 mg, FW = 262.28, 19.5 μmol, 1.0 eq.) were added to a 2-dram vial and dissolved in 0.7 mL of anhydrous C_6D_6. The reaction was monitored by ^{1}H NMR, with **5.15** being completely consumed within 2.5 hours at 25°C. No isomers were observed. Recrystallization was achieved by layering the benzene solution with excess acetonitrile to give 7.4 mg (41%) as orange crystals.$C_{53}H_{68}NOPPt$, FW = 961.16. **^{1}H NMR** (CD_2Cl_2; 300.0 MHz) δ 0.53-0.62 (m, 12H), 3.954 (sept., 2H, $^3J_{HH}$ = 6.6 Hz), 6.555 (dd, 1H, $^3J_{HH}$ = 6.9 Hz, $^3J_{HH}$ = 7.8 Hz), 6.986 (dd, 2H, $^3J_{HH}$ = 6.6 Hz, $^4J_{HH}$ = 1.2 Hz), 7.015 (dd, 1H, $^3J_{HH}$ = 6.3 Hz, $^4J_{HH}$ = 1.2 Hz), 7.15-7.24 (m, 5H), 7.828 (d, 2H, $^3J_{HH}$ = 8.7 Hz), 8.064 (dd, 2H, $^3J_{HH}$ = 8.7 Hz, $^4J_{HH}$ = 0.9 Hz), 8.221 (s, 1H), 8.278 (d, 1H, $^4J_{PH}$ = 10.5 Hz). **^{13}C NMR** (CD_2Cl_2; 75.4 MHz) δ 7.87 ($^1J_{PtC}$ = 686.4 Hz), 16.45 ($^2J_{PtC}$ = 37.4 Hz), 26.05, 26.79 ($^3J_{PtC}$ = 31.1 Hz), 60.70 ($^1J_{PtC}$ = 227.7 Hz), 99.33 ($^3J_{PtC}$ = 47.4 Hz), 123.25, 125.15, 125.25, 126.16, 127.88, 128.52, 149.61, 151.71, 158.06, 160.43. **^{31}P NMR** (CD_2Cl_2, 121.5 MHz) δ 13.35 ($^1J_{PtP}$ = 4329 Hz). **EA** (Calcd. for $C_{53}H_{68}NOPPt$ C_6H_6/ Found): C 68.19 (68.45), H 7.18 (7.31), N 1.35 (1.39).

5.18. References

(1) Herzog, T. A.; Zubris, D. L.; Bercaw, J. E. *Journal of the American Chemical Society* **1996**, *118*, 11988-11989.

(2) Grubbs, R. H.; Coates, G. W. *Accounts of Chemical Research* **1996**, *29*, 85-93.

(3) Coates, G. W. *Chemical Reviews* **2000**, *100*, 1223-1252.

(4) Crabtree, R. H. *The Organometallic Chemistry of the Transition Metals*; 3rd ed. ed.; John Wiley & Sons, Inc.: New York, NY, 2001.

(5) Brookhart, M.; Green, M. L. H.; Wong, L. L. *Progress in Inorganic Chemistry* **1988**, *36*, 1-124.

(6) Conroylewis, F. M.; Mole, L.; Redhouse, A. D.; Litster, S. A.; Spencer, J. L. *Journal of the Chemical Society-Chemical Communications* **1991**, 1601-1603.

(7) Carr, N.; Mole, L.; Orpen, A. G.; Spencer, J. L. *Journal of the Chemical Society-Dalton Transactions* **1992**, 2653-2662.

(8) Tempel, D. J.; Brookhart, M. *Organometallics* **1998**, *17*, 2290-2296.

(9) Scott, J. D.; Puddephatt, R. J. *Journal of the Chemical Society-Chemical Communications* **1984**, 193-195.

(10) Scott, J. D.; Puddephatt, R. J. *Organometallics* **1986**, *5*, 1253-1257.

(11) Orabona, I.; Panunzi, A.; Ruffo, F. *Journal of Organometallic Chemistry* **1996**, *525*, 295-298.

(12) Basickes, N.; Hutson, A. C.; Sen, A.; Yap, G. P. A.; Rheingold, A. L. *Organometallics* **1996**, *15*, 4116-4118.

(13) Dias, E. L.; Brookhart, M.; White, P. S. *Organometallics* **2000**, *19*, 4995-5004.

(14) Brookhart, M.; Volpe, A. F.; Lincoln, D. M. *Journal of the American Chemical Society* **1990**, *112*, 5634-5636.

(15) Brookhart, M.; Hauptman, E.; Lincoln, D. M. *Journal of the American Chemical Society* **1992**, *114*, 10394-10401.

(16) Doherty, N. M.; Bercaw, J. E. *Journal of the American Chemical Society* **1985**, *107*, 2670-2682.

(17) Burger, B. J.; Santarsiero, B. D.; Trimmer, M. S.; Bercaw, J. E. *Journal of the American Chemical Society* **1988**, *110*, 3134-3146.

(18) Bercaw, J. E.; Burger, B. J.; Green, M. L. H.; Santarsiero, B. D.; Sella, A.; Trimmer, M. S.; Wong, L. L. *Journal of the Chemical Society-Chemical Communications* **1989**, 734-736.

(19) Britovsek, G. J. P.; Gibson, V. C.; Wass, D. F. *Angewandte Chemie-International Edition* **1999**, *38*, 429-447.

(20) Ittel, S. D.; Johnson, L. K.; Brookhart, M. *Chemical Reviews* **2000**, *100*, 1169-1203.

(21) Boffa, L. S.; Novak, B. M. *Chemical Reviews* **2000**, *100*, 1479-1493.

(22) Jandeleit, B.; Schaefer, D. J.; Powers, T. S.; Turner, H. W.; Weinberg, W. H. *Angewandte Chemie-International Edition* **1999**, *38*, 2495-2532.

(23) McLain, S. J.; Feldman, J.; McCord, E. F.; Gardner, K. H.; Teasley, M. F.; Coughlin, E. B.; Sweetman, B. J.; Johnson, L. K.; Brookhart, M. *Macromolecules* **1998**, *31*, 6705-6707.

(24) Svejda, S. A.; Johnson, L. K.; Brookhart, M. *Journal of the American Chemical Society* **1999**, *121*, 10634-10635.

(25) Tempel, D. J.; Johnson, L. K.; Huff, R. L.; White, P. S.; Brookhart, M. *Journal of the American Chemical Society* **2000**, *122*, 6686-6700.

(26) Mecking, S.; Johnson, L. K.; Wang, L.; Brookhart, M. *Journal of the American Chemical Society* **1998**, *120*, 888-899.

(27) Watson, P. L.; Roe, D. C. *Journal of the American Chemical Society* **1982**, *104*, 6471-6473.

(28) Fusto, M.; Giordano, F.; Orabona, I.; Ruffo, F.; Panunzi, A. *Organometallics* **1997**, *16*, 5981-5987.

(29) Ganis, P.; Orabona, I.; Ruffo, F.; Vitagliano, A. *Organometallics* **1998**, *17*, 2646-2650.

(30) Zuccaccia, C.; Macchioni, A.; Orabona, I.; Ruffo, F. *Organometallics* **1999**, *18*, 4367-4372.

(31) Hartley, F. R. In *Comprehensive Organometallic Chemistry*; Abel, E. W., Stone, F. G. A., Wilkinson, G., Eds.; Pergamon: Oxford, UK, 1982.

(32) Defelice, V.; Derenzi, A.; Tesauro, D.; Vitagliano, A. *Organometallics* **1992**, *11*, 3669-3676.

(33) Flood, T. C.; Bitler, S. P. *Journal of the American Chemical Society* **1984**, *106*, 6076-6077.

(34) Ermer, S. P.; Struck, G. E.; Bitler, S. P.; Richards, R.; Bau, R.; Flood, T. C. *Organometallics* **1993**, *12*, 2634-2643.

(35) Clark, H. C.; Puddephatt, R. J. *Inorganic Chemistry* **1970**, *9*, 2670-2675.

(36) Appleton, T. G.; Hall, J. R.; Neale, D. W.; Williams, M. A. *Journal of Organometallic Chemistry* **1984**, *276*, C73-C76.

(37) Appleton, T. G.; Hall, J. R.; Williams, M. A. *Journal of Organometallic Chemistry* **1986**, *303*, 139-149.

(38) Albano, V. G.; Natile, G.; Panunzi, A. *Coordination Chemistry Reviews* **1994**, *133*, 67-114.

(39) Romeo, R.; Alibrandi, G. *Inorganic Chemistry* **1997**, *36*, 4822-4830.

(40) Haar, C. M.; Nolan, S. P.; Marshall, W. J.; Moloy, K. G.; Prock, A.; Giering, W. P. *Organometallics* **1999**, *18*, 474-479.

(41) Wong-Foy, A., Unpublished Results.

(42) Cotton, F. A.; Wilkinson, G. *Advanced Inorganic Chemistry*; 6th ed.; Wiley Interscience, Inc.: New York, NY, 1999.

(43) March, J. In *Advanced Organic Chemistry*; John Wiley & Sons, Inc.: New York, NY, 1992.

(44) Vanleeuwen, P.; Roobeek, C. F.; Vanderheijden, H. *Journal of the American Chemical Society* **1994**, *116*, 12117-12118.

(45) Vanleeuwen, P.; Roobeek, K. F. *Recueil Des Travaux Chimiques Des Pays-Bas-Journal of the Royal Netherlands Chemical Society* **1995**, *114*, 73-75.

(46) Heinicke, J.; He, M. Z.; Dal, A.; Klein, H. F.; Hetche, O.; Keim, W.; Florke, U.; Haupt, H. J. *European Journal of Inorganic Chemistry* **2000**, 431-440.

(47) Keim, W. *Angewandte Chemie-International Edition in English* **1990**, *29*, 235-244.

(48) Akermark, B.; Martin, J.; Nystrom, J. E.; Stromberg, S.; Svensson, M.; Zetterberg, K.; Zuber, M. *Organometallics* **1998**, *17*, 5367-5373.

(49) Desjardins, S. Y.; Cavell, K. J.; Jin, H.; Skelton, B. W.; White, A. H. *Journal of Organometallic Chemistry* **1996**, *515*, 233-243.

(50) Desjardins, S. Y.; Cavell, K. J.; Hoare, J. L.; Skelton, B. W.; Sobolev, A. N.; White, A. H.; Keim, W. *Journal of Organometallic Chemistry* **1997**, *544*, 163-174.

(51) Wiencko, H. L.; Warren, T. H. *Abstracts of Papers of the American Chemical Society* **2001**, *220*, U509-U509.

(52) Warren, T. H.; Dai, X. L.; Wiencko, H. L.; Puiu, S. *Abstracts of Papers of the American Chemical Society* **2001**, *220*, U522-U522.

(53) Jin, H.; Cavell, K. J. *Journal of the Chemical Society-Dalton Transactions* **1994**, 415-421.

(54) Jin, H.; Cavell, K. J.; Skelton, B. W.; White, A. H. *Journal of the Chemical Society-Dalton Transactions* **1995**, 2159-2169.

(55) Keim, W.; Kowaldt, F. H.; Goddard, R.; Krüger, C. *Angew. Chem. Int. Ed. Engl.* **1978**, *17*, 466-467.

(56) Bouaoud, S.-H.; Braunstein, P.; Grandjean, D.; Matt, D.; Nobel, D. *Inorganic Chemistry* **1986**, *25*, 3765.

(57) Cavell, K. J.; Jin, H.; Skelton, B. W.; White, A. H. *J. Chem. Soc. Dalton Trans.* **1993**, 1973-1978.

(58) Parks, J. E.; Holm, R. H. *Inorganic Chemistry* **1968**, *7*, 1408-1416.

(59) McGeachin, S. G. *Can. J. Chem.* **1968**, *46*, 1903-1912.

(60) Reinartz, S.; White, P. S.; Brookhart, M.; Templeton, J. L. *Organometallics* **2000**, *19*, 3854-3866.

(61) Li, R. T. Darn Good, California Institute of Technology, 1997.

(62) Darensbourg, D. J.; Rainey, P.; Yarbrough, J. *Inorganic Chemistry* **2001**, *40*, 986-993.

Appendix A

X-Ray Analysis of

(^{Anthr,H}Sal)Ni(PPh$_3$)Ph

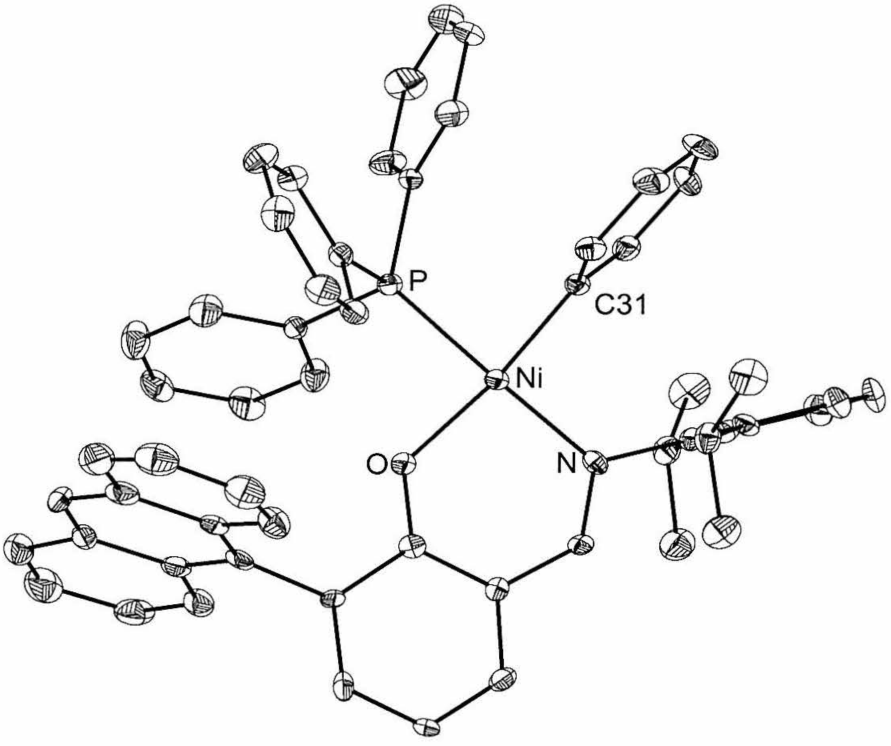

Table 1. Crystal data and structure refinement for SKF1 (CCDC .

Empirical formula	$C_{71}H_{66}NNiOP$
Formula weight	1038.93
Crystallization solvent	Toluene
Crystal Habit	Colunmar
Crystal size	0.48 x 0.10 x 0.07 mm^3
Crystal color	Yellow

Data Collection

Preliminary photos	None	
Type of diffractometer	CAD-4	
Wavelength	0.71073Å MoKα	
Data collection temperature	160 K	
Lattice determination from	25 reflections	
θ range for reflections used in lattice determination	8.6 to 10.9^3	
Unit cell dimensions	a = 20.397(9)Å	α = 90°
	b = 10.994(5)Å	β = 107.85(4)°
	c = 26.028(13)Å	γ = 90°
Volume	5556(5) Å^3	
Z	4	
Crystal system and space group	Monoclinic P2(1)/c	
Density (calculated)	1.242 g/cm^3	
Absorption coefficient	0.424 mm^{-1}	
F(000)	2200	
θ range for data collection	1.6 to 22.5^3	
Index ranges	0<=h<=-20, -11<=k<=11, -28<=l<=28	
Data collection scan type	Omega scans	
Reflections collected	16164	
Independent reflections	7238 [R(merge) = 0.073 GOF(merge) = 1.08]	
Absorption correction	None	
Number of standards	3 reflections measured every 60 min.	
Variation of standards	2.0%	

Table 1 (cont).

Structure Solution and Refinement

Structure solution program	SHELXS-86 (Sheldrick, 1990)
Primary solution method	Direct methods
Secondary solution method	Difference Fourier map
Hydrogen placement	Geometric calculated sites
Structure refinement program	SHELXL-93 (Sheldrick, 1993)
Refinement method	Full matrix least-squares on F^2
Data / restraints / parameters	7234 / 0 / 731
Treatment of hydrogen atoms	Geometric calculated sites
Goodness-of-fit on F^2	1.149
Final R indices [$I>2\sigma(I)$]	R1 = 0.0620, wR2 = 0.0896
R indices (all data)	R1 = 0.1126, wR2 = 0.1067
Max shift/error	1.623
Average shift/error	0.015
Extinction coefficient	0.00009(6)
Largest diff. peak and hole	0.330 and -0.298 e.Å^3

Special Refinement Details

The coordination geometry around the Nickel is very nearly square planar with the Nickel displaced approximately 0.03 Å. from the plane of its ligands. The RMS deviation from the plane for the four ligand atoms (O, N, P and C31) is 0.16 Å. The plane defined by the atoms of the anthracene moiety forms an approximately 80° angle with plane defined by the atoms of salicylaldiminato fragment. The triphenyl phosphine ligand lies trans- to N and cis- to the anthracene fragment while the phenyl ligand lies trans- to O and cis- to the bis-isopropylphenyl group.

Refinement on F^2 for ALL reflections except for 4 with very negative F^2 or flagged by the user for potential systematic errors. Weighted R-factors (*w*R) and all goodnesses of fit (S) are based on F^2, conventional R-factors (R) are based on F, with F set to zero for negative F^2. The observed criterion of $F^2 > 2\sigma(F^2)$ is used only for calculating R-factor$_{obs}$ etc. and is not relevant to the choice of reflections for refinement. R-factors based on F^2 are statistically about twice as large as those based on F, and R-factors based on ALL data will be even larger.

All esds (except the esd in the dihedral angle between two l.s. planes) are estimated using the full covariance matrix. The cell esds are taken into account individually in the estimation of esds in distances, angles, and torsion angles; correlations between esds in cell parameters are only used when they are defined by crystal symmetry. An approximate (isotropic) treatment of cell esds is used for estimating esds involving l.s. planes.

Table 2. Atomic coordinates (x 10^4) and equivalent isotropic displacement parameters ($Å^2$ x 10^3) for SKF1. U(eq) is defined as one third of the trace of the orthogonalized U^{ij} tensor.

	x	y	z	U(eq)
Ni	7098(1)	2298(1)	9321(1)	17(1)
P	8163(1)	2382(1)	9321(1)	18(1)
O	7439(2)	2346(3)	10091(1)	21(1)
N	6141(2)	2454(4)	9290(1)	17(1)
C(1)	8210(3)	2075(5)	11214(2)	21(1)
C(2)	8628(3)	3066(5)	11447(2)	22(1)
C(3)	8364(3)	4275(5)	11447(2)	28(1)
C(4)	8778(3)	5204(6)	11695(2)	36(2)
C(5)	9485(3)	5007(6)	11958(2)	44(2)
C(6)	9763(3)	3892(6)	11960(2)	34(2)
C(7)	9353(3)	2887(5)	11698(2)	25(1)
C(8)	9635(3)	1738(5)	11695(2)	30(2)
C(9)	9221(3)	738(5)	11470(2)	28(1)
C(10)	9502(3)	-461(6)	11493(2)	39(2)
C(11)	9082(3)	-1430(6)	11306(2)	42(2)
C(12)	8373(3)	-1266(6)	11087(2)	39(2)
C(13)	8080(3)	-150(5)	11039(2)	30(2)
C(14)	8491(3)	908(5)	11231(2)	21(1)
C(21)	7087(2)	2359(4)	10428(2)	16(1)
C(22)	6361(2)	2504(4)	10268(2)	14(1)
C(23)	6009(3)	2545(5)	10655(2)	22(1)
C(24)	6356(2)	2444(5)	11195(2)	26(1)
C(25)	7065(2)	2299(5)	11355(2)	25(1)
C(26)	7444(2)	2248(5)	11002(2)	18(1)
C(31)	6883(3)	1899(4)	8580(2)	19(1)
C(32)	6904(3)	676(5)	8437(2)	23(1)
C(33)	6727(3)	313(5)	7905(2)	30(2)
C(34)	6528(3)	1172(5)	7496(2)	36(2)
C(35)	6509(3)	2386(6)	7631(2)	30(2)
C(36)	6688(2)	2740(5)	8164(2)	23(1)
C(41)	8583(3)	903(4)	9475(2)	19(1)
C(42)	9173(3)	583(5)	9343(2)	26(1)
C(43)	9446(3)	-568(5)	9450(2)	30(2)
C(44)	9126(3)	-1433(5)	9686(2)	31(2)
C(45)	8556(3)	-1113(5)	9831(2)	30(2)
C(46)	8281(3)	44(5)	9733(2)	24(1)
C(51)	8392(2)	2861(5)	8725(2)	20(1)
C(52)	8333(3)	2046(5)	8303(2)	29(2)
C(53)	8502(3)	2396(6)	7847(2)	36(2)
C(54)	8718(3)	3570(6)	7803(2)	43(2)
C(55)	8777(3)	4379(6)	8216(2)	43(2)
C(56)	8620(3)	4023(5)	8675(2)	30(2)
C(61)	8663(3)	3428(4)	9843(2)	16(1)
C(62)	8377(3)	4530(5)	9915(2)	29(2)

C(63)	8746(3)	5379(5)	10272(2)	34(2)
C(64)	9416(3)	5139(5)	10572(2)	32(2)
C(65)	9709(3)	4046(5)	10516(2)	39(2)
C(66)	9328(3)	3208(5)	10145(2)	33(2)
C(71)	5578(2)	2527(4)	8790(2)	17(1)
C(72)	5383(3)	3655(4)	8543(2)	19(1)
C(721)	5729(3)	4823(4)	8800(2)	24(1)
C(722)	5335(3)	5409(5)	9155(2)	35(2)
C(723)	5797(3)	5763(5)	8380(2)	38(2)
C(74)	4506(3)	2621(5)	7836(2)	31(1)
C(75)	4711(3)	1521(5)	8086(2)	29(2)
C(76)	5249(3)	1445(4)	8567(2)	19(1)
C(73)	4835(3)	3677(5)	8068(2)	29(2)
C(761)	5442(3)	236(4)	8855(2)	24(1)
C(762)	5373(3)	-847(5)	8474(2)	36(2)
C(763)	5019(3)	6(5)	9243(2)	34(2)
C(81)	5950(2)	2580(4)	9716(2)	15(1)
C(101)	3457(4)	4096(7)	8850(3)	75(2)
C(102)	3381(3)	3351(6)	9314(3)	46(2)
C(103)	3584(3)	2151(7)	9359(3)	61(2)
C(104)	3514(4)	1450(7)	9780(4)	73(3)
C(105)	3240(4)	1924(7)	10156(3)	59(2)
C(106)	3031(3)	3110(6)	10110(3)	47(2)
C(107)	3104(3)	3821(6)	9692(3)	44(2)
C(201)	2822(4)	503(7)	7859(3)	75(2)
C(202)	2493(3)	1461(6)	7465(3)	46(2)
C(203)	2540(4)	1466(7)	6949(3)	58(2)
C(204)	2231(4)	2336(7)	6576(3)	66(2)
C(205)	1861(4)	3255(6)	6725(3)	60(2)
C(206)	1798(4)	3273(6)	7236(3)	58(2)
C(207)	2120(3)	2391(7)	7599(3)	55(2)

Table 3. Selected bond lengths [Å] and angles [°] for SKF1.

Ni-C(31)	1.895(5)	C(31)-Ni-O	166.2(2)
Ni-O	1.910(3)	C(31)-Ni-N	93.5(2)
Ni-N	1.937(4)	O-Ni-N	94.5(2)
Ni-P	2.172(2)	C(31)-Ni-P	86.0(2)
		O-Ni-P	87.51(11)
		N-Ni-P	172.16(12)

Symmetry transformations used to generate equivalent atoms:

Table 4. Bond lengths [Å] and angles [°] for SKF1.

Ni-C(31)	1.895(5)	N-C(71)	1.451(5)
Ni-O	1.910(3)	C(1)-C(2)	1.401(7)
Ni-N	1.937(4)	C(1)-C(14)	1.401(7)
Ni-P	2.172(2)	C(1)-C(26)	1.501(6)
P-C(41)	1.824(5)	C(2)-C(7)	1.436(7)
P-C(61)	1.832(5)	C(2)-C(3)	1.434(7)
P-C(51)	1.830(5)	C(3)-C(4)	1.357(7)
O-C(21)	1.293(5)	C(3)-H(3A)	0.94(5)
N-C(81)	1.291(5)	C(4)-C(5)	1.409(8)

C(4)-H(4A)	0.90(5)
C(5)-C(6)	1.350(8)
C(5)-H(5A)	0.91(5)
C(6)-C(7)	1.427(7)
C(6)-H(6A)	0.98(5)
C(7)-C(8)	1.389(7)
C(8)-C(9)	1.401(7)
C(8)-H(8A)	0.98(5)
C(9)-C(10)	1.431(8)
C9)-C(14)	1.437(7)
C(10)-C(11)	1.361(8)
C(10)-H(10A)	1.04(5)
C(11)-C(12)	1.394(8)
C(11)-H(11A)	0.96(5)
C(12)-C(13)	1.353(7)
C(12)-H(12A)	0.92(5)
C(13)-C(14)	1.431(7)
C(13)-H(13A)	0.97(5)
C(21)-C(22)	1.418(6)
C(21)-C(26)	1.454(6)
C(22)-C(23)	1.405(6)
C(22)-C(81)	1.427(6)
C(23)-C(24)	1.370(6)
C(23)-H(23A)	0.99(4)
C(24)-C(25)	1.387(6)
C(24)-H(24A)	0.92(4)
C(25)-C(26)	1.370(6)
C(25)-H(25A)	0.97(4)
C31)-C(36)	1.386(6)
C(31)-C(32)	1.399(7)
C(32)-C(33)	1.380(7)
C(32)-H(32A)	0.95(4)
C(33)-C(34)	1.387(7)
C(33)-H(33A)	1.00(5)
C(34)-C(35)	1.384(7)
C(34)-H(34A)	0.94(5)
C(35)-C(36)	1.376(6)
C(35)-H(35A)	0.96(5)
C(36)-H(36A)	0.93(5)
C(41)-C(42)	1.395(7)
C(41)-C(46)	1.404(7)
C(42)-C(43)	1.376(7)
C(42)-H(42A)	0.99(5)
C(43)-C(44)	1.396(7)
C(43)-H(43A)	0.98(5)
C(44)-C(45)	1.374(7)
C(44)-H(44A)	0.97(5)
C(45)-C(46)	1.382(7)
C(45)-H(45A)	0.93(5)
C(46)-H(46A)	1.07(5)
C(51)-C(56)	1.380(7)
C(51)-C(52)	1.395(6)
C(52)-C(53)	1.389(7)
C(52)-H(52A)	0.88(5)
C(53)-C(54)	1.379(8)
C(53)-H(53A)	0.88(5)
C(54)-C(55)	1.372(8)
C(54)-H(54A)	0.96(5)
C(55)-C(56)	1.384(7)
C(55)-H(55A)	0.94(5)
C(56)-H(56A)	1.04(5)
C(61)-C(66)	1.366(7)
C(61)-C(62)	1.381(7)
C(62)-C(63)	1.369(7)
C(62)-H(62A)	0.87(5)
C(63)-C(64)	1.377(7)
C(63)-H(63A)	0.83(5)
C(64)-C(65)	1.369(7)
C(64)-H(64A)	0.94(5)
C(65)-C(66)	1.388(7)
C(65)-H(65A)	0.97(5)
C(66)-H(66A)	0.90(5)
C(71)-C(72)	1.397(7)
C(71)-C(76)	1.401(7)
C(72)-C(73)	1.390(7)
C(72)-C(721)	1.518(7)
C(721)-C(722)	1.539(7)
C(721)-C(723)	1.541(7)
C(721)-H(72A)	1.03(5)
C(722)-H(72B)	0.96
C(722)-H(72C)	0.96
C(722)-H(72D)	0.96
C(723)-H(72E)	0.96
C(723)-H(72F)	0.96
C(723)-H(72G)	0.96
C(74)-C(73)	1.383(7)
C(74)-C(75)	1.376(7)
C(74)-H(74A)	0.97(4)
C(75)-C(76)	1.390(7)
C(75)-H(75A)	0.97(5)
C(76)-C(761)	1.519(7)
C(73)-H(73A)	0.86(5)
C(761)-C(762)	1.528(7)
C(761)-C(763)	1.537(7)
C(761)-H(76A)	0.99(5)
C(762)-H(76B)	0.96
C(762)-H(76C)	0.96
C(762)-H(76D)	0.96
C(763)-H(76E)	0.96
C(763)-H(76F)	0.96
C(763)-H(76G)	0.96
C(81)-H(81A)	0.97(4)
C(101)-C(102)	1.507(8)
C(101)-H(10B)	0.96
C(101)-H(10C)	0.96
C(101)-H(10D)	0.96
C(102)-C(107)	1.377(8)
C(102)-C(103)	1.376(8)
C(103)-C(104)	1.382(10)
C(103)-H(10E)	0.91(6)
C(104)-C(105)	1.370(10)
C(104)-H(10F)	0.85(6)

C(105)-C(106)	1.366(9)
C(105)-H(10G)	1.02(6)
C(106)-C(107)	1.386(8)
C(106)-H(10H)	0.92(5)
C(107)-H(10I)	0.90(5)
C(201)-C(202)	1.480(8)
C(201)-H(20A)	0.96
C(201)-H(20B)	0.96
C(201)-H(20C)	0.96
C(202)-C(207)	1.383(8)
C(202)-C(203)	1.374(8)
C(203)-C(204)	1.371(9)
C(203)-H(20D)	0.93(6)
C(204)-C(205)	1.385(9)
C(204)-H(20E)	1.01(6)
C(205)-C(206)	1.372(9)
C(205)-H(20F)	0.87(6)
C(206)-C(207)	1.373(8)
C(206)-H(20G)	1.08(6)
C(207)-H(20H)	0.89(5)

C(31)-Ni-O	166.2(2)
C(31)-Ni-N	93.5(2)
O-Ni-N	94.5(2)
C(31)-Ni-P	86.0(2)
O-Ni-P	87.51(11)
N-Ni-P	172.16(12)
C(41)-P-C(61)	106.2(2)
C(41)-P-C(51)	102.6(2)
C(61)-P-C(51)	102.6(2)
C(41)-P-Ni	111.4(2)
C(61)-P-Ni	110.9(2)
C(51)-P-Ni	121.8(2)
C(21)-O-Ni	127.8(3)
C(81)-N-C(71)	113.7(4)
C(81)-N-Ni	122.6(3)
C(71)-N-Ni	123.6(3)
C(2)-C(1)-C(14)	120.6(5)
C(2)-C(1)-C(26)	119.1(5)
C(14)-C(1)-C(26)	119.9(5)
C(1)-C(2)-C(7)	119.7(5)
C(1)-C(2)-C(3)	122.8(5)
C(7)-C(2)-C(3)	117.5(5)
C(4)-C(3)-C(2)	121.2(6)
C(4)-C(3)-H(3A)	119.4(4)
C(2)-C(3)-H(3A)	119.4(3)
C(3)-C(4)-C(5)	120.7(6)
C(3)-C(4)-H(4A)	119.6(4)
C(5)-C(4)-H(4A)	119.6(4)
C(6)-C(5)-C(4)	120.5(6)
C(6)-C(5)-H(5A)	119.7(4)
C(4)-C(5)-H(5A)	119.7(4)
C(5)-C(6)-C(7)	121.1(6)
C(5)-C(6)-H(6A)	119.5(4)
C(7)-C(6)-H(6A)	119.5(4)
C(8)-C(7)-C(6)	121.6(5)
C(8)-C(7)-C(2)	119.5(5)
C(6)-C(7)-C(2)	118.9(5)
C(7)-C(8)-C(9)	121.2(5)
C(7)-C(8)-H(8A)	119.4(3)
C(9)-C(8)-H(8A)	119.4(3)
C(8)-C(9)-C(10)	121.5(6)
C(8)-C(9)-C(14)	119.4(5)
C(10)-C(9)-C(14)	119.1(6)
C(11)-C(10)-C(9)	120.4(6)
C(11)-C(10)-H(10A)	119.8(4)
C(9)-C(10)-H(10A)	119.8(4)
C(10)-C(11)-C(12)	120.3(6)
C(10)-C(11)-H(11A)	119.8(4)
C(12)-C(11)-H(11A)	119.8(4)
C(13)-C(12)-C(11)	121.9(6)
C(13)-C(12)-H(12A)	119.1(4)
C(11)-C(12)-H(12A)	119.0(4)
C(12)-C(13)-C(14)	120.6(6)
C(12)-C(13)-H(13A)	119.7(4)
C(14)-C(13)-H(13A)	119.7(3)
C(1)-C(14)-C(13)	122.8(5)
C(1)-C(14)-C(9)	119.5(5)
C(13)-C(14)-C(9)	117.6(5)
O-C(21)-C(22)	123.3(4)
O-C(21)-C(26)	119.3(4)
C(22)-C(21)-C(26)	117.4(4)
C(23)-C(22)-C(21)	120.7(4)
C(23)-C(22)-C(81)	116.6(4)
C(21)-C(22)-C(81)	122.7(4)
C(24)-C(23)-C(22)	121.0(5)
C(24)-C(23)-H(23A)	119.5(3)
C(22)-C(23)-H(23A)	119.5(3)
C(23)-C(24)-C(25)	118.8(5)
C(23)-C(24)-H(24A)	120.6(3)
C(25)-C(24)-H(24A)	120.6(3)
C(26)-C(25)-C(24)	123.6(5)
C(26)-C(25)-H(25A)	118.2(3)
C(24)-C(25)-H(25A)	118.2(3)
C(25)-C(26)-C(21)	118.6(4)
C(25)-C(26)-C(1)	119.8(4)
C(21)-C(26)-C(1)	121.7(4)
C(36)-C(31)-C(32)	117.3(5)
C(36)-C(31)-Ni	124.3(4)
C(32)-C(31)-Ni	118.4(4)
C(33)-C(32)-C(31)	121.6(5)
C(33)-C(32)-H(32A)	119.2(3)
C(31)-C(32)-H(32A)	119.2(3)
C(32)-C(33)-C(34)	119.9(5)
C(32)-C(33)-H(33A)	120.0(3)
C(34)-C(33)-H(33A)	120.1(3)
C(35)-C(34)-C(33)	119.1(5)
C(35)-C(34)-H(34A)	120.5(3)
C(33)-C(34)-H(34A)	120.5(3)
C(36)-C(35)-C(34)	120.6(5)
C(36)-C(35)-H(35A)	119.7(3)
C(34)-C(35)-H(35A)	119.7(3)

C(35)-C(36)-C(31)	121.5(5)
C(35)-C(36)-H(36A)	119.2(3)
C(31)-C(36)-H(36A)	119.2(3)
C(42)-C(41)-C(46)	119.0(5)
C(42)-C(41)-P	123.6(4)
C(46)-C(41)-P	117.4(4)
C(43)-C(42)-C(41)	120.6(5)
C(43)-C(42)-H(42A)	119.7(3)
C(41)-C(42)-H(42A)	119.7(3)
C(42)-C(43)-C(44)	120.0(5)
C(42)-C(43)-H(43A)	120.0(3)
C(44)-C(43)-H(43A)	120.0(3)
C(45)-C(44)-C(43)	119.7(5)
C(45)-C(44)-H(44A)	120.2(3)
C(43)-C(44)-H(44A)	120.1(3)
C(44)-C(45)-C(46)	120.9(5)
C(44)-C(45)-H(45A)	119.5(3)
C(46)-C(45)-H(45A)	119.6(3)
C(45)-C(46)-C(41)	119.8(5)
C(45)-C(46)-H(46A)	120.1(3)
C(41)-C(46)-H(46A)	120.1(3)
C(56)-C(51)-C(52)	118.0(5)
C(56)-C(51)-P	121.9(4)
C(52)-C(51)-P	120.1(4)
C(53)-C(52)-C(51)	120.8(5)
C(53)-C(52)-H(52A)	119.6(4)
C(51)-C(52)-H(52A)	119.6(3)
C(54)-C(53)-C(52)	120.0(6)
C(54)-C(53)-H(53A)	120.0(3)
C(52)-C(53)-H(53A)	120.0(4)
C(55)-C(54)-C(53)	119.7(6)
C(55)-C(54)-H(54A)	120.1(4)
C(53)-C(54)-H(54A)	120.1(3)
C(54)-C(55)-C(56)	120.3(6)
C(54)-C(55)-H(55A)	119.9(4)
C(56)-C(55)-H(55A)	119.9(4)
C(51)-C(56)-C(55)	121.2(6)
C(51)-C(56)-H(56A)	119.4(3)
C(55)-C(56)-H(56A)	119.4(4)
C(66)-C(61)-C(62)	117.6(5)
C(66)-C(61)-P	123.0(4)
C(62)-C(61)-P	119.2(4)
C(63)-C(62)-C(61)	121.5(5)
C(63)-C(62)-H(62A)	119.2(3)
C(61)-C(62)-H(62A)	119.2(3)
C(62)-C(63)-C(64)	119.9(5)
C(62)-C(63)-H(63A)	120.1(4)
C(64)-C(63)-H(63A)	120.1(3)
C(65)-C(64)-C(63)	119.9(5)
C(65)-C(64)-H(64A)	120.1(3)
C(63)-C(64)-H(64A)	120.1(3)
C(64)-C(65)-C(66)	119.1(6)
C(64)-C(65)-H(65A)	120.4(3)
C(66)-C(65)-H(65A)	120.4(3)
C(61)-C(66)-C(65)	121.9(5)
C(61)-C(66)-H(66A)	119.1(3)
C(65)-C(66)-H(66A)	119.1(4)
C(72)-C(71)-C(76)	122.0(4)
C(72)-C(71)-N	119.8(4)
C(76)-C(71)-N	118.2(4)
C(73)-C(72)-C(71)	117.6(5)
C(73)-C(72)-C(721)	121.0(5)
C(71)-C(72)-C(721)	121.4(4)
C(72)-C(721)-C(722)	111.2(4)
C(72)-C(721)-C(723)	112.7(4)
C(722)-C(721)-C(723)	108.8(4)
C(72)-C(721)-H(72A)	108.0(3)
C(722)-C(721)-H(72A)	108.0(3)
C(723)-C(721)-H(72A)	108.0(3)
C(721)-C(722)-H(72B)	109.5(3)
C(721)-C(722)-H(72C)	109.5(3)
H(72B)-C(722)-H(72C)	109.5
C(721)-C(722)-H(72D)	109.5(3)
H(72B)-C(722)-H(72D)	109.5
H(72C)-C(722)-H(72D)	109.5
C(721)-C(723)-H(72E)	109.5(3)
C(721)-C(723)-H(72F)	109.5(3)
H(72E)-C(723)-H(72F)	109.5
C(721)-C(723)-H(72G)	109.5(3)
H(72E)-C(723)-H(72G)	109.5
H(72F)-C(723)-H(72G)	109.5
C(73)-C(74)-C(75)	119.7(5)
C(73)-C(74)-H(74A)	120.1(3)
C(75)-C(74)-H(74A)	120.2(3)
C(74)-C(75)-C(76)	121.3(5)
C(74)-C(75)-H(75A)	119.4(3)
C(76)-C(75)-H(75A)	119.4(3)
C(75)-C(76)-C(71)	117.9(5)
C(75)-C(76)-C(761)	120.7(5)
C(71)-C(76)-C(761)	121.3(4)
C(74)-C(73)-C(72)	121.5(5)
C(74)-C(73)-H(73A)	119.2(3)
C(72)-C(73)-H(73A)	119.2(3)
C(76)-C(761)-C(762)	113.8(4)
C(76)-C(761)-C(763)	110.8(4)
C(762)-C(761)-C(763)	109.9(4)
C(76)-C(761)-H(76A)	107.4(3)
C(762)-C(761)-H(76A)	107.4(3)
C(763)-C(761)-H(76A)	107.4(3)
C(761)-C(762)-H(76B)	109.5(3)
C(761)-C(762)-H(76C)	109.5(3)
H(76B)-C(762)-H(76C)	109.5
C(761)-C(762)-H(76D)	109.5(3)
H(76B)-C(762)-H(76D)	109.5
H(76C)-C(762)-H(76D)	109.5
C(761)-C(763)-H(76E)	109.5(3)
C(761)-C(763)-H(76F)	109.5(3)
H(76E)-C(763)-H(76F)	109.5
C(761)-C(763)-H(76G)	109.5(3)
H(76E)-C(763)-H(76G)	109.5
H(76F)-C(763)-H(76G)	109.5
N-C(81)-C(22)	128.4(4)

N-C(81)-H(81A)	115.8(3)	C(106)-C(107)-H(10I)	119.5(4)
C(22)-C(81)-H(81A)	115.8(3)	C(202)-C(201)-H(20A)	109.5(4)
C(102)-C(101)-H(10B)	109.5(4)	C(202)-C(201)-H(20B)	109.5(4)
C(102)-C(101)-H(10C)	109.5(4)	H(20A)-C(201)-H(20B)	109.4
H(10B)-C(101)-H(10C)	109.5	C(202)-C(201)-H(20C)	109.5(4)
C(102)-C(101)-H(10D)	109.5(4)	H(20A)-C(201)-H(20C)	109.4
H(10B)-C(101)-H(10D)	109.47(6)	H(20B)-C(201)-H(20C)	109.4
H(10C)-C(101)-H(10D)	109.5	C(207)-C(202)-C(203)	116.9(6)
C(107)-C(102)-C(103)	118.5(7)	C(207)-C(202)-C(201)	121.2(6)
C(107)-C(102)-C(101)	122.3(6)	C(203)-C(202)-C(201)	121.9(6)
C(103)-C(102)-C(101)	119.2(7)	C(202)-C(203)-C(204)	122.6(7)
C(104)-C(103)-C(102)	120.1(8)	C(202)-C(203)-H(20D)	118.7(4)
C(104)-C(103)-H(10E)	120.0(5)	C(204)-C(203)-H(20D)	118.7(5)
C(102)-C(103)-H(10E)	120.0(5)	C(205)-C(204)-C(203)	118.9(7)
C(105)-C(104)-C(103)	121.2(7)	C(205)-C(204)-H(20E)	120.6(4)
C(105)-C(104)-H(10F)	119.4(5)	C(203)-C(204)-H(20E)	120.6(5)
C(103)-C(104)-H(10F)	119.4(5)	C(206)-C(205)-C(204)	120.1(7)
C(104)-C(105)-C(106)	119.1(8)	C(206)-C(205)-H(20F)	119.9(4)
C(104)-C(105)-H(10G)	120.5(5)	C(204)-C(205)-H(20F)	119.9(4)
C(106)-C(105)-H(10G)	120.5(5)	C(205)-C(206)-C(207)	119.3(7)
C(105)-C(106)-C(107)	120.1(7)	C(205)-C(206)-H(20G)	120.3(4)
C(105)-C(106)-H(10H)	119.9(5)	C(207)-C(206)-H(20G)	120.3(4)
C(107)-C(106)-H(10H)	120.0(4)	C(206)-C(207)-C(202)	122.2(6)
C(102)-C(107)-C(106)	121.1(6)	C(206)-C(207)-H(20H)	118.9(4)
C(102)-C(107)-H(10I)	119.5(4)	C(202)-C(207)-H(20H)	118.9(4)

Symmetry transformations used to generate equivalent atoms:

Table 5. Anisotropic displacement parameters (Å^2 x 10^4) for SKF1. The anisotropic displacement factor exponent takes the form: $-2\pi^2[h^2a^{*2}U^{11}+...+2hka^*b^*U^{12}]$

	U^{11}	U^{22}	U^{33}	U^{23}	U^{13}	U^{12}
Ni	17(1)	21(1)	14(1)	1(1)	6(1)	2(1)
P	17(1)	21(1)	17(1)	1(1)	7(1)	2(1)
O	17(2)	31(2)	16(2)	2(2)	6(2)	3(2)
N	22(2)	13(2)	14(2)	-1(2)	3(2)	0(2)
C(1)	26(3)	30(4)	9(3)	4(2)	8(2)	-3(3)
C(2)	26(3)	28(4)	15(3)	1(2)	10(3)	2(3)
C(3)	29(4)	34(4)	20(3)	4(3)	8(3)	-4(3)
C(4)	43(4)	37(4)	35(4)	-13(3)	22(3)	-6(3)
C(5)	46(5)	52(5)	36(4)	-12(3)	14(4)	-21(4)
C(6)	28(4)	47(4)	27(4)	-1(3)	7(3)	-10(3)
C(7)	19(3)	41(4)	15(3)	0(3)	6(3)	-12(3)
C(8)	14(3)	55(5)	23(3)	5(3)	6(3)	3(3)
C(9)	35(4)	36(4)	17(3)	10(3)	13(3)	11(3)
C(10)	37(4)	51(5)	30(4)	14(3)	11(3)	13(4)
C(11)	57(5)	37(4)	38(4)	5(3)	22(4)	6(4)
C(12)	49(5)	33(4)	35(4)	2(3)	16(3)	1(3)
C(13)	35(4)	29(4)	24(3)	2(3)	6(3)	4(3)
C(14)	26(3)	28(4)	12(3)	3(2)	10(3)	0(3)
C(21)	21(3)	10(3)	19(3)	6(2)	9(2)	-1(2)
C(22)	15(3)	9(3)	19(3)	-2(2)	4(2)	1(2)
C(23)	16(3)	26(3)	26(3)	-7(3)	10(2)	-2(3)

C(24)	22(3)	47(4)	13(3)	-3(3)	9(2)	-1(3)
C(25)	16(3)	37(4)	19(3)	0(3)	-1(2)	-3(3)
C(26)	15(3)	27(3)	14(3)	4(2)	9(2)	-1(3)
C(31)	18(3)	25(3)	15(3)	3(2)	6(2)	5(2)
C(32)	25(3)	23(3)	24(3)	0(3)	11(3)	-1(3)
C(33)	36(4)	26(4)	33(4)	-13(3)	17(3)	-6(3)
C(34)	42(4)	47(4)	19(3)	-16(3)	11(3)	-5(3)
C(35)	29(3)	44(4)	13(3)	10(3)	2(2)	4(3)
C(36)	20(3)	25(3)	23(3)	2(3)	8(2)	6(3)
C(41)	20(3)	19(3)	17(3)	-1(2)	4(3)	2(2)
C(42)	24(3)	31(4)	25(3)	-1(3)	10(3)	2(3)
C(43)	26(4)	26(4)	41(4)	0(3)	15(3)	5(3)
C(44)	32(4)	21(3)	38(4)	0(3)	7(3)	4(3)
C(45)	37(4)	26(4)	28(3)	6(3)	12(3)	0(3)
C(46)	26(3)	28(4)	17(3)	-1(3)	6(3)	5(3)
C(51)	17(3)	29(3)	15(3)	-3(2)	7(2)	-4(3)
C(52)	29(3)	32(4)	28(4)	-1(3)	13(3)	1(3)
C(53)	31(3)	63(5)	16(3)	-1(3)	10(3)	2(4)
C(54)	34(4)	71(5)	26(4)	13(4)	14(3)	-3(4)
C(55)	50(4)	49(4)	39(4)	13(3)	25(4)	-19(4)
C(56)	32(4)	32(4)	33(4)	1(3)	21(3)	-6(3)
C(61)	16(3)	18(3)	16(3)	1(2)	5(2)	-4(2)
C(62)	24(4)	26(4)	33(4)	-1(3)	4(3)	5(3)
C(63)	42(4)	20(3)	37(4)	-15(3)	10(3)	-3(3)
C(64)	40(4)	28(4)	25(4)	-10(3)	7(3)	-12(3)
C(65)	27(4)	39(4)	44(4)	-19(3)	-1(3)	6(3)
C(66)	30(4)	29(4)	38(4)	-10(3)	10(3)	6(3)
C(71)	15(3)	19(3)	17(3)	2(2)	5(2)	4(3)
C(72)	16(3)	19(3)	23(3)	-2(3)	9(3)	0(2)
C(721)	20(3)	23(3)	26(3)	2(3)	5(3)	8(3)
C(722)	32(4)	35(4)	41(4)	-13(3)	14(3)	-3(3)
C(723)	41(4)	24(3)	51(4)	10(3)	17(3)	3(3)
C(74)	26(3)	40(4)	20(3)	-1(3)	-6(3)	-2(3)
C(75)	28(4)	32(4)	23(3)	-6(3)	2(3)	-4(3)
C(76)	24(3)	22(3)	12(3)	1(2)	7(3)	-2(3)
C(73)	30(4)	31(4)	22(3)	9(3)	4(3)	10(3)
C(761)	21(3)	20(3)	28(3)	-3(3)	2(3)	-1(3)
C(762)	41(4)	24(3)	43(4)	-1(3)	12(3)	-2(3)
C(763)	36(4)	27(3)	42(4)	7(3)	17(3)	-5(3)
C(81)	17(3)	12(3)	18(3)	-2(2)	8(2)	5(2)
C(101)	55(5)	80(6)	99(7)	-4(5)	37(5)	-12(4)
C(102)	24(4)	40(4)	69(5)	-4(4)	8(4)	-7(3)
C(103)	40(4)	57(6)	72(6)	-13(5)	-7(4)	14(4)
C(104)	47(5)	39(5)	102(7)	-1(5)	-22(5)	13(4)
C(105)	37(5)	51(6)	73(6)	16(4)	-9(4)	-7(4)
C(106)	29(4)	63(5)	47(5)	8(4)	8(3)	0(3)
C(107)	34(4)	33(4)	60(5)	-5(4)	5(4)	-1(3)
C(201)	61(6)	85(6)	79(6)	26(5)	19(5)	11(5)
C(202)	36(4)	46(4)	57(5)	11(4)	16(4)	5(3)
C(203)	66(5)	54(5)	65(6)	-6(4)	39(5)	-1(4)
C(204)	95(6)	53(5)	51(5)	1(4)	25(4)	-12(5)
C(205)	68(6)	39(5)	58(6)	16(4)	-1(4)	6(4)
C(206)	56(5)	54(5)	63(6)	-5(4)	15(4)	16(4)
C(207)	55(5)	65(5)	42(4)	-6(4)	12(4)	9(4)

Table 6. Hydrogen coordinates (x 10^4) and isotropic displacement parameters (Å^{2}x 10^3) for SKF 1.

	x	y	z	U(eq)
H(3A)	7893(25)	4427(9)	11270(9)	30
H(4A)	8601(11)	5951(44)	11692(2)	40
H(5A)	9756(16)	5637(38)	12127(10)	49
H(6A)	10256(26)	3770(9)	12145(10)	38
H(8A)	10134(26)	1624(8)	11854(8)	33
H(10A)	10033(27)	-592(8)	11655(8)	43
H(11A)	9276(11)	-2234(45)	11324(3)	46
H(12A)	8098(16)	-1932(37)	10972(7)	42
H(13A)	7588(25)	-67(7)	10873(9)	33
H(23A)	5504(22)	2647(6)	10536(6)	24
H(24A)	6122(12)	2473(5)	11446(12)	29
H(25A)	7307(11)	2230(6)	11738(18)	28
H(32A)	7043(7)	81(29)	8714(13)	25
H(33A)	6743(3)	-568(43)	7813(5)	33
H(34A)	6407(7)	933(14)	7131(20)	39
H(35A)	6370(7)	2987(31)	7352(14)	33
H(36A)	6679(2)	3559(42)	8246(5)	25
H(42A)	9398(11)	1192(30)	9170(9)	29
H(43A)	9866(22)	-781(12)	9361(5)	33
H(44A)	9306(9)	-2257(42)	9746(4)	34
H(45A)	8352(11)	-1684(30)	9999(9)	33
H(46A)	7839(19)	284(11)	9852(5)	26
H(52A)	8188(9)	1304(42)	8326(2)	32
H(53A)	8471(3)	1871(31)	7586(15)	39
H(54A)	8827(7)	3820(15)	7484(18)	47
H(55A)	8926(9)	5182(46)	8187(3)	48
H(56A)	8676(4)	4645(29)	8988(15)	33
H(62A)	7952(25)	4687(10)	9729(11)	32
H(63A)	8566(12)	6036(41)	10307(3)	37
H(64A)	9672(14)	5724(31)	10816(13)	35
H(65A)	10179(25)	3860(11)	10734(12)	43
H(66A)	9525(11)	2498(41)	10103(3)	36
H(72A)	6218(23)	4609(11)	9045(11)	26
H(72B)	5329(13)	4861(12)	9441(7)	39
H(72C)	4871(5)	5580(25)	8939(3)	39
H(72D)	5559(9)	6153(14)	9306(10)	39
H(72E)	5970(15)	5369(7)	8119(7)	42
H(72F)	6110(12)	6393(15)	8558(3)	42
H(72G)	5354(4)	6111(20)	8202(9)	42
H(74A)	4134(18)	2656(5)	7501(16)	34
H(75A)	4476(12)	787(38)	7924(8)	32
H(73A)	4698(8)	4362(40)	7914(9)	32
H(76A)	5933(23)	289(5)	9076(11)	27
H(76B)	5609(13)	-673(12)	8215(8)	40
H(76C)	4895(3)	-993(18)	8289(9)	40
H(76D)	5571(14)	-1556(8)	8678(3)	40
H(76E)	5082(12)	671(14)	9492(8)	37
H(76F)	5170(11)	-735(15)	9438(9)	37
H(76G)	4540(3)	-61(27)	9040(2)	37
H(81A)	5464(22)	2749(8)	9653(3)	17
H(10B)	3553(21)	4926(10)	8962(6)	82

H(10C)	3037(8)	4058(31)	8554(7)	82
H(10D)	3829(14)	3778(24)	8736(11)	82
H(10E)	3764(12)	1819(22)	9111(17)	68
H(10F)	3643(11)	710(58)	9806(4)	80
H(10G)	3193(5)	1396(31)	10467(18)	65
H(10H)	2840(12)	3438(21)	10359(15)	52
H(10I)	2968(9)	4603(48)	9667(3)	49
H(20A)	2532(10)	316(27)	8078(11)	83
H(20B)	3260(10)	787(15)	8086(11)	83
H(20C)	2887(19)	-214(14)	7671(3)	83
H(20D)	2791(17)	856(40)	6849(7)	63
H(20E)	2272(5)	2308(7)	6200(22)	73
H(20F)	1667(14)	3821(40)	6495(16)	66
H(20G)	1501(17)	3972(39)	7350(7)	64
H(20H)	2086(4)	2419(7)	7933(20)	60

Appendix B

X-Ray Diffraction Analysis of

$(^{\mathrm{Anthr,H}}\mathrm{Sal})\mathrm{Pd}(\mathrm{PPh}_3)\mathrm{Ph}$

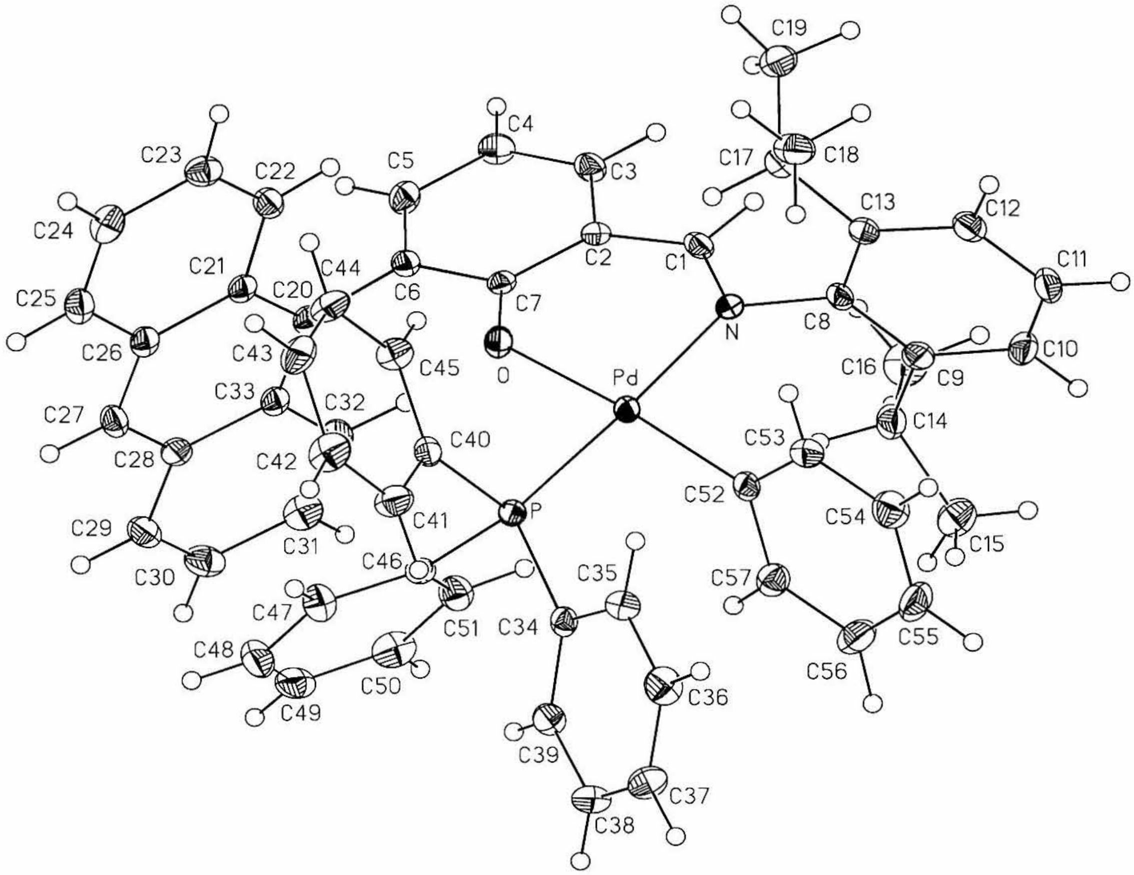

Table 1. Crystal data and structure refinement for TRY5 (CCDC 161496).

Empirical formula	$C_{51}H_{44}NOPPd \cdot C_6H_6$	
Formula weight	902.35	
Crystallization Solvent	Benzene/pentane	
Crystal Habit	Square prism	
Crystal size	148.00 x 0.39 x 0.15 mm^3	
Crystal color	Yellow	

Data Collection

Preliminary Photos	Rotation	
Type of diffractometer	CCD area detector	
Wavelength	0.71073 Å MoKα	
Data Collection Temperature	98(2) K	
θ range for 26106 reflections used in lattice determination	2.25 to 28.18°	
Unit cell dimensions	a = 9.5473(5) Å	α= 73.9060(10)°
	b = 13.2077(7) Å	β= 87.2070(10)°
	c = 20.2788(10) Å	γ = 89.7660(10)°
Volume	2453.9(2) Å^3	
Z	2	
Crystal system	Triclinic	
Space group	P-1	
Density (calculated)	1.221 Mg/m^3	
F(000)	936	
Data collection program	Bruker SMART	
θ range for data collection	1.60 to 28.26°	
Completeness to θ = 28.26°	91.4 %	
Index ranges	-12 h 12, -17 k 16, -26 l 26	
Data collection scan type	ω scans at 6 ϕ settings	
Data reduction program	Bruker SAINT v6.2	
Reflections collected	42656	
Independent reflections	11102 [R_{int}= 0.0420]	
Absorption coefficient	0.449 mm^{-1}	
Absorption correction	None	
Max. and min. transmission (calculated)	0.9353 and 0.0096	

Table 1 (cont.)

Structure Solution and Refinement

Structure solution program	SHELXS-97 (Sheldrick, 1990)
Primary solution method	Patterson method
Secondary solution method	Difference Fourier map
Hydrogen placement	Difference Fourier map
Structure refinement program	SHELXL-97 (Sheldrick, 1997)
Refinement method	Full matrix least-squares on F^2
Data / restraints / parameters	11102 / 0 / 828
Treatment of hydrogen atoms	Unrestrained
Goodness-of-fit on F^2	1.811
Final R indices [$I>2\sigma(I)$, 9752 reflections]	R1 = 0.0301, *w*R2 = 0.0622
R indices (all data)	R1 = 0.0356, *w*R2 = 0.0629
Type of weighting scheme used	Sigma
Weighting scheme used	$w=1/\sigma^2(Fo^2)$
Max shift/error	0.002
Average shift/error	0.000
Largest diff. peak and hole	0.784 and -0.415 e.Å^{-3}

Special Refinement Details

One molecule of benzene is included in the asymmetric unit as solvent of crystallization.

Refinement of F^2 against ALL reflections. The weighted R-factor (*w*R) and goodness of fit (S) are based on F^2, conventional R-factors (R) are based on F, with F set to zero for negative F^2. The threshold expression of $F^2 > 2\sigma(F^2)$ is used only for calculating R-factors(gt) etc. and is not relevant to the choice of reflections for refinement. R-factors based on F^2 are statistically about twice as large as those based on F, and R-factors based on ALL data will be even larger.

All esds (except the esd in the dihedral angle between two l.s. planes) are estimated using the full covariance matrix. The cell esds are taken into account individually in the estimation of esds in distances, angles and torsion angles; correlations between esds in cell parameters are only used when they are defined by crystal symmetry. An approximate (isotropic) treatment of cell esds is used for estimating esds involving l.s. planes.

Table 2. Atomic coordinates (x 10^4) and equivalent isotropic displacement parameters (Å^{2}x 10^3) for TRY5 (CCDC 161496). U(eq) is defined as the trace of the orthogonalized U^{ij} tensor.

	x	y	z	U_{eq}
Pd	3554(1)	2815(1)	3235(1)	13(1)
P	5017(1)	3662(1)	2344(1)	13(1)
O	3680(1)	1481(1)	2877(1)	16(1)
N	2277(1)	1972(1)	4079(1)	12(1)
C(1)	1775(2)	1047(2)	4129(1)	15(1)
C(2)	1929(2)	412(1)	3658(1)	14(1)
C(3)	1104(2)	-526(2)	3822(1)	17(1)
C(4)	1173(2)	-1204(2)	3420(1)	20(1)
C(5)	2068(2)	-957(2)	2829(1)	19(1)
C(6)	2885(2)	-54(1)	2642(1)	14(1)
C(7)	2861(2)	660(1)	3059(1)	13(1)
C(8)	1973(2)	2386(1)	4661(1)	14(1)
C(9)	786(2)	3014(1)	4661(1)	17(1)
C(10)	565(2)	3447(2)	5211(1)	20(1)
C(11)	1483(2)	3265(2)	5736(1)	21(1)
C(12)	2638(2)	2633(2)	5727(1)	19(1)
C(13)	2907(2)	2179(1)	5190(1)	16(1)
C(14)	-248(2)	3181(2)	4098(1)	21(1)
C(15)	-913(2)	4269(2)	3930(1)	29(1)
C(16)	-1392(2)	2331(2)	4295(1)	30(1)
C(17)	4151(2)	1459(2)	5202(1)	19(1)
C(18)	5441(2)	1815(2)	5497(1)	24(1)
C(19)	3747(2)	324(2)	5602(1)	23(1)
C(20)	3725(2)	212(1)	1973(1)	14(1)
C(21)	5177(2)	17(1)	1951(1)	15(1)
C(22)	5914(2)	-429(1)	2554(1)	17(1)
C(23)	7303(2)	-651(2)	2521(1)	20(1)
C(24)	8058(2)	-430(2)	1878(1)	21(1)
C(25)	7403(2)	-3(2)	1290(1)	19(1)
C(26)	5943(2)	236(1)	1296(1)	16(1)
C(27)	5237(2)	620(2)	697(1)	18(1)
C(28)	3801(2)	805(1)	709(1)	16(1)
C(29)	3061(2)	1172(2)	94(1)	20(1)
C(30)	1663(2)	1342(2)	111(1)	23(1)
C(31)	909(2)	1176(2)	753(1)	23(1)
C(32)	1563(2)	825(2)	1351(1)	19(1)
C(33)	3029(2)	609(1)	1360(1)	15(1)
C(34)	5269(2)	5084(1)	2162(1)	15(1)
C(35)	5973(2)	5482(2)	2627(1)	18(1)
C(36)	6168(2)	6551(2)	2506(1)	24(1)
C(37)	5655(2)	7242(2)	1928(1)	26(1)
C(38)	4938(2)	6862(2)	1471(1)	23(1)
C(39)	4745(2)	5783(2)	1586(1)	19(1)
C(40)	6808(2)	3165(1)	2391(1)	15(1)
C(41)	7958(2)	3828(2)	2130(1)	23(1)
C(42)	9306(2)	3427(2)	2174(1)	27(1)
C(43)	9526(2)	2367(2)	2474(1)	23(1)

C(44)	8389(2)	1706(2)	2719(1)	24(1)
C(45)	7037(2)	2095(2)	2684(1)	19(1)
C(46)	4432(2)	3525(1)	1532(1)	15(1)
C(47)	5362(2)	3570(2)	972(1)	22(1)
C(48)	4851(2)	3605(2)	339(1)	27(1)
C(49)	3432(2)	3595(2)	256(1)	26(1)
C(50)	2503(2)	3523(2)	810(1)	26(1)
C(51)	3001(2)	3481(2)	1447(1)	21(1)
C(52)	3338(2)	4166(1)	3488(1)	15(1)
C(53)	3992(2)	4384(2)	4030(1)	20(1)
C(54)	3793(2)	5334(2)	4188(1)	26(1)
C(55)	2933(2)	6095(2)	3804(1)	27(1)
C(56)	2276(2)	5898(2)	3261(1)	25(1)
C(57)	2473(2)	4948(2)	3104(1)	19(1)
C(61)	8420(3)	2050(2)	9156(2)	58(1)
C(62)	8187(3)	2540(2)	9674(2)	47(1)
C(63)	8832(3)	3458(2)	9645(2)	48(1)
C(64)	9750(3)	3913(2)	9095(2)	56(1)
C(65)	10001(3)	3455(2)	8572(2)	55(1)
C(66)	9335(3)	2532(2)	8588(2)	55(1)

Table 3. Selected bond lengths [Å] and angles [°] for TRY5 (CCDC 161496).

Pd-C(52)	1.9956(17)	C(52)-Pd-O	174.04(6)
Pd-O	2.0843(11)	C(52)-Pd-N	93.06(6)
Pd-N	2.0991(14)	O-Pd-N	89.74(5)
Pd-P	2.2613(5)	C(52)-Pd-P	88.64(5)
		O-Pd-P	88.79(3)
		N-Pd-P	177.11(4)

Table 4. Bond lengths [Å] and angles [°] for TRY5 (CCDC 161496).

Pd-C(52)	1.9956(17)	C(3)-C(4)	1.367(3)
Pd-O	2.0843(11)	C(3)-H(3)	0.999(17)
Pd-N	2.0991(14)	C(4)-C(5)	1.400(3)
Pd-P	2.2613(5)	C(4)-H(4)	0.90(2)
P-C(46)	1.8185(17)	C(5)-C(6)	1.379(2)
P-C(40)	1.8263(18)	C(5)-H(5)	0.887(18)
P-C(34)	1.8264(18)	C(6)-C(7)	1.429(2)
O-C(7)	1.297(2)	C(6)-C(20)	1.497(2)
N-C(1)	1.290(2)	C(8)-C(13)	1.397(2)
N-C(8)	1.448(2)	C(8)-C(9)	1.402(2)
C(1)-C(2)	1.438(2)	C(9)-C(10)	1.395(2)
C(1)-H(1)	0.970(17)	C(9)-C(14)	1.515(3)
C(2)-C(3)	1.421(2)	C(10)-C(11)	1.380(3)
C(2)-C(7)	1.432(2)	C(10)-H(10)	0.98(2)

C(11)-C(12)	1.382(3)	C(37)-C(38)	1.380(3)
C(11)-H(11)	0.949(18)	C(37)-H(37)	0.91(2)
C(12)-C(13)	1.396(2)	C(38)-C(39)	1.390(3)
C(12)-H(12)	0.917(19)	C(38)-H(38)	0.90(2)
C(13)-C(17)	1.516(3)	C(39)-H(39)	0.886(17)
C(14)-C(15)	1.525(3)	C(40)-C(45)	1.394(3)
C(14)-C(16)	1.527(3)	C(40)-C(41)	1.395(2)
C(14)-H(14)	0.940(17)	C(41)-C(42)	1.387(3)
C(15)-H(15A)	0.92(2)	C(41)-H(41)	0.982(18)
C(15)-H(15B)	0.98(2)	C(42)-C(43)	1.383(3)
C(15)-H(15C)	1.00(2)	C(42)-H(42)	0.98(2)
C(16)-H(16A)	1.00(2)	C(43)-C(44)	1.379(3)
C(16)-H(16B)	0.96(2)	C(43)-H(43)	0.93(2)
C(16)-H(16C)	0.94(2)	C(44)-C(45)	1.385(3)
C(17)-C(18)	1.526(3)	C(44)-H(44)	0.899(19)
C(17)-C(19)	1.534(3)	C(45)-H(45)	0.891(19)
C(17)-H(17)	0.961(17)	C(46)-C(51)	1.389(3)
C(18)-H(18A)	0.99(2)	C(46)-C(47)	1.396(2)
C(18)-H(18B)	0.98(2)	C(47)-C(48)	1.384(3)
C(18)-H(18C)	0.93(2)	C(47)-H(47)	0.929(18)
C(19)-H(19A)	0.98(2)	C(48)-C(49)	1.374(3)
C(19)-H(19B)	0.96(2)	C(48)-H(48)	0.93(2)
C(19)-H(19C)	0.985(19)	C(49)-C(50)	1.379(3)
C(20)-C(33)	1.407(2)	C(49)-H(49)	0.89(2)
C(20)-C(21)	1.410(2)	C(50)-C(51)	1.385(3)
C(21)-C(22)	1.422(2)	C(50)-H(50)	0.980(19)
C(21)-C(26)	1.440(2)	C(51)-H(51)	0.956(19)
C(22)-C(23)	1.359(3)	C(52)-C(53)	1.389(2)
C(22)-H(22)	0.927(18)	C(52)-C(57)	1.402(3)
C(23)-C(24)	1.416(3)	C(53)-C(54)	1.389(3)
C(23)-H(23)	0.931(18)	C(53)-H(53)	0.93(2)
C(24)-C(25)	1.353(3)	C(54)-C(55)	1.383(3)
C(24)-H(24)	0.898(18)	C(54)-H(54)	0.899(19)
C(25)-C(26)	1.428(3)	C(55)-C(56)	1.380(3)
C(25)-H(25)	0.935(18)	C(55)-H(55)	0.95(2)
C(26)-C(27)	1.387(2)	C(56)-C(57)	1.387(3)
C(27)-C(28)	1.392(3)	C(56)-H(56)	1.00(2)
C(27)-H(27)	0.936(17)	C(57)-H(57)	0.919(18)
C(28)-C(29)	1.428(2)	C(61)-C(62)	1.387(4)
C(28)-C(33)	1.439(2)	C(61)-C(66)	1.412(4)
C(29)-C(30)	1.353(3)	C(61)-H(61)	1.04(3)
C(29)-H(29)	0.935(19)	C(62)-C(63)	1.348(4)
C(30)-C(31)	1.419(3)	C(62)-H(62)	0.99(3)
C(30)-H(30)	0.922(18)	C(63)-C(64)	1.381(4)
C(31)-C(32)	1.353(3)	C(63)-H(63)	1.13(2)
C(31)-H(31)	0.926(18)	C(64)-C(65)	1.372(4)
C(32)-C(33)	1.427(2)	C(64)-H(64)	0.96(3)
C(32)-H(32)	0.986(18)	C(65)-C(66)	1.369(4)
C(34)-C(39)	1.385(2)	C(65)-H(65)	1.08(4)
C(34)-C(35)	1.399(2)	C(66)-H(66)	0.89(3)
C(35)-C(36)	1.376(3)		
C(35)-H(35)	0.911(18)	C(52)-Pd-O	174.04(6)
C(36)-C(37)	1.380(3)	C(52)-Pd-N	93.06(6)
C(36)-H(36)	0.914(19)	O-Pd-N	89.74(5)

C(52)-Pd-P	88.64(5)
O-Pd-P	88.79(3)
N-Pd-P	177.11(4)
C(46)-P-C(40)	104.61(8)
C(46)-P-C(34)	102.49(8)
C(40)-P-C(34)	103.09(8)
C(46)-P-Pd	111.51(6)
C(40)-P-Pd	114.31(6)
C(34)-P-Pd	119.19(6)
C(7)-O-Pd	126.85(11)
C(1)-N-C(8)	116.08(15)
C(1)-N-Pd	122.88(12)
C(8)-N-Pd	120.96(11)
N-C(1)-C(2)	129.54(17)
N-C(1)-H(1)	115.7(10)
C(2)-C(1)-H(1)	114.7(10)
C(3)-C(2)-C(7)	119.65(15)
C(3)-C(2)-C(1)	116.06(16)
C(7)-C(2)-C(1)	124.28(16)
C(4)-C(3)-C(2)	121.68(17)
C(4)-C(3)-H(3)	119.2(10)
C(2)-C(3)-H(3)	119.1(10)
C(3)-C(4)-C(5)	118.78(17)
C(3)-C(4)-H(4)	118.8(13)
C(5)-C(4)-H(4)	122.4(13)
C(6)-C(5)-C(4)	122.06(17)
C(6)-C(5)-H(5)	120.0(12)
C(4)-C(5)-H(5)	118.0(12)
C(5)-C(6)-C(7)	120.52(16)
C(5)-C(6)-C(20)	119.36(15)
C(7)-C(6)-C(20)	119.99(15)
O-C(7)-C(6)	118.53(15)
O-C(7)-C(2)	124.19(15)
C(6)-C(7)-C(2)	117.28(15)
C(13)-C(8)-C(9)	122.23(16)
C(13)-C(8)-N	118.68(15)
C(9)-C(8)-N	119.03(15)
C(10)-C(9)-C(8)	117.63(17)
C(10)-C(9)-C(14)	121.22(17)
C(8)-C(9)-C(14)	121.11(16)
C(11)-C(10)-C(9)	121.15(18)
C(11)-C(10)-H(10)	121.9(11)
C(9)-C(10)-H(10)	116.9(11)
C(10)-C(11)-C(12)	120.15(17)
C(10)-C(11)-H(11)	118.5(11)
C(12)-C(11)-H(11)	121.4(11)
C(11)-C(12)-C(13)	121.02(18)
C(11)-C(12)-H(12)	117.6(12)
C(13)-C(12)-H(12)	121.3(12)
C(12)-C(13)-C(8)	117.81(17)
C(12)-C(13)-C(17)	120.25(16)
C(8)-C(13)-C(17)	121.90(15)
C(9)-C(14)-C(15)	113.03(17)
C(9)-C(14)-C(16)	110.21(17)
C(15)-C(14)-C(16)	109.79(18)
C(9)-C(14)-H(14)	110.5(11)
C(15)-C(14)-H(14)	106.1(11)
C(16)-C(14)-H(14)	107.1(11)
C(14)-C(15)-H(15A)	116.2(13)
C(14)-C(15)-H(15B)	109.4(12)
H(15A)-C(15)-H(15B)	105.8(17)
C(14)-C(15)-H(15C)	114.0(12)
H(15A)-C(15)-H(15C)	105.3(18)
H(15B)-C(15)-H(15C)	105.2(17)
C(14)-C(16)-H(16A)	107.9(11)
C(14)-C(16)-H(16B)	113.4(13)
H(16A)-C(16)-H(16B)	106.0(18)
C(14)-C(16)-H(16C)	111.2(13)
H(16A)-C(16)-H(16C)	113.1(17)
H(16B)-C(16)-H(16C)	105.3(18)
C(13)-C(17)-C(18)	113.16(16)
C(13)-C(17)-C(19)	110.22(16)
C(18)-C(17)-C(19)	110.20(16)
C(13)-C(17)-H(17)	106.8(10)
C(18)-C(17)-H(17)	106.5(10)
C(19)-C(17)-H(17)	109.9(10)
C(17)-C(18)-H(18A)	113.6(11)
C(17)-C(18)-H(18B)	111.4(11)
H(18A)-C(18)-H(18B)	107.3(16)
C(17)-C(18)-H(18C)	111.3(12)
H(18A)-C(18)-H(18C)	103.6(17)
H(18B)-C(18)-H(18C)	109.3(17)
C(17)-C(19)-H(19A)	110.9(11)
C(17)-C(19)-H(19B)	112.8(12)
H(19A)-C(19)-H(19B)	106.3(16)
C(17)-C(19)-H(19C)	112.0(11)
H(19A)-C(19)-H(19C)	106.9(15)
H(19B)-C(19)-H(19C)	107.5(16)
C(33)-C(20)-C(21)	120.16(16)
C(33)-C(20)-C(6)	118.86(15)
C(21)-C(20)-C(6)	120.90(15)
C(20)-C(21)-C(22)	122.20(16)
C(20)-C(21)-C(26)	119.52(16)
C(22)-C(21)-C(26)	118.24(16)
C(23)-C(22)-C(21)	121.42(17)
C(23)-C(22)-H(22)	120.2(11)
C(21)-C(22)-H(22)	118.3(11)
C(22)-C(23)-C(24)	120.34(18)
C(22)-C(23)-H(23)	121.3(11)
C(24)-C(23)-H(23)	118.4(11)
C(25)-C(24)-C(23)	120.40(18)
C(25)-C(24)-H(24)	122.2(12)
C(23)-C(24)-H(24)	117.4(12)
C(24)-C(25)-C(26)	121.42(18)
C(24)-C(25)-H(25)	121.8(11)
C(26)-C(25)-H(25)	116.8(11)
C(27)-C(26)-C(25)	122.23(17)
C(27)-C(26)-C(21)	119.53(16)

C(25)-C(26)-C(21)	118.17(16)	C(45)-C(44)-H(44)	119.7(12)
C(26)-C(27)-C(28)	121.71(17)	C(44)-C(45)-C(40)	120.13(18)
C(26)-C(27)-H(27)	119.3(10)	C(44)-C(45)-H(45)	119.7(12)
C(28)-C(27)-H(27)	119.0(10)	C(40)-C(45)-H(45)	120.1(12)
C(27)-C(28)-C(29)	122.03(17)	C(51)-C(46)-C(47)	118.91(17)
C(27)-C(28)-C(33)	119.32(16)	C(51)-C(46)-P	118.57(14)
C(29)-C(28)-C(33)	118.65(16)	C(47)-C(46)-P	122.20(14)
C(30)-C(29)-C(28)	121.58(18)	C(48)-C(47)-C(46)	119.95(19)
C(30)-C(29)-H(29)	121.3(11)	C(48)-C(47)-H(47)	120.0(11)
C(28)-C(29)-H(29)	117.1(11)	C(46)-C(47)-H(47)	120.0(11)
C(29)-C(30)-C(31)	119.70(18)	C(49)-C(48)-C(47)	120.6(2)
C(29)-C(30)-H(30)	120.9(11)	C(49)-C(48)-H(48)	121.3(12)
C(31)-C(30)-H(30)	119.4(11)	C(47)-C(48)-H(48)	118.1(12)
C(32)-C(31)-C(30)	120.93(19)	C(48)-C(49)-C(50)	120.02(19)
C(32)-C(31)-H(31)	120.2(11)	C(48)-C(49)-H(49)	120.3(13)
C(30)-C(31)-H(31)	118.9(11)	C(50)-C(49)-H(49)	119.6(13)
C(31)-C(32)-C(33)	121.50(18)	C(49)-C(50)-C(51)	119.96(19)
C(31)-C(32)-H(32)	120.9(11)	C(49)-C(50)-H(50)	119.0(11)
C(33)-C(32)-H(32)	117.6(11)	C(51)-C(50)-H(50)	121.0(11)
C(20)-C(33)-C(32)	122.65(16)	C(50)-C(51)-C(46)	120.55(18)
C(20)-C(33)-C(28)	119.75(16)	C(50)-C(51)-H(51)	122.0(11)
C(32)-C(33)-C(28)	117.60(16)	C(46)-C(51)-H(51)	117.4(11)
C(39)-C(34)-C(35)	119.03(17)	C(53)-C(52)-C(57)	117.13(17)
C(39)-C(34)-P	121.84(13)	C(53)-C(52)-Pd	123.85(15)
C(35)-C(34)-P	119.11(14)	C(57)-C(52)-Pd	119.02(13)
C(36)-C(35)-C(34)	120.34(19)	C(54)-C(53)-C(52)	121.5(2)
C(36)-C(35)-H(35)	120.5(11)	C(54)-C(53)-H(53)	119.7(12)
C(34)-C(35)-H(35)	119.1(11)	C(52)-C(53)-H(53)	118.7(12)
C(35)-C(36)-C(37)	120.36(18)	C(55)-C(54)-C(53)	120.53(19)
C(35)-C(36)-H(36)	116.8(13)	C(55)-C(54)-H(54)	119.0(13)
C(37)-C(36)-H(36)	122.8(13)	C(53)-C(54)-H(54)	120.4(13)
C(38)-C(37)-C(36)	119.91(19)	C(56)-C(55)-C(54)	119.07(19)
C(38)-C(37)-H(37)	118.0(13)	C(56)-C(55)-H(55)	118.4(12)
C(36)-C(37)-H(37)	122.0(13)	C(54)-C(55)-H(55)	122.5(12)
C(37)-C(38)-C(39)	120.2(2)	C(55)-C(56)-C(57)	120.4(2)
C(37)-C(38)-H(38)	121.4(13)	C(55)-C(56)-H(56)	120.5(11)
C(39)-C(38)-H(38)	118.4(13)	C(57)-C(56)-H(56)	119.1(11)
C(34)-C(39)-C(38)	120.18(18)	C(56)-C(57)-C(52)	121.43(18)
C(34)-C(39)-H(39)	121.1(12)	C(56)-C(57)-H(57)	119.1(12)
C(38)-C(39)-H(39)	118.7(12)	C(52)-C(57)-H(57)	119.5(12)
C(45)-C(40)-C(41)	118.89(17)	C(62)-C(61)-C(66)	119.2(3)
C(45)-C(40)-P	119.46(14)	C(62)-C(61)-H(61)	119.2(15)
C(41)-C(40)-P	121.65(14)	C(66)-C(61)-H(61)	121.5(15)
C(42)-C(41)-C(40)	120.28(19)	C(63)-C(62)-C(61)	120.8(3)
C(42)-C(41)-H(41)	121.0(11)	C(63)-C(62)-H(62)	120.7(15)
C(40)-C(41)-H(41)	118.7(11)	C(61)-C(62)-H(62)	118.3(15)
C(43)-C(42)-C(41)	120.46(19)	C(62)-C(63)-C(64)	119.7(3)
C(43)-C(42)-H(42)	122.0(12)	C(62)-C(63)-H(63)	118.5(11)
C(41)-C(42)-H(42)	117.6(12)	C(64)-C(63)-H(63)	121.4(11)
C(44)-C(43)-C(42)	119.40(19)	C(65)-C(64)-C(63)	121.1(3)
C(44)-C(43)-H(43)	120.8(12)	C(65)-C(64)-H(64)	127(2)
C(42)-C(43)-H(43)	119.8(12)	C(63)-C(64)-H(64)	112(2)
C(43)-C(44)-C(45)	120.8(2)	C(66)-C(65)-C(64)	120.0(3)
C(43)-C(44)-H(44)	119.4(12)	C(66)-C(65)-H(65)	108.2(19)

C(64)-C(65)-H(65)	131.8(19)	C(65)-C(66)-H(66)	115.7(18)
C(65)-C(66)-C(61)	119.1(3)	C(61)-C(66)-H(66)	125.2(18)

Table 5. Anisotropic displacement parameters ($Å^2 x\ 10^4$) for TRY5 (CCDC 161496). The anisotropic displacement factor exponent takes the form: $-2\pi^2$ [$h^2 a^{*2}U^{11}$ + ... + 2 h k a* b* U^{12}]

	U^{11}	U^{22}	U^{33}	U^{23}	U^{13}	U^{12}
Pd	147(1)	113(1)	122(1)	-34(1)	21(1)	-6(1)
P	133(2)	120(2)	132(2)	-31(2)	8(2)	-6(2)
O	176(7)	135(7)	179(6)	-60(5)	46(5)	-29(5)
N	133(8)	111(8)	125(7)	-27(6)	-7(6)	19(6)
C(1)	131(9)	182(10)	115(9)	-1(8)	17(7)	13(8)
C(2)	153(9)	110(9)	128(9)	-9(7)	-9(7)	12(7)
C(3)	154(10)	184(10)	154(9)	-13(8)	28(8)	-4(8)
C(4)	216(10)	129(10)	229(10)	-31(8)	27(8)	-65(8)
C(5)	226(10)	153(10)	197(10)	-83(8)	1(8)	-10(8)
C(6)	138(9)	147(10)	134(9)	-28(8)	-7(7)	16(7)
C(7)	125(9)	116(9)	133(9)	-15(7)	-15(7)	29(7)
C(8)	183(9)	116(9)	120(9)	-22(7)	51(7)	-34(7)
C(9)	164(10)	145(10)	171(9)	-11(8)	38(7)	-21(8)
C(10)	192(10)	181(11)	227(10)	-58(9)	59(8)	26(8)
C(11)	299(11)	199(11)	155(10)	-80(9)	56(8)	-16(9)
C(12)	241(11)	178(11)	140(9)	-35(8)	-9(8)	-19(8)
C(13)	182(10)	121(10)	148(9)	-8(8)	44(7)	-27(8)
C(14)	182(10)	252(11)	188(10)	-76(9)	13(8)	48(8)
C(15)	252(12)	322(14)	305(13)	-80(11)	-19(10)	111(10)
C(16)	219(12)	361(15)	342(13)	-122(11)	-48(10)	2(10)
C(17)	214(10)	199(11)	135(9)	-31(8)	6(8)	37(8)
C(18)	218(11)	233(12)	229(11)	3(10)	-13(9)	17(9)
C(19)	285(12)	189(11)	222(11)	-56(9)	-37(9)	38(9)
C(20)	176(9)	95(9)	160(9)	-56(8)	19(7)	-22(7)
C(21)	181(10)	92(9)	173(9)	-54(8)	12(7)	-19(7)
C(22)	211(10)	154(10)	153(9)	-47(8)	17(8)	-20(8)
C(23)	220(11)	160(10)	209(10)	-45(8)	-48(8)	-3(8)
C(24)	151(10)	211(11)	285(11)	-106(9)	0(8)	-7(8)
C(25)	191(10)	185(11)	207(10)	-83(9)	44(8)	-28(8)
C(26)	183(10)	118(10)	179(9)	-63(8)	26(7)	-35(7)
C(27)	207(10)	168(10)	156(9)	-61(8)	56(8)	-42(8)
C(28)	213(10)	112(10)	165(9)	-45(8)	1(8)	-22(8)
C(29)	256(11)	180(11)	150(10)	-37(8)	11(8)	-35(8)
C(30)	269(12)	217(11)	184(10)	-27(9)	-67(9)	-9(9)
C(31)	164(11)	230(11)	281(11)	-62(9)	-23(8)	0(9)
C(32)	191(10)	181(11)	196(10)	-65(8)	19(8)	-27(8)
C(33)	179(10)	111(9)	168(9)	-60(8)	9(7)	-22(7)
C(34)	140(9)	143(10)	158(9)	-48(8)	37(7)	-19(7)
C(35)	180(10)	176(11)	170(10)	-23(8)	-17(8)	-5(8)
C(36)	278(11)	229(12)	231(11)	-104(9)	-26(9)	-57(9)
C(37)	362(13)	119(11)	291(11)	-54(9)	21(9)	-33(9)
C(38)	278(11)	170(11)	200(10)	11(9)	-11(9)	15(9)

C(39)	202(10)	182(11)	173(10)	-53(8)	0(8)	-21(8)
C(40)	155(9)	174(10)	136(9)	-53(8)	8(7)	7(8)
C(41)	193(11)	180(11)	284(11)	-14(9)	28(8)	14(8)
C(42)	148(10)	253(12)	374(12)	-62(10)	36(9)	-15(9)
C(43)	164(11)	257(12)	300(11)	-116(9)	-39(9)	65(9)
C(44)	256(11)	148(11)	303(12)	-51(9)	-20(9)	42(9)
C(45)	165(10)	171(11)	233(10)	-48(9)	-11(8)	-23(8)
C(46)	200(10)	102(9)	150(9)	-33(7)	-6(7)	-13(7)
C(47)	213(11)	256(12)	207(10)	-81(9)	20(8)	-14(9)
C(48)	366(13)	271(12)	171(10)	-78(9)	35(9)	-4(10)
C(49)	429(14)	182(11)	165(10)	-54(9)	-91(9)	5(9)
C(50)	251(12)	227(12)	299(12)	-74(9)	-88(9)	-2(9)
C(51)	205(11)	223(11)	204(10)	-60(9)	11(8)	-17(8)
C(52)	166(10)	132(10)	152(9)	-35(8)	62(7)	-29(7)
C(53)	266(11)	157(11)	172(10)	-25(8)	12(8)	2(9)
C(54)	362(13)	223(12)	219(11)	-99(9)	-6(9)	-34(10)
C(55)	329(12)	175(11)	333(12)	-126(10)	58(10)	10(9)
C(56)	231(11)	187(11)	323(12)	-56(9)	11(9)	46(9)
C(57)	184(10)	181(11)	213(10)	-61(9)	10(8)	-4(8)
C(61)	367(16)	384(17)	980(30)	-123(17)	-292(17)	57(13)
C(62)	292(14)	395(16)	631(19)	2(15)	-38(13)	45(12)
C(63)	400(15)	392(16)	580(18)	-9(14)	1(13)	22(12)
C(64)	620(20)	396(17)	588(19)	-12(15)	47(15)	-38(15)
C(65)	700(20)	452(18)	471(17)	-56(14)	-39(15)	67(15)
C(66)	505(18)	580(20)	610(20)	-230(17)	-224(16)	215(16)

Table 6. Hydrogen coordinates (x 10^4) and isotropic displacement parameters ($Å^2$x 10^3) for TRY5 (CCDC 161496).

	x	y	z	U_{iso}
H(1)	1186(17)	737(13)	4538(9)	10(4)
H(3)	480(17)	-704(13)	4248(9)	9(4)
H(4)	640(20)	-1790(16)	3544(10)	25(5)
H(5)	2092(18)	-1397(14)	2569(9)	16(5)
H(10)	-290(20)	3866(15)	5214(10)	28(6)
H(11)	1287(18)	3566(14)	6104(9)	15(5)
H(12)	3220(19)	2525(15)	6086(10)	22(5)
H(14)	204(18)	3127(13)	3687(9)	12(5)
H(15A)	-1540(20)	4390(16)	4257(11)	31(6)
H(15B)	-1430(20)	4380(16)	3512(11)	30(6)
H(15C)	-220(20)	4866(17)	3829(10)	35(6)
H(16A)	-1800(20)	2320(15)	4760(11)	28(6)
H(16B)	-1040(20)	1631(19)	4335(11)	39(7)
H(16C)	-2070(20)	2443(16)	3959(10)	29(6)
H(17)	4406(17)	1492(13)	4732(9)	13(5)
H(18A)	5310(20)	1786(15)	5988(11)	26(5)
H(18B)	5716(19)	2542(16)	5247(10)	21(5)
H(18C)	6190(20)	1372(16)	5486(10)	30(6)
H(19A)	4570(20)	-132(15)	5663(9)	22(5)

H(19B)	3080(20)	11(16)	5370(10)	33(6)
H(19C)	3336(19)	280(14)	6064(10)	20(5)
H(22)	5415(18)	-592(14)	2975(9)	15(5)
H(23)	7773(19)	-972(14)	2916(9)	16(5)
H(24)	8977(19)	-576(14)	1881(9)	14(5)
H(25)	7881(18)	150(14)	860(9)	14(5)
H(27)	5732(17)	738(13)	272(9)	9(4)
H(29)	3587(19)	1306(14)	-323(10)	20(5)
H(30)	1194(18)	1575(14)	-289(9)	17(5)
H(31)	-41(19)	1318(14)	758(9)	15(5)
H(32)	1040(19)	711(14)	1797(10)	20(5)
H(35)	6279(18)	5025(14)	3016(9)	12(5)
H(36)	6650(20)	6768(15)	2822(10)	26(5)
H(37)	5740(20)	7951(17)	1845(10)	33(6)
H(38)	4590(20)	7298(16)	1094(10)	26(6)
H(39)	4274(18)	5555(14)	1289(9)	14(5)
H(41)	7795(18)	4584(15)	1934(9)	16(5)
H(42)	10090(20)	3926(16)	1997(10)	30(6)
H(43)	10430(20)	2104(15)	2493(10)	24(5)
H(44)	8531(19)	1015(16)	2911(10)	20(5)
H(45)	6317(19)	1662(15)	2860(9)	18(5)
H(47)	6322(19)	3601(14)	1020(9)	13(5)
H(48)	5490(20)	3652(15)	-26(10)	28(6)
H(49)	3110(20)	3596(15)	-148(10)	27(6)
H(50)	1490(20)	3535(15)	740(9)	23(5)
H(51)	2390(20)	3425(14)	1842(10)	21(5)
H(53)	4610(20)	3891(16)	4279(10)	26(6)
H(54)	4240(20)	5469(16)	4537(10)	28(6)
H(55)	2770(20)	6753(16)	3903(10)	32(6)
H(56)	1660(20)	6436(16)	2973(10)	25(5)
H(57)	2048(19)	4839(15)	2732(10)	20(5)
H(61)	7900(30)	1340(20)	9190(13)	66(8)
H(62)	7580(30)	2180(20)	10081(13)	62(8)
H(63)	8710(20)	3780(16)	10103(11)	32(6)
H(64)	10180(40)	4550(30)	9144(18)	112(13)a
H(65)	10660(40)	3690(30)	8104(18)	122(13)
H(66)	9520(30)	2280(20)	8226(13)	56(8)

Appendix C

X-Ray Diffraction Analysis of

$(^{Anthr,H}Sal)Ni(PCy_3)H$

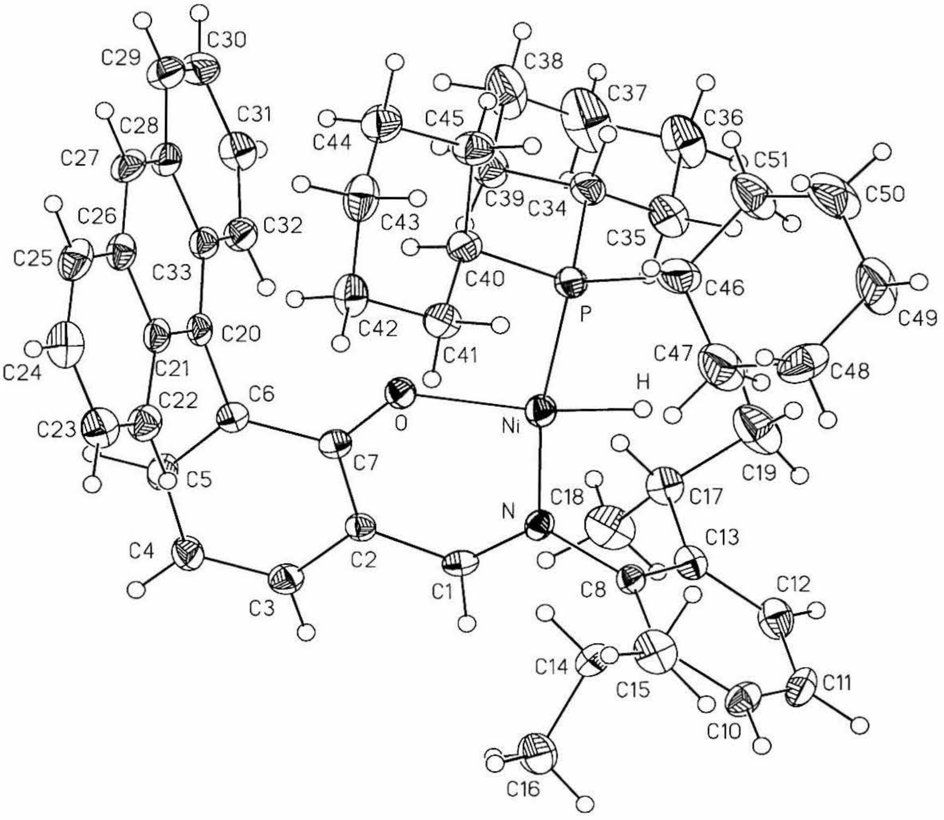

Table 1. Crystal data and structure refinement for TRY11 (CCDC 161167).

Empirical formula	$C_{51}H_{63}NOPNi \cdot 4(C_6H_6)$
Formula weight	1108.14
Crystallization Solvent	Benzene/acetonitrile
Crystal Habit	Column
Crystal size	0.31 x 0.19 x 0.19 mm^3
Crystal color	Orange

Data Collection

Preliminary Photos	Rotation	
Type of diffractometer	CCD area detector	
Wavelength	0.71073 Å MoKα	
Data Collection Temperature	98(2) K	
θ range for 27201 reflections used in lattice determination	2.19 to 26.44°	
Unit cell dimensions	a = 10.2643(6) Å b = 23.5700(13) Å c = 26.2323(15) Å	β= 99.6420(10)°
Volume	6256.7(6) Å^3	
Z	4	
Crystal system	Monoclinic	
Space group	$P2_1/n$	
Density (calculated)	1.176 Mg/m^3	
F(000)	2380	
Data collection program	Bruker SMART	
θ range for data collection	1.57 to 28.54°	
Completeness to θ = 28.54°	94.5 %	
Index ranges	-13 h 13, -31 k 30, -35 l 33	
Data collection scan type	ω scans at 7 ϕ settings	
Data reduction program	Bruker SAINT v6.2	
Reflections collected	127512	
Independent reflections	15058 [R_{int}= 0.0814]	
Absorption coefficient	0.380 mm^{-1}	
Absorption correction	None	
Max. and min. transmission (calculated)	0.9317 and 0.8897	

Table 1 (cont.)

Structure Solution and Refinement

Structure solution program	SHELXS-97 (Sheldrick, 1990)
Primary solution method	Patterson method
Secondary solution method	Difference Fourier map
Hydrogen placement	Difference Fourier map
Structure refinement program	SHELXL-97 (Sheldrick, 1997)
Refinement method	Full matrix least-squares on F^2
Data / restraints / parameters	15058 / 0 / 1060
Treatment of hydrogen atoms	Unrestrained
Goodness-of-fit on F^2	1.562
Final R indices [$I>2\sigma(I)$, 10020 reflections]	R1 = 0.0475, *w*R2 = 0.0664
R indices (all data)	R1 = 0.0795, *w*R2 = 0.0690
Type of weighting scheme used	Sigma
Weighting scheme used	$w=1/\sigma^2(Fo^2)$
Max shift/error	0.003
Average shift/error	0.000
Largest diff. peak and hole	1.030 and -0.590 e.Å^{-3}

Special Refinement Details

The asymmetric unit contains four benzene molecules. One of these appears as two half molecules on two inequivalent centers of symmetry. The benzene designated as C(91)-C(93) sits at the center located at ½, ½, ½ or 0,0,0 and the benzene designated by C(94)-C(96) sits at the center located at 0, ½, ½ or ½, 0, 0.

Refinement of F^2 against ALL reflections. The weighted R-factor (*w*R) and goodness of fit (S) are based on F^2, conventional R-factors (R) are based on F, with F set to zero for negative F^2. The threshold expression of $F^2 > 2\sigma(F^2)$ is used only for calculating R-factors(gt) etc. and is not relevant to the choice of reflections for refinement. R-factors based on F^2 are statistically about twice as large as those based on F, and R-factors based on ALL data will be even larger.

All esds (except the esd in the dihedral angle between two l.s. planes) are estimated using the full covariance matrix. The cell esds are taken into account individually in the estimation of esds in distances, angles and torsion angles; correlations between esds in cell parameters are only used when they are defined by crystal symmetry. An approximate (isotropic) treatment of cell esds is used for estimating esds involving l.s. planes.

Table 2. Atomic coordinates (x 10^4) and equivalent isotropic displacement parameters (Å^{2}x 10^3) for TRY11 (CCDC 161167). U(eq) is defined as the trace of the orthogonalized U^{ij} tensor.

	x	y	z	U_{eq}
Ni	6869(1)	4930(1)	8001(1)	21(1)
P	6542(1)	5048(1)	7183(1)	21(1)
O	6793(1)	5715(1)	8157(1)	21(1)
N	7085(1)	4688(1)	8696(1)	17(1)
C(1)	7069(2)	5019(1)	9088(1)	18(1)
C(2)	6898(2)	5621(1)	9074(1)	17(1)
C(3)	6889(2)	5897(1)	9548(1)	22(1)
C(4)	6778(2)	6472(1)	9582(1)	25(1)
C(5)	6662(2)	6788(1)	9126(1)	25(1)
C(6)	6652(2)	6541(1)	8649(1)	18(1)
C(7)	6783(2)	5942(1)	8607(1)	18(1)
C(8)	7337(2)	4093(1)	8825(1)	18(1)
C(9)	8641(2)	3902(1)	8910(1)	20(1)
C(10)	8862(2)	3337(1)	9053(1)	25(1)
C(11)	7837(2)	2981(1)	9107(1)	28(1)
C(12)	6550(2)	3175(1)	9003(1)	27(1)
C(13)	6271(2)	3733(1)	8855(1)	21(1)
C(14)	9778(2)	4294(1)	8857(1)	23(1)
C(15)	10647(2)	4050(1)	8493(1)	33(1)
C(16)	10573(2)	4432(1)	9382(1)	32(1)
C(17)	4858(2)	3941(1)	8726(1)	25(1)
C(18)	4332(2)	4095(1)	9216(1)	39(1)
C(19)	3960(2)	3516(1)	8401(1)	44(1)
C(20)	6473(2)	6910(1)	8177(1)	19(1)
C(21)	7557(2)	7207(1)	8044(1)	21(1)
C(22)	8856(2)	7166(1)	8338(1)	25(1)
C(23)	9877(2)	7471(1)	8214(1)	29(1)
C(24)	9681(2)	7836(1)	7781(1)	31(1)
C(25)	8478(2)	7888(1)	7485(1)	29(1)
C(26)	7366(2)	7579(1)	7605(1)	23(1)
C(27)	6101(2)	7646(1)	7324(1)	25(1)
C(28)	5010(2)	7376(1)	7464(1)	23(1)
C(29)	3695(2)	7478(1)	7206(1)	29(1)
C(30)	2646(2)	7227(1)	7360(1)	30(1)
C(31)	2834(2)	6847(1)	7782(1)	28(1)
C(32)	4061(2)	6730(1)	8036(1)	24(1)
C(33)	5206(2)	6993(1)	7896(1)	20(1)
C(34)	4744(2)	5040(1)	6953(1)	25(1)
C(35)	4127(2)	4501(1)	7127(1)	31(1)
C(36)	2638(2)	4482(1)	6958(1)	43(1)
C(37)	1988(2)	4998(1)	7143(1)	59(1)
C(38)	2575(2)	5536(1)	6971(1)	51(1)
C(39)	4074(2)	5562(1)	7145(1)	33(1)
C(40)	7127(2)	5747(1)	7005(1)	22(1)
C(41)	8619(2)	5804(1)	7189(1)	26(1)
C(42)	9122(2)	6388(1)	7073(1)	29(1)
C(43)	8756(2)	6535(1)	6503(1)	33(1)

C(44)	7272(2)	6487(1)	6322(1)	32(1)
C(45)	6770(2)	5900(1)	6433(1)	28(1)
C(46)	7306(2)	4550(1)	6771(1)	40(1)
C(47)	8368(3)	4194(1)	7047(1)	55(1)
C(48)	9069(3)	3825(1)	6713(1)	40(1)
C(49)	8217(3)	3551(1)	6272(1)	53(1)
C(50)	7193(3)	3912(1)	5997(1)	67(1)
C(51)	6438(2)	4278(1)	6316(1)	44(1)
C(61)	1620(3)	5650(1)	8585(1)	39(1)
C(62)	2847(2)	5614(1)	8881(1)	43(1)
C(63)	3021(2)	5761(1)	9396(1)	43(1)
C(64)	1952(3)	5941(1)	9612(1)	40(1)
C(65)	720(2)	5974(1)	9309(1)	35(1)
C(66)	557(2)	5826(1)	8800(1)	35(1)
C(71)	3508(2)	7756(1)	8979(1)	43(1)
C(72)	3018(3)	7357(1)	9271(1)	55(1)
C(73)	2046(4)	7498(1)	9550(1)	75(1)
C(74)	1563(3)	8045(1)	9539(1)	69(1)
C(75)	2062(3)	8448(1)	9250(1)	56(1)
C(76)	3043(2)	8301(1)	8972(1)	45(1)
C(81)	3344(3)	6849(1)	5995(1)	49(1)
C(82)	2003(3)	6822(1)	6001(1)	47(1)
C(83)	1120(2)	6950(1)	5564(1)	37(1)
C(84)	1567(2)	7104(1)	5116(1)	35(1)
C(85)	2915(2)	7133(1)	5108(1)	38(1)
C(86)	3801(2)	7006(1)	5548(1)	41(1)
C(91)	5462(3)	5533(1)	5134(1)	55(1)
C(92)	6273(3)	5151(1)	4948(1)	56(1)
C(93)	5795(3)	4614(1)	4807(1)	57(1)
C(94)	327(3)	5407(1)	5374(1)	57(1)
C(95)	240(3)	4852(1)	5510(1)	57(1)
C(96)	-85(2)	4441(1)	5139(1)	54(1)

Table 3. Selected bond lengths [Å] and angles [°] for TRY11. (CCDC 161167)

Ni-N	1.8861(14)	N-Ni-O	95.15(5)
Ni-O	1.8983(11)	N-Ni-P	169.68(5)
Ni-P	2.1339(5)	O-Ni-P	94.81(4)
Ni-H	1.360(16)	N-Ni-H	92.9(6)
		O-Ni-H	171.2(6)
		P-Ni-H	77.0(6)

Table 4. Bond lengths [Å] and angles [°] for TRY11. (CCDC 161167)

Ni-N	1.8861(14)	C(20)-C(33)	1.398(2)
Ni-O	1.8983(11)	C(20)-C(21)	1.407(2)
Ni-P	2.1339(5)	C(21)-C(22)	1.428(2)
Ni-H	1.360(16)	C(21)-C(26)	1.434(2)
P-C(40)	1.8403(19)	C(22)-C(23)	1.356(3)
P-C(34)	1.8426(18)	C(22)-H(22)	0.959(14)
P-C(46)	1.858(2)	C(23)-C(24)	1.413(3)
O-C(7)	1.3000(19)	C(23)-H(23)	0.916(17)
N-C(1)	1.294(2)	C(24)-C(25)	1.350(3)
N-C(8)	1.455(2)	C(24)-H(24)	0.948(16)
C(1)-C(2)	1.428(2)	C(25)-C(26)	1.433(2)
C(1)-H(1)	0.959(14)	C(25)-H(25)	0.937(16)
C(2)-C(3)	1.404(2)	C(26)-C(27)	1.390(3)
C(2)-C(7)	1.428(2)	C(27)-C(28)	1.390(2)
C(3)-C(4)	1.365(2)	C(27)-H(27)	0.933(16)
C(3)-H(3)	0.920(15)	C(28)-C(29)	1.425(3)
C(4)-C(5)	1.396(2)	C(28)-C(33)	1.436(2)
C(4)-H(4)	0.952(15)	C(29)-C(30)	1.348(3)
C(5)-C(6)	1.377(2)	C(29)-H(29)	0.917(16)
C(5)-H(5)	0.980(15)	C(30)-C(31)	1.412(3)
C(6)-C(7)	1.425(2)	C(30)-H(30)	0.923(16)
C(6)-C(20)	1.498(2)	C(31)-C(32)	1.351(3)
C(8)-C(9)	1.394(2)	C(31)-H(31)	0.905(15)
C(8)-C(13)	1.397(2)	C(32)-C(33)	1.430(2)
C(9)-C(10)	1.392(2)	C(32)-H(32)	0.922(15)
C(9)-C(14)	1.513(2)	C(34)-C(35)	1.525(3)
C(10)-C(11)	1.373(3)	C(34)-C(39)	1.535(3)
C(10)-H(10)	0.947(16)	C(34)-H(34)	0.928(14)
C(11)-C(12)	1.381(3)	C(35)-C(36)	1.519(3)
C(11)-H(11)	0.967(15)	C(35)-H(35A)	0.966(17)
C(12)-C(13)	1.389(2)	C(35)-H(35B)	0.976(16)
C(12)-H(12)	0.924(16)	C(36)-C(37)	1.507(3)
C(13)-C(17)	1.514(2)	C(36)-H(36A)	0.976(18)
C(14)-C(16)	1.516(3)	C(36)-H(36B)	1.00(2)
C(14)-C(15)	1.525(3)	C(37)-C(38)	1.505(4)
C(14)-H(14)	0.922(14)	C(37)-H(37A)	0.98(2)
C(15)-H(15A)	1.004(19)	C(37)-H(37B)	0.95(2)
C(15)-H(15B)	0.980(18)	C(38)-C(39)	1.531(3)
C(15)-H(15C)	0.951(18)	C(38)-H(38A)	0.97(2)
C(16)-H(16A)	0.973(19)	C(38)-H(38B)	1.005(19)
C(16)-H(16B)	0.965(17)	C(39)-H(39A)	0.961(16)
C(16)-H(16C)	0.961(18)	C(39)-H(39B)	0.984(16)
C(17)-C(18)	1.518(3)	C(40)-C(45)	1.527(3)
C(17)-C(19)	1.523(3)	C(40)-C(41)	1.532(3)
C(17)-H(17)	0.952(15)	C(40)-H(40)	0.933(15)
C(18)-H(18A)	1.006(19)	C(41)-C(42)	1.519(3)
C(18)-H(18B)	0.951(19)	C(41)-H(41A)	0.934(15)
C(18)-H(18C)	1.01(2)	C(41)-H(41B)	0.970(17)
C(19)-H(19A)	0.92(2)	C(42)-C(43)	1.520(3)
C(19)-H(19B)	1.002(18)	C(42)-H(42A)	0.981(16)
C(19)-H(19C)	1.07(2)	C(42)-H(42B)	0.932(17)

C(43)-C(44)	1.522(3)	C(83)-H(83)	1.020(18)
C(43)-H(43A)	0.969(17)	C(84)-C(85)	1.389(3)
C(43)-H(43B)	0.994(17)	C(84)-H(84)	0.980(19)
C(44)-C(45)	1.521(3)	C(85)-C(86)	1.377(3)
C(44)-H(44A)	0.985(18)	C(85)-H(85)	1.001(19)
C(44)-H(44B)	0.969(18)	C(86)-H(86)	0.989(18)
C(45)-H(45A)	0.971(16)	C(91)-C(93)#1	1.369(4)
C(45)-H(45B)	1.002(16)	C(91)-C(92)	1.373(4)
C(46)-C(47)	1.467(3)	C(91)-H(91)	0.91(2)
C(46)-C(51)	1.507(3)	C(92)-C(93)	1.383(3)
C(46)-H(46)	1.04(3)	C(92)-H(92)	1.08(2)
C(47)-C(48)	1.502(3)	C(93)-C(91)#1	1.369(4)
C(47)-H(47A)	1.02(3)	C(93)-H(93)	0.92(2)
C(47)-H(47B)	0.947(17)	C(94)-C(95)	1.364(3)
C(48)-C(49)	1.477(3)	C(94)-C(96)#2	1.373(3)
C(48)-H(48A)	0.97(2)	C(94)-H(94)	0.99(2)
C(48)-H(48B)	0.91(2)	C(95)-C(96)	1.374(3)
C(49)-C(50)	1.448(3)	C(95)-H(95)	0.99(2)
C(49)-H(49)	0.853(17)	C(96)-C(94)#2	1.373(3)
C(50)-C(51)	1.504(3)	C(96)-H(96)	1.05(2)
C(50)-H(50A)	0.96(2)		
C(50)-H(50B)	1.05(3)	N-Ni-O	95.15(5)
C(51)-H(51A)	1.03(3)	N-Ni-P	169.68(5)
C(51)-H(51B)	0.90(2)	O-Ni-P	94.81(4)
C(61)-C(62)	1.366(3)	N-Ni-H	92.9(6)
C(61)-C(66)	1.373(3)	O-Ni-H	171.2(6)
C(61)-H(61)	0.948(18)	P-Ni-H	77.0(6)
C(62)-C(63)	1.378(3)	C(40)-P-C(34)	106.09(9)
C(62)-H(62)	0.922(18)	C(40)-P-C(46)	103.27(11)
C(63)-C(64)	1.383(3)	C(34)-P-C(46)	107.50(9)
C(63)-H(63)	0.937(18)	C(40)-P-Ni	111.66(6)
C(64)-C(65)	1.379(3)	C(34)-P-Ni	107.98(6)
C(64)-H(64)	0.902(18)	C(46)-P-Ni	119.52(7)
C(65)-C(66)	1.364(3)	C(7)-O-Ni	127.15(11)
C(65)-H(65)	0.936(18)	C(1)-N-C(8)	114.97(14)
C(66)-H(66)	0.939(17)	C(1)-N-Ni	124.76(12)
C(71)-C(72)	1.363(3)	C(8)-N-Ni	120.23(11)
C(71)-C(76)	1.368(3)	N-C(1)-C(2)	126.68(16)
C(71)-H(71)	1.03(2)	N-C(1)-H(1)	118.0(9)
C(72)-C(73)	1.373(4)	C(2)-C(1)-H(1)	115.1(9)
C(72)-H(72)	0.98(2)	C(3)-C(2)-C(1)	117.23(16)
C(73)-C(74)	1.379(4)	C(3)-C(2)-C(7)	120.06(17)
C(73)-H(73)	0.94(2)	C(1)-C(2)-C(7)	122.67(16)
C(74)-C(75)	1.367(3)	C(4)-C(3)-C(2)	122.11(18)
C(74)-H(74)	1.06(2)	C(4)-C(3)-H(3)	121.0(10)
C(75)-C(76)	1.383(3)	C(2)-C(3)-H(3)	116.8(10)
C(75)-H(75)	0.97(2)	C(3)-C(4)-C(5)	117.99(18)
C(76)-H(76)	0.95(2)	C(3)-C(4)-H(4)	122.6(10)
C(81)-C(82)	1.380(3)	C(5)-C(4)-H(4)	119.3(10)
C(81)-C(86)	1.385(3)	C(6)-C(5)-C(4)	122.66(19)
C(81)-H(81)	0.95(2)	C(6)-C(5)-H(5)	120.0(9)
C(82)-C(83)	1.372(3)	C(4)-C(5)-H(5)	117.3(9)
C(82)-H(82)	1.02(2)	C(5)-C(6)-C(7)	120.10(17)
C(83)-C(84)	1.378(3)	C(5)-C(6)-C(20)	119.14(16)

C(7)-C(6)-C(20)	120.75(15)	H(19A)-C(19)-H(19B)	106.4(16)
O-C(7)-C(6)	119.60(15)	C(17)-C(19)-H(19C)	106.0(12)
O-C(7)-C(2)	123.33(16)	H(19A)-C(19)-H(19C)	112.4(18)
C(6)-C(7)-C(2)	117.07(16)	H(19B)-C(19)-H(19C)	110.5(16)
C(9)-C(8)-C(13)	122.34(16)	C(33)-C(20)-C(21)	120.21(16)
C(9)-C(8)-N	118.45(15)	C(33)-C(20)-C(6)	119.49(16)
C(13)-C(8)-N	119.21(15)	C(21)-C(20)-C(6)	120.10(16)
C(10)-C(9)-C(8)	117.47(17)	C(20)-C(21)-C(22)	122.48(17)
C(10)-C(9)-C(14)	120.99(17)	C(20)-C(21)-C(26)	119.74(17)
C(8)-C(9)-C(14)	121.54(16)	C(22)-C(21)-C(26)	117.75(17)
C(11)-C(10)-C(9)	121.32(18)	C(23)-C(22)-C(21)	121.58(19)
C(11)-C(10)-H(10)	119.3(10)	C(23)-C(22)-H(22)	118.4(9)
C(9)-C(10)-H(10)	119.4(10)	C(21)-C(22)-H(22)	120.0(9)
C(10)-C(11)-C(12)	120.10(19)	C(22)-C(23)-C(24)	120.3(2)
C(10)-C(11)-H(11)	120.9(10)	C(22)-C(23)-H(23)	121.3(11)
C(12)-C(11)-H(11)	119.0(10)	C(24)-C(23)-H(23)	118.4(11)
C(11)-C(12)-C(13)	120.99(19)	C(25)-C(24)-C(23)	120.7(2)
C(11)-C(12)-H(12)	119.1(10)	C(25)-C(24)-H(24)	119.7(10)
C(13)-C(12)-H(12)	119.9(10)	C(23)-C(24)-H(24)	119.5(10)
C(12)-C(13)-C(8)	117.68(17)	C(24)-C(25)-C(26)	120.9(2)
C(12)-C(13)-C(17)	120.91(17)	C(24)-C(25)-H(25)	122.2(10)
C(8)-C(13)-C(17)	121.41(16)	C(26)-C(25)-H(25)	116.9(10)
C(9)-C(14)-C(16)	110.72(16)	C(27)-C(26)-C(25)	122.18(18)
C(9)-C(14)-C(15)	111.64(16)	C(27)-C(26)-C(21)	119.05(17)
C(16)-C(14)-C(15)	111.61(18)	C(25)-C(26)-C(21)	118.73(18)
C(9)-C(14)-H(14)	109.0(9)	C(28)-C(27)-C(26)	121.99(18)
C(16)-C(14)-H(14)	106.9(10)	C(28)-C(27)-H(27)	118.0(10)
C(15)-C(14)-H(14)	106.8(9)	C(26)-C(27)-H(27)	119.9(10)
C(14)-C(15)-H(15A)	110.6(11)	C(27)-C(28)-C(29)	122.61(18)
C(14)-C(15)-H(15B)	108.0(10)	C(27)-C(28)-C(33)	118.93(17)
H(15A)-C(15)-H(15B)	110.4(15)	C(29)-C(28)-C(33)	118.43(18)
C(14)-C(15)-H(15C)	114.6(11)	C(30)-C(29)-C(28)	121.7(2)
H(15A)-C(15)-H(15C)	105.9(15)	C(30)-C(29)-H(29)	122.1(11)
H(15B)-C(15)-H(15C)	107.3(15)	C(28)-C(29)-H(29)	116.3(11)
C(14)-C(16)-H(16A)	112.1(11)	C(29)-C(30)-C(31)	120.1(2)
C(14)-C(16)-H(16B)	112.2(10)	C(29)-C(30)-H(30)	121.6(10)
H(16A)-C(16)-H(16B)	105.4(15)	C(31)-C(30)-H(30)	118.3(10)
C(14)-C(16)-H(16C)	109.3(11)	C(32)-C(31)-C(30)	120.6(2)
H(16A)-C(16)-H(16C)	110.7(16)	C(32)-C(31)-H(31)	118.8(10)
H(16B)-C(16)-H(16C)	107.0(15)	C(30)-C(31)-H(31)	120.6(10)
C(13)-C(17)-C(18)	110.62(17)	C(31)-C(32)-C(33)	121.55(19)
C(13)-C(17)-C(19)	112.29(17)	C(31)-C(32)-H(32)	120.6(10)
C(18)-C(17)-C(19)	111.33(19)	C(33)-C(32)-H(32)	117.9(10)
C(13)-C(17)-H(17)	107.9(10)	C(20)-C(33)-C(32)	122.36(17)
C(18)-C(17)-H(17)	106.9(10)	C(20)-C(33)-C(28)	119.98(16)
C(19)-C(17)-H(17)	107.6(10)	C(32)-C(33)-C(28)	117.59(17)
C(17)-C(18)-H(18A)	107.3(11)	C(35)-C(34)-C(39)	109.83(17)
C(17)-C(18)-H(18B)	110.7(11)	C(35)-C(34)-P	110.67(14)
H(18A)-C(18)-H(18B)	106.5(16)	C(39)-C(34)-P	111.36(13)
C(17)-C(18)-H(18C)	110.9(11)	C(35)-C(34)-H(34)	109.1(10)
H(18A)-C(18)-H(18C)	112.5(16)	C(39)-C(34)-H(34)	107.9(10)
H(18B)-C(18)-H(18C)	108.9(16)	P-C(34)-H(34)	107.9(9)
C(17)-C(19)-H(19A)	110.1(13)	C(36)-C(35)-C(34)	112.59(19)
C(17)-C(19)-H(19B)	111.5(10)	C(36)-C(35)-H(35A)	110.6(10)

C(34)-C(35)-H(35A)	107.2(10)	C(43)-C(44)-H(44A)	109.2(11)
C(36)-C(35)-H(35B)	109.2(10)	C(45)-C(44)-H(44B)	106.1(11)
C(34)-C(35)-H(35B)	111.3(10)	C(43)-C(44)-H(44B)	111.8(11)
H(35A)-C(35)-H(35B)	105.7(14)	H(44A)-C(44)-H(44B)	111.0(15)
C(37)-C(36)-C(35)	111.1(2)	C(44)-C(45)-C(40)	111.74(17)
C(37)-C(36)-H(36A)	106.7(11)	C(44)-C(45)-H(45A)	112.1(10)
C(35)-C(36)-H(36A)	109.0(12)	C(40)-C(45)-H(45A)	110.3(10)
C(37)-C(36)-H(36B)	113.3(12)	C(44)-C(45)-H(45B)	106.8(10)
C(35)-C(36)-H(36B)	108.9(12)	C(40)-C(45)-H(45B)	110.6(9)
H(36A)-C(36)-H(36B)	107.6(16)	H(45A)-C(45)-H(45B)	105.1(13)
C(38)-C(37)-C(36)	111.2(2)	C(47)-C(46)-C(51)	116.2(2)
C(38)-C(37)-H(37A)	110.7(13)	C(47)-C(46)-P	115.10(16)
C(36)-C(37)-H(37A)	103.8(13)	C(51)-C(46)-P	118.56(16)
C(38)-C(37)-H(37B)	111.7(13)	C(47)-C(46)-H(46)	88.6(15)
C(36)-C(37)-H(37B)	109.3(12)	C(51)-C(46)-H(46)	104.3(15)
H(37A)-C(37)-H(37B)	109.9(17)	P-C(46)-H(46)	108.5(15)
C(37)-C(38)-C(39)	112.2(2)	C(46)-C(47)-C(48)	115.5(2)
C(37)-C(38)-H(38A)	111.9(12)	C(46)-C(47)-H(47A)	99(2)
C(39)-C(38)-H(38A)	106.7(12)	C(48)-C(47)-H(47A)	102(2)
C(37)-C(38)-H(38B)	112.2(12)	C(46)-C(47)-H(47B)	114.6(10)
C(39)-C(38)-H(38B)	107.1(12)	C(48)-C(47)-H(47B)	114.4(10)
H(38A)-C(38)-H(38B)	106.4(17)	H(47A)-C(47)-H(47B)	109(2)
C(38)-C(39)-C(34)	110.65(18)	C(49)-C(48)-C(47)	115.6(2)
C(38)-C(39)-H(39A)	110.2(10)	C(49)-C(48)-H(48A)	112.4(14)
C(34)-C(39)-H(39A)	110.4(10)	C(47)-C(48)-H(48A)	101.8(14)
C(38)-C(39)-H(39B)	107.5(10)	C(49)-C(48)-H(48B)	116.7(14)
C(34)-C(39)-H(39B)	109.7(10)	C(47)-C(48)-H(48B)	114.9(13)
H(39A)-C(39)-H(39B)	108.2(14)	H(48A)-C(48)-H(48B)	91.5(17)
C(45)-C(40)-C(41)	110.63(17)	C(50)-C(49)-C(48)	114.7(2)
C(45)-C(40)-P	115.30(14)	C(50)-C(49)-H(49)	113.1(13)
C(41)-C(40)-P	110.51(13)	C(48)-C(49)-H(49)	114.1(13)
C(45)-C(40)-H(40)	109.5(10)	C(49)-C(50)-C(51)	117.3(2)
C(41)-C(40)-H(40)	106.6(10)	C(49)-C(50)-H(50A)	113.5(13)
P-C(40)-H(40)	103.7(10)	C(51)-C(50)-H(50A)	104.0(12)
C(42)-C(41)-C(40)	111.85(17)	C(49)-C(50)-H(50B)	95(2)
C(42)-C(41)-H(41A)	109.3(10)	C(51)-C(50)-H(50B)	109(2)
C(40)-C(41)-H(41A)	109.9(10)	H(50A)-C(50)-H(50B)	118(2)
C(42)-C(41)-H(41B)	109.5(10)	C(50)-C(51)-C(46)	113.1(2)
C(40)-C(41)-H(41B)	107.7(10)	C(50)-C(51)-H(51A)	101.9(15)
H(41A)-C(41)-H(41B)	108.5(14)	C(46)-C(51)-H(51A)	97.0(15)
C(41)-C(42)-C(43)	111.64(18)	C(50)-C(51)-H(51B)	116.9(15)
C(41)-C(42)-H(42A)	109.6(9)	C(46)-C(51)-H(51B)	119.3(15)
C(43)-C(42)-H(42A)	110.8(9)	H(51A)-C(51)-H(51B)	104(2)
C(41)-C(42)-H(42B)	108.4(10)	C(62)-C(61)-C(66)	120.4(2)
C(43)-C(42)-H(42B)	111.1(11)	C(62)-C(61)-H(61)	119.4(11)
H(42A)-C(42)-H(42B)	105.0(14)	C(66)-C(61)-H(61)	120.2(12)
C(42)-C(43)-C(44)	111.05(18)	C(61)-C(62)-C(63)	119.8(2)
C(42)-C(43)-H(43A)	108.8(11)	C(61)-C(62)-H(62)	117.1(12)
C(44)-C(43)-H(43A)	111.6(10)	C(63)-C(62)-H(62)	123.1(12)
C(42)-C(43)-H(43B)	109.1(10)	C(62)-C(63)-C(64)	119.9(2)
C(44)-C(43)-H(43B)	108.9(10)	C(62)-C(63)-H(63)	120.8(12)
H(43A)-C(43)-H(43B)	107.3(14)	C(64)-C(63)-H(63)	119.3(12)
C(45)-C(44)-C(43)	111.21(18)	C(65)-C(64)-C(63)	119.7(2)
C(45)-C(44)-H(44A)	107.5(11)	C(65)-C(64)-H(64)	118.7(13)

C(63)-C(64)-H(64)	121.7(13)	C(82)-C(83)-C(84)	120.2(2)
C(66)-C(65)-C(64)	120.1(2)	C(82)-C(83)-H(83)	120.8(11)
C(66)-C(65)-H(65)	122.0(12)	C(84)-C(83)-H(83)	118.9(11)
C(64)-C(65)-H(65)	117.9(12)	C(83)-C(84)-C(85)	119.9(2)
C(65)-C(66)-C(61)	120.2(2)	C(83)-C(84)-H(84)	120.3(12)
C(65)-C(66)-H(66)	121.4(11)	C(85)-C(84)-H(84)	119.7(12)
C(61)-C(66)-H(66)	118.4(11)	C(86)-C(85)-C(84)	119.8(2)
C(72)-C(71)-C(76)	119.7(3)	C(86)-C(85)-H(85)	118.1(12)
C(72)-C(71)-H(71)	117.6(12)	C(84)-C(85)-H(85)	122.1(12)
C(76)-C(71)-H(71)	122.7(13)	C(85)-C(86)-C(81)	119.9(2)
C(71)-C(72)-C(73)	120.1(3)	C(85)-C(86)-H(86)	118.1(11)
C(71)-C(72)-H(72)	117.3(15)	C(81)-C(86)-H(86)	121.9(11)
C(73)-C(72)-H(72)	122.6(15)	C(93)#1-C(91)-C(92)	120.8(3)
C(72)-C(73)-C(74)	120.4(3)	C(93)#1-C(91)-H(91)	120.0(14)
C(72)-C(73)-H(73)	122.2(15)	C(92)-C(91)-H(91)	119.1(14)
C(74)-C(73)-H(73)	117.4(15)	C(91)-C(92)-C(93)	119.1(3)
C(75)-C(74)-C(73)	119.7(3)	C(91)-C(92)-H(92)	121.0(13)
C(75)-C(74)-H(74)	118.9(13)	C(93)-C(92)-H(92)	119.5(13)
C(73)-C(74)-H(74)	121.3(13)	C(91)#1-C(93)-C(92)	120.1(3)
C(74)-C(75)-C(76)	119.4(3)	C(91)#1-C(93)-H(93)	123.9(14)
C(74)-C(75)-H(75)	120.9(15)	C(92)-C(93)-H(93)	116.0(14)
C(76)-C(75)-H(75)	119.7(15)	C(95)-C(94)-C(96)#2	119.8(3)
C(71)-C(76)-C(75)	120.8(2)	C(95)-C(94)-H(94)	119.2(13)
C(71)-C(76)-H(76)	120.6(14)	C(96)#2-C(94)-H(94)	120.9(13)
C(75)-C(76)-H(76)	118.6(13)	C(94)-C(95)-C(96)	120.7(3)
C(82)-C(81)-C(86)	120.1(2)	C(94)-C(95)-H(95)	118.6(12)
C(82)-C(81)-H(81)	120.7(14)	C(96)-C(95)-H(95)	120.7(13)
C(86)-C(81)-H(81)	119.0(14)	C(94)#2-C(96)-C(95)	119.4(2)
C(83)-C(82)-C(81)	120.0(2)	C(94)#2-C(96)-H(96)	119.3(12)
C(83)-C(82)-H(82)	120.1(12)	C(95)-C(96)-H(96)	121.3(12)
C(81)-C(82)-H(82)	119.8(12)		

Symmetry transformations used to generate equivalent atoms:
#1 -x+1,-y+1,-z+1 #2 -x,-y+1,-z+1

Table 5. Anisotropic displacement parameters (Å^{2}x 10^4) for TRY11 (CCDC 161167). The anisotropic displacement factor exponent takes the form: $-2\pi^2$ [h^2 $a^{*2}U^{11}$ + ... + 2 h k a* b* U^{12}]

	U^{11}	U^{22}	U^{33}	U^{23}	U^{13}	U^{12}
Ni	242(1)	185(1)	194(1)	-11(1)	46(1)	16(1)
P	230(3)	214(3)	190(3)	-20(2)	32(2)	28(2)
O	287(7)	188(7)	166(7)	-13(5)	39(6)	27(6)
N	145(8)	151(8)	220(9)	5(7)	34(7)	14(6)
C(1)	149(9)	231(11)	158(9)	46(9)	31(7)	18(8)
C(2)	139(10)	183(10)	182(10)	-7(8)	12(8)	-3(8)
C(3)	245(11)	225(12)	183(11)	30(9)	36(9)	-3(9)
C(4)	363(13)	214(11)	178(11)	-28(9)	49(9)	5(9)
C(5)	314(12)	173(11)	254(12)	-4(9)	66(9)	22(9)
C(6)	158(10)	196(10)	192(10)	5(8)	41(8)	8(8)

C(7)	128(10)	205(10)	201(10)	7(8)	29(8)	15(8)
C(8)	231(11)	164(10)	155(10)	-11(8)	34(8)	16(8)
C(9)	192(10)	193(11)	211(10)	-13(8)	54(8)	10(8)
C(10)	238(12)	229(12)	292(12)	10(9)	56(9)	74(9)
C(11)	370(13)	157(11)	310(12)	22(9)	93(10)	30(10)
C(12)	292(13)	236(12)	292(12)	-17(9)	94(10)	-88(10)
C(13)	216(11)	217(11)	194(10)	-25(8)	69(8)	-30(9)
C(14)	213(11)	199(11)	274(11)	43(9)	44(9)	38(9)
C(15)	293(13)	369(15)	350(14)	-31(12)	114(11)	-31(12)
C(16)	295(14)	297(14)	362(14)	-15(11)	33(11)	-72(11)
C(17)	219(11)	270(12)	280(12)	-16(10)	76(9)	-19(9)
C(18)	269(14)	537(18)	368(14)	-73(13)	96(11)	46(13)
C(19)	257(14)	584(19)	475(17)	-240(15)	48(13)	-9(13)
C(20)	280(11)	144(10)	164(10)	-42(8)	54(9)	28(8)
C(21)	251(11)	153(10)	222(11)	-43(8)	64(9)	32(8)
C(22)	277(12)	222(11)	250(12)	-11(9)	71(10)	36(9)
C(23)	250(13)	297(13)	329(13)	-43(10)	69(10)	-1(10)
C(24)	282(13)	273(13)	396(14)	-48(10)	165(11)	-34(10)
C(25)	402(14)	195(12)	311(13)	37(10)	159(11)	15(10)
C(26)	289(12)	175(11)	230(11)	-27(8)	99(9)	18(9)
C(27)	375(13)	193(11)	189(11)	57(9)	73(10)	48(10)
C(28)	271(12)	185(11)	221(11)	-24(8)	43(9)	40(9)
C(29)	353(13)	256(12)	241(12)	36(10)	20(10)	50(10)
C(30)	254(13)	319(13)	303(13)	-22(10)	-34(10)	68(10)
C(31)	245(12)	285(13)	302(12)	-34(10)	63(10)	-17(10)
C(32)	312(13)	213(11)	204(11)	-2(9)	49(9)	24(9)
C(33)	242(11)	168(10)	187(10)	-18(8)	52(8)	20(8)
C(34)	263(11)	267(12)	210(10)	-44(10)	21(8)	29(9)
C(35)	281(13)	349(14)	316(14)	-72(11)	94(11)	-40(10)
C(36)	304(14)	468(17)	527(18)	-165(14)	127(13)	-78(12)
C(37)	231(14)	660(20)	910(20)	-350(19)	130(14)	-48(14)
C(38)	286(14)	464(17)	740(20)	-280(15)	16(14)	94(12)
C(39)	264(13)	320(14)	396(15)	-105(11)	21(11)	27(10)
C(40)	241(11)	233(11)	199(11)	2(9)	50(9)	29(9)
C(41)	239(12)	286(13)	255(12)	-16(10)	47(10)	18(9)
C(42)	272(13)	244(13)	378(14)	-59(10)	96(11)	-10(10)
C(43)	409(14)	229(13)	376(14)	-4(11)	181(11)	-31(11)
C(44)	421(15)	294(13)	260(13)	44(10)	71(11)	5(11)
C(45)	298(13)	313(13)	235(12)	46(10)	35(10)	-11(11)
C(46)	459(15)	448(15)	258(12)	-109(11)	-27(11)	205(12)
C(47)	421(17)	581(19)	578(18)	-316(16)	-97(15)	217(14)
C(48)	455(16)	457(16)	321(14)	74(12)	143(12)	229(14)
C(49)	504(17)	498(17)	599(18)	-341(14)	128(14)	127(13)
C(50)	660(20)	800(20)	463(17)	-410(17)	-140(16)	352(19)
C(51)	323(15)	539(18)	428(16)	-269(13)	9(13)	79(13)
C(61)	608(18)	296(13)	290(14)	51(11)	144(13)	47(12)
C(62)	407(16)	320(14)	632(19)	117(12)	288(15)	27(12)
C(63)	295(14)	317(14)	630(18)	155(13)	-78(14)	-92(11)
C(64)	612(18)	262(13)	295(14)	38(11)	19(13)	-70(12)
C(65)	415(15)	243(12)	407(15)	44(10)	135(12)	21(11)
C(66)	343(14)	283(13)	393(14)	51(11)	-7(12)	17(11)
C(71)	340(14)	351(15)	570(17)	-99(12)	26(13)	-15(11)

C(72)	790(20)	293(16)	530(18)	28(13)	-8(15)	26(15)
C(73)	1460(30)	448(19)	394(17)	-29(14)	301(19)	-350(20)
C(74)	960(20)	600(20)	635(19)	-220(16)	508(18)	-250(18)
C(75)	698(19)	313(16)	740(20)	-3(14)	325(16)	27(14)
C(76)	483(16)	326(15)	582(17)	93(12)	206(13)	-6(12)
C(81)	554(18)	578(17)	308(15)	-44(12)	-25(14)	93(14)
C(82)	554(18)	579(17)	273(14)	-19(12)	99(13)	-15(14)
C(83)	421(15)	352(14)	350(14)	-19(11)	111(12)	-39(12)
C(84)	446(15)	290(13)	317(14)	18(10)	38(12)	-11(11)
C(85)	501(16)	293(13)	376(14)	8(11)	145(13)	4(11)
C(86)	399(15)	383(14)	437(16)	-79(11)	64(13)	26(12)
C(91)	830(20)	397(18)	366(16)	38(13)	-92(14)	-215(17)
C(92)	570(18)	640(20)	444(16)	119(14)	-4(14)	-157(16)
C(93)	740(20)	530(20)	424(17)	42(14)	72(16)	58(18)
C(94)	730(20)	494(18)	502(18)	-143(15)	136(15)	-156(15)
C(95)	690(18)	640(20)	367(16)	81(15)	31(14)	-186(15)
C(96)	579(17)	381(17)	660(20)	89(15)	65(15)	-38(13)

Table 6. Hydrogen coordinates (x 10^4) and isotropic displacement parameters (Å^{2}x 10^3) for TRY11 (CCDC 161167).

	x	y	z	U_{iso}
H	6821(15)	4389(7)	7817(6)	36(5)
H(1)	7253(13)	4857(6)	9427(6)	9(4)
H(3)	6973(15)	5672(6)	9838(6)	17(5)
H(4)	6820(15)	6665(6)	9903(6)	21(5)
H(5)	6577(15)	7200(7)	9154(6)	16(5)
H(10)	9740(17)	3198(7)	9123(6)	26(5)
H(11)	7999(15)	2592(7)	9215(6)	18(5)
H(12)	5869(16)	2927(7)	9034(6)	23(5)
H(14)	9444(14)	4632(6)	8714(6)	9(4)
H(15A)	11091(18)	3692(8)	8640(7)	44(6)
H(15B)	11307(17)	4336(7)	8445(6)	30(5)
H(15C)	10187(18)	3951(7)	8159(7)	34(6)
H(16A)	10041(19)	4618(8)	9607(7)	45(6)
H(16B)	11289(16)	4691(7)	9359(6)	22(5)
H(16C)	10962(18)	4090(8)	9539(7)	37(6)
H(17)	4856(15)	4280(7)	8529(6)	21(5)
H(18A)	4313(18)	3737(8)	9423(7)	47(7)
H(18B)	3440(20)	4224(8)	9135(7)	43(6)
H(18C)	4890(19)	4402(8)	9414(7)	53(7)
H(19A)	4340(20)	3398(8)	8126(8)	53(7)
H(19B)	3090(19)	3690(7)	8251(7)	33(6)
H(19C)	3820(20)	3173(10)	8656(9)	81(9)
H(22)	9020(14)	6921(6)	8635(6)	8(4)
H(23)	10709(17)	7445(7)	8405(7)	32(6)

H(24)	10401(16)	8052(7)	7701(6)	17(5)
H(25)	8326(15)	8128(7)	7196(6)	21(5)
H(27)	5961(15)	7892(7)	7041(6)	22(5)
H(29)	3605(16)	7720(7)	6929(6)	21(5)
H(30)	1794(16)	7296(7)	7194(6)	21(5)
H(31)	2132(15)	6688(6)	7895(6)	16(5)
H(32)	4184(15)	6478(7)	8308(6)	18(5)
H(34)	4604(14)	5052(6)	6595(6)	14(4)
H(35A)	4352(16)	4484(7)	7500(7)	29(5)
H(35B)	4519(16)	4162(7)	7000(6)	27(5)
H(36A)	2439(18)	4488(8)	6581(7)	42(6)
H(36B)	2290(20)	4117(9)	7076(8)	57(7)
H(37A)	2170(20)	4964(9)	7522(8)	59(8)
H(37B)	1060(20)	4980(8)	7025(7)	53(6)
H(38A)	2211(19)	5870(8)	7109(7)	50(7)
H(38B)	2400(20)	5579(8)	6584(8)	53(7)
H(39A)	4422(16)	5905(7)	7021(6)	21(5)
H(39B)	4243(16)	5571(7)	7525(7)	22(5)
H(40)	6719(15)	6000(7)	7201(6)	18(5)
H(41A)	8817(15)	5736(6)	7545(6)	18(5)
H(41B)	9055(16)	5517(7)	7012(6)	28(5)
H(42A)	10082(17)	6405(7)	7185(6)	21(5)
H(42B)	8778(17)	6652(7)	7278(7)	28(5)
H(43A)	9074(17)	6914(8)	6448(7)	33(6)
H(43B)	9215(16)	6270(7)	6297(6)	31(5)
H(44A)	7075(17)	6546(7)	5945(7)	41(6)
H(44B)	6785(18)	6753(8)	6500(7)	43(6)
H(45A)	5825(17)	5863(7)	6318(6)	23(5)
H(45B)	7184(16)	5626(7)	6215(6)	24(5)
H(46)	8020(30)	4770(11)	6607(10)	115(11)
H(47A)	7810(40)	3904(15)	7203(14)	184(18)
H(47B)	8934(17)	4381(7)	7318(7)	23(5)
H(48A)	9690(20)	4090(9)	6603(9)	72(9)
H(48B)	9730(20)	3613(9)	6886(8)	57(7)
H(49)	8640(17)	3368(7)	6071(7)	28(6)
H(50A)	6520(20)	3708(8)	5773(8)	51(7)
H(50B)	7840(40)	4167(15)	5824(14)	179(18)
H(51A)	6010(30)	3979(11)	6523(10)	104(11)
H(51B)	5740(20)	4474(10)	6144(9)	75(9)
H(61)	1511(17)	5556(7)	8229(7)	37(6)
H(62)	3527(18)	5491(7)	8719(7)	34(6)
H(63)	3861(19)	5751(7)	9601(7)	39(6)
H(64)	2038(18)	6040(8)	9948(7)	39(6)
H(65)	14(19)	6098(8)	9464(7)	45(7)
H(66)	-272(18)	5848(7)	8586(7)	32(6)
H(71)	4210(20)	7628(9)	8762(8)	77(8)
H(72)	3350(20)	6971(10)	9257(9)	83(9)
H(73)	1660(20)	7227(10)	9743(9)	83(9)
H(74)	770(20)	8154(10)	9729(10)	93(9)
H(75)	1770(20)	8839(10)	9254(9)	90(9)
H(76)	3390(20)	8585(9)	8775(8)	70(8)

H(81)	3960(20)	6788(9)	6303(8)	67(8)
H(82)	1670(20)	6717(8)	6336(8)	65(7)
H(83)	127(19)	6934(8)	5563(7)	50(6)
H(84)	937(19)	7181(8)	4799(8)	53(7)
H(85)	3274(19)	7240(8)	4790(8)	55(7)
H(86)	4753(18)	7006(7)	5526(7)	36(6)
H(91)	5790(20)	5883(9)	5237(8)	55(7)
H(92)	7230(20)	5276(10)	4868(9)	94(9)
H(93)	6360(20)	4378(9)	4670(8)	55(8)
H(94)	610(20)	5692(9)	5646(8)	70(8)
H(95)	430(20)	4750(9)	5879(9)	66(8)
H(96)	-140(20)	4013(9)	5239(8)	72(8)

Appendix D

X-Ray Diffraction Analysis of

$[(^{Anthr,H}Sal)Ni(\mu\text{-}OH)]_2$

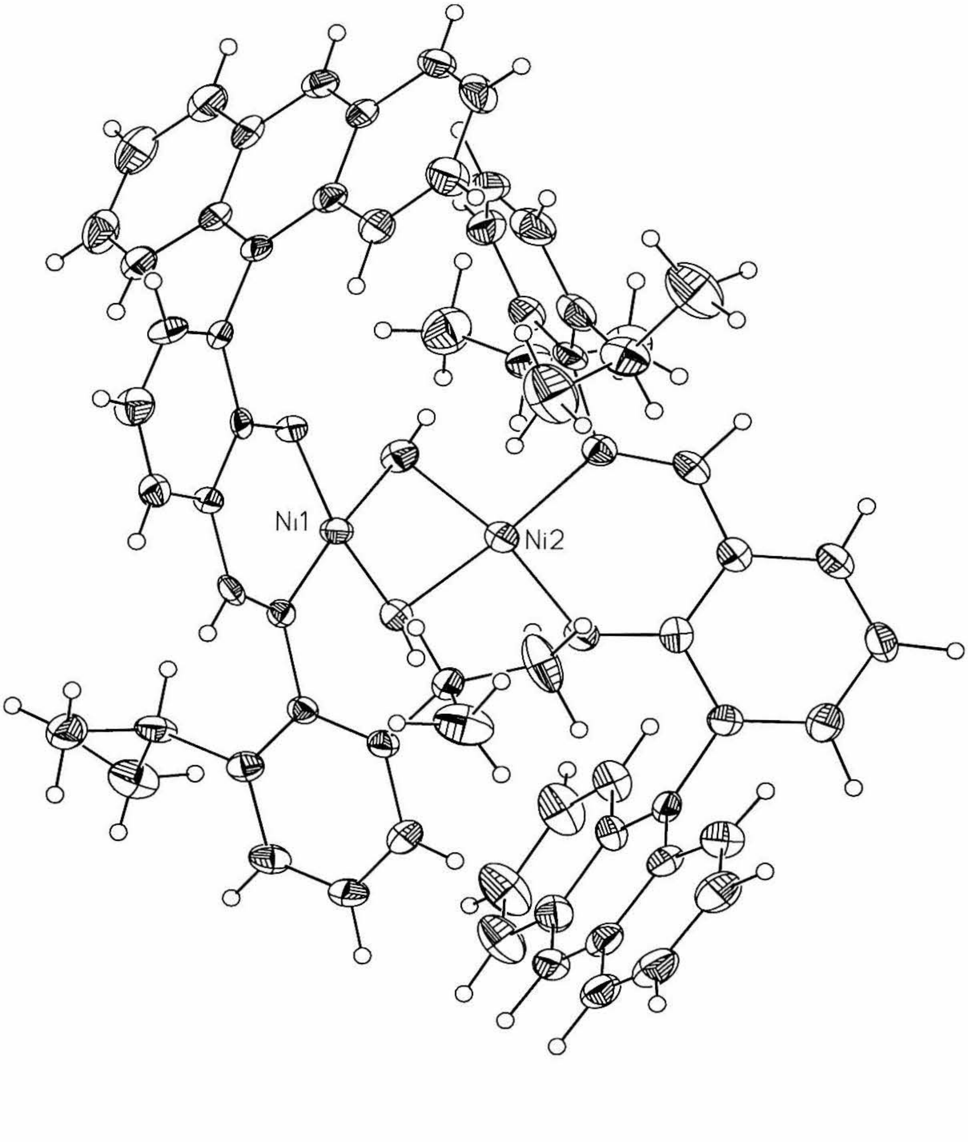

Table 1. Crystal data and structure refinement for TRY9 (CCDC No. 142964).

Empirical formula	$C_{66}H_{62}N_2Ni_2O_4 \cdot \frac{1}{2}(N{\equiv}CCH_3)$	
Formula weight	1083.61	
Crystallization Solvent	Acetonitrile	
Crystal Habit	Square needle	
Crystal size	0.44 x 0.07 x 0.05 mm^3	
Crystal color	Reddish brown	

Data Collection

Preliminary Photos	Rotation	
Type of diffractometer	CCD area detector	
Wavelength	0.71073 Å MoKα	
Data Collection Temperature	98 K	
θ range for 6923 reflections used in lattice determination	2.31 to 26.75°	
Unit cell dimensions	a = 9.0540(9) Å b = 20.512(2) Å c = 29.299(3) Å	 β= 93.573(2)°
Volume	5430.6(9) Å^3	
Z	4	
Crystal system	Monoclinic	
Space group	$P2_1/n$	
Density (calculated)	1.325 Mg/m^3	
F(000)	2278	
θ range for data collection	1.39 to 25.00°	
Completeness to θ = 25.00°	100.0 %	
Index ranges	$-10 \leq h \leq 10$, $-24 \leq k \leq 23$, $-34 \leq l \leq 34$	
Data collection scan type	ω scans at 3 ϕ settings	
Reflections collected	38083	
Independent reflections	9567 [R_{int}= 0.0793]	
Absorption coefficient	0.746 mm^{-1}	
Absorption correction	None	

Table 1 (cont.)

Structure Solution and Refinement

Structure solution program	SHELXS-97 (Sheldrick, 1990)
Primary solution method	Direct methods
Secondary solution method	Difference Fourier map
Hydrogen placement	Difference Fourier map
Structure refinement program	SHELXL-97 (Sheldrick, 1997)
Refinement method	Full-matrix least-squares on F^2
Data / restraints / parameters	9567 / 0 / 931
Treatment of hydrogen atoms	Unrestrained
Goodness-of-fit on F^2	1.124
Final R indices [$I>2\sigma(I)$, 5876 reflections]	$R1 = 0.0466$, $wR2 = 0.0706$
R indices (all data)	$R1 = 0.0886$, $wR2 = 0.0762$
Type of weighting scheme used	Sigma
Weighting scheme used	$w=1/\sigma^2(Fo^2)$
Max shift/error	0.365
Average shift/error	0.001
Largest diff. peak and hole	0.698 and -0.559 e.Å^{-3}

Special Refinement Details

The crystals contain a solvent molecule at a center of symmetry.

Refinement of F^2 against ALL reflections. The weighted R-factor (wR) and goodness of fit (S) are based on F^2, conventional R-factors (R) are based on F, with F set to zero for negative F^2. The threshold expression of $F^2 > 2\sigma(F^2)$ is used only for calculating R-factors(gt) etc. and is not relevant to the choice of reflections for refinement. R-factors based on F^2 are statistically about twice as large as those based on F, and R-factors based on ALL data will be even larger.

All esds (except the esd in the dihedral angle between two l.s. planes) are estimated using the full covariance matrix. The cell esds are taken into account individually in the estimation of esds in distances, angles and torsion angles; correlations between esds in cell parameters are only used when they are defined by crystal symmetry. An approximate (isotropic) treatment of cell esds is used for estimating esds involving l.s. planes.

Table 2. Atomic coordinates (x 10^4) and equivalent isotropic displacement parameters (Å^{2}x 10^3) for TRY9 (CCDC No. 142964). U(eq) is defined as the trace of the orthogonalized U^{ij} tensor.

	x	y	z	U_{eq}	Occ
Ni(1)	1167(1)	8851(1)	1616(1)	20(1)	1
Ni(2)	1296(1)	7537(1)	1604(1)	23(1)	1
O(1)	29(2)	9319(1)	1996(1)	20(1)	1
O(2)	1578(2)	7030(1)	1106(1)	25(1)	1
O(3)	1248(2)	8183(1)	2051(1)	26(1)	1
O(4)	2323(3)	8226(1)	1342(1)	24(1)	1
N(1)	1123(3)	9460(1)	1147(1)	17(1)	1
N(2)	144(3)	6927(1)	1896(1)	23(1)	1
N(100)	3111(12)	4630(7)	50(4)	145(6)	0.50
C(100)	4249(6)	4903(4)	2(2)	98(2)	1
C(1)	406(4)	10007(2)	1155(1)	20(1)	1
C(2)	-452(4)	10246(2)	1514(1)	18(1)	1
C(3)	-1167(4)	10849(2)	1446(1)	26(1)	1
C(4)	-2054(4)	11089(2)	1765(1)	31(1)	1
C(5)	-2226(4)	10725(2)	2157(1)	29(1)	1
C(6)	-1554(4)	10139(2)	2249(1)	19(1)	1
C(7)	-617(4)	9880(2)	1917(1)	18(1)	1
C(8)	-1871(4)	9772(2)	2673(1)	21(1)	1
C(9)	-3273(4)	9493(2)	2716(1)	23(1)	1
C(10)	-4436(4)	9517(2)	2357(1)	30(1)	1
C(11)	-5766(5)	9238(2)	2409(2)	37(1)	1
C(12)	-6083(5)	8924(2)	2818(2)	34(1)	1
C(13)	-5046(4)	8893(2)	3164(1)	27(1)	1
C(14)	-3605(4)	9168(2)	3130(1)	22(1)	1
C(15)	-2519(4)	9127(2)	3481(1)	25(1)	1
C(16)	-1118(4)	9394(2)	3448(1)	25(1)	1
C(17)	19(5)	9328(2)	3807(1)	34(1)	1
C(18)	1363(5)	9594(2)	3770(2)	41(1)	1
C(19)	1680(5)	9944(2)	3371(2)	38(1)	1
C(20)	650(4)	10003(2)	3022(1)	28(1)	1
C(21)	-782(4)	9722(2)	3036(1)	22(1)	1
C(22)	1765(4)	9303(2)	719(1)	18(1)	1
C(23)	3256(4)	9441(2)	662(1)	23(1)	1
C(24)	3820(4)	9276(2)	246(1)	27(1)	1
C(25)	2955(4)	8974(2)	-93(1)	30(1)	1
C(26)	1504(4)	8834(2)	-29(1)	30(1)	1
C(27)	855(4)	9002(2)	377(1)	20(1)	1
C(28)	4225(4)	9789(2)	1034(1)	27(1)	1
C(29)	5852(5)	9602(3)	1035(2)	40(1)	1
C(30)	4070(5)	10532(2)	995(2)	38(1)	1
C(31)	-763(4)	8834(2)	433(1)	25(1)	1
C(32)	-960(5)	8112(2)	513(2)	48(1)	1
C(33)	-1753(5)	9073(3)	37(2)	46(1)	1
C(34)	-268(4)	6365(2)	1728(1)	25(1)	1
C(35)	111(4)	6100(2)	1305(1)	22(1)	1
C(36)	-454(4)	5493(2)	1174(1)	28(1)	1
C(37)	-165(4)	5214(2)	767(1)	30(1)	1

C(38)	751(4)	5556(2)	474(1)	31(1)	1
C(39)	1331(4)	6159(2)	586(1)	23(1)	1
C(40)	1009(4)	6454(2)	1008(1)	21(1)	1
C(41)	2298(4)	6508(2)	272(1)	22(1)	1
C(42)	3826(4)	6557(2)	386(1)	25(1)	1
C(43)	4499(4)	6257(2)	788(1)	32(1)	1
C(44)	5980(5)	6288(2)	885(2)	44(1)	1
C(45)	6891(5)	6631(2)	593(2)	49(1)	1
C(46)	6314(5)	6924(2)	214(2)	47(1)	1
C(47)	4764(4)	6903(2)	93(1)	32(1)	1
C(48)	4135(5)	7207(2)	-301(1)	31(1)	1
C(49)	2639(4)	7166(2)	-416(1)	29(1)	1
C(50)	1993(5)	7485(2)	-816(1)	34(1)	1
C(51)	528(5)	7427(2)	-936(1)	40(1)	1
C(52)	-422(5)	7054(2)	-668(1)	38(1)	1
C(53)	148(4)	6754(2)	-278(1)	32(1)	1
C(54)	1687(4)	6803(2)	-134(1)	28(1)	1
C(55)	-427(4)	7128(2)	2322(1)	28(1)	1
C(56)	535(4)	7109(2)	2722(1)	30(1)	1
C(57)	36(5)	7397(2)	3112(1)	36(1)	1
C(58)	-1339(6)	7693(2)	3107(2)	44(1)	1
C(59)	-2273(5)	7684(2)	2723(2)	41(1)	1
C(60)	-1866(4)	7400(2)	2318(1)	33(1)	1
C(61)	2024(4)	6770(2)	2711(1)	35(1)	1
C(62)	1853(6)	6029(2)	2762(2)	42(1)	1
C(63)	3161(6)	7029(3)	3072(2)	51(1)	1
C(64)	-2918(4)	7408(2)	1895(2)	36(1)	1
C(65)	-2996(7)	8080(3)	1676(2)	62(2)	1
C(66)	-4467(6)	7179(3)	1996(2)	65(2)	1

Table 3. Selected bond lengths [Å] and angles [°] for TRY9 (CCDC No. 142964).

Ni(1)-O(1)	1.835(2)	O(1)-Ni(1)-N(1)	96.25(11)
Ni(1)-N(1)	1.857(3)	O(1)-Ni(1)-O(3)	88.31(10)
Ni(1)-O(3)	1.868(3)	N(1)-Ni(1)-O(3)	175.06(12)
Ni(1)-O(4)	1.867(3)	O(1)-Ni(1)-O(4)	166.29(10)
Ni(1)-Ni(2)	2.6966(7)	N(1)-Ni(1)-O(4)	97.46(11)
Ni(2)-O(2)	1.824(2)	O(3)-Ni(1)-O(4)	77.98(10)
Ni(2)-O(3)	1.865(3)	O(1)-Ni(1)-Ni(2)	123.91(7)
Ni(2)-N(2)	1.870(3)	N(1)-Ni(1)-Ni(2)	131.44(9)
Ni(2)-O(4)	1.882(3)	O(3)-Ni(1)-Ni(2)	43.69(8)
Ni(2)-H(3OH)	2.13(4)	O(4)-Ni(1)-Ni(2)	44.23(8)
		O(2)-Ni(2)-O(3)	167.90(11)
		O(2)-Ni(2)-N(2)	95.36(12)
		O(3)-Ni(2)-N(2)	96.74(11)
		O(2)-Ni(2)-O(4)	90.25(10)
		O(3)-Ni(2)-O(4)	77.67(10)
		N(2)-Ni(2)-O(4)	173.36(12)
		O(2)-Ni(2)-Ni(1)	126.08(8)
		O(3)-Ni(2)-Ni(1)	43.78(8)
		N(2)-Ni(2)-Ni(1)	129.59(9)
		O(4)-Ni(2)-Ni(1)	43.77(8)
		O(2)-Ni(2)-H(3OH)	167.6(10)
		O(3)-Ni(2)-H(3OH)	20.9(10)
		N(2)-Ni(2)-H(3OH)	79.0(11)
		O(4)-Ni(2)-H(3OH)	94.8(11)
		Ni(1)-Ni(2)-H(3OH)	54.3(11

Table 4. Bond lengths [Å] and angles [°] for TRY9 (CCDC No. 142964).

Ni(1)-O(1)	1.835(2)	C(1)-C(2)	1.432(4)
Ni(1)-N(1)	1.857(3)	C(1)-H(1)	0.90(3)
Ni(1)-O(3)	1.868(3)	C(2)-C(3)	1.405(5)
Ni(1)-O(4)	1.867(3)	C(2)-C(7)	1.416(4)
Ni(1)-Ni(2)	2.6966(7)	C(3)-C(4)	1.361(5)
Ni(2)-O(2)	1.824(2)	C(3)-H(3)	0.94(3)
Ni(2)-O(3)	1.865(3)	C(4)-C(5)	1.389(5)
Ni(2)-N(2)	1.870(3)	C(4)-H(4)	0.87(3)
Ni(2)-O(4)	1.882(3)	C(5)-C(6)	1.367(5)
Ni(2)-H(3OH)	2.13(4)	C(5)-H(5)	0.84(3)
O(1)-C(7)	1.305(4)	C(6)-C(7)	1.432(4)
O(2)-C(40)	1.313(4)	C(6)-C(8)	1.495(4)
O(3)-H(3OH)	0.77(3)	C(8)-C(9)	1.405(4)
O(4)-H(4OH)	0.75(3)	C(8)-C(21)	1.409(4)
N(1)-C(1)	1.296(4)	C(9)-C(14)	1.434(4)
N(1)-C(22)	1.452(4)	C(9)-C(10)	1.440(5)
N(2)-C(34)	1.299(4)	C(10)-C(11)	1.350(5)
N(2)-C(55)	1.442(4)	C(10)-H(10)	1.02(3)
N(100)-C(100)	1.189(12)	C(11)-C(12)	1.405(5)
C(100)-C(100)#1	1.417(12)	C(11)-H(11)	0.86(3)

C(12)-C(13)	1.340(5)	C(38)-C(39)	1.375(5)
C(12)-H(12)	0.82(4)	C(38)-H(38)	1.03(3)
C(13)-C(14)	1.431(5)	C(39)-C(40)	1.424(4)
C(13)-H(13)	0.88(3)	C(39)-C(41)	1.491(4)
C(14)-C(15)	1.379(5)	C(41)-C(54)	1.416(4)
C(15)-C(16)	1.390(5)	C(41)-C(42)	1.407(5)
C(15)-H(15)	0.85(3)	C(42)-C(47)	1.433(5)
C(16)-C(17)	1.430(5)	C(42)-C(43)	1.431(5)
C(16)-C(21)	1.430(5)	C(43)-C(44)	1.355(5)
C(17)-C(18)	1.344(5)	C(43)-H(43)	0.95(3)
C(17)-H(17)	0.94(3)	C(44)-C(45)	1.412(5)
C(18)-C(19)	1.416(6)	C(44)-H(44)	1.01(3)
C(18)-H(18)	0.91(3)	C(45)-C(46)	1.340(5)
C(19)-C(20)	1.346(5)	C(45)-H(45)	0.97(3)
C(19)-H(19)	0.90(3)	C(46)-C(47)	1.426(5)
C(20)-C(21)	1.421(5)	C(46)-H(46)	0.97(4)
C(20)-H(20)	0.87(3)	C(47)-C(48)	1.403(5)
C(22)-C(23)	1.400(4)	C(48)-C(49)	1.378(5)
C(22)-C(27)	1.401(4)	C(48)-H(48)	1.04(3)
C(23)-C(24)	1.392(5)	C(49)-C(50)	1.435(5)
C(23)-C(28)	1.532(5)	C(49)-C(54)	1.439(5)
C(24)-C(25)	1.372(5)	C(50)-C(51)	1.356(5)
C(24)-H(24)	0.94(3)	C(50)-H(50)	1.01(3)
C(25)-C(26)	1.368(5)	C(51)-C(52)	1.424(5)
C(25)-H(25)	0.96(3)	C(51)-H(51)	0.91(3)
C(26)-C(27)	1.401(5)	C(52)-C(53)	1.370(5)
C(26)-H(26)	0.89(3)	C(52)-H(52)	1.07(3)
C(27)-C(31)	1.524(4)	C(53)-C(54)	1.434(5)
C(28)-C(29)	1.522(5)	C(53)-H(53)	0.93(3)
C(28)-C(30)	1.533(6)	C(55)-C(56)	1.415(5)
C(28)-H(28)	0.93(3)	C(55)-C(60)	1.417(5)
C(29)-H(29A)	0.82(4)	C(56)-C(57)	1.389(5)
C(29)-H(29B)	1.09(3)	C(56)-C(61)	1.518(5)
C(29)-H(29C)	1.10(4)	C(57)-C(58)	1.383(6)
C(30)-H(30A)	0.99(4)	C(57)-H(57)	0.91(3)
C(30)-H(30B)	0.96(4)	C(58)-C(59)	1.364(6)
C(30)-H(30C)	0.98(3)	C(58)-H(58)	0.92(3)
C(31)-C(33)	1.504(5)	C(59)-C(60)	1.392(5)
C(31)-C(32)	1.511(6)	C(59)-H(59)	1.00(3)
C(31)-H(31)	0.95(3)	C(60)-C(64)	1.516(5)
C(32)-H(32A)	1.10(4)	C(61)-C(63)	1.525(6)
C(32)-H(32B)	0.98(3)	C(61)-C(62)	1.536(6)
C(32)-H(32C)	1.04(4)	C(61)-H(61)	0.93(3)
C(33)-H(33A)	1.04(4)	C(62)-H(62A)	0.97(3)
C(33)-H(33B)	0.97(3)	C(62)-H(62B)	0.95(3)
C(33)-H(33C)	0.90(4)	C(62)-H(62C)	1.01(4)
C(34)-C(35)	1.414(5)	C(63)-H(63A)	0.97(3)
C(34)-H(34)	0.98(3)	C(63)-H(63B)	1.04(4)
C(35)-C(36)	1.390(5)	C(63)-H(63C)	1.05(3)
C(35)-C(40)	1.426(4)	C(64)-C(65)	1.521(6)
C(36)-C(37)	1.363(5)	C(64)-C(66)	1.525(6)
C(36)-H(36)	0.92(3)	C(64)-H(64)	0.92(3)
C(37)-C(38)	1.417(5)	C(65)-H(65A)	1.04(4)
C(37)-H(37)	1.05(3)	C(65)-H(65B)	1.03(4)

C(65)-H(65C)	1.04(5)
C(66)-H(66A)	1.05(4)
C(66)-H(66B)	0.92(4)
C(66)-H(66C)	1.09(4)

O(1)-Ni(1)-N(1)	96.25(11)
O(1)-Ni(1)-O(3)	88.31(10)
N(1)-Ni(1)-O(3)	175.06(12)
O(1)-Ni(1)-O(4)	166.29(10)
N(1)-Ni(1)-O(4)	97.46(11)
O(3)-Ni(1)-O(4)	77.98(10)
O(1)-Ni(1)-Ni(2)	123.91(7)
N(1)-Ni(1)-Ni(2)	131.44(9)
O(3)-Ni(1)-Ni(2)	43.69(8)
O(4)-Ni(1)-Ni(2)	44.23(8)
O(2)-Ni(2)-O(3)	167.90(11)
O(2)-Ni(2)-N(2)	95.36(12)
O(3)-Ni(2)-N(2)	96.74(11)
O(2)-Ni(2)-O(4)	90.25(10)
O(3)-Ni(2)-O(4)	77.67(10)
N(2)-Ni(2)-O(4)	173.36(12)
O(2)-Ni(2)-Ni(1)	126.08(8)
O(3)-Ni(2)-Ni(1)	43.78(8)
N(2)-Ni(2)-Ni(1)	129.59(9)
O(4)-Ni(2)-Ni(1)	43.77(8)
O(2)-Ni(2)-H(3OH)	167.6(10)
O(3)-Ni(2)-H(3OH)	20.9(10)
N(2)-Ni(2)-H(3OH)	79.0(11)
O(4)-Ni(2)-H(3OH)	94.8(11)
Ni(1)-Ni(2)-H(3OH)	54.3(11)
C(7)-O(1)-Ni(1)	128.1(2)
C(40)-O(2)-Ni(2)	127.9(2)
Ni(2)-O(3)-Ni(1)	92.52(10)
Ni(2)-O(3)-H(3OH)	99(3)
Ni(1)-O(3)-H(3OH)	111(3)
Ni(1)-O(4)-Ni(2)	92.00(10)
Ni(1)-O(4)-H(4OH)	118(3)
Ni(2)-O(4)-H(4OH)	107(3)
C(1)-N(1)-C(22)	115.8(3)
C(1)-N(1)-Ni(1)	123.8(2)
C(22)-N(1)-Ni(1)	119.9(2)
C(34)-N(2)-C(55)	118.2(3)
C(34)-N(2)-Ni(2)	125.2(3)
C(55)-N(2)-Ni(2)	116.4(2)
N(100)-C(100)-C(100)#1	166.4(13)
N(1)-C(1)-C(2)	127.2(3)
N(1)-C(1)-H(1)	120.2(18)
C(2)-C(1)-H(1)	112.6(17)
C(3)-C(2)-C(7)	120.8(3)
C(3)-C(2)-C(1)	117.7(3)
C(7)-C(2)-C(1)	121.4(3)
C(4)-C(3)-C(2)	120.5(4)
C(4)-C(3)-H(3)	118.2(18)
C(2)-C(3)-H(3)	121.1(18)
C(3)-C(4)-C(5)	118.5(4)
C(3)-C(4)-H(4)	123(2)
C(5)-C(4)-H(4)	119(2)
C(6)-C(5)-C(4)	124.4(4)
C(6)-C(5)-H(5)	123(2)
C(4)-C(5)-H(5)	113(2)
C(5)-C(6)-C(7)	117.8(3)
C(5)-C(6)-C(8)	120.0(3)
C(7)-C(6)-C(8)	122.1(3)
O(1)-C(7)-C(2)	123.0(3)
O(1)-C(7)-C(6)	118.9(3)
C(2)-C(7)-C(6)	118.0(3)
C(9)-C(8)-C(21)	119.8(3)
C(9)-C(8)-C(6)	119.9(3)
C(21)-C(8)-C(6)	120.2(3)
C(8)-C(9)-C(14)	120.1(3)
C(8)-C(9)-C(10)	123.1(3)
C(14)-C(9)-C(10)	116.8(3)
C(11)-C(10)-C(9)	121.4(4)
C(11)-C(10)-H(10)	118.3(17)
C(9)-C(10)-H(10)	120.3(17)
C(10)-C(11)-C(12)	121.3(4)
C(10)-C(11)-H(11)	119(2)
C(12)-C(11)-H(11)	120(2)
C(13)-C(12)-C(11)	119.8(4)
C(13)-C(12)-H(12)	124(3)
C(11)-C(12)-H(12)	116(3)
C(12)-C(13)-C(14)	121.8(4)
C(12)-C(13)-H(13)	123(2)
C(14)-C(13)-H(13)	115(2)
C(15)-C(14)-C(13)	122.4(3)
C(15)-C(14)-C(9)	118.8(3)
C(13)-C(14)-C(9)	118.9(3)
C(14)-C(15)-C(16)	122.5(4)
C(14)-C(15)-H(15)	121(2)
C(16)-C(15)-H(15)	117(2)
C(15)-C(16)-C(17)	122.0(4)
C(15)-C(16)-C(21)	119.0(4)
C(17)-C(16)-C(21)	118.9(4)
C(18)-C(17)-C(16)	121.1(4)
C(18)-C(17)-H(17)	120.3(19)
C(16)-C(17)-H(17)	118.5(19)
C(17)-C(18)-C(19)	120.2(4)
C(17)-C(18)-H(18)	118(2)
C(19)-C(18)-H(18)	122(2)
C(20)-C(19)-C(18)	120.4(4)
C(20)-C(19)-H(19)	123.0(19)
C(18)-C(19)-H(19)	116.6(19)
C(19)-C(20)-C(21)	122.1(4)
C(19)-C(20)-H(20)	121.7(19)
C(21)-C(20)-H(20)	116.1(19)
C(8)-C(21)-C(20)	123.0(3)
C(8)-C(21)-C(16)	119.7(3)
C(20)-C(21)-C(16)	117.3(3)

C(23)-C(22)-C(27)	122.1(3)
C(23)-C(22)-N(1)	120.0(3)
C(27)-C(22)-N(1)	117.9(3)
C(24)-C(23)-C(22)	117.7(3)
C(24)-C(23)-C(28)	120.7(3)
C(22)-C(23)-C(28)	121.6(3)
C(25)-C(24)-C(23)	121.2(4)
C(25)-C(24)-H(24)	119.4(19)
C(23)-C(24)-H(24)	119.3(19)
C(26)-C(25)-C(24)	120.4(4)
C(26)-C(25)-H(25)	121.5(19)
C(24)-C(25)-H(25)	118.2(19)
C(25)-C(26)-C(27)	121.4(4)
C(25)-C(26)-H(26)	118(2)
C(27)-C(26)-H(26)	120(2)
C(26)-C(27)-C(22)	117.1(3)
C(26)-C(27)-C(31)	119.6(3)
C(22)-C(27)-C(31)	123.2(3)
C(29)-C(28)-C(30)	109.6(4)
C(29)-C(28)-C(23)	113.3(3)
C(30)-C(28)-C(23)	111.4(3)
C(29)-C(28)-H(28)	104.2(17)
C(30)-C(28)-H(28)	109.0(17)
C(23)-C(28)-H(28)	108.9(17)
C(28)-C(29)-H(29A)	109(3)
C(28)-C(29)-H(29B)	109.5(17)
H(29A)-C(29)-H(29B)	113(3)
C(28)-C(29)-H(29C)	107(2)
H(29A)-C(29)-H(29C)	113(4)
H(29B)-C(29)-H(29C)	105(3)
C(28)-C(30)-H(30A)	107(2)
C(28)-C(30)-H(30B)	113(2)
H(30A)-C(30)-H(30B)	103(3)
C(28)-C(30)-H(30C)	109(2)
H(30A)-C(30)-H(30C)	113(3)
H(30B)-C(30)-H(30C)	111(3)
C(33)-C(31)-C(32)	111.6(4)
C(33)-C(31)-C(27)	111.9(3)
C(32)-C(31)-C(27)	111.2(3)
C(33)-C(31)-H(31)	105.0(19)
C(32)-C(31)-H(31)	108.4(19)
C(27)-C(31)-H(31)	108.4(19)
C(31)-C(32)-H(32A)	106(2)
C(31)-C(32)-H(32B)	109.0(19)
H(32A)-C(32)-H(32B)	107(3)
C(31)-C(32)-H(32C)	112(2)
H(32A)-C(32)-H(32C)	111(3)
H(32B)-C(32)-H(32C)	111(3)
C(31)-C(33)-H(33A)	106(2)
C(31)-C(33)-H(33B)	107(2)
H(33A)-C(33)-H(33B)	103(3)
C(31)-C(33)-H(33C)	107(3)
H(33A)-C(33)-H(33C)	127(4)
H(33B)-C(33)-H(33C)	106(3)
N(2)-C(34)-C(35)	126.4(4)
N(2)-C(34)-H(34)	124.5(17)
C(35)-C(34)-H(34)	109.1(17)
C(36)-C(35)-C(34)	118.8(3)
C(36)-C(35)-C(40)	120.1(3)
C(34)-C(35)-C(40)	121.1(3)
C(37)-C(36)-C(35)	122.1(4)
C(37)-C(36)-H(36)	123(2)
C(35)-C(36)-H(36)	114(2)
C(36)-C(37)-C(38)	118.2(4)
C(36)-C(37)-H(37)	124.9(17)
C(38)-C(37)-H(37)	116.2(17)
C(39)-C(38)-C(37)	122.0(4)
C(39)-C(38)-H(38)	114.3(19)
C(37)-C(38)-H(38)	123.6(19)
C(38)-C(39)-C(40)	119.6(3)
C(38)-C(39)-C(41)	121.0(3)
C(40)-C(39)-C(41)	119.5(3)
O(2)-C(40)-C(35)	123.9(3)
O(2)-C(40)-C(39)	118.2(3)
C(35)-C(40)-C(39)	118.0(3)
C(54)-C(41)-C(42)	119.8(3)
C(54)-C(41)-C(39)	120.6(3)
C(42)-C(41)-C(39)	119.6(3)
C(41)-C(42)-C(47)	120.2(3)
C(41)-C(42)-C(43)	121.8(3)
C(47)-C(42)-C(43)	117.9(3)
C(44)-C(43)-C(42)	121.1(4)
C(44)-C(43)-H(43)	120.2(18)
C(42)-C(43)-H(43)	118.7(18)
C(43)-C(44)-C(45)	120.3(4)
C(43)-C(44)-H(44)	116.2(19)
C(45)-C(44)-H(44)	123.5(19)
C(46)-C(45)-C(44)	120.8(4)
C(46)-C(45)-H(45)	122(2)
C(44)-C(45)-H(45)	117(2)
C(45)-C(46)-C(47)	121.3(4)
C(45)-C(46)-H(46)	123(2)
C(47)-C(46)-H(46)	116(2)
C(48)-C(47)-C(46)	122.3(4)
C(48)-C(47)-C(42)	119.2(4)
C(46)-C(47)-C(42)	118.5(4)
C(49)-C(48)-C(47)	121.1(4)
C(49)-C(48)-H(48)	121.4(17)
C(47)-C(48)-H(48)	117.5(17)
C(48)-C(49)-C(50)	121.1(4)
C(48)-C(49)-C(54)	120.4(4)
C(50)-C(49)-C(54)	118.5(4)
C(51)-C(50)-C(49)	120.9(4)
C(51)-C(50)-H(50)	123(2)
C(49)-C(50)-H(50)	116(2)
C(50)-C(51)-C(52)	121.3(4)
C(50)-C(51)-H(51)	121(2)
C(52)-C(51)-H(51)	118(2)

C(53)-C(52)-C(51)	119.5(4)
C(53)-C(52)-H(52)	115.5(16)
C(51)-C(52)-H(52)	125.0(16)
C(52)-C(53)-C(54)	121.5(4)
C(52)-C(53)-H(53)	116(2)
C(54)-C(53)-H(53)	123(2)
C(41)-C(54)-C(53)	122.6(3)
C(41)-C(54)-C(49)	119.2(3)
C(53)-C(54)-C(49)	118.2(3)
C(56)-C(55)-C(60)	122.4(3)
C(56)-C(55)-N(2)	118.3(3)
C(60)-C(55)-N(2)	119.0(3)
C(57)-C(56)-C(55)	117.0(4)
C(57)-C(56)-C(61)	123.2(4)
C(55)-C(56)-C(61)	119.8(3)
C(58)-C(57)-C(56)	121.1(4)
C(58)-C(57)-H(57)	125(2)
C(56)-C(57)-H(57)	114(2)
C(59)-C(58)-C(57)	121.0(4)
C(59)-C(58)-H(58)	120(2)
C(57)-C(58)-H(58)	119(2)
C(58)-C(59)-C(60)	121.6(4)
C(58)-C(59)-H(59)	126(2)
C(60)-C(59)-H(59)	111(2)
C(59)-C(60)-C(55)	116.7(4)
C(59)-C(60)-C(64)	120.4(4)
C(55)-C(60)-C(64)	122.8(3)
C(56)-C(61)-C(63)	112.9(4)
C(56)-C(61)-C(62)	110.8(4)
C(63)-C(61)-C(62)	110.1(4)
C(56)-C(61)-H(61)	106(2)
C(63)-C(61)-H(61)	106(2)
C(62)-C(61)-H(61)	110(2)
C(61)-C(62)-H(62A)	106(2)
C(61)-C(62)-H(62B)	107(2)
H(62A)-C(62)-H(62B)	110(3)
C(61)-C(62)-H(62C)	109(2)
H(62A)-C(62)-H(62C)	110(3)
H(62B)-C(62)-H(62C)	114(3)
C(61)-C(63)-H(63A)	116(2)
C(61)-C(63)-H(63B)	107(2)
H(63A)-C(63)-H(63B)	107(3)
C(61)-C(63)-H(63C)	102.2(18)
H(63A)-C(63)-H(63C)	104(3)
H(63B)-C(63)-H(63C)	121(3)
C(60)-C(64)-C(65)	111.4(4)
C(60)-C(64)-C(66)	112.2(4)
C(65)-C(64)-C(66)	109.9(4)
C(60)-C(64)-H(64)	109(2)
C(65)-C(64)-H(64)	100(2)
C(66)-C(64)-H(64)	113(2)
C(64)-C(65)-H(65A)	101(2)
C(64)-C(65)-H(65B)	112(2)
H(65A)-C(65)-H(65B)	105(3)
C(64)-C(65)-H(65C)	106(3)
H(65A)-C(65)-H(65C)	128(4)
H(65B)-C(65)-H(65C)	105(3)
C(64)-C(66)-H(66A)	109(2)
C(64)-C(66)-H(66B)	113(3)
H(66A)-C(66)-H(66B)	95(4)
C(64)-C(66)-H(66C)	107.7(19)
H(66A)-C(66)-H(66C)	119(3)
H(66B)-C(66)-H(66C)	113(4)

Symmetry transformations used to generate equivalent atoms:
#1 -x+1,-y+1,-z

Table 5. Anisotropic displacement parameters ($Å^2$x 10^4) for TRY9 (CCDC No. 142964). The anisotropic displacement factor exponent takes the form: $-2\pi^2$ [h^2 $a^{*2}U^{11}$ + ... + 2 h k a* b* U^{12}]

	U^{11}	U^{22}	U^{33}	U^{23}	U^{13}	U^{12}
Ni(1)	232(3)	199(3)	179(3)	10(2)	56(2)	11(2)
Ni(2)	220(3)	230(3)	238(3)	17(2)	35(2)	-3(2)
O(1)	225(14)	224(15)	155(13)	-10(11)	30(11)	-13(12)
O(2)	231(15)	261(15)	245(15)	4(12)	29(11)	-21(12)
O(3)	298(16)	260(15)	220(14)	-4(13)	12(12)	33(15)
O(4)	284(14)	215(14)	221(14)	7(14)	36(13)	-26(13)
N(1)	156(17)	172(17)	186(17)	-10(13)	20(13)	-9(14)
N(2)	204(17)	230(20)	245(18)	6(14)	34(14)	18(15)
N(100)	700(80)	2450(170)	1170(100)	-580(100)	-80(80)	330(100)
C(100)	650(50)	1470(70)	840(40)	-300(40)	140(50)	100(60)
C(1)	190(20)	200(20)	210(20)	44(18)	16(17)	-87(18)
C(2)	170(20)	200(20)	180(20)	-5(17)	33(16)	-12(17)
C(3)	340(20)	210(20)	240(20)	7(19)	29(19)	-51(19)
C(4)	350(30)	230(30)	340(30)	-10(20)	40(20)	80(20)
C(5)	320(30)	320(30)	250(20)	-90(20)	130(20)	30(20)
C(6)	210(20)	190(20)	180(20)	-61(17)	20(16)	-42(17)
C(7)	130(20)	180(20)	220(20)	-42(17)	-3(16)	-71(17)
C(8)	200(20)	220(20)	210(20)	-71(17)	74(17)	9(17)
C(9)	280(20)	200(20)	210(20)	-36(17)	46(18)	38(18)
C(10)	310(30)	360(30)	220(20)	-30(20)	-16(19)	-70(20)
C(11)	290(30)	530(30)	290(30)	20(20)	-40(20)	-110(20)
C(12)	210(30)	350(30)	470(30)	-20(20)	90(20)	-60(20)
C(13)	340(30)	240(20)	250(20)	40(20)	120(20)	0(20)
C(14)	240(20)	180(20)	230(20)	-53(17)	68(18)	44(17)
C(15)	390(30)	180(20)	190(20)	14(18)	80(20)	57(19)
C(16)	280(20)	210(20)	240(20)	-90(18)	16(18)	33(19)
C(17)	440(30)	300(30)	260(30)	-50(20)	0(20)	20(20)
C(18)	390(30)	420(30)	390(30)	-120(20)	-120(30)	50(20)
C(19)	240(30)	430(30)	470(30)	-180(20)	0(20)	-70(20)
C(20)	310(30)	300(30)	230(20)	-60(20)	20(20)	-10(20)
C(21)	260(20)	200(20)	210(20)	-64(17)	61(18)	28(18)
C(22)	210(20)	170(20)	180(20)	23(16)	42(16)	6(17)
C(23)	260(20)	250(20)	180(20)	29(17)	10(17)	33(18)
C(24)	190(20)	370(30)	260(20)	12(19)	77(19)	20(20)
C(25)	270(20)	370(30)	270(20)	-40(20)	120(20)	-20(20)
C(26)	350(30)	330(30)	210(20)	-70(20)	-1(19)	-60(20)
C(27)	210(20)	190(20)	210(20)	-2(17)	69(17)	4(17)
C(28)	230(20)	440(30)	160(20)	30(20)	36(18)	-40(20)
C(29)	300(30)	560(40)	330(30)	90(30)	10(20)	0(20)
C(30)	330(30)	510(30)	310(30)	-110(20)	50(20)	-120(30)
C(31)	240(20)	270(20)	250(20)	-70(20)	36(18)	-40(19)
C(32)	240(30)	390(30)	790(40)	140(30)	-60(30)	-100(20)
C(33)	260(30)	670(40)	460(30)	140(30)	60(20)	120(30)
C(34)	220(20)	260(30)	270(20)	93(19)	18(18)	-20(19)
C(35)	180(20)	250(20)	220(20)	47(18)	-50(16)	-5(18)
C(36)	250(20)	330(30)	260(20)	80(20)	-9(19)	-80(20)
C(37)	320(20)	270(30)	310(20)	40(20)	-22(19)	-110(20)

C(38)	300(20)	330(30)	280(20)	-30(20)	-30(20)	-30(20)
C(39)	180(20)	320(20)	190(20)	-7(19)	-10(16)	-38(19)
C(40)	160(20)	210(20)	260(20)	16(18)	-39(17)	26(18)
C(41)	220(20)	220(20)	210(20)	-60(17)	9(17)	-37(17)
C(42)	280(20)	190(20)	280(20)	18(17)	25(18)	-28(18)
C(43)	290(30)	300(30)	380(30)	40(20)	-10(20)	-20(20)
C(44)	300(30)	450(30)	550(30)	140(20)	-90(20)	-10(20)
C(45)	200(30)	630(40)	640(30)	220(30)	-80(20)	-70(20)
C(46)	290(30)	490(30)	620(30)	140(30)	30(20)	-70(20)
C(47)	280(20)	300(30)	390(20)	-30(20)	59(19)	0(20)
C(48)	400(30)	260(20)	270(20)	7(19)	110(20)	-30(20)
C(49)	400(30)	230(20)	240(20)	-54(18)	38(19)	50(20)
C(50)	520(30)	290(20)	200(20)	-30(20)	30(20)	0(20)
C(51)	650(30)	330(30)	220(20)	-30(20)	0(20)	70(30)
C(52)	410(30)	420(30)	290(30)	-40(20)	-60(20)	60(20)
C(53)	260(20)	400(30)	290(20)	20(20)	-9(19)	20(20)
C(54)	350(20)	270(20)	210(20)	-60(20)	48(18)	0(20)
C(55)	410(30)	190(20)	260(20)	42(18)	170(20)	-50(19)
C(56)	390(30)	250(20)	270(20)	64(19)	70(20)	-40(20)
C(57)	560(30)	300(30)	240(30)	-10(20)	70(20)	-50(20)
C(58)	730(40)	260(30)	360(30)	-10(20)	310(30)	-10(20)
C(59)	480(30)	270(30)	500(30)	70(20)	240(30)	50(20)
C(60)	340(20)	240(20)	420(30)	80(20)	130(20)	0(20)
C(61)	370(30)	450(30)	230(20)	0(20)	30(20)	20(20)
C(62)	430(30)	430(30)	400(30)	20(30)	10(30)	160(30)
C(63)	570(40)	560(40)	390(30)	-20(30)	-40(30)	-40(30)
C(64)	270(20)	410(30)	420(30)	60(20)	80(20)	100(20)
C(65)	580(40)	550(40)	720(40)	210(30)	-70(40)	-20(30)
C(66)	370(30)	770(50)	820(50)	130(40)	70(30)	-110(30)

Table 6. Hydrogen coordinates (x 10^4) and isotropic displacement parameters (Å^{2}x 10^3) for TRY9 (CCDC No. 142964).

	x	y	z	U_{iso}
H(3OH)	470(40)	8120(20)	2136(13)	50
H(4OH)	2220(40)	8180(20)	1086(12)	50
H(1)	400(30)	10279(13)	913(9)	0(8)
H(3)	-1120(30)	11078(14)	1169(10)	14(9)
H(4)	-2510(40)	11460(16)	1734(11)	32(12)
H(5)	-2790(30)	10902(16)	2337(11)	25(11)
H(10)	-4270(30)	9748(14)	2056(10)	18(9)
H(11)	-6420(30)	9247(15)	2182(10)	14(10)
H(12)	-6920(40)	8770(19)	2828(13)	54(15)
H(13)	-5190(30)	8694(14)	3422(10)	9(9)
H(15)	-2690(30)	8947(14)	3734(10)	8(9)
H(17)	-220(30)	9118(15)	4080(10)	19(10)
H(18)	2050(40)	9547(15)	4009(11)	23(10)
H(19)	2610(30)	10099(14)	3359(9)	9(9)
H(20)	810(30)	10232(13)	2779(9)	1(8)
H(24)	4810(30)	9376(15)	195(10)	21(10)
H(25)	3390(30)	8872(15)	-375(11)	28(10)
H(26)	970(30)	8643(14)	-254(10)	14(9)
H(28)	3940(30)	9657(12)	1318(9)	2(8)
H(31)	-1080(30)	9062(15)	692(10)	26(10)
H(34)	-860(30)	6045(14)	1886(9)	14(9)
H(36)	-1000(30)	5295(15)	1387(10)	23(10)
H(37)	-430(30)	4733(15)	673(10)	23(9)
H(38)	1030(40)	5382(16)	160(12)	44(12)
H(43)	3890(30)	6029(14)	987(10)	16(9)
H(44)	6370(40)	6054(16)	1172(11)	38(11)
H(45)	7940(40)	6645(17)	682(11)	46(12)
H(46)	6910(40)	7163(18)	8(13)	58(14)
H(48)	4830(30)	7481(15)	-496(10)	28(9)
H(50)	2700(40)	7735(16)	-1006(11)	41(11)
H(51)	140(40)	7597(18)	-1205(12)	48(13)
H(52)	-1570(30)	6977(14)	-749(9)	20(9)
H(53)	-520(40)	6510(17)	-120(12)	43(12)
H(57)	680(40)	7357(16)	3363(11)	30(11)
H(58)	-1640(30)	7884(15)	3370(11)	29(11)
H(59)	-3330(40)	7818(16)	2702(11)	34(11)
H(61)	2390(40)	6869(18)	2430(11)	41(11)
H(64)	-2510(40)	7175(17)	1664(12)	40(12)
H(29A)	6180(40)	9731(19)	798(13)	50(15)
H(30A)	4700(40)	10725(17)	1247(12)	45(12)
H(32A)	-640(40)	7868(18)	199(13)	58(14)
H(33A)	-1710(40)	9578(19)	55(12)	45(13)
H(62A)	1360(30)	5962(16)	3041(11)	30(11)
H(63A)	3250(40)	7498(18)	3091(11)	34(12)
H(65A)	-3560(40)	8339(18)	1916(12)	49(14)
H(66A)	-4400(40)	6700(20)	2122(14)	70(16)
H(29B)	5970(30)	9079(16)	1085(10)	22(9)
H(30B)	3100(40)	10684(17)	1059(12)	43(12)

H(32B)	-2010(40)	8021(15)	543(10)	31(10)
H(33B)	-2760(40)	8978(17)	106(11)	38(11)
H(62B)	2820(40)	5851(17)	2793(11)	35(12)
H(63B)	4190(40)	6855(18)	2990(11)	49(12)
H(65B)	-3680(40)	8090(19)	1383(13)	61(14)
H(66B)	-5040(50)	7070(20)	1736(15)	80(20)
H(29C)	6400(40)	9824(19)	1342(14)	66(14)
H(30C)	4340(40)	10672(17)	693(12)	43(12)
H(32C)	-320(50)	7945(19)	797(14)	71(15)
H(33C)	-1560(50)	8820(20)	-205(14)	64(17)
H(62C)	1220(40)	5856(17)	2492(13)	48(13)
H(63C)	2700(30)	6893(16)	3379(11)	32(10)
H(65C)	-1940(50)	8170(20)	1566(15)	97(18)
H(66C)	-4960(40)	7553(18)	2201(12)	46(13)

Appendix E

X-Ray Analysis of

$(^{H,H}Sal)_2Ni$

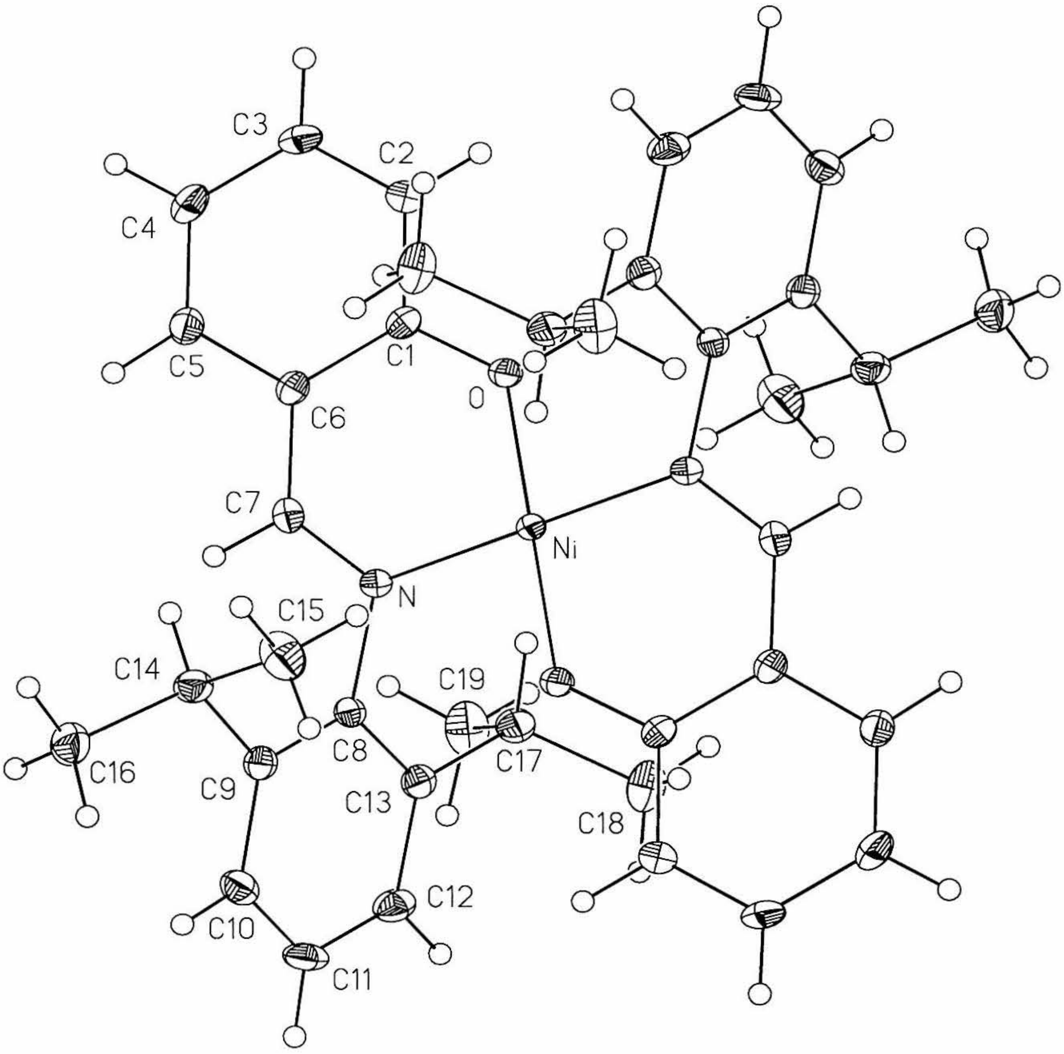

Table 1. Crystal data and structure refinement for TRY1 (CCDC No. 162674).

Empirical formula	$C_{38}H_{44}N_2NiO_2$	
Formula weight	619.46	
Crystallization Solvent	Acetonitrile	
Crystal Habit	Rhomboid	
Crystal size	0.370 x 0.270 x 0.185 mm^3	
Crystal color	Olive green	

Data Collection

Preliminary Photos	None	
Type of diffractometer	CCD area detector	
Wavelength	0.71073 Å MoKα	
Data Collection Temperature	93 K	
θ range for 7378 reflections used in lattice determination	2.24 to 27.73°	
Unit cell dimensions	a = 8.0050(5) Å	α= 113.5190(10)°
	b = 10.1054(6) Å	β= 97.4260(10)°
	c = 11.0123(7) Å	γ = 97.6730(10)°
Volume	793.01(8) Å^3	
Z	1	
Crystal system	Triclinic	
Space group	P-1	
Density (calculated)	1.297 Mg/m^3	
F(000)	330	
Data collection program	Bruker SMART	
θ range for data collection	2.06 to 27.73°	
Completeness to θ = 27.73°	90.5 %	
Index ranges	$-9 \leq h \leq 9$, $-12 \leq k \leq 12$, $-14 \leq l \leq 14$	
Data collection scan type	ω scans at 4 ϕ settings	
Data reduction program	Bruker SAINT v. 6.2	
Reflections collected	8648	
Independent reflections	3382 [R_{int}= 0.0346]	
Absorption coefficient	0.648 mm^{-1}	
Absorption correction	None	

Table 1 (cont.)

Structure Solution and Refinement

Structure solution program	SHELXS-97 (Sheldrick, 1990)
Primary solution method	Direct methods
Secondary solution method	Direct methods
Hydrogen placement	Difference Fourier map
Structure refinement program	SHELXL-97 (Sheldrick, 1997)
Refinement method	Full matrix least-squares on F^2
Data / restraints / parameters	3382 / 0 / 284
Treatment of hydrogen atoms	Unrestrained
Goodness-of-fit on F^2	2.406
Final R indices [$I>2\sigma(I)$, 3260 reflections]	$R1 = 0.0288$, $wR2 = 0.0711$
R indices (all data)	$R1 = 0.0297$, $wR2 = 0.0713$
Type of weighting scheme used	Sigma
Weighting scheme used	$w=1/\sigma^2(Fo^2)$
Max shift/error	0.000
Average shift/error	0.000
Largest diff. peak and hole	0.471 and -0.267 e.Å^{-3}

Special Refinement Details

Refinement of F^2 against ALL reflections. The weighted R-factor (wR) and goodness of fit (S) are based on F^2, conventional R-factors (R) are based on F, with F set to zero for negative F^2. The threshold expression of $F^2 > 2\sigma(F^2)$ is used only for calculating R-factors(gt) etc. and is not relevant to the choice of reflections for refinement. R-factors based on F^2 are statistically about twice as large as those based on F, and R-factors based on ALL data will be even larger.

All esds (except the esd in the dihedral angle between two l.s. planes) are estimated using the full covariance matrix. The cell esds are taken into account individually in the estimation of esds in distances, angles and torsion angles; correlations between esds in cell parameters are only used when they are defined by crystal symmetry. An approximate (isotropic) treatment of cell esds is used for estimating esds involving l.s. planes.

Table 2. Atomic coordinates (x 10^4) and equivalent isotropic displacement parameters (Å^{2}x 10^3) for TRY1 (CCDC No. 162674). U(eq) is defined as the trace of the orthogonalized U^{ij} tensor.

	x	y	z	U_{eq}
Ni	5000	5000	5000	11(1)
O	5996(1)	3478(1)	4060(1)	16(1)
N	5462(1)	4733(1)	6623(1)	12(1)
C(1)	6502(2)	2459(1)	4384(1)	13(1)
C(2)	7057(2)	1300(2)	3392(2)	17(1)
C(3)	7594(2)	195(2)	3675(2)	18(1)
C(4)	7620(2)	188(2)	4950(2)	19(1)
C(5)	7092(2)	1305(2)	5926(2)	17(1)
C(6)	6532(2)	2460(1)	5671(1)	13(1)
C(7)	6067(2)	3635(1)	6727(1)	13(1)
C(8)	5171(2)	5821(1)	7877(1)	13(1)
C(9)	3735(2)	5499(1)	8398(1)	15(1)
C(10)	3521(2)	6590(2)	9609(1)	17(1)
C(11)	4663(2)	7939(2)	10252(2)	19(1)
C(12)	6048(2)	8235(2)	9706(2)	18(1)
C(13)	6331(2)	7182(1)	8500(1)	15(1)
C(14)	2428(2)	4046(2)	7646(2)	18(1)
C(15)	1258(2)	4034(2)	6426(2)	26(1)
C(16)	1350(2)	3664(2)	8558(2)	24(1)
C(17)	7878(2)	7518(2)	7921(2)	18(1)
C(18)	7925(2)	8935(2)	7712(2)	26(1)
C(19)	9548(2)	7598(2)	8810(2)	28(1)

Table 3. Selected bond lengths [Å] and angles [°] for TRY1 (CCDC No. 162674).

Ni-O	1.8285(9)	O-Ni-O#1	180.0
Ni-O#1	1.8285(9)	O-Ni-N	93.03(4)
Ni-N	1.9087(11)	O#1-Ni-N	86.97(4)
Ni-N#1	1.9087(11)	O-Ni-N#1	86.97(4)
		O#1-Ni-N#1	93.03(4)
		N-Ni-N#1	180.0

Symmetry transformations used to generate equivalent atoms:
#1 -x+1,-y+1,-z+1

Table 4. Bond lengths [Å] and angles [°] for TRY1 (CCDC No. 162674).

Ni-O	1.8285(9)	O#1-Ni-N	86.97(4)
Ni-O#1	1.8285(9)	O-Ni-N#1	86.97(4)
Ni-N	1.9087(11)	O#1-Ni-N#1	93.03(4)
Ni-N#1	1.9087(11)	N-Ni-N#1	180.0
O-C(1)	1.3107(15)	C(1)-O-Ni	130.01(9)
N-C(7)	1.3074(16)	C(7)-N-C(8)	114.96(11)
N-C(8)	1.4528(16)	C(7)-N-Ni	125.34(9)
C(1)-C(6)	1.4147(19)	C(8)-N-Ni	119.69(8)
C(1)-C(2)	1.4159(18)	O-C(1)-C(6)	123.54(12)
C(2)-C(3)	1.3785(19)	O-C(1)-C(2)	118.18(12)
C(2)-H(2)	0.955(15)	C(6)-C(1)-C(2)	118.28(12)
C(3)-C(4)	1.404(2)	C(3)-C(2)-C(1)	120.63(13)
C(3)-H(3)	0.903(16)	C(3)-C(2)-H(2)	121.3(9)
C(4)-C(5)	1.373(2)	C(1)-C(2)-H(2)	118.0(9)
C(4)-H(4)	0.967(18)	C(2)-C(3)-C(4)	121.31(13)
C(5)-C(6)	1.4187(18)	C(2)-C(3)-H(3)	118.1(10)
C(5)-H(5)	0.959(15)	C(4)-C(3)-H(3)	120.6(10)
C(6)-C(7)	1.4242(18)	C(5)-C(4)-C(3)	118.98(13)
C(7)-H(7)	0.967(16)	C(5)-C(4)-H(4)	119.0(11)
C(8)-C(13)	1.4019(19)	C(3)-C(4)-H(4)	122.0(11)
C(8)-C(9)	1.4059(19)	C(4)-C(5)-C(6)	121.26(13)
C(9)-C(10)	1.3998(19)	C(4)-C(5)-H(5)	120.9(9)
C(9)-C(14)	1.528(2)	C(6)-C(5)-H(5)	117.8(9)
C(10)-C(11)	1.387(2)	C(1)-C(6)-C(5)	119.54(12)
C(10)-H(10)	0.932(16)	C(1)-C(6)-C(7)	120.75(11)
C(11)-C(12)	1.381(2)	C(5)-C(6)-C(7)	119.67(12)
C(11)-H(11)	0.897(16)	N-C(7)-C(6)	126.27(12)
C(12)-C(13)	1.4003(19)	N-C(7)-H(7)	116.8(9)
C(12)-H(12)	0.949(17)	C(6)-C(7)-H(7)	116.9(9)
C(13)-C(17)	1.5235(19)	C(13)-C(8)-C(9)	122.60(12)
C(14)-C(15)	1.531(2)	C(13)-C(8)-N	117.70(12)
C(14)-C(16)	1.5319(19)	C(9)-C(8)-N	119.68(12)
C(14)-H(14)	0.956(14)	C(10)-C(9)-C(8)	117.13(13)
C(15)-H(15A)	0.945(19)	C(10)-C(9)-C(14)	121.45(12)
C(15)-H(15B)	0.969(17)	C(8)-C(9)-C(14)	121.37(12)
C(15)-H(15C)	0.968(18)	C(11)-C(10)-C(9)	121.28(13)
C(16)-H(16A)	0.972(17)	C(11)-C(10)-H(10)	118.9(10)
C(16)-H(16B)	0.989(18)	C(9)-C(10)-H(10)	119.8(10)
C(16)-H(16C)	0.972(18)	C(12)-C(11)-C(10)	120.35(13)
C(17)-C(19)	1.524(2)	C(12)-C(11)-H(11)	118.9(10)
C(17)-C(18)	1.5345(19)	C(10)-C(11)-H(11)	120.7(10)
C(17)-H(17)	0.957(17)	C(11)-C(12)-C(13)	120.85(14)
C(18)-H(18A)	1.009(18)	C(11)-C(12)-H(12)	119.7(10)
C(18)-H(18B)	0.97(2)	C(13)-C(12)-H(12)	119.5(10)
C(18)-H(18C)	0.969(18)	C(12)-C(13)-C(8)	117.77(13)
C(19)-H(19A)	0.977(17)	C(12)-C(13)-C(17)	120.19(13)
C(19)-H(19B)	1.03(2)	C(8)-C(13)-C(17)	122.03(12)
C(19)-H(19C)	0.955(19)	C(9)-C(14)-C(15)	111.35(12)
		C(9)-C(14)-C(16)	113.14(13)
O-Ni-O#1	180.0	C(15)-C(14)-C(16)	110.38(13)
O-Ni-N	93.03(4)	C(9)-C(14)-H(14)	105.7(9)

C(15)-C(14)-H(14)	109.0(9)	C(19)-C(17)-C(18)	110.84(13)
C(16)-C(14)-H(14)	107.0(8)	C(13)-C(17)-H(17)	107.7(10)
C(14)-C(15)-H(15A)	111.3(11)	C(19)-C(17)-H(17)	107.7(10)
C(14)-C(15)-H(15B)	111.0(10)	C(18)-C(17)-H(17)	107.5(10)
H(15A)-C(15)-H(15B)	107.7(14)	C(17)-C(18)-H(18A)	109.8(10)
C(14)-C(15)-H(15C)	112.2(11)	C(17)-C(18)-H(18B)	110.0(11)
H(15A)-C(15)-H(15C)	109.3(15)	H(18A)-C(18)-H(18B)	108.8(15)
H(15B)-C(15)-H(15C)	105.1(14)	C(17)-C(18)-H(18C)	110.6(10)
C(14)-C(16)-H(16A)	111.4(10)	H(18A)-C(18)-H(18C)	110.4(14)
C(14)-C(16)-H(16B)	109.0(10)	H(18B)-C(18)-H(18C)	107.2(15)
H(16A)-C(16)-H(16B)	106.1(14)	C(17)-C(19)-H(19A)	112.2(10)
C(14)-C(16)-H(16C)	110.7(10)	C(17)-C(19)-H(19B)	110.3(11)
H(16A)-C(16)-H(16C)	106.5(14)	H(19A)-C(19)-H(19B)	109.3(15)
H(16B)-C(16)-H(16C)	113.1(14)	C(17)-C(19)-H(19C)	110.5(11)
C(13)-C(17)-C(19)	110.84(12)	H(19A)-C(19)-H(19C)	108.8(15)
C(13)-C(17)-C(18)	111.98(12)	H(19B)-C(19)-H(19C)	105.4(15)

Symmetry transformations used to generate equivalent atoms:
#1 -x+1,-y+1,-z+1

Table 5. Anisotropic displacement parameters ($Å^2 x 10^4$) for TRY1 (CCDC No. 162674). The anisotropic displacement factor exponent takes the form: $-2\pi^2$ [$h^2 a^{*2}U^{11}$ + ... + 2 h k a* b* U^{12}]

	U^{11}	U^{22}	U^{33}	U^{23}	U^{13}	U^{12}
Ni	152(2)	99(1)	97(1)	42(1)	32(1)	45(1)
O	235(6)	144(5)	115(5)	59(4)	51(4)	87(4)
N	140(6)	105(5)	108(6)	35(5)	27(5)	23(5)
C(1)	109(7)	109(6)	146(7)	46(6)	6(6)	14(5)
C(2)	200(8)	158(7)	146(8)	52(6)	54(6)	47(6)
C(3)	206(8)	133(7)	190(8)	31(6)	65(7)	72(6)
C(4)	204(8)	143(7)	253(8)	107(6)	48(7)	65(6)
C(5)	180(8)	156(7)	180(8)	90(6)	43(6)	39(6)
C(6)	113(7)	119(6)	152(7)	61(6)	14(6)	10(5)
C(7)	131(7)	147(7)	130(7)	72(6)	20(6)	16(6)
C(8)	173(7)	133(6)	84(7)	51(6)	9(6)	59(6)
C(9)	167(7)	150(6)	136(7)	74(6)	22(6)	57(6)
C(10)	187(8)	217(7)	150(7)	88(6)	63(6)	86(6)
C(11)	252(8)	187(7)	107(7)	14(6)	32(6)	100(6)
C(12)	215(8)	135(7)	151(8)	26(6)	-5(6)	33(6)
C(13)	168(7)	145(6)	123(7)	61(6)	1(6)	41(6)
C(14)	184(8)	150(7)	196(8)	59(6)	80(6)	43(6)
C(15)	221(9)	294(9)	213(9)	96(7)	21(7)	-51(8)
C(16)	256(9)	220(8)	283(9)	139(7)	118(8)	59(7)
C(17)	201(8)	140(7)	149(8)	35(6)	22(6)	2(6)
C(18)	243(9)	245(8)	326(10)	179(8)	46(8)	16(7)
C(19)	203(9)	360(10)	343(10)	224(9)	62(8)	70(7)

Table 6. Hydrogen coordinates (x 10^4) and isotropic displacement parameters ($\AA^2$x 10^3) for TRY1 (CCDC No. 162674).

	x	y	z	U_{iso}
H(2)	7036(19)	1304(15)	2525(16)	16(4)
H(3)	7919(19)	-536(17)	3013(16)	20(4)
H(4)	7990(20)	-584(19)	5158(19)	37(5)
H(5)	7125(19)	1345(15)	6814(16)	19(4)
H(7)	6250(19)	3639(16)	7614(16)	16(4)
H(10)	2570(20)	6430(16)	9975(16)	19(4)
H(11)	4480(20)	8650(17)	11004(16)	20(4)
H(12)	6810(20)	9168(18)	10145(17)	28(5)
H(14)	3091(18)	3300(15)	7336(15)	12(4)
H(17)	7780(20)	6721(18)	7053(17)	27(4)
H(15A)	1900(20)	4208(19)	5825(18)	36(5)
H(16A)	580(20)	4346(18)	8864(17)	27(4)
H(18A)	8960(20)	9117(18)	7321(17)	31(5)
H(19A)	10560(20)	7816(18)	8458(17)	30(4)
H(15B)	580(20)	4791(18)	6708(16)	23(4)
H(16B)	600(20)	2680(20)	8029(18)	33(5)
H(18B)	6890(30)	8841(19)	7092(19)	41(5)
H(19B)	9660(20)	8380(20)	9780(20)	40(5)
H(15C)	420(20)	3120(20)	5939(18)	36(5)
H(16C)	2090(20)	3736(18)	9366(18)	28(5)
H(18C)	7960(20)	9770(20)	8558(19)	33(5)
H(19C)	9540(20)	6690(20)	8891(18)	39(5)

Appendix F

X-Ray Diffraction Analysis of

$(^{\text{Anthr,H}}$Sal)Ni(NCMe)Me

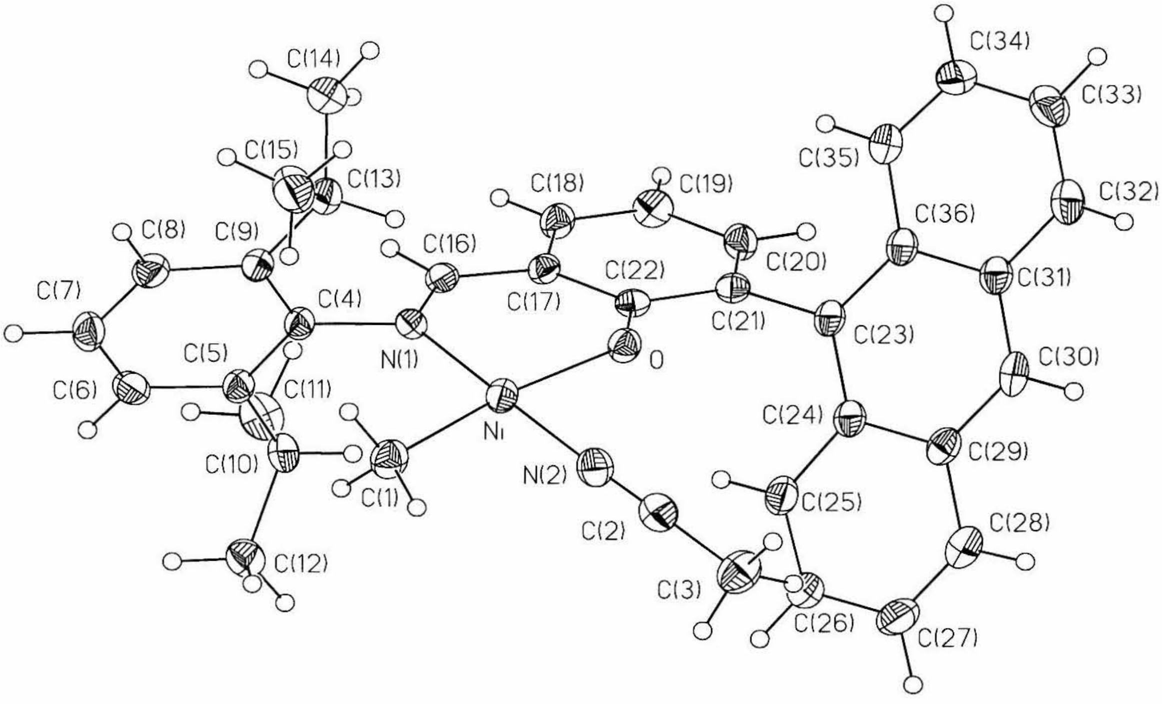

Table 1. Crystal data and structure refinement for EFC1 (CCDC No. 139263).

Empirical formula	$C_{36}H_{36}N_2NiO$	
Formula weight	571.38	
Crystallization Solvent	Acetonitrile	
Crystal Habit	Blade	
Crystal size	0.36 x 0.22 x 0.06 mm^3	
Crystal color	Dichroic yellow/brown	

Data Collection

Type of diffractometer	CCD area detector	
Wavelength	0.71073 Å MoKα	
Data Collection Temperature	98(2) K	
θ range for 5843 reflections used in lattice determination	2.66 to 23.30°	
Unit cell dimensions	a = 18.0982(13) Å	α= 90°
	b = 14.4000(10) Å	β= 90°
	c = 22.3830(16) Å	γ = 90°
Volume	5833.3(7) Å^3	
Z	8	
Crystal system	Orthorhombic	
Space group	Pbca	
Density (calculated)	1.301 Mg/m^3	
F(000)	2416	
Data collection program	Bruker SMART	
θ range for data collection	1.82 to 23.32°	
Completeness to θ = 23.32°	99.9 %	
Index ranges	$-20 \leq h \leq 20$, $-16 \leq k \leq 16$, $-24 \leq l \leq 24$	
Data collection scan type	ω scans at 4 ϕ settings	
Data reduction program	Bruker SAINT v 6.01	
Reflections collected	47311	
Independent reflections	4213 [R_{int}= 0.0614]	
Absorption coefficient	0.696 mm^{-1}	
Absorption correction	None	

Table 1 (cont.)

Structure Solution and Refinement

Structure solution program	SHELXS-97 (Sheldrick, 1990)
Primary solution method	Direct methods
Secondary solution method	Direct methods
Hydrogen placement	Difference Fourier map
Structure refinement program	SHELXL-97 (Sheldrick, 1997)
Refinement method	Full-matrix least-squares on F^2
Data / restraints / parameters	4213 / 0 / 505
Treatment of hydrogen atoms	Unrestrained
Goodness-of-fit on F^2	1.913
Final R indices [$I>2\sigma(I)$]	R1 = 0.0287, *w*R2 = 0.0518
R indices (all data)	R1 = 0.0387, *w*R2 = 0.0527
Type of weighting scheme used	Sigma
Weighting scheme used	$w=1/\sigma^2(Fo^2)$
Max shift/error	0.001
Average shift/error	0.000
Largest diff. peak and hole	0.274 and -0.309 e.Å^{-3}

Special Refinement Details

Refinement of F^2 against ALL reflections. The weighted R-factor (*w*R) and goodness of fit (S) are based on F^2, conventional R-factors (R) are based on F, with F set to zero for negative F^2. The threshold expression of $F^2 > 2\sigma(F^2)$ is used only for calculating R-factors(gt) etc. and is not relevant to the choice of reflections for refinement. R-factors based on F^2 are statistically about twice as large as those based on F, and R-factors based on ALL data will be even larger.

All esds (except the esd in the dihedral angle between two l.s. planes) are estimated using the full covariance matrix. The cell esds are taken into account individually in the estimation of esds in distances, angles and torsion angles; correlations between esds in cell parameters are only used when they are defined by crystal symmetry. An approximate (isotropic) treatment of cell esds is used for estimating esds involving l.s. planes.

Table 2. Atomic coordinates (x 10^4) and equivalent isotropic displacement parameters (Å^{2}x 10^3) for EFC1 (CCDC No. 139263). U(eq) is defined as the trace of the orthogonalized U^{ij} tensor.

	x	y	z	U_{eq}
Ni	1842(1)	542(1)	4277(1)	22(1)
N(1)	2579(1)	280(1)	3705(1)	20(1)
N(2)	1088(1)	822(1)	4812(1)	26(1)
O	1048(1)	168(1)	3768(1)	22(1)
C(1)	2550(1)	997(2)	4852(1)	27(1)
C(2)	583(1)	1031(2)	5082(1)	26(1)
C(3)	-59(2)	1325(2)	5420(1)	34(1)
C(4)	3364(1)	351(1)	3841(1)	21(1)
C(5)	3738(1)	1157(1)	3671(1)	22(1)
C(6)	4484(1)	1227(2)	3831(1)	26(1)
C(7)	4827(1)	537(2)	4151(1)	28(1)
C(8)	4445(1)	-251(2)	4312(1)	26(1)
C(9)	3704(1)	-364(1)	4162(1)	23(1)
C(10)	3365(1)	1951(2)	3346(1)	27(1)
C(11)	3588(2)	1992(2)	2695(1)	36(1)
C(12)	3516(2)	2879(2)	3652(1)	31(1)
C(13)	3291(1)	-1244(1)	4325(1)	29(1)
C(14)	3402(2)	-1972(2)	3839(2)	41(1)
C(15)	3498(2)	-1624(2)	4937(1)	41(1)
C(16)	2433(1)	98(1)	3150(1)	22(1)
C(17)	1730(1)	34(1)	2863(1)	19(1)
C(18)	1711(1)	-104(1)	2244(1)	24(1)
C(19)	1061(1)	-189(2)	1942(1)	26(1)
C(20)	398(1)	-158(1)	2264(1)	25(1)
C(21)	378(1)	-39(1)	2873(1)	20(1)
C(22)	1058(1)	65(1)	3194(1)	20(1)
C(23)	-344(1)	-53(1)	3198(1)	21(1)
C(24)	-599(1)	742(1)	3505(1)	21(1)
C(25)	-201(1)	1599(2)	3522(1)	26(1)
C(26)	-473(1)	2359(2)	3798(1)	31(1)
C(27)	-1162(1)	2326(2)	4101(1)	33(1)
C(28)	-1556(1)	1532(2)	4105(1)	30(1)
C(29)	-1301(1)	717(1)	3806(1)	24(1)
C(30)	-1717(1)	-89(2)	3788(1)	25(1)
C(31)	-1479(1)	-881(1)	3492(1)	23(1)
C(32)	-1910(1)	-1712(2)	3477(1)	29(1)
C(33)	-1671(1)	-2488(2)	3203(1)	32(1)
C(34)	-975(1)	-2485(2)	2917(1)	29(1)
C(35)	-547(1)	-1712(2)	2907(1)	26(1)
C(36)	-778(1)	-867(1)	3191(1)	21(1)

Table 3. Selected bond lengths [Å] and angles [°] for EFC1 (CCDC No. 139263).

Ni-N(2)	1.8588(19)
Ni-N(1)	1.8872(16)
Ni-O	1.9107(13)
Ni-C(1)	1.931(2)
N(2)-Ni-N(1)	177.34(7)
N(2)-Ni-O	83.87(6)
N(1)-Ni-O	94.12(6)
N(2)-Ni-C(1)	89.07(9)
N(1)-Ni-C(1)	92.88(9)
O-Ni-C(1)	172.72(9)

Table 4. Bond lengths [Å] and angles [°] for EFC1 (CCDC No. 139263).

Ni-N(2)	1.8588(19)	C(14)-H(14A)	0.96(3)
Ni-N(1)	1.8872(16)	C(14)-H(14B)	0.95(2)
Ni-O	1.9107(13)	C(14)-H(14C)	1.01(2)
Ni-C(1)	1.931(2)	C(15)-H(15A)	0.97(2)
N(1)-C(16)	1.299(3)	C(15)-H(15B)	1.03(2)
N(1)-C(4)	1.455(2)	C(15)-H(15C)	0.96(2)
N(2)-C(2)	1.136(3)	C(16)-C(17)	1.427(3)
O-C(22)	1.294(2)	C(16)-H(16)	0.928(18)
C(1)-H(1A)	0.96(2)	C(17)-C(18)	1.401(3)
C(1)-H(1B)	1.01(2)	C(17)-C(22)	1.426(3)
C(1)-H(1C)	0.98(2)	C(18)-C(19)	1.362(3)
C(2)-C(3)	1.451(3)	C(18)-H(18)	0.934(18)
C(3)-H(3A)	0.96(2)	C(19)-C(20)	1.400(3)
C(3)-H(3B)	0.96(2)	C(19)-H(19)	0.916(19)
C(3)-H(3C)	1.00(2)	C(20)-C(21)	1.375(3)
C(4)-C(9)	1.398(3)	C(20)-H(20)	0.928(18)
C(4)-C(5)	1.397(3)	C(21)-C(22)	1.432(3)
C(5)-C(6)	1.399(3)	C(21)-C(23)	1.495(3)
C(5)-C(10)	1.514(3)	C(23)-C(24)	1.414(3)
C(6)-C(7)	1.373(3)	C(23)-C(36)	1.411(3)
C(6)-H(6)	0.958(18)	C(24)-C(29)	1.439(3)
C(7)-C(8)	1.376(3)	C(24)-C(25)	1.429(3)
C(7)-H(7)	0.976(18)	C(25)-C(26)	1.351(3)
C(8)-C(9)	1.392(3)	C(25)-H(25)	0.919(18)
C(8)-H(8)	0.953(18)	C(26)-C(27)	1.419(3)
C(9)-C(13)	1.516(3)	C(26)-H(26)	0.935(19)
C(10)-C(12)	1.526(3)	C(27)-C(28)	1.348(3)
C(10)-C(11)	1.514(3)	C(27)-H(27)	0.97(2)
C(10)-H(10)	0.902(17)	C(28)-C(29)	1.426(3)
C(11)-H(11A)	1.01(2)	C(28)-H(28)	0.940(19)
C(11)-H(11B)	0.92(2)	C(29)-C(30)	1.385(3)
C(11)-H(11C)	0.96(2)	C(30)-C(31)	1.387(3)
C(12)-H(12A)	0.98(2)	C(30)-H(30)	0.920(18)
C(12)-H(12B)	0.981(19)	C(31)-C(36)	1.437(3)
C(12)-H(12C)	0.99(2)	C(31)-C(32)	1.428(3)
C(13)-C(15)	1.522(3)	C(32)-C(33)	1.346(3)
C(13)-C(14)	1.524(3)	C(32)-H(32)	0.87(2)
C(13)-H(13)	0.950(18)	C(33)-C(34)	1.414(3)

C(33)-H(33)	0.978(19)
C(34)-C(35)	1.357(3)
C(34)-H(34)	0.898(18)
C(35)-C(36)	1.435(3)
C(35)-H(35)	0.926(17)

N(2)-Ni-N(1)	177.34(7)
N(2)-Ni-O	83.87(6)
N(1)-Ni-O	94.12(6)
N(2)-Ni-C(1)	89.07(9)
N(1)-Ni-C(1)	92.88(9)
O-Ni-C(1)	172.72(9)
C(16)-N(1)-C(4)	114.45(17)
C(16)-N(1)-Ni	123.03(15)
C(4)-N(1)-Ni	122.29(13)
C(2)-N(2)-Ni	171.95(18)
C(22)-O-Ni	127.87(13)
Ni-C(1)-H(1A)	109.3(11)
Ni-C(1)-H(1B)	112.2(12)
H(1A)-C(1)-H(1B)	106.3(16)
Ni-C(1)-H(1C)	109.5(11)
H(1A)-C(1)-H(1C)	111.5(16)
H(1B)-C(1)-H(1C)	108.0(16)
N(2)-C(2)-C(3)	178.3(3)
C(2)-C(3)-H(3A)	113.4(13)
C(2)-C(3)-H(3B)	103.1(14)
H(3A)-C(3)-H(3B)	113(2)
C(2)-C(3)-H(3C)	107.5(14)
H(3A)-C(3)-H(3C)	107.8(19)
H(3B)-C(3)-H(3C)	112.4(19)
C(9)-C(4)-C(5)	122.51(19)
C(9)-C(4)-N(1)	119.11(17)
C(5)-C(4)-N(1)	118.30(18)
C(6)-C(5)-C(4)	117.3(2)
C(6)-C(5)-C(10)	119.88(19)
C(4)-C(5)-C(10)	122.82(18)
C(7)-C(6)-C(5)	121.1(2)
C(7)-C(6)-H(6)	119.8(11)
C(5)-C(6)-H(6)	119.1(11)
C(6)-C(7)-C(8)	120.4(2)
C(6)-C(7)-H(7)	120.6(11)
C(8)-C(7)-H(7)	119.0(11)
C(7)-C(8)-C(9)	121.1(2)
C(7)-C(8)-H(8)	120.9(11)
C(9)-C(8)-H(8)	117.9(11)
C(4)-C(9)-C(8)	117.55(19)
C(4)-C(9)-C(13)	121.42(18)
C(8)-C(9)-C(13)	121.01(19)
C(5)-C(10)-C(12)	111.52(19)
C(5)-C(10)-C(11)	112.0(2)
C(12)-C(10)-C(11)	110.4(2)
C(5)-C(10)-H(10)	106.5(11)
C(12)-C(10)-H(10)	106.6(11)
C(11)-C(10)-H(10)	109.6(11)
C(10)-C(11)-H(11A)	114.1(12)
C(10)-C(11)-H(11B)	109.9(13)
H(11A)-C(11)-H(11B)	107.8(18)
C(10)-C(11)-H(11C)	112.4(12)
H(11A)-C(11)-H(11C)	106.2(17)
H(11B)-C(11)-H(11C)	106.1(17)
C(10)-C(12)-H(12A)	108.9(11)
C(10)-C(12)-H(12B)	111.1(11)
H(12A)-C(12)-H(12B)	109.7(16)
C(10)-C(12)-H(12C)	114.0(12)
H(12A)-C(12)-H(12C)	107.2(17)
H(12B)-C(12)-H(12C)	105.8(17)
C(9)-C(13)-C(15)	113.29(19)
C(9)-C(13)-C(14)	109.7(2)
C(15)-C(13)-C(14)	111.3(2)
C(9)-C(13)-H(13)	109.8(10)
C(15)-C(13)-H(13)	105.4(11)
C(14)-C(13)-H(13)	107.1(11)
C(13)-C(14)-H(14A)	110.8(14)
C(13)-C(14)-H(14B)	112.7(13)
H(14A)-C(14)-H(14B)	108.4(19)
C(13)-C(14)-H(14C)	113.5(12)
H(14A)-C(14)-H(14C)	104.2(19)
H(14B)-C(14)-H(14C)	106.9(18)
C(13)-C(15)-H(15A)	108.8(13)
C(13)-C(15)-H(15B)	113.9(13)
H(15A)-C(15)-H(15B)	109.6(18)
C(13)-C(15)-H(15C)	109.9(14)
H(15A)-C(15)-H(15C)	106.9(19)
H(15B)-C(15)-H(15C)	107.6(19)
N(1)-C(16)-C(17)	128.7(2)
N(1)-C(16)-H(16)	115.4(11)
C(17)-C(16)-H(16)	115.8(11)
C(18)-C(17)-C(22)	119.83(19)
C(18)-C(17)-C(16)	118.5(2)
C(22)-C(17)-C(16)	121.65(19)
C(19)-C(18)-C(17)	121.7(2)
C(19)-C(18)-H(18)	118.7(12)
C(17)-C(18)-H(18)	119.6(12)
C(20)-C(19)-C(18)	118.8(2)
C(20)-C(19)-H(19)	119.8(12)
C(18)-C(19)-H(19)	121.4(12)
C(21)-C(20)-C(19)	122.5(2)
C(21)-C(20)-H(20)	118.6(12)
C(19)-C(20)-H(20)	118.9(12)
C(20)-C(21)-C(22)	119.2(2)
C(20)-C(21)-C(23)	120.25(19)
C(22)-C(21)-C(23)	120.50(18)
O-C(22)-C(17)	122.11(18)
O-C(22)-C(21)	119.91(18)
C(17)-C(22)-C(21)	117.97(19)
C(24)-C(23)-C(36)	119.76(18)
C(24)-C(23)-C(21)	120.72(18)
C(36)-C(23)-C(21)	119.52(18)

C(23)-C(24)-C(29)	119.74(18)	C(29)-C(30)-H(30)	119.5(11)
C(23)-C(24)-C(25)	123.20(19)	C(30)-C(31)-C(36)	119.13(19)
C(29)-C(24)-C(25)	117.04(19)	C(30)-C(31)-C(32)	122.0(2)
C(26)-C(25)-C(24)	121.8(2)	C(36)-C(31)-C(32)	118.9(2)
C(26)-C(25)-H(25)	119.7(11)	C(33)-C(32)-C(31)	122.0(2)
C(24)-C(25)-H(25)	118.4(11)	C(33)-C(32)-H(32)	121.1(13)
C(25)-C(26)-C(27)	120.8(2)	C(31)-C(32)-H(32)	116.8(13)
C(25)-C(26)-H(26)	119.6(12)	C(32)-C(33)-C(34)	119.4(2)
C(27)-C(26)-H(26)	119.6(12)	C(32)-C(33)-H(33)	121.2(11)
C(28)-C(27)-C(26)	119.8(2)	C(34)-C(33)-H(33)	119.3(11)
C(28)-C(27)-H(27)	119.5(12)	C(35)-C(34)-C(33)	121.2(2)
C(26)-C(27)-H(27)	120.7(12)	C(35)-C(34)-H(34)	120.4(12)
C(27)-C(28)-C(29)	121.5(2)	C(33)-C(34)-H(34)	118.4(12)
C(27)-C(28)-H(28)	122.4(12)	C(34)-C(35)-C(36)	121.5(2)
C(29)-C(28)-H(28)	116.1(12)	C(34)-C(35)-H(35)	120.1(11)
C(30)-C(29)-C(24)	119.18(19)	C(36)-C(35)-H(35)	118.4(11)
C(30)-C(29)-C(28)	121.8(2)	C(23)-C(36)-C(35)	123.12(19)
C(24)-C(29)-C(28)	119.0(2)	C(23)-C(36)-C(31)	119.90(19)
C(31)-C(30)-C(29)	122.3(2)	C(35)-C(36)-C(31)	116.96(19)
C(31)-C(30)-H(30)	118.2(11)		

Table 5. Anisotropic displacement parameters ($Å^2$x 10^4) for EFC1 (CCDC No. 139263). The anisotropic displacement factor exponent takes the form: $-2\pi^2$ [$h^2 a^{*2}U^{11}$ + ... + 2 h k a* b* U^{12}]

	U^{11}	U^{22}	U^{33}	U^{23}	U^{13}	U^{12}
Ni	176(2)	243(2)	237(2)	-13(1)	7(1)	7(1)
N(1)	177(10)	168(10)	243(11)	-6(8)	-15(8)	-13(7)
N(2)	245(11)	297(11)	245(11)	1(9)	-33(9)	-10(9)
O	190(8)	254(8)	205(9)	-17(7)	11(7)	8(6)
C(1)	241(14)	323(15)	255(16)	-8(13)	44(12)	2(12)
C(2)	274(14)	273(14)	237(14)	18(11)	-27(12)	-15(11)
C(3)	311(16)	388(18)	328(17)	8(15)	79(14)	40(13)
C(4)	155(12)	258(13)	225(12)	-70(10)	21(9)	-3(9)
C(5)	171(12)	257(13)	215(13)	-51(10)	26(10)	-4(10)
C(6)	247(14)	253(13)	288(14)	-76(12)	55(11)	-57(11)
C(7)	180(13)	382(14)	277(15)	-105(12)	-34(11)	-5(12)
C(8)	233(13)	257(14)	276(14)	-32(12)	-41(11)	47(10)
C(9)	173(12)	253(13)	265(14)	-64(11)	-6(10)	15(9)
C(10)	179(14)	291(14)	324(15)	-1(11)	24(11)	-53(10)
C(11)	368(18)	405(18)	312(17)	48(14)	-12(14)	-70(14)
C(12)	277(16)	252(15)	398(19)	18(13)	-7(14)	-33(12)
C(13)	194(14)	249(13)	417(15)	0(12)	-52(12)	16(10)
C(14)	289(17)	293(16)	640(20)	-112(15)	-55(15)	3(13)
C(15)	328(17)	339(17)	550(20)	89(15)	-91(15)	-54(14)
C(16)	184(13)	162(12)	312(16)	-2(11)	59(12)	-6(10)
C(17)	175(13)	166(11)	241(13)	16(10)	10(10)	13(9)
C(18)	200(14)	239(12)	272(15)	20(11)	54(11)	-4(10)
C(19)	285(15)	306(14)	193(15)	-4(11)	-12(12)	17(10)
C(20)	201(14)	237(13)	303(16)	14(11)	-57(12)	-3(10)
C(21)	204(13)	154(11)	245(14)	22(10)	-1(10)	9(9)
C(22)	219(13)	140(12)	254(14)	10(10)	-10(11)	15(9)
C(23)	163(12)	246(12)	209(13)	35(10)	-50(10)	29(10)
C(24)	179(12)	253(13)	211(13)	29(10)	-53(10)	19(10)
C(25)	182(14)	295(14)	315(15)	15(11)	-15(12)	19(11)
C(26)	243(14)	250(14)	429(16)	-21(13)	-56(12)	27(12)
C(27)	300(15)	323(15)	378(16)	-70(12)	-27(12)	104(12)
C(28)	219(14)	376(16)	303(15)	4(12)	13(12)	65(12)
C(29)	197(12)	293(14)	217(13)	15(11)	-26(10)	57(10)
C(30)	137(13)	382(15)	217(13)	54(11)	5(10)	1(11)
C(31)	189(12)	265(13)	230(13)	42(11)	-37(10)	13(10)
C(32)	199(14)	359(15)	313(15)	64(12)	15(12)	-43(12)
C(33)	299(15)	285(14)	374(15)	45(12)	-12(13)	-85(12)
C(34)	293(15)	236(14)	338(16)	-15(12)	-18(12)	24(12)
C(35)	189(14)	306(15)	271(14)	16(11)	-15(11)	13(11)
C(36)	169(12)	264(13)	206(13)	34(10)	-52(10)	23(10)

Table 6. Hydrogen coordinates (x 10^4) and isotropic displacement parameters (Å^{2}x 10^3) for EFC1 (CCDC No. 139263).

	x	y	z	U_{iso}
H(1A)	2292(10)	1248(13)	5190(9)	21(6)
H(1B)	2877(11)	485(15)	5012(9)	38(6)
H(1C)	2868(11)	1464(13)	4663(8)	26(6)
H(3A)	-275(12)	836(16)	5655(11)	55(8)
H(3B)	129(12)	1825(16)	5660(11)	49(8)
H(3C)	-440(13)	1538(16)	5127(11)	57(8)
H(6)	4755(10)	1771(12)	3717(8)	19(5)
H(7)	5347(11)	592(12)	4260(8)	25(5)
H(8)	4678(10)	-731(12)	4536(8)	18(5)
H(10)	2875(10)	1849(11)	3374(7)	6(5)
H(11A)	3442(11)	1428(16)	2457(9)	41(7)
H(11B)	4093(12)	2060(14)	2664(9)	33(7)
H(11C)	3377(10)	2515(15)	2492(9)	30(6)
H(12A)	4034(12)	3044(13)	3593(8)	29(6)
H(12B)	3198(11)	3370(13)	3489(8)	22(5)
H(12C)	3424(11)	2876(14)	4087(10)	39(7)
H(13)	2776(10)	-1120(12)	4346(8)	17(5)
H(14A)	3917(15)	-2118(16)	3793(10)	57(8)
H(14B)	3143(12)	-2530(15)	3917(9)	34(6)
H(14C)	3244(12)	-1755(15)	3427(10)	42(7)
H(15A)	4002(13)	-1849(15)	4922(9)	43(7)
H(15B)	3446(12)	-1145(17)	5279(11)	56(8)
H(15C)	3190(13)	-2147(17)	5033(10)	53(7)
H(16)	2841(10)	15(11)	2904(8)	13(5)
H(18)	2153(10)	-136(12)	2029(8)	21(6)
H(19)	1051(10)	-295(12)	1538(9)	18(6)
H(20)	-45(10)	-233(12)	2060(8)	19(6)
H(25)	249(10)	1630(11)	3332(8)	14(5)
H(26)	-204(11)	2913(13)	3792(8)	23(6)
H(27)	-1346(11)	2862(14)	4315(9)	29(6)
H(28)	-2010(11)	1477(13)	4307(8)	26(6)
H(30)	-2162(10)	-113(12)	3987(8)	14(5)
H(32)	-2334(11)	-1700(13)	3664(9)	24(6)
H(33)	-1959(10)	-3062(13)	3214(8)	26(6)
H(34)	-815(10)	-3014(13)	2748(8)	18(6)
H(35)	-97(10)	-1718(11)	2711(8)	13(5)

Appendix G

X-Ray Diffraction Analysis of

$({}^{\text{Anthr,H}}\text{Sal}^{\text{Ph}})_2\text{Ni(tmeda)}$

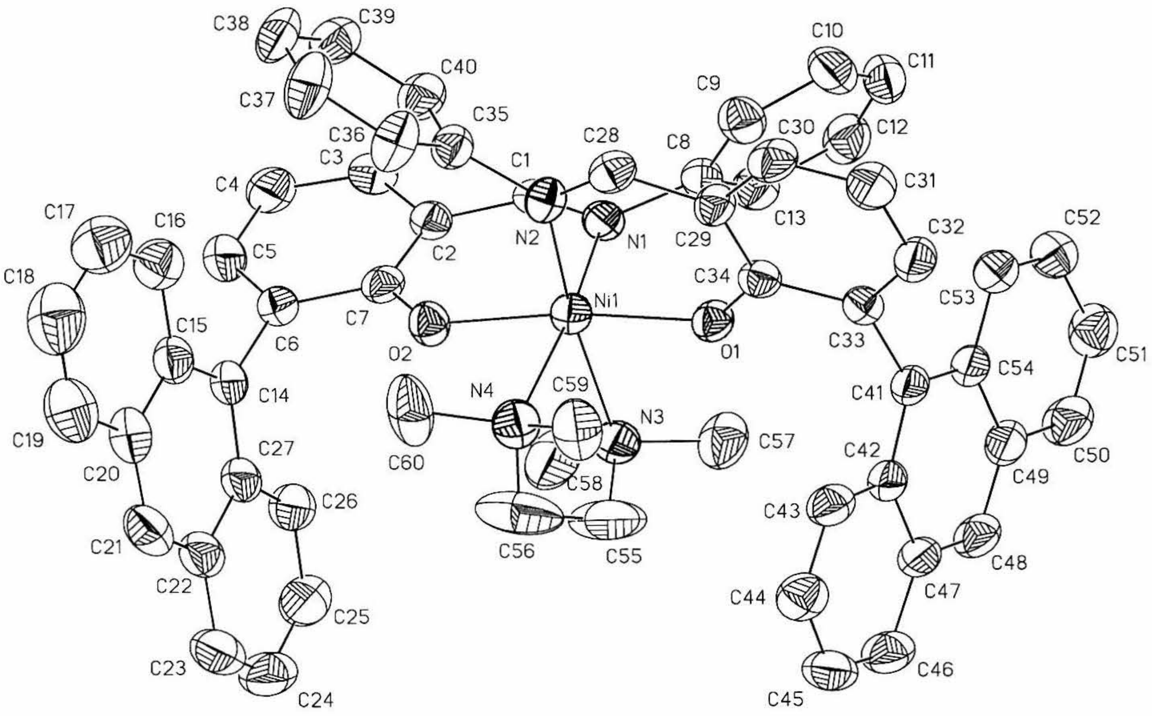

Table 1. Crystal data and structure refinement for TRY12 (CCDC 161495).

Empirical formula	$C_{60}H_{52}N_4O_2Ni$
Formula weight	919.77
Crystallization Solvent	CH_2Cl_2/CH_3C N
Crystal Habit	Needle
Crystal size	0.37 x 0.22 x 0.19 mm^3
Crystal color	Greenish yellow

Data Collection

Preliminary Photos	Rotation
Type of diffractometer	CCD area detector
Wavelength	0.71073 Å MoKα
Data Collection Temperature	98(2) K
θ range for 33100 reflections used in lattice determination	2.16 to 27.01°
Unit cell dimensions	a = 17.8013(6) Å b = 19.2789(6) Å c = 27.0247(9) Å
Volume	9274.6(5) $Å^3$
Z	8
Crystal system	Orthorhombic
Space group	Pbca
Density (calculated)	1.317 Mg/m^3
F(000)	3872
Data collection program	Bruker SMART
θ range for data collection	1.89 to 28.59°
Completeness to θ = 28.59°	94.4 %
Index ranges	-23 h 22, -25 k 25, -36 l 36
Data collection scan type	ω scans at 6 ϕ settings
Data reduction program	Bruker SAINT v6.2
Reflections collected	154074
Independent reflections	11208 [R_{int}= 0.0780]
Absorption coefficient	0.469 mm^{-1}
Absorption correction	None
Max. and min. transmission	0.9183 and 0.8471

Table 1 (cont.)

Structure Solution and Refinement

Structure solution program	SHELXS-97 (Sheldrick, 1990)
Primary solution method	Direct methods
Secondary solution method	Difference Fourier map
Hydrogen placement	Difference Fourier map
Structure refinement program	SHELXL-97 (Sheldrick, 1997)
Refinement method	Full matrix least-squares on F^2
Data / restraints / parameters	11208 / 0 / 812
Treatment of hydrogen atoms	Unrestrained
Goodness-of-fit on F^2	1.805
Final R indices [$I>2\sigma(I)$, 7057 reflections]	R1 = 0.0439, *w*R2 = 0.0566
R indices (all data)	R1 = 0.0833, *w*R2 = 0.0589
Type of weighting scheme used	Sigma
Weighting scheme used	$w=1/\sigma^2(Fo^2)$
Max shift/error	0.005
Average shift/error	0.000
Largest diff. peak and hole	1.016 and -0.510 e.Å^{-3}

Special Refinement Details

Refinement of F^2 against ALL reflections. The weighted R-factor (*w*R) and goodness of fit (S) are based on F^2, conventional R-factors (R) are based on F, with F set to zero for negative F^2. The threshold expression of $F^2 > 2\sigma(F^2)$ is used only for calculating R-factors(gt) etc. and is not relevant to the choice of reflections for refinement. R-factors based on F^2 are statistically about twice as large as those based on F, and R-factors based on ALL data will be even larger.

All esds (except the esd in the dihedral angle between two l.s. planes) are estimated using the full covariance matrix. The cell esds are taken into account individually in the estimation of esds in distances, angles and torsion angles; correlations between esds in cell parameters are only used when they are defined by crystal symmetry. An approximate (isotropic) treatment of cell esds is used for estimating esds involving l.s. planes.

Table 2. Atomic coordinates (x 10^4) and equivalent isotropic displacement parameters (Å^{2}x 10^3) for TRY12 (CCDC 161495). U(eq) is defined as the trace of the orthogonalized U^{ij} tensor.

	x	y	z	U_{eq}
Ni(1)	7254(1)	1538(1)	3826(1)	33(1)
O(1)	8132(1)	1583(1)	4284(1)	34(1)
O(2)	6391(1)	1621(1)	3356(1)	36(1)
N(1)	6521(1)	992(1)	4311(1)	33(1)
N(2)	7739(1)	616(1)	3524(1)	36(1)
N(3)	6939(1)	2560(1)	4172(1)	41(1)
N(4)	7821(1)	2214(1)	3272(1)	44(1)
C(1)	5819(1)	870(1)	4214(1)	34(1)
C(2)	5408(1)	1010(1)	3768(1)	32(1)
C(3)	4681(1)	730(1)	3730(1)	39(1)
C(4)	4247(1)	827(1)	3321(1)	45(1)
C(5)	4524(1)	1244(1)	2940(1)	45(1)
C(6)	5226(1)	1535(1)	2955(1)	34(1)
C(7)	5714(1)	1393(1)	3365(1)	32(1)
C(8)	6761(1)	730(1)	4782(1)	34(1)
C(9)	7345(1)	257(1)	4797(1)	42(1)
C(10)	7543(1)	-58(1)	5237(1)	48(1)
C(11)	7167(1)	102(1)	5668(1)	51(1)
C(12)	6605(1)	589(1)	5659(1)	49(1)
C(13)	6401(1)	901(1)	5218(1)	41(1)
C(14)	5499(1)	2012(1)	2559(1)	36(1)
C(15)	5830(1)	1752(1)	2126(1)	41(1)
C(16)	5906(1)	1029(1)	2037(1)	54(1)
C(17)	6209(2)	795(2)	1607(1)	71(1)
C(18)	6460(2)	1263(2)	1242(1)	76(1)
C(19)	6419(1)	1945(2)	1315(1)	64(1)
C(20)	6110(1)	2221(1)	1759(1)	46(1)
C(21)	6079(1)	2929(1)	1848(1)	50(1)
C(22)	5747(1)	3199(1)	2269(1)	43(1)
C(23)	5692(1)	3928(1)	2357(1)	54(1)
C(24)	5352(1)	4180(1)	2764(1)	58(1)
C(25)	5038(1)	3728(1)	3111(1)	52(1)
C(26)	5073(1)	3032(1)	3047(1)	43(1)
C(27)	5437(1)	2737(1)	2628(1)	37(1)
C(28)	8388(1)	372(1)	3658(1)	37(1)
C(29)	8895(1)	625(1)	4030(1)	34(1)
C(30)	9560(1)	250(1)	4110(1)	43(1)
C(31)	10074(1)	440(1)	4455(1)	48(1)
C(32)	9940(1)	1035(1)	4735(1)	43(1)
C(33)	9300(1)	1423(1)	4678(1)	33(1)
C(34)	8742(1)	1224(1)	4322(1)	32(1)
C(35)	7372(1)	206(1)	3152(1)	37(1)
C(36)	7707(1)	68(1)	2703(1)	54(1)
C(37)	7351(1)	-359(1)	2364(1)	62(1)
C(38)	6670(1)	-647(1)	2469(1)	54(1)
C(39)	6333(1)	-509(1)	2915(1)	48(1)
C(40)	6686(1)	-85(1)	3254(1)	42(1)

C(41)	9158(1)	2065(1)	4975(1)	34(1)
C(42)	9317(1)	2716(1)	4767(1)	36(1)
C(43)	9685(1)	2792(1)	4302(1)	40(1)
C(44)	9773(1)	3423(1)	4087(1)	46(1)
C(45)	9507(1)	4022(1)	4326(1)	50(1)
C(46)	9187(1)	3984(1)	4778(1)	47(1)
C(47)	9078(1)	3333(1)	5018(1)	37(1)
C(48)	8738(1)	3278(1)	5476(1)	43(1)
C(49)	8620(1)	2643(1)	5705(1)	39(1)
C(50)	8292(1)	2583(1)	6183(1)	49(1)
C(51)	8155(1)	1964(1)	6391(1)	52(1)
C(52)	8333(1)	1351(1)	6129(1)	50(1)
C(53)	8653(1)	1378(1)	5677(1)	44(1)
C(54)	8823(1)	2021(1)	5444(1)	35(1)
C(55)	7453(2)	3042(1)	3906(1)	85(1)
C(56)	7533(2)	2904(1)	3381(1)	85(1)
C(57)	7120(2)	2611(2)	4700(1)	57(1)
C(58)	6156(2)	2745(2)	4112(1)	74(1)
C(59)	8644(1)	2184(2)	3300(1)	59(1)
C(60)	7628(2)	2053(2)	2755(1)	71(1)

Table 3. Selected bond lengths [Å] and angles [°] for TRY12 (CCDC 161495).

Ni(1)-O(1)	1.9959(11)	O(1)-Ni(1)-O(2)	172.87(5)
Ni(1)-O(2)	1.9991(11)	O(1)-Ni(1)-N(1)	96.84(5)
Ni(1)-N(1)	2.1289(14)	O(2)-Ni(1)-N(1)	87.67(5)
Ni(1)-N(2)	2.1383(14)	O(1)-Ni(1)-N(2)	87.51(5)
Ni(1)-N(4)	2.2263(14)	O(2)-Ni(1)-N(2)	97.70(5)
Ni(1)-N(3)	2.2517(14)	N(1)-Ni(1)-N(2)	94.10(5)
		O(1)-Ni(1)-N(4)	92.10(5)
		O(2)-Ni(1)-N(4)	82.84(5)
		N(1)-Ni(1)-N(4)	168.98(6)
		N(2)-Ni(1)-N(4)	92.71(6)
		O(1)-Ni(1)-N(3)	84.20(5)
		O(2)-Ni(1)-N(3)	90.19(5)
		N(1)-Ni(1)-N(3)	91.34(5)
		N(2)-Ni(1)-N(3)	170.57(6)
		N(4)-Ni(1)-N(3)	83.13(6)

Table 4. Bond lengths [Å] and angles [°] for TRY12 (CCDC 161495).

Ni(1)-O(1)	1.9959(11)	C(19)-C(20)	1.424(3)
Ni(1)-O(2)	1.9991(11)	C(19)-H(19)	0.937(17)
Ni(1)-N(1)	2.1289(14)	C(20)-C(21)	1.388(3)
Ni(1)-N(2)	2.1383(14)	C(21)-C(22)	1.384(3)
Ni(1)-N(4)	2.2263(14)	C(21)-H(21)	0.933(15)
Ni(1)-N(3)	2.2517(14)	C(22)-C(23)	1.428(3)
O(1)-C(34)	1.2913(18)	C(22)-C(27)	1.429(2)
O(2)-C(7)	1.2839(18)	C(23)-C(24)	1.346(3)
N(1)-C(1)	1.298(2)	C(23)-H(23)	0.901(16)
N(1)-C(8)	1.435(2)	C(24)-C(25)	1.398(3)
N(2)-C(28)	1.299(2)	C(24)-H(24)	0.946(17)
N(2)-C(35)	1.437(2)	C(25)-C(26)	1.354(3)
N(3)-C(58)	1.448(3)	C(25)-H(25)	0.946(15)
N(3)-C(57)	1.466(3)	C(26)-C(27)	1.422(2)
N(3)-C(55)	1.489(3)	C(26)-H(26)	0.934(14)
N(4)-C(56)	1.456(3)	C(28)-C(29)	1.436(2)
N(4)-C(59)	1.467(3)	C(28)-H(28)	0.962(14)
N(4)-C(60)	1.474(3)	C(29)-C(30)	1.404(2)
C(1)-C(2)	1.436(2)	C(29)-C(34)	1.425(2)
C(1)-H(1)	0.978(13)	C(30)-C(31)	1.357(2)
C(2)-C(3)	1.407(2)	C(30)-H(30)	0.929(15)
C(2)-C(7)	1.423(2)	C(31)-C(32)	1.394(2)
C(3)-C(4)	1.363(2)	C(31)-H(31)	0.945(15)
C(3)-H(3)	0.981(13)	C(32)-C(33)	1.372(2)
C(4)-C(5)	1.396(3)	C(32)-H(32)	0.929(15)
C(4)-H(4)	0.939(15)	C(33)-C(34)	1.434(2)
C(5)-C(6)	1.371(2)	C(33)-C(41)	1.497(2)
C(5)-H(5)	0.916(14)	C(35)-C(40)	1.373(2)
C(6)-C(7)	1.433(2)	C(35)-C(36)	1.377(2)
C(6)-C(14)	1.493(2)	C(36)-C(37)	1.385(3)
C(8)-C(13)	1.379(2)	C(36)-H(36)	0.937(16)
C(8)-C(9)	1.384(2)	C(37)-C(38)	1.364(3)
C(9)-C(10)	1.382(2)	C(37)-H(37)	0.985(18)
C(9)-H(9)	0.955(14)	C(38)-C(39)	1.373(3)
C(10)-C(11)	1.378(3)	C(38)-H(38)	0.915(17)
C(10)-H(10)	0.948(15)	C(39)-C(40)	1.380(2)
C(11)-C(12)	1.372(3)	C(39)-H(39)	0.948(16)
C(11)-H(11)	0.953(16)	C(40)-H(40)	0.930(14)
C(12)-C(13)	1.384(3)	C(41)-C(54)	1.403(2)
C(12)-H(12)	0.933(15)	C(41)-C(42)	1.405(2)
C(13)-H(13)	0.921(14)	C(42)-C(43)	1.424(2)
C(14)-C(15)	1.403(2)	C(42)-C(47)	1.434(2)
C(14)-C(27)	1.415(2)	C(43)-C(44)	1.358(2)
C(15)-C(16)	1.422(3)	C(43)-H(43)	0.931(13)
C(15)-C(20)	1.431(2)	C(44)-C(45)	1.405(3)
C(16)-C(17)	1.357(3)	C(44)-H(44)	1.003(15)
C(16)-H(16)	0.942(16)	C(45)-C(46)	1.348(3)
C(17)-C(18)	1.409(3)	C(45)-H(45)	0.908(15)
C(17)-H(17)	0.961(18)	C(46)-C(47)	1.426(2)
C(18)-C(19)	1.332(3)	C(46)-H(46)	0.946(15)
C(18)-H(18)	0.924(19)	C(47)-C(48)	1.383(2)

C(48)-C(49)	1.388(2)	C(58)-N(3)-C(55)	112.4(2)
C(48)-H(48)	0.927(15)	C(57)-N(3)-C(55)	107.1(2)
C(49)-C(50)	1.423(2)	C(58)-N(3)-Ni(1)	114.07(14)
C(49)-C(54)	1.436(2)	C(57)-N(3)-Ni(1)	114.20(13)
C(50)-C(51)	1.342(3)	C(55)-N(3)-Ni(1)	101.08(13)
C(50)-H(50)	0.925(15)	C(56)-N(4)-C(59)	112.2(2)
C(51)-C(52)	1.415(3)	C(56)-N(4)-C(60)	107.6(2)
C(51)-H(51)	0.958(15)	C(59)-N(4)-C(60)	105.9(2)
C(52)-C(53)	1.346(3)	C(56)-N(4)-Ni(1)	103.85(14)
C(52)-H(52)	0.923(16)	C(59)-N(4)-Ni(1)	113.22(13)
C(53)-C(54)	1.425(2)	C(60)-N(4)-Ni(1)	114.06(14)
C(53)-H(53)	0.958(14)	N(1)-C(1)-C(2)	128.74(17)
C(55)-C(56)	1.451(4)	N(1)-C(1)-H(1)	117.4(8)
C(55)-H(55A)	1.066(18)	C(2)-C(1)-H(1)	113.8(8)
C(55)-H(55B)	1.03(3)	C(3)-C(2)-C(7)	119.75(16)
C(56)-H(56A)	0.969(19)	C(3)-C(2)-C(1)	117.16(16)
C(56)-H(56B)	1.14(3)	C(7)-C(2)-C(1)	123.06(16)
C(57)-H(57A)	0.92(2)	C(4)-C(3)-C(2)	121.78(19)
C(57)-H(57B)	0.98(2)	C(4)-C(3)-H(3)	120.4(8)
C(57)-H(57C)	0.990(18)	C(2)-C(3)-H(3)	117.8(8)
C(58)-H(58A)	0.981(18)	C(3)-C(4)-C(5)	118.57(19)
C(58)-H(58B)	0.980(17)	C(3)-C(4)-H(4)	120.8(10)
C(58)-H(58C)	0.98(2)	C(5)-C(4)-H(4)	120.6(10)
C(59)-H(59A)	0.968(17)	C(6)-C(5)-C(4)	122.35(19)
C(59)-H(59B)	0.96(2)	C(6)-C(5)-H(5)	117.6(10)
C(59)-H(59C)	0.946(18)	C(4)-C(5)-H(5)	120.0(10)
C(60)-H(60A)	0.95(2)	C(5)-C(6)-C(7)	119.86(17)
C(60)-H(60B)	0.97(3)	C(5)-C(6)-C(14)	121.74(16)
C(60)-H(60C)	0.997(17)	C(7)-C(6)-C(14)	118.38(15)
		O(2)-C(7)-C(2)	123.38(15)
O(1)-Ni(1)-O(2)	172.87(5)	O(2)-C(7)-C(6)	119.31(16)
O(1)-Ni(1)-N(1)	96.84(5)	C(2)-C(7)-C(6)	117.30(16)
O(2)-Ni(1)-N(1)	87.67(5)	C(13)-C(8)-C(9)	118.76(18)
O(1)-Ni(1)-N(2)	87.51(5)	C(13)-C(8)-N(1)	122.36(17)
O(2)-Ni(1)-N(2)	97.70(5)	C(9)-C(8)-N(1)	118.77(16)
N(1)-Ni(1)-N(2)	94.10(5)	C(10)-C(9)-C(8)	120.4(2)
O(1)-Ni(1)-N(4)	92.10(5)	C(10)-C(9)-H(9)	119.3(9)
O(2)-Ni(1)-N(4)	82.84(5)	C(8)-C(9)-H(9)	120.2(9)
N(1)-Ni(1)-N(4)	168.98(6)	C(11)-C(10)-C(9)	120.3(2)
N(2)-Ni(1)-N(4)	92.71(6)	C(11)-C(10)-H(10)	121.6(10)
O(1)-Ni(1)-N(3)	84.20(5)	C(9)-C(10)-H(10)	118.1(10)
O(2)-Ni(1)-N(3)	90.19(5)	C(12)-C(11)-C(10)	119.6(2)
N(1)-Ni(1)-N(3)	91.34(5)	C(12)-C(11)-H(11)	120.1(10)
N(2)-Ni(1)-N(3)	170.57(6)	C(10)-C(11)-H(11)	120.3(10)
N(4)-Ni(1)-N(3)	83.13(6)	C(11)-C(12)-C(13)	120.2(2)
C(34)-O(1)-Ni(1)	133.18(11)	C(11)-C(12)-H(12)	121.1(10)
C(7)-O(2)-Ni(1)	133.09(11)	C(13)-C(12)-H(12)	118.7(10)
C(1)-N(1)-C(8)	113.69(15)	C(8)-C(13)-C(12)	120.7(2)
C(1)-N(1)-Ni(1)	123.72(12)	C(8)-C(13)-H(13)	119.1(10)
C(8)-N(1)-Ni(1)	122.59(11)	C(12)-C(13)-H(13)	120.2(10)
C(28)-N(2)-C(35)	113.57(15)	C(15)-C(14)-C(27)	119.79(17)
C(28)-N(2)-Ni(1)	123.64(12)	C(15)-C(14)-C(6)	120.95(16)
C(35)-N(2)-Ni(1)	122.79(11)	C(27)-C(14)-C(6)	119.24(16)
C(58)-N(3)-C(57)	107.7(2)	C(14)-C(15)-C(16)	122.19(19)

C(14)-C(15)-C(20)	119.87(18)	C(32)-C(33)-C(41)	122.02(16)
C(16)-C(15)-C(20)	117.94(19)	C(34)-C(33)-C(41)	117.62(15)
C(17)-C(16)-C(15)	120.6(2)	O(1)-C(34)-C(29)	123.43(16)
C(17)-C(16)-H(16)	120.6(11)	O(1)-C(34)-C(33)	119.50(15)
C(15)-C(16)-H(16)	118.9(11)	C(29)-C(34)-C(33)	117.07(16)
C(16)-C(17)-C(18)	120.9(3)	C(40)-C(35)-C(36)	118.97(19)
C(16)-C(17)-H(17)	118.7(12)	C(40)-C(35)-N(2)	119.20(17)
C(18)-C(17)-H(17)	120.4(12)	C(36)-C(35)-N(2)	121.75(18)
C(19)-C(18)-C(17)	120.7(3)	C(35)-C(36)-C(37)	120.0(2)
C(19)-C(18)-H(18)	118.1(13)	C(35)-C(36)-H(36)	118.7(10)
C(17)-C(18)-H(18)	121.1(13)	C(37)-C(36)-H(36)	121.3(11)
C(18)-C(19)-C(20)	120.9(3)	C(38)-C(37)-C(36)	120.7(2)
C(18)-C(19)-H(19)	123.8(12)	C(38)-C(37)-H(37)	121.0(11)
C(20)-C(19)-H(19)	115.1(12)	C(36)-C(37)-H(37)	118.3(11)
C(21)-C(20)-C(19)	121.9(2)	C(37)-C(38)-C(39)	119.5(2)
C(21)-C(20)-C(15)	119.20(19)	C(37)-C(38)-H(38)	119.7(11)
C(19)-C(20)-C(15)	118.9(2)	C(39)-C(38)-H(38)	120.8(11)
C(22)-C(21)-C(20)	122.0(2)	C(38)-C(39)-C(40)	120.0(2)
C(22)-C(21)-H(21)	118.1(10)	C(38)-C(39)-H(39)	121.4(10)
C(20)-C(21)-H(21)	120.0(10)	C(40)-C(39)-H(39)	118.6(10)
C(21)-C(22)-C(23)	122.5(2)	C(35)-C(40)-C(39)	120.8(2)
C(21)-C(22)-C(27)	119.28(19)	C(35)-C(40)-H(40)	121.7(9)
C(23)-C(22)-C(27)	118.3(2)	C(39)-C(40)-H(40)	117.5(9)
C(24)-C(23)-C(22)	121.5(2)	C(54)-C(41)-C(42)	120.03(16)
C(24)-C(23)-H(23)	121.1(11)	C(54)-C(41)-C(33)	120.49(16)
C(22)-C(23)-H(23)	117.4(11)	C(42)-C(41)-C(33)	119.34(16)
C(23)-C(24)-C(25)	120.1(2)	C(41)-C(42)-C(43)	122.52(17)
C(23)-C(24)-H(24)	119.6(11)	C(41)-C(42)-C(47)	119.48(17)
C(25)-C(24)-H(24)	120.3(11)	C(43)-C(42)-C(47)	117.95(17)
C(26)-C(25)-C(24)	121.0(2)	C(44)-C(43)-C(42)	121.47(19)
C(26)-C(25)-H(25)	115.7(10)	C(44)-C(43)-H(43)	118.6(9)
C(24)-C(25)-H(25)	123.3(10)	C(42)-C(43)-H(43)	119.9(9)
C(25)-C(26)-C(27)	121.2(2)	C(43)-C(44)-C(45)	120.1(2)
C(25)-C(26)-H(26)	120.3(10)	C(43)-C(44)-H(44)	119.6(10)
C(27)-C(26)-H(26)	118.5(10)	C(45)-C(44)-H(44)	120.3(10)
C(14)-C(27)-C(26)	122.37(18)	C(46)-C(45)-C(44)	120.9(2)
C(14)-C(27)-C(22)	119.73(18)	C(46)-C(45)-H(45)	121.1(10)
C(26)-C(27)-C(22)	117.89(18)	C(44)-C(45)-H(45)	118.0(10)
N(2)-C(28)-C(29)	129.08(18)	C(45)-C(46)-C(47)	121.1(2)
N(2)-C(28)-H(28)	116.8(9)	C(45)-C(46)-H(46)	122.1(9)
C(29)-C(28)-H(28)	114.1(9)	C(47)-C(46)-H(46)	116.7(9)
C(30)-C(29)-C(34)	119.59(17)	C(48)-C(47)-C(46)	122.31(18)
C(30)-C(29)-C(28)	117.49(17)	C(48)-C(47)-C(42)	119.35(18)
C(34)-C(29)-C(28)	122.91(17)	C(46)-C(47)-C(42)	118.32(18)
C(31)-C(30)-C(29)	122.33(19)	C(47)-C(48)-C(49)	122.18(18)
C(31)-C(30)-H(30)	121.0(10)	C(47)-C(48)-H(48)	119.4(10)
C(29)-C(30)-H(30)	116.6(10)	C(49)-C(48)-H(48)	118.4(10)
C(30)-C(31)-C(32)	118.7(2)	C(48)-C(49)-C(50)	122.56(18)
C(30)-C(31)-H(31)	121.4(9)	C(48)-C(49)-C(54)	118.67(17)
C(32)-C(31)-H(31)	119.9(9)	C(50)-C(49)-C(54)	118.76(18)
C(33)-C(32)-C(31)	121.97(19)	C(51)-C(50)-C(49)	121.9(2)
C(33)-C(32)-H(32)	117.7(10)	C(51)-C(50)-H(50)	120.5(10)
C(31)-C(32)-H(32)	120.3(10)	C(49)-C(50)-H(50)	117.7(10)
C(32)-C(33)-C(34)	120.36(17)	C(50)-C(51)-C(52)	119.5(2)

C(50)-C(51)-H(51)	121.3(10)	N(3)-C(57)-H(57B)	109.0(14)
C(52)-C(51)-H(51)	119.2(10)	H(57A)-C(57)-H(57B)	113.2(19)
C(53)-C(52)-C(51)	121.1(2)	N(3)-C(57)-H(57C)	111.2(10)
C(53)-C(52)-H(52)	120.6(11)	H(57A)-C(57)-H(57C)	107.1(16)
C(51)-C(52)-H(52)	118.2(11)	H(57B)-C(57)-H(57C)	105.6(17)
C(52)-C(53)-C(54)	121.6(2)	N(3)-C(58)-H(58A)	110.5(11)
C(52)-C(53)-H(53)	120.7(9)	N(3)-C(58)-H(58B)	109.6(12)
C(54)-C(53)-H(53)	117.7(9)	H(58A)-C(58)-H(58B)	110.3(16)
C(41)-C(54)-C(53)	122.82(17)	N(3)-C(58)-H(58C)	109.8(13)
C(41)-C(54)-C(49)	120.05(17)	H(58A)-C(58)-H(58C)	109.1(17)
C(53)-C(54)-C(49)	117.11(17)	H(58B)-C(58)-H(58C)	107.4(18)
C(56)-C(55)-N(3)	114.8(2)	N(4)-C(59)-H(59A)	109.9(11)
C(56)-C(55)-H(55A)	111.0(10)	N(4)-C(59)-H(59B)	112.6(14)
N(3)-C(55)-H(55A)	104.2(10)	H(59A)-C(59)-H(59B)	110.4(17)
C(56)-C(55)-H(55B)	104.8(19)	N(4)-C(59)-H(59C)	106.3(12)
N(3)-C(55)-H(55B)	108.4(18)	H(59A)-C(59)-H(59C)	109.4(15)
H(55A)-C(55)-H(55B)	114(2)	H(59B)-C(59)-H(59C)	108.3(18)
C(55)-C(56)-N(4)	113.5(2)	N(4)-C(60)-H(60A)	106.7(14)
C(55)-C(56)-H(56A)	110.0(11)	N(4)-C(60)-H(60B)	107.5(18)
N(4)-C(56)-H(56A)	112.4(11)	H(60A)-C(60)-H(60B)	114(2)
C(55)-C(56)-H(56B)	80.1(15)	N(4)-C(60)-H(60C)	109.8(10)
N(4)-C(56)-H(56B)	119.5(14)	H(60A)-C(60)-H(60C)	108.5(17)
H(56A)-C(56)-H(56B)	116.9(18)	H(60B)-C(60)-H(60C)	110(2)
N(3)-C(57)-H(57A)	110.7(12)		

Table 5. Anisotropic displacement parameters ($Å^2 x 10^4$) for TRY12 (CCDC 161495). The anisotropic displacement factor exponent takes the form: $-2\pi^2$ [$h^2 a^{*2}U^{11}$ + ... + 2 h k a* b* U^{12}]

	U^{11}	U^{22}	U^{33}	U^{23}	U^{13}	U^{12}
Ni(1)	327(1)	347(1)	319(1)	-2(1)	-16(1)	-4(1)
O(1)	336(7)	331(7)	361(7)	-60(6)	-45(5)	42(6)
O(2)	308(7)	431(8)	343(7)	52(6)	-35(6)	-40(6)
N(1)	370(9)	313(9)	309(9)	4(7)	-8(7)	22(7)
N(2)	367(9)	412(9)	300(8)	-46(7)	-7(8)	-15(8)
N(3)	420(10)	357(9)	454(10)	-12(8)	-45(8)	47(8)
N(4)	387(10)	513(11)	425(10)	43(8)	-4(8)	-70(8)
C(1)	379(12)	274(11)	368(12)	9(9)	77(10)	0(9)
C(2)	322(10)	300(10)	338(11)	-3(9)	-11(9)	15(8)
C(3)	377(12)	353(11)	429(13)	24(10)	33(10)	3(9)
C(4)	347(13)	445(13)	567(14)	24(11)	-69(11)	-96(10)
C(5)	419(13)	467(13)	456(14)	36(11)	-122(11)	0(10)
C(6)	364(11)	318(10)	349(11)	-7(9)	-52(8)	15(10)
C(7)	340(11)	275(11)	355(11)	-57(8)	-11(9)	21(8)
C(8)	359(11)	340(11)	320(11)	40(9)	-22(9)	-70(9)
C(9)	421(13)	464(13)	374(12)	46(10)	27(11)	-13(10)
C(10)	447(14)	487(14)	511(14)	142(12)	-81(11)	4(11)
C(11)	585(15)	551(15)	386(13)	114(12)	-132(12)	-154(13)
C(12)	613(16)	540(14)	310(13)	-24(11)	24(12)	-124(12)
C(13)	444(13)	393(13)	386(12)	-9(10)	4(11)	-14(10)
C(14)	331(11)	393(12)	357(11)	24(9)	-110(9)	11(9)
C(15)	396(12)	467(13)	366(12)	-3(10)	-93(9)	43(10)
C(16)	628(16)	515(16)	463(15)	-44(13)	-51(12)	43(12)
C(17)	850(20)	627(19)	646(18)	-176(16)	-35(15)	164(16)
C(18)	766(19)	1010(20)	493(18)	-168(18)	48(15)	181(17)
C(19)	625(17)	850(20)	450(16)	52(16)	32(12)	70(16)
C(20)	397(12)	624(15)	361(13)	13(11)	-52(10)	50(11)
C(21)	442(14)	586(16)	479(14)	207(13)	-34(11)	-30(12)
C(22)	374(12)	445(13)	475(13)	83(11)	-87(10)	-1(10)
C(23)	481(15)	463(16)	687(18)	191(14)	-95(13)	-46(12)
C(24)	519(15)	375(15)	850(20)	-24(15)	-157(14)	29(12)
C(25)	451(14)	490(15)	613(16)	-96(13)	-77(12)	64(11)
C(26)	363(13)	443(14)	488(14)	21(12)	-64(10)	-12(11)
C(27)	323(11)	401(12)	395(12)	44(10)	-92(9)	17(9)
C(28)	401(12)	357(12)	356(12)	-77(9)	55(9)	8(10)
C(29)	354(11)	349(11)	304(10)	-56(9)	-7(8)	12(9)
C(30)	472(13)	351(12)	458(13)	-128(10)	-3(10)	73(10)
C(31)	435(13)	416(13)	585(15)	-73(11)	-108(11)	165(11)
C(32)	434(13)	410(13)	444(13)	-74(10)	-127(11)	42(10)
C(33)	366(11)	305(11)	315(10)	2(9)	-29(9)	27(9)
C(34)	345(11)	303(10)	316(11)	10(9)	14(9)	-3(9)
C(35)	385(12)	384(11)	354(11)	-60(9)	-45(9)	43(9)
C(36)	431(14)	748(16)	426(13)	-168(11)	0(12)	-83(13)
C(37)	558(16)	869(18)	421(14)	-254(13)	-30(13)	13(14)
C(38)	530(15)	561(15)	521(15)	-230(12)	-170(12)	30(12)
C(39)	415(14)	433(13)	591(15)	-81(11)	-58(12)	-27(11)
C(40)	430(13)	416(12)	420(13)	-92(10)	10(11)	30(10)

C(41)	335(11)	309(11)	362(11)	-52(9)	-100(9)	33(9)
C(42)	344(11)	341(11)	379(11)	-19(9)	-95(9)	-3(9)
C(43)	406(12)	336(13)	460(13)	-66(11)	-22(10)	8(10)
C(44)	434(13)	477(14)	481(14)	-5(12)	25(10)	-61(11)
C(45)	521(14)	352(14)	618(16)	87(13)	-40(12)	-35(11)
C(46)	481(14)	338(13)	576(15)	-74(12)	-30(12)	35(10)
C(47)	367(11)	311(12)	437(12)	-46(9)	-83(9)	-2(9)
C(48)	461(13)	357(13)	472(14)	-135(11)	-60(10)	49(10)
C(49)	401(12)	404(12)	379(12)	-69(10)	-72(9)	13(10)
C(50)	545(14)	472(14)	455(14)	-130(13)	0(11)	24(11)
C(51)	593(15)	596(16)	364(13)	-39(12)	15(11)	-48(12)
C(52)	630(15)	483(15)	401(13)	51(12)	-49(12)	-85(11)
C(53)	560(14)	371(13)	387(12)	-54(10)	-64(11)	25(10)
C(54)	368(11)	348(11)	342(11)	-36(9)	-86(9)	0(9)
C(55)	1410(30)	331(15)	800(20)	20(14)	180(20)	-116(17)
C(56)	1140(30)	415(16)	990(20)	201(15)	449(19)	1(16)
C(57)	594(19)	571(17)	541(16)	-220(13)	-109(14)	180(15)
C(58)	650(20)	640(20)	940(20)	-327(19)	-306(18)	259(16)
C(59)	447(15)	850(20)	472(16)	159(16)	-21(12)	-188(15)
C(60)	551(18)	1190(30)	391(15)	289(16)	-50(13)	-293(19)

Table 6. Hydrogen coordinates (x 10^4) and isotropic displacement parameters ($Å^2$x 10^3) for TRY12 (CCDC 161495).

	x	y	z	U_{iso}
H(1)	5523(8)	637(7)	4469(5)	26(4)
H(3)	4493(8)	456(7)	4010(5)	24(4)
H(4)	3762(9)	637(8)	3302(6)	43(5)
H(5)	4226(8)	1347(7)	2673(5)	34(5)
H(9)	7604(8)	133(7)	4500(5)	25(4)
H(10)	7927(9)	-398(8)	5230(6)	39(5)
H(11)	7309(9)	-109(8)	5973(6)	49(5)
H(12)	6343(9)	707(8)	5946(6)	37(5)
H(13)	6025(8)	1229(7)	5212(5)	29(5)
H(16)	5746(9)	714(9)	2281(6)	48(6)
H(17)	6262(10)	304(10)	1560(7)	67(7)
H(18)	6659(11)	1106(10)	947(7)	78(8)
H(19)	6550(11)	2276(9)	1075(7)	62(7)
H(21)	6281(9)	3239(8)	1619(6)	41(5)
H(23)	5890(9)	4214(8)	2128(6)	45(6)
H(24)	5325(10)	4666(9)	2813(6)	60(6)
H(25)	4783(9)	3880(8)	3398(6)	41(6)
H(26)	4861(8)	2733(8)	3281(5)	33(5)
H(28)	8552(8)	-49(8)	3500(5)	36(5)
H(30)	9627(8)	-147(8)	3920(6)	38(5)
H(31)	10507(9)	170(8)	4516(5)	35(5)
H(32)	10286(9)	1179(8)	4970(6)	38(5)
H(36)	8175(10)	268(8)	2633(6)	52(6)
H(37)	7600(10)	-443(9)	2044(7)	67(6)
H(38)	6445(10)	-932(9)	2242(6)	57(6)
H(39)	5858(9)	-699(8)	2997(6)	48(6)
H(40)	6449(8)	-20(7)	3558(5)	30(5)
H(43)	9859(8)	2401(7)	4135(5)	24(4)
H(44)	10003(9)	3456(8)	3749(6)	45(5)
H(45)	9560(9)	4435(8)	4168(6)	38(5)
H(46)	9004(8)	4382(8)	4944(5)	38(5)
H(48)	8575(9)	3676(8)	5636(5)	37(5)
H(50)	8172(9)	2988(8)	6348(6)	42(5)
H(51)	7922(9)	1928(8)	6710(6)	45(5)
H(52)	8219(9)	930(9)	6273(6)	51(6)
H(53)	8771(8)	960(8)	5501(5)	30(5)
H(55A)	7216(10)	3542(10)	3969(6)	65(6)
H(55B)	7985(18)	2984(17)	4049(12)	187(18)
H(56A)	7829(10)	3267(10)	3227(6)	63(6)
H(56B)	6900(17)	2991(14)	3401(11)	158(12)
H(57A)	7615(12)	2498(10)	4756(7)	76(8)
H(57B)	6767(13)	2323(12)	4888(8)	110(11)
H(57C)	7045(9)	3090(10)	4824(6)	54(6)
H(58A)	6063(10)	3215(10)	4236(6)	61(6)
H(58B)	5840(10)	2409(9)	4287(7)	55(8)
H(58C)	6020(12)	2725(11)	3762(8)	90(9)
H(59A)	8862(10)	2505(9)	3065(6)	58(6)
H(59B)	8836(12)	1724(11)	3246(8)	91(10)

H(59C)	8774(10)	2322(9)	3625(7)	64(7)
H(60A)	7102(13)	2109(11)	2725(8)	92(9)
H(60B)	7807(17)	1586(15)	2686(11)	164(16)
H(60C)	7879(9)	2389(9)	2529(6)	55(6)

Appendix H

X-Ray Diffraction Analysis of

$(^{\text{Anthr,H}}\text{Sal})_2\text{Ni}\cdot\ 2\ \text{CH}_3\text{CN}$

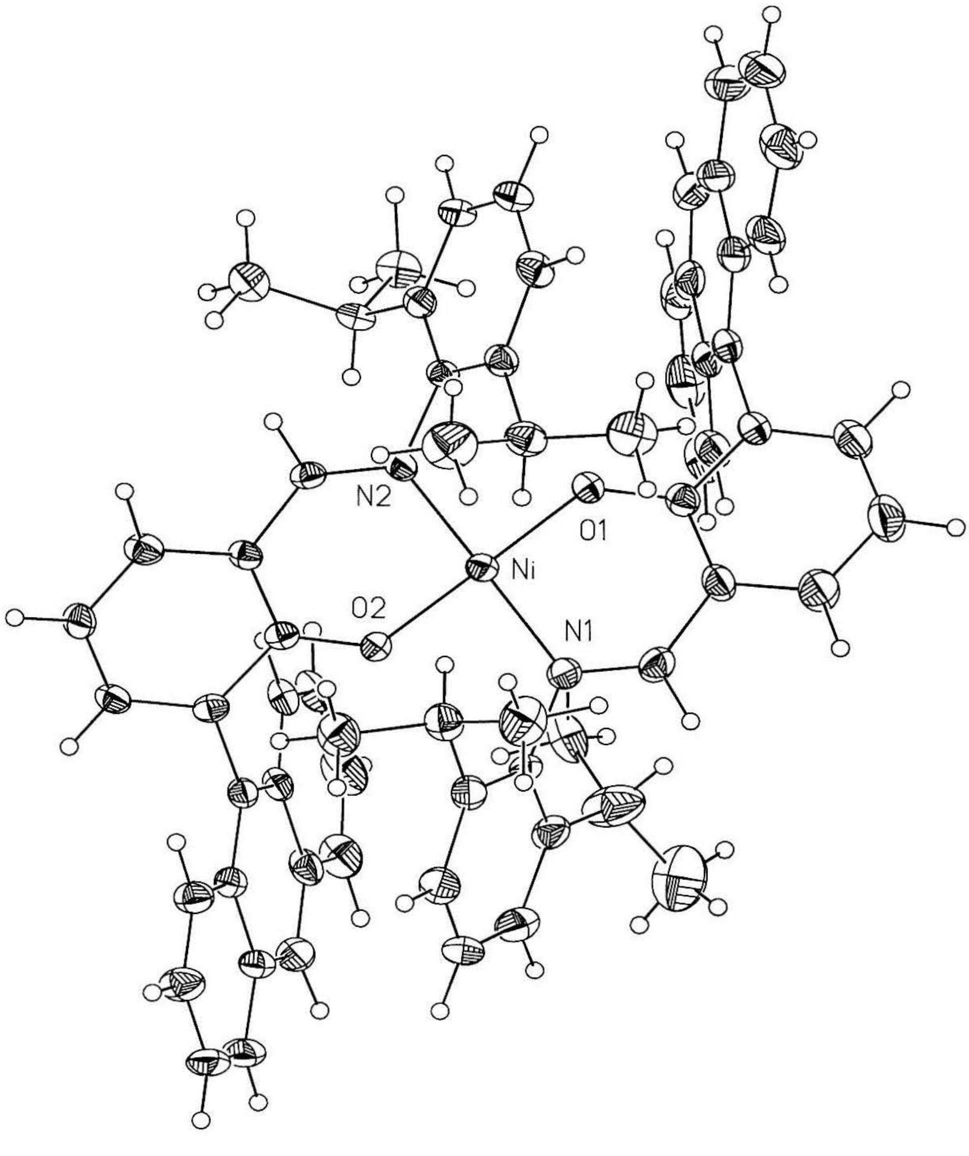

Table 1. Crystal data and structure refinement for TRY4 (CCDC No. 141446)

Empirical formula	$C_{66}H_{60}N_2NiO_2$ $(CH_3C\ \ N)_2$
Formula weight	971.91 (82.06)
Crystallization Solvent	Acetonitrile
Crystal Habit	Thin chunk
Crystal size	0.259 x 0.185 x 0.148 mm^3
Crystal color	Dark brown

Data Collection

Preliminary Photos	Rotation	
Type of diffractometer	CCD area detector	
Wavelength	0.71073 Å MoKα	
Data Collection Temperature	93 K	
θ range for 5769 reflections used in lattice determination	2.35 to 26.39°	
Unit cell dimensions	a = 10.8701(8) Å b = 28.890(2) Å c = 18.3122(14) Å	 β= 97.8390(10)°
Volume	5697.0(7) Å^3	
Z	4	
Crystal system	Monoclinic	
Space group	$P2_1/c$	
Density (calculated)	1.229 Mg/m^3	
F(000)	2232	
Data collection program	Bruker SMART	
θ range for data collection	1.80 to 28.58°	
Completeness to θ = 28.58°	94.5 %	
Index ranges	$-14 \leq h \leq 14$, $-38 \leq k \leq 38$, $-24 \leq l \leq 24$	
Data collection scan type	ω scans at eight ϕ settings	
Data reduction program	Bruker SAINT v 6.2	
Reflections collected	104083	
Independent reflections	13770 [R_{int}= 0.0967]	
Absorption coefficient	0.390 mm^{-1}	
Absorption correction	None	

Table 1 (cont.)

Structure Solution and Refinement

Structure solution program	SHELXS-97 (Sheldrick, 1990)
Primary solution method	Patterson method
Secondary solution method	Difference Fourier map
Hydrogen placement	Difference Fourier map
Structure refinement program	SHELXL-97 (Sheldrick, 1997)
Refinement method	Full matrix least-squares on F^2
Data / restraints / parameters	13770 / 15 / 901
Treatment of hydrogen atoms	Unrestrained
Goodness-of-fit on F^2	1.499
Final R indices [$I>2\sigma(I)$, 8132 reflections]	$R1 = 0.0499$, $wR2 = 0.0778$
R indices (all data)	$R1 = 0.0985$, $wR2 = 0.0818$
Type of weighting scheme used	Sigma
Weighting scheme used	$w=1/\sigma^2(Fo^2)$
Max shift/error	0.001
Average shift/error	0.000
Largest diff. peak and hole	0.689 and -0.860 e.Å^{-3}

Special Refinement Details

The crystals contain solvent at two sites. At one site (solvent 100) the solvent is well behaved and the has been refined anisotropically without any restraints whatsoever (including hydrogen atoms). At the second site (solvents 200 and 300) there is disorder with respect to the orientation of the nitrile in the two molecules which occupy the site. Therefore these two aetonitrile molecules were refined as rigid bodies with the total population of the site set equal to one.

Additionally, disorder is present in the isopropyl group which is bonded to C9, labeled C28, C29 and C30. The disorder is a rotation about the C9-C28 bond, resulting in alternate orientations for the methyl groups C29 and C30 with the maps indicating an approximate 2:1 ratio for the two orientations. This disorder was successfully modeled with riding hydrogen atoms and a light restraint on the isopropyl geometry. The refined ratio of occupancies for the two orientations was 0.69:0.31 which is in excellent agreement with the density maps. Please refer to the enclosed figures for density maps showing this disorder.

Refinement of F^2 against ALL reflections. The weighted R-factor (wR) and goodness of fit (S) are based on F^2, conventional R-factors (R) are based on F, with F set to zero for negative F^2. The threshold expression of $F^2 > 2\sigma(F^2)$ is used only for calculating R-factors(gt) etc. and is not relevant to the choice of reflections for refinement. R-factors based on F^2 are statistically about twice as large as those based on F, and R-factors based on ALL data will be even larger.

All esds (except the esd in the dihedral angle between two l.s. planes) are estimated using the full covariance matrix. The cell esds are taken into account individually in the estimation of esds in distances, angles and torsion angles; correlations between esds in cell parameters are only used when they are defined by crystal symmetry. An approximate (isotropic) treatment of cell esds is used for estimating esds involving l.s. planes.

Table 2. Atomic coordinates (x 10^4) and equivalent isotropic displacement parameters (Å^{2}x 10^3) for TRY4 (CCDC No. 141446). U(eq) is defined as the trace of the orthogonalized U^{ij} tensor.

	x	y	z	U_{eq}	Occ
Ni	7472(1)	8252(1)	7815(1)	20(1)	1
O(1)	6917(2)	8846(1)	7597(2)	23(1)	1
O(2)	7619(2)	7674(1)	8235(1)	20(1)	1
N(1)	6575(3)	7993(1)	6952(2)	23(1)	1
N(2)	8919(3)	8488(1)	8391(2)	20(1)	1
C(1)	6389(4)	9010(1)	6967(2)	22(1)	1
C(2)	6038(4)	9485(1)	6908(2)	24(1)	1
C(3)	5568(4)	9661(2)	6227(3)	34(1)	1
C(4)	5387(5)	9392(2)	5590(3)	45(1)	1
C(5)	5646(5)	8927(2)	5655(3)	42(1)	1
C(6)	6120(4)	8733(1)	6333(2)	28(1)	1
C(7)	6219(4)	8239(2)	6371(2)	28(1)	1
C(8)	6443(4)	7496(1)	6831(2)	24(1)	1
C(9)	5275(4)	7296(2)	6819(2)	31(1)	1
C(10)	5168(5)	6824(2)	6662(3)	36(1)	1
C(11)	6170(5)	6570(2)	6513(3)	34(1)	1
C(12)	7311(5)	6777(2)	6529(2)	32(1)	1
C(13)	7486(4)	7242(1)	6697(2)	26(1)	1
C(14)	6089(4)	9787(1)	7572(2)	26(1)	1
C(15)	6844(4)	10182(1)	7653(3)	30(1)	1
C(16)	7617(4)	10318(2)	7118(3)	38(1)	1
C(17)	8242(5)	10724(2)	7173(4)	47(2)	1
C(18)	8191(5)	11018(2)	7783(4)	57(2)	1
C(19)	7515(5)	10901(2)	8317(4)	48(2)	1
C(20)	6777(4)	10487(2)	8266(3)	37(1)	1
C(21)	5978(5)	10386(2)	8768(3)	37(1)	1
C(22)	5178(4)	10010(2)	8678(2)	31(1)	1
C(23)	4238(5)	9940(2)	9138(3)	40(1)	1
C(24)	3395(5)	9599(2)	9009(3)	43(1)	1
C(25)	3436(5)	9295(2)	8406(3)	38(1)	1
C(26)	4327(4)	9342(2)	7961(3)	30(1)	1
C(27)	5236(4)	9702(1)	8072(2)	27(1)	1
C(28)	4171(4)	7571(2)	6942(3)	56(2)	1
C(29)	4190(5)	7771(2)	7702(3)	36(2)	0.693(8)

C(30)	2959(5)	7426(3)	6557(4)	64(3)	0.693(8)
C(29B)	3715(13)	7424(7)	7650(6)	68(7)	0.307(8)
C(30B)	3205(10)	7663(6)	6314(5)	33(5)	0.307(8)
C(31)	8767(4)	7469(2)	6693(2)	29(1)	1
C(32)	9806(5)	7161(2)	7045(3)	37(1)	1
C(33)	8899(6)	7643(2)	5950(3)	44(1)	1
C(34)	8554(4)	7496(1)	8668(2)	18(1)	1
C(35)	8479(4)	7028(1)	8922(2)	20(1)	1
C(36)	9499(4)	6833(1)	9338(2)	22(1)	1
C(37)	10602(4)	7073(2)	9527(3)	27(1)	1
C(38)	10683(4)	7525(2)	9319(2)	26(1)	1
C(39)	9663(4)	7742(1)	8896(2)	19(1)	1
C(40)	9768(4)	8225(1)	8739(2)	20(1)	1
C(41)	9256(3)	8976(1)	8371(2)	20(1)	1
C(42)	9671(4)	9153(1)	7740(2)	22(1)	1
C(43)	10048(4)	9615(2)	7765(3)	27(1)	1
C(44)	9988(4)	9885(2)	8380(3)	28(1)	1
C(45)	9545(4)	9702(1)	8987(3)	24(1)	1
C(46)	9168(4)	9239(1)	9002(2)	21(1)	1
C(47)	7316(3)	6751(1)	8736(2)	20(1)	1
C(48)	6219(4)	6889(1)	8996(2)	22(1)	1
C(49)	6157(4)	7284(1)	9457(2)	22(1)	1
C(50)	5098(4)	7398(2)	9730(3)	29(1)	1
C(51)	4004(5)	7138(2)	9542(3)	39(1)	1
C(52)	4004(4)	6761(2)	9109(3)	38(1)	1
C(53)	5113(4)	6615(1)	8828(2)	27(1)	1
C(54)	5152(4)	6210(2)	8428(3)	31(1)	1
C(55)	6247(4)	6060(1)	8189(2)	27(1)	1
C(56)	6300(5)	5639(2)	7793(3)	34(1)	1
C(57)	7346(5)	5496(2)	7551(3)	36(1)	1
C(58)	8431(5)	5760(2)	7691(3)	33(1)	1
C(59)	8432(4)	6168(2)	8065(2)	27(1)	1
C(60)	7351(4)	6335(1)	8341(2)	22(1)	1
C(61)	9748(4)	8861(2)	7062(2)	29(1)	1
C(62)	9396(6)	9123(2)	6340(3)	42(1)	1
C(63)	11019(6)	8640(2)	7083(4)	49(2)	1
C(64)	8724(4)	9045(2)	9687(2)	25(1)	1
C(65)	7822(5)	9365(2)	10001(3)	32(1)	1
C(66)	9822(5)	8940(2)	10282(3)	33(1)	1
C(101)	5317(5)	8561(2)	9464(4)	54(2)	1
C(100)	4044(5)	8491(2)	9625(3)	46(2)	1
N(100)	3053(4)	8437(1)	9742(3)	60(1)	1
N(200)	7895	10019	4474	112	0.24
C(200)	8384	10296	4862	169	0.24
C(201)	9062	10615	5379	131	0.24
N(300)	8898	10441	5371	116	0.76
C(300)	8496	10130	5025	102	0.76
C(301)	8044	9740	4568	83	0.76

Table 3. Selected bond lengths [Å] and angles [°] for TRY4 (CCDC No. 141446).

Ni-O(2)	1.836(3)	O(2)-Ni-O(1)	160.71(12)
Ni-O(1)	1.844(2)	O(2)-Ni-N(1)	89.69(13)
Ni-N(1)	1.895(3)	O(1)-Ni-N(1)	94.10(13)
Ni-N(2)	1.896(3)	O(2)-Ni-N(2)	94.32(12)
		O(1)-Ni-N(2)	90.52(12)
		N(1)-Ni-N(2)	154.05(14)

Table 4. Bond lengths [Å] and angles [°] for TRY4 (CCDC No. 141446).

Ni-O(2)	1.836(3)	C(15)-C(16)	1.430(7)
Ni-O(1)	1.844(2)	C(15)-C(20)	1.436(6)
Ni-N(1)	1.895(3)	C(16)-C(17)	1.353(6)
Ni-N(2)	1.896(3)	C(16)-H(16)	0.93(4)
O(1)-C(1)	1.305(4)	C(17)-C(18)	1.411(8)
O(2)-C(34)	1.306(4)	C(17)-H(17)	0.96(4)
N(1)-C(7)	1.295(5)	C(18)-C(19)	1.344(8)
N(1)-C(8)	1.457(5)	C(18)-H(18)	0.87(4)
N(2)-C(40)	1.294(5)	C(19)-C(20)	1.436(7)
N(2)-C(41)	1.459(4)	C(19)-H(19)	0.97(4)
C(1)-C(6)	1.407(5)	C(20)-C(21)	1.380(7)
C(1)-C(2)	1.427(5)	C(21)-C(22)	1.387(6)
C(2)-C(3)	1.379(6)	C(21)-H(21)	0.94(4)
C(2)-C(14)	1.490(5)	C(22)-C(23)	1.424(6)
C(3)-C(4)	1.392(6)	C(22)-C(27)	1.430(6)
C(3)-H(3)	0.97(4)	C(23)-C(24)	1.344(7)
C(4)-C(5)	1.375(6)	C(23)-H(23)	0.98(4)
C(4)-H(4)	0.95(4)	C(24)-C(25)	1.415(7)
C(5)-C(6)	1.394(6)	C(24)-H(24)	0.98(5)
C(5)-H(5)	0.97(4)	C(25)-C(26)	1.354(6)
C(6)-C(7)	1.431(6)	C(25)-H(25)	0.96(4)
C(7)-H(7)	0.99(3)	C(26)-C(27)	1.430(6)
C(8)-C(9)	1.392(5)	C(26)-H(26)	1.02(4)
C(8)-C(13)	1.399(5)	C(28)-C(30)	1.468(5)
C(9)-C(10)	1.396(6)	C(28)-C(29)	1.505(5)
C(9)-C(28)	1.483(6)	C(28)-H(28)	0.9800
C(10)-C(11)	1.371(6)	C(28)-C(30B)	1.4719(47)
C(10)-H(10)	0.99(4)	C(28)-C(29B)	1.5095(47)
C(11)-C(12)	1.374(6)	C(28)-H(28B)	0.9800
C(11)-H(11)	0.93(4)	C(29)-H(29A)	0.9600
C(12)-C(13)	1.384(6)	C(29)-H(29B)	0.9600
C(12)-H(12)	0.92(4)	C(29)-H(29C)	0.9600
C(13)-C(31)	1.541(6)	C(30)-H(30A)	0.9600
C(14)-C(15)	1.403(5)	C(30)-H(30B)	0.9600
C(14)-C(27)	1.410(6)	C(30)-H(30C)	0.9600

C(29B)-H(29D)	0.9600	C(55)-C(60)	1.435(5)
C(29B)-H(29E)	0.9600	C(56)-C(57)	1.341(6)
C(29B)-H(29F)	0.9600	C(56)-H(56)	0.92(4)
C(30B)-H(30D)	0.9600	C(57)-C(58)	1.399(6)
C(30B)-H(30E)	0.9600	C(57)-H(57)	0.94(3)
C(30B)-H(30F)	0.9600	C(58)-C(59)	1.362(6)
C(31)-C(33)	1.476(5)	C(58)-H(58)	0.98(4)
C(31)-C(32)	1.511(5)	C(59)-C(60)	1.426(5)
C(31)-H(31)	0.97(3)	C(59)-H(59)	0.98(4)
C(32)-H(32A)	1.06(5)	C(61)-C(63)	1.519(7)
C(32)-H(32B)	0.92(4)	C(61)-C(62)	1.526(6)
C(32)-H(32C)	0.95(4)	C(61)-H(61)	0.98(4)
C(33)-H(33A)	1.06(5)	C(62)-H(62A)	1.01(5)
C(33)-H(33B)	1.00(4)	C(62)-H(62B)	0.98(4)
C(33)-H(33C)	0.92(4)	C(62)-H(62C)	1.05(4)
C(34)-C(39)	1.413(5)	C(63)-H(63A)	1.00(5)
C(34)-C(35)	1.436(5)	C(63)-H(63B)	0.99(5)
C(35)-C(36)	1.377(5)	C(63)-H(63C)	0.97(4)
C(35)-C(47)	1.496(5)	C(64)-C(65)	1.517(6)
C(36)-C(37)	1.388(5)	C(64)-C(66)	1.532(6)
C(36)-H(36)	0.93(3)	C(64)-H(64)	0.88(4)
C(37)-C(38)	1.366(5)	C(65)-H(65A)	0.95(3)
C(37)-H(37)	0.89(3)	C(65)-H(65B)	1.06(4)
C(38)-C(39)	1.410(5)	C(65)-H(65C)	1.01(4)
C(38)-H(38)	0.99(3)	C(66)-H(66A)	1.02(4)
C(39)-C(40)	1.431(5)	C(66)-H(66B)	1.00(4)
C(40)-H(40)	1.00(3)	C(66)-H(66C)	0.95(4)
C(41)-C(42)	1.394(5)	C(101)-C(100)	1.467(7)
C(41)-C(46)	1.396(5)	C(101)-H(10A)	1.05(6)
C(42)-C(43)	1.396(5)	C(101)-H(10B)	0.97(5)
C(42)-C(61)	1.513(6)	C(101)-H(10C)	1.09(6)
C(43)-C(44)	1.377(6)	C(100)-N(100)	1.136(6)
C(43)-H(43)	0.95(3)	N(200)-C(200)	1.1514
C(44)-C(45)	1.376(6)	N(200)-H(30D)	1.2557
C(44)-H(44)	0.97(3)	N(200)-H(30F)	1.0507
C(45)-C(46)	1.401(5)	C(200)-C(201)	1.4491
C(45)-H(45)	0.92(3)	C(201)-H(20A)	0.9600
C(46)-C(64)	1.512(6)	C(201)-H(20B)	0.9600
C(47)-C(48)	1.401(5)	C(201)-H(20C)	0.9600
C(47)-C(60)	1.405(5)	N(300)-C(300)	1.1500
C(48)-C(49)	1.427(5)	N(300)-H(20A)	1.0623
C(48)-C(53)	1.438(5)	N(300)-H(20B)	1.0809
C(49)-C(50)	1.356(5)	N(300)-H(20C)	1.4475
C(49)-H(49)	0.98(3)	C(300)-C(301)	1.4500
C(50)-C(51)	1.409(6)	C(301)-H(30D)	0.9600
C(50)-H(50)	0.96(3)	C(301)-H(30E)	0.9600
C(51)-C(52)	1.347(6)	C(301)-H(30F)	0.9600
C(51)-H(51)	0.96(4)		
C(52)-C(53)	1.438(6)	O(2)-Ni-O(1)	160.71(12)
C(52)-H(52)	1.02(4)	O(2)-Ni-N(1)	89.69(13)
C(53)-C(54)	1.384(6)	O(1)-Ni-N(1)	94.10(13)
C(54)-C(55)	1.392(6)	O(2)-Ni-N(2)	94.32(12)
C(54)-H(54)	1.02(4)	O(1)-Ni-N(2)	90.52(12)
C(55)-C(56)	1.422(6)	N(1)-Ni-N(2)	154.05(14)

C(1)-O(1)-Ni	128.3(3)
C(34)-O(2)-Ni	128.9(2)
C(7)-N(1)-C(8)	113.9(4)
C(7)-N(1)-Ni	121.9(3)
C(8)-N(1)-Ni	123.1(3)
C(40)-N(2)-C(41)	114.5(3)
C(40)-N(2)-Ni	123.0(3)
C(41)-N(2)-Ni	121.7(2)
O(1)-C(1)-C(6)	122.7(4)
O(1)-C(1)-C(2)	119.8(4)
C(6)-C(1)-C(2)	117.5(4)
C(3)-C(2)-C(1)	119.0(4)
C(3)-C(2)-C(14)	119.4(4)
C(1)-C(2)-C(14)	121.4(4)
C(2)-C(3)-C(4)	123.1(5)
C(2)-C(3)-H(3)	118(2)
C(4)-C(3)-H(3)	119(2)
C(5)-C(4)-C(3)	117.9(5)
C(5)-C(4)-H(4)	119(2)
C(3)-C(4)-H(4)	122(2)
C(4)-C(5)-C(6)	121.1(5)
C(4)-C(5)-H(5)	121(2)
C(6)-C(5)-H(5)	118(2)
C(5)-C(6)-C(1)	121.1(4)
C(5)-C(6)-C(7)	117.4(4)
C(1)-C(6)-C(7)	121.3(4)
N(1)-C(7)-C(6)	127.0(4)
N(1)-C(7)-H(7)	117(2)
C(6)-C(7)-H(7)	116(2)
C(9)-C(8)-C(13)	122.6(4)
C(9)-C(8)-N(1)	118.8(4)
C(13)-C(8)-N(1)	118.5(4)
C(8)-C(9)-C(10)	117.3(4)
C(8)-C(9)-C(28)	122.1(4)
C(10)-C(9)-C(28)	120.6(4)
C(11)-C(10)-C(9)	121.2(5)
C(11)-C(10)-H(10)	121(2)
C(9)-C(10)-H(10)	118(2)
C(10)-C(11)-C(12)	120.1(5)
C(10)-C(11)-H(11)	120(2)
C(12)-C(11)-H(11)	120(2)
C(11)-C(12)-C(13)	121.6(5)
C(11)-C(12)-H(12)	120(2)
C(13)-C(12)-H(12)	118(2)
C(12)-C(13)-C(8)	117.1(4)
C(12)-C(13)-C(31)	120.6(4)
C(8)-C(13)-C(31)	122.1(4)
C(15)-C(14)-C(27)	119.9(4)
C(15)-C(14)-C(2)	121.2(4)
C(27)-C(14)-C(2)	118.4(4)
C(14)-C(15)-C(16)	122.8(4)
C(14)-C(15)-C(20)	119.4(5)
C(16)-C(15)-C(20)	117.6(4)
C(17)-C(16)-C(15)	121.6(6)
C(17)-C(16)-H(16)	119(3)
C(15)-C(16)-H(16)	120(3)
C(16)-C(17)-C(18)	120.4(6)
C(16)-C(17)-H(17)	116(3)
C(18)-C(17)-H(17)	123(3)
C(19)-C(18)-C(17)	120.6(6)
C(19)-C(18)-H(18)	122(3)
C(17)-C(18)-H(18)	118(3)
C(18)-C(19)-C(20)	121.2(6)
C(18)-C(19)-H(19)	126(3)
C(20)-C(19)-H(19)	113(3)
C(21)-C(20)-C(19)	122.0(5)
C(21)-C(20)-C(15)	119.6(4)
C(19)-C(20)-C(15)	118.3(5)
C(20)-C(21)-C(22)	121.9(5)
C(20)-C(21)-H(21)	120(2)
C(22)-C(21)-H(21)	118(2)
C(21)-C(22)-C(23)	122.0(5)
C(21)-C(22)-C(27)	119.0(5)
C(23)-C(22)-C(27)	118.8(5)
C(24)-C(23)-C(22)	121.8(5)
C(24)-C(23)-H(23)	124(3)
C(22)-C(23)-H(23)	114(3)
C(23)-C(24)-C(25)	119.9(6)
C(23)-C(24)-H(24)	123(3)
C(25)-C(24)-H(24)	118(3)
C(26)-C(25)-C(24)	120.5(5)
C(26)-C(25)-H(25)	117(3)
C(24)-C(25)-H(25)	122(3)
C(25)-C(26)-C(27)	121.6(5)
C(25)-C(26)-H(26)	119(2)
C(27)-C(26)-H(26)	119(2)
C(14)-C(27)-C(22)	120.0(4)
C(14)-C(27)-C(26)	122.4(4)
C(22)-C(27)-C(26)	117.4(4)
C(30)-C(28)-C(9)	117.7(4)
C(30)-C(28)-C(29)	117.0(4)
C(9)-C(28)-C(29)	115.9(4)
C(30)-C(28)-H(28)	100.3
C(9)-C(28)-H(28)	100.3
C(29)-C(28)-H(28)	100.3
C(30B)-C(28)-C(9)	118.87(69)
C(30B)-C(28)-C(29B)	116.07(39)
C(9)-C(28)-C(29B)	110.29(74)
C(30B)-C(28)-H(28B)	103.00
C(9)-C(28)-H(28B)	103.00
C(29B)-C(28)-H(28B)	103.00
C(28)-C(29)-H(29A)	109.5
C(28)-C(29)-H(29B)	109.5
H(29A)-C(29)-H(29B)	109.5
C(28)-C(29)-H(29C)	109.5
H(29A)-C(29)-H(29C)	109.5
H(29B)-C(29)-H(29C)	109.5
C(28)-C(30)-H(30A)	109.5

C(28)-C(30)-H(30B)	109.5
H(30A)-C(30)-H(30B)	109.5
C(28)-C(30)-H(30C)	109.5
H(30A)-C(30)-H(30C)	109.5
H(30B)-C(30)-H(30C)	109.5
H(29D)-C(29B)-H(29E)	109.5
H(29D)-C(29B)-H(29F)	109.5
H(29E)-C(29B)-H(29F)	109.5
H(30D)-C(30B)-H(30E)	109.5
H(30D)-C(30B)-H(30F)	109.5
H(30E)-C(30B)-H(30F)	109.5
C(33)-C(31)-C(32)	115.6(4)
C(33)-C(31)-C(13)	110.5(4)
C(32)-C(31)-C(13)	111.7(4)
C(33)-C(31)-H(31)	110.8(18)
C(32)-C(31)-H(31)	107.0(18)
C(13)-C(31)-H(31)	100.1(18)
C(31)-C(32)-H(32A)	118(3)
C(31)-C(32)-H(32B)	108(2)
H(32A)-C(32)-H(32B)	112(4)
C(31)-C(32)-H(32C)	109(2)
H(32A)-C(32)-H(32C)	109(3)
H(32B)-C(32)-H(32C)	99(3)
C(31)-C(33)-H(33A)	122(3)
C(31)-C(33)-H(33B)	109(2)
H(33A)-C(33)-H(33B)	107(3)
C(31)-C(33)-H(33C)	112(2)
H(33A)-C(33)-H(33C)	105(4)
H(33B)-C(33)-H(33C)	100(3)
O(2)-C(34)-C(39)	122.9(3)
O(2)-C(34)-C(35)	119.6(3)
C(39)-C(34)-C(35)	117.5(3)
C(36)-C(35)-C(34)	119.1(4)
C(36)-C(35)-C(47)	119.9(4)
C(34)-C(35)-C(47)	120.9(3)
C(35)-C(36)-C(37)	122.5(4)
C(35)-C(36)-H(36)	117(2)
C(37)-C(36)-H(36)	120(2)
C(38)-C(37)-C(36)	119.6(4)
C(38)-C(37)-H(37)	122(2)
C(36)-C(37)-H(37)	119(2)
C(37)-C(38)-C(39)	120.2(4)
C(37)-C(38)-H(38)	123(2)
C(39)-C(38)-H(38)	116(2)
C(38)-C(39)-C(34)	120.9(4)
C(38)-C(39)-C(40)	117.8(4)
C(34)-C(39)-C(40)	121.2(4)
N(2)-C(40)-C(39)	126.9(4)
N(2)-C(40)-H(40)	119.0(18)
C(39)-C(40)-H(40)	114.0(18)
C(42)-C(41)-C(46)	123.5(4)
C(42)-C(41)-N(2)	119.1(4)
C(46)-C(41)-N(2)	117.4(4)
C(41)-C(42)-C(43)	116.8(4)
C(41)-C(42)-C(61)	122.4(4)
C(43)-C(42)-C(61)	120.7(4)
C(44)-C(43)-C(42)	121.4(4)
C(44)-C(43)-H(43)	117(2)
C(42)-C(43)-H(43)	121(2)
C(45)-C(44)-C(43)	120.2(4)
C(45)-C(44)-H(44)	121(2)
C(43)-C(44)-H(44)	119(2)
C(44)-C(45)-C(46)	121.3(4)
C(44)-C(45)-H(45)	119(2)
C(46)-C(45)-H(45)	120(2)
C(41)-C(46)-C(45)	116.7(4)
C(41)-C(46)-C(64)	123.4(4)
C(45)-C(46)-C(64)	119.9(4)
C(48)-C(47)-C(60)	120.2(4)
C(48)-C(47)-C(35)	120.1(4)
C(60)-C(47)-C(35)	119.5(3)
C(47)-C(48)-C(49)	122.7(4)
C(47)-C(48)-C(53)	119.7(4)
C(49)-C(48)-C(53)	117.5(4)
C(50)-C(49)-C(48)	121.5(4)
C(50)-C(49)-H(49)	121(2)
C(48)-C(49)-H(49)	118(2)
C(49)-C(50)-C(51)	120.8(5)
C(49)-C(50)-H(50)	118(2)
C(51)-C(50)-H(50)	121(2)
C(52)-C(51)-C(50)	120.4(5)
C(52)-C(51)-H(51)	120(3)
C(50)-C(51)-H(51)	119(3)
C(51)-C(52)-C(53)	121.1(5)
C(51)-C(52)-H(52)	125(2)
C(53)-C(52)-H(52)	113(2)
C(54)-C(53)-C(52)	121.7(4)
C(54)-C(53)-C(48)	119.6(4)
C(52)-C(53)-C(48)	118.6(4)
C(53)-C(54)-C(55)	121.2(4)
C(53)-C(54)-H(54)	118(2)
C(55)-C(54)-H(54)	121(2)
C(54)-C(55)-C(56)	121.5(4)
C(54)-C(55)-C(60)	119.7(4)
C(56)-C(55)-C(60)	118.8(4)
C(57)-C(56)-C(55)	121.8(4)
C(57)-C(56)-H(56)	123(2)
C(55)-C(56)-H(56)	116(2)
C(56)-C(57)-C(58)	120.3(5)
C(56)-C(57)-H(57)	123(2)
C(58)-C(57)-H(57)	117(2)
C(59)-C(58)-C(57)	120.4(5)
C(59)-C(58)-H(58)	120(2)
C(57)-C(58)-H(58)	119(2)
C(58)-C(59)-C(60)	121.9(4)
C(58)-C(59)-H(59)	120(2)
C(60)-C(59)-H(59)	118(2)
C(47)-C(60)-C(59)	123.7(4)

C(47)-C(60)-C(55)	119.5(4)	H(66A)-C(66)-H(66B)	104(3)
C(59)-C(60)-C(55)	116.8(4)	C(64)-C(66)-H(66C)	114(3)
C(42)-C(61)-C(63)	111.5(4)	H(66A)-C(66)-H(66C)	107(3)
C(42)-C(61)-C(62)	113.6(4)	H(66B)-C(66)-H(66C)	109(3)
C(63)-C(61)-C(62)	110.5(5)	C(100)-C(101)-H(10A)	109(3)
C(42)-C(61)-H(61)	107(2)	C(100)-C(101)-H(10B)	104(3)
C(63)-C(61)-H(61)	107(2)	H(10A)-C(101)-H(10B)	111(4)
C(62)-C(61)-H(61)	106(2)	C(100)-C(101)-H(10C)	106(3)
C(61)-C(62)-H(62A)	114(3)	H(10A)-C(101)-H(10C)	109(4)
C(61)-C(62)-H(62B)	111(3)	H(10B)-C(101)-H(10C)	117(4)
H(62A)-C(62)-H(62B)	108(4)	N(100)-C(100)-C(101)	179.2(7)
C(61)-C(62)-H(62C)	116(2)	C(200)-N(200)-H(30D)	131.0
H(62A)-C(62)-H(62C)	106(3)	C(200)-N(200)-H(30F)	135.0
H(62B)-C(62)-H(62C)	101(3)	H(30D)-N(200)-H(30F)	85.2
C(61)-C(63)-H(63A)	114(3)	N(200)-C(200)-C(201)	175.4
C(61)-C(63)-H(63B)	109(3)	C(200)-C(201)-H(20A)	109.5
H(63A)-C(63)-H(63B)	109(4)	C(200)-C(201)-H(20B)	109.5
C(61)-C(63)-H(63C)	108(3)	H(20A)-C(201)-H(20B)	109.5
H(63A)-C(63)-H(63C)	109(4)	C(200)-C(201)-H(20C)	109.5
H(63B)-C(63)-H(63C)	107(4)	H(20A)-C(201)-H(20C)	109.5
C(46)-C(64)-C(65)	112.6(4)	H(20B)-C(201)-H(20C)	109.5
C(46)-C(64)-C(66)	111.0(4)	C(300)-N(300)-H(20A)	124.0
C(65)-C(64)-C(66)	109.5(4)	C(300)-N(300)-H(20B)	137.0
C(46)-C(64)-H(64)	110(3)	H(20A)-N(300)-H(20B)	94.0
C(65)-C(64)-H(64)	107(3)	C(300)-N(300)-H(20C)	129.4
C(66)-C(64)-H(64)	107(3)	H(20A)-N(300)-H(20C)	75.6
C(64)-C(65)-H(65A)	108(2)	H(20B)-N(300)-H(20C)	75.1
C(64)-C(65)-H(65B)	112(2)	N(300)-C(300)-C(301)	177.0
H(65A)-C(65)-H(65B)	110(3)	C(300)-C(301)-H(30D)	109.5
C(64)-C(65)-H(65C)	111(2)	C(300)-C(301)-H(30E)	109.5
H(65A)-C(65)-H(65C)	112(3)	H(30D)-C(301)-H(30E)	109.5
H(65B)-C(65)-H(65C)	104(3)	C(300)-C(301)-H(30F)	109.5
C(64)-C(66)-H(66A)	111(2)	H(30D)-C(301)-H(30F)	109.5
C(64)-C(66)-H(66B)	110(2)	H(30E)-C(301)-H(30F)	109.5

Table 5. Anisotropic displacement parameters (Å^{2}x 10^4) for TRY4 (CCDC No. 141446). The anisotropic displacement factor exponent takes the form: $-2\pi^2$ [$h^2 a^{*2}U^{11}$ + ... + 2 h k a* b* U^{12}]

	U^{11}	U^{22}	U^{33}	U^{23}	U^{13}	U^{12}
Ni	209(3)	162(3)	233(3)	-26(3)	3(2)	13(3)
O(1)	242(17)	188(16)	243(17)	-8(13)	-6(14)	36(13)
O(2)	187(16)	185(15)	228(17)	-3(13)	-20(13)	-3(12)
N(1)	200(20)	210(20)	260(20)	-34(17)	-1(17)	30(16)
N(2)	210(20)	157(18)	240(20)	1(16)	34(16)	16(15)
C(1)	190(20)	220(20)	260(30)	0(20)	30(20)	21(19)
C(2)	250(30)	200(20)	270(30)	0(20)	10(20)	46(19)
C(3)	440(30)	240(30)	340(30)	30(20)	20(30)	60(20)
C(4)	670(40)	360(30)	300(30)	60(30)	-30(30)	120(30)

C(5)	650(40)	340(30)	240(30)	-40(30)	-10(30)	90(30)
C(6)	370(30)	210(20)	240(30)	10(20)	20(20)	80(20)
C(7)	310(30)	290(30)	220(30)	-50(20)	-20(20)	40(20)
C(8)	280(30)	190(20)	230(30)	-70(19)	-50(20)	20(20)
C(9)	230(30)	290(30)	370(30)	-100(20)	-70(20)	60(20)
C(10)	330(30)	320(30)	410(30)	-70(20)	-40(20)	-60(20)
C(11)	460(30)	200(30)	350(30)	-90(20)	-30(30)	10(20)
C(12)	380(30)	270(30)	310(30)	-90(20)	30(20)	110(30)
C(13)	320(30)	240(30)	220(30)	-40(20)	20(20)	50(20)
C(14)	250(30)	190(20)	310(30)	0(20)	-50(20)	80(20)
C(15)	220(30)	230(30)	420(30)	10(20)	-70(20)	60(20)
C(16)	260(30)	240(30)	610(40)	30(30)	-60(30)	70(20)
C(17)	260(30)	340(30)	780(50)	130(30)	-60(30)	20(30)
C(18)	310(40)	260(30)	1030(60)	30(40)	-270(40)	-30(30)
C(19)	300(30)	310(30)	760(50)	-140(30)	-190(30)	70(30)
C(20)	270(30)	210(30)	580(40)	-70(30)	-170(30)	70(20)
C(21)	390(30)	310(30)	370(30)	-130(30)	-120(30)	160(20)
C(22)	330(30)	290(30)	290(30)	-30(20)	-80(20)	150(20)
C(23)	450(40)	400(30)	320(30)	-20(30)	-10(30)	230(30)
C(24)	430(40)	470(40)	380(40)	90(30)	90(30)	190(30)
C(25)	370(30)	340(30)	420(30)	100(30)	50(30)	80(30)
C(26)	350(30)	230(30)	320(30)	20(20)	30(20)	70(20)
C(27)	280(30)	220(20)	290(30)	0(20)	-40(20)	100(20)
C(28)	310(30)	550(40)	800(50)	-260(30)	10(30)	-30(30)
C(29)	290(40)	380(50)	450(50)	150(40)	170(30)	110(30)
C(30)	350(50)	900(80)	690(70)	70(60)	110(50)	120(50)
C(31)	330(30)	270(30)	270(30)	-30(20)	70(20)	60(20)
C(32)	310(30)	370(30)	430(40)	-10(30)	60(30)	90(30)
C(33)	470(40)	550(40)	310(30)	50(30)	110(30)	-30(30)
C(34)	160(20)	180(20)	190(20)	-52(18)	53(19)	13(18)
C(35)	180(20)	200(20)	210(20)	-47(19)	43(19)	-15(19)
C(36)	200(20)	160(30)	300(30)	-10(20)	40(20)	8(19)
C(37)	170(30)	230(30)	380(30)	20(20)	-30(20)	40(20)
C(38)	170(20)	210(30)	380(30)	-30(20)	30(20)	-10(20)
C(39)	150(20)	160(20)	270(30)	-22(19)	44(19)	24(18)
C(40)	170(20)	190(20)	250(20)	-40(20)	19(19)	-30(20)
C(41)	150(20)	150(20)	290(30)	0(20)	0(20)	-16(18)
C(42)	200(20)	200(20)	270(30)	10(20)	30(20)	14(19)
C(43)	300(30)	250(30)	280(30)	80(20)	70(20)	-50(20)
C(44)	310(30)	190(30)	340(30)	10(20)	20(20)	-60(20)
C(45)	290(30)	160(20)	270(30)	-40(20)	30(20)	-10(20)
C(46)	160(20)	200(20)	270(30)	10(20)	22(19)	2(18)
C(47)	170(20)	180(20)	230(20)	20(20)	9(18)	-2(19)
C(48)	180(20)	180(20)	280(30)	62(19)	20(20)	5(18)
C(49)	210(30)	200(20)	260(30)	70(20)	50(20)	40(20)
C(50)	290(30)	240(30)	360(30)	70(20)	90(20)	80(20)
C(51)	240(30)	340(30)	610(40)	70(30)	170(30)	110(20)
C(52)	180(30)	350(30)	600(40)	80(30)	40(20)	0(20)
C(53)	180(20)	220(30)	390(30)	70(20)	20(20)	19(19)
C(54)	170(30)	270(30)	460(30)	30(20)	-40(20)	-50(20)
C(55)	250(30)	180(20)	340(30)	-10(20)	-20(20)	-30(20)
C(56)	280(30)	220(30)	500(30)	-40(20)	-50(30)	-70(20)
C(57)	400(30)	200(30)	440(30)	-130(20)	-70(30)	10(20)
C(58)	290(30)	280(30)	410(30)	-110(20)	40(20)	30(20)

C(59)	230(30)	240(30)	330(30)	-40(20)	30(20)	-20(20)
C(60)	200(20)	190(20)	250(30)	1(19)	0(20)	-1(19)
C(61)	340(30)	250(30)	280(30)	-20(20)	90(20)	-10(20)
C(62)	540(40)	440(40)	310(30)	-10(30)	140(30)	-30(30)
C(63)	480(40)	510(40)	490(40)	-140(40)	130(30)	80(30)
C(64)	290(30)	150(20)	300(30)	-30(20)	40(20)	-30(20)
C(65)	310(30)	300(30)	350(30)	-30(30)	90(30)	-20(20)
C(66)	360(30)	290(30)	330(30)	20(30)	70(30)	20(30)
C(101)	330(40)	400(40)	840(50)	220(40)	-50(30)	-70(30)
C(100)	410(40)	290(30)	640(40)	120(30)	-100(30)	10(30)
N(100)	440(30)	430(30)	900(40)	150(30)	10(30)	-20(20)

Table 6. Hydrogen coordinates (x 10^4) and isotropic displacement para-meters (Å^{2}x 10 ^{3}) for TRY4 (CCDC No. 141446).

	x	y	z	U_{iso}
H(10A)	5940(50)	8492(18)	9950(30)	100(20)
H(10B)	5340(40)	8885(18)	9330(30)	71(18)
H(10C)	5450(50)	8300(20)	9050(30)	100(20)
H(3)	5350(30)	9987(13)	6190(20)	35(13)
H(4)	5000(40)	9511(13)	5130(20)	34(13)
H(5)	5490(30)	8725(13)	5230(20)	31(12)
H(7)	5930(30)	8072(11)	5910(20)	20(11)
H(10)	4340(40)	6677(13)	6650(20)	34(12)
H(11)	6090(30)	6253(13)	6420(20)	32(12)
H(12)	7980(30)	6610(13)	6420(20)	28(12)
H(16)	7670(30)	10130(13)	6710(20)	30(14)
H(17)	8690(40)	10801(13)	6770(20)	30(14)
H(18)	8620(40)	11272(15)	7800(20)	41(15)
H(19)	7430(40)	11084(14)	8750(20)	36(14)
H(21)	5980(30)	10570(13)	9190(20)	29(12)
H(23)	4270(40)	10159(14)	9550(20)	45(14)
H(24)	2750(40)	9543(16)	9330(30)	68(18)
H(25)	2870(40)	9041(14)	8310(20)	44(14)
H(26)	4350(30)	9116(13)	7540(20)	36(13)
H(31)	8700(30)	7723(10)	7029(17)	2(9)
H(32A)	9720(40)	7007(16)	7560(30)	71(17)
H(32B)	10540(40)	7320(13)	7050(20)	29(13)
H(32C)	9950(40)	6924(13)	6700(20)	33(13)
H(33A)	8270(40)	7891(17)	5680(30)	71(17)
H(33B)	8910(30)	7375(13)	5610(20)	30(13)
H(33C)	9680(40)	7764(13)	5930(20)	26(13)
H(36)	9430(30)	6530(12)	9491(19)	20(11)
H(37)	11220(30)	6934(11)	9810(20)	19(11)
H(38)	11430(30)	7719(12)	9453(19)	27(12)
H(40)	10580(30)	8366(11)	8952(17)	10(9)
H(43)	10340(30)	9758(12)	7357(19)	17(11)
H(44)	10240(30)	10205(12)	8369(18)	17(10)
H(45)	9500(30)	9889(11)	9389(18)	8(10)

H(49)	6910(30)	7471(11)	9577(18)	16(10)
H(50)	5120(30)	7659(12)	10060(20)	22(11)
H(51)	3280(40)	7220(14)	9760(20)	45(14)
H(52)	3260(40)	6551(13)	8960(20)	38(13)
H(54)	4340(40)	6032(13)	8290(20)	35(12)
H(56)	5580(30)	5466(12)	7730(20)	26(12)
H(57)	7390(30)	5224(12)	7280(20)	23(11)
H(58)	9200(40)	5642(13)	7540(20)	32(12)
H(59)	9200(30)	6353(12)	8150(20)	28(12)
H(61)	9140(30)	8609(12)	7060(20)	27(12)
H(62A)	8570(40)	9292(15)	6300(20)	58(16)
H(62B)	9370(40)	8914(14)	5920(20)	44(14)
H(62C)	10040(40)	9370(14)	6210(20)	39(13)
H(63A)	11260(40)	8440(15)	7520(30)	56(17)
H(63B)	11650(40)	8887(16)	7070(20)	57(17)
H(63C)	11020(40)	8457(14)	6640(20)	44(15)
H(64)	8340(30)	8781(13)	9580(20)	29(12)
H(65A)	7180(30)	9444(12)	9620(20)	18(11)
H(65B)	8270(30)	9669(13)	10230(20)	31(12)
H(65C)	7480(40)	9217(13)	10430(20)	40(14)
H(66A)	10370(40)	8684(14)	10110(20)	46(14)
H(66B)	9520(40)	8810(13)	10730(20)	36(13)
H(66C)	10340(40)	9199(14)	10420(20)	43(14)
H(28)	4310	7852	6664	84
H(29A)	3374	7877	7763	43
H(29B)	4761	8026	7766	43
H(29C)	4449	7537	8064	43
H(30A)	2352	7660	6611	77
H(30B)	2715	7141	6764	77
H(30C)	3018	7382	6043	77
H(28B)	4519	7879	7062	84
H(29D)	3002	7605	7723	81
H(29E)	4361	7472	8055	81
H(29F)	3494	7102	7620	81
H(30D)	3590	7744	5890	50
H(30E)	2689	7913	6433	50
H(30F)	2707	7390	6208	50
H(20A)	9859	10486	5560	158
H(20B)	8603	10667	5783	158
H(20C)	9173	10903	5135	158
H(30D)	7176	9696	4593	100
H(30E)	8493	9466	4741	100
H(30F)	8164	9799	4066	100

Appendix I

X-Ray Diffraction Analysis of

(^{Anthr,H}Sal)Pt(CH_2CH_3)(CH_2=CH_2)

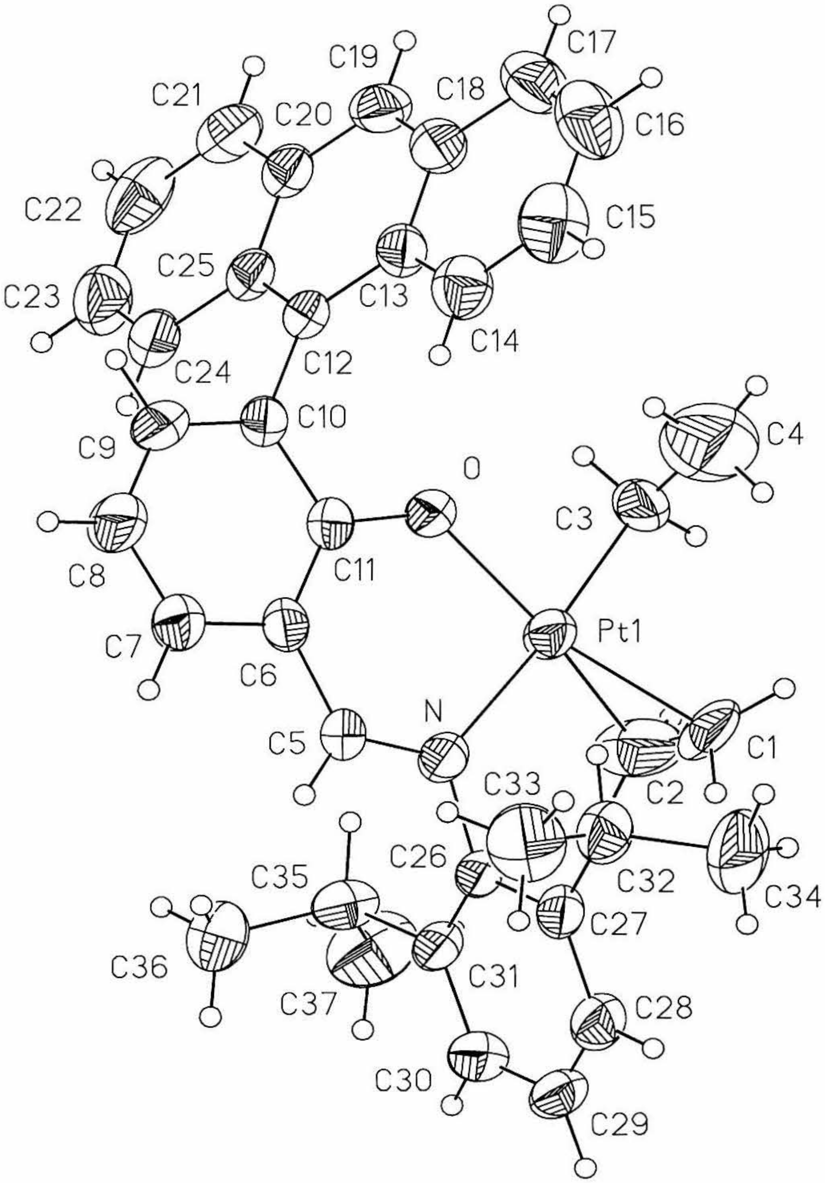

Table 1. Crystal data and structure refinement for TRY13 (CCDC No. 150671).

Empirical formula	$C_{37}H_{39}NOPt$
Formula weight	708.78
Crystallization Solvent	Toluene/hexane
Crystal Habit	Prism
Crystal size	0.326 x 0.215 x 0.178 mm^3
Crystal color	Yellow

Data Collection

Preliminary Photos	Rotation	
Type of diffractometer	CCD area detector	
Wavelength	0.71073 Å MoKα	
Data Collection Temperature	293(2) K	
θ range for 14777 reflections used in lattice determination	2.37 to 27.17°	
Unit cell dimensions	a = 11.8674(12) Å	
	b = 17.1171(18) Å	β= 95.320(2)°
	c = 15.1623(16) Å	
Volume	3066.7(6) Å^3	
Z	4	
Crystal system	Monoclinic	
Space group	$P2_1/c$	
Density (calculated)	1.535 Mg/m^3	
F(000)	1416	
Data collection program	Bruker SMART	
θ range for data collection	1.72 to 28.41°	
Completeness to θ = 28.41°	95.0 %	
Index ranges	-15 *h* 15, -22 *k* 22, -20 *l* 20	
Data collection scan type	ω scans at 5 ϕ settings	
Data reduction program	Bruker SAINT v6.2	
Reflections collected	45188	
Independent reflections	7322 [R_{int}= 0.0997]	
Absorption coefficient	4.605 mm^{-1}	
Absorption correction	None	

Table 1 (cont.)

Structure Solution and Refinement

Structure solution program	SHELXS-97 (Sheldrick, 1990)
Primary solution method	Direct methods
Secondary solution method	Difference Fourier map
Hydrogen placement	Geometric positions
Structure refinement program	SHELXL-97 (Sheldrick, 1997)
Refinement method	Full matrix least-squares on F^2
Data / restraints / parameters	7322 / 0 / 366
Treatment of hydrogen atoms	Riding
Goodness-of-fit on F^2	1.364
Final R indices [$I>2\sigma(I)$, 5009 reflections]	R1 = 0.0363, *w*R2 = 0.0712
R indices (all data)	R1 = 0.0599, *w*R2 = 0.0738
Type of weighting scheme used	Sigma
Weighting scheme used	$w=1/\sigma^2(Fo^2)$
Max shift/error	0.002
Average shift/error	0.000
Largest diff. peak and hole	1.580 and -1.256 e.Å^{-3}

Special Refinement Details

Refinement of F^2 against ALL reflections. The weighted R-factor (*w*R) and goodness of fit (S) are based on F^2, conventional R-factors (R) are based on F, with F set to zero for negative F^2. The threshold expression of $F^2 > 2\sigma(F^2)$ is used only for calculating R-factors(gt) etc. and is not relevant to the choice of reflections for refinement. R-factors based on F^2 are statistically about twice as large as those based on F, and R-factors based on ALL data will be even larger.

All esds (except the esd in the dihedral angle between two l.s. planes) are estimated using the full covariance matrix. The cell esds are taken into account individually in the estimation of esds in distances, angles and torsion angles; correlations between esds in cell parameters are only used when they are defined by crystal symmetry. An approximate (isotropic) treatment of cell esds is used for estimating esds involving l.s. planes.

Table 2. Atomic coordinates (x 10^4) and equivalent isotropic displacement parameters (Å^{2}x 10^3) for TRY13 (CCDC No. 150671). U(eq) is defined as the trace of the orthogonalized U^{ij} tensor.

	x	y	z	U_{eq}
Pt(1)	8991(1)	1978(1)	9098(1)	43(1)
O	7632(2)	2208(2)	9746(2)	38(1)
N	9547(3)	3152(2)	9281(2)	38(1)
C(1)	10017(6)	1699(4)	8100(5)	91(2)
C(2)	10580(5)	1507(4)	8926(5)	93(2)
C(3)	8335(4)	881(3)	8982(3)	58(1)
C(4)	7452(7)	861(4)	8270(5)	126(3)
C(5)	9003(3)	3677(3)	9689(2)	37(1)
C(6)	7949(4)	3576(3)	10087(3)	39(1)
C(7)	7516(4)	4254(3)	10468(3)	53(1)
C(8)	6511(4)	4235(3)	10845(3)	67(2)
C(9)	5944(4)	3538(3)	10877(3)	61(2)
C(10)	6312(4)	2854(3)	10518(3)	40(1)
C(11)	7344(4)	2870(3)	10098(2)	37(1)
C(12)	5681(4)	2111(3)	10574(3)	39(1)
C(13)	4990(4)	1821(3)	9842(3)	42(1)
C(14)	4881(4)	2227(3)	9015(3)	53(1)
C(15)	4200(5)	1935(4)	8325(3)	68(2)
C(16)	3579(5)	1249(4)	8402(4)	72(2)
C(17)	3656(4)	852(4)	9161(4)	61(2)
C(18)	4363(4)	1125(3)	9912(3)	46(1)
C(19)	4459(4)	715(3)	10714(3)	49(1)
C(20)	5155(4)	981(3)	11443(3)	42(1)
C(21)	5267(4)	558(3)	12258(3)	55(1)
C(22)	5950(5)	820(4)	12955(3)	69(2)
C(23)	6570(5)	1518(4)	12886(3)	64(2)
C(24)	6485(4)	1943(3)	12133(3)	53(1)
C(25)	5766(4)	1683(3)	11369(3)	41(1)
C(26)	10583(4)	3410(3)	8961(3)	39(1)
C(27)	10586(4)	3670(3)	8082(3)	45(1)
C(28)	11614(5)	3866(3)	7789(3)	58(1)
C(29)	12604(5)	3820(3)	8324(3)	59(2)
C(30)	12599(4)	3564(3)	9193(3)	57(1)
C(31)	11583(4)	3361(3)	9518(3)	45(1)
C(32)	9489(4)	3730(3)	7481(3)	55(1)
C(33)	8997(5)	4544(4)	7503(3)	79(2)
C(34)	9625(5)	3498(5)	6525(3)	98(2)
C(35)	11561(4)	3105(3)	10490(3)	50(1)
C(36)	11544(5)	3812(4)	11092(3)	71(2)
C(37)	12552(5)	2565(4)	10799(4)	86(2)

Table 3. Selected bond lengths [Å] and angles [°] for TRY13 (CCDC No. 150671).

Pt(1)-O	2.004(3)	O-Pt(1)-C(3)	84.54(16)
Pt(1)-C(3)	2.033(5)	O-Pt(1)-C(1)	162.2(2)
Pt(1)-C(1)	2.084(5)	C(3)-Pt(1)-C(1)	88.3(2)
Pt(1)-C(2)	2.090(6)	O-Pt(1)-C(2)	156.0(2)
Pt(1)-N	2.126(4)	C(3)-Pt(1)-C(2)	88.6(2)
O-C(11)	1.311(5)	C(1)-Pt(1)-C(2)	39.3(2)
N-C(5)	1.296(5)	O-Pt(1)-N	90.25(13)
N-C(26)	1.432(5)	C(3)-Pt(1)-N	174.79(16)
C(1)-C(2)	1.404(8)	C(1)-Pt(1)-N	96.66(19)
		C(2)-Pt(1)-N	96.2(2)

Table 4. Bond lengths [Å] and angles [°] for TRY13 (CCDC No. 150671).

Pt(1)-O	2.004(3)	C(14)-C(15)	1.356(7)
Pt(1)-C(3)	2.033(5)	C(14)-H(14)	0.9300
Pt(1)-C(1)	2.084(5)	C(15)-C(16)	1.398(8)
Pt(1)-C(2)	2.090(6)	C(15)-H(15)	0.9300
Pt(1)-N	2.126(4)	C(16)-C(17)	1.332(7)
O-C(11)	1.311(5)	C(16)-H(16)	0.9300
N-C(5)	1.296(5)	C(17)-C(18)	1.430(6)
N-C(26)	1.432(5)	C(17)-H(17)	0.9300
C(1)-C(2)	1.404(8)	C(18)-C(19)	1.399(6)
C(1)-H(1A)	0.9700	C(19)-C(20)	1.393(6)
C(1)-H(1B)	0.9700	C(19)-H(19)	0.9300
C(2)-H(2A)	0.9700	C(20)-C(25)	1.413(6)
C(2)-H(2B)	0.9700	C(20)-C(21)	1.428(6)
C(3)-C(4)	1.433(8)	C(21)-C(22)	1.348(6)
C(3)-H(3A)	0.9700	C(21)-H(21)	0.9300
C(3)-H(3B)	0.9700	C(22)-C(23)	1.412(8)
C(4)-H(4A)	0.9600	C(22)-H(22)	0.9300
C(4)-H(4B)	0.9600	C(23)-C(24)	1.350(7)
C(4)-H(4C)	0.9600	C(23)-H(23)	0.9300
C(5)-C(6)	1.449(5)	C(24)-C(25)	1.444(6)
C(5)-H(5)	0.9300	C(24)-H(24)	0.9300
C(6)-C(11)	1.406(6)	C(26)-C(31)	1.394(6)
C(6)-C(7)	1.414(6)	C(26)-C(27)	1.406(6)
C(7)-C(8)	1.370(6)	C(27)-C(28)	1.378(6)
C(7)-H(7)	0.9300	C(27)-C(32)	1.521(6)
C(8)-C(9)	1.372(7)	C(28)-C(29)	1.366(7)
C(8)-H(8)	0.9300	C(28)-H(28)	0.9300
C(9)-C(10)	1.379(7)	C(29)-C(30)	1.390(6)
C(9)-H(9)	0.9300	C(29)-H(29)	0.9300
C(10)-C(11)	1.432(6)	C(30)-C(31)	1.389(6)
C(10)-C(12)	1.483(6)	C(30)-H(30)	0.9300
C(12)-C(25)	1.407(6)	C(31)-C(35)	1.540(6)
C(12)-C(13)	1.408(6)	C(32)-C(33)	1.512(7)
C(13)-C(18)	1.413(6)	C(32)-C(34)	1.526(6)
C(13)-C(14)	1.429(6)	C(32)-H(32)	0.9800

C(33)-H(33A)	0.9600
C(33)-H(33B)	0.9600
C(33)-H(33C)	0.9600
C(34)-H(34A)	0.9600
C(34)-H(34B)	0.9600
C(34)-H(34C)	0.9600
C(35)-C(36)	1.516(7)
C(35)-C(37)	1.535(7)
C(35)-H(35)	0.9800
C(36)-H(36A)	0.9600
C(36)-H(36B)	0.9600
C(36)-H(36C)	0.9600
C(37)-H(37A)	0.9600
C(37)-H(37B)	0.9600
C(37)-H(37C)	0.9600
O-Pt(1)-C(3)	84.54(16)
O-Pt(1)-C(1)	162.2(2)
C(3)-Pt(1)-C(1)	88.3(2)
O-Pt(1)-C(2)	156.0(2)
C(3)-Pt(1)-C(2)	88.6(2)
C(1)-Pt(1)-C(2)	39.3(2)
O-Pt(1)-N	90.25(13)
C(3)-Pt(1)-N	174.79(16)
C(1)-Pt(1)-N	96.66(19)
C(2)-Pt(1)-N	96.2(2)
C(11)-O-Pt(1)	128.4(3)
C(5)-N-C(26)	115.5(4)
C(5)-N-Pt(1)	123.7(3)
C(26)-N-Pt(1)	120.8(3)
C(2)-C(1)-Pt(1)	70.6(3)
C(2)-C(1)-H(1A)	116.6
Pt(1)-C(1)-H(1A)	116.6
C(2)-C(1)-H(1B)	116.6
Pt(1)-C(1)-H(1B)	116.6
H(1A)-C(1)-H(1B)	113.6
C(1)-C(2)-Pt(1)	70.1(3)
C(1)-C(2)-H(2A)	116.6
Pt(1)-C(2)-H(2A)	116.6
C(1)-C(2)-H(2B)	116.6
Pt(1)-C(2)-H(2B)	116.6
H(2A)-C(2)-H(2B)	113.6
C(4)-C(3)-Pt(1)	109.6(4)
C(4)-C(3)-H(3A)	109.8
Pt(1)-C(3)-H(3A)	109.8
C(4)-C(3)-H(3B)	109.8
Pt(1)-C(3)-H(3B)	109.8
H(3A)-C(3)-H(3B)	108.2
C(3)-C(4)-H(4A)	109.5
C(3)-C(4)-H(4B)	109.5
H(4A)-C(4)-H(4B)	109.5
C(3)-C(4)-H(4C)	109.5
H(4A)-C(4)-H(4C)	109.5
H(4B)-C(4)-H(4C)	109.5

N-C(5)-C(6)	127.1(4)
N-C(5)-H(5)	116.4
C(6)-C(5)-H(5)	116.4
C(11)-C(6)-C(7)	119.7(4)
C(11)-C(6)-C(5)	124.7(4)
C(7)-C(6)-C(5)	115.6(4)
C(8)-C(7)-C(6)	120.9(5)
C(8)-C(7)-H(7)	119.5
C(6)-C(7)-H(7)	119.5
C(7)-C(8)-C(9)	119.0(5)
C(7)-C(8)-H(8)	120.5
C(9)-C(8)-H(8)	120.5
C(8)-C(9)-C(10)	123.3(5)
C(8)-C(9)-H(9)	118.3
C(10)-C(9)-H(9)	118.3
C(9)-C(10)-C(11)	118.4(4)
C(9)-C(10)-C(12)	121.7(4)
C(11)-C(10)-C(12)	119.9(4)
O-C(11)-C(6)	125.8(4)
O-C(11)-C(10)	115.5(4)
C(6)-C(11)-C(10)	118.7(4)
C(25)-C(12)-C(13)	118.8(4)
C(25)-C(12)-C(10)	120.0(4)
C(13)-C(12)-C(10)	121.2(4)
C(12)-C(13)-C(18)	120.6(4)
C(12)-C(13)-C(14)	121.3(5)
C(18)-C(13)-C(14)	118.1(4)
C(15)-C(14)-C(13)	119.8(5)
C(15)-C(14)-H(14)	120.1
C(13)-C(14)-H(14)	120.1
C(14)-C(15)-C(16)	121.8(5)
C(14)-C(15)-H(15)	119.1
C(16)-C(15)-H(15)	119.1
C(17)-C(16)-C(15)	120.4(5)
C(17)-C(16)-H(16)	119.8
C(15)-C(16)-H(16)	119.8
C(16)-C(17)-C(18)	120.6(6)
C(16)-C(17)-H(17)	119.7
C(18)-C(17)-H(17)	119.7
C(19)-C(18)-C(13)	119.2(4)
C(19)-C(18)-C(17)	121.5(5)
C(13)-C(18)-C(17)	119.3(4)
C(20)-C(19)-C(18)	121.3(5)
C(20)-C(19)-H(19)	119.4
C(18)-C(19)-H(19)	119.4
C(19)-C(20)-C(25)	119.1(4)
C(19)-C(20)-C(21)	121.4(5)
C(25)-C(20)-C(21)	119.5(4)
C(22)-C(21)-C(20)	120.8(5)
C(22)-C(21)-H(21)	119.6
C(20)-C(21)-H(21)	119.6
C(21)-C(22)-C(23)	120.2(5)
C(21)-C(22)-H(22)	119.9
C(23)-C(22)-H(22)	119.9

C(24)-C(23)-C(22)	121.4(5)
C(24)-C(23)-H(23)	119.3
C(22)-C(23)-H(23)	119.3
C(23)-C(24)-C(25)	120.3(5)
C(23)-C(24)-H(24)	119.9
C(25)-C(24)-H(24)	119.9
C(12)-C(25)-C(20)	120.9(4)
C(12)-C(25)-C(24)	121.1(5)
C(20)-C(25)-C(24)	118.0(4)
C(31)-C(26)-C(27)	121.1(4)
C(31)-C(26)-N	119.0(4)
C(27)-C(26)-N	119.8(4)
C(28)-C(27)-C(26)	117.6(4)
C(28)-C(27)-C(32)	121.6(4)
C(26)-C(27)-C(32)	120.8(4)
C(29)-C(28)-C(27)	122.2(5)
C(29)-C(28)-H(28)	118.9
C(27)-C(28)-H(28)	118.9
C(28)-C(29)-C(30)	120.2(5)
C(28)-C(29)-H(29)	119.9
C(30)-C(29)-H(29)	119.9
C(31)-C(30)-C(29)	119.7(5)
C(31)-C(30)-H(30)	120.2
C(29)-C(30)-H(30)	120.2
C(30)-C(31)-C(26)	119.3(4)
C(30)-C(31)-C(35)	120.2(4)
C(26)-C(31)-C(35)	120.5(4)
C(33)-C(32)-C(27)	111.1(4)
C(33)-C(32)-C(34)	109.6(5)
C(27)-C(32)-C(34)	113.0(4)
C(33)-C(32)-H(32)	107.6
C(27)-C(32)-H(32)	107.6
C(34)-C(32)-H(32)	107.6
C(32)-C(33)-H(33A)	109.5
C(32)-C(33)-H(33B)	109.5
H(33A)-C(33)-H(33B)	109.5
C(32)-C(33)-H(33C)	109.5
H(33A)-C(33)-H(33C)	109.5
H(33B)-C(33)-H(33C)	109.5
C(32)-C(34)-H(34A)	109.5
C(32)-C(34)-H(34B)	109.5
H(34A)-C(34)-H(34B)	109.5
C(32)-C(34)-H(34C)	109.5
H(34A)-C(34)-H(34C)	109.5
H(34B)-C(34)-H(34C)	109.5
C(36)-C(35)-C(37)	110.5(5)
C(36)-C(35)-C(31)	110.6(4)
C(37)-C(35)-C(31)	112.5(4)
C(36)-C(35)-H(35)	107.7
C(37)-C(35)-H(35)	107.7
C(31)-C(35)-H(35)	107.7
C(35)-C(36)-H(36A)	109.5
C(35)-C(36)-H(36B)	109.5
H(36A)-C(36)-H(36B)	109.5
C(35)-C(36)-H(36C)	109.5
H(36A)-C(36)-H(36C)	109.5
H(36B)-C(36)-H(36C)	109.5
C(35)-C(37)-H(37A)	109.5
C(35)-C(37)-H(37B)	109.5
H(37A)-C(37)-H(37B)	109.5
C(35)-C(37)-H(37C)	109.5
H(37A)-C(37)-H(37C)	109.5
H(37B)-C(37)-H(37C)	109.5

Table 5. Anisotropic displacement parameters ($Å^2$x 10^4) for TRY13 (CCDC No. 150671). The anisotropic displacement factor exponent takes the form: $-2\pi^2$ [$h^2 a^{*2}U^{11}$ + ... + 2 h k a* b* U^{12}]

	U^{11}	U^{22}	U^{33}	U^{23}	U^{13}	U^{12}
Pt(1)	462(1)	325(1)	534(1)	-82(1)	209(1)	-38(1)
O	353(17)	376(18)	424(16)	-60(13)	102(13)	-25(14)
N	410(20)	360(20)	374(19)	-20(16)	120(16)	-7(18)
C(1)	1140(60)	460(40)	1310(50)	-410(40)	1000(50)	-290(40)
C(2)	620(40)	490(40)	1740(70)	-230(50)	510(50)	-40(30)
C(3)	400(30)	540(40)	800(40)	-330(30)	140(30)	-80(30)
C(4)	1410(70)	830(60)	1610(70)	-90(50)	540(60)	-340(60)
C(5)	400(30)	400(30)	320(20)	-78(19)	61(19)	-10(20)
C(6)	490(30)	380(30)	320(20)	-69(19)	70(20)	-60(20)
C(7)	600(30)	450(30)	590(30)	-170(20)	220(30)	-90(30)
C(8)	630(40)	550(40)	900(40)	-290(30)	380(30)	-60(30)

C(9)	510(30)	620(40)	740(30)	-240(30)	330(30)	-150(30)
C(10)	350(20)	480(30)	380(20)	-130(20)	59(19)	-20(20)
C(11)	410(30)	420(30)	280(20)	-46(19)	39(19)	-20(20)
C(12)	340(20)	440(30)	400(20)	-120(20)	118(19)	-20(20)
C(13)	350(30)	490(30)	400(30)	-100(20)	30(20)	10(20)
C(14)	560(30)	580(40)	460(30)	-20(20)	20(30)	30(30)
C(15)	770(40)	750(50)	510(30)	50(30)	-60(30)	170(40)
C(16)	680(40)	770(50)	650(40)	-170(30)	-200(30)	130(40)
C(17)	490(30)	620(40)	700(40)	-160(30)	-80(30)	-20(30)
C(18)	350(30)	500(30)	540(30)	-110(20)	30(20)	50(20)
C(19)	380(30)	440(30)	670(30)	-80(30)	150(20)	-40(20)
C(20)	380(30)	490(30)	400(30)	-60(20)	100(20)	30(20)
C(21)	530(30)	560(40)	600(30)	30(30)	220(30)	30(30)
C(22)	690(40)	980(50)	410(30)	130(30)	160(30)	220(40)
C(23)	620(40)	880(50)	410(30)	-120(30)	20(30)	20(30)
C(24)	470(30)	700(40)	420(30)	-160(30)	110(20)	-30(30)
C(25)	340(30)	510(30)	390(30)	-100(20)	100(20)	30(20)
C(26)	430(30)	350(30)	410(30)	-90(20)	170(20)	-80(20)
C(27)	580(30)	390(30)	420(30)	-110(20)	200(20)	-100(20)
C(28)	760(40)	490(30)	530(30)	-100(20)	310(30)	-180(30)
C(29)	640(40)	500(30)	710(40)	-160(30)	400(30)	-200(30)
C(30)	530(30)	540(40)	670(30)	-140(30)	210(30)	-160(30)
C(31)	470(30)	430(30)	480(30)	-110(20)	230(20)	-70(20)
C(32)	680(40)	600(40)	380(30)	-30(20)	130(30)	-80(30)
C(33)	1050(50)	610(40)	720(40)	120(30)	110(30)	-40(40)
C(34)	1010(50)	1510(70)	430(30)	-290(40)	130(30)	-110(50)
C(35)	400(30)	570(40)	540(30)	60(30)	90(20)	-60(30)
C(36)	810(40)	870(50)	460(30)	-70(30)	150(30)	-80(40)
C(37)	710(40)	1020(60)	860(40)	230(40)	100(30)	160(40)

Table 6. Hydrogen coordinates (x 10^4) and isotropic displacement parameters ($Å^2$x 10^3) for TRY13 (CCDC No. 150671).

	x	y	z	U_{iso}
H(1A)	9771	1266	7716	109
H(1B)	10321	2135	7788	109
H(2A)	11232	1823	9126	111
H(2B)	10682	955	9054	111
H(3A)	8925	513	8866	69
H(3B)	8034	731	9531	69
H(4A)	6842	1194	8410	189
H(4B)	7179	335	8189	189
H(4C)	7741	1040	7736	189
H(5)	9324	4173	9731	44
H(7)	7919	4719	10462	64
H(8)	6218	4687	11076	81
H(9)	5277	3526	11154	73
H(14)	5276	2689	8950	64
H(15)	4144	2200	7787	82

H(16)	3109	1068	7920	86
H(17)	3245	393	9202	73
H(19)	4051	255	10761	59
H(21)	4863	97	12309	67
H(22)	6014	540	13483	82
H(23)	7047	1688	13369	77
H(24)	6891	2406	12106	63
H(28)	11635	4034	7207	69
H(29)	13282	3962	8106	71
H(30)	13274	3528	9555	68
H(32)	8944	3370	7709	66
H(33A)	8731	4637	8072	119
H(33B)	8378	4591	7052	119
H(33C)	9570	4920	7398	119
H(34A)	10104	3869	6267	147
H(34B)	8896	3490	6193	147
H(34C)	9961	2988	6515	147
H(35)	10858	2813	10537	60
H(36A)	11495	3642	11691	106
H(36B)	10902	4132	10906	106
H(36C)	12226	4108	11060	106
H(37A)	12560	2126	10405	129
H(37B)	12466	2383	11388	129
H(37C)	13251	2847	10796	129

Appendix J

X-Ray Diffraction Analysis of

$(^{NO_2,NO_2}Sal)Pt(CH_2CH_3)(CH_2{=}CH_2)$

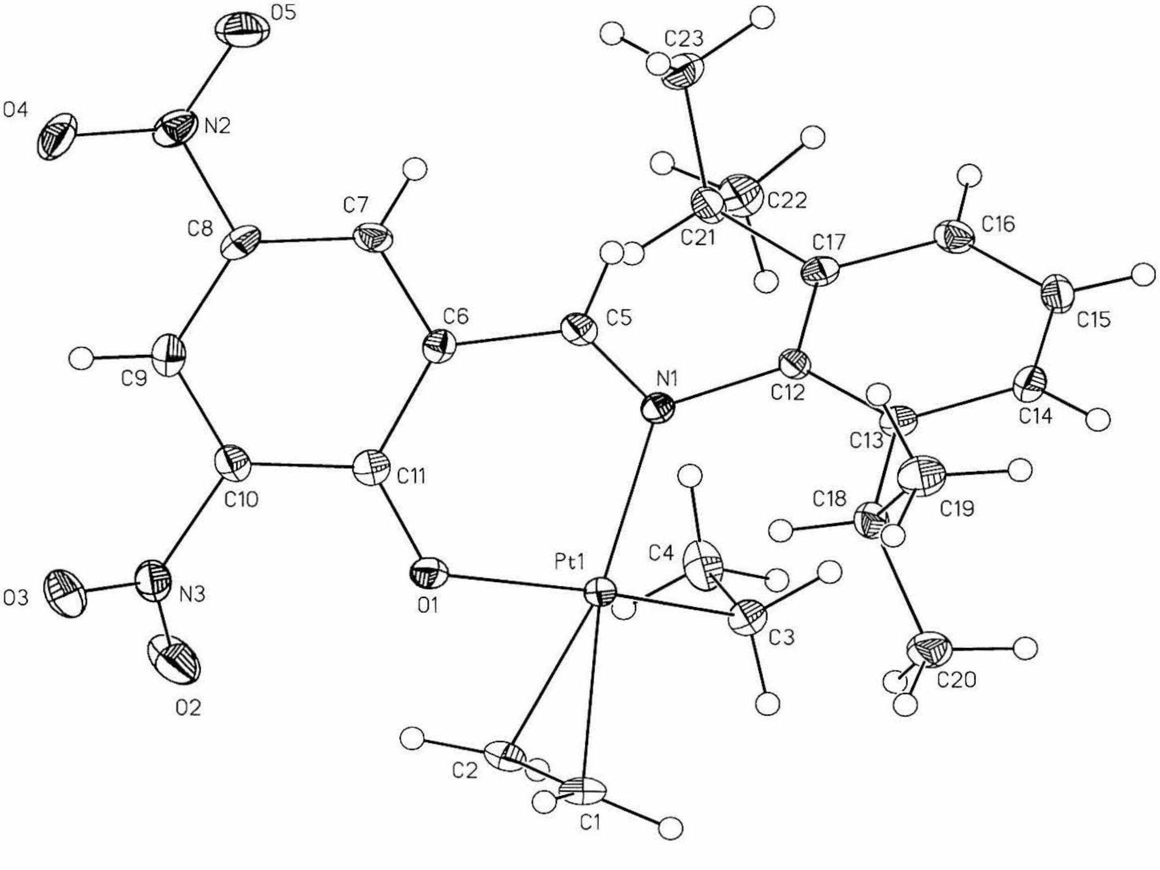

Table 1. Crystal data and structure refinement for TRY16 (CCDC 160844).

Empirical formula	$C_{23}H_{29}N_3O_5Pt$
Formula weight	622.58
Crystallization Solvent	Benzene/hexanes
Crystal Habit	Blocks
Crystal size	0.23 x 0.19 x 0.13 mm^3
Crystal color	Deep yellow

Data Collection

Preliminary Photos	Rotation	
Type of diffractometer	CCD area detector	
Wavelength	0.71073 Å MoKα	
Data Collection Temperature	98(2) K	
θ range for 17920 reflections used in lattice determination	2.41 to 28.17°	
Unit cell dimensions	a = 8.1765(5) Å	α= 85.3990(10)°
	b = 12.3539(7) Å	β= 73.4250(10)°
	c = 12.5292(7) Å	γ = 70.7300(10)°
Volume	1144.91(11) Å^3	
Z	2	
Crystal system	Triclinic	
Space group	P-1	
Density (calculated)	1.806 Mg/m^3	
F(000)	612	
Data collection program	Bruker SMART	
θ range for data collection	1.70 to 28.29°	
Completeness to θ = 28.29°	93.4 %	
Index ranges	-10 h 10, -16 k 16, -16 l 16	
Data collection scan type	ω scans at 7 ϕ settings	
Data reduction program	Bruker SAINT v6.2	
Reflections collected	23715	
Independent reflections	5316 [R_{int}= 0.0400]	
Absorption coefficient	6.167 mm^{-1}	
Absorption correction	SADABS	
Max. and min. transmission	1.000000 and 0.737708	

Table 1 (cont.)

Structure Solution and Refinement

Structure solution program	SHELXS-97 (Sheldrick, 1990)
Primary solution method	Patterson method
Secondary solution method	Difference Fourier map
Hydrogen placement	Difference Fourier map
Structure refinement program	SHELXL-97 (Sheldrick, 1997)
Refinement method	Full matrix least-squares on F^2
Data / restraints / parameters	5316 / 0 / 405
Treatment of hydrogen atoms	Unrestrained
Goodness-of-fit on F^2	1.464
Final R indices [$I > 2\sigma(I)$, 4959 reflections]	$R1 = 0.0204$, $wR2 = 0.0408$
R indices (all data)	$R1 = 0.0225$, $wR2 = 0.0411$
Type of weighting scheme used	Sigma
Weighting scheme used	$w=1/\sigma^2(Fo^2)$
Max shift/error	0.003
Average shift/error	0.000
Largest diff. peak and hole	1.328 and -0.678 e.Å^{-3}

Special Refinement Details

All difference Fourier peaks with heights over 1 e$^-$/Å^3 are within 1 Å of the platinum and are assumed to be absorption ripples.

Refinement of F^2 against ALL reflections. The weighted R-factor (*w*R) and goodness of fit (S) are based on F^2, conventional R-factors (R) are based on F, with F set to zero for negative F^2. The threshold expression of $F^2 > 2\sigma(F^2)$ is used only for calculating R-factors(gt) etc. and is not relevant to the choice of reflections for refinement. R-factors based on F^2 are statistically about twice as large as those based on F, and R-factors based on ALL data will be even larger.

All esds (except the esd in the dihedral angle between two l.s. planes) are estimated using the full covariance matrix. The cell esds are taken into account individually in the estimation of esds in distances, angles and torsion angles; correlations between esds in cell parameters are only used when they are defined by crystal symmetry. An approximate (isotropic) treatment of cell esds is used for estimating esds involving l.s. planes.

Table 2. Atomic coordinates (x 10^4) and equivalent isotropic displacement parameters (Å^{2}x 10^3) for TRY16 (CCDC 160844). U(eq) is defined as the trace of the orthogonalized U^{ij} tensor.

	x	y	z	U_{eq}
Pt(1)	7113(1)	8308(1)	6967(1)	12(1)
O(1)	7688(3)	7117(2)	5677(2)	15(1)
O(2)	5801(3)	7015(2)	4243(2)	30(1)
O(3)	7384(3)	5493(2)	3226(2)	24(1)
O(4)	8383(3)	1995(2)	5321(2)	25(1)
O(5)	9209(3)	1941(2)	6826(2)	28(1)
N(1)	8226(3)	6981(2)	7927(2)	11(1)
N(2)	8641(3)	2458(2)	6057(2)	18(1)
N(3)	6835(3)	6033(2)	4115(2)	17(1)
C(1)	7174(4)	9560(3)	5710(3)	21(1)
C(2)	5456(4)	9487(3)	6087(3)	19(1)
C(3)	6230(4)	9524(3)	8182(3)	18(1)
C(4)	4387(4)	9548(3)	8926(3)	22(1)
C(5)	8614(4)	5910(2)	7676(2)	12(1)
C(6)	8252(4)	5428(2)	6781(2)	12(1)
C(7)	8532(4)	4252(2)	6826(2)	14(1)
C(8)	8264(4)	3698(2)	6015(2)	15(1)
C(9)	7710(4)	4283(2)	5126(2)	15(1)
C(10)	7444(4)	5438(2)	5061(2)	14(1)
C(11)	7758(4)	6073(2)	5846(2)	13(1)
C(12)	8751(4)	7202(2)	8882(2)	11(1)
C(13)	10177(4)	7657(2)	8673(2)	13(1)
C(14)	10617(4)	7926(2)	9589(2)	16(1)
C(15)	9692(4)	7752(2)	10660(2)	16(1)
C(16)	8318(4)	7284(2)	10846(2)	15(1)
C(17)	7799(4)	7008(2)	9963(2)	13(1)
C(18)	11236(4)	7850(2)	7502(2)	15(1)
C(19)	13232(4)	7151(3)	7269(3)	21(1)
C(20)	10981(5)	9118(3)	7276(3)	20(1)
C(21)	6289(4)	6482(2)	10201(2)	15(1)
C(22)	4653(4)	7115(3)	11142(3)	21(1)
C(23)	6973(5)	5212(3)	10490(3)	19(1)

Table 3. Selected bond lengths [Å] and angles [°] for TRY16 (CCDC 160844).

Pt(1)-C(3)	2.029(3)	C(3)-Pt(1)-N(1)	94.85(11)
Pt(1)-N(1)	2.070(2)	C(3)-Pt(1)-C(2)	87.97(13)
Pt(1)-C(2)	2.114(3)	N(1)-Pt(1)-C(2)	165.85(10)
Pt(1)-O(1)	2.1196(18)	C(3)-Pt(1)-O(1)	172.51(10)
Pt(1)-C(1)	2.120(3)	N(1)-Pt(1)-O(1)	89.84(8)
C(1)-C(2)	1.380(4)	C(2)-Pt(1)-O(1)	86.08(10)
		C(3)-Pt(1)-C(1)	91.46(13)
		N(1)-Pt(1)-C(1)	155.21(11)
		C(2)-Pt(1)-C(1)	38.04(12)
		O(1)-Pt(1)-C(1)	86.66(10)

Table 4. Bond lengths [Å] and angles [°] for TRY16 (CCDC 160844).

Pt(1)-C(3)	2.029(3)	C(19)-H(19C)	1.00(3)
Pt(1)-N(1)	2.070(2)	C(20)-H(20A)	0.96(3)
Pt(1)-C(2)	2.114(3)	C(20)-H(20B)	1.02(4)
Pt(1)-O(1)	2.1196(18)	C(20)-H(20C)	0.87(4)
Pt(1)-C(1)	2.120(3)	C(21)-C(23)	1.533(4)
O(1)-C(11)	1.275(3)	C(21)-C(22)	1.532(4)
O(2)-N(3)	1.220(3)	C(21)-H(21)	0.92(3)
O(3)-N(3)	1.234(3)	C(22)-H(22A)	1.01(3)
O(4)-N(2)	1.224(3)	C(22)-H(22B)	0.97(3)
O(5)-N(2)	1.230(3)	C(22)-H(22C)	0.95(3)
N(1)-C(5)	1.298(3)	C(23)-H(23A)	0.91(4)
N(1)-C(12)	1.453(3)	C(23)-H(23B)	0.93(3)
N(2)-C(8)	1.459(3)	C(23)-H(23C)	0.98(3)
N(3)-C(10)	1.467(3)		
C(1)-C(2)	1.380(4)	C(3)-Pt(1)-N(1)	94.85(11)
C(1)-H(1A)	1.03(3)	C(3)-Pt(1)-C(2)	87.97(13)
C(1)-H(1B)	0.97(3)	N(1)-Pt(1)-C(2)	165.85(10)
C(2)-H(2A)	0.95(3)	C(3)-Pt(1)-O(1)	172.51(10)
C(2)-H(2B)	0.93(3)	N(1)-Pt(1)-O(1)	89.84(8)
C(3)-C(4)	1.521(4)	C(2)-Pt(1)-O(1)	86.08(10)
C(3)-H(3A)	0.99(3)	C(3)-Pt(1)-C(1)	91.46(13)
C(3)-H(3B)	0.93(4)	N(1)-Pt(1)-C(1)	155.21(11)
C(4)-H(4A)	0.97(4)	C(2)-Pt(1)-C(1)	38.04(12)
C(4)-H(4B)	1.02(3)	O(1)-Pt(1)-C(1)	86.66(10)
C(4)-H(4C)	0.96(3)	C(11)-O(1)-Pt(1)	123.68(17)
C(5)-C(6)	1.453(4)	C(5)-N(1)-C(12)	115.9(2)
C(5)-H(5)	0.91(3)	C(5)-N(1)-Pt(1)	122.71(19)
C(6)-C(7)	1.393(4)	C(12)-N(1)-Pt(1)	121.21(17)
C(6)-C(11)	1.442(4)	O(4)-N(2)-O(5)	124.0(2)
C(7)-C(8)	1.374(4)	O(4)-N(2)-C(8)	118.0(2)
C(7)-H(7)	0.83(3)	O(5)-N(2)-C(8)	118.0(2)
C(8)-C(9)	1.382(4)	O(2)-N(3)-O(3)	123.4(2)
C(9)-C(10)	1.370(4)	O(2)-N(3)-C(10)	119.3(2)
C(9)-H(9)	0.90(3)	O(3)-N(3)-C(10)	117.2(2)
C(10)-C(11)	1.431(4)	C(2)-C(1)-Pt(1)	70.74(17)
C(12)-C(17)	1.402(4)	C(2)-C(1)-H(1A)	123.1(18)
C(12)-C(13)	1.407(4)	Pt(1)-C(1)-H(1A)	105.7(17)
C(13)-C(14)	1.390(4)	C(2)-C(1)-H(1B)	122.6(17)
C(13)-C(18)	1.521(4)	Pt(1)-C(1)-H(1B)	108.3(17)
C(14)-C(15)	1.378(4)	H(1A)-C(1)-H(1B)	113(2)
C(14)-H(14)	0.89(3)	C(1)-C(2)-Pt(1)	71.22(17)
C(15)-C(16)	1.382(4)	C(1)-C(2)-H(2A)	123.3(18)
C(15)-H(15)	0.90(3)	Pt(1)-C(2)-H(2A)	104.4(18)
C(16)-C(17)	1.394(4)	C(1)-C(2)-H(2B)	119.6(19)
C(16)-H(16)	0.91(3)	Pt(1)-C(2)-H(2B)	108.3(19)
C(17)-C(21)	1.524(4)	H(2A)-C(2)-H(2B)	115(3)
C(18)-C(20)	1.524(4)	C(4)-C(3)-Pt(1)	110.2(2)
C(18)-C(19)	1.527(4)	C(4)-C(3)-H(3A)	109.9(18)
C(18)-H(18)	0.90(3)	Pt(1)-C(3)-H(3A)	108.7(17)
C(19)-H(19A)	0.94(4)	C(4)-C(3)-H(3B)	111(2)
C(19)-H(19B)	0.98(3)	Pt(1)-C(3)-H(3B)	109(2)

H(3A)-C(3)-H(3B)	108(3)
C(3)-C(4)-H(4A)	112(2)
C(3)-C(4)-H(4B)	110.1(19)
H(4A)-C(4)-H(4B)	106(3)
C(3)-C(4)-H(4C)	109.8(19)
H(4A)-C(4)-H(4C)	111(3)
H(4B)-C(4)-H(4C)	107(3)
N(1)-C(5)-C(6)	128.5(3)
N(1)-C(5)-H(5)	118.9(16)
C(6)-C(5)-H(5)	112.6(16)
C(7)-C(6)-C(11)	120.0(2)
C(7)-C(6)-C(5)	115.8(2)
C(11)-C(6)-C(5)	124.0(2)
C(8)-C(7)-C(6)	121.0(3)
C(8)-C(7)-H(7)	119(2)
C(6)-C(7)-H(7)	120(2)
C(7)-C(8)-C(9)	121.4(3)
C(7)-C(8)-N(2)	119.8(3)
C(9)-C(8)-N(2)	118.7(2)
C(10)-C(9)-C(8)	118.5(3)
C(10)-C(9)-H(9)	119.9(19)
C(8)-C(9)-H(9)	121.6(19)
C(9)-C(10)-C(11)	123.8(3)
C(9)-C(10)-N(3)	117.0(2)
C(11)-C(10)-N(3)	119.3(2)
O(1)-C(11)-C(10)	121.0(2)
O(1)-C(11)-C(6)	123.7(2)
C(10)-C(11)-C(6)	115.1(2)
C(17)-C(12)-C(13)	122.4(2)
C(17)-C(12)-N(1)	120.2(2)
C(13)-C(12)-N(1)	117.3(2)
C(14)-C(13)-C(12)	117.4(3)
C(14)-C(13)-C(18)	119.8(3)
C(12)-C(13)-C(18)	122.8(2)
C(15)-C(14)-C(13)	121.3(3)
C(15)-C(14)-H(14)	118.9(18)
C(13)-C(14)-H(14)	119.8(18)
C(14)-C(15)-C(16)	120.4(3)
C(14)-C(15)-H(15)	120.0(19)
C(16)-C(15)-H(15)	119.6(19)
C(17)-C(16)-C(15)	121.1(3)
C(17)-C(16)-H(16)	116.6(17)
C(15)-C(16)-H(16)	122.3(17)
C(16)-C(17)-C(12)	117.4(3)
C(16)-C(17)-C(21)	119.5(2)
C(12)-C(17)-C(21)	123.0(2)
C(13)-C(18)-C(20)	112.0(2)
C(13)-C(18)-C(19)	111.7(2)
C(20)-C(18)-C(19)	111.2(3)
C(13)-C(18)-H(18)	103.5(19)
C(20)-C(18)-H(18)	105.1(19)
C(19)-C(18)-H(18)	113.1(19)
C(18)-C(19)-H(19A)	108(2)
C(18)-C(19)-H(19B)	111.4(18)
H(19A)-C(19)-H(19B)	109(3)
C(18)-C(19)-H(19C)	111.4(19)
H(19A)-C(19)-H(19C)	105(3)
H(19B)-C(19)-H(19C)	111(3)
C(18)-C(20)-H(20A)	113.0(19)
C(18)-C(20)-H(20B)	112(2)
H(20A)-C(20)-H(20B)	104(3)
C(18)-C(20)-H(20C)	108(2)
H(20A)-C(20)-H(20C)	111(3)
H(20B)-C(20)-H(20C)	108(3)
C(17)-C(21)-C(23)	110.5(2)
C(17)-C(21)-C(22)	112.4(2)
C(23)-C(21)-C(22)	109.6(2)
C(17)-C(21)-H(21)	107.9(17)
C(23)-C(21)-H(21)	109.6(16)
C(22)-C(21)-H(21)	106.7(17)
C(21)-C(22)-H(22A)	111.5(18)
C(21)-C(22)-H(22B)	108.8(19)
H(22A)-C(22)-H(22B)	109(3)
C(21)-C(22)-H(22C)	111.0(19)
H(22A)-C(22)-H(22C)	109(3)
H(22B)-C(22)-H(22C)	107(3)
C(21)-C(23)-H(23A)	118(2)
C(21)-C(23)-H(23B)	109.5(18)
H(23A)-C(23)-H(23B)	104(3)
C(21)-C(23)-H(23C)	110.6(19)
H(23A)-C(23)-H(23C)	105(3)
H(23B)-C(23)-H(23C)	108(3)

Table 5. Anisotropic displacement parameters ($Å^2$x 10^4) for TRY16 (CCDC 160844). The anisotropic displacement factor exponent takes the form: $-2\pi^2$ [h^2 $a^{*2}U^{11}$ + ... + 2 h k a* b* U^{12}]

	U^{11}	U^{22}	U^{33}	U^{23}	U^{13}	U^{12}
Pt(1)	144(1)	112(1)	130(1)	27(1)	-61(1)	-57(1)
O(1)	198(11)	139(10)	122(10)	27(8)	-49(8)	-69(8)
O(2)	357(14)	259(12)	250(12)	-14(10)	-169(11)	13(11)
O(3)	311(13)	291(12)	120(10)	-27(9)	-69(9)	-99(10)
O(4)	364(14)	194(11)	247(12)	-36(9)	-84(10)	-165(10)
O(5)	487(15)	152(11)	209(12)	39(9)	-124(11)	-89(10)
N(1)	108(12)	137(11)	104(11)	20(9)	-20(9)	-65(9)
N(2)	243(14)	156(12)	143(13)	-9(10)	10(11)	-101(11)
N(3)	177(13)	220(13)	152(13)	3(10)	-56(10)	-92(11)
C(1)	289(18)	153(15)	205(16)	92(12)	-108(14)	-93(13)
C(2)	235(17)	167(15)	189(16)	77(12)	-122(14)	-69(13)
C(3)	212(16)	140(15)	193(16)	11(12)	-84(13)	-60(12)
C(4)	201(17)	237(17)	230(17)	-56(14)	-95(14)	-28(14)
C(5)	100(14)	174(14)	97(13)	28(11)	-11(11)	-63(11)
C(6)	108(14)	132(13)	116(13)	-6(10)	-14(11)	-51(11)
C(7)	151(15)	161(14)	106(14)	44(11)	-30(12)	-67(12)
C(8)	165(15)	118(13)	150(14)	-6(11)	7(12)	-76(11)
C(9)	140(15)	215(15)	119(14)	-32(11)	-7(12)	-89(12)
C(10)	119(14)	203(15)	102(14)	15(11)	-19(11)	-72(12)
C(11)	96(14)	165(14)	103(13)	-3(11)	10(11)	-52(11)
C(12)	130(14)	105(13)	111(13)	4(10)	-51(11)	-29(11)
C(13)	127(14)	113(13)	134(14)	8(10)	-28(11)	-34(11)
C(14)	174(16)	153(14)	198(16)	17(11)	-85(13)	-85(12)
C(15)	178(16)	148(14)	167(15)	-18(11)	-85(13)	-39(12)
C(16)	177(15)	157(14)	109(14)	16(11)	-29(12)	-52(12)
C(17)	121(14)	95(13)	148(14)	12(10)	-32(11)	-25(11)
C(18)	146(15)	190(15)	158(15)	26(11)	-63(12)	-86(12)
C(19)	197(17)	211(17)	195(17)	17(13)	-24(14)	-73(13)
C(20)	197(17)	218(16)	199(17)	66(13)	-61(14)	-107(14)
C(21)	152(15)	200(15)	125(14)	21(11)	-58(12)	-75(12)
C(22)	182(17)	257(18)	180(17)	24(13)	-33(13)	-94(14)
C(23)	247(18)	170(16)	185(16)	26(12)	-48(14)	-117(14)

Table 6. Hydrogen coordinates (x 10^4) and isotropic displacement parameters ($Å^2$x 10^3) for TRY16 (CCDC 160844).

	x	y	z	U_{iso}
H(1A)	8110(40)	9130(30)	5010(30)	22(8)
H(1B)	7510(40)	10160(20)	5960(20)	13(8)
H(2A)	5030(40)	9030(30)	5730(20)	18(8)
H(2B)	4570(40)	10040(30)	6590(30)	20(8)
H(3A)	7110(40)	9340(30)	8630(30)	19(8)
H(3B)	6190(50)	10230(30)	7850(30)	33(10)
H(4A)	3490(50)	9730(30)	8520(30)	32(10)
H(4B)	3930(40)	10170(30)	9530(30)	31(9)
H(4C)	4480(40)	8830(30)	9300(30)	23(9)
H(5)	9190(40)	5360(20)	8090(20)	3(7)
H(7)	8910(40)	3870(20)	7340(20)	12(8)
H(9)	7500(40)	3930(20)	4610(20)	16(8)
H(14)	11500(40)	8230(20)	9490(20)	10(7)
H(15)	9950(40)	7970(20)	11240(20)	10(7)
H(16)	7700(40)	7140(20)	11540(20)	6(7)
H(18)	10680(40)	7640(20)	7060(20)	17(8)
H(19A)	13790(50)	7230(30)	6510(30)	30(10)
H(19B)	13820(40)	7420(30)	7730(30)	21(8)
H(19C)	13410(40)	6310(30)	7360(30)	31(9)
H(20A)	11390(40)	9460(30)	7760(30)	21(8)
H(20B)	9660(50)	9590(30)	7410(30)	45(11)
H(20C)	11530(50)	9190(30)	6580(30)	32(10)
H(21)	5900(40)	6550(20)	9570(20)	4(7)
H(22A)	4230(40)	7970(30)	11010(30)	29(9)
H(22B)	3690(50)	6810(30)	11190(30)	24(9)
H(22C)	4930(40)	6990(30)	11840(30)	22(8)
H(23A)	7920(50)	4730(30)	9980(30)	37(10)
H(23B)	6050(40)	4890(20)	10600(20)	10(7)
H(23C)	7350(40)	5130(30)	11170(30)	31(9)

Appendix K

X-Ray Diffraction Analysis of

(pyca)Pt(CH_2CH_3)(CH_2=CH_2)

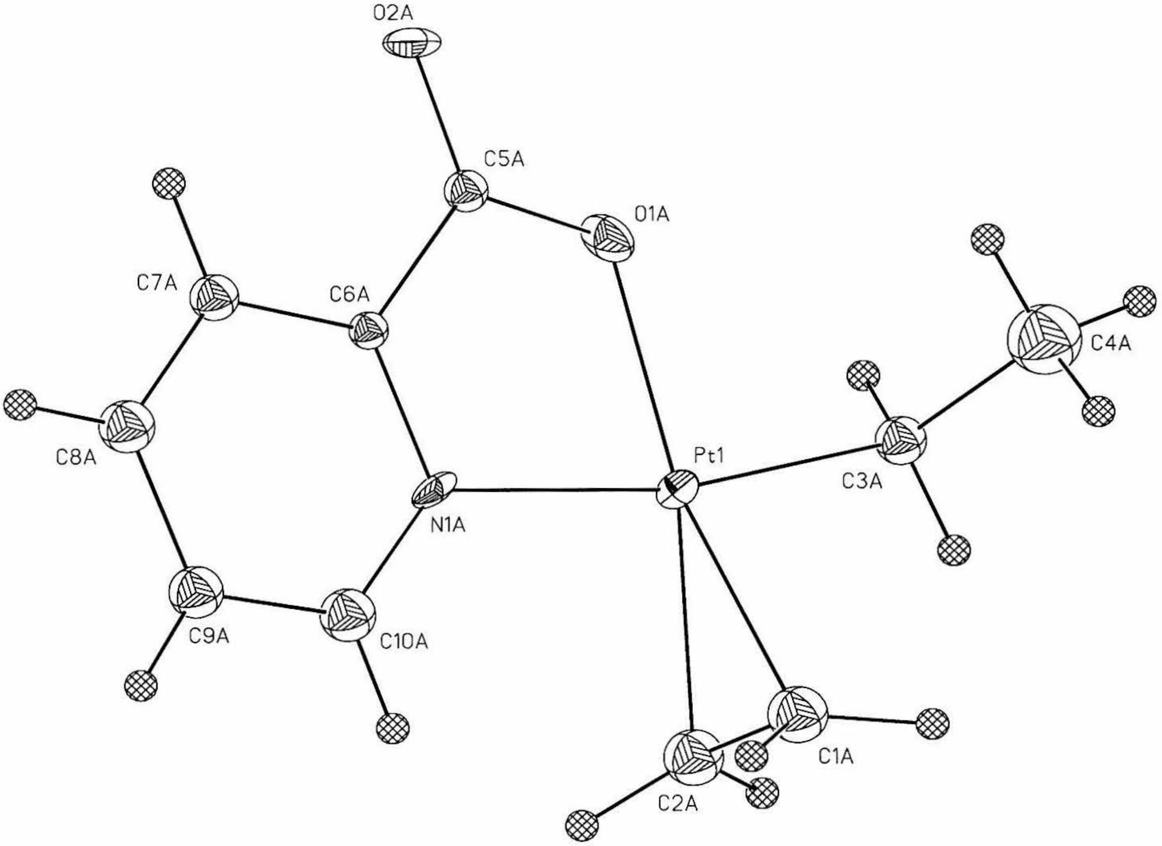

Table 1. Crystal data and structure refinement for TRY15 (CCDC No. 153076)

Empirical formula	$C_{10}H_{13}NO_2Pt$
Formula weight	374.30
Crystallization Solvent	Pentane/dichloromethane
Crystal Habit	Blade
Crystal size	0.24 x 0.18 x 0.14 mm^3
Crystal color	Colorless

Data Collection

Preliminary Photos	Rotation	
Type of diffractometer	CCD area detector	
Wavelength	0.71073 Å MoKα	
Data Collection Temperature	98(2) K	
θ range for 23883 reflections used in lattice determination	2.43 to 28.40°	
Unit cell dimensions	a = 8.0940(4) Å b = 16.8013(8) Å c = 15.1965(7) Å	β= 90.4890(10)°
Volume	2066.49(17) Å^3	
Z	8	
Crystal system	Monoclinic	
Space group	$P2_1$	
Density (calculated)	2.406 Mg/m^3	
F(000)	1392	
Data collection program	Bruker SMART	
θ range for data collection	1.81 to 28.48°	
Completeness to θ = 28.48°	94.2 %	
Index ranges	-10 h 10, -21 k 22, -20 l 19	
Data collection scan type	ω scans at 6 φ settings	
Data reduction program	Bruker SAINT v.62	
Reflections collected	30908	
Independent reflections	9591 [R_{int}= 0.0425]	
Absorption coefficient	13.553 mm^{-1}	
Absorption correction	SADABS	
Max. and min. transmission	1.00000 and 0.63725	

Table 1 (cont.)

Structure Solution and Refinement

Structure solution program	SHELXS-97 (Sheldrick, 1990)
Primary solution method	Direct methods
Secondary solution method	Difference Fourier map
Hydrogen placement	Geometric positions
Structure refinement program	SHELXL-97 (Sheldrick, 1997)
Refinement method	Full matrix least-squares on F^2
Data / restraints / parameters	9591 / 1 / 310
Treatment of hydrogen atoms	Riding
Goodness-of-fit on F^2	1.947
Final R indices [$I>2\sigma(I)$, 9423 reflections]	$R1 = 0.0324$, $wR2 = 0.0687$
R indices (all data)	$R1 = 0.0331$, $wR2 = 0.0688$
Type of weighting scheme used	Sigma
Weighting scheme used	$w=1/\sigma^2(Fo^2)$
Max shift/error	0.001
Average shift/error	0.000
Absolute structure parameter	0.211(10)
Largest diff. peak and hole	2.060 and -2.130 e.Å^{-3}

Special Refinement Details

There are four molecules in the asymmetric unit. The ethyl group of three molecules is oriented out of the molecular plane while the fourth molecule appears to have its ethyl group nearly in the molecular plane. The diffraction pattern is convincingly of 2/m Laue symmetry and NOT mmm symmetry. Therefore, even though the beta angle is near 90° the correct choice of crystal system is monoclinic and NOT orthorhombic.

Refinement of F^2 against ALL reflections. The weighted R-factor (wR) and goodness of fit (S) are based on F^2, conventional R-factors (R) are based on F, with F set to zero for negative F^2. The threshold expression of $F^2 > 2\sigma(F^2)$ is used only for calculating R-factors(gt) etc. and is not relevant to the choice of reflections for refinement. R-factors based on F^2 are statistically about twice as large as those based on F, and R-factors based on ALL data will be even larger.

All esds (except the esd in the dihedral angle between two l.s. planes) are estimated using the full covariance matrix. The cell esds are taken into account individually in the estimation of esds in distances, angles and torsion angles; correlations between esds in cell parameters are only used when they are defined by crystal symmetry. An approximate (isotropic) treatment of cell esds is used for estimating esds involving l.s. planes.

Table 2. Atomic coordinates (x 10^4) and equivalent isotropic displacement parameters (Å^{2}x 10^3) for TRY15 (CCDC No. 153076). U(eq) is defined as the trace of the orthogonalized U^{ij} tensor.

	x	y	z	U_{eq}
Pt(1)	6445(1)	8813(1)	900(1)	11(1)
O(1A)	8491(7)	8296(4)	1440(4)	16(1)
O(2A)	10944(7)	7780(4)	1127(4)	21(2)
N(1A)	7758(8)	8513(4)	-270(5)	10(2)
C(1A)	4885(11)	9700(6)	378(6)	20(2)
C(2A)	4059(11)	8969(6)	324(6)	20(2)
C(3A)	5579(10)	9009(5)	2127(5)	15(2)
C(4A)	6539(13)	9665(7)	2598(7)	31(3)
C(5A)	9617(10)	8071(5)	899(5)	11(2)
C(6A)	9252(10)	8204(5)	-68(5)	9(2)
C(7A)	10342(11)	7982(5)	-712(5)	14(2)
C(8A)	9945(11)	8089(6)	-1575(6)	18(2)
C(9A)	8422(11)	8423(6)	-1792(6)	17(2)
C(10A)	7376(11)	8606(5)	-1107(6)	18(2)
Pt(2)	3423(1)	9016(1)	5806(1)	12(1)
O(1B)	1440(7)	8538(4)	6415(4)	15(1)
O(2B)	-1014(7)	7953(4)	6186(4)	21(2)
N(1B)	2084(8)	8570(4)	4686(5)	12(2)
C(1B)	4841(11)	9838(6)	5127(7)	25(2)
C(2B)	5755(10)	9122(5)	5205(6)	16(2)
C(3B)	4401(11)	9432(6)	6957(6)	20(2)
C(4B)	3376(11)	9300(6)	7763(6)	18(2)
C(5B)	292(11)	8260(6)	5898(6)	15(2)
C(6B)	569(11)	8291(5)	4931(6)	16(2)
C(7B)	-606(11)	8031(5)	4315(5)	13(2)
C(8B)	-229(11)	8082(6)	3432(6)	18(2)
C(9B)	1334(10)	8356(5)	3203(6)	15(2)
C(10B)	2420(10)	8603(5)	3851(5)	14(2)
Pt(3)	8563(1)	6146(1)	-425(1)	12(1)
O(1C)	6557(7)	6661(4)	-1013(4)	18(1)
O(2C)	4083(7)	7187(4)	-759(4)	19(1)
N(1C)	7148(8)	6459(4)	714(5)	14(2)
C(1C)	10064(11)	5253(6)	122(6)	20(2)
C(2C)	10832(12)	5985(6)	205(6)	24(2)
C(3C)	9588(11)	5939(6)	-1631(6)	22(2)
C(4C)	8608(12)	5319(6)	-2144(7)	28(2)
C(5C)	5345(11)	6886(6)	-500(6)	15(2)
C(6C)	5684(11)	6799(6)	483(6)	18(2)
C(7C)	4520(11)	6969(5)	1092(6)	14(2)
C(8C)	4882(10)	6877(5)	1985(6)	13(2)
C(9C)	6406(11)	6556(6)	2212(6)	19(2)
C(10C)	7500(10)	6346(5)	1556(6)	17(2)
Pt(4)	1308(1)	6226(1)	4603(1)	11(1)
O(1D)	3316(7)	6696(4)	3983(4)	16(1)
O(2D)	5764(8)	7247(4)	4218(4)	21(2)
N(1D)	2723(8)	6608(4)	5705(5)	11(2)
C(1D)	-153(11)	5368(6)	5231(6)	20(2)

C(2D)	-963(11)	6088(6)	5235(6)	20(2)
C(3D)	252(11)	5912(6)	3421(6)	19(2)
C(4D)	1238(11)	5296(6)	2937(6)	21(2)
C(5D)	4460(10)	6956(5)	4498(5)	8(2)
C(6D)	4184(9)	6949(5)	5472(5)	6(2)
C(7D)	5349(11)	7170(5)	6086(6)	15(2)
C(8D)	4996(11)	7123(6)	6969(6)	18(2)
C(9D)	3450(11)	6831(5)	7229(6)	17(2)
C(10D)	2361(10)	6574(5)	6571(5)	15(2)

Table 3. Selected bond lengths [Å] and angles [°] for TRY15 (CCDC No. 153076).

Pt(1)-C(3A)	2.025(8)	C(1A)-Pt(1)-N(1A)	98.9(3)
Pt(1)-O(1A)	2.036(6)	C(2A)-Pt(1)-N(1A)	98.2(3)
Pt(1)-C(1A)	2.105(9)	C(3B)-Pt(2)-O(1B)	92.7(3)
Pt(1)-C(2A)	2.130(9)	C(3B)-Pt(2)-C(1B)	89.2(4)
Pt(1)-N(1A)	2.138(7)	O(1B)-Pt(2)-C(1B)	159.2(3)
C(1A)-C(2A)	1.401(13)	C(3B)-Pt(2)-C(2B)	90.0(4)
Pt(2)-C(3B)	2.039(9)	O(1B)-Pt(2)-C(2B)	161.0(3)
Pt(2)-O(1B)	2.025(6)	C(1B)-Pt(2)-C(2B)	39.6(4)
Pt(2)-C(1B)	2.076(10)	C(3B)-Pt(2)-N(1B)	172.3(3)
Pt(2)-C(2B)	2.111(8)	O(1B)-Pt(2)-N(1B)	80.0(2)
Pt(2)-N(1B)	2.144(7)	C(1B)-Pt(2)-N(1B)	96.7(3)
C(1B)-C(2B)	1.418(13)	C(2B)-Pt(2)-N(1B)	97.7(3)
Pt(3)-C(3C)	2.048(9)	C(3C)-Pt(3)-O(1C)	90.4(3)
Pt(3)-O(1C)	2.039(6)	C(3C)-Pt(3)-C(2C)	91.5(4)
Pt(3)-C(2C)	2.082(9)	O(1C)-Pt(3)-C(2C)	162.3(3)
Pt(3)-C(1C)	2.098(9)	C(3C)-Pt(3)-C(1C)	89.7(4)
Pt(3)-N(1C)	2.148(7)	O(1C)-Pt(3)-C(1C)	159.0(3)
C(1C)-C(2C)	1.383(13)	C(2C)-Pt(3)-C(1C)	38.6(4)
Pt(4)-O(1D)	2.044(6)	C(3C)-Pt(3)-N(1C)	170.1(3)
Pt(4)-C(3D)	2.051(9)	O(1C)-Pt(3)-N(1C)	79.7(3)
Pt(4)-C(1D)	2.099(9)	C(2C)-Pt(3)-N(1C)	97.8(3)
Pt(4)-C(2D)	2.094(9)	C(1C)-Pt(3)-N(1C)	99.6(3)
Pt(4)-N(1D)	2.120(7)	O(1D)-Pt(4)-C(3D)	91.3(3)
C(1D)-C(2D)	1.375(13)	O(1D)-Pt(4)-C(1D)	158.1(3)
		C(3D)-Pt(4)-C(1D)	89.4(4)
C(3A)-Pt(1)-O(1A)	89.1(3)	O(1D)-Pt(4)-C(2D)	163.5(3)
C(3A)-Pt(1)-C(1A)	91.1(4)	C(3D)-Pt(4)-C(2D)	90.7(3)
O(1A)-Pt(1)-C(1A)	159.6(3)	C(1D)-Pt(4)-C(2D)	38.3(4)
C(3A)-Pt(1)-C(2A)	92.2(3)	O(1D)-Pt(4)-N(1D)	79.7(3)
O(1A)-Pt(1)-C(2A)	161.8(3)	C(3D)-Pt(4)-N(1D)	171.0(3)
C(1A)-Pt(1)-C(2A)	38.6(3)	C(1D)-Pt(4)-N(1D)	98.7(3)
C(3A)-Pt(1)-N(1A)	169.1(3)	C(2D)-Pt(4)-N(1D)	98.1(3)
O(1A)-Pt(1)-N(1A)	80.0(2)		

Table 4. Bond lengths [Å] and angles [°] for TRY15 (CCDC No. 153076).

Pt(1)-C(3A)	2.025(8)	C(6B)-C(7B)	1.399(12)
Pt(1)-O(1A)	2.036(6)	C(7B)-C(8B)	1.381(12)
Pt(1)-C(1A)	2.105(9)	C(7B)-H(7B)	0.9500
Pt(1)-C(2A)	2.130(9)	C(8B)-C(9B)	1.393(12)
Pt(1)-N(1A)	2.138(7)	C(8B)-H(8B)	0.9500
O(1A)-C(5A)	1.289(10)	C(9B)-C(10B)	1.378(11)
O(2A)-C(5A)	1.227(10)	C(9B)-H(9B)	0.9500
N(1A)-C(10A)	1.316(11)	C(10B)-H(10B)	0.9500
N(1A)-C(6A)	1.348(10)	Pt(3)-C(3C)	2.048(9)
C(1A)-C(2A)	1.401(13)	Pt(3)-O(1C)	2.039(6)
C(1A)-H(1A1)	0.9900	Pt(3)-C(2C)	2.082(9)
C(1A)-H(1A2)	0.9900	Pt(3)-C(1C)	2.098(9)
C(2A)-H(2A1)	0.9900	Pt(3)-N(1C)	2.148(7)
C(2A)-H(2A2)	0.9900	O(1C)-C(5C)	1.314(10)
C(3A)-C(4A)	1.523(13)	O(2C)-C(5C)	1.203(10)
C(3A)-H(3A1)	0.9900	N(1C)-C(10C)	1.323(11)
C(3A)-H(3A2)	0.9900	N(1C)-C(6C)	1.359(11)
C(4A)-H(4A1)	0.9800	C(1C)-C(2C)	1.383(13)
C(4A)-H(4A2)	0.9800	C(1C)-H(1C1)	0.9900
C(4A)-H(4A3)	0.9800	C(1C)-H(1C2)	0.9900
C(5A)-C(6A)	1.513(11)	C(2C)-H(2C1)	0.9900
C(6A)-C(7A)	1.376(11)	C(2C)-H(2C2)	0.9900
C(7A)-C(8A)	1.359(12)	C(3C)-C(4C)	1.520(13)
C(7A)-H(7A)	0.9500	C(3C)-H(3C1)	0.9900
C(8A)-C(9A)	1.392(12)	C(3C)-H(3C2)	0.9900
C(8A)-H(8A)	0.9500	C(4C)-H(4C1)	0.9800
C(9A)-C(10A)	1.382(12)	C(4C)-H(4C2)	0.9800
C(9A)-H(9A)	0.9500	C(4C)-H(4C3)	0.9800
C(10A)-H(10A)	0.9500	C(5C)-C(6C)	1.523(12)
Pt(2)-C(3B)	2.039(9)	C(6C)-C(7C)	1.357(12)
Pt(2)-O(1B)	2.025(6)	C(7C)-C(8C)	1.394(12)
Pt(2)-C(1B)	2.076(10)	C(7C)-H(7C)	0.9500
Pt(2)-C(2B)	2.111(8)	C(8C)-C(9C)	1.388(12)
Pt(2)-N(1B)	2.144(7)	C(8C)-H(8C)	0.9500
O(1B)-C(5B)	1.299(10)	C(9C)-C(10C)	1.384(12)
O(2B)-C(5B)	1.258(10)	C(9C)-H(9C)	0.9500
N(1B)-C(10B)	1.301(11)	C(10C)-H(10C)	0.9500
N(1B)-C(6B)	1.368(11)	Pt(4)-O(1D)	2.044(6)
C(1B)-C(2B)	1.418(13)	Pt(4)-C(3D)	2.051(9)
C(1B)-H(1B1)	0.9900	Pt(4)-C(1D)	2.099(9)
C(1B)-H(1B2)	0.9900	Pt(4)-C(2D)	2.094(9)
C(2B)-H(2B1)	0.9900	Pt(4)-N(1D)	2.120(7)
C(2B)-H(2B2)	0.9900	O(1D)-C(5D)	1.284(9)
C(3B)-C(4B)	1.502(12)	O(2D)-C(5D)	1.241(10)
C(3B)-H(3B1)	0.9900	N(1D)-C(10D)	1.351(11)
C(3B)-H(3B2)	0.9900	N(1D)-C(6D)	1.363(10)
C(4B)-H(4B1)	0.9800	C(1D)-C(2D)	1.375(13)
C(4B)-H(4B2)	0.9800	C(1D)-H(1D1)	0.9900
C(4B)-H(4B3)	0.9800	C(1D)-H(1D2)	0.9900
C(5B)-C(6B)	1.489(12)	C(2D)-H(2D1)	0.9900

C(2D)-H(2D2)	0.9900
C(3D)-C(4D)	1.502(12)
C(3D)-H(3D1)	0.9900
C(3D)-H(3D2)	0.9900
C(4D)-H(4D1)	0.9800
C(4D)-H(4D2)	0.9800
C(4D)-H(4D3)	0.9800
C(5D)-C(6D)	1.499(11)
C(6D)-C(7D)	1.373(11)
C(7D)-C(8D)	1.376(12)
C(7D)-H(7D)	0.9500
C(8D)-C(9D)	1.405(12)
C(8D)-H(8D)	0.9500
C(9D)-C(10D)	1.396(12)
C(9D)-H(9D)	0.9500
C(10D)-H(10D)	0.9500

C(3A)-Pt(1)-O(1A)	89.1(3)
C(3A)-Pt(1)-C(1A)	91.1(4)
O(1A)-Pt(1)-C(1A)	159.6(3)
C(3A)-Pt(1)-C(2A)	92.2(3)
O(1A)-Pt(1)-C(2A)	161.8(3)
C(1A)-Pt(1)-C(2A)	38.6(3)
C(3A)-Pt(1)-N(1A)	169.1(3)
O(1A)-Pt(1)-N(1A)	80.0(2)
C(1A)-Pt(1)-N(1A)	98.9(3)
C(2A)-Pt(1)-N(1A)	98.2(3)
C(5A)-O(1A)-Pt(1)	116.4(5)
C(10A)-N(1A)-C(6A)	117.9(7)
C(10A)-N(1A)-Pt(1)	131.4(6)
C(6A)-N(1A)-Pt(1)	110.7(5)
C(2A)-C(1A)-Pt(1)	71.7(5)
C(2A)-C(1A)-H(1A1)	116.4
Pt(1)-C(1A)-H(1A1)	116.4
C(2A)-C(1A)-H(1A2)	116.4
Pt(1)-C(1A)-H(1A2)	116.4
H(1A1)-C(1A)-H(1A2)	113.4
C(1A)-C(2A)-Pt(1)	69.7(5)
C(1A)-C(2A)-H(2A1)	116.7
Pt(1)-C(2A)-H(2A1)	116.7
C(1A)-C(2A)-H(2A2)	116.7
Pt(1)-C(2A)-H(2A2)	116.7
H(2A1)-C(2A)-H(2A2)	113.7
C(4A)-C(3A)-Pt(1)	111.8(6)
C(4A)-C(3A)-H(3A1)	109.3
Pt(1)-C(3A)-H(3A1)	109.3
C(4A)-C(3A)-H(3A2)	109.3
Pt(1)-C(3A)-H(3A2)	109.3
H(3A1)-C(3A)-H(3A2)	107.9
C(3A)-C(4A)-H(4A1)	109.5
C(3A)-C(4A)-H(4A2)	109.5
H(4A1)-C(4A)-H(4A2)	109.5
C(3A)-C(4A)-H(4A3)	109.5
H(4A1)-C(4A)-H(4A3)	109.5
H(4A2)-C(4A)-H(4A3)	109.5
O(2A)-C(5A)-O(1A)	123.9(8)
O(2A)-C(5A)-C(6A)	119.8(8)
O(1A)-C(5A)-C(6A)	116.3(7)
N(1A)-C(6A)-C(7A)	121.5(8)
N(1A)-C(6A)-C(5A)	116.4(7)
C(7A)-C(6A)-C(5A)	122.0(7)
C(8A)-C(7A)-C(6A)	120.2(8)
C(8A)-C(7A)-H(7A)	119.9
C(6A)-C(7A)-H(7A)	119.9
C(7A)-C(8A)-C(9A)	118.9(9)
C(7A)-C(8A)-H(8A)	120.5
C(9A)-C(8A)-H(8A)	120.5
C(10A)-C(9A)-C(8A)	117.3(8)
C(10A)-C(9A)-H(9A)	121.4
C(8A)-C(9A)-H(9A)	121.4
N(1A)-C(10A)-C(9A)	124.2(8)
N(1A)-C(10A)-H(10A)	117.9
C(9A)-C(10A)-H(10A)	117.9
C(3B)-Pt(2)-O(1B)	92.7(3)
C(3B)-Pt(2)-C(1B)	89.2(4)
O(1B)-Pt(2)-C(1B)	159.2(3)
C(3B)-Pt(2)-C(2B)	90.0(4)
O(1B)-Pt(2)-C(2B)	161.0(3)
C(1B)-Pt(2)-C(2B)	39.6(4)
C(3B)-Pt(2)-N(1B)	172.3(3)
O(1B)-Pt(2)-N(1B)	80.0(2)
C(1B)-Pt(2)-N(1B)	96.7(3)
C(2B)-Pt(2)-N(1B)	97.7(3)
C(5B)-O(1B)-Pt(2)	115.6(5)
C(10B)-N(1B)-C(6B)	118.4(7)
C(10B)-N(1B)-Pt(2)	130.6(6)
C(6B)-N(1B)-Pt(2)	110.6(6)
C(2B)-C(1B)-Pt(2)	71.6(6)
C(2B)-C(1B)-H(1B1)	116.4
Pt(2)-C(1B)-H(1B1)	116.4
C(2B)-C(1B)-H(1B2)	116.4
Pt(2)-C(1B)-H(1B2)	116.4
H(1B1)-C(1B)-H(1B2)	113.4
C(1B)-C(2B)-Pt(2)	68.9(5)
C(1B)-C(2B)-H(2B1)	116.8
Pt(2)-C(2B)-H(2B1)	116.8
C(1B)-C(2B)-H(2B2)	116.8
Pt(2)-C(2B)-H(2B2)	116.8
H(2B1)-C(2B)-H(2B2)	113.8
C(4B)-C(3B)-Pt(2)	115.8(6)
C(4B)-C(3B)-H(3B1)	108.3
Pt(2)-C(3B)-H(3B1)	108.3
C(4B)-C(3B)-H(3B2)	108.3
Pt(2)-C(3B)-H(3B2)	108.3
H(3B1)-C(3B)-H(3B2)	107.4
C(3B)-C(4B)-H(4B1)	109.5
C(3B)-C(4B)-H(4B2)	109.5
H(4B1)-C(4B)-H(4B2)	109.5

C(3B)-C(4B)-H(4B3)	109.5
H(4B1)-C(4B)-H(4B3)	109.5
H(4B2)-C(4B)-H(4B3)	109.5
O(2B)-C(5B)-O(1B)	122.4(8)
O(2B)-C(5B)-C(6B)	119.4(8)
O(1B)-C(5B)-C(6B)	118.1(8)
N(1B)-C(6B)-C(7B)	122.1(8)
N(1B)-C(6B)-C(5B)	115.0(8)
C(7B)-C(6B)-C(5B)	122.9(8)
C(8B)-C(7B)-C(6B)	118.5(8)
C(8B)-C(7B)-H(7B)	120.8
C(6B)-C(7B)-H(7B)	120.8
C(7B)-C(8B)-C(9B)	118.1(8)
C(7B)-C(8B)-H(8B)	120.9
C(9B)-C(8B)-H(8B)	120.9
C(10B)-C(9B)-C(8B)	119.8(8)
C(10B)-C(9B)-H(9B)	120.1
C(8B)-C(9B)-H(9B)	120.1
N(1B)-C(10B)-C(9B)	123.1(8)
N(1B)-C(10B)-H(10B)	118.4
C(9B)-C(10B)-H(10B)	118.4
C(3C)-Pt(3)-O(1C)	90.4(3)
C(3C)-Pt(3)-C(2C)	91.5(4)
O(1C)-Pt(3)-C(2C)	162.3(3)
C(3C)-Pt(3)-C(1C)	89.7(4)
O(1C)-Pt(3)-C(1C)	159.0(3)
C(2C)-Pt(3)-C(1C)	38.6(4)
C(3C)-Pt(3)-N(1C)	170.1(3)
O(1C)-Pt(3)-N(1C)	79.7(3)
C(2C)-Pt(3)-N(1C)	97.8(3)
C(1C)-Pt(3)-N(1C)	99.6(3)
C(5C)-O(1C)-Pt(3)	117.2(5)
C(10C)-N(1C)-C(6C)	119.3(8)
C(10C)-N(1C)-Pt(3)	129.2(6)
C(6C)-N(1C)-Pt(3)	111.4(6)
C(2C)-C(1C)-Pt(3)	70.1(6)
C(2C)-C(1C)-H(1C1)	116.6
Pt(3)-C(1C)-H(1C1)	116.6
C(2C)-C(1C)-H(1C2)	116.6
Pt(3)-C(1C)-H(1C2)	116.6
H(1C1)-C(1C)-H(1C2)	113.6
C(1C)-C(2C)-Pt(3)	71.3(6)
C(1C)-C(2C)-H(2C1)	116.5
Pt(3)-C(2C)-H(2C1)	116.5
C(1C)-C(2C)-H(2C2)	116.5
Pt(3)-C(2C)-H(2C2)	116.5
H(2C1)-C(2C)-H(2C2)	113.5
C(4C)-C(3C)-Pt(3)	111.2(6)
C(4C)-C(3C)-H(3C1)	109.4
Pt(3)-C(3C)-H(3C1)	109.4
C(4C)-C(3C)-H(3C2)	109.4
Pt(3)-C(3C)-H(3C2)	109.4
H(3C1)-C(3C)-H(3C2)	108.0
C(3C)-C(4C)-H(4C1)	109.5
C(3C)-C(4C)-H(4C2)	109.5
H(4C1)-C(4C)-H(4C2)	109.5
C(3C)-C(4C)-H(4C3)	109.5
H(4C1)-C(4C)-H(4C3)	109.5
H(4C2)-C(4C)-H(4C3)	109.5
O(2C)-C(5C)-O(1C)	124.2(8)
O(2C)-C(5C)-C(6C)	120.5(8)
O(1C)-C(5C)-C(6C)	115.1(7)
C(7C)-C(6C)-N(1C)	121.4(8)
C(7C)-C(6C)-C(5C)	121.9(8)
N(1C)-C(6C)-C(5C)	116.3(8)
C(6C)-C(7C)-C(8C)	119.9(8)
C(6C)-C(7C)-H(7C)	120.0
C(8C)-C(7C)-H(7C)	120.0
C(9C)-C(8C)-C(7C)	117.7(8)
C(9C)-C(8C)-H(8C)	121.2
C(7C)-C(8C)-H(8C)	121.2
C(8C)-C(9C)-C(10C)	119.5(8)
C(8C)-C(9C)-H(9C)	120.2
C(10C)-C(9C)-H(9C)	120.2
N(1C)-C(10C)-C(9C)	121.8(8)
N(1C)-C(10C)-H(10C)	119.1
C(9C)-C(10C)-H(10C)	119.1
O(1D)-Pt(4)-C(3D)	91.3(3)
O(1D)-Pt(4)-C(1D)	158.1(3)
C(3D)-Pt(4)-C(1D)	89.4(4)
O(1D)-Pt(4)-C(2D)	163.5(3)
C(3D)-Pt(4)-C(2D)	90.7(3)
C(1D)-Pt(4)-C(2D)	38.3(4)
O(1D)-Pt(4)-N(1D)	79.7(3)
C(3D)-Pt(4)-N(1D)	171.0(3)
C(1D)-Pt(4)-N(1D)	98.7(3)
C(2D)-Pt(4)-N(1D)	98.1(3)
C(5D)-O(1D)-Pt(4)	115.0(5)
C(10D)-N(1D)-C(6D)	117.8(7)
C(10D)-N(1D)-Pt(4)	129.5(6)
C(6D)-N(1D)-Pt(4)	112.7(5)
C(2D)-C(1D)-Pt(4)	70.7(6)
C(2D)-C(1D)-H(1D1)	116.5
Pt(4)-C(1D)-H(1D1)	116.5
C(2D)-C(1D)-H(1D2)	116.5
Pt(4)-C(1D)-H(1D2)	116.5
H(1D1)-C(1D)-H(1D2)	113.5
C(1D)-C(2D)-Pt(4)	71.0(5)
C(1D)-C(2D)-H(2D1)	116.5
Pt(4)-C(2D)-H(2D1)	116.5
C(1D)-C(2D)-H(2D2)	116.5
Pt(4)-C(2D)-H(2D2)	116.5
H(2D1)-C(2D)-H(2D2)	113.5
C(4D)-C(3D)-Pt(4)	112.8(6)
C(4D)-C(3D)-H(3D1)	109.0
Pt(4)-C(3D)-H(3D1)	109.0
C(4D)-C(3D)-H(3D2)	109.0
Pt(4)-C(3D)-H(3D2)	109.0

H(3D1)-C(3D)-H(3D2)	107.8
C(3D)-C(4D)-H(4D1)	109.5
C(3D)-C(4D)-H(4D2)	109.5
H(4D1)-C(4D)-H(4D2)	109.5
C(3D)-C(4D)-H(4D3)	109.5
H(4D1)-C(4D)-H(4D3)	109.5
H(4D2)-C(4D)-H(4D3)	109.5
O(2D)-C(5D)-O(1D)	122.4(7)
O(2D)-C(5D)-C(6D)	118.4(7)
O(1D)-C(5D)-C(6D)	119.1(7)
N(1D)-C(6D)-C(7D)	122.0(7)
N(1D)-C(6D)-C(5D)	113.4(7)
C(7D)-C(6D)-C(5D)	124.1(7)
C(6D)-C(7D)-C(8D)	120.0(8)
C(6D)-C(7D)-H(7D)	120.0
C(8D)-C(7D)-H(7D)	120.0
C(7D)-C(8D)-C(9D)	119.2(9)
C(7D)-C(8D)-H(8D)	120.4
C(9D)-C(8D)-H(8D)	120.4
C(10D)-C(9D)-C(8D)	117.7(8)
C(10D)-C(9D)-H(9D)	121.1
C(8D)-C(9D)-H(9D)	121.1
N(1D)-C(10D)-C(9D)	122.9(8)
N(1D)-C(10D)-H(10D)	118.5
C(9D)-C(10D)-H(10D)	118.5

Table 5. Anisotropic displacement parameters (Å^{2}x 10^4) for TRY15 (CCDC No. 153076). The anisotropic displacement factor exponent takes the form: $-2\pi^2$ [$h^2 a^{*2}U^{11}$ + ... + 2 h k a* b* U^{12}]

	U^{11}	U^{22}	U^{33}	U^{23}	U^{13}	U^{12}
Pt(1)	95(2)	109(2)	130(2)	-6(1)	-1(1)	25(1)
O(1A)	160(30)	240(40)	80(30)	-10(30)	0(20)	-10(30)
O(2A)	150(30)	350(40)	140(30)	-40(30)	-70(30)	120(30)
N(1A)	70(30)	40(30)	200(40)	10(30)	-20(30)	20(30)
Pt(2)	80(2)	122(2)	144(2)	-9(1)	-16(1)	-13(1)
O(1B)	80(30)	220(40)	160(30)	30(30)	-40(20)	-40(30)
O(2B)	120(30)	250(40)	250(40)	30(30)	0(30)	-100(30)
N(1B)	110(40)	50(40)	200(40)	10(30)	10(30)	20(30)
Pt(3)	95(2)	102(2)	160(2)	-11(1)	13(1)	13(1)
O(1C)	180(30)	190(40)	170(30)	0(30)	0(30)	30(30)
O(2C)	140(30)	260(40)	180(30)	-20(30)	-70(30)	90(30)
N(1C)	130(40)	150(40)	150(40)	-80(30)	10(30)	20(30)
Pt(4)	86(1)	98(2)	138(2)	-8(1)	-31(1)	-6(1)
O(1D)	180(30)	170(30)	130(30)	20(30)	0(20)	-30(30)
O(2D)	170(30)	320(40)	120(30)	-50(30)	10(30)	-90(30)
N(1D)	80(30)	50(40)	210(40)	10(30)	-70(30)	-10(30)

Table 6. Hydrogen coordinates (x 10^4) and isotropic displacement parameters (Å^{2}x 10^3) for TRY15 (CCDC No. 153076).

	x	y	z	U_{iso}
H(1A1)	4441	10091	802	24
H(1A2)	5226	9941	-187	24
H(2A1)	3888	8746	-273	24
H(2A2)	3101	8896	717	24
H(3A1)	4398	9161	2089	18
H(3A2)	5660	8511	2473	18

H(4A1)	7726	9557	2558	47
H(4A2)	6219	9681	3218	47
H(4A3)	6291	10178	2322	47
H(7A)	11377	7754	-554	16
H(8A)	10695	7938	-2023	21
H(9A)	8113	8521	-2387	20
H(10A)	6314	8812	-1249	21
H(1B1)	4451	9982	4529	30
H(1B2)	5256	10299	5470	30
H(2B1)	6731	9131	5602	19
H(2B2)	5925	8813	4658	19
H(3B1)	5490	9176	7052	24
H(3B2)	4596	10011	6894	24
H(4B1)	2318	9577	7696	26
H(4B2)	3965	9506	8281	26
H(4B3)	3176	8728	7838	26
H(7B)	-1640	7825	4499	16
H(8B)	-1014	7934	2993	21
H(9B)	1650	8372	2603	18
H(10B)	3464	8807	3679	17
H(1C1)	9670	5003	671	24
H(1C2)	10565	4872	-295	24
H(2C1)	11828	6070	-156	29
H(2C2)	10935	6202	809	29
H(3C1)	9616	6442	-1970	26
H(3C2)	10739	5752	-1550	26
H(4C1)	8467	4843	-1780	42
H(4C2)	9205	5179	-2680	42
H(4C3)	7522	5536	-2301	42
H(7C)	3460	7152	911	16
H(8C)	4112	7028	2422	15
H(9C)	6697	6481	2813	23
H(10C)	8530	6114	1716	20
H(1D1)	-633	4947	4852	24
H(1D2)	257	5170	5806	24
H(2D1)	-1076	6352	5814	24
H(2D2)	-1966	6128	4860	24
H(3D1)	-871	5701	3527	23
H(3D2)	140	6392	3048	23
H(4D1)	2361	5496	2843	31
H(4D2)	711	5186	2367	31
H(4D3)	1287	4806	3285	31
H(7D)	6399	7356	5902	18
H(8D)	5789	7287	7397	22
H(9D)	3155	6809	7832	20
H(10D)	1319	6365	6739	18

Appendix L

X-Ray Diffraction Analysis of

$[(^{\mathrm{Anthr,H}}\mathrm{Sal})\mathrm{Pt}(\mu\text{-COD})\mathrm{Me}]_2$

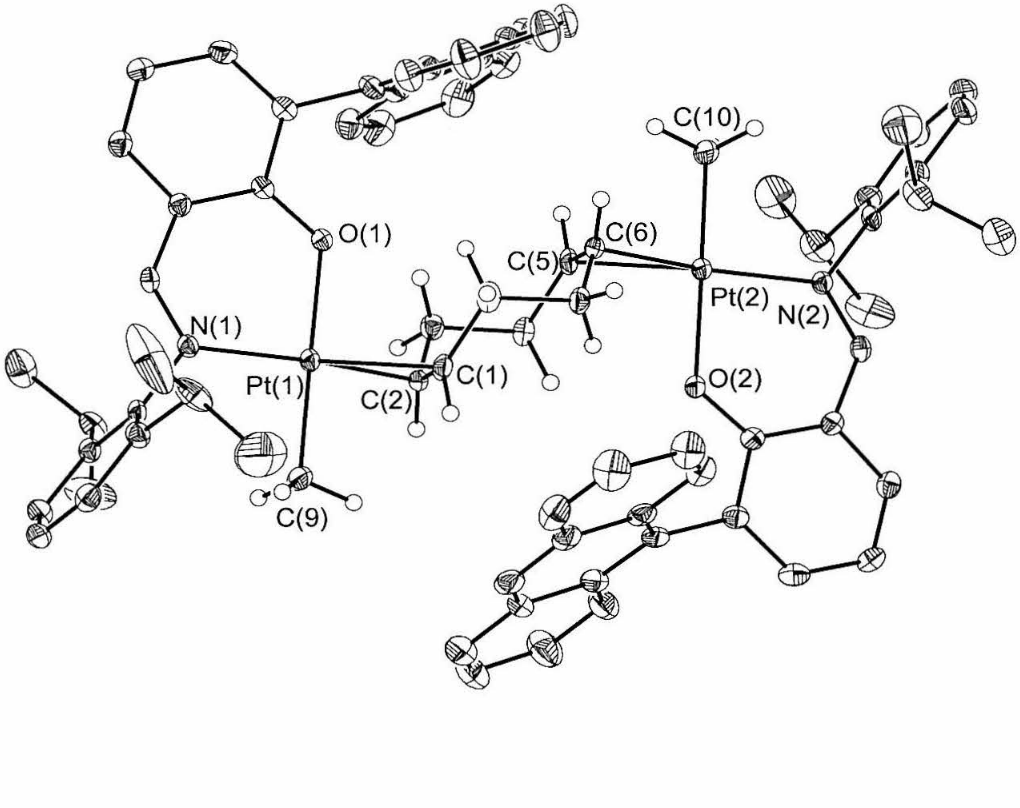

Table 1. Crystal data and structure refinement for TRY17 (CCDC 163158).

Empirical formula	$C_{76}H_{78}N_2O_2Pt_2\cdot$ 2½(C6H6)
Formula weight	1636.85
Crystallization Solvent	Benzene/hexane
Crystal Habit	Block
Crystal size	0.24 x 0.22 x 0.21 mm^3
Crystal color	Yellow/orange

Data Collection

Preliminary Photos	None	
Type of diffractometer	CCD area detector	
Wavelength	0.71073 Å MoKα	
Data Collection Temperature	98(2) K	
θ range for 50003 reflections used in lattice determination	2.23 to 28.52°	
Unit cell dimensions	a = 14.8073(12) Å b = 18.2407(15) Å c = 28.508(2) Å	β= 102.0860(10)°
Volume	7529.3(11) $Å^3$	
Z	4	
Crystal system	Monoclinic	
Space group	$P2_1/n$	
Density (calculated)	1.444 Mg/m^3	
F(000)	3300	
Data collection program	Bruker SMART	
θ range for data collection	1.46 to 28.53°	
Completeness to θ = 28.53°	95.0 %	
Index ranges	-19 h 19, -24 k 24, -38 l 38	
Data collection scan type	ω scans at 7 φ settings	
Data reduction program	Bruker SAINT v6.2	
Reflections collected	154834	
Independent reflections	18204 [R_{int}= 0.0694]	
Absorption coefficient	3.762 mm^{-1}	
Absorption correction	None	
Max. and min. transmission	0.5098 and 0.4705	

Table 1 (cont.)

Structure Solution and Refinement

Structure solution program	SHELXS-97 (Sheldrick, 1990)
Primary solution method	Direct methods
Secondary solution method	Difference Fourier map
Hydrogen placement	Difference Fourier map
Structure refinement program	SHELXL-97 (Sheldrick, 1997)
Refinement method	Full matrix least-squares on F^2
Data / restraints / parameters	18204 / 0 / 1076
Treatment of hydrogen atoms	Methyl and solvent hydrogens riding, all others unrestrained
Goodness-of-fit on F^2	1.802
Final R indices [$I>2\sigma(I)$, 13902 reflections]	R1 = 0.0419, *w*R2 = 0.0630
R indices (all data)	R1 = 0.0626, *w*R2 = 0.0649
Type of weighting scheme used	Sigma
Weighting scheme used	$w=1/\sigma^2(Fo^2)$
Max shift/error	0.011
Average shift/error	0.000
Largest diff. peak and hole	2.799 and -2.403 e.Å^{-3}

Special Refinement Details

Refinement of F^2 against ALL reflections. The weighted R-factor (*w*R) and goodness of fit (S) are based on F^2, conventional R-factors (R) are based on F, with F set to zero for negative F^2. The threshold expression of $F^2 > 2\sigma(F^2)$ is used only for calculating R-factors(gt) etc. and is not relevant to the choice of reflections for refinement. R-factors based on F^2 are statistically about twice as large as those based on F, and R-factors based on ALL data will be even larger.

All esds (except the esd in the dihedral angle between two l.s. planes) are estimated using the full covariance matrix. The cell esds are taken into account individually in the estimation of esds in distances, angles and torsion angles; correlations between esds in cell parameters are only used when they are defined by crystal symmetry. An approximate (isotropic) treatment of cell esds is used for estimating esds involving l.s. planes.

Table 2. Atomic coordinates (x 10^4) and equivalent isotropic displacement parameters ($Å^2$x 10^3) for TRY17 (CCDC 163158). U(eq) is defined as the trace of the orthogonalized U^{ij} tensor.

	x	y	z	U_{eq}
Pt(1)	7666(1)	7201(1)	10605(1)	29(1)
Pt(2)	8777(1)	7945(1)	8423(1)	28(1)
O(1)	6543(2)	7681(1)	10136(1)	27(1)
O(2)	9956(2)	7599(1)	8919(1)	27(1)
N(1)	6886(2)	7101(2)	11118(1)	25(1)
N(2)	9516(2)	7993(2)	7892(1)	25(1)
C(1)	8561(3)	7662(3)	10177(2)	33(1)
C(2)	8315(3)	6954(3)	10019(2)	31(1)
C(3)	7688(3)	6757(3)	9556(2)	31(1)
C(4)	8213(3)	6845(2)	9140(2)	30(1)
C(5)	7893(3)	7517(2)	8864(1)	31(1)
C(6)	8141(3)	8222(3)	9010(2)	30(1)
C(7)	8755(3)	8433(3)	9477(2)	30(1)
C(8)	8245(3)	8341(3)	9896(2)	32(1)
C(9)	8757(3)	6695(3)	11037(2)	66(2)
C(10)	7623(3)	8302(3)	7957(2)	49(1)
C(11)	6015(3)	7271(2)	11045(1)	26(1)
C(12)	5419(3)	7544(2)	10626(1)	26(1)
C(13)	4476(3)	7609(2)	10646(2)	31(1)
C(14)	3827(3)	7853(2)	10265(2)	36(1)
C(15)	4109(3)	8064(2)	9848(2)	35(1)
C(16)	5016(3)	8020(2)	9802(1)	29(1)
C(17)	5693(2)	7733(2)	10193(1)	20(1)
C(18)	7276(3)	6807(2)	11590(1)	26(1)
C(19)	7730(3)	7283(2)	11948(1)	32(1)
C(20)	8084(3)	6985(3)	12397(2)	35(1)
C(21)	7982(3)	6250(3)	12487(2)	36(1)
C(22)	7539(3)	5797(3)	12124(2)	33(1)
C(23)	7187(3)	6061(2)	11667(1)	28(1)
C(24)	7858(4)	8083(3)	11846(2)	53(1)
C(25)	7443(7)	8575(3)	12131(2)	154(4)
C(26)	8923(4)	8252(4)	11899(3)	132(3)
C(27)	6718(3)	5557(2)	11261(2)	35(1)
C(28)	5685(3)	5451(3)	11277(2)	57(1)
C(29)	7179(4)	4826(3)	11270(2)	72(2)
C(30)	5286(3)	8256(2)	9348(1)	31(1)
C(31)	5619(3)	8969(2)	9307(1)	29(1)
C(32)	5809(3)	9459(3)	9696(2)	43(1)
C(33)	6167(4)	10142(3)	9655(2)	57(2)
C(34)	6324(4)	10382(3)	9202(2)	60(2)
C(35)	6128(3)	9934(3)	8817(2)	45(1)
C(36)	5762(3)	9217(2)	8851(2)	32(1)
C(37)	5595(3)	8746(3)	8463(2)	43(1)
C(38)	5377(3)	8013(2)	8514(1)	31(1)
C(39)	5345(3)	7503(3)	8135(2)	40(1)
C(40)	5221(4)	6781(3)	8204(2)	53(1)
C(41)	5081(3)	6520(3)	8651(2)	53(1)

C(42)	5092(3)	7002(3)	9026(2)	41(1)
C(43)	5244(3)	7752(2)	8972(1)	30(1)
C(44)	10379(3)	7803(2)	7953(1)	26(1)
C(45)	10993(3)	7541(2)	8371(1)	24(1)
C(46)	11890(3)	7361(2)	8314(2)	30(1)
C(47)	12553(3)	7117(2)	8684(2)	34(1)
C(48)	12340(3)	7061(2)	9141(2)	35(1)
C(49)	11476(3)	7238(2)	9224(1)	29(1)
C(50)	10761(3)	7466(2)	8832(1)	25(1)
C(51)	9115(3)	8248(2)	7416(1)	29(1)
C(52)	8673(3)	7743(2)	7070(1)	35(1)
C(53)	8273(3)	8014(3)	6614(2)	43(1)
C(54)	8318(3)	8744(3)	6506(2)	50(1)
C(55)	8736(3)	9236(3)	6854(2)	46(1)
C(56)	9136(3)	9005(2)	7320(2)	35(1)
C(57)	8653(3)	6940(3)	7188(2)	47(1)
C(58)	9475(4)	6536(3)	7056(2)	69(2)
C(59)	7750(4)	6562(3)	6952(2)	78(2)
C(60)	9594(3)	9543(3)	7703(2)	45(1)
C(61)	10538(3)	9776(3)	7620(2)	60(1)
C(62)	9000(4)	10205(3)	7749(2)	73(2)
C(63)	11302(3)	7178(2)	9720(1)	32(1)
C(64)	11231(3)	6481(3)	9923(2)	38(1)
C(65)	11275(4)	5818(3)	9665(2)	49(1)
C(66)	11231(4)	5152(3)	9876(2)	64(2)
C(67)	11123(4)	5098(4)	10358(2)	67(2)
C(68)	11075(4)	5713(3)	10614(2)	56(1)
C(69)	11134(3)	6422(3)	10415(2)	43(1)
C(70)	11078(3)	7063(3)	10673(2)	45(1)
C(71)	11117(3)	7747(3)	10477(2)	37(1)
C(72)	11045(3)	8408(3)	10740(2)	51(1)
C(73)	11103(4)	9067(3)	10547(2)	61(2)
C(74)	11258(4)	9134(3)	10074(2)	52(1)
C(75)	11311(3)	8524(3)	9808(2)	39(1)
C(76)	11239(3)	7807(2)	9990(1)	33(1)
C(81)	8559(3)	5402(3)	8167(2)	48(1)
C(82)	9348(3)	5810(3)	8289(2)	43(1)
C(83)	10166(3)	5530(3)	8236(2)	50(1)
C(84)	10203(4)	4832(3)	8064(2)	57(1)
C(85)	9429(4)	4412(3)	7948(2)	54(1)
C(86)	8598(4)	4695(3)	8000(2)	55(1)
C(91)	1669(5)	9693(4)	8849(2)	74(2)
C(92)	1870(5)	10395(4)	9036(2)	82(2)
C(93)	2728(6)	10627(3)	9114(2)	75(2)
C(94)	3445(4)	10197(4)	8997(2)	74(2)
C(95)	3236(4)	9513(3)	8810(2)	65(2)
C(96)	2338(4)	9281(3)	8750(2)	58(2)
C(101)	5913(4)	4908(3)	-30(2)	52(1)
C(102)	5559(3)	5597(3)	0(2)	47(1)
C(103)	4654(3)	5699(3)	31(2)	49(1)

Table 3. Selected bond lengths [Å] and angles [°] for TRY17 (CCDC 163158).

Pt(1)-N(1)	2.053(3)	Pt(2)-N(2)	2.047(3)
Pt(1)-C(9)	2.036(4)	Pt(2)-C(10)	2.040(4)
Pt(1)-O(1)	2.095(2)	Pt(2)-O(2)	2.101(2)
Pt(1)-C(2)	2.143(4)	Pt(2)-C(5)	2.142(4)
Pt(1)-C(1)	2.152(4)	Pt(2)-C(6)	2.146(4)
C(1)-C(2)	1.391(6)	C(4)-C(5)	1.481(6)
C(1)-C(8)	1.496(6)	C(4)-H(4A)	1.05(3)
C(1)-H(1)	0.97(3)	C(4)-H(4B)	0.84(4)
C(2)-C(3)	1.489(6)	C(5)-C(6)	1.378(6)
C(2)-H(2)	0.88(4)	C(5)-H(5)	1.00(4)
C(3)-C(4)	1.556(5)	C(6)-C(7)	1.497(6)
C(3)-H(3A)	0.89(3)	C(6)-H(6)	0.88(4)
C(3)-H(3B)	0.93(4)	C(7)-C(8)	1.547(6)
N(1)-Pt(1)-C(9)	91.28(15)	N(2)-Pt(2)-C(10)	90.49(14)
N(1)-Pt(1)-O(1)	90.14(11)	N(2)-Pt(2)-O(2)	90.80(11)
C(9)-Pt(1)-O(1)	177.17(17)	C(10)-Pt(2)-O(2)	178.25(15)
N(1)-Pt(1)-C(2)	161.43(15)	N(2)-Pt(2)-C(5)	159.42(15)
C(9)-Pt(1)-C(2)	87.00(17)	C(10)-Pt(2)-C(5)	88.13(17)
O(1)-Pt(1)-C(2)	90.87(13)	O(2)-Pt(2)-C(5)	91.08(14)
N(1)-Pt(1)-C(1)	160.78(15)	N(2)-Pt(2)-C(6)	163.05(15)
C(9)-Pt(1)-C(1)	90.87(17)	C(10)-Pt(2)-C(6)	89.34(16)
O(1)-Pt(1)-C(1)	88.59(14)	O(2)-Pt(2)-C(6)	89.08(13)
C(2)-Pt(1)-C(1)	37.78(15)	C(5)-Pt(2)-C(6)	37.49(15)

Table 4. Bond lengths [Å] and angles [°] for TRY17 (CCDC 163158).

Pt(1)-N(1)	2.053(3)	N(2)-C(51)	1.438(4)
Pt(1)-C(9)	2.036(4)	C(1)-C(2)	1.391(6)
Pt(1)-O(1)	2.095(2)	C(1)-C(8)	1.496(6)
Pt(1)-C(2)	2.143(4)	C(1)-H(1)	0.97(3)
Pt(1)-C(1)	2.152(4)	C(2)-C(3)	1.489(6)
Pt(2)-N(2)	2.047(3)	C(2)-H(2)	0.88(4)
Pt(2)-C(10)	2.040(4)	C(3)-C(4)	1.556(5)
Pt(2)-O(2)	2.101(2)	C(3)-H(3A)	0.89(3)
Pt(2)-C(5)	2.142(4)	C(3)-H(3B)	0.93(4)
Pt(2)-C(6)	2.146(4)	C(4)-C(5)	1.481(6)
O(1)-C(17)	1.306(4)	C(4)-H(4A)	1.05(3)
O(2)-C(50)	1.291(4)	C(4)-H(4B)	0.84(4)
N(1)-C(11)	1.301(5)	C(5)-C(6)	1.378(6)
N(1)-C(18)	1.452(4)	C(5)-H(5)	1.00(4)
N(2)-C(44)	1.301(5)	C(6)-C(7)	1.497(6)

C(6)-H(6)	0.88(4)	C(30)-C(43)	1.404(5)
C(7)-C(8)	1.547(6)	C(31)-C(32)	1.406(6)
C(7)-H(7A)	0.94(3)	C(31)-C(36)	1.434(5)
C(7)-H(7B)	0.85(3)	C(32)-C(33)	1.369(6)
C(8)-H(8A)	0.86(4)	C(32)-H(32)	1.04(4)
C(8)-H(8B)	0.97(4)	C(33)-C(34)	1.427(6)
C(9)-H(9A)	0.9800	C(33)-H(33)	1.18(6)
C(9)-H(9B)	0.9800	C(34)-C(35)	1.350(7)
C(9)-H(9C)	0.9800	C(34)-H(34)	1.03(5)
C(10)-H(10A)	0.9800	C(35)-C(36)	1.427(6)
C(10)-H(10B)	0.9800	C(35)-H(35)	0.98(4)
C(10)-H(10C)	0.9800	C(36)-C(37)	1.381(6)
C(11)-C(12)	1.418(5)	C(37)-C(38)	1.389(6)
C(11)-H(11)	0.98(3)	C(37)-H(37)	1.03(4)
C(12)-C(13)	1.414(5)	C(38)-C(39)	1.417(6)
C(12)-C(17)	1.420(5)	C(38)-C(43)	1.443(5)
C(13)-C(14)	1.364(6)	C(39)-C(40)	1.351(6)
C(13)-H(13)	0.94(4)	C(39)-H(39)	1.02(4)
C(14)-C(15)	1.395(6)	C(40)-C(41)	1.415(7)
C(14)-H(14)	0.97(4)	C(40)-H(40)	0.99(4)
C(15)-C(16)	1.380(5)	C(41)-C(42)	1.382(6)
C(15)-H(15)	0.97(4)	C(41)-H(41)	0.98(4)
C(16)-C(17)	1.433(5)	C(42)-C(43)	1.401(6)
C(16)-C(30)	1.495(5)	C(42)-H(42)	1.02(4)
C(18)-C(23)	1.388(5)	C(44)-C(45)	1.422(5)
C(18)-C(19)	1.399(5)	C(44)-H(44)	0.87(3)
C(19)-C(20)	1.388(5)	C(45)-C(46)	1.409(5)
C(19)-C(24)	1.508(6)	C(45)-C(50)	1.433(5)
C(20)-C(21)	1.379(6)	C(46)-C(47)	1.357(6)
C(20)-H(20)	1.00(4)	C(46)-H(46)	0.90(4)
C(21)-C(22)	1.378(6)	C(47)-C(48)	1.405(6)
C(21)-H(21)	0.95(4)	C(47)-H(47)	0.97(3)
C(22)-C(23)	1.383(5)	C(48)-C(49)	1.387(5)
C(22)-H(22)	0.95(4)	C(48)-H(48)	0.95(4)
C(23)-C(27)	1.526(5)	C(49)-C(50)	1.431(5)
C(24)-C(25)	1.432(7)	C(49)-C(63)	1.492(5)
C(24)-C(26)	1.582(8)	C(51)-C(52)	1.408(5)
C(24)-H(24)	0.95(4)	C(51)-C(56)	1.409(5)
C(25)-H(25A)	0.9800	C(52)-C(53)	1.401(6)
C(25)-H(25B)	0.9800	C(52)-C(57)	1.505(6)
C(25)-H(25C)	0.9800	C(53)-C(54)	1.371(7)
C(26)-H(26A)	0.9800	C(53)-H(53)	0.95(4)
C(26)-H(26B)	0.9800	C(54)-C(55)	1.384(7)
C(26)-H(26C)	0.9800	C(54)-H(54)	1.00(4)
C(27)-C(29)	1.496(6)	C(55)-C(56)	1.401(6)
C(27)-C(28)	1.552(6)	C(55)-H(55)	1.00(4)
C(27)-H(27)	1.00(4)	C(56)-C(60)	1.517(6)
C(28)-H(28A)	0.9800	C(57)-C(59)	1.528(6)
C(28)-H(28B)	0.9800	C(57)-C(58)	1.535(7)
C(28)-H(28C)	0.9800	C(57)-H(57)	1.01(4)
C(29)-H(29A)	0.9800	C(58)-H(58A)	0.9800
C(29)-H(29B)	0.9800	C(58)-H(58B)	0.9800
C(29)-H(29C)	0.9800	C(58)-H(58C)	0.9800
C(30)-C(31)	1.404(5)	C(59)-H(59A)	0.9800

C(59)-H(59B)	0.9800	C(93)-H(93)	0.9500
C(59)-H(59C)	0.9800	C(94)-C(95)	1.366(7)
C(60)-C(62)	1.517(6)	C(94)-H(94)	0.9500
C(60)-C(61)	1.526(6)	C(95)-C(96)	1.373(7)
C(60)-H(60)	0.98(4)	C(95)-H(95)	0.9500
C(61)-H(61A)	0.9800	C(96)-H(96)	0.9500
C(61)-H(61B)	0.9800	C(101)-C(102)	1.371(6)
C(61)-H(61C)	0.9800	C(101)-C(103)#1	1.389(6)
C(62)-H(62A)	0.9800	C(101)-H(101)	0.9500
C(62)-H(62B)	0.9800	C(102)-C(103)	1.375(6)
C(62)-H(62C)	0.9800	C(102)-H(102)	0.9500
C(63)-C(76)	1.396(5)	C(103)-C(101)#1	1.389(6)
C(63)-C(64)	1.411(6)	C(103)-H(103)	0.9500
C(64)-C(65)	1.423(6)		
C(64)-C(69)	1.443(6)	N(1)-Pt(1)-C(9)	91.28(15)
C(65)-C(66)	1.363(7)	N(1)-Pt(1)-O(1)	90.14(11)
C(65)-H(65)	0.92(4)	C(9)-Pt(1)-O(1)	177.17(17)
C(66)-C(67)	1.419(7)	N(1)-Pt(1)-C(2)	161.43(15)
C(66)-H(66)	0.98(4)	C(9)-Pt(1)-C(2)	87.00(17)
C(67)-C(68)	1.348(7)	O(1)-Pt(1)-C(2)	90.87(13)
C(67)-H(67)	1.00(5)	N(1)-Pt(1)-C(1)	160.78(15)
C(68)-C(69)	1.421(6)	C(9)-Pt(1)-C(1)	90.87(17)
C(68)-H(68)	1.05(5)	O(1)-Pt(1)-C(1)	88.59(14)
C(69)-C(70)	1.395(6)	C(2)-Pt(1)-C(1)	37.78(15)
C(70)-C(71)	1.373(6)	N(2)-Pt(2)-C(10)	90.49(14)
C(70)-H(70)	0.96(4)	N(2)-Pt(2)-O(2)	90.80(11)
C(71)-C(72)	1.435(6)	C(10)-Pt(2)-O(2)	178.25(15)
C(71)-C(76)	1.443(6)	N(2)-Pt(2)-C(5)	159.42(15)
C(72)-C(73)	1.331(7)	C(10)-Pt(2)-C(5)	88.13(17)
C(72)-H(72)	0.89(5)	O(2)-Pt(2)-C(5)	91.08(14)
C(73)-C(74)	1.422(7)	N(2)-Pt(2)-C(6)	163.05(15)
C(73)-H(73)	1.03(5)	C(10)-Pt(2)-C(6)	89.34(16)
C(74)-C(75)	1.358(6)	O(2)-Pt(2)-C(6)	89.08(13)
C(74)-H(74)	1.03(5)	C(5)-Pt(2)-C(6)	37.49(15)
C(75)-C(76)	1.418(6)	C(17)-O(1)-Pt(1)	127.3(2)
C(75)-H(75)	0.91(4)	C(50)-O(2)-Pt(2)	126.6(2)
C(81)-C(82)	1.368(6)	C(11)-N(1)-C(18)	115.1(3)
C(81)-C(86)	1.381(6)	C(11)-N(1)-Pt(1)	123.5(3)
C(81)-H(81)	0.9500	C(18)-N(1)-Pt(1)	121.3(2)
C(82)-C(83)	1.352(6)	C(44)-N(2)-C(51)	114.3(3)
C(82)-H(82)	0.9500	C(44)-N(2)-Pt(2)	123.5(3)
C(83)-C(84)	1.371(6)	C(51)-N(2)-Pt(2)	122.2(2)
C(83)-H(83)	0.9500	C(2)-C(1)-C(8)	124.3(4)
C(84)-C(85)	1.360(7)	C(2)-C(1)-Pt(1)	70.7(2)
C(84)-H(84)	0.9500	C(8)-C(1)-Pt(1)	117.8(3)
C(85)-C(86)	1.369(7)	C(2)-C(1)-H(1)	117(2)
C(85)-H(85)	0.9500	C(8)-C(1)-H(1)	114(2)
C(86)-H(86)	0.9500	Pt(1)-C(1)-H(1)	103(2)
C(91)-C(96)	1.320(7)	C(1)-C(2)-C(3)	125.7(4)
C(91)-C(92)	1.394(8)	C(1)-C(2)-Pt(1)	71.5(2)
C(91)-H(91)	0.9500	C(3)-C(2)-Pt(1)	116.4(3)
C(92)-C(93)	1.314(8)	C(1)-C(2)-H(2)	119(3)
C(92)-H(92)	0.9500	C(3)-C(2)-H(2)	109(3)
C(93)-C(94)	1.416(8)	Pt(1)-C(2)-H(2)	108(2)

C(2)-C(3)-C(4)	109.4(4)	C(14)-C(13)-C(12)	122.3(4)
C(2)-C(3)-H(3A)	112(2)	C(14)-C(13)-H(13)	121(2)
C(4)-C(3)-H(3A)	108(2)	C(12)-C(13)-H(13)	117(2)
C(2)-C(3)-H(3B)	103(2)	C(13)-C(14)-C(15)	118.7(4)
C(4)-C(3)-H(3B)	110(2)	C(13)-C(14)-H(14)	122(2)
H(3A)-C(3)-H(3B)	114(3)	C(15)-C(14)-H(14)	120(2)
C(5)-C(4)-C(3)	109.6(4)	C(16)-C(15)-C(14)	122.4(4)
C(5)-C(4)-H(4A)	112.5(18)	C(16)-C(15)-H(15)	117(3)
C(3)-C(4)-H(4A)	110.3(18)	C(14)-C(15)-H(15)	121(3)
C(5)-C(4)-H(4B)	110(3)	C(15)-C(16)-C(17)	119.0(4)
C(3)-C(4)-H(4B)	110(3)	C(15)-C(16)-C(30)	120.4(4)
H(4A)-C(4)-H(4B)	105(3)	C(17)-C(16)-C(30)	120.5(3)
C(6)-C(5)-C(4)	125.2(4)	O(1)-C(17)-C(12)	123.4(3)
C(6)-C(5)-Pt(2)	71.4(2)	O(1)-C(17)-C(16)	117.6(3)
C(4)-C(5)-Pt(2)	116.5(3)	C(12)-C(17)-C(16)	119.0(3)
C(6)-C(5)-H(5)	116(2)	C(23)-C(18)-C(19)	122.7(4)
C(4)-C(5)-H(5)	115(2)	C(23)-C(18)-N(1)	118.4(3)
Pt(2)-C(5)-H(5)	100(2)	C(19)-C(18)-N(1)	118.9(3)
C(5)-C(6)-C(7)	125.6(4)	C(20)-C(19)-C(18)	117.3(4)
C(5)-C(6)-Pt(2)	71.1(2)	C(20)-C(19)-C(24)	121.2(4)
C(7)-C(6)-Pt(2)	118.1(3)	C(18)-C(19)-C(24)	121.4(4)
C(5)-C(6)-H(6)	121(2)	C(21)-C(20)-C(19)	121.2(4)
C(7)-C(6)-H(6)	108(2)	C(21)-C(20)-H(20)	120(2)
Pt(2)-C(6)-H(6)	105(2)	C(19)-C(20)-H(20)	119(2)
C(6)-C(7)-C(8)	110.8(4)	C(22)-C(21)-C(20)	119.7(4)
C(6)-C(7)-H(7A)	115(2)	C(22)-C(21)-H(21)	115(2)
C(8)-C(7)-H(7A)	109(2)	C(20)-C(21)-H(21)	125(2)
C(6)-C(7)-H(7B)	108(2)	C(21)-C(22)-C(23)	121.7(4)
C(8)-C(7)-H(7B)	111(2)	C(21)-C(22)-H(22)	122(2)
H(7A)-C(7)-H(7B)	103(3)	C(23)-C(22)-H(22)	117(2)
C(1)-C(8)-C(7)	110.7(4)	C(22)-C(23)-C(18)	117.4(4)
C(1)-C(8)-H(8A)	110(3)	C(22)-C(23)-C(27)	121.7(4)
C(7)-C(8)-H(8A)	108(3)	C(18)-C(23)-C(27)	120.9(4)
C(1)-C(8)-H(8B)	113(2)	C(25)-C(24)-C(19)	114.2(5)
C(7)-C(8)-H(8B)	107(2)	C(25)-C(24)-C(26)	111.2(6)
H(8A)-C(8)-H(8B)	108(3)	C(19)-C(24)-C(26)	109.4(4)
Pt(1)-C(9)-H(9A)	109.5	C(25)-C(24)-H(24)	111(2)
Pt(1)-C(9)-H(9B)	109.5	C(19)-C(24)-H(24)	110(2)
H(9A)-C(9)-H(9B)	109.5	C(26)-C(24)-H(24)	100(2)
Pt(1)-C(9)-H(9C)	109.5	C(24)-C(25)-H(25A)	109.5
H(9A)-C(9)-H(9C)	109.5	C(24)-C(25)-H(25B)	109.5
H(9B)-C(9)-H(9C)	109.5	H(25A)-C(25)-H(25B)	109.5
Pt(2)-C(10)-H(10A)	109.5	C(24)-C(25)-H(25C)	109.5
Pt(2)-C(10)-H(10B)	109.5	H(25A)-C(25)-H(25C)	109.5
H(10A)-C(10)-H(10B)	109.5	H(25B)-C(25)-H(25C)	109.5
Pt(2)-C(10)-H(10C)	109.5	C(24)-C(26)-H(26A)	109.5
H(10A)-C(10)-H(10C)	109.5	C(24)-C(26)-H(26B)	109.5
H(10B)-C(10)-H(10C)	109.5	H(26A)-C(26)-H(26B)	109.5
N(1)-C(11)-C(12)	129.7(4)	C(24)-C(26)-H(26C)	109.5
N(1)-C(11)-H(11)	115.4(17)	H(26A)-C(26)-H(26C)	109.5
C(12)-C(11)-H(11)	114.8(17)	H(26B)-C(26)-H(26C)	109.5
C(13)-C(12)-C(11)	116.2(4)	C(29)-C(27)-C(23)	113.0(4)
C(13)-C(12)-C(17)	118.5(4)	C(29)-C(27)-C(28)	109.8(4)
C(11)-C(12)-C(17)	125.2(3)	C(23)-C(27)-C(28)	110.4(4)

C(29)-C(27)-H(27)	108(2)	C(42)-C(43)-C(30)	122.6(4)
C(23)-C(27)-H(27)	105(2)	C(42)-C(43)-C(38)	118.5(4)
C(28)-C(27)-H(27)	111(2)	C(30)-C(43)-C(38)	119.0(4)
C(27)-C(28)-H(28A)	109.5	N(2)-C(44)-C(45)	129.8(4)
C(27)-C(28)-H(28B)	109.5	N(2)-C(44)-H(44)	116(2)
H(28A)-C(28)-H(28B)	109.5	C(45)-C(44)-H(44)	115(2)
C(27)-C(28)-H(28C)	109.5	C(46)-C(45)-C(44)	115.7(4)
H(28A)-C(28)-H(28C)	109.5	C(46)-C(45)-C(50)	119.8(4)
H(28B)-C(28)-H(28C)	109.5	C(44)-C(45)-C(50)	124.5(3)
C(27)-C(29)-H(29A)	109.5	C(47)-C(46)-C(45)	122.1(4)
C(27)-C(29)-H(29B)	109.5	C(47)-C(46)-H(46)	119(3)
H(29A)-C(29)-H(29B)	109.5	C(45)-C(46)-H(46)	119(3)
C(27)-C(29)-H(29C)	109.5	C(46)-C(47)-C(48)	118.6(4)
H(29A)-C(29)-H(29C)	109.5	C(46)-C(47)-H(47)	121(2)
H(29B)-C(29)-H(29C)	109.5	C(48)-C(47)-H(47)	120(2)
C(31)-C(30)-C(43)	120.2(4)	C(49)-C(48)-C(47)	122.3(4)
C(31)-C(30)-C(16)	120.1(4)	C(49)-C(48)-H(48)	124(2)
C(43)-C(30)-C(16)	119.7(4)	C(47)-C(48)-H(48)	114(2)
C(30)-C(31)-C(32)	122.6(4)	C(48)-C(49)-C(50)	119.5(4)
C(30)-C(31)-C(36)	119.3(4)	C(48)-C(49)-C(63)	119.6(4)
C(32)-C(31)-C(36)	118.1(4)	C(50)-C(49)-C(63)	120.9(3)
C(33)-C(32)-C(31)	121.9(5)	O(2)-C(50)-C(49)	117.8(3)
C(33)-C(32)-H(32)	122(2)	O(2)-C(50)-C(45)	124.6(3)
C(31)-C(32)-H(32)	116(2)	C(49)-C(50)-C(45)	117.6(3)
C(32)-C(33)-C(34)	119.8(5)	C(52)-C(51)-C(56)	122.0(4)
C(32)-C(33)-H(33)	118(3)	C(52)-C(51)-N(2)	119.3(4)
C(34)-C(33)-H(33)	122(3)	C(56)-C(51)-N(2)	118.6(4)
C(35)-C(34)-C(33)	120.1(5)	C(53)-C(52)-C(51)	117.7(4)
C(35)-C(34)-H(34)	116(3)	C(53)-C(52)-C(57)	121.7(4)
C(33)-C(34)-H(34)	124(3)	C(51)-C(52)-C(57)	120.6(4)
C(34)-C(35)-C(36)	121.3(5)	C(54)-C(53)-C(52)	121.2(5)
C(34)-C(35)-H(35)	124(2)	C(54)-C(53)-H(53)	124(2)
C(36)-C(35)-H(35)	114(2)	C(52)-C(53)-H(53)	114(2)
C(37)-C(36)-C(35)	121.5(4)	C(53)-C(54)-C(55)	120.4(5)
C(37)-C(36)-C(31)	119.6(4)	C(53)-C(54)-H(54)	124(3)
C(35)-C(36)-C(31)	118.7(4)	C(55)-C(54)-H(54)	116(3)
C(36)-C(37)-C(38)	121.5(4)	C(54)-C(55)-C(56)	121.4(5)
C(36)-C(37)-H(37)	118(2)	C(54)-C(55)-H(55)	122(3)
C(38)-C(37)-H(37)	120(2)	C(56)-C(55)-H(55)	116(3)
C(37)-C(38)-C(39)	121.6(4)	C(55)-C(56)-C(51)	117.2(4)
C(37)-C(38)-C(43)	119.3(4)	C(55)-C(56)-C(60)	121.6(4)
C(39)-C(38)-C(43)	119.0(4)	C(51)-C(56)-C(60)	121.2(4)
C(40)-C(39)-C(38)	120.9(5)	C(52)-C(57)-C(59)	113.4(4)
C(40)-C(39)-H(39)	120(2)	C(52)-C(57)-C(58)	111.1(4)
C(38)-C(39)-H(39)	118(2)	C(59)-C(57)-C(58)	109.9(4)
C(39)-C(40)-C(41)	120.5(5)	C(52)-C(57)-H(57)	108(2)
C(39)-C(40)-H(40)	116(3)	C(59)-C(57)-H(57)	101(2)
C(41)-C(40)-H(40)	124(3)	C(58)-C(57)-H(57)	113(2)
C(42)-C(41)-C(40)	120.2(5)	C(57)-C(58)-H(58A)	109.5
C(42)-C(41)-H(41)	116(3)	C(57)-C(58)-H(58B)	109.5
C(40)-C(41)-H(41)	123(3)	H(58A)-C(58)-H(58B)	109.5
C(41)-C(42)-C(43)	120.8(5)	C(57)-C(58)-H(58C)	109.5
C(41)-C(42)-H(42)	117(2)	H(58A)-C(58)-H(58C)	109.5
C(43)-C(42)-H(42)	122(2)	H(58B)-C(58)-H(58C)	109.5

C(57)-C(59)-H(59A)	109.5	C(72)-C(73)-C(74)	120.3(5)
C(57)-C(59)-H(59B)	109.5	C(72)-C(73)-H(73)	119(3)
H(59A)-C(59)-H(59B)	109.5	C(74)-C(73)-H(73)	120(3)
C(57)-C(59)-H(59C)	109.5	C(75)-C(74)-C(73)	119.9(5)
H(59A)-C(59)-H(59C)	109.5	C(75)-C(74)-H(74)	119(3)
H(59B)-C(59)-H(59C)	109.5	C(73)-C(74)-H(74)	121(3)
C(62)-C(60)-C(56)	113.4(4)	C(74)-C(75)-C(76)	122.3(5)
C(62)-C(60)-C(61)	111.0(4)	C(74)-C(75)-H(75)	117(2)
C(56)-C(60)-C(61)	110.8(4)	C(76)-C(75)-H(75)	120(2)
C(62)-C(60)-H(60)	113(2)	C(63)-C(76)-C(75)	122.5(4)
C(56)-C(60)-H(60)	106(2)	C(63)-C(76)-C(71)	120.3(4)
C(61)-C(60)-H(60)	102(2)	C(75)-C(76)-C(71)	117.1(4)
C(60)-C(61)-H(61A)	109.5	C(82)-C(81)-C(86)	120.0(5)
C(60)-C(61)-H(61B)	109.5	C(82)-C(81)-H(81)	120.0
H(61A)-C(61)-H(61B)	109.5	C(86)-C(81)-H(81)	120.0
C(60)-C(61)-H(61C)	109.5	C(83)-C(82)-C(81)	120.3(5)
H(61A)-C(61)-H(61C)	109.5	C(83)-C(82)-H(82)	119.9
H(61B)-C(61)-H(61C)	109.5	C(81)-C(82)-H(82)	119.9
C(60)-C(62)-H(62A)	109.5	C(82)-C(83)-C(84)	119.7(5)
C(60)-C(62)-H(62B)	109.5	C(82)-C(83)-H(83)	120.2
H(62A)-C(62)-H(62B)	109.5	C(84)-C(83)-H(83)	120.2
C(60)-C(62)-H(62C)	109.5	C(85)-C(84)-C(83)	121.0(5)
H(62A)-C(62)-H(62C)	109.5	C(85)-C(84)-H(84)	119.5
H(62B)-C(62)-H(62C)	109.5	C(83)-C(84)-H(84)	119.5
C(76)-C(63)-C(64)	119.7(4)	C(84)-C(85)-C(86)	119.6(5)
C(76)-C(63)-C(49)	120.5(4)	C(84)-C(85)-H(85)	120.2
C(64)-C(63)-C(49)	119.8(4)	C(86)-C(85)-H(85)	120.2
C(63)-C(64)-C(65)	122.6(4)	C(81)-C(86)-C(85)	119.5(5)
C(63)-C(64)-C(69)	119.9(4)	C(81)-C(86)-H(86)	120.3
C(65)-C(64)-C(69)	117.5(4)	C(85)-C(86)-H(86)	120.3
C(66)-C(65)-C(64)	121.3(5)	C(96)-C(91)-C(92)	119.7(6)
C(66)-C(65)-H(65)	119(3)	C(96)-C(91)-H(91)	120.2
C(64)-C(65)-H(65)	119(3)	C(92)-C(91)-H(91)	120.2
C(65)-C(66)-C(67)	120.8(6)	C(93)-C(92)-C(91)	118.8(7)
C(65)-C(66)-H(66)	117(3)	C(93)-C(92)-H(92)	120.6
C(67)-C(66)-H(66)	123(3)	C(91)-C(92)-H(92)	120.6
C(68)-C(67)-C(66)	119.8(5)	C(92)-C(93)-C(94)	121.9(6)
C(68)-C(67)-H(67)	119(3)	C(92)-C(93)-H(93)	119.1
C(66)-C(67)-H(67)	121(3)	C(94)-C(93)-H(93)	119.1
C(67)-C(68)-C(69)	121.7(5)	C(95)-C(94)-C(93)	118.6(6)
C(67)-C(68)-H(68)	122(3)	C(95)-C(94)-H(94)	120.7
C(69)-C(68)-H(68)	116(3)	C(93)-C(94)-H(94)	120.7
C(70)-C(69)-C(68)	122.5(5)	C(94)-C(95)-C(96)	117.7(6)
C(70)-C(69)-C(64)	118.7(4)	C(94)-C(95)-H(95)	121.2
C(68)-C(69)-C(64)	118.9(5)	C(96)-C(95)-H(95)	121.2
C(71)-C(70)-C(69)	122.3(4)	C(91)-C(96)-C(95)	123.3(6)
C(71)-C(70)-H(70)	119(2)	C(91)-C(96)-H(96)	118.4
C(69)-C(70)-H(70)	118(3)	C(95)-C(96)-H(96)	118.4
C(70)-C(71)-C(72)	122.5(5)	C(102)-C(101)-C(103)#1	119.6(5)
C(70)-C(71)-C(76)	119.1(4)	C(102)-C(101)-H(101)	120.2
C(72)-C(71)-C(76)	118.4(5)	C(103)#1-C(101)-H(101)	120.2
C(73)-C(72)-C(71)	121.8(5)	C(101)-C(102)-C(103)	121.2(5)
C(73)-C(72)-H(72)	127(3)	C(101)-C(102)-H(102)	119.4
C(71)-C(72)-H(72)	111(3)	C(103)-C(102)-H(102)	119.4

C(102)-C(103)-C(101)#1	119.2(5)	C(101)#1-C(103)-H(103)	120.4
C(102)-C(103)-H(103)	120.4		

Symmetry transformations used to generate equivalent atoms:
#1 -x+1,-y+1,-z

Table 5. Anisotropic displacement parameters (Å^{2}x 10^4) for TRY17 (CCDC 163158). The anisotropic displacement factor exponent takes the form: $-2\pi^2$ [$h^2 a^{*2}U^{11}$ + ... + 2 h k a* b* U^{12}]

	U^{11}	U^{22}	U^{33}	U^{23}	U^{13}	U^{12}
Pt(1)	236(1)	453(1)	192(1)	77(1)	65(1)	-2(1)
Pt(2)	233(1)	426(1)	203(1)	77(1)	76(1)	23(1)
O(1)	249(15)	351(16)	204(14)	53(12)	57(12)	12(12)
O(2)	228(14)	353(16)	226(15)	47(12)	71(12)	-5(12)
N(1)	256(18)	310(20)	178(17)	18(14)	47(14)	-24(15)
N(2)	241(18)	330(20)	191(17)	23(15)	63(14)	-14(15)
C(1)	230(20)	560(30)	210(20)	40(20)	82(19)	-50(20)
C(2)	270(20)	430(30)	280(20)	160(20)	142(19)	120(20)
C(3)	350(30)	250(30)	350(30)	0(20)	140(20)	0(20)
C(4)	320(30)	330(30)	290(30)	-40(20)	140(20)	-80(20)
C(5)	290(20)	440(30)	220(20)	60(20)	118(19)	-40(20)
C(6)	270(20)	410(30)	260(20)	100(20)	154(19)	100(20)
C(7)	300(30)	270(30)	380(30)	30(20)	160(20)	-40(20)
C(8)	380(30)	310(30)	300(30)	-90(20)	130(20)	-110(20)
C(9)	290(30)	1340(50)	360(30)	400(30)	130(20)	230(30)
C(10)	340(30)	880(40)	300(30)	210(30)	150(20)	190(30)
C(11)	290(20)	290(20)	200(20)	9(18)	112(18)	-35(18)
C(12)	270(20)	300(20)	230(20)	-11(18)	74(18)	3(18)
C(13)	330(30)	340(30)	290(20)	0(20)	120(20)	0(20)
C(14)	280(20)	450(30)	360(30)	50(20)	60(20)	70(20)
C(15)	330(30)	380(30)	300(30)	40(20)	-10(20)	20(20)
C(16)	340(20)	260(20)	250(20)	14(18)	42(18)	-11(19)
C(17)	260(20)	170(20)	135(19)	-48(15)	3(16)	-46(16)
C(18)	270(20)	360(20)	190(20)	33(18)	104(17)	-15(18)
C(19)	350(20)	370(30)	240(20)	13(19)	70(19)	-20(20)
C(20)	320(20)	520(30)	230(20)	-60(20)	66(19)	-30(20)
C(21)	360(30)	510(30)	210(20)	80(20)	80(20)	60(20)
C(22)	370(30)	340(30)	280(30)	60(20)	70(20)	10(20)
C(23)	280(20)	340(30)	220(20)	0(18)	82(18)	-11(19)
C(24)	790(40)	360(30)	320(30)	40(20)	-120(30)	-140(30)
C(25)	3600(130)	330(40)	1130(60)	100(40)	1510(80)	420(60)
C(26)	820(50)	880(50)	2160(90)	450(60)	110(60)	-340(40)
C(27)	460(30)	340(30)	240(20)	30(20)	30(20)	-20(20)
C(28)	630(40)	640(40)	420(30)	10(30)	40(30)	-290(30)
C(29)	980(50)	510(30)	500(30)	-140(30)	-180(30)	220(30)
C(30)	400(30)	310(20)	230(20)	55(19)	71(19)	70(20)
C(31)	320(20)	290(20)	260(20)	0(19)	77(19)	25(19)
C(32)	520(30)	420(30)	360(30)	30(20)	110(20)	-80(20)
C(33)	790(40)	500(30)	430(30)	10(30)	170(30)	-230(30)

C(34)	800(40)	490(40)	540(40)	20(30)	210(30)	-250(30)
C(35)	590(30)	440(30)	390(30)	100(20)	230(30)	-10(30)
C(36)	350(20)	340(30)	270(20)	40(20)	70(20)	100(20)
C(37)	520(30)	460(30)	280(30)	70(20)	20(20)	100(20)
C(38)	230(20)	400(30)	260(20)	-10(20)	-35(17)	45(19)
C(39)	340(30)	460(30)	420(30)	-100(20)	100(20)	-30(20)
C(40)	620(40)	530(40)	480(30)	-190(30)	220(30)	-60(30)
C(41)	540(30)	380(30)	690(40)	-80(30)	220(30)	-80(30)
C(42)	440(30)	390(30)	410(30)	-30(20)	130(20)	-40(20)
C(43)	200(20)	350(30)	330(20)	-20(20)	22(18)	-34(19)
C(44)	330(20)	270(20)	200(20)	-31(18)	114(18)	-49(19)
C(45)	230(20)	210(20)	280(20)	-33(17)	65(18)	-35(17)
C(46)	330(20)	270(20)	330(30)	-40(20)	130(20)	-18(19)
C(47)	250(20)	390(30)	390(30)	-50(20)	80(20)	30(20)
C(48)	300(20)	380(30)	350(30)	0(20)	-20(20)	40(20)
C(49)	290(20)	260(20)	300(20)	-4(18)	38(18)	6(18)
C(50)	260(20)	190(20)	290(20)	-14(17)	63(18)	-4(17)
C(51)	320(20)	420(30)	140(20)	29(18)	96(18)	0(20)
C(52)	300(20)	490(30)	270(20)	0(20)	55(19)	40(20)
C(53)	360(30)	720(40)	210(20)	0(30)	50(20)	70(30)
C(54)	430(30)	820(40)	270(30)	150(30)	150(20)	220(30)
C(55)	540(30)	540(40)	360(30)	190(30)	240(30)	180(30)
C(56)	370(30)	410(30)	290(20)	50(20)	150(20)	70(20)
C(57)	570(30)	500(30)	310(30)	-60(20)	-10(20)	-90(30)
C(58)	970(50)	490(30)	500(30)	-160(30)	-110(30)	60(30)
C(59)	810(40)	840(40)	590(40)	-20(30)	-50(30)	-360(40)
C(60)	620(30)	370(30)	350(30)	60(20)	130(30)	40(30)
C(61)	710(40)	590(40)	500(30)	40(30)	130(30)	-110(30)
C(62)	920(50)	510(40)	800(40)	-10(30)	300(40)	90(30)
C(63)	230(20)	420(30)	280(20)	30(20)	-20(17)	30(20)
C(64)	340(30)	460(30)	340(30)	80(20)	70(20)	110(20)
C(65)	600(30)	430(30)	480(30)	130(30)	180(30)	100(30)
C(66)	930(50)	450(40)	590(40)	120(30)	280(30)	130(30)
C(67)	810(40)	570(40)	640(40)	290(30)	200(30)	80(30)
C(68)	560(30)	650(40)	480(40)	170(30)	140(30)	140(30)
C(69)	380(30)	520(30)	390(30)	200(20)	100(20)	110(20)
C(70)	290(20)	770(40)	290(30)	30(30)	10(20)	80(30)
C(71)	230(20)	560(30)	300(20)	-30(20)	-14(18)	-30(20)
C(72)	420(30)	810(40)	300(30)	-180(30)	90(20)	-100(30)
C(73)	730(40)	610(40)	490(40)	-250(30)	140(30)	-150(30)
C(74)	600(30)	550(40)	420(30)	-170(30)	120(30)	-150(30)
C(75)	350(30)	490(30)	340(30)	-110(20)	60(20)	-70(20)
C(76)	190(20)	450(30)	300(20)	-30(20)	-30(17)	0(20)
C(81)	430(30)	640(40)	380(30)	-110(30)	110(20)	120(30)
C(82)	470(30)	420(30)	410(30)	-50(20)	130(20)	50(20)
C(83)	410(30)	530(30)	530(30)	-10(30)	70(20)	40(30)
C(84)	540(30)	620(40)	570(40)	-70(30)	120(30)	170(30)
C(85)	850(40)	410(30)	350(30)	-140(20)	90(30)	100(30)
C(86)	670(40)	670(40)	300(30)	-160(30)	110(30)	-180(30)
C(91)	860(50)	1000(50)	370(30)	140(30)	150(30)	50(40)
C(92)	1120(60)	1050(60)	210(30)	-130(30)	-40(30)	140(50)
C(93)	1540(70)	310(30)	320(30)	-30(20)	-10(40)	150(40)
C(94)	900(50)	890(50)	320(30)	-10(30)	-90(30)	-220(40)
C(95)	790(40)	740(40)	370(30)	-20(30)	0(30)	180(40)

C(96)	620(40)	380(30)	640(40)	10(30)	-90(30)	-60(30)
C(101)	580(30)	660(40)	280(30)	20(20)	10(20)	-80(30)
C(102)	560(30)	480(30)	310(30)	20(20)	-30(20)	-160(30)
C(103)	560(30)	550(30)	310(30)	30(20)	0(20)	-80(30)

Table 6. Hydrogen coordinates (x 10^4) and isotropic displacement parameters ($\AA^2$x 10^3) for TRY17 (CCDC 163158).

	x	y	z	U_{iso}
H(9A)	8937	6969	11337	79
H(9B)	9279	6677	10874	79
H(9C)	8582	6195	11106	79
H(10A)	7761	8762	7808	59
H(10B)	7127	8385	8131	59
H(10C)	7427	7932	7707	59
H(25A)	6779	8475	12078	231
H(25B)	7541	9081	12039	231
H(25C)	7725	8503	12471	231
H(26A)	9001	8741	11772	197
H(26B)	9199	7886	11720	197
H(26C)	9229	8232	12239	197
H(28A)	5385	5149	11004	86
H(28B)	5380	5930	11259	86
H(28C)	5637	5207	11577	86
H(29A)	7824	4895	11244	107
H(29B)	6857	4530	10999	107
H(29C)	7160	4575	11571	107
H(58A)	9430	6564	6708	104
H(58B)	9466	6021	7153	104
H(58C)	10052	6765	7222	104
H(59A)	7229	6828	7034	116
H(59B)	7754	6057	7070	116
H(59C)	7690	6559	6604	116
H(61A)	10912	9340	7595	90
H(61B)	10851	10080	7888	90
H(61C)	10459	10058	7321	90
H(62A)	8881	10481	7447	109
H(62B)	9323	10520	8009	109
H(62C)	8413	10043	7820	109
H(1)	9140(20)	7715(17)	10405(12)	21(10)
H(2)	8710(30)	6600(20)	10107(13)	33(12)
H(3A)	7180(20)	7041(19)	9493(12)	24(11)
H(3B)	7560(30)	6260(20)	9597(13)	36(12)
H(4A)	8930(20)	6844(17)	9275(11)	17(9)
H(4B)	8120(30)	6480(20)	8957(14)	34(13)
H(5)	7300(30)	7465(19)	8619(13)	30(11)
H(6)	7780(20)	8600(20)	8906(13)	29(11)
H(7A)	9000(20)	8911(19)	9486(12)	21(10)
H(7B)	9230(20)	8168(16)	9520(11)	1(9)

H(8A)	8360(30)	8720(20)	10077(14)	37(13)
H(8B)	7590(30)	8335(18)	9754(12)	25(10)
H(11)	5719(19)	7182(15)	11315(10)	4(8)
H(13)	4310(30)	7470(20)	10934(14)	38(12)
H(14)	3180(30)	7890(20)	10280(14)	41(12)
H(15)	3680(30)	8280(20)	9583(15)	53(14)
H(20)	8460(30)	7305(19)	12648(13)	31(11)
H(21)	8170(30)	6020(20)	12790(14)	38(12)
H(22)	7460(30)	5290(20)	12174(14)	44(13)
H(24)	7650(30)	8180(20)	11515(15)	40(12)
H(27)	6780(20)	5817(19)	10960(13)	34(11)
H(32)	5710(30)	9260(20)	10024(16)	57(14)
H(33)	6220(40)	10540(30)	9980(20)	130(20)
H(34)	6530(30)	10910(30)	9137(16)	71(16)
H(35)	6240(30)	10060(20)	8499(15)	43(12)
H(37)	5730(30)	8930(20)	8144(14)	44(12)
H(39)	5490(30)	7690(20)	7822(16)	59(15)
H(40)	5210(30)	6460(20)	7922(16)	62(15)
H(41)	5060(30)	6000(20)	8726(15)	58(15)
H(42)	5000(30)	6790(20)	9344(14)	43(12)
H(44)	10630(20)	7846(18)	7701(13)	21(10)
H(46)	12040(30)	7430(20)	8028(14)	36(12)
H(47)	13180(20)	7037(17)	8642(11)	19(9)
H(48)	12830(20)	6865(18)	9377(13)	28(11)
H(53)	7960(30)	7650(20)	6398(13)	30(12)
H(54)	8020(30)	8960(20)	6188(16)	58(14)
H(55)	8790(30)	9770(20)	6784(15)	58(15)
H(57)	8630(20)	6892(19)	7538(14)	29(11)
H(60)	9760(30)	9260(20)	7998(15)	46(13)
H(65)	11330(30)	5840(20)	9350(17)	63(16)
H(66)	11280(30)	4720(20)	9676(15)	53(15)
H(67)	11090(30)	4610(30)	10513(17)	74(17)
H(68)	11010(30)	5690(20)	10974(17)	72(16)
H(70)	11040(30)	7020(20)	11004(15)	48(13)
H(72)	10940(30)	8310(20)	11028(17)	62(16)
H(73)	11120(30)	9520(30)	10762(17)	74(16)
H(74)	11360(30)	9640(30)	9934(18)	86(19)
H(75)	11410(30)	8590(20)	9506(13)	32(12)
H(81)	7983	5606	8196	58
H(82)	9322	6292	8412	51
H(83)	10713	5816	8318	59
H(84)	10778	4638	8024	69
H(85)	9464	3926	7833	65
H(86)	8053	4406	7921	66
H(91)	1054	9513	8793	89
H(92)	1394	10699	9106	99
H(93)	2871	11098	9253	90
H(94)	4059	10380	9048	88
H(95)	3697	9209	8724	78
H(96)	2190	8800	8632	70
H(101)	6541	4846	-49	62
H(102)	5948	6012	-1	56
H(103)	4418	6180	54	58

Appendix M

X-Ray Diffraction Analysis of

$(^{\mathrm{Anthr,H}}\mathrm{Sal})\mathrm{Pt}(\mathrm{PPh_3})\mathrm{Et}$

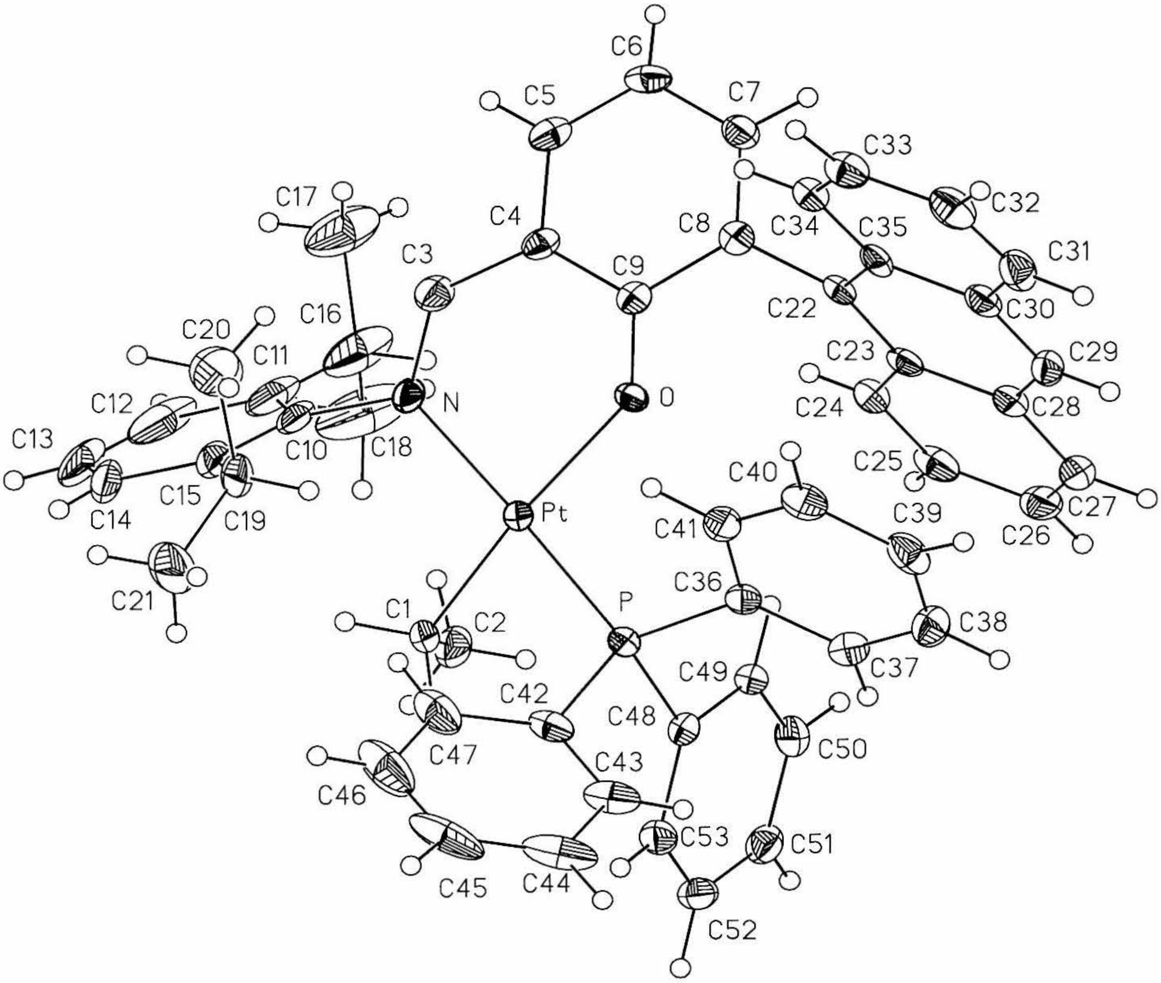

Table 1. Crystal data and structure refinement for TRY14 (CCDC 160843).

Empirical formula	$C_{53}H_{49}NOPPt\cdot C_6H_6$
Formula weight	1020.10
Crystallization Solvent	Benzene
Crystal Habit	Trapezoidal
Crystal size	0.30 x 0.22 x 0.16 mm^3
Crystal color	Canary yellow

Data Collection

Preliminary Photos	Rotation	
Type of diffractometer	CCD area detector	
Wavelength	0.71073 Å MoKα	
Data Collection Temperature	98(2) K	
θ range for 24539 reflections used in lattice determination	2.23 to 28.35°	
Unit cell dimensions	a = 9.9116(8) Å	α= 74.8710(10)°
	b = 12.0112(9) Å	β= 79.6870(10)°
	c = 22.3876(17) Å	γ = 67.6700(10)°
Volume	2370.4(3) Å^3	
Z	2	
Crystal system	Triclinic	
Space group	P-1	
Density (calculated)	1.429 Mg/m^3	
F(000)	1034	
Data collection program	Bruker SMART	
θ range for data collection	1.88 to 28.34°	
Completeness to θ = 28.34°	91.0 %	
Index ranges	-12 h 13, -15 k 16, -29 l 29	
Data collection scan type	ω scans at 5 ϕ settings	
Data reduction program	Bruker SAINT v6.2	
Reflections collected	34869	
Independent reflections	10776 [R_{int}= 0.0365]	
Absorption coefficient	3.035 mm^{-1}	
Absorption correction	SADABS	
Max. and min. transmission	1.000000 and 0.778883	

Table 1 (cont.)

Structure Solution and Refinement

Structure solution program	SHELXS-97 (Sheldrick, 1990)
Primary solution method	Patterson method
Secondary solution method	Difference Fourier map
Hydrogen placement	Difference Fourier map
Structure refinement program	SHELXL-97 (Sheldrick, 1997)
Refinement method	Full matrix least-squares on F^2
Data / restraints / parameters	10776 / 0 / 788
Treatment of hydrogen atoms	Unrestrained
Goodness-of-fit on F^2	1.455
Final R indices [$I>2\sigma(I)$, 9839 reflections]	$R1 = 0.0248$, $wR2 = 0.0489$
R indices (all data)	$R1 = 0.0282$, $wR2 = 0.0493$
Type of weighting scheme used	Sigma
Weighting scheme used	$w=1/\sigma^2(Fo^2)$
Max shift/error	0.004
Average shift/error	0.000
Largest diff. peak and hole	1.598 and -0.571 e.Å^{-3}

Special Refinement Details

Refinement of F^2 against ALL reflections. The weighted R-factor (*w*R) and goodness of fit (S) are based on F^2, conventional R-factors (R) are based on F, with F set to zero for negative F^2. The threshold expression of $F^2 > 2\sigma(F^2)$ is used only for calculating R-factors(gt) etc. and is not relevant to the choice of reflections for refinement. R-factors based on F^2 are statistically about twice as large as those based on F, and R-factors based on ALL data will be even larger.

All esds (except the esd in the dihedral angle between two l.s. planes) are estimated using the full covariance matrix. The cell esds are taken into account individually in the estimation of esds in distances, angles and torsion angles; correlations between esds in cell parameters are only used when they are defined by crystal symmetry. An approximate (isotropic) treatment of cell esds is used for estimating esds involving l.s. planes.

Table 2. Atomic coordinates (x 10^4) and equivalent isotropic displacement parameters (Å^{2}x 10^3) for TRY14 (CCDC 160843). U(eq) is defined as the trace of the orthogonalized U^{ij} tensor.

	x	y	z	U_{eq}
Pt	5918(1)	8364(1)	2818(1)	17(1)
P	6508(1)	7991(1)	1874(1)	17(1)
O	5853(2)	10180(1)	2475(1)	17(1)
N	5574(2)	8648(2)	3726(1)	22(1)
C(1)	5681(3)	6666(2)	3102(1)	23(1)
C(2)	4072(4)	6813(3)	3202(1)	30(1)
C(3)	5334(3)	9716(2)	3848(1)	24(1)
C(4)	5056(3)	10896(2)	3431(1)	18(1)
C(5)	4510(3)	11931(2)	3713(1)	22(1)
C(6)	4157(3)	13099(2)	3366(1)	25(1)
C(7)	4365(3)	13278(2)	2721(1)	21(1)
C(8)	4910(3)	12317(2)	2418(1)	17(1)
C(9)	5290(3)	11072(2)	2772(1)	16(1)
C(10)	5632(4)	7670(3)	4275(1)	37(1)
C(11)	4343(5)	7722(3)	4667(1)	48(1)
C(12)	4471(8)	6742(5)	5185(2)	75(2)
C(13)	5737(9)	5793(5)	5306(2)	96(2)
C(14)	6967(8)	5772(4)	4921(2)	73(2)
C(15)	6979(5)	6703(3)	4394(2)	48(1)
C(16)	2909(5)	8732(4)	4550(2)	55(1)
C(17)	2491(7)	9679(5)	4968(2)	62(1)
C(18)	1630(7)	8282(7)	4612(2)	80(2)
C(19)	8357(5)	6699(3)	3996(2)	50(1)
C(20)	9094(6)	7435(4)	4204(2)	62(1)
C(21)	9474(8)	5417(4)	3954(3)	80(2)
C(22)	5099(3)	12570(2)	1725(1)	17(1)
C(23)	4134(3)	12420(2)	1385(1)	18(1)
C(24)	3028(3)	11919(2)	1681(1)	21(1)
C(25)	2078(3)	11807(2)	1352(1)	25(1)
C(26)	2160(3)	12193(2)	696(1)	27(1)
C(27)	3189(3)	12679(2)	392(1)	26(1)
C(28)	4206(3)	12813(2)	724(1)	20(1)
C(29)	5241(3)	13334(2)	420(1)	23(1)
C(30)	6243(3)	13447(2)	737(1)	20(1)
C(31)	7357(3)	13927(2)	425(1)	26(1)
C(32)	8355(3)	13993(2)	738(1)	27(1)
C(33)	8318(3)	13594(2)	1391(1)	25(1)
C(34)	7265(3)	13154(2)	1712(1)	20(1)
C(35)	6185(3)	13057(2)	1404(1)	18(1)
C(36)	6919(3)	9180(2)	1257(1)	19(1)
C(37)	6457(3)	9487(2)	666(1)	24(1)
C(38)	6999(3)	10240(3)	184(1)	29(1)
C(39)	7999(3)	10695(2)	291(1)	28(1)
C(40)	8444(3)	10418(2)	881(1)	25(1)
C(41)	7915(3)	9668(2)	1361(1)	21(1)
C(42)	8224(3)	6710(2)	1788(1)	23(1)
C(43)	8842(3)	6503(3)	1202(2)	30(1)

C(44)	10226(3)	5631(3)	1127(2)	41(1)
C(45)	10987(4)	4964(3)	1640(2)	48(1)
C(46)	10394(4)	5149(3)	2211(2)	47(1)
C(47)	9011(3)	6023(3)	2294(2)	35(1)
C(48)	5076(3)	7682(2)	1610(1)	18(1)
C(49)	3704(3)	8612(2)	1593(1)	20(1)
C(50)	2510(3)	8426(2)	1460(1)	24(1)
C(51)	2670(3)	7298(2)	1346(1)	25(1)
C(52)	4025(3)	6372(2)	1362(1)	25(1)
C(53)	5224(3)	6562(2)	1490(1)	22(1)
C(61)	-954(4)	405(3)	3037(1)	40(1)
C(62)	541(4)	-196(3)	2915(1)	40(1)
C(63)	1517(4)	282(3)	3013(2)	47(1)
C(64)	1028(4)	1342(4)	3231(2)	48(1)
C(65)	-460(4)	1942(4)	3351(2)	46(1)
C(66)	-1443(4)	1471(3)	3254(1)	38(1)

Table 3. Selected bond lengths [Å] and angles [°] for TRY14 (CCDC 160843).

Pt-C(1)	2.062(2)	C(1)-Pt-O	171.33(9)
Pt-O	2.0954(15)	C(1)-Pt-N	93.21(9)
Pt-N	2.094(2)	O-Pt-N	89.69(7)
Pt-P	2.2047(7)	C(1)-Pt-P	87.11(8)
C(1)-C(2)	1.518(4)	O-Pt-P	90.78(5)
		N-Pt-P	174.51(6)

Table 4. Bond lengths [Å] and angles [°] for TRY14 (CCDC 160843).

Pt-C(1)	2.062(2)	C(5)-C(6)	1.360(4)
Pt-O	2.0954(15)	C(5)-H(5)	0.92(2)
Pt-N	2.094(2)	C(6)-C(7)	1.393(4)
Pt-P	2.2047(7)	C(6)-H(6)	0.85(3)
P-C(36)	1.824(3)	C(7)-C(8)	1.374(3)
P-C(48)	1.821(3)	C(7)-H(7)	0.91(3)
P-C(42)	1.830(3)	C(8)-C(9)	1.438(3)
O-C(9)	1.298(3)	C(8)-C(22)	1.492(3)
N-C(3)	1.307(3)	C(10)-C(11)	1.404(5)
N-C(10)	1.454(3)	C(10)-C(15)	1.411(5)
C(1)-C(2)	1.518(4)	C(11)-C(12)	1.404(5)
C(1)-H(1A)	0.93(3)	C(11)-C(16)	1.489(6)
C(1)-H(1B)	0.97(3)	C(12)-C(13)	1.350(8)
C(2)-H(2A)	0.89(3)	C(12)-H(12)	0.82(3)
C(2)-H(2B)	0.98(3)	C(13)-C(14)	1.357(8)
C(2)-H(2C)	0.96(3)	C(13)-H(13)	0.89(4)
C(3)-C(4)	1.435(3)	C(14)-C(15)	1.400(5)
C(4)-C(9)	1.424(3)	C(14)-H(14)	0.89(3)
C(4)-C(5)	1.419(3)	C(15)-C(19)	1.490(5)

C(16)-C(18)	1.530(5)	C(42)-C(47)	1.382(4)
C(16)-C(17)	1.548(5)	C(42)-C(43)	1.389(4)
C(16)-H(16)	0.88(3)	C(43)-C(44)	1.386(4)
C(17)-H(17A)	0.94(4)	C(43)-H(43)	0.87(3)
C(17)-H(17B)	1.00(4)	C(44)-C(45)	1.378(5)
C(17)-H(17C)	0.89(3)	C(44)-H(44)	0.96(3)
C(18)-H(18A)	0.98(4)	C(45)-C(46)	1.346(5)
C(18)-H(18B)	0.98(5)	C(45)-H(45)	0.82(3)
C(18)-H(18C)	0.99(5)	C(46)-C(47)	1.390(4)
C(19)-C(21)	1.532(6)	C(46)-H(46)	0.84(3)
C(19)-C(20)	1.535(5)	C(47)-H(47)	0.94(3)
C(19)-H(19)	0.87(3)	C(48)-C(49)	1.393(3)
C(20)-H(20A)	0.97(3)	C(48)-C(53)	1.388(3)
C(20)-H(20B)	0.96(4)	C(49)-C(50)	1.380(4)
C(20)-H(20C)	1.00(4)	C(49)-H(49)	0.96(2)
C(21)-H(21A)	0.96(4)	C(50)-C(51)	1.389(4)
C(21)-H(21B)	0.85(5)	C(50)-H(50)	0.97(3)
C(21)-H(21C)	0.90(4)	C(51)-C(52)	1.379(4)
C(22)-C(35)	1.414(3)	C(51)-H(51)	0.90(3)
C(22)-C(23)	1.410(3)	C(52)-C(53)	1.381(4)
C(23)-C(28)	1.429(3)	C(52)-H(52)	0.98(3)
C(23)-C(24)	1.426(4)	C(53)-H(53)	0.81(2)
C(24)-C(25)	1.358(4)	C(61)-C(66)	1.370(5)
C(24)-H(24)	0.84(2)	C(61)-C(62)	1.392(4)
C(25)-C(26)	1.419(4)	C(61)-H(61)	0.85(3)
C(25)-H(25)	0.92(3)	C(62)-C(63)	1.370(5)
C(26)-C(27)	1.357(4)	C(62)-H(62)	1.00(3)
C(26)-H(26)	0.87(3)	C(63)-C(64)	1.366(5)
C(27)-C(28)	1.432(4)	C(63)-H(63)	0.92(3)
C(27)-H(27)	0.95(3)	C(64)-C(65)	1.385(5)
C(28)-C(29)	1.387(4)	C(64)-H(64)	0.89(3)
C(29)-C(30)	1.384(4)	C(65)-C(66)	1.370(5)
C(29)-H(29)	0.84(2)	C(65)-H(65)	0.84(3)
C(30)-C(31)	1.427(4)	C(66)-H(66)	0.89(3)
C(30)-C(35)	1.442(3)		
C(31)-C(32)	1.346(4)	C(1)-Pt-O	171.33(9)
C(31)-H(31)	0.87(3)	C(1)-Pt-N	93.21(9)
C(32)-C(33)	1.414(4)	O-Pt-N	89.69(7)
C(32)-H(32)	0.90(3)	C(1)-Pt-P	87.11(8)
C(33)-C(34)	1.355(4)	O-Pt-P	90.78(5)
C(33)-H(33)	0.95(3)	N-Pt-P	174.51(6)
C(34)-C(35)	1.427(4)	C(36)-P-C(48)	105.67(11)
C(34)-H(34)	0.89(2)	C(36)-P-C(42)	98.68(12)
C(36)-C(37)	1.390(4)	C(48)-P-C(42)	107.70(11)
C(36)-C(41)	1.402(4)	C(36)-P-Pt	117.29(8)
C(37)-C(38)	1.386(4)	C(48)-P-Pt	111.89(8)
C(37)-H(37)	0.89(3)	C(42)-P-Pt	114.39(9)
C(38)-C(39)	1.381(4)	C(9)-O-Pt	126.15(15)
C(38)-H(38)	0.91(3)	C(3)-N-C(10)	113.9(2)
C(39)-C(40)	1.385(4)	C(3)-N-Pt	122.69(17)
C(39)-H(39)	0.90(3)	C(10)-N-Pt	123.33(16)
C(40)-C(41)	1.377(4)	C(2)-C(1)-Pt	110.49(19)
C(40)-H(40)	0.92(2)	C(2)-C(1)-H(1A)	108.1(15)
C(41)-H(41)	0.95(2)	Pt-C(1)-H(1A)	115.2(15)

C(2)-C(1)-H(1B)	109.9(15)
Pt-C(1)-H(1B)	109.6(15)
H(1A)-C(1)-H(1B)	103(2)
C(1)-C(2)-H(2A)	115.6(18)
C(1)-C(2)-H(2B)	109.6(16)
H(2A)-C(2)-H(2B)	104(2)
C(1)-C(2)-H(2C)	107.8(17)
H(2A)-C(2)-H(2C)	108(2)
H(2B)-C(2)-H(2C)	111(2)
N-C(3)-C(4)	129.1(2)
C(9)-C(4)-C(5)	119.8(2)
C(9)-C(4)-C(3)	124.3(2)
C(5)-C(4)-C(3)	115.9(2)
C(6)-C(5)-C(4)	121.3(2)
C(6)-C(5)-H(5)	120.0(15)
C(4)-C(5)-H(5)	118.5(15)
C(5)-C(6)-C(7)	119.2(2)
C(5)-C(6)-H(6)	121.1(18)
C(7)-C(6)-H(6)	119.7(18)
C(8)-C(7)-C(6)	122.5(2)
C(8)-C(7)-H(7)	116.7(17)
C(6)-C(7)-H(7)	120.8(17)
C(7)-C(8)-C(9)	119.6(2)
C(7)-C(8)-C(22)	119.9(2)
C(9)-C(8)-C(22)	120.4(2)
O-C(9)-C(4)	124.1(2)
O-C(9)-C(8)	118.3(2)
C(4)-C(9)-C(8)	117.6(2)
C(11)-C(10)-C(15)	122.4(3)
C(11)-C(10)-N	118.7(3)
C(15)-C(10)-N	118.9(3)
C(10)-C(11)-C(12)	115.8(5)
C(10)-C(11)-C(16)	123.4(3)
C(12)-C(11)-C(16)	120.8(4)
C(13)-C(12)-C(11)	123.2(5)
C(13)-C(12)-H(12)	132(2)
C(11)-C(12)-H(12)	105(3)
C(12)-C(13)-C(14)	119.6(4)
C(12)-C(13)-H(13)	119(2)
C(14)-C(13)-H(13)	121(2)
C(13)-C(14)-C(15)	122.4(5)
C(13)-C(14)-H(14)	125(2)
C(15)-C(14)-H(14)	112(2)
C(14)-C(15)-C(10)	116.5(4)
C(14)-C(15)-C(19)	121.6(4)
C(10)-C(15)-C(19)	121.8(3)
C(11)-C(16)-C(18)	113.9(4)
C(11)-C(16)-C(17)	113.5(4)
C(18)-C(16)-C(17)	108.1(4)
C(11)-C(16)-H(16)	110(2)
C(18)-C(16)-H(16)	103(2)
C(17)-C(16)-H(16)	108(2)
C(16)-C(17)-H(17A)	110(2)
C(16)-C(17)-H(17B)	108(2)
H(17A)-C(17)-H(17B)	106(3)
C(16)-C(17)-H(17C)	113(2)
H(17A)-C(17)-H(17C)	110(3)
H(17B)-C(17)-H(17C)	110(3)
C(16)-C(18)-H(18A)	112(2)
C(16)-C(18)-H(18B)	115(4)
H(18A)-C(18)-H(18B)	112(4)
C(16)-C(18)-H(18C)	106(3)
H(18A)-C(18)-H(18C)	98(3)
H(18B)-C(18)-H(18C)	112(4)
C(15)-C(19)-C(21)	114.9(4)
C(15)-C(19)-C(20)	111.2(4)
C(21)-C(19)-C(20)	109.4(4)
C(15)-C(19)-H(19)	108.0(19)
C(21)-C(19)-H(19)	106.3(19)
C(20)-C(19)-H(19)	106.7(19)
C(19)-C(20)-H(20A)	108(2)
C(19)-C(20)-H(20B)	106(2)
H(20A)-C(20)-H(20B)	112(3)
C(19)-C(20)-H(20C)	108(2)
H(20A)-C(20)-H(20C)	115(3)
H(20B)-C(20)-H(20C)	108(3)
C(19)-C(21)-H(21A)	112(2)
C(19)-C(21)-H(21B)	109(4)
H(21A)-C(21)-H(21B)	111(4)
C(19)-C(21)-H(21C)	109(3)
H(21A)-C(21)-H(21C)	100(3)
H(21B)-C(21)-H(21C)	116(5)
C(35)-C(22)-C(23)	119.5(2)
C(35)-C(22)-C(8)	119.6(2)
C(23)-C(22)-C(8)	120.7(2)
C(22)-C(23)-C(28)	120.3(2)
C(22)-C(23)-C(24)	122.1(2)
C(28)-C(23)-C(24)	117.6(2)
C(25)-C(24)-C(23)	121.8(3)
C(25)-C(24)-H(24)	121.4(18)
C(23)-C(24)-H(24)	116.8(17)
C(24)-C(25)-C(26)	120.3(3)
C(24)-C(25)-H(25)	119.5(16)
C(26)-C(25)-H(25)	120.0(16)
C(27)-C(26)-C(25)	120.2(3)
C(27)-C(26)-H(26)	121.1(17)
C(25)-C(26)-H(26)	118.7(17)
C(26)-C(27)-C(28)	120.9(3)
C(26)-C(27)-H(27)	120.7(17)
C(28)-C(27)-H(27)	118.3(17)
C(29)-C(28)-C(23)	119.4(2)
C(29)-C(28)-C(27)	121.5(2)
C(23)-C(28)-C(27)	119.1(2)
C(28)-C(29)-C(30)	121.8(2)
C(28)-C(29)-H(29)	119.1(17)
C(30)-C(29)-H(29)	119.1(17)
C(29)-C(30)-C(31)	122.2(2)
C(29)-C(30)-C(35)	119.5(2)

C(31)-C(30)-C(35)	118.2(2)	C(46)-C(45)-H(45)	115(3)
C(32)-C(31)-C(30)	121.5(3)	C(44)-C(45)-H(45)	125(3)
C(32)-C(31)-H(31)	122.2(19)	C(45)-C(46)-C(47)	120.6(4)
C(30)-C(31)-H(31)	116.3(19)	C(45)-C(46)-H(46)	123(2)
C(31)-C(32)-C(33)	120.5(3)	C(47)-C(46)-H(46)	117(3)
C(31)-C(32)-H(32)	117.2(17)	C(42)-C(47)-C(46)	120.2(3)
C(33)-C(32)-H(32)	122.2(17)	C(42)-C(47)-H(47)	118.1(17)
C(34)-C(33)-C(32)	120.4(3)	C(46)-C(47)-H(47)	121.6(18)
C(34)-C(33)-H(33)	116.5(16)	C(49)-C(48)-C(53)	118.9(2)
C(32)-C(33)-H(33)	123.0(16)	C(49)-C(48)-P	115.94(18)
C(33)-C(34)-C(35)	121.6(3)	C(53)-C(48)-P	124.8(2)
C(33)-C(34)-H(34)	118.5(16)	C(50)-C(49)-C(48)	120.6(2)
C(35)-C(34)-H(34)	120.0(16)	C(50)-C(49)-H(49)	118.0(14)
C(22)-C(35)-C(34)	122.7(2)	C(48)-C(49)-H(49)	121.3(14)
C(22)-C(35)-C(30)	119.5(2)	C(49)-C(50)-C(51)	119.8(3)
C(34)-C(35)-C(30)	117.8(2)	C(49)-C(50)-H(50)	121.2(15)
C(37)-C(36)-C(41)	118.9(2)	C(51)-C(50)-H(50)	118.9(15)
C(37)-C(36)-P	122.7(2)	C(52)-C(51)-C(50)	119.8(3)
C(41)-C(36)-P	117.78(19)	C(52)-C(51)-H(51)	120.7(17)
C(38)-C(37)-C(36)	120.5(3)	C(50)-C(51)-H(51)	119.5(17)
C(38)-C(37)-H(37)	116.8(18)	C(51)-C(52)-C(53)	120.4(2)
C(36)-C(37)-H(37)	122.6(18)	C(51)-C(52)-H(52)	116.9(15)
C(37)-C(38)-C(39)	119.9(3)	C(53)-C(52)-H(52)	122.8(15)
C(37)-C(38)-H(38)	120.6(17)	C(52)-C(53)-C(48)	120.4(3)
C(39)-C(38)-H(38)	119.5(17)	C(52)-C(53)-H(53)	119.7(18)
C(40)-C(39)-C(38)	120.1(3)	C(48)-C(53)-H(53)	119.8(18)
C(40)-C(39)-H(39)	122.5(18)	C(66)-C(61)-C(62)	119.9(4)
C(38)-C(39)-H(39)	117.4(18)	C(66)-C(61)-H(61)	120.3(19)
C(41)-C(40)-C(39)	120.3(3)	C(62)-C(61)-H(61)	120(2)
C(41)-C(40)-H(40)	119.7(15)	C(63)-C(62)-C(61)	119.7(4)
C(39)-C(40)-H(40)	120.0(15)	C(63)-C(62)-H(62)	120.3(18)
C(40)-C(41)-C(36)	120.2(3)	C(61)-C(62)-H(62)	119.9(18)
C(40)-C(41)-H(41)	120.2(15)	C(64)-C(63)-C(62)	120.3(3)
C(36)-C(41)-H(41)	119.5(14)	C(64)-C(63)-H(63)	120.5(19)
C(47)-C(42)-C(43)	118.6(3)	C(62)-C(63)-H(63)	119.1(19)
C(47)-C(42)-P	120.8(2)	C(63)-C(64)-C(65)	120.0(4)
C(43)-C(42)-P	120.2(2)	C(63)-C(64)-H(64)	124(2)
C(44)-C(43)-C(42)	120.4(3)	C(65)-C(64)-H(64)	116(2)
C(44)-C(43)-H(43)	120.0(18)	C(66)-C(65)-C(64)	120.1(4)
C(42)-C(43)-H(43)	119.6(18)	C(66)-C(65)-H(65)	120(2)
C(45)-C(44)-C(43)	119.7(3)	C(64)-C(65)-H(65)	120(2)
C(45)-C(44)-H(44)	120(2)	C(65)-C(66)-C(61)	120.0(3)
C(43)-C(44)-H(44)	120(2)	C(65)-C(66)-H(66)	120.6(18)
C(46)-C(45)-C(44)	120.4(3)	C(61)-C(66)-H(66)	119.2(17)

Table 5. Anisotropic displacement parameters ($Å^2 x\ 10^4$) for TRY14 (CCDC 160843). The anisotropic displacement factor exponent takes the form: $-2\pi^2$ [$h^2 a^{*2}U^{11}$ + ... + 2 h k a* b* U^{12}]

	U^{11}	U^{22}	U^{33}	U^{23}	U^{13}	U^{12}
Pt	240(1)	135(1)	149(1)	-13(1)	-61(1)	-68(1)
P	194(4)	133(3)	178(3)	-38(3)	-39(3)	-30(3)
O	209(9)	119(8)	160(9)	-37(7)	-1(7)	-50(7)
N	373(14)	205(11)	145(11)	13(9)	-75(10)	-175(11)
C(1)	387(18)	147(13)	176(14)	14(11)	-105(13)	-102(12)
C(2)	450(20)	295(17)	202(15)	17(13)	-83(14)	-216(15)
C(3)	313(16)	255(14)	201(14)	-36(11)	-22(12)	-173(13)
C(4)	202(14)	229(13)	170(13)	-65(10)	-15(10)	-117(11)
C(5)	261(15)	285(15)	180(14)	-91(11)	19(12)	-148(12)
C(6)	270(16)	214(14)	283(16)	-158(12)	9(12)	-55(12)
C(7)	221(15)	160(13)	253(15)	-41(11)	-52(12)	-45(11)
C(8)	122(12)	184(12)	196(13)	-40(10)	-16(10)	-55(10)
C(9)	125(12)	196(13)	181(13)	-42(10)	-19(10)	-81(10)
C(10)	830(30)	298(16)	148(14)	14(12)	-150(16)	-375(18)
C(11)	1020(30)	540(20)	164(16)	-65(15)	-39(18)	-590(20)
C(12)	1700(60)	860(40)	179(19)	-80(20)	30(30)	-1070(40)
C(13)	2520(80)	590(30)	220(20)	210(20)	-510(40)	-1050(50)
C(14)	1700(50)	310(20)	400(20)	172(18)	-660(30)	-500(30)
C(15)	1030(30)	255(16)	297(18)	69(13)	-380(20)	-330(20)
C(16)	920(30)	860(30)	194(17)	-192(18)	211(19)	-740(30)
C(17)	960(40)	890(40)	330(20)	-270(20)	210(20)	-710(40)
C(18)	1130(50)	1320(50)	500(30)	-530(30)	450(30)	-1050(50)
C(19)	810(30)	242(17)	470(20)	27(15)	-510(20)	-73(18)
C(20)	810(40)	400(20)	740(30)	-80(20)	-510(30)	-140(20)
C(21)	1170(50)	290(20)	920(40)	-40(20)	-820(50)	30(30)
C(22)	183(13)	91(11)	198(13)	-29(10)	-28(10)	-10(10)
C(23)	175(13)	96(11)	245(14)	-53(10)	-28(11)	-11(10)
C(24)	213(15)	151(13)	228(15)	-39(11)	-36(12)	-27(11)
C(25)	190(15)	149(13)	411(18)	-68(12)	-67(13)	-38(12)
C(26)	253(16)	211(14)	367(17)	-94(12)	-152(13)	-37(12)
C(27)	321(17)	186(14)	242(15)	-56(11)	-104(13)	-27(12)
C(28)	226(14)	131(12)	231(14)	-43(10)	-50(11)	-25(11)
C(29)	298(16)	181(13)	148(14)	-27(11)	-28(12)	-30(12)
C(30)	213(14)	121(12)	219(14)	-37(10)	-1(11)	-21(11)
C(31)	288(16)	203(14)	213(15)	-5(11)	13(13)	-61(12)
C(32)	243(16)	212(14)	340(17)	-27(12)	47(13)	-112(13)
C(33)	211(15)	205(14)	334(16)	-76(12)	-33(13)	-61(12)
C(34)	224(15)	153(13)	215(15)	-32(11)	-32(12)	-45(11)
C(35)	167(13)	96(11)	214(13)	-18(10)	-22(11)	4(10)
C(36)	208(14)	157(12)	178(13)	-70(10)	0(11)	-19(11)
C(37)	299(16)	225(14)	227(15)	-75(11)	-30(12)	-91(13)
C(38)	377(18)	277(15)	176(15)	-41(12)	-21(13)	-77(14)
C(39)	308(17)	180(14)	265(16)	-12(12)	76(13)	-67(13)
C(40)	201(15)	212(14)	320(16)	-87(12)	21(12)	-65(12)
C(41)	195(14)	203(13)	214(14)	-66(11)	-19(11)	-25(11)
C(42)	187(14)	155(13)	368(16)	-96(12)	-39(12)	-41(11)
C(43)	232(16)	251(15)	460(20)	-188(14)	27(14)	-100(13)

C(44)	257(18)	325(18)	760(30)	-339(19)	172(18)	-164(15)
C(45)	177(17)	181(16)	1060(40)	-230(19)	10(20)	-20(14)
C(46)	292(19)	223(17)	820(30)	5(18)	-190(20)	-18(14)
C(47)	295(18)	191(15)	500(20)	-38(14)	-93(16)	-22(13)
C(48)	223(14)	182(13)	132(12)	-29(10)	-22(10)	-67(11)
C(49)	271(15)	150(13)	171(13)	-37(10)	-46(11)	-54(11)
C(50)	227(15)	217(14)	236(15)	-11(11)	-70(12)	-43(12)
C(51)	304(17)	274(15)	207(14)	-19(11)	-73(12)	-153(13)
C(52)	355(17)	218(14)	200(14)	-56(11)	-17(12)	-135(13)
C(53)	237(16)	186(14)	200(14)	-58(11)	-5(12)	-39(12)
C(61)	310(19)	510(20)	284(18)	22(15)	-40(14)	-117(17)
C(62)	370(20)	420(20)	267(17)	56(14)	20(14)	-80(16)
C(63)	268(19)	510(20)	450(20)	68(17)	83(16)	-102(18)
C(64)	360(20)	540(20)	500(20)	-21(18)	60(17)	-231(19)
C(65)	430(20)	480(20)	400(20)	-57(17)	68(16)	-171(19)
C(66)	249(18)	520(20)	243(16)	9(15)	4(14)	-59(16)

Table 6. Hydrogen coordinates (x 10^4) and isotropic displacement parameters (Å^{2}x 10^3) for TRY14 (CCDC 160843).

	x	y	z	U_{iso}
H(1A)	6150(30)	6130(20)	2834(12)	17(7)
H(1B)	6140(30)	6230(20)	3482(12)	22(7)
H(2A)	3560(30)	7220(20)	2873(13)	28(8)
H(2B)	3580(30)	7300(20)	3521(13)	29(8)
H(2C)	4010(30)	6000(30)	3323(12)	31(8)
H(5)	4350(20)	11800(20)	4138(11)	11(6)
H(6)	3780(30)	13710(20)	3535(12)	21(7)
H(7)	4130(30)	14050(30)	2478(12)	26(8)
H(12)	3650(30)	6900(30)	5368(15)	27(10)
H(13)	5740(40)	5170(30)	5629(17)	62(11)
H(14)	7840(30)	5180(30)	4965(15)	34(10)
H(16)	2920(30)	9130(30)	4163(15)	39(9)
H(17A)	1590(40)	10300(40)	4874(18)	64(15)
H(17B)	2340(40)	9250(30)	5407(19)	73(12)
H(17C)	3170(40)	10020(30)	4935(15)	46(10)
H(18A)	1880(40)	7590(30)	4409(18)	72(12)
H(18B)	710(60)	8930(50)	4490(30)	140(30)
H(18C)	1550(50)	7830(40)	5050(20)	90(15)
H(19)	8130(30)	7070(30)	3619(13)	28(8)
H(20A)	8400(40)	8270(30)	4183(15)	52(10)
H(20B)	9320(40)	7020(30)	4621(18)	64(12)
H(20C)	10030(50)	7360(40)	3939(19)	84(16)
H(21A)	9040(40)	4890(40)	3866(18)	75(13)
H(21B)	10160(50)	5500(50)	3680(20)	100(20)
H(21C)	9740(50)	5010(40)	4340(20)	80(14)
H(24)	3000(30)	11690(20)	2068(12)	14(7)
H(25)	1340(30)	11520(20)	1560(12)	20(7)
H(26)	1520(30)	12130(20)	497(12)	17(7)

H(27)	3250(30)	12940(30)	-49(14)	36(8)
H(29)	5280(30)	13560(20)	31(12)	15(7)
H(31)	7370(30)	14160(20)	22(13)	27(8)
H(32)	9020(30)	14320(20)	514(12)	25(7)
H(33)	9040(30)	13570(20)	1627(12)	28(8)
H(34)	7270(30)	12910(20)	2122(12)	13(6)
H(37)	5810(30)	9220(20)	576(13)	30(8)
H(38)	6710(30)	10430(20)	-205(13)	26(8)
H(39)	8340(30)	11170(20)	-36(13)	28(8)
H(40)	9080(30)	10740(20)	954(11)	12(6)
H(41)	8220(30)	9480(20)	1768(12)	13(6)
H(43)	8340(30)	6900(20)	881(12)	21(8)
H(44)	10660(40)	5500(30)	720(16)	57(11)
H(45)	11810(40)	4440(30)	1629(16)	55(11)
H(46)	10840(40)	4760(30)	2533(16)	52(11)
H(47)	8600(30)	6190(20)	2686(13)	29(8)
H(49)	3560(30)	9390(20)	1677(11)	14(6)
H(50)	1550(30)	9070(20)	1446(12)	25(7)
H(51)	1880(30)	7170(20)	1270(12)	26(8)
H(52)	4080(30)	5590(20)	1283(11)	21(7)
H(53)	6020(30)	6020(20)	1494(11)	16(7)
H(61)	-1550(30)	80(20)	3007(13)	23(8)
H(62)	900(30)	-1000(30)	2781(14)	44(9)
H(63)	2500(30)	-130(30)	2942(13)	36(9)
H(64)	1610(30)	1670(30)	3323(14)	39(10)
H(65)	-760(30)	2610(30)	3470(14)	35(9)
H(66)	-2400(30)	1880(20)	3300(12)	22(7)

Appendix N

X-Ray Diffraction Analysis of

$(^{NO_2,NO_2}Sal)_2Ni \cdot 2\,B(C_6F_5)_3$

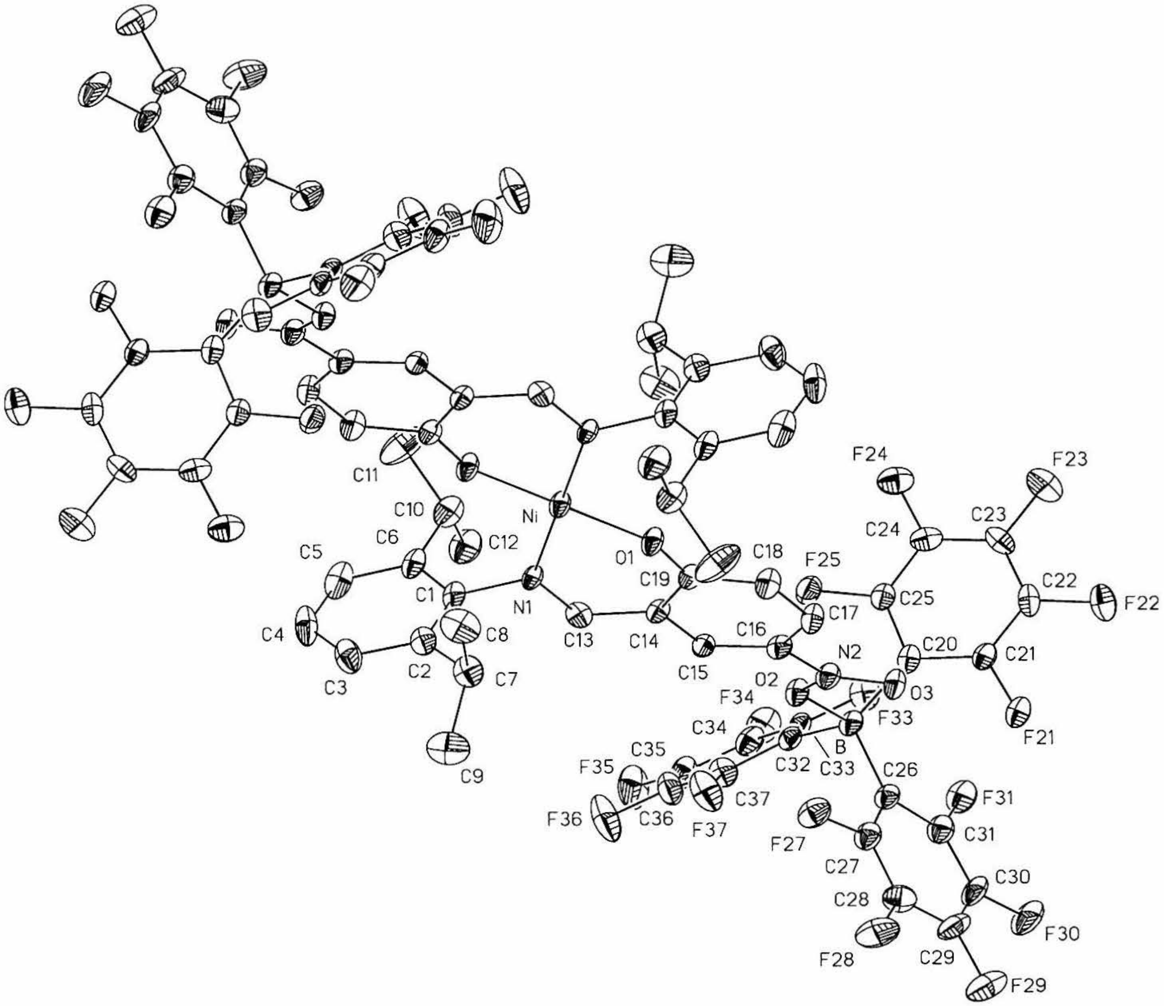

Table 1. Crystal data and structure refinement for TRY2 (CCDC No. 140826)

Empirical formula	$C_{74}H_{42}B_2F_{30}N_4NiO_8$ $2H_2O$ C_7H_{16}
Formula weight	1865.64
Crystallization Solvent	CH_2Cl_2/Heptane
Crystal Habit	Plates
Crystal size	0.33 x 0.15 x 0.07 mm^3
Crystal color	Dark red

Data Collection

Preliminary Photos	Rotation	
Type of diffractometer	CCD area detector	
Wavelength	0.71073 Å MoKα	
Data Collection Temperature	95 K	
θ range for reflections used in lattice determination	2.27 to 24.71°	
Unit cell dimensions	a = 16.2240(13)Å b = 17.8530(15)Å c = 15.4684(13)Å	 β= 104.095(2)°
Volume	4345.5(6) $Å^3$	
Z	2	
Crystal system	Monoclinic	
Space group	$P2_1/c$	
Density (calculated)	1.426 Mg/m^3	
F(000)	1888	
Data collection program	Bruker SMART	
θ range for data collection	1.77 to 28.49°	
Completeness to θ = 28.49°	93.2 %	
Index ranges	$-21 \leq h \leq 21$, $-23 \leq k \leq 22$, $-20 \leq l \leq 20$	
Data collection scan type	ω scans at 3 ϕ settings	
Data reduction program	Bruker SAINT v6.2	
Reflections collected	50756	
Independent reflections	10262 [R_{int}= 0.0815]	
Absorption coefficient	0.342 mm^{-1}	
Absorption correction	None	

Table 1 (cont.)

Structure Solution and Refinement

Structure solution program	SHELXS-97 (Sheldrick, 1990)
Primary solution method	Direct methods
Secondary solution method	Difference Fourier map
Hydrogen placement	Geometric positions
Structure refinement program	SHELXL-97 (Sheldrick, 1997)
Refinement method	Full matrix least-squares on F^2
Data / restraints / parameters	10262 / 15 / 560
Treatment of hydrogen atoms	Riding
Goodness-of-fit on F^2	2.355
Final R indices [$I>2\sigma(I)$, 5984 reflections]	R1 = 0.0625, *w*R2 = 0.1368
R indices (all data)	R1 = 0.1109, *w*R2 = 0.1399
Type of weighting scheme used	Sigma
Weighting scheme used	$w=1/\sigma^2(\mathrm{Fo}^2)$
Max shift/error	0.003
Average shift/error	0.000
Extinction coefficient	0.0024(2)
Largest diff. peak and hole	1.293 and -0.770 e.Å^{-3}

Special Refinement Details

The unit cell contains disordered heptane which has an adverse effect on the overall refinement. The heptane model was restrained to known distances and angles and to near planarity. It occupies channels that run throughout the crystal lattice along the *c*-axis at both *a* and *b*=¼ & ¾. The occupancy in these channels is approximately 45% and since the length of the *c*-axis is too short to accommodate two repeats of the heptane molecule the ends of the disordered solvents appear to overlap. This can be seen clearly in Figures 2 and 3. There also appears to be two molecules of water co-crystallized with each organometallic molecule.

Refinement of F^2 against ALL reflections. The weighted R-factor (*w*R) and goodness of fit (S) are based on F^2, conventional R-factors (R) are based on F, with F set to zero for negative F^2. The threshold expression of $F^2 > 2\sigma(F^2)$ is used only for calculating R-factors(gt) etc. and is not relevant to the choice of reflections for refinement. R-factors based on F^2 are statistically about twice as large as those based on F, and R-factors based on ALL data will be even larger.

All esds (except the esd in the dihedral angle between two l.s. planes) are estimated using the full covariance matrix. The cell esds are taken into account individually in the estimation of esds in distances, angles and torsion angles; correlations between esds in cell parameters are only used when they are defined by crystal symmetry. An approximate (isotropic) treatment of cell esds is used for estimating esds involving l.s. planes.

Table 2. Atomic coordinates (x 10^4) and equivalent isotropic displacement parameters (Å^{2}x 10^3) for TRY2 (CCDC No. 140826). U(eq) is defined as the trace of the orthogonalized U^{ij} tensor.

	x	y	z	U_{eq}
Ni	0	5000	5000	20(1)
F(21)	2542(2)	6436(1)	-366(2)	29(1)
F(22)	1214(2)	6855(1)	-1636(2)	38(1)
F(23)	-209(2)	6002(1)	-2057(2)	40(1)
F(24)	-270(2)	4689(1)	-1171(2)	36(1)
F(25)	1048(2)	4256(1)	105(2)	30(1)
F(27)	3751(2)	5645(1)	2436(1)	33(1)
F(28)	5214(2)	6319(2)	2587(2)	46(1)
F(29)	5878(2)	6518(2)	1150(2)	50(1)
F(30)	5044(2)	5959(1)	-459(2)	43(1)
F(31)	3565(2)	5233(1)	-627(2)	32(1)
F(33)	2308(2)	3957(1)	-889(2)	31(1)
F(34)	2687(2)	2511(1)	-869(2)	38(1)
F(35)	3429(2)	1811(1)	674(2)	51(1)
F(36)	3803(2)	2608(1)	2229(2)	56(1)
F(37)	3481(2)	4058(1)	2228(2)	43(1)
O(1)	455(2)	5778(1)	4501(2)	23(1)
O(2)	2289(2)	5023(2)	1571(2)	22(1)
O(3)	2196(2)	6250(1)	1421(2)	25(1)
N(1)	882(2)	4342(2)	4883(2)	18(1)
N(2)	2096(2)	5685(2)	1822(2)	23(1)
B	2666(3)	4981(3)	705(3)	20(1)
C(1)	1096(3)	3702(2)	5486(3)	21(1)
C(2)	1644(3)	3833(2)	6314(3)	26(1)
C(3)	1822(3)	3229(3)	6895(3)	34(1)
C(4)	1452(3)	2535(3)	6656(3)	39(1)
C(5)	906(3)	2435(2)	5833(3)	34(1)
C(6)	706(3)	3020(2)	5227(3)	23(1)
C(7)	2014(3)	4600(2)	6593(3)	30(1)
C(8)	1466(3)	5022(3)	7111(3)	41(1)
C(9)	2944(3)	4567(3)	7137(3)	48(1)
C(10)	80(3)	2913(2)	4338(3)	31(1)
C(11)	-720(3)	2502(3)	4408(3)	52(2)
C(12)	501(3)	2521(2)	3669(3)	37(1)
C(13)	1338(3)	4423(2)	4305(2)	21(1)
C(14)	1296(2)	5063(2)	3732(2)	19(1)
C(15)	1717(2)	5053(2)	3054(2)	19(1)
C(16)	1739(3)	5695(2)	2566(2)	21(1)
C(17)	1395(3)	6376(2)	2764(3)	26(1)
C(18)	969(3)	6386(2)	3421(3)	26(1)

C(19)	881(3)	5729(2)	3907(3)	22(1)
C(20)	1890(3)	5294(2)	-88(2)	20(1)
C(21)	1866(3)	5966(2)	-552(3)	21(1)
C(22)	1182(3)	6197(2)	-1195(3)	26(1)
C(23)	457(3)	5773(2)	-1416(3)	26(1)
C(24)	436(3)	5123(2)	-973(3)	25(1)
C(25)	1133(3)	4908(2)	-324(3)	22(1)
C(26)	3561(3)	5428(2)	879(3)	22(1)
C(27)	4035(3)	5708(2)	1681(3)	27(1)
C(28)	4799(3)	6067(2)	1790(3)	31(1)
C(29)	5146(3)	6160(2)	1074(3)	36(1)
C(30)	4712(3)	5878(2)	251(3)	30(1)
C(31)	3958(3)	5519(2)	185(3)	27(1)
C(32)	2847(3)	4084(2)	674(3)	21(1)
C(33)	2682(3)	3647(2)	-81(3)	23(1)
C(34)	2875(3)	2904(2)	-102(3)	27(1)
C(35)	3256(3)	2546(2)	681(3)	33(1)
C(36)	3448(3)	2945(3)	1457(3)	35(1)
C(37)	3255(3)	3695(2)	1431(3)	29(1)
O(10)	3915(7)	4526(6)	4459(7)	297(5)
C(101)	7029(3)	3604(4)	4832(5)	90
C(102)	6368(3)	3468(5)	3946(5)	90
C(103)	6793(2)	3043(4)	3303(5)	90
C(104)	6137(2)	2924(4)	2410(5)	90
C(105)	6570(2)	2524(4)	1756(5)	90
C(106)	5885(3)	2264(8)	936(6)	90
C(107)	6320(4)	1890(8)	266(6)	90

Table 3. Bond lengths [Å] and angles [°] for TRY2 (CCDC No. 140826).

Ni-O(1)	1.830(2)	F(37)-C(37)	1.360(5)
Ni-O(1)#1	1.830(2)	O(1)-C(19)	1.279(4)
Ni-N(1)#1	1.894(3)	O(2)-N(2)	1.306(4)
Ni-N(1)	1.894(3)	O(2)-B	1.605(5)
F(21)-C(21)	1.355(4)	O(3)-N(2)	1.216(4)
F(22)-C(22)	1.366(4)	N(1)-C(13)	1.300(4)
F(23)-C(23)	1.341(5)	N(1)-C(1)	1.462(5)
F(24)-C(24)	1.355(4)	N(2)-C(16)	1.409(5)
F(25)-C(25)	1.364(4)	B-C(26)	1.621(6)
F(27)-C(27)	1.361(4)	B-C(20)	1.627(6)
F(28)-C(28)	1.331(5)	B-C(32)	1.630(6)
F(29)-C(29)	1.328(5)	C(1)-C(6)	1.384(5)
F(30)-C(30)	1.344(4)	C(1)-C(2)	1.391(5)
F(31)-C(31)	1.363(4)	C(2)-C(3)	1.389(5)
F(33)-C(33)	1.366(4)	C(2)-C(7)	1.513(6)
F(34)-C(34)	1.348(4)	C(3)-C(4)	1.387(6)
F(35)-C(35)	1.343(4)	C(3)-H(3)	0.9300
F(36)-C(36)	1.337(5)	C(4)-C(5)	1.375(6)

C(4)-H(4)	0.9300
C(5)-C(6)	1.388(5)
C(5)-H(5)	0.9300
C(6)-C(10)	1.511(6)
C(7)-C(8)	1.532(5)
C(7)-C(9)	1.539(6)
C(7)-H(7)	0.9800
C(8)-H(8A)	0.9600
C(8)-H(8B)	0.9600
C(8)-H(8C)	0.9600
C(9)-H(9A)	0.9600
C(9)-H(9B)	0.9600
C(9)-H(9C)	0.9600
C(10)-C(11)	1.517(6)
C(10)-C(12)	1.540(5)
C(10)-H(10)	0.9800
C(11)-H(11A)	0.9600
C(11)-H(11B)	0.9600
C(11)-H(11C)	0.9600
C(12)-H(12A)	0.9600
C(12)-H(12B)	0.9600
C(12)-H(12C)	0.9600
C(13)-C(14)	1.438(5)
C(13)-H(13)	0.9300
C(14)-C(15)	1.383(5)
C(14)-C(19)	1.424(5)
C(15)-C(16)	1.378(5)
C(15)-H(15)	0.9300
C(16)-C(17)	1.401(5)
C(17)-C(18)	1.361(5)
C(17)-H(17)	0.9300
C(18)-C(19)	1.420(5)
C(18)-H(18)	0.9300
C(20)-C(25)	1.378(5)
C(20)-C(21)	1.394(5)
C(21)-C(22)	1.361(6)
C(22)-C(23)	1.370(6)
C(23)-C(24)	1.351(5)
C(24)-C(25)	1.371(6)
C(26)-C(27)	1.385(6)
C(26)-C(31)	1.389(5)
C(27)-C(28)	1.369(6)
C(28)-C(29)	1.369(6)
C(29)-C(30)	1.389(6)
C(30)-C(31)	1.363(6)
C(32)-C(33)	1.377(5)
C(32)-C(37)	1.384(5)
C(33)-C(34)	1.364(5)
C(34)-C(35)	1.377(6)
C(35)-C(36)	1.364(6)
C(36)-C(37)	1.374(6)
C(101)-C(102)	1.54000(14)
C(101)-H(10A)	0.9600
C(101)-H(10B)	0.9600
C(101)-H(10C)	0.9600
C(102)-C(103)	1.53999(13)
C(102)-H(10G)	0.9700
C(102)-H(10H)	0.9700
C(103)-C(104)	1.54000(14)
C(103)-H(10I)	0.9700
C(103)-H(10J)	0.9700
C(104)-C(105)	1.53999(13)
C(104)-H(10K)	0.9700
C(104)-H(10L)	0.9700
C(105)-C(106)	1.53999(13)
C(105)-H(10M)	0.9700
C(105)-H(10N)	0.9700
C(106)-C(107)	1.54000(14)
C(106)-H(10O)	0.9700
C(106)-H(10P)	0.9700
C(107)-H(10D)	0.9600
C(107)-H(10E)	0.9600
C(107)-H(10F)	0.9600

O(1)-Ni-O(1)#1	180.00(10)
O(1)-Ni-N(1)#1	87.75(12)
O(1)#1-Ni-N(1)#1	92.25(12)
O(1)-Ni-N(1)	92.25(12)
O(1)#1-Ni-N(1)	87.75(12)
N(1)#1-Ni-N(1)	180.00(18)
C(19)-O(1)-Ni	126.4(2)
N(2)-O(2)-B	117.3(3)
C(13)-N(1)-C(1)	116.1(3)
C(13)-N(1)-Ni	124.5(3)
C(1)-N(1)-Ni	119.4(2)
O(3)-N(2)-O(2)	121.9(3)
O(3)-N(2)-C(16)	122.6(3)
O(2)-N(2)-C(16)	115.5(3)
O(2)-B-C(26)	110.3(3)
O(2)-B-C(20)	103.3(3)
C(26)-B-C(20)	117.0(3)
O(2)-B-C(32)	100.2(3)
C(26)-B-C(32)	109.2(3)
C(20)-B-C(32)	115.2(3)
C(6)-C(1)-C(2)	124.0(4)
C(6)-C(1)-N(1)	118.8(4)
C(2)-C(1)-N(1)	117.1(3)
C(3)-C(2)-C(1)	116.8(4)
C(3)-C(2)-C(7)	120.8(4)
C(1)-C(2)-C(7)	122.4(4)
C(4)-C(3)-C(2)	120.9(4)
C(4)-C(3)-H(3)	119.6
C(2)-C(3)-H(3)	119.6
C(5)-C(4)-C(3)	120.2(4)
C(5)-C(4)-H(4)	119.9
C(3)-C(4)-H(4)	119.9
C(4)-C(5)-C(6)	121.3(4)
C(4)-C(5)-H(5)	119.3

C(6)-C(5)-H(5)	119.3
C(1)-C(6)-C(5)	116.8(4)
C(1)-C(6)-C(10)	122.2(4)
C(5)-C(6)-C(10)	120.9(4)
C(2)-C(7)-C(8)	110.8(4)
C(2)-C(7)-C(9)	112.9(4)
C(8)-C(7)-C(9)	110.4(4)
C(2)-C(7)-H(7)	107.5
C(8)-C(7)-H(7)	107.5
C(9)-C(7)-H(7)	107.5
C(7)-C(8)-H(8A)	109.5
C(7)-C(8)-H(8B)	109.5
H(8A)-C(8)-H(8B)	109.5
C(7)-C(8)-H(8C)	109.5
H(8A)-C(8)-H(8C)	109.5
H(8B)-C(8)-H(8C)	109.5
C(7)-C(9)-H(9A)	109.5
C(7)-C(9)-H(9B)	109.5
H(9A)-C(9)-H(9B)	109.5
C(7)-C(9)-H(9C)	109.5
H(9A)-C(9)-H(9C)	109.5
H(9B)-C(9)-H(9C)	109.5
C(6)-C(10)-C(11)	113.2(4)
C(6)-C(10)-C(12)	111.1(4)
C(11)-C(10)-C(12)	110.8(4)
C(6)-C(10)-H(10)	107.2
C(11)-C(10)-H(10)	107.2
C(12)-C(10)-H(10)	107.2
C(10)-C(11)-H(11A)	109.5
C(10)-C(11)-H(11B)	109.5
H(11A)-C(11)-H(11B)	109.5
C(10)-C(11)-H(11C)	109.5
H(11A)-C(11)-H(11C)	109.5
H(11B)-C(11)-H(11C)	109.5
C(10)-C(12)-H(12A)	109.5
C(10)-C(12)-H(12B)	109.5
H(12A)-C(12)-H(12B)	109.5
C(10)-C(12)-H(12C)	109.5
H(12A)-C(12)-H(12C)	109.5
H(12B)-C(12)-H(12C)	109.5
N(1)-C(13)-C(14)	124.4(4)
N(1)-C(13)-H(13)	117.8
C(14)-C(13)-H(13)	117.8
C(15)-C(14)-C(19)	119.9(3)
C(15)-C(14)-C(13)	120.0(4)
C(19)-C(14)-C(13)	119.9(3)
C(16)-C(15)-C(14)	119.2(4)
C(16)-C(15)-H(15)	120.4
C(14)-C(15)-H(15)	120.4
C(15)-C(16)-C(17)	122.5(3)
C(15)-C(16)-N(2)	120.5(3)
C(17)-C(16)-N(2)	117.1(3)
C(18)-C(17)-C(16)	118.4(4)
C(18)-C(17)-H(17)	120.8
C(16)-C(17)-H(17)	120.8
C(17)-C(18)-C(19)	121.3(4)
C(17)-C(18)-H(18)	119.3
C(19)-C(18)-H(18)	119.3
O(1)-C(19)-C(18)	117.7(4)
O(1)-C(19)-C(14)	123.9(3)
C(18)-C(19)-C(14)	118.4(3)
C(25)-C(20)-C(21)	112.4(4)
C(25)-C(20)-B	120.3(3)
C(21)-C(20)-B	127.1(4)
F(21)-C(21)-C(22)	116.2(4)
F(21)-C(21)-C(20)	120.2(4)
C(22)-C(21)-C(20)	123.5(4)
C(21)-C(22)-F(22)	120.1(4)
C(21)-C(22)-C(23)	120.8(4)
F(22)-C(22)-C(23)	119.1(4)
F(23)-C(23)-C(24)	121.4(4)
F(23)-C(23)-C(22)	120.2(4)
C(24)-C(23)-C(22)	118.3(4)
C(23)-C(24)-F(24)	120.1(4)
C(23)-C(24)-C(25)	119.5(4)
F(24)-C(24)-C(25)	120.4(4)
F(25)-C(25)-C(24)	115.6(4)
F(25)-C(25)-C(20)	119.1(4)
C(24)-C(25)-C(20)	125.3(4)
C(27)-C(26)-C(31)	112.9(4)
C(27)-C(26)-B	127.3(3)
C(31)-C(26)-B	119.6(4)
F(27)-C(27)-C(28)	114.8(4)
F(27)-C(27)-C(26)	120.6(4)
C(28)-C(27)-C(26)	124.6(4)
F(28)-C(28)-C(27)	120.7(4)
F(28)-C(28)-C(29)	119.6(4)
C(27)-C(28)-C(29)	119.7(4)
F(29)-C(29)-C(28)	121.4(5)
F(29)-C(29)-C(30)	119.9(4)
C(28)-C(29)-C(30)	118.8(4)
F(30)-C(30)-C(31)	121.4(4)
F(30)-C(30)-C(29)	119.7(4)
C(31)-C(30)-C(29)	118.9(4)
C(30)-C(31)-F(31)	117.1(4)
C(30)-C(31)-C(26)	125.0(4)
F(31)-C(31)-C(26)	117.9(4)
C(33)-C(32)-C(37)	112.8(4)
C(33)-C(32)-B	125.7(4)
C(37)-C(32)-B	121.4(4)
C(34)-C(33)-F(33)	115.2(4)
C(34)-C(33)-C(32)	125.0(4)
F(33)-C(33)-C(32)	119.8(4)
F(34)-C(34)-C(33)	121.5(4)
F(34)-C(34)-C(35)	119.3(4)
C(33)-C(34)-C(35)	119.1(4)
F(35)-C(35)-C(36)	121.0(4)
F(35)-C(35)-C(34)	119.7(4)

C(36)-C(35)-C(34)	119.3(4)
F(36)-C(36)-C(35)	120.5(4)
F(36)-C(36)-C(37)	120.7(4)
C(35)-C(36)-C(37)	118.8(4)
F(37)-C(37)-C(36)	115.4(4)
F(37)-C(37)-C(32)	119.7(4)
C(36)-C(37)-C(32)	124.9(4)
C(102)-C(101)-H(10A)	109.5
C(102)-C(101)-H(10B)	109.5
H(10A)-C(101)-H(10B)	109.5
C(102)-C(101)-H(10C)	109.5
H(10A)-C(101)-H(10C)	109.5
H(10B)-C(101)-H(10C)	109.5
C(103)-C(102)-C(101)	109.162(12)
C(103)-C(102)-H(10G)	109.8
C(101)-C(102)-H(10G)	109.8
C(103)-C(102)-H(10H)	109.8
C(101)-C(102)-H(10H)	109.8
H(10G)-C(102)-H(10H)	108.3
C(102)-C(103)-C(104)	109.163(12)
C(102)-C(103)-H(10I)	109.8
C(104)-C(103)-H(10I)	109.8
C(102)-C(103)-H(10J)	109.8
C(104)-C(103)-H(10J)	109.8
H(10I)-C(103)-H(10J)	108.3
C(103)-C(104)-C(105)	109.162(12)
C(103)-C(104)-H(10K)	109.8
C(105)-C(104)-H(10K)	109.8
C(103)-C(104)-H(10L)	109.8
C(105)-C(104)-H(10L)	109.8
H(10K)-C(104)-H(10L)	108.3
C(104)-C(105)-C(106)	109.163(12)
C(104)-C(105)-H(10M)	109.8
C(106)-C(105)-H(10M)	109.8
C(104)-C(105)-H(10N)	109.8
C(106)-C(105)-H(10N)	109.8
H(10M)-C(105)-H(10N)	108.3
C(105)-C(106)-C(107)	109.162(12)
C(105)-C(106)-H(10O)	109.8
C(107)-C(106)-H(10O)	109.8
C(105)-C(106)-H(10P)	109.8
C(107)-C(106)-H(10P)	109.8
H(10O)-C(106)-H(10P)	108.3
C(106)-C(107)-H(10D)	109.5
C(106)-C(107)-H(10E)	109.5
H(10D)-C(107)-H(10E)	109.5
C(106)-C(107)-H(10F)	109.5
H(10D)-C(107)-H(10F)	109.5
H(10E)-C(107)-H(10F)	109.5

Symmetry transformations used to generate equivalent atoms:
#1 -x,-y+1,-z+1

Table 4. Anisotropic displacement parameters (Å^{2}x 10^4) for TRY2 (CCDC No. 140826). The anisotropic displacement factor exponent takes the form: $-2\pi^2$ [$h^2 a^{*2}U^{11}$ + ... + 2 h k a* b* U^{12}]

	U^{11}	U^{22}	U^{33}	U^{23}	U^{13}	U^{12}
Ni	270(5)	170(4)	205(4)	13(3)	140(3)	13(4)
F(21)	358(16)	220(13)	326(14)	31(11)	127(12)	-55(12)
F(22)	522(18)	241(14)	373(15)	87(12)	89(13)	57(13)
F(23)	414(18)	380(16)	338(15)	-26(12)	-24(13)	90(13)
F(24)	280(16)	377(15)	418(16)	-64(12)	64(13)	-41(13)
F(25)	312(16)	240(14)	364(15)	57(11)	133(12)	-23(11)
F(27)	336(16)	423(16)	255(14)	-48(11)	147(12)	-57(13)
F(28)	339(18)	554(18)	487(18)	-165(14)	111(14)	-139(14)
F(29)	347(18)	528(19)	670(20)	-33(15)	212(15)	-152(15)
F(30)	455(18)	466(17)	499(17)	46(13)	355(15)	-36(14)
F(31)	403(17)	335(15)	282(14)	-38(11)	189(13)	-8(12)
F(33)	427(17)	288(14)	251(14)	-36(11)	132(12)	42(12)
F(34)	499(19)	252(14)	447(16)	-87(12)	218(14)	-10(13)
F(35)	750(20)	226(15)	636(19)	100(13)	341(17)	173(14)
F(36)	830(20)	412(17)	429(18)	175(14)	160(17)	289(16)
F(37)	630(20)	367(15)	270(15)	7(12)	89(14)	177(14)

O(1)	310(18)	184(15)	266(16)	30(12)	189(14)	28(13)
O(2)	292(17)	188(14)	218(15)	3(13)	144(13)	23(14)
O(3)	355(19)	199(16)	245(16)	38(13)	160(14)	7(14)
N(1)	230(20)	177(18)	161(17)	-5(14)	109(16)	-22(15)
N(2)	260(20)	230(20)	218(19)	7(16)	117(17)	-1(17)
B	240(30)	220(20)	190(20)	0(20)	140(20)	10(20)
C(1)	290(30)	220(20)	180(20)	13(18)	180(20)	50(20)
C(2)	300(30)	290(30)	230(20)	30(20)	170(20)	90(20)
C(3)	460(30)	390(30)	210(20)	70(20)	140(20)	120(20)
C(4)	630(40)	290(30)	340(30)	140(20)	310(30)	190(30)
C(5)	530(40)	180(20)	420(30)	-20(20)	330(30)	40(20)
C(6)	340(30)	190(20)	240(20)	-18(18)	210(20)	10(20)
C(7)	380(30)	360(30)	170(20)	-40(20)	80(20)	10(20)
C(8)	460(30)	400(30)	380(30)	-130(20)	110(20)	90(30)
C(9)	410(40)	580(40)	430(30)	-120(30)	80(30)	20(30)
C(10)	370(30)	230(20)	350(30)	-50(20)	150(20)	-40(20)
C(11)	550(40)	580(40)	540(30)	-250(30)	380(30)	-260(30)
C(12)	450(30)	390(30)	340(30)	-40(20)	210(30)	-10(20)
C(13)	250(30)	180(20)	210(20)	-36(17)	70(20)	45(19)
C(14)	220(20)	150(20)	220(20)	-20(18)	109(18)	-9(19)
C(15)	200(20)	180(20)	220(20)	10(18)	77(18)	-1(19)
C(16)	230(30)	250(20)	180(20)	-12(18)	121(19)	10(20)
C(17)	360(30)	190(20)	270(20)	38(19)	150(20)	10(20)
C(18)	360(30)	190(20)	290(20)	-3(19)	180(20)	30(20)
C(19)	240(30)	230(20)	200(20)	13(18)	90(20)	-20(20)
C(20)	310(30)	160(20)	170(20)	-22(17)	130(20)	11(19)
C(21)	270(30)	210(20)	190(20)	-16(18)	110(20)	-20(20)
C(22)	410(30)	190(20)	220(20)	47(19)	150(20)	80(20)
C(23)	280(30)	260(30)	210(20)	-17(19)	0(20)	100(20)
C(24)	210(30)	250(30)	290(20)	-100(20)	80(20)	-10(20)
C(25)	270(30)	180(20)	250(20)	8(19)	130(20)	20(20)
C(26)	240(30)	220(20)	250(20)	11(18)	140(20)	18(19)
C(27)	300(30)	260(20)	290(30)	20(20)	150(20)	20(20)
C(28)	280(30)	320(30)	320(30)	-70(20)	40(20)	-20(20)
C(29)	260(30)	320(30)	530(30)	0(20)	170(30)	-100(20)
C(30)	330(30)	290(30)	370(30)	40(20)	260(30)	-10(20)
C(31)	310(30)	260(20)	270(20)	0(20)	120(20)	0(20)
C(32)	220(30)	250(20)	210(20)	37(18)	120(20)	4(19)
C(33)	230(30)	250(20)	250(20)	69(19)	140(20)	20(20)
C(34)	330(30)	220(20)	330(30)	-40(20)	180(20)	-30(20)
C(35)	420(30)	160(20)	490(30)	50(20)	260(30)	50(20)
C(36)	420(30)	320(30)	340(30)	130(20)	170(20)	150(20)
C(37)	330(30)	290(30)	260(20)	0(20)	100(20)	40(20)

Table 5. Hydrogen coordinates (x 10^4) and isotropic displacement parameters ($Å^2$x 10^3) for TRY2 (CCDC No. 140826).

	x	y	z	U_{iso}
H(3)	2195	3290	7452	41
H(4)	1575	2136	7054	46

H(5)	665	1966	5679	41
H(7)	2002	4885	6049	36
H(8A)	889	5040	6762	62
H(8B)	1679	5523	7231	62
H(8C)	1487	4769	7663	62
H(9A)	2974	4300	7683	72
H(9B)	3155	5066	7270	72
H(9C)	3282	4313	6798	72
H(10)	-94	3413	4099	37
H(11A)	-590	1983	4538	78
H(11B)	-1141	2543	3854	78
H(11C)	-935	2719	4877	78
H(12A)	983	2807	3605	56
H(12B)	99	2482	3101	56
H(12C)	683	2029	3884	56
H(13)	1716	4043	4260	25
H(15)	1981	4618	2929	23
H(17)	1457	6810	2454	31
H(18)	731	6832	3554	31
H(10A)	6775	3889	5226	135
H(10B)	7503	3877	4720	135
H(10C)	7224	3132	5103	135
H(10G)	5898	3177	4053	108
H(10H)	6147	3943	3685	108
H(10I)	7001	2563	3559	108
H(10J)	7271	3329	3208	108
H(10K)	5914	3404	2165	108
H(10L)	5668	2624	2502	108
H(10M)	6889	2096	2046	108
H(10N)	6962	2863	1572	108
H(10O)	5552	2690	659	108
H(10P)	5506	1910	1117	108
H(10D)	5895	1725	-246	135
H(10E)	6646	1468	543	135
H(10F)	6689	2245	83	135